

**Aqueous solvent-gel cleaning of poly (methyl methacrylate)  
surfaces in museum collections**

***Stefani Kavda***

A thesis submitted for  
the degree of Doctor of Philosophy  
in Art Conservation Science

**University College London**

November 2019

## **Declaration of originality**

I, Stefani Kavda, confirm that the work presented in this thesis is my own. Where information has been derived from other sources, I confirm that this has been indicated in the thesis.

Stefani Kavda

## Acknowledgements

---

First and foremost I want to thank my supervisors Dr. Stavroula Golfomitsou and Dr. Emma Richardson for mentoring me over the past five years. Thank you both for always encouraging my research, shaping me into a researcher and proofreading so many drafts. Voula thank you for enduring my endless chapters and Emma thank you for always understanding my made-up words! I appreciate all your contributions of time and ideas in formulating my research topic, as well as your patience and guidance. I would like to express my special appreciation and thanks to Professor Dr. Thilo Rehren for his invaluable academic advice and for always being so supportive of my work.

My thanks also go out to the support I received from Dr. Lora Angelova, who was always keen to share her materials with me, as well as her expert knowledge on polymer chemistry and gel making. I am grateful for her interest in my work and her helpful comments. The study of the oxidative degradation of PMMA under UV radiation discussed in this thesis would have not been possible without the Pyrolysis-Gas Chromatography/Mass Spectrometry analysis carried out by Dr. Rachel Rivenc at the Getty Research Institute. I am especially grateful to Benedict Barbour, artist curator at the Msheireb Art Centre for kindly trusting me to treat three PMMA objects from the collection. Many thanks also to Peter Swartjes from Atlas, for always being available to assist me with the use of the weathering chamber.

I would like to thank Arianne Panton, the Conservation and Laboratory Technician at UCL Qatar for her willingness to help, but mostly for always being smiley and making my days in the lab fun. I also want to thank the conservators who took the time and interest to participate in my survey about plastics in museum collections: my work would not be so pertinent without their participation. I am also very grateful to the staff at UCL for taking care of all the logistics and administration during various stages of my PhD. I am happy to have worked with fellow PhDs and Post-Docs at the Materials Studies Laboratory at the UCL History of Art Department, not only for being a source of good advice and collaboration, but also for their friendship. I would also like to acknowledge Professor Dr. JoAnn Peters for introducing me to the world of polymer chemistry and inspiring me, and Tim Bechthold for introducing me to the fascinating world of plastics in design at Die Neue Sammlung. Special thanks go to my colleagues at the Deutsches Museum for their understanding and the warmth they extended to me during the final stages of writing up and submission.

I gratefully acknowledge the funding source that made my PhD work possible. My numerous travels, conferences, research materials and equipment were generously funded by Qatar Foundation. I would like to take this opportunity to thank UCL Qatar and Dr. Sam Evans, Director of UCL Qatar for supporting my work.

Although working on the PhD and carrying out experimental work in the labs in Doha has been a very challenging and often lonely process, my time there was made so wonderful due to my friends who quickly became family. I am grateful for the time spent with you ya habibis. I would like to say a very big thank you to Ghaida for the long nights she spent with me preparing samples for artificial ageing and tying them - one by one - on the sample holders! And to Theo, for the fruitful discussions about my chapters. Thank you both for your comfort and friendship. A heartfelt thank you goes to Mateusz, who has been by my side throughout this PhD, during tough moments but also happy explorations. Whose profound belief in my abilities, his patience and care, have kept me going. Thank you. Finally, words cannot express the huge debt of gratitude I owe to my Mum, Dad and Brother for all their love, nurturing and support in all my pursuits and particularly over these challenging past five years. For all the comfort food my Mum has cooked, all the flights my Dad has tracked and all the intergalactic talks with my brother. For always lending a sympathetic ear to my complaints. You are always there for me. For this, I am extremely grateful.

## Abstract

---

This research explores the use of aqueous solvent-gel systems for cleaning transparent and highly polished poly(methyl methacrylate) (PMMA) surfaces found in historical, technological, art and design museum collections. Surface transparency and glossiness were identified as conservators' priorities when cleaning plastics, in a survey conducted for the purposes of this research. The absence of established conservation cleaning treatments for plastics has led to the inappropriate use of methods employed on other materials. Gels are used here as solvent carriers for their potential to optimise cleaning with their purported abilities to control solvent diffusion and limit mechanical stresses.

Factors affecting cleaning are investigated through a series of statistically designed laboratory-based experiments on unaged and accelerated light-aged PMMA samples. A range of polar and nonpolar solvents, and natural as well as synthetic polymeric matrices are tested independently and in combination. Artificial oily dirt and pressure-sensitive adhesive are applied to surfaces to respectively simulate human fingerprints and labels/package tape remains. PMMA is mechanically and chemically characterised with Dynamic Mechanical Analysis, tensile testing and pyrolysis-Gas Chromatography/Mass Spectrometry. Macroscopic observation, stereomicroscopy and Scanning Electron Microscopy imaging are used to evaluate visual change. Weight and gloss measurements offer quantitative evidence of post-treatment changes. Surface chemical modifications are detected with Attenuated Total Reflection Fourier Transform Infrared spectroscopy and bulk mechanical changes are monitored with Nuclear Magnetic Resonance Mobile Universal Surface Explorer. Finally, three PMMA museum objects with a user life are treated with the successful gels to test the validity of lab-based results.

The research has shown that direct application of deionised water, ethanol, isopropanol and petroleum ether with cotton swabs causes dissolution of PMMA components and is to be avoided. Solvents dispersed in Agar, Gellan, Pemulen TR2/triethanolamine and 80 % Poly(vinyl acetate)/borax gels regulate the damaging solvent effect and reduce visual damage. Carbopol E22/Ethomeen C-25 is unsuitable due to inducing numerous scratches and leaving gel residues. Pemulen performed the best; with isopropanol being the most efficient at oily dirt removal and petroleum ether at adhesive removal. Repeated gel applications are recommended for improved results. This research recommends the use of Poly(vinyl acetate)/borax ethanol and Pemulen TR2/triethanolamine gels/emulsions with isopropanol or petroleum ether for cleaning transparent and glossy PMMA in museum collections.

## Impact statement

---

The increasing proportion of plastics in everyday life and museums has led to an ever-growing need for their preservation. The research presented in this thesis is the first systematic piece of work on the use of gel systems for the cleaning of transparent and highly polished (glossy) plastic surfaces. Due to the lack of an established approach, common cleaning treatments widely used on different types of object surfaces or methods developed for industrial purposes are often being employed. While these may be safe on other materials, they might compromise the physical and visual characteristics of plastics, particularly pristine surfaces; Simple mechanical cleaning can introduce abrasions and in turn reduce gloss, and wet cleaning may cause swelling, dissolution, or extraction of components. These types of damage cause loss of aesthetic qualities integral to transparent PMMA objects and artworks, leading to change of perception and loss of their artistic and aesthetic value. This research thus responds to the necessity of identifying safe treatments and systematising their application for use on pristine PMMA surfaces.

The research carried out in this thesis confirmed that gel systems can offer more control over the solvent action and cleaning. Moreover, it proved that the effect of cleaning with a range of gels is safer than application of free solvent with the conventional use of cotton swabs. Up until now cleaning of such objects was empirical. This study provides scientific evidence that elucidates the processes involved in cleaning using solvent-gel systems, and provides unprecedented data regarding the visual, chemical and physical changes that can occur on PMMA surfaces as a result of cleaning. In relation to contributions in academia, this research provides data that can be used to further research on gels and cleaning of other materials used in museum objects. Moreover, it will allow professionals in the field to pursue the targeted development of cleaning treatments for different plastics.

Outside of academia, this thesis contributes to the conservation profession and the advancement of the conservation of modern materials. Findings of this research offer conservators and conservation scientists a range of optimised gel treatments with different properties that are safe for use on immaculate PMMA surfaces and successful at removing a mixture of surface dirt and oily fingerprints, as well as adhesive remains from packaging tapes and self-adhesive labels. By disseminating the work to conservation practitioners, dealing with the hands-on treatment of plastics, this research provides a methodical and practical approach for the conservation of PMMA. It discusses the properties of different gel formulations, sets forth possible risks and offers a variety of protocols involving practical information and knowledge sharing on how to best prepare gel cleaning systems, what to avoid and what to expect, all of which can be consulted or followed by conservators.

## Table of contents

---

<b>Chapter 1. INTRODUCTION</b>	1
1.1. CONSERVATION CLEANING OF MUSEUM OBJECTS	3
1.2. STATING THE PROBLEM	5
1.3. RESEARCH AIMS & OBJECTIVES	8
1.4. THESIS STRUCTURE	10
<b>Chapter 2. RESEARCH DESIGN &amp; METHODS</b>	13
2.1. OPEN-ENDED SURVEY (RESEARCH METHOD I)	13
2.2. LITERATURE REVIEW (RESEARCH METHOD II)	14
2.3. EXPERIMENTAL WORK (RESEARCH METHOD III)	14
2.3.1. Selection of PMMA & artificial ageing	14
2.3.2. Sample preparation & artificial dirt	16
2.3.3. Gels & solvents for cleaning	18
2.3.4. Design of cleaning experiments	19
2.3.5. Evaluation methods & data analysis	19
2.4. CASE STUDY CLEANING APPLICATION OF MUSEUM OBJECTS	20
<b>Chapter 3. PLASTICS &amp; POLY (METHYL METHACRYLATE)</b>	21
3.1. BRIEF REVIEW OF PLASTICS	21
3.1.1. Overview of historical development	21
3.1.2. Application in industry, art & design	24
3.2. DEVELOPMENT & USE OF POLY (METHYL METHACRYLATE)	27
3.3. POLY (METHYL METHACRYLATE): PROPERTIES, STRUCTURE & DEGRADATION	31
3.3.1. Chemical & physical properties	33
3.3.2. Mechanical behaviour	39
3.3.3. Degradation	42
3.3.3.1. Physical ageing	43
3.3.3.2. Chemical degradation	47
<b>Chapter 4. CLEANING OF POLY (METHYL METHACRYLATE)</b>	51
4.1. OPEN-ENDED SURVEY OF EXPERTS OPINIONS	51
4.2. INDUSTRIAL & CONSERVATION CLEANING OF PLASTICS	54
4.2.1. Review of cleaning poly (methyl methacrylate)	55
4.2.2. The use of cleaning agents on poly (methyl methacrylate)	56
4.3. INTRODUCTION TO GEL CLEANING IN CONSERVATION OF CULTURAL HERITAGE	60
4.3.1. Gels: chemistry & properties	65
<b>Chapter 5. ARTIFICIAL AGEING, SAMPLE PREPARATION &amp; ARTIFICIAL DIRT</b>	76
5.1. LIGHT AGEING REGIME	76
5.1.1. Mechanical testing of poly (methyl methacrylate)	79
5.1.1.1. Preliminary tensile test: fine tuning the method	80
5.1.1.2. Main tensile test of exponentially aged material	80

5.1.1.3. Dynamic Mechanical Analysis of exponentially aged material	87
5.1.2. Characterisation of poly (methyl methacrylate)	92
5.1.2.1. <i>Attenuated total reflectance</i> Fourier transform infrared spectroscopy	92
5.1.2.1.a. New poly (methyl methacrylate)	93
5.1.2.1.b. UV-aged/irradiated poly (methyl methacrylate)	95
5.1.2.1.c. Tacticity of poly (methyl methacrylate)	97
5.1.2.2. Pyrolysis-Gas Chromatography/Mass Spectrometry	98
5.1.2.3. Discussion of gravimetric study, mechanical testing & chemical analysis	100
5.2. SAMPLE PREWASHING: RESIDUE REMOVAL	104
5.3. ARTIFICIAL DIRT: PREPARATION & APPLICATION	105
5.3.1. Synthetic sebum soil/carbon black	106
5.3.2. Pressure-sensitive spray adhesive	109
<b>Chapter 6. CLEANING EVALUATION &amp; ANALYTICAL METHODS</b>	<b>114</b>
6.1. VISUAL ASSESSMENT	115
6.1.1. Macroscopic evaluation	115
6.1.2. Stereomicroscopy under raking light	115
6.1.3. Scanning electron microscopy imaging	116
6.1.4. Criterion anchored ranking system (CARS)	118
6.2. GLOSS MEASUREMENTS	123
6.3. WEIGHT CHANGE MEASUREMENTS	127
6.4. ATTENUATED TOTAL REFLECTANCE FOURIER TRANSFORM INFRARED SPECTROSCOPY	129
6.5. NUCLEAR MAGNETIC RESONANCE MOBILE UNIVERSAL SURFACE EXPLORER	132
6.6. EXPERIMENTAL DESIGN & ANALYSIS OF VARIANCE	145
<b>Chapter 7. CLEANING: MATERIALS &amp; PROTOCOLS</b>	<b>149</b>
7.1. CLEANING MATERIALS	149
7.1.1. Synthesis of gels	149
7.1.1.1. Fourier Transform Infrared Spectroscopy characterisation of gels	153
7.1.2. Solvent effects: immersion study	162
7.2. CLEANING PROTOCOL	172
<b>Chapter 8. PRELIMINARY EXPERIMENTS</b>	<b>176</b>
8.1. UNAGED, UNSOILED POLY (METHYL METHACRYLATE)	176
8.1.1. Experimental design	176
8.1.2. Discussion of results	177
8.2. REPLICATION OF TREATMENTS	178
8.2.1. Experimental design	179
8.2.2. Results & interpretation	179
8.2.3. Discussion of results	198
8.3. APPLICATION TIME: 5 MINUTES VERSUS 60 MINUTES	200
8.3.1. Experimental design	201
8.3.2. Results & discussion	201



<b>8.4. 5 MINUTES: REPEATED APPLICATIONS</b>	201
<b>8.4.1. Experimental design</b>	202
<b>8.4.2. Results &amp; discussion</b>	202
<b>8.5. PRELIMINARY SOLVENT TESTING</b>	203
<b>Chapter 9. MAIN EXPERIMENTS: UNAGED &amp; AGED DIRT</b>	204
<b>9.1. POLY (METHYL METHACRYLATE) WITH UNAGED DIRT</b>	204
<b>9.1.1. Experimental design</b>	204
<b>9.1.2. Results and interpretation</b>	205
<b>9.1.2.a. Synthetic sebum soil</b>	205
<b>9.1.2.b. Spray adhesive</b>	217
<b>9.1.3. Conclusion</b>	229
<b>9.2. POLY (METHYL METHACRYLATE) WITH AGED DIRT</b>	231
<b>9.2.1. Experimental design</b>	231
<b>9.2.2. Results &amp; interpretation</b>	233
<b>9.2.2.a. Aged synthetic sebum soil</b>	233
<b>9.2.2.b. Aged spray adhesive</b>	244
<b>9.2.3. Conclusion</b>	255
<b>Chapter 10. MAIN EXPERIMENTS: REPEATED APPLICATIONS</b>	257
<b>10.1. POLY (METHYL METHACRYLATE) WITH AGED DIRT</b>	257
<b>10.1.1. Experimental design</b>	261
<b>10.1.2. Results &amp; interpretation</b>	263
<b>10.1.2.a. Aged synthetic sebum soil</b>	263
<b>10.1.2.b. Aged spray adhesive</b>	275
<b>10.1.3. Conclusion</b>	285
<b>10.1.4. Nuclear Magnetic Resonance Mobile Universal Surface Explorer</b>	286
<b>Chapter 11. CASE STUDY: CLEANING OF MUSEUM OBJECTS</b>	289
<b>11.1. CASE STUDIES</b>	289
<b>11.1.1. Neon shop sign C550</b>	290
<b>11.1.2. Lamp shade C553</b>	297
<b>11.1.3. Lamp shade C554</b>	303
<b>11.2. CONCLUSIONS</b>	306
<b>Chapter 12. DISCUSSION &amp; CONCLUSION</b>	308
<b>12.1. DISCUSSION OF EXPERIMENTAL RESULTS</b>	308
<b>12.1.1. The effects of free liquids, hydrogels &amp; solvent gels on pristine PMMA</b>	308
<b>12.1.2. Removal of synthetic sebum soil &amp; pressure-sensitive spray adhesive</b>	311
<b>12.1.3. Optimisation of treatments with three consecutive 3-minute gel applications</b>	313
<b>12.2. REVIEW OF CLEANING EVALUATION METHODS</b>	316
<b>12.3. CASE STUDIES: CLEANING OF THREE-DIMENSIONAL MUSEUM OBJECTS</b>	317
<b>12.4. EXPERIMENTAL CRITIQUE &amp; LIMITATIONS</b>	319

<b>12.5. CONCLUSION &amp; FURTHER RESEARCH</b>	320
<b>12.5.1. Recommendations for future research</b>	324
<b>Appendix A. Primary photooxidation routes of PMMA relating to the movement of free radicals</b>	325
<b>Appendix B. Conservation survey questionnaire &amp; answers</b>	326
<b>Appendix C. Mounting samples in the Atlas ageing chamber</b>	337
<b>Appendix D. Preliminary tensile test: fine tuning the method</b>	341
<b>Appendix E. Diagram of the mounting positions of PMMA samples in the Atlas chamber for exponential ageing</b>	344
<b>Appendix F. Tensile test of exponentially aged material</b>	345
<b>Appendix G. Residues on received samples &amp; pre-washing</b>	349
<b>Appendix H. Conditioning of samples &amp; weighing protocol</b>	354
<b>Appendix I. Physical characteristics of gels</b>	362
<b>Appendix J. Smoothing of NMR MOUSE data</b>	364
<b>Appendix K. Gel recipes</b>	365
<b>Appendix L. NMR MOUSE profile scans of gel systems</b>	367
<b>Appendix M. Preliminary cleaning experiments on unaged, unsoiled PMMA samples</b>	368
<b>Appendix N. Macroscopic observation of PMMA samples synthetic sebum soil treated with gels for 5 &amp; 60 minutes</b>	379
<b>Appendix O. NMR results of 2<sup>nd</sup> replicates: line graphs of profile scans after gel treatment</b>	380
<b>Appendix P. Msheireb Arts Centre, Doha</b>	381
<b>Appendix Q. Characterisation of objects with ATR-FTIR analysis</b>	384
<b>Appendix R. Treatment reports of Msheireb Art Centre case studies</b>	386
<b>BIBLIOGRAPHY</b>	395

## List of figures

---

Figure 1.1. Advertising signs made of PMMA in the District Line of the London Tube. ....	2
Figure 1.2. Double Loop (1946) by László Moholy-Nagy. ....	2
Figure 3.1. Posters in the U.S. showing the benefits of plastics. ....	23
Figure 3.2. László Moholy-Nagy and his studies of light through the use of acrylics. ....	27
Figure 3.3. Charles Biederman's geometric relief ( <a href="https://blog.dma.org/tag/charles-biederman/">https://blog.dma.org/tag/charles-biederman/</a> ). ....	28
Figure 3.4. Bruce Beasley in front of Apolymon in Sacramento, 1970 ( <a href="http://brucebeasley.com/apolymon/">http://brucebeasley.com/apolymon/</a> ). ....	29
Figure 3.5. Craig Kauffman next to his acrylic sheet ( <a href="https://www.nytimes.com/2010/05/15/arts/design/15kauffman.html">https://www.nytimes.com/2010/05/15/arts/design/15kauffman.html</a> ). ....	29
Figure 3.6. a. Heat-formed mineral-coated PMMA by Chamberlain ( <a href="https://theartstack.com/artist/john-chamberlain/luna-luna-luna-in-memory-of-elaine-chamberlain-1970-mineral-coated-synthetic-polymer-resin-photograph-by-katy-hamer-image-courtesy-of-the-guggenheim-ny">https://theartstack.com/artist/john-chamberlain/luna-luna-luna-in-memory-of-elaine-chamberlain-1970-mineral-coated-synthetic-polymer-resin-photograph-by-katy-hamer-image-courtesy-of-the-guggenheim-ny</a> ), b. Giraffa artificiale con fiore by Marotta ( <a href="https://www.vogue.it/en/people-are-talking-about/vogue-arts/2012/11/tribute-to-gino-marotta?refresh_ce=#ad-image234871">https://www.vogue.it/en/people-are-talking-about/vogue-arts/2012/11/tribute-to-gino-marotta?refresh_ce=#ad-image234871</a> ), Transparent PMMA stools and chairs made by Kartell: .....	30
Figure 3.7. Helen Pashgian sanding one of her transparent sculptures at the California Institute of Technology, 1970 ( <a href="https://blogs.getty.edu/pacificstandardtime/explore-the-era/archives/i130/">https://blogs.getty.edu/pacificstandardtime/explore-the-era/archives/i130/</a> ). .....	31
Figure 3.8. Addition polymerisation is reliant on the presence of unsaturation. The double bond between the two carbon atoms of the monomer (a) break and form two new bonding sites (b). .....	32
Figure 3.9. Two distinct physical structures found in polymers: amorphous and crystalline (Wager and Hoffman 2011). ....	32
Figure 3.10. The perfect three-dimensional network of a diamond. ( <a href="https://tex.stackexchange.com/questions/141363/draw-realistic-3d-crystal-structures-diamond">https://tex.stackexchange.com/questions/141363/draw-realistic-3d-crystal-structures-diamond</a> ). ....	32
Figure 3.11. Crystalline regions of closely packed chains and amorphous regions of random tangles (Bryant 1947, p. 549). ....	33
Figure 3.12. Methyl methacrylate: the monomer of PMMA. The methyl side group attached to the $\alpha$ -carbon is highlighted in red and its ester side group (methoxycarbonyl) with a methyl as its R group (in blue) is highlighted in yellow. ....	34
Figure 3.13. The chemical structure of PMMA monomer methyl methacrylate. ....	34
Figure 3.14. Schematic diagram of an unoriented (a) and oriented (b) amorphous polymer. (Ward and Sweeney 2013, p. 11). ....	36
Figure 3.15. The volume of crystalline and amorphous polymers in relation to their transition regions: $T_m$ for crystalline and $T_g$ for amorphous (Shashoua 2008, p. 108). ....	37
Figure 3.16. Diagram of PMMA, typical of all linear-amorphous polymers, exhibiting the distinguishable states of deformation: liquid, rubbery, elastic, glassy-solid (Ashby 2012, p. 429). .....	37

<i>Figure 3.17. The T<sub>g</sub> is the point of break in the slope of free volume plotted versus temperature (Ward and Sweeney 2013, p. 151).</i>	38
<i>Figure 3.18. Mechanical deformation (elongation) of a solid under an applied pulling force (stress).</i>	40
<i>Figure 3.19. Stress-strain curves displaying three typically different types of stress-strain polymer behaviour: A. brittle, B. plastic and C. highly elastic (Callister and Rethwisch 2014, p. 571).</i>	41
<i>Figure 3.20. Load-elongation curves displaying a typical polymer mechanical behaviour at four different temperatures: (a) brittle fracture, (b) ductile failure, (c) necking and cold-drawing and (d) rubbery behaviour (Ward and Sweeney 2013, p. 380).</i>	42
<i>Figure 3.21. PMMA dome-cover of cake plate with visible scratches on its surface (a), parallel microcrazes (b) and crack formation (c).</i>	45
<i>Figure 3.22. Transparent PMMA bracelet exhibiting crack formation (Laganà and van Oosten 2011, 7).</i>	46
<i>Figure 3.23. Transparent PMMA architectural model exhibited at the</i>	46
<i>Figure 3.24. Structures of a craze and a crack in comparison (Andrews and Bevan 1972, p. 337).</i>	47
<i>Figure 4.1. Agarose repeat unit: 1, 3 linked D-galactose (a) and 1, 4 linked 3, 6 anhydro L-galactose (b) (Varshosaz et al. 2015, p. 2).</i>	68
<i>Figure 4.2. 1, 3 linked D-galactose (a) and sulfated 1, 4 linked 3, 6 anhydro L-galactose with D-glucuronic acid and pyruvic acid (b) (Varshosaz et al. 2015, p. 2).</i>	68
<i>Figure 4.3. Primary chemical structure of deacetylated Gellan gel; linear anionic heteropolysaccharide made of repeating units of two molecules of β-D-Glucose (a,b), one molecule of α-L-Rhamnose (c) and one molecule of β-D-Glucuronic acid (d) (ICF Consulting 2006, p. 1).</i>	70
<i>Figure 4.4. Gellan gel coil helix and its transition scheme (Iannuccelli and Sotgiu 2010, p. 31).</i>	71
<i>Figure 4.5. Partially hydrolysed poly(vinyl acetate) (xPVA) (a) and fully hydrolysed poly(vinyl alcohol) (PVA) (b) (Ben Halima 2016, p. 39823).</i>	74
<i>Figure 4.6. Borate ion.</i>	74
<i>Figure 5.1. Spectral power distributions of xenon arc with Atlas Right Light/Quartz filters compared to normalised ASTM G177 sunlight (After Pickett 2018, p. 177).</i>	79
<i>Figure 5.2. Instron 5944 Single Column.</i>	79
<i>Figure 5.3. Samples for exponential artificial ageing, cut for subsequent tensile testing, were mounted on the holders with nylon thread. Labelling used permanent marking to endure the artificial weathering.</i>	81
<i>Figure 5.4. Schematic diagram of the DMA curve of the unaged PMMA sample analysed in this study (Ehrenstein et al. 2004, p. 239).</i>	88
<i>Figure 5.5. DMA curve of amorphous PMMA exhibiting two relaxation processes:</i>	89
<i>Figure 5.6. DMA 8000 Perkin Elmer.</i>	90
<i>Figure 5.7. Spectra of unaged (pink line) and 32 days UV-aged (green line) reference PMMA. Peaks were enlarged and labelled inset. The spectra were averaged from three replicates.</i>	94
<i>Figure 5.8. Conformational characteristics of isotactic and syndiotactic polymers (Reusch 2013).</i>	99

<i>Figure 5.9. Normalised comparison between unaged and UV-aged PMMA. With ageing two peaks were altered substantially: at 3.33 minutes appearance of Methyl pyruvate (or Propanoic acid, 2-oxo-, methyl ester) and at 4.74 appearance of 2-Methoxyirane-2-carboxylic acid, methyl ester. ....</i>	100
<i>Figure 5.11. ....</i>	101
<i>Figure 5.10.....</i>	101
<i>Figure 5.12. Spectra of unaged and UV-aged PMMA for 4, 8, 16, 32, 64 and 96 days. Spectra are averaged from three replicates for each stage of ageing. For absorption bands and assignments of new and exponentially UV-aged PMMA see Table 5.4. ....</i>	104
<i>Figure 5.13. PMMA coupons immediately after being removed from the black hard-plastic, on which they were attached when received. Transparent and black (dust) residues are visible on all the coupons. ....</i>	105
<i>Figure 5.14. Ultrasonic bath cleaning of PMMA coupons in deionised water. ....</i>	106
<i>Figure 5.15. Different mixtures of sebum oil with carbon black pigment after one application with different consistencies. The circled mixture shows pigment globules. Mixture 2 (2 % carbon black) shows the best homogeneity. ....</i>	108
<i>Figure 5.16. Test applications of the four different sebum oil/carbon black mixtures with airbrush on transparent PMMA surrogate surface. ....</i>	109
<i>Figure 5.17. Step/comb gauge to measure synthetic sebum soil thickness. ....</i>	109
<i>Figure 5.18. Dried synthetic sebum soil (sebum oil and carbon black pigment) at 180 °C for 24 hours. ....</i>	110
<i>Figure 5.19. Spectrum of sebum oil and 2wt.% carbon black pigment formulation with 16 scans at ambient temperature and pressure, with a resolution of 4 cm<sup>-1</sup> equating to a penetration depth of 0.5-5 µm. Labelled absorption bands correspond to assignments in Table 5.5. ....</i>	110
<i>Figure 5.20. IR spectra of PSA under study (pink) in ATR mode matched with reference commercial product BYK 358 (black): a polyacrylate-based solution with 52 % solid content in naphtha, petroleum, light aromatic and isopropyl benzene. Absorption bands and assignments available in Table 5.6. ....</i>	112
<i>Figure 6.1. Microimages of treated PMMA samples captured under the stereomicroscope (x78.1) with raking light. Samples were mounted on a clip and a mask placed on them defined the area to image. EtOH left PMMA with large areas of non-uniform loss of transparency. Agar EtOH after 5 and 60 minutes left deposits of fine nature and imprints of post-treatment swabbing. ....</i>	117
<i>Figure 6.2. PMMA sample observed under 10kV/high vacuum showed damage (deformation and loss of volatile components) in a squared-like shape due to irradiation of the electron beam. ....</i>	119
<i>Figure 6.3. PMMA sample after Agar hydrogel treatment at 1kV/high vacuum. SEM micrograph at a magnification of 100x appeared sharp, while at 500x was blurry. ....</i>	119
<i>Figure 6.4. Glossmeter with options of incident angles at 20°, 60° and 85°. ....</i>	125
<i>Figure 6.5. Example of raw gloss values expressed in gloss units (GU) at measuring angle of 20 degrees. ....</i>	126
<i>Figure 6.6. ATR-FTIR reference spectrum of PMMA (Shashoua 2008, 264). ....</i>	133
<i>Figure 6.7. Relaxation times (<math>T_{2eff}</math>) of rigid and soft materials, as obtained by unilateral NMR. The harder the material, the shorter the relaxation (Meldrum 2013). ....</i>	138

<i>Figure 6.8. Sketch of experimental set up of PMMA sample on the NMR MOUSE lift ready for scanning. ....</i>	<i>139</i>
<i>Figure 6.9. 2D colour-intensity contour heat map of the aged PMMA with aged synthetic soil before (left) and 24 h after (right) treatment with Pemulen H<sub>2</sub>O. The first 2 echoes (between 0.06 – 0.08) showed the highest proton density. The material has fully relaxed by the 6<sup>th</sup> echo. ....</i>	<i>140</i>
<i>Figure 6.10. 2D colour-intensity contour heat maps of the dynamic scans of aged PMMA with aged synthetic soil immediately after treatment with Pem hydrogel. The scans were acquired only for the first 2 echoes. Each increment (sampling depth) equates to 50 μm. Changes in the signal amplitude are either nonexistent or difficult to observe. ....</i>	<i>141</i>
<i>Figure 6.11. Issues arising from analytical depth resolution not representing signal and set step size. (A) depicts the ideal situation, while (B) and (C) instances where resolution is bigger or smaller than the step size. ....</i>	<i>144</i>
<i>Figure 6.12. The 7<sup>th</sup> segment (highlighted with a red arrow) is 350 μm from the sample surface and shows signal of approximately 0.05 based on the colour intensity scale. ....</i>	<i>145</i>
<i>Figure 6.13. The main effects plot of new and aged PMMA samples on CARS scores. Points represented the mean values for all runs per factorial level. Horizontal dotted line represented the mean value of all factorial runs in the experiment. ....</i>	<i>150</i>
<i>Figure 7.1. Glass jars with lids for storage of Carbopol/Ethomeen, Pemulen/TEA and PVA/borax hydro- and solvent-gels. ....</i>	<i>152</i>
<i>Figure 7.2. Physical, solid Agar and Gellan hydrogels and solvent-gels prepared as rectangular pieces ready to be used. Gels were refrigerated in resealable polyethylene zip lock bags. ....</i>	<i>153</i>
<i>Figure 7.3. Carbopol/Ethomeen C-25 hydrogels and solvent-gels prepared and stored in glass jars with lids. ....</i>	<i>154</i>
<i>Figure 7.4. Pemulen/TEA hydrogels and solvent-gels prepared and stored in glass jars with lids. ....</i>	<i>154</i>
<i>Figure 7.5. PVA/borax hydrogels and solvent-gels prepared and stored in glass jars with lids or flat plastic containers allowing them to spread in pre-formed sheets. ....</i>	<i>155</i>
<i>Figure 7.6. IR spectrum of Agar analysed as a KBr pellet in transmittance mode. Absorption bands and assignments available in Table 7.1. Monomer chemical structure inset. ....</i>	<i>157</i>
<i>Figure 7.7. IR spectra of Gellan analysed as a KBr pellet in transmittance mode (green) and a dried hydrogel in ATR mode (red). Absorption bands and assignments available in Table 7.2. Monomer chemical structure inset. ....</i>	<i>159</i>
<i>Figure 7.8. IR spectrum of Carbopol/Ethomeen hydrogel system analysed in dried state in ATR mode. Absorption bands and assignments available in Table 7.3. Carbopol EZ2 chemical structure inset. ....</i>	<i>160</i>
<i>Figure 7.9. IR spectrum of pure Ethomeen C-25 prepared as a KBr pellet and analysed in transmittance mode. Ethomeen C-25 chemical structure inset. ....</i>	<i>160</i>
<i>Figure 7.10. IR spectrum of Pemulen TR-2/TEA hydrogel system analysed in dried state in ATR mode. Absorption bands and assignments available in Table 7.4. Chemical structures of Pemulen and TEA monomers inset. ....</i>	<i>162</i>

<i>Figure 7.11. IR spectrum of PVA/borax hydrogel system analysed in their dried state in ATR mode. Absorption bands and assignments available in Table 7.5. Chemical structures of PVA and crosslinked PVA/borax network inset. ....</i>	<i>164</i>
<i>Figure 7.12. Overlay of spectra of unaged and aged PMMA and all hydrogel systems (Agar, Gellan, Carbopol/Ethomeen, Pemulen/TEA, PVA/borax). Spectral overlap/similarities are highlighted with a dotted line in red and absorptions are labelled. ....</i>	<i>166</i>
<i>Figure 7.13. Microimages under the Leica M205 A 3D stereomicroscope (x78.1) showing the PMMA sample immersed in EtOH at different time intervals. At Day 7 a network of cracks was visible. ....</i>	<i>168</i>
<i>Figure 7.14. Microimages under the Leica DM 2500P optical microscope showing the PMMA sample immersed in EtOH for a month, at different magnifications. The organised network of cracks showed fine fibrils. ....</i>	<i>169</i>
<i>Figure 7.15. Microimages under the stereomicroscope (x78.1) showing PMMA sample after 2 and 15 days: 5 h after removal from PET and after moistened cotton swab clearance of the surface. Images after immersion showed dust-like residues, which were removed after use of swabs. The longer PMMA stayed in the liquid environment, the less the residues. ....</i>	<i>169</i>
<i>Figure 7.16. Weight change % of untreated control PMMA (black) and samples immersed in liquid environments: EtOH (green), H<sub>2</sub>O (pink), IPA (blue) and PET (yellow) for 30 days. Changes % are relative to the initial weight (pre-immersion) set at zero. ....</i>	<i>171</i>
<i>Figure 7.17. Spectra of PMMA samples: unaged control (orange), 32-days UV-aged control (grey) and 30-days immersed samples in EtOH (green), H<sub>2</sub>O (blue), IPA (pink) and PET (yellow). Regions 3700-2800 cm<sup>-1</sup> and 1000-700 cm<sup>-1</sup> were enlarged and presented in detail. MMA monomer chemical structure inset. ....</i>	<i>172</i>
<i>Figure 7.18. Detail of spectra of PMMA samples with the new peaks formed after immersion in EtOH (green) and IPA (purple) for 30 days. ....</i>	<i>172</i>
<i>Figure 7.19. PMMA sample surfaces during cleaning treatments: putty PVA/borax gel and paste Carbopol/Ethomeen flattened with a glass slide, rigid Agar and Gellan gels placed with a Teflon spatula. ....</i>	<i>178</i>
<i>Figure 7.20. Comparing wiping of a Teflon spatula against rolling dry cotton swabs to standardise the safe removal of gels and solvents from treated PMMA surfaces. Teflon spatula produced significantly less to non-existent scratches compared to cotton swabs. ....</i>	<i>179</i>
<i>Figure 7.21. Comparing rolling moistened cotton swabs against blotting with dry filter paper for post-treatment clearance of gel and solvent residues from the treated PMMA. Rolling moistened swabs in linear motions towards one direction was less damaging and more effective at removing dirt for the transparent surface. ....</i>	<i>180</i>
<i>Figure 8.1. Unaged and unsoiled PMMA samples before treatment with hydrogels, free solvents or solvent gels for 5 or 60 minutes. The samples were labelled at the back. ....</i>	<i>182</i>
<i>Figure 8.2. Microimages under the stereomicroscope (x78.1) with raking light. Aged PMMA samples treated with organic solvents (EtOH, IPA or PET) for 5 minutes, display comparable damage: few deposits, discolouration and intense stains. ....</i>	<i>187</i>
<i>Figure 8.3. Microimages under the stereomicroscope (x78.1) with raking light. All five replicates for each treatment are presented. Agar and Gellan gels coupled with water, IPA or PET, for 5 minutes, induced similar types of surface damage to new PMMA samples: deposits and intense surface imprints of swabbing. Gellan caused more intense damage. ....</i>	<i>188</i>

Figure 8.4. Microimages under the stereomicroscope (x78.1) with raking light. All five replicates for each treatment are presented. Agar and Gellan gels coupled with IPA or PET, for 5 minutes induced comparable damage to aged PMMA samples: a lot of deposits and residues, discolouration and surface imprints of swabbing. .... 189

Figure 8.5. Microimages under the stereomicroscope (x78.1) with raking light. All five replicates for each treatment are presented. Carbopol solvent gels for 5 minutes left aged PMMA samples in a very poor visual condition: deposits and residues, discolouration and surface imprints of swabbing. .... 190

Figure 8.6. SEM micrographs: Unaged, unsoiled PMMA control under magnification x100 (left) and x1000 (right). .... 191

Figure 8.7. SEM micrographs: Aged, unsoiled PMMA control under magnification x100 (left) and x1000 (right). .... 191

Figure 8.8. SEM micrographs of unaged, treated PMMA. Left: Agar H<sub>2</sub>O for 5 minutes rarely left minute gel residues and surface discoloration around them. Right: Carbopol solvent gels left a large amount of gel residues and surface discoloration. .... 192

Figure 8.9. SEM micrographs of aged, treated PMMA. A-C: PMMA surfaces that were left with ring-like stains because of gel treatment leaving behind liquid that upon evaporation left solutes, visible as fine matter; both after Agar and Gellan solvent gels. D-E: Carbopol and Pemulen solvent gels left large amounts of gel. F-G: Samples after PVA appeared to bare thin layers of gel giving the impression they were swabbed or spread around the surface, possibly during the post-treatment clearance. Some solvents such as IPA in PVA caused cloudiness of the transparent surface due to entrapment of solvent. .... 194

Figure 8.10. SEM micrographs of treated PMMA with organic solvents. A: PET left surfaces with deposited material, either precipitates of non-volatile PMMA components or contaminants found on the pre-treated surface. B-C: New PMMA surfaces treated with EtOH and IPA appeared very cloudy due to real time evaporation of solvents (see red arrow) under the SEM beam. .... 195

Figure 8.11. Spectra of new PMMA samples after gel treatments with EtOH (and Pemulen hydrogel). The spectra are averaged from 3 replicates for each treatment. Each replicate is averaged from 3 spot ATR analyses. .... 200

Figure 8.12. Spectra of aged PMMA samples after Carbopol gel treatments. Spectra are averaged from 3 replicates for each treatment. Each replicate is averaged from 3 spot ATR analyses. The spectrum of Carbopol hydrogel (analysed in dried state in ATR mode) is included for comparison. Carbopol left such extensive gel residue that FTIR analysis was unable to absorb PMMA peaks and detected only Carbopol peaks. .... 200

Figure 8.13. New PMMA samples with synthetic soil are treated with Agar and Carbopol solvent gels (12 samples for each gel type). Sets of 4 samples are treated with different repetitions of 5-minute applications: one, two and three. Three applications left samples cleaner than two, which left samples cleaner than one. .... 207

Figure 9.1. SEM micrographs: Unaged PMMA control with synthetic soil under magnification x40 (left) and aged PMMA control under magnification x35 (right). .... 213

Figure 9.2. SEM micrographs: A-D: Agar EtOH left all PMMA clean with limited gel residue. E-H: Agar IPA failed to remove synthetic soil from PMMA and deposited cotton threads and gel residue. .... 215



Figure 9.1. SEM micrographs: Unaged PMMA control with synthetic soil under magnification x40 (left) and aged PMMA control under magnification x35 (right). .....	213
Figure 9.2. SEM micrographs: A-D: Agar EtOH left all PMMA clean with limited gel residue. E-H: Agar IPA failed to remove synthetic soil from PMMA and deposited cotton threads and gel residue. ....	215
Figure 9.3. SEM micrographs: A-B: Agar PET failed to clean synthetic soil from new PMMA and deposited tiny gel residue. C: Agar PET cleaned aged PMMA depositing minute gel residue. D: Pemulen EtOH deposited extensive residue leaving new surfaces hazy. E: Pemulen EtOH cleaned aged PMMA depositing limited gel residue. F, G: Pemulen IPA failed to clean new PMMA and deposited extensive gel residue. H: Pemulen IPA cleaned aged PMMA with limited gel residue. ....	216
Figure 9.4. SEM micrographs: A: Minute Pemulen IPA gel residue macroscopically seen as discolouration. B: Pemulen PET failed to clean new PMMA and deposited gel residue. C: Pemulen PET cleaned aged PMMA. D: Pemulen PET gel residue on aged PMMA. E, G, I: PVA with EtOH, IPA and PET all failed to remove synthetic soil from new PMMA. F: PVA EtOH cleaned aged PMMA. H, J: PVA with IPA and PET failed to clean aged PMMA and deposited extensive gel residue. ....	218
Figure 9.5. Spectra of new PMMA samples with synthetic soil after gel treatment. The spectra are averaged from 3 replicates for each treatment. Each replicate is averaged from 3 spot ATR analyses. The spectrum of synthetic soil is included for comparison. ....	222
Figure 9.6. SEM micrographs: Unaged PMMA control with PSA under magnification x40 (left) and aged PMMA control under magnification x35 (right). ....	226
Figure 9.7 A, D: Agar with EtOH and IPA failed to removed PSA from new PMMA. B: Agar EtOH left aged PMMA partly clean. C: Agar EtOH gel residue entrapped on PSA. E, G, H: Agar with IPA and PET failed to remove PSA from aged PMMA. ....	228
Figure 9.8. A-B: Pemulen EtOH left new and aged PMMA clean, the latter with limited discolouration. C-D: Pemulen IPA deposited extensive gel residue on new and aged PMMA. E: Pemulen IPA left aged PMMA partly clean and F: other areas with gel residue entrapped on PSA remains. G: Pemulen PET left new PMMA clean, but H: with some scratches. ....	229
Figure 9.9. Pemulen PET left aged PMMA clean. B-C: PVA EtOH removed PSA from new PMMA. D-E: PVA EtOH left extensive gel residue on aged PMMA. F: PVA IPA left PSA remains on new PMMA and G-H: extensive gel residue and solute deposits from droplet evaporation. ....	230
Figure 9.10. A-C: PVA IPA failed to remove PSA leaving extensive gel residue. D: PVA PET left new PMMA clean and E: with limited gel residue. F: PVA PET partly removed PSA from aged PMMA, leaving gel residue entrapped on PSA remains. ....	231
Figure 9.11. Spectra of new PMMA samples with PSA after solvent-gel treatment. The spectra are averaged from 3 replicates for each treatment. Each replicate is averaged from 3 spot ATR analyses. The spectrum of PSA is included for comparison. ....	235
Figure 9.12. SEM micrographs: Unaged PMMA control (left) and aged PMMA control (right) with aged synthetic soil under magnification x100. ....	242
Figure 9.13. SEM micrographs: A-D: Agar with EtOH and IPA failed to clean PMMA. E: Pemulen EtOH left new surfaces covered with layers of gel residue and scratches. F: Pemulen EtOH left some areas clean. ....	243
Figure 9.14. SEM micrographs: A: Pemulen IPA cleaned aged samples. B: Pemulen PET failed to clean aged PMMA. C-D: Pemulen PET partly cleaned new PMMA and deposited extensive gel residue. E: PVA EtOH cleaned new PMMA and F: deposited extensive gel residue and scratches.	

*Figure 9.15. Spectra of new PMMA samples with aged synthetic soil after gel treatment. The spectra are averaged from 3 replicates for each treatment. Each replicate is averaged from 3 spot ATR analyses. Peaks are enlarged and labelled. The spectrum of 32-days aged control (untreated, unsoiled) is included for comparison.....* 249

*Figure 9.16. Spectra of aged PMMA samples with aged synthetic soil after solvent-gel treatment. The spectra are averaged from 3 replicates for each treatment. Each replicate is averaged from 3 spot ATR analyses. Peaks are enlarged and labelled. The spectrum of 32-days aged control (untreated, unsoiled) is included for comparison. ....* 250

*Figure 9.17. SEM micrographs: PMMA controls with aged PSA: Unaged under magnification x80 (left) and aged under magnification x45 (right). ....* 253

*Figure 9.18. SEM micrographs: A, B: Agar PET failed to clean PMMA and deposited gel residue. C, D: Pemulen EtOH residues on new PMMA causing the haziness of images. E: Pemulen IPA left aged PMMA clean and F: with limited scratches. G: Pemulen IPA deposited gel residue and caused scratches to new PMMA. H: Pemulen IPA residues on aged PMMA causing the haziness of images. ....* 255

*Figure 9.19. SEM micrographs: A: Pemulen PET left new PMMA clean with limited gel residue. B: Clean new PMMA with solute deposition from droplet evaporation. C, D: Pemulen PET cleaned aged PMMA and induced some discolouration. E, F: PVA PET failed to remove PSA and caused discolouration around gel residues. G: PVA PET caused discolouration around gel deposits on aged PMMA and H: induced scratches. ....* 256

*Figure 10.1. SEM micrographs: A-D: Agar IPA failed to remove synthetic soil from all PMMA surfaces. E-G: Agar PET failed to remove synthetic soil from all PMMA surfaces. H: Pemulen H<sub>2</sub>O left new PMMA surfaces clean. ....* 273

*Figure 10.2. SEM micrographs: A: Tiny Pemulen H<sub>2</sub>O residues on cleaned new surfaces. B: Pemulen H<sub>2</sub>O left aged PMMA surfaces clean with limited synthetic soil remains. C: Pemulen IPA left new PMMA with some soil remains but also D: clean areas. E: Pemulen IPA left aged samples clean. F: Pemulen PET left new PMMA with some soil remains. G: Pemulen PET caused solute deposition from droplet evaporation on clean areas of new and aged PMMA. This resembled stains to the naked eye. ....* 274

*Figure 10.3 SEM micrographs: A, B: Stains formed after Pemulen PET identified as minute gel residues and solute deposition from droplet evaporation. C: PVA EtOH left new surfaces clean with limited synthetic soil remains. D: PVA EtOH left aged PMMA clean. ....* 275

*Figure 10.1. SEM micrographs: A-D: Agar IPA failed to remove synthetic soil from all PMMA surfaces. E-G: Agar PET failed to remove synthetic soil from all PMMA surfaces. H: Pemulen H<sub>2</sub>O left new PMMA surfaces clean. ....* 273

*Figure 10.2. SEM micrographs: A: Tiny Pemulen H<sub>2</sub>O residues on cleaned new surfaces. B: Pemulen H<sub>2</sub>O left aged PMMA surfaces clean with limited synthetic soil remains. C: Pemulen IPA left new PMMA with some soil remains but also D: clean areas. E: Pemulen IPA left aged samples clean. F: Pemulen PET left new PMMA with some soil remains. G: Pemulen PET caused solute deposition from droplet evaporation on clean areas of new and aged PMMA. This resembled stains to the naked eye. ....* 274

Figure 10.3 SEM micrographs: A, B: Stains formed after Pemulen PET identified as minute gel residues and solute deposition from droplet evaporation. C: PVA EtOH left new surfaces clean with limited synthetic soil remains. D: PVA EtOH left aged PMMA clean. ....	275
Figure 10.4. Spectra of new (upper) and aged (bottom) PMMA samples with aged synthetic soil after treatment. The spectra are averaged from 3 replicates for each treatment. Each replicate is averaged from 3 spot ATR analyses. Peaks are enlarged and labelled. The spectrum of 32-days aged control (untreated, unsoiled) is included for comparison. ....	281
Figure 10.5. SEM micrographs: A: Pemulen H <sub>2</sub> O left PSA remains. B: Salt-like structures after Pemulen H <sub>2</sub> O. C: Pemulen H <sub>2</sub> O cleaned aged PMMA. D: Areas of discoloration identified as tiny specks of PSA remains. E: Pemulen EtOH residue on clean new PMMA. F: Formation of a network of cracks on aged PSA remains on aged PMMA. G: Solvent penetrating upper micron PMMA layers resembling stain/discholoration. H: Pemulen PET cleaned new PMMA. ....	285
Figure 10.6. SEM micrographs: A, B: Pemulen PET left aged PMMA clean with limited PSA remains. C: PVA PET failed to remove PSA from new PMMA. D, E: Stains to the naked eye around remaining PSA after PVA PET, identified as solutes and minute gel residues. F: PVA PET failed to remove PSA from aged PMMA. ....	286
Figure 10.7. Spectra of new (upper) and aged (bottom) PMMA samples with aged PSA after gel treatment. The spectra are averaged from 3 replicates for each treatment. Each replicate is averaged from 3 spot ATR analyses. Peaks are enlarged and labelled. The spectra of 32-days aged control (untreated, unsoiled) are included for comparison. ....	291
Figure 11.1. Neon shop sign C550 (front side) before treatment. ....	297
Figure 11.2. Neon shop sign C550 (back side) before treatment. ....	298
Figure 11.3. During treatment of C550 with Pemulen/TEA hydrogel. ....	299
Figure 11.4. During treatment of C550 with Pemulen/TEA hydrogel. ....	300
Figure 11.5. Visibly darkened Pemulen gels after use on the shop sign C550 with entrapped dirt compared to fresh, unused gel: Pemulen/TEA (a) and PVA/borax (b). ....	300
Figure 11.6. PVA/borax EtOH before application (a-b). Gel during treatment of the shop sign C550 (c-d). ....	301
Figure 11.7. The surface of the shop sign C550 before, during and after cleaning. ....	301
Figure 11.8. Neon shop sign C550 (front side) after treatment. ....	302
Figure 11.9. Neon shop sign C550 (back side) after treatment. ....	303
Figure 11.10. Light shade C553 (internally) before treatment. ....	304
Figure 11.11. Light shade C553 (externally) before treatment. ....	305
Figure 11.12. During treatment of C553 with Pemulen/TEA hydrogel (a-b). Before and after treatment with Pemulen/TEA hydrogel (c). Transparent adhesive tape (d-e). Treatment of adhesive tape with Pemulen/TEA hydrogel (f) and Pemulen/TEA PET (g). ....	307
Figure 11.13. Light shade C553 (internally) after treatment. ....	308
Figure 11.14. Light shade C553 (externally) after treatment. ....	309
Figure 11.15. Light shade C554 (internally) before treatment. ....	310
Figure 11.16. Light shade C554 (externally) before treatment. ....	310
Figure 11.17. During treatment of C554 with Pemulen/TEA IPA (a-b). Before and after treatment with Pemulen/TEA IPA (c). ....	311
Figure 11.18. Dirt removed from object C554 and entrapped in used Pemulen/TEA (a). Cotton swabs used for clearance after treatment (b). PVA/borax before use on the metallic element (c). ....	312
Figure 11.19. Light shade C554 internally after treatment. ....	312
Figure 11.20. Light shade C554 externally after treatment. ....	313

## List of graphs

---

<i>Graph 4.2. Types of plastic surfaces mentioned as more problematic to clean in an open-ended survey of conservators of modern materials and plastics.</i> .....	53
<i>Graph 4.3. Types of dirt mentioned as more commonly encountered on plastics in an open-ended survey of conservators of modern materials and plastics.</i> .....	53
<i>Figure 5.1. Spectral power distributions of xenon arc with Atlas Right Light/Quartz filters compared to normalised ASTM G177 sunlight (After Pickett 2018, p. 177).</i> .....	80
<i>Figure 5.2. Instron 5944 Single Column.</i> .....	80
<i>Figure 5.3. Samples for exponential artificial ageing, cut for subsequent tensile testing, were mounted on the holders with nylon thread. Labelling used permanent marking to endure the artificial weathering.</i> .....	82
<i>Figure 5.4. Schematic diagram of the DMA curve of the unaged PMMA sample analysed in this study (Ehrenstein et al. 2004, p. 239).</i> .....	89
<i>Figure 5.5. DMA curve of amorphous PMMA exhibiting two relaxation processes:</i> .....	90
<i>Figure 5.6. DMA 8000 Perkin Elmer.</i> .....	91
<i>Figure 5.7. Spectra of unaged (pink line) and 32 days UV-aged (green line) reference PMMA. Peaks were enlarged and labelled inset. The spectra were averaged from three replicates.</i> ....	95
<i>Figure 5.8. Conformational characteristics of isotactic and syndiotactic polymers (Reusch 2013).</i> .....	100
<i>Figure 5.9. Normalised comparison between unaged and UV-aged PMMA. With ageing two peaks were altered substantially: at 3.33 minutes appearance of Methyl pyruvate (or Propanoic acid, 2-oxo-, methyl ester) and at 4.74 appearance of 2-Methyloxirane-2-carboxylic acid, methyl ester.</i> .....	101
<i>Figure 5.11.</i> .....	102
<i>Figure 5.10.</i> .....	102
<i>Figure 5.12. Spectra of unaged and UV-aged PMMA for 4, 8, 16, 32, 64 and 96 days. Spectra are averaged from three replicates for each stage of ageing. For absorption bands and assignments of new and exponentially UV-aged PMMA see Table 5.4.</i> .....	105
<i>Figure 5.13. PMMA coupons immediately after being removed from the black hard-plastic, on which they were attached when received. Transparent and black (dust) residues are visible on all the coupons.</i> .....	106
<i>Figure 5.14. Ultrasonic bath cleaning of PMMA coupons in deionised water.</i> .....	107
<i>Figure 5.15. Different mixtures of sebum oil with carbon black pigment after one application with different consistencies. The circled mixture shows pigment globules. Mixture 2 (2 % carbon black) shows the best homogeneity.</i> .....	109
<i>Figure 5.16. Test applications of the four different sebum oil/carbon black mixtures with airbrush on transparent PMMA surrogate surface.</i> .....	110
<i>Figure 5.17. Step/comb gauge to measure synthetic sebum soil thickness.</i> .....	110
<i>Figure 5.18. Dried synthetic sebum soil (sebum oil and carbon black pigment) at 180 °C for 24 hours.</i> .....	111
<i>Figure 5.19. Spectrum of sebum oil and 2wt.% carbon black pigment formulation with 16 scans at ambient temperature and pressure, with a resolution of 4 cm<sup>-1</sup> equating to a penetration depth of 0.5-5 µm. Labelled absorption bands correspond to assignments in Table 5.5.</i> .....	111
<i>Figure 5.20. IR spectra of PSA under study (pink) in ATR mode matched with reference commercial product BYK 358 (black): a polyacrylate-based solution with 52 % solid content in naphtha, petroleum, light aromatic and isopropyl benzene. Absorption bands and assignments available in Table 5.6.</i> .....	113

<i>Graph 6.1. Bar chart of average gloss values of an untreated-clean (blue) and a solvent-treated/dull (purple) PMMA sample against a variety of backgrounds. Gloss measurements were carried out at an incident angle of 20° on five spots repeated five times. Error bars represent the standard deviation. ....</i>	<i>129</i>
<i>Graph 6.2. Example of a bar chart displaying the averaged weight changes % from Table 6.9. Changes % were averaged from five replicates after spraying of PSA (blue), ageing of samples with PSA (grey) and cleaning (light blue). Changes % are normalised to the starting/initial weight. Error bars show the standard deviation. ....</i>	<i>131</i>
<i>Graph 6.3. An example of the 2D colour-intensity contour heat map (left) obtained for a new PMMA sample with aged synthetic soil. A vertical slice through the 2D data at the 1<sup>st</sup> (green arrow) and 6<sup>th</sup> (yellow arrow) echo yields a profile of the proton density through the scan depth (1<sup>st</sup> echo: black line, 6<sup>th</sup> echo: yellow line). The central line graph is before smoothing and the one on the right is after smoothing using Savitzky-Golay filtering with a 9-point convolute. ...</i>	<i>143</i>
<i>Graph 6.4. Smoothed line graphs of NMR profile scans of 1<sup>st</sup> and 6<sup>th</sup> echoes: unaged PMMA control (purple tones) and aged PMMA control (green tones). Control samples are unsoiled and untreated. ....</i>	<i>147</i>
<i>Graph 6.5. Smoothed line graphs of NMR profile scans of PMMA samples immersed in H<sub>2</sub>O, EtOH, IPA or PET for 30 days. Samples were scanned 24 h after conditioning in lab environment to allow liquid evaporation. The scans represent the extreme damage these liquids are capable of inducing - when applied free-standing. Liquids were used thickened in the present cleaning treatments, so data are presented for comparative purposes. ....</i>	<i>147</i>
<i>Graph 6.6. Smoothed line graphs of NMR profile scans of the PMMA sample immersed in EtOH for 30 days: 1<sup>st</sup> and 6<sup>th</sup> echoes 24 h after (pink tones) and 96 h after (blue tones) standing in lab environment. ....</i>	<i>148</i>
<i>Graph 7.1. Ratios between the peak heights at 1723 cm<sup>-1</sup> and 750 cm<sup>-1</sup> of new and aged untreated PMMA controls and PMMA samples immersed in H<sub>2</sub>O, PET, IPA and EtOH for 30 days. Ratios were based on the loss of carbonyl bands (C=O) in relation to a constant peak. The smaller the ratio, the bigger the chemical change. ....</i>	<i>175</i>
<i>Graph 8.1. CARS scores of the unsoiled, new and aged PMMA samples. Scores are based on a five-point progressive ranking from 0 (worst) to 4 (best). The scores, expressed as a bar chart, are averaged from 5 replicates for each treatment. The untreated PMMA controls scored the highest possible CARS 12 in categories 'Abrasion' and 'Gel residue'. Error bars show the standard deviation. ....</i>	<i>186</i>
<i>Graph 8.2. The mean CARS scores of free solvents (no) are above the mean value, while that of PVA below the mean value, indicating they affected cleaning of PMMA in a positive and a negative manner, respectively. ....</i>	<i>188</i>
<i>Graph 8.3. Gloss measurements of new and aged PMMA samples treated for 5 minutes, plotted as bar charts. Gloss units (GU) are averaged from 3 repetitions of 3 spot measurements on 5 replicates. Differences &lt; 15 GU are non-detectable by the human eye. The PMMA controls are highly glossy with a value of 146 GU for the unaged and 138 GU for the aged. Red lines show below which point change is visible. Error bars show the standard deviation. ....</i>	<i>197</i>

<i>Graph 8.4. The mean gloss scores of Carbopol are the lowest indicating it affected cleaning of PMMA in a negative manner. ....</i>	<i>198</i>
<i>Graph 8.5. Average weight change % of new and aged, unsoiled PMMA – averaged from five replicates – after cleaning treatment with free solvents and solvent gels for 5 and 60 minutes (yellow tones for new and blue tones for aged samples). Changes % are normalised to the starting/initial weight. Error bars show the standard deviation. ....</i>	<i>199</i>
<i>Graph 8.6. The surface condition of PMMA aged samples significantly impacted cleaning of PMMA. Application time was another significant factor in the cleaning process. ....</i>	<i>200</i>
<i>Graph 8.7. Ratios between the peak heights at 1723 cm<sup>-1</sup> and 750 cm<sup>-1</sup> of new and aged: untreated PMMA controls (in fuchsia) and treated PMMA samples for 5 (green) and 60 (blue) minutes. Ratios are based on the loss of carbonyl bands (C=O) in relation to a constant peak (750 cm<sup>-1</sup>). The lower the ratio, the bigger the chemical change. Error bars show the standard deviation. ....</i>	<i>203</i>
<i>Graph 9.1. CARS scores of treated new and aged PMMA samples with unaged synthetic soil. Scores are based on a five-point progressive ranking from 0 (worst) to 4 (best). Scores, expressed as a bar chart, are averaged from 5 replicates for each treatment. Untreated new and aged PMMA controls scored the highest possible CARS 20 in categories ‘Dirt residue’, ‘Abrasion’ and ‘Gel residue’. Red line shows below which point treatments failed to remove synthetic soil. Error bars show the standard deviation. ....</i>	<i>213</i>
<i>Graph 9.2. Interaction plot showing the significant interactions between gels and solvents on PMMA CARS. ....</i>	<i>214</i>
<i>Graph 9.3. Interaction plot showing the significant interactions between gels and condition on PMMA CARS. ....</i>	<i>215</i>
<i>Graph 9.4. The mean CARS scores of Pemulen are the highest, while that of PVA the lowest, indicating they affected cleaning of PMMA with PSA in a positive and a negative manner, respectively. PET scored below the means CARS value having a negative impact on PMMA. .</i>	<i>215</i>
<i>Graph 9.5. Gloss measurements of new and aged PMMA with synthetic soil after treatment, plotted as bar charts. Gloss units (GU) are averaged from 3 repetitions of 3 spot measurements on 5 replicates. Differences &lt; 15 GU are non-detectable by the human eye. The PMMA controls are highly glossy with a value of 146 GU for the unaged and 138 GU for the aged. Red line shows below which point change is visible for aged PMMA and blue line does the same for new PMMA. Error bars show the standard deviation. ....</i>	<i>221</i>
<i>Graph 9.6. Interaction plot showing the significant interactions between gels and solvents on PMMA gloss. ....</i>	<i>223</i>
<i>Graph 9.7. The mean gloss scores of EtOH are the highest, while that of IPA the lowest, indicating they affected cleaning of PMMA with PSA in a positive and a negative manner, respectively. ....</i>	<i>223</i>
<i>Graph 9.8. Average weight change % of new and aged PMMA - averaged from five replicates - after application of synthetic soil and after cleaning (purple tones: new - yellow tones: aged samples). Changes % are normalised to the starting/initial weight. Error bars show the standard deviation. ....</i>	<i>224</i>

<i>Graph 9.9. CARS scores of new and aged PMMA samples with unaged PSA. Scores are based on a five-point progressive ranking from 0 (worst) to 4 (best). Scores, expressed as a bar chart, are averaged from 5 replicates for each treatment. Untreated new and aged PMMA controls scored the highest possible CARS 20 in categories 'Dirt residue', 'Abrasion' and 'Gel residue'. Red line shows below which point treatments failed to remove PSA. Error bars show the standard deviation. ....</i>	<i>227</i>
<i>Graph 9.10. Interaction plot showing the significant interactions between gels and condition on PMMA gloss. ....</i>	<i>228</i>
<i>Graph 9.11. The mean CARS scores of Pemulen are the highest, while that of IPA the lowest, indicating they affected cleaning of PMMA with PSA in a positive and a negative manner, respectively. PET scored below the means CARS value having a negative impact on PMMA. .</i>	<i>228</i>
<i>Graph 9.12. Gloss measurements of new and aged PMMA with PSA after treatment, plotted as bar charts. Gloss units (GU) are averaged from 3 repetitions of 3 spot measurements on 5 replicates. Differences &lt; 15 GU are non-detectable by the human eye. The PMMA controls are highly glossy with a value of 146 GU for the unaged and 138 GU for the aged. Blue line shows below which point change is visible for aged PMMA and green line does the same for new PMMA. Error bars show the standard deviation. ....</i>	<i>235</i>
<i>Graph 9.13. The mean gloss scores of Agar and IPA are the lowest indicating they affected cleaning of PMMA with PSA in a negative manner. ....</i>	<i>236</i>
<i>Graph 9.14. Average weight change % of new and aged PMMA - averaged from five replicates - after application of PSA and after cleaning treatment (blue tones: new - green tones: aged samples). Changes % are normalised to the starting/initial weight. Error bars show the standard deviation. ....</i>	<i>237</i>
<i>Graph 9.15. CARS scores of treated new and aged PMMA samples with aged synthetic soil. Scores are based on a five-point progressive ranking from 0 (worst) to 4 (best). Scores, expressed as a bar chart, are averaged from 5 replicates for each treatment. Untreated new and aged PMMA controls scored the highest possible CARS 20 in all categories 'Dirt residue', 'Abrasion' and 'Gel residue'. Red line shows below which point treatments failed to remove synthetic soil. Error bars show the standard deviation. ....</i>	<i>243</i>
<i>Graph 9.16. The mean CARS scores of Pemulen EtOH and Pemulen IPA are the highest, while that of Agar IPA and Pemulen PET the lowest, indicating they affected cleaning of PMMA with aged synthetic soil in a positive and a negative manner, respectively. ....</i>	<i>244</i>
<i>Graph 9.17. Gloss measurements of new and aged PMMA samples with aged synthetic soil after treatment, plotted as bar charts. Gloss units (GU) are averaged from 3 repetitions of 3 spot measurements on 3 replicates. Differences &lt; 15 GU are non-detectable by the human eye. The PMMA controls are highly glossy with a value of 146 GU for the unaged and 138 GU for the aged. Red line shows below which point change is visible for aged PMMA and blue line does the same for new PMMA. Error bars show the standard deviation. ....</i>	<i>248</i>
<i>Graph 9.18. Average weight change % of new (upper) and aged (bottom) PMMA - averaged from five replicates - after application of synthetic soil (blue), ageing of the soil (green) and cleaning treatment (grey). Changes % are normalised to the starting/initial weight. Error bars show the standard deviation. ....</i>	<i>250</i>
<i>Graph 9.19. Average weight change % of new and aged PMMA with aged synthetic soil after the cleaning treatments - averaged from five replicates. Changes % are calculated as the change between the soiled surface after ageing and the surface after treatment. Error bars show the standard deviation. ....</i>	<i>251</i>

Graph 9.20. CARS scores of treated new and aged PMMA samples with aged PSA. Scores are based on a five-point progressive ranking from 0 (worst) to 4 (best). Scores, expressed as a bar chart, are averaged from 5 replicates for each treatment. Untreated new and aged PMMA controls scored the highest possible CARS 20 in all categories ‘Dirt residue’, ‘Abrasion’ and ‘Gel residue’. Red line shows below which point treatments failed to remove PSA. Error bars show the standard deviation. .... 254

Graph 9.21. The mean CARS scores of Pemulen PET and Pemulen EtOH are the highest, while that of Agar PET and PVA PET the lowest, indicating they affected cleaning of PMMA with aged PSA in a positive and a negative manner, respectively. .... 255

Graph 9.22. Gloss measurements of new and aged PMMA samples with aged PSA after treatment, plotted as bar charts. Gloss units (GU) are averaged from 3 repetitions of 3 spot measurements on 3 replicates. Differences < 15 GU are non-detectable by the human eye. The PMMA controls are highly glossy with a value of 146 GU for the unaged and 138 GU for the aged. Blue line shows below which point change is visible for aged PMMA and green line does the same for new PMMA. Error bars show the standard deviation. .... 260

Graph 9.23. Average weight change % of new (upper) and aged (bottom) PMMA - averaged from five replicates - after application of PSA (blue), ageing of the PSA (green) and cleaning treatment (grey). Changes % are normalised to the starting/initial weight. Error bars show the standard deviation. .... 262

Graph 9.24. Average weight change % of new and aged PMMA with aged PSA after the cleaning treatments - averaged from five replicates. Changes % are calculated as the change between the sprayed surface after ageing and the surface after treatment. Error bars show the standard deviation. .... 263

Graph 9.25. Spectra of new PMMA samples with aged PSA after gel treatment. The spectra are averaged from 3 replicates for each treatment. Each replicate is averaged from 3 spot ATR analyses. Peaks are enlarged and labelled. The spectra of 32-days aged control (untreated, unsoiled) and 32-days aged PSA on PMMA are included for comparison. .... 264

Graph 9.26. Spectra of aged PMMA samples with aged PSA after gel treatment. The spectra are averaged from 3 replicates for each treatment. Each replicate is averaged from 3 spot ATR analyses. Peaks are enlarged and labelled. The spectra of 32-days aged control (untreated, unsoiled) and 32-days aged PSA on PMMA are included for comparison. .... 265

Graph 10.1. CARS scores of treated new and aged PMMA samples with aged synthetic soil. Scores are based on a five-point progressive ranking from 0 (worst) to 4 (best). Scores, expressed as a bar chart, are averaged from 5 replicates for each treatment. Untreated new and aged PMMA controls scored the highest possible CARS 20 in all categories ‘Dirt residue’, ‘Abrasion’ and ‘Gel residue’. Error bars show the standard deviation. .... 272

Graph 10.2. The mean CARS scores of Pemulen IPA is the highest, while that of Agar IPA, Agar PET and Pemulen PET the lowest, indicating they affected cleaning of PMMA with aged synthetic soil in a positive and a negative manner, respectively. .... 273

Graph 10.3. Gloss measurements of new and aged PMMA samples with aged synthetic soil after treatment, plotted as bar charts. Gloss units (GU) are averaged from 3 repetitions of 3 spot measurements on 3 replicates. Differences < 15 GU are non-detectable by the human eye. The PMMA controls are highly glossy with a value of 146 GU for the unaged and 138 GU for the aged. Red line shows below which point change is visible for aged PMMA and blue line does the same for new PMMA. Error bars show the standard deviation. .... 278

Graph 10.4. Interaction plot showing the significant interactions between treatments and condition on PMMA gloss. .... 279



<i>Graph 10.5. The mean CARS scores of Pemulen H<sub>2</sub>O and Pemulen IPA is the highest, while that of Agar IPA the lowest, indicating they affected cleaning of PMMA with aged synthetic soil in a positive and a negative manner, respectively. ....</i>	<i>279</i>
<i>Graph 10.6. Average weight change % of new (upper) and aged (bottom) PMMA - averaged from five replicates - after application of synthetic soil (green), ageing of the soil (grey) and cleaning treatment (blue). Changes % are normalised to the starting/initial weight. Error bars show the standard deviation. ....</i>	<i>281</i>
<i>Graph 10.7. Average weight change % of new and aged PMMA with aged synthetic soil after the cleaning treatments - averaged from five replicates. Changes % are calculated as the change between the soiled surface after ageing and the surface after treatment. Error bars show the standard deviation. ....</i>	<i>282</i>
<i>Graph 10.8. CARS scores of new and aged PMMA samples with aged PSA. Scores are based on a five-point progressive ranking from 0 (worst) to 4 (best). Scores, expressed as a bar chart, are averaged from 5 replicates for each treatment. Untreated new and aged PMMA controls scored the highest possible CARS 20 in categories 'Dirt residue', 'Abrasion' and 'Gel residue'. Error bars show the standard deviation. ....</i>	<i>284</i>
<i>Graph 10.9. The mean CARS scores of Pemulen EtOH is the highest, while that of Pemulen H<sub>2</sub>O and PVA PET the lowest, indicating they affected cleaning of PMMA with aged PSA in a positive and a negative manner, respectively. ....</i>	<i>285</i>
<i>Graph 10.10. Gloss measurements of new and aged PMMA with aged PSA after treatment, plotted as bar charts. Gloss units (GU) are averaged from 3 repetitions of 3 spot measurements on 5 replicates. Differences &lt; 15 GU are non-detectable by the human eye. The PMMA controls are highly glossy with a value of 146 GU for the unaged and 138 GU for the aged. Blue line shows below which point change is visible for aged PMMA and green line does the same for new PMMA. Error bars show the standard deviation. ....</i>	<i>289</i>
<i>Graph 10.11. The mean CARS scores of Pemulen hydrogel and Pemulen PET are the highest, while that of PVA PET the lowest, indicating they affected cleaning of PMMA with aged PSA in a positive and a negative manner, respectively. ....</i>	<i>290</i>
<i>Graph 10.12. Average weight change % of new (upper) and aged (bottom) PMMA - averaged from five replicates - after application of PSA (blue), ageing of the PSA (yellow) and cleaning treatment (green). Changes % are normalised to the starting/initial weight. Error bars show the standard deviation. ....</i>	<i>291</i>
<i>Graph 10.13. Average weight change % of new and aged PMMA with aged PSA after the cleaning treatments - averaged from five replicates. Changes % are calculated as the change between the sprayed surface after ageing and the surface after treatment. Error bars show the standard deviation. ....</i>	<i>292</i>
<i>Graph 10.14. Smoothed line graphs of NMR profile scans of PMMA with aged synthetic soil before and 24 hours after treatment with Pemulen hydrogel, Pemulen IPA and PVA EtOH. Profile scans of new samples (left) in black (1<sup>st</sup> echo) and yellow (6<sup>th</sup> echo) tones and of aged samples (right) in orange (1<sup>st</sup> echo) and purple (6<sup>th</sup> echo) tones. ....</i>	<i>296</i>
<i>Graph 10.15. Smoothed line graphs of NMR profile scans of PMMA samples with aged PSA before and 24 hours after gel treatment with Pemulen H<sub>2</sub>O, Pemulen EtOH and Pemulen PET. Profile scans of new samples (left) in blue (1<sup>st</sup> echo) and yellow (6<sup>th</sup> echo) tones and aged samples (right) in purple (1<sup>st</sup> echo) and green (6<sup>th</sup> echo) tones. ....</i>	<i>297</i>

## List of tables

---

Table 3.1. Generic information about PMMA. ....	34
Table 3.2. Main factors (degradation agents) causing either chemical degradation or physical ageing to PMMA, their processes and chemical and physical effects. ....	44
Table 4.1. Hildebrand solubility parameters of selected solvents appropriate for the safe cleaning of PMMA. ....	59
Table 5.1. ISO 4892-2:2013 Test Method A: Exposure using daylight filters (artificial weathering) selected in this study for accelerated ageing of PMMA, included two phases: one dry and one wet. ....	79
Table 5.2. Experimental parameters used in tensile test. ....	81
Table 5.3. A range of exemplary Tg values of different materials and PMMA molecular arrangements/tacticities (Biroš et al. 1982; O'Reilly et al. 1982; Cowie 1991; Brydson 1999; Shaw and MacKnight 2005; Shin et al. 2005; Shashoua 2008; Villalobos and Debling 2013; Ionita et al. 2015). ....	90
Table 5.4. Assignments of diagnostic IR absorptions of the unaged (unirradiated) and aged (irradiated) PMMA reference analysed with ATR-FTIR. The new bands formed with ageing are circled in blue. ....	96
Table 5.5. Assignments of diagnostic IR absorptions of reference sebum in ATR mode. ....	111
Table 5.6. Assignments of diagnostic IR absorptions of the PSA used in this study analysed in ATR mode. It consisted of two solid components: the acrylic adhesive and a terpene tackifier. ....	113
Table 6.1. Qualitative and quantitative techniques, including analytical methods, performed on PMMA samples for the evaluation of cleaning experiments. Measurements and analysis were carried out on all samples before and after treatment, and sometimes during treatment. ....	116
Table 6.2. Example of visual macroscopic evaluation of treated samples based on the level of dirt removal. ....	117
Table 6.3. List of the untreated PMMA controls, per type of condition and dirt, imaged under the SEM. ....	119
Table 6.4. Criterion anchored rating scale (CARS) comprised of five categories: three (highlighted in blue) concerning surface condition of treated PMMA samples and the effect of treatments and two (in white) referring to the quality/handling of gel treatments. ....	122
Table 6.5. Matrix showing the weighing factors used in the assessment of cleaning experiments for the condition categories describing the surfaces of samples after treatment. Criteria Ease of use and Control are missing as this is the control. ....	123
Table 6.6. Condition survey sheet: examples of samples assessed and scored based on CARS ranking system, immediately after treatment. ....	124
Table 6.7. Raw gloss data of an untreated-clean and a solvent-treated/dull PMMA sample measured at an incident angle of 20° against a variety of backgrounds. Table includes averages and standard deviations of five measurements repeated for each of the five spots per sample. ....	128
Table 6.8. Raw gloss data of the averages and standard deviations of the untreated-clean and the solvent-treated/dull PMMA samples measured at an incident angle of 20° against the darker matte backgrounds: black foam, black textile and grey matte. Total average and standard deviation are calculated from the five spot measurements per sample. ....	129

<i>Table 6.9. Example of weight measurements on new and aged PMMA samples treated with solvent gels. Weight changes % were calculated according to the above formula. Averages and standard deviation of changes % were also estimated. ....</i>	131
<i>Table 6.10. Analytical set up for NMR MOUSE scanning experiments of PMMA samples. Before and after treatment scans were longer and more optimised, while the dynamic scans were shorter and consisted of 10 experiments. ....</i>	144
<i>Table 7.1. Assignments of diagnostic IR absorptions of raw Agar analysed as a KBr pellet in transmittance mode. ....</i>	159
<i>Table 7.2. Assignments of diagnostic IR absorptions of Gellan analysed as a KBr pellet (raw form) in transmittance mode and as a dried gel in ATR mode. ....</i>	161
<i>Table 7.3. Assignments of diagnostic IR absorptions of Carbopol EZ2-Ethomeen C-25 system analysed in its dried state in ATR mode. ....</i>	163
<i>Table 7.4. Assignments of diagnostic IR absorptions of the Pemulen TR-2/TEA system analysed in its dried state in ATR mode. ....</i>	164
<i>Table 7.5. Assignments of diagnostic IR absorptions of the PVA/borax system analysed in its dried state in ATR mode. ....</i>	166
<i>Table 7.6. Assignments of diagnostic IR absorptions of PMMA samples immersed in EtOH, H<sub>2</sub>O, IPA and PET environments for 30 days. ....</i>	174
<i>Table 8.1. Experimental variables in the two-factorial design used for the preliminary cleaning experiments of unaged and unsoiled PMMA. ....</i>	182
<i>Table 8.2. Experimental variables in the multilevel full-factorial design used for the preliminary cleaning experiment with replication of treatments on new and aged unsoiled PMMA with 5 replicates. Number of levels: 6, 4, 2, 2. ....</i>	185
<i>Table 8.3. Areas of interest identified under the stereomicroscope (visual effects) are understood and described under the SEM (description/interpretation). ....</i>	204
<i>Table 8.4. Experimental variables in the multilevel full-factorial design used for the preliminary cleaning experiment on new PMMA with synthetic soil. ....</i>	207
<i>Table 8.5. Experimental variables in the multilevel full-factorial design used for the preliminary cleaning experiment on new PMMA with synthetic soil. ....</i>	208
<i>Table 9.1. Experimental variables in the multilevel full-factorial design used for the main cleaning experiment on new and aged PMMA with synthetic soil or PSA and 5 replicates. Number of levels: 3, 3, 2, 2. ....</i>	210
<i>Table 9.2. Macroscopic observation of the overall impression of unaged synthetic soil removal from new and aged PMMA after treatment. ....</i>	211
<i>Table 9.3. Evaluation based on SEM imaging of treated new PMMA samples with synthetic soil. ....</i>	215
<i>Table 9.4. Evaluation based on SEM imaging of treated aged PMMA samples with synthetic soil. ....</i>	215
<i>Table 9.5. Macroscopic observation of the overall impression of unaged PSA removal from new and aged PMMA after treatment. ....</i>	224
<i>Table 9.6. Cleaning trials testing treatments - previously discarded as ineffective on PMMA with unaged synthetic soil and PSA - on their ability to remove aged synthetic soil and aged PSA. ....</i>	240
<i>Table 9.7. Experimental variables in the multilevel two-factorial design used for the main cleaning experiment on new and aged PMMA with aged synthetic soil (5 replicates). Number of levels: 6, 2. ....</i>	240

<i>Table 9.8. Experimental variables in the multilevel two-factorial design used for the main cleaning experiment on new and aged PMMA with aged PSA (5 replicates). Number of levels: 5, 2.</i>	241
<i>Table 9.9. Macroscopic observation of the overall impression of aged synthetic soil removal from new and aged PMMA after treatment.</i>	241
<i>Table 9.10. Evaluation based on SEM imaging of treated new PMMA samples with aged synthetic soil.</i>	244
<i>Table 9.11. Evaluation based on SEM imaging of treated aged PMMA samples with aged synthetic soil.</i>	244
<i>Table 9.12. Macroscopic observation of the overall impression of the aged PSA removal from new and aged PMMA after treatment.</i>	253
<i>Table 9.13. Evaluation based on SEM imaging of treated new PMMA samples with aged PSA.</i>	254
<i>Table 9.14. Evaluation based on SEM imaging of treated aged PMMA samples with aged PSA.</i>	255
<i>Table 10.1. Treatments unable to remove unaged or aged synthetic soil and PSA from PMMA after one 5-minute application, were tested with three repeated 5-minute applications.</i>	266
<i>Table 10.2. Duplicate trials with three repeated 5-minute applications on PMMA with aged synthetic soil.</i>	266
<i>Table 10.3. Duplicate trials with three repeated 5-minute applications on PMMA with aged PSA.</i>	267
<i>Table 10.4. Duplicate cleaning trials tested three repeated applications of 1 and 3 minutes on PMMA with aged synthetic soil.</i>	268
<i>Table 10.5. Duplicate cleaning trials tested three repeated applications of 1 and 3 minutes on PMMA with aged PSA.</i>	268
<i>Table 10.6. Duplicate cleaning trials tested three repeated applications of 3 and 5 minutes on PMMA with aged synthetic soil.</i>	268
<i>Table 10.7. Duplicate cleaning trials tested three repeated applications of 3 and 5 minutes on PMMA with aged PSA.</i>	269
<i>Table 10.8. Successful treatments at removing aged synthetic soil and PSA from PMMA tested in the final cleaning experiment. Marked treatments with * are reinserted after cleaning trials.</i>	269
<i>Table 10.9. Experimental variables in the multilevel two-factorial design used for the main cleaning experiment on new and aged PMMA with aged synthetic soil (5 replicates). Number of levels: 6, 2.</i>	270
<i>Table 10.10. Experimental variables in the multilevel two-factorial design used for the main cleaning experiment on new and aged PMMA with aged PSA (5 replicates). Number of levels: 4, 2.</i>	270
<i>Table 10.11. Macroscopic observation of the overall impression of aged synthetic soil removal from new and aged PMMA after three treatment applications of three minutes each.</i>	271
<i>Table 10.13. Macroscopic observation of the overall impression of aged PSA removal from new and aged PMMA after treatment.</i>	283
<i>Table 12.1. Summary of results of cleaning experiments on unaged and aged (32 days under UV) PMMA with unaged and aged (32 days under UV) synthetic sebum soil or pressure-sensitive spray adhesive.</i>	319

## Chapter 1. INTRODUCTION

---

Plastics<sup>1</sup> (Newman 1965; Meikle 1992; Andrady and Neal 2009) have had a significant impact on industrial, technological, scientific, historical, domestic and cultural aspects of everyday life in the 20<sup>th</sup> and 21<sup>st</sup> centuries (Sale 1993; Shashoua 2008; García Fernández-Villa 2012; Cecchini and Hansen 2014). Although having a short history compared to other materials, nowadays, plastics can be found in numerous and different types of museum collections (Pavitt 1998). These may consist of anything from plastic food containers to Barbie dolls, furniture, housewares, medical and sports equipment (Shashoua 2006), consumer goods, and other 20<sup>th</sup> century paraphernalia (Coghlan 1996), or uniquely created objects by celebrated artists with broad influence as iconic works of art (Pugliese and Waentig 2012). Plastic objects are often seen as documents which in the context of historic heritage are held in high esteem internationally (Albus *et al.* 2008), and can tell stories about a city, its political situation, or history (Etherington 2013). Such objects can be of technological and cultural history, such as the first total artificial heart implanted in a human body in 1969 (Lim 2018) and spacesuits (Lantry 2001). Collections can also comprise mundane objects that have little (economic) value, including material that was once mass-produced (Pearce 2012), and has either acquired a collectible value due to its scarcity and unconventional design (Pugliese and Waentig 2012), or if not collected would otherwise disappear. These can be seen as the documentation of human life, and include objects such as rotary telephones, coffee cup lids, Tupperware products (Lim 2018).

Poly (methyl methacrylate) (PMMA) is one of the plastics commonly found in collections ranging from modern and contemporary art, industrial design and decorative arts to social history, science and technology (Sale 1993; Shashoua 2008; Waentig 2008a; Ward 2008). PMMA as a material has numerous advantages; being thermoplastic, it has the capacity to be softened with temperature, making it easy to be molded into various shapes (Comiotto and Egger 2009), while being amorphous, it has the ability to transmit light (Brydson 1999; Rogerson 2009; Bodurov *et al.* 2013). In addition, it can be formed into opaque, clear/transparent, or coloured objects (Lenz 2012). For all these qualities PMMA has been cherished (Laganà *et al.* 2017) by the industry, designers and artists. An example of 'everyday' objects of historical importance are the signs used for advertising and information in the London Underground (Fig.1.1), currently collected and exhibited in the London Transport

---

<sup>1</sup> According to Plastics Historical Society and American Chemistry Council 'plastic' is a synthetic, man-made material based on polymers; large molecules (macromolecules) made up of smaller units (monomers) joined together to create long chains. Plastics can be manipulated to form films, fibres, foams or three-dimensional objects. Originally the term referred to any substance that is malleable when soft and hardened upon cooling. Plastics form a fifth class to the materials, metal, wood, glass and ceramics.

Museum (<https://www.ltmuseum.co.uk/>). Examples of PMMA works of modern art are creations by László Moholy-Nagy (Fig.1.2), a Hungarian artist known for his unconventional use of industrial materials in painting and sculpture, and his experiments with light, transparency and space (The Solomon R. Guggenheim Foundation 2020).



Figure 1.1. Advertising signs made of PMMA in the District Line of the London Tube. Available at: <https://www.ltmuseum.co.uk/collections/collections-online/signs?q=acrylic>.



Figure 1.2. Double Loop (1946) by László Moholy-Nagy. Artwork made of PMMA found at MoMA, New York. Available at: [https://www.moma.org/collection/works/81115?artist\\_id=4048&locale=en&page=2&sov\\_referrer=artist](https://www.moma.org/collection/works/81115?artist_id=4048&locale=en&page=2&sov_referrer=artist).

### 1.1. CONSERVATION CLEANING OF MUSEUM OBJECTS

The aims of plastics conservation are no different to those for other cultural materials. Museums and cultural institutions conserve objects for future generations (Hodin 2009, 8) and to preserve information about past materials and technologies (Shashoua 2008). In addition to

preserving the material itself, there are numerous reasons for conserving plastics, including and not limited to preserving the design, concept or intention reflected by an object, along with its artistic, historical and financial values (Laurenson 2006; Shashoua 2008). Conservation is a process of understanding, and managing change rather than merely an arresting process. A major objective in conservation of plastics, is to increase their chemical and mechanical stability (Shashoua 1999; Khandekar 2004; Barros García 2015). According to Jones and Holden:

It (conservation) seeks to retain, reveal and enhance what people value about the material past, and sustain those values for future generations (2008, 27).

Plastics, just like any other museum object, are subject to soiling and accumulation of surface deposits (Caminati 2013) during their lifetime of use/handling, display and storage. Surface deposits might consist of superficial soil, dirt, dust, grime, soot, adhesives, stains, grease, insect excreta, accretions, past repairs and restoration interventions, as well as anything not part of the original object (Moncrieff and Weaver 1987; Oddy 1999; Caple 2000; Baglioni *et al.* 2012). Products of alteration of the object's surface can also be considered undesirable deposits. Once settled on the plastic surface, either by being adhered, mechanically trapped, or held on by electrostatic attraction (Moncrieff and Weaver 1987), deposits affect stability, significance (Shashoua 2008) or/and aesthetics. Presence of deposits on a plastic object impact on its surface nature causing visual modifications, by obscuring the topography and colour, and alterations in the underlying chemistry and physical properties (AIC-BPG 1992; Khandekar 2004b). Additionally, they can trap moisture and acidic pollutants, providing a favourable environment for degradation mechanisms (Caple 2000). Hence, surface deposits require removal, rendering cleaning an essential part of a conservation strategy.

Surface cleaning, according to the American Institute for the Conservation of Historic and Artistic Works (AIC) (1992), is a technique used to reduce the potential for damage by removing/reducing surface deposits. The purpose of cleaning varies, and the approaches/treatments available for cleaning vary too. Often, cleaning treatments aim to remove anything that dulls gloss or transparency (Koller 2000), reveal appearance and uncover information. Sometimes cleaning decisions attempt to maximise the most valuable aspect of an object: whether this is to approximate it as closely as possible to its initial original appearance (Rhyne 2006; Caple 2011), make it more displayable (Hedley 1994; Shashoua 1999; Barros García 2015) or maintain its artistic integrity (Fricker 2016). For instance, collectors are particularly interested in the aesthetic aspect of plastics, which affects both commercial value and interpretation of works (Shashoua 2008).

As a technique, cleaning is inherently irreversible (Iannuccelli and Sotgiu 2010) and can compromise the integrity of an object (Oddy 1999). It requires first of all technical skill (e.g. manual dexterity) and experience on the part of the conservator (Moncrieff and Weaver 1987). Conservators need to evaluate the cleaning options and provide an effective and safe method to perform this operation. This must be controlled and selective (Baglioni *et al.* 2012), removing deposits from targeted areas of the substrate, while leaving others intact. However, cleaning also requires critical judgement, as well as an ethical, historic and philosophical understanding (Moncrieff and Weaver 1987), and must be understood within the larger context of a conservation project (Cremonesi 2010).

The question to clean any historical or artistic work is filtered through by multiple considerations, which are uniquely overlapping in each artefact. Cleaning is ethically questionable (Oddy 199), because it has serious implications in terms of aesthetics and physical changes to the object being cleaned (Koller 2000). The dirt to be removed, where/when to stop, and the appearance after cleaning are issues of primary importance to be considered in advance, as not all traces of age should be removed (Beerkens and Thompson 2005). Should an artwork/historical artefact be bearing the patina of time? Should it be free of large dust particles? How does someone distinguish between what is acceptable and what is not? These are rather subjective formulations which are open to discussion/interpretation (Beerkens and Thompson 2005). A significant difference between objects made of traditional materials and of plastic is that in the former, the patinas may be cherished, while in the latter what is mostly cherished are the original aesthetics. A patina on a plastic object is considered unpleasant, as we expect plastics to have fresh, unaltered surfaces (Albus *et al.* 2008; Fricker 2016). In addition, since the significance of an artwork/historical artefact is determined by its aesthetic appearance, one may consider that changes instigated by cleaning could compromise the work and be considered as damage (Bollard *et al.* 2011).

Conservation has moved to less aggressive techniques and nowadays it is accepted that no cleaning should proceed without thorough scientific and historic research (Rhyne 2006). This demands an intense cooperation between conservators, art and design historians, curators and scientists, for a balanced and complementary understanding of the problems of cleaning (Koller 2000; Baglioni *et al.* 2012). According to Otero-Pailos (2007) conservation cleaning needs to be re-considered within a larger context, that of a field that borrows methods and concepts from disciplines such as art, history, design, engineering, materials science, to name but a few. Additionally, the understanding of the surface condition from a scientific point of view has expanded (Considine *et al.* 2000), and the quest for better cleaning methods and tools is constant (Baglioni *et al.* 2012).



## 1.2. STATING THE PROBLEM

Despite all issues discussed above, cleaning is nevertheless the most common task for conservators (Charola and Koestler 2006). It may be an independent treatment, or a prelude to another (i.e. stabilisation) (Szmelter 2009), without which dirt may set irreversibly in the substrate (AIC-BPG 1992). According to Teutonico (2006, 7), current associate director of the Getty Conservation Institute, cleaning is among the most important and critical treatment processes conducted by conservators. According to Shashoua (2008) it was estimated - a little over a decade ago, that approximately 75 % of plastics in British and Scandinavian museum collections needed cleaning.

Several studies have addressed the degradation and conservation of plastics (Blank 1990; Quye and Williamson 1999), however only a few have provided guidelines for their cleaning (Morgan 1991b; Shashoua 2008; Fricker 2016). The topic has been approached with caution due to the fact that cleaning can be uncontrollable, potentially aggressive and with a high risk of causing irreversible damage (Considine *et al.* 2000; Sun *et al.* 2014). Due to such reasons, there is a general lack of well-defined and established treatments for plastics, with limited publications evaluating aqueous and non-aqueous techniques and their effectiveness at removing contaminants (Lavédrine and Shashoua 2012). Given the increasing proportion of plastics in museum and other collections, up until this point, there have not been any systematic cleaning strategies developed by the conservation field.

Previous conservation research has focused on documentation of the material condition, ageing studies and identification of plastics in collections. A significant proportion of publications are dedicated to the characterisation of (semi) synthetic polymers with the use of analytical techniques. A lot of research has been carried out on consolidation of polyurethane (PUR) foam by Winkelmeyer (2002), De Groot *et al.* (2011), and Van Oosten (2011). Adhesion issues are also popular among conservation professionals; bonding of PMMA has been researched by Comiotto and Egger (2009) and Müller-Wuesten (2011), polyester resins by Laganà and Van Oosten (2009, 2011), and rubber by Duboisset (2011). Studies by Laganà and Van Oosten (2011), Debik *et al.* (2013) and Laganà *et al.* (2017) (ongoing) have been exploring the use of adhesives for the repair of scratches and cracks in PMMA. Available treatment reports mostly discuss works of plasticised poly (vinyl chloride) (PVC) (Van Oosten and Huys 2005; Bechthold 2009; Morales-Muñoz 2010; Rovetta *et al.* 2014), polyester resins (Knuutinen and Kyllonen 2006; Graner 2009; Rivenc *et al.* 2011) and PUR foam (Bützer 2002; Bechthold 2005; Jonge *et al.* 2005; Snijders *et al.* 2011).

To date, the most extensive study on the cleaning of plastics is the Preservation of Plastic Artefacts in Museum Collections (POPART)<sup>2</sup>, a 42-month international research project that started in 2008. POPART aimed to contribute in establishing a strategy for the preventive conservation and maintenance of modern materials in museum collections (Lavédrine *et al.* 2009). POPART addressed issues related to the wet cleaning of PMMA, among numerous other plastics. Prior to POPART, research into conservation and cleaning of plastics was scarce. Among the limited publications available is that of Nagy *et al.* (2011) discussing the conservation of Donald Judd's PMMA artwork *Untitled 1977*, presented at the American Institute for Conservation of Historic & Artistic Works (AIC) conference of the same year. A recently published doctoral research on plastics by Fricker (2016) investigated the effect of conventional cleaning treatments used in the POPART project, with a particular focus on polystyrene and PMMA.

Fricker (2016) established that - until 2016 - there were no universally accepted cleaning protocols for plastic artefacts in museum collections. This is still true today, with interventive conservation treatments not yet established. Common conservation cleaning treatments employed on other cultural heritage materials have often been applied on plastics; soft brushes and cloths for removal of loose surface particles, dry cleaning with cotton swabs or microfibre cloths, dampening of cloths with deionised water (Fricker 2016). While these are successful and safe on most materials, on plastics the mechanical action and use of liquids can cause irreversible damage (Shashoua 2008, 2012).

Mechanical cleaning of plastic surfaces is challenging as it can introduce abrasions that decrease the light reflective properties and reduce gloss (Shashoua 2012). Even the widely employed cotton swab is not entirely safe for use due to the mechanical friction it produces (Shashoua 1999). When removing accumulated surface dirt, some of the particles become attached only by static electricity forces, while others get embedded in the material by attractive forces, such as van der Waals. In practice it is rarely possible to separate dirt, i.e. secondary adhesive residues, from objects by mechanical or chemical means without affecting the original surface (Moncrieff and Weaver 1987), as any vigorous action to remove them would result in scratches (Wypych 2013).

The scarce publications on cleaning PMMA in museum collections are mostly limited to industrial applications (Shashoua *et al.* 2009, 51). Approaches for treating plastics developed for industrial purposes include mechanical processing, namely sanding and polishing. Use of commercial abrasive products, except for being rarely satisfactory (Kim 2007, O'Connor 2015), especially when scratches and chips are very deep (Laganà *et al.* 2017), has never been

---

<sup>2</sup> <http://popart-highlights.mnhn.fr/>

evaluated for use on museum plastics (Shashoua 2008). Sanding and polishing, often used in traditional materials conservation (Buys and Oakley 1993, 87) such as historic metals, are invasive and inevitably remove original material (Learner *et al.* 2011). They have also been documented to remove significant material quantities from PMMA (Laganà *et al.* 2017). Such approaches not only increase surface and internal stresses (Shashoua 2008; Comiotto and Egger 2009, 245) that initiate crazing and cracking, but can cause distortion and softening/melting of plastics due to their low heat conductivity (Shashoua 2008). Abrasive products may also be chemically incompatible with plastics, with the potential to cause irreversible changes that are impossible to re-treat (Shashoua 2008). Lastly, to repair even a small area, the entire surface needs sanding off (Rivenc 2016) and to maintain a perfect finish, routine re-sanding/polishing is required (Learner *et al.* 2011). Based on these arguments, and according to current conservation ethics and canons, industrial 'cleaning' is considered inappropriate for plastic museum objects.

Wet cleaning treatments also affect plastic surfaces by chemically and physically reacting with them (Shashoua 2008). Liquids, such as organic solvents and even water (Shashoua 1999), may cause swelling, softening, dissolution, or extraction of components, i.e. additives (Quye and Keneghan 1999). Diffusion of a liquid (cleaning agent) into a plastic can cause plasticisation, a localised reduction in yield strength, which in turn leads to formation of crazes and, finally, fracture (Akhurst 2008). All these kinds of damage render cleaning one of the most delicate and complex operations in conservation (Dei 2013).

Having discussed potential damages and irreversible changes, it may well be argued that cleaning treatments could result in loss of qualities integral to museum objects, whether every day, historical or technological artefacts, or works of art. Conservators of modern materials and plastics surveyed for the purposes of this research suggested that transparent and/or highly polished surfaces are particularly difficult to clean, placing them in their top cleaning priorities. Being pristine they have a very low tolerance to physical damage (Rivenc *et al.* 2011; Dei 2013), and once damaged, they readily show it (Shashoua 2012).

Archival research and consultation with conservation professionals indicated that a large portion of PMMA museum objects/artworks are often both transparent and highly polished. Transparency and glossiness offer optical clarity, transmission of light and weightlessness. Often, the need to transmit such properties has dictated the use of PMMA by artists and designers, and for that reason they are seen as critical and integral to the character of PMMA objects and works of art (Rogerson 2009; Learner *et al.* 2011; Rivenc *et al.* 2011; Chiantore and Rava 2012; Lenz 2012). Therefore, loss of these aesthetic qualities can change the perception of an object, risking losing values assigned to it by different audiences. The

importance of the pristine surface qualities of such materials was accurately discussed by artist Helen Pashgian (2010 cited in Rivenc *et al.* 2011, 6) who stated about her PMMA sculptures that “On any of these works, if there is a scratch... that’s all you see”. Similarly, artist De Wain Valentine explained in an interview with the Getty Conservation Institute that:

The surface needs to disappear as much as possible, so you can look through it to the inside of the piece and out to the other side. A scratch or other damage only draws attention to the object’s surface (Learner *et al.* 2011).

This thesis is based on the quest to find a safe method to clean this type of surfaces considering POPART recommendations that PMMA could be cleaned easier following prolonged exposure to solvents (Balcar *et al.* 2012).

### 1.3. RESEARCH AIMS & OBJECTIVES

The present doctoral research investigates the cleaning of PMMA museum objects in historical, technological, art and design collections to establish safe practices. A range of aqueous gel systems carrying deionised water or organic solvents were employed. The idea to investigate the use of gels for the removal of surface deposits from PMMA, originated from the necessity to identify treatments that could be safely used on transparent and highly polished plastic surfaces, standardise their application and evaluate all possible risks. Artificial dirt and adhesive were applied to PMMA surfaces to respectively simulate oily human fingerprints and adhesive remains from labels, packaging and sticky tapes. These types were selected based on a survey carried out for the purposes of this research, where expert conservators identified them as the two most common surface deposits found on museum plastics.

Gels have been employed in the conservation field over the last decade because they have the potential to optimise cleaning treatments due to their presumed advantages; gels were purported to immobilise solvents and increase the surface contact time, retarding the solvent evaporation rate (Gorel 2010) and penetration (capillary suction rate), while introducing them gradually and uniformly into the bulk of the treated material (Carretti *et al.* 2008; Baglioni *et al.* 2013; Angelova *et al.* 2015). Such alleged abilities render gels safer and more efficient (Callister and Rethwisch 2014) compared to free solvent cleaning with cotton swabs. Of primary concern in the literature was the ability to control the diffusion of the thickened liquid to affect only targeted areas and limit, ideally eliminate, the deposition of residues from the gel on the treated surface (Khanjian *et al.* 2004). Both of these aspects were likely to depend on the interactions between the gel system and the surface/dirt to be treated/removed – another largely unexplored topic. This supported the decision in this research to focus on the cleaning of

one particular plastic, as the characteristics of the surface material was of importance and in need of investigation in a case-by-case study.

The main issue arising from the nature of PMMA is that being amorphous, it could, during a routine wet cleaning, allow the penetration of low-molecular-weight liquids (Shashoua 2008). This depends on the miscibility of solvents and the difference between the Hildebrand solubility parameters of PMMA and cleaning agents. Penetration in either the surface layers or the bulk could cause swelling, or extraction and dissolution of PMMA (Chuang *et al.* 2016), almost always leading to irreversible stress cracking and embrittlement (McGlinchey 1993; Akhurst 2008). Such phenomena compromise not only the visual characteristics of objects, especially aggravated in cases of transparent surfaces, but their physical structure too. The vulnerability of PMMA to solvents and the possibility of instigating cracking, demanded a more controlled application of solvents. This was expected to be offered through the use of gels, which have been very seldom studied in relation to plastics; there is only one published work on the application of gels on plastics by Bollard *et al.* (2011). The aim of this research is to methodically examine all the critical factors that could affect the cleaning of pristine PMMA with the use of aqueous solvent-gels and investigate their efficiency and safety at removing artificial surface dirt. This research intends to establish an optimised cleaning methodology and document the potential risks and damage that the solvents and gels could cause to PMMA. The results of the study will be significant to the profession and the advancement of the conservation of modern materials discipline.

The hypothesis that solvents encapsulated in gels would offer a sufficient, but restricted amount of free-flowing solvent penetration into cracks and pores of the plastic surface, while minimising the risk of material dissolution, seemed very promising and is thus explored in this study. The main research objectives were:

- to identify the most effective and safe gel cleaning system(s) at removing surface deposits of oily and adhesive nature from PMMA surfaces,
- to develop a methodology to test gel cleaning systems on plastic substrates,
- to evaluate potential changes and risks on the PMMA macro/microscopic levels and
- to identify changes in the chemical and mechanical properties of PMMA following gel cleaning.

The topic was explored through laboratory-based experiments on PMMA specimens. A number of samples were artificially light-aged in a controlled environment under ultraviolet (UV) radiation, following standards simulating accelerated outdoor weathering conditions. Degraded surfaces were known to behave differently to new, so it was important to examine both surface conditions. Aged plastics were expected to be more vulnerable to wet cleaning treatments and

mechanical action, and to show increased solubility in liquid agents compared to modern surfaces (Grattan 1993). This approach was not intended to reflect the real compositions of objects/artworks in museum collections, but shed light on the processes occurring during ageing and conservation treatments. Cleaning treatments were performed with controlled variables on controlled surfaces and included a wide range of gel systems of different, known composition and properties, commonly employed by conservators, as well as more recently developed gel matrices (Carretti *et al.* 2010b; Cremonesi 2010; Domingues *et al.* 2013a; Bonaldo 2015; Angelova *et al.* 2017a; Barkovic *et al.* 2017; Bertasa *et al.* 2017). Gels were coupled with deionised water and polar and nonpolar organic solvents.

It is essential to highlight that the focus of the study was the surface condition of PMMA. Weathering and soiling affecting the chemical and physical structure, composition and aesthetics of materials, initiate on the surface of objects (Caminati 2013). For these reasons, evaluation methods and analytical techniques were selected based on their ability to examine the surface material alterations. The suitability and efficiency of the gel cleaning treatments were assessed both quantitatively and qualitatively. The surface response to treatment was optically assessed through macroscopic examination conveyed numerically using a ranking system developed for this study, according to which treated surfaces were ascribed scores representative of their condition. Stereomicroscopy and scanning electron microscope (SEM) imaging were employed for evaluation of treatments at higher magnification. Quantitative evidence of the changes taking place in the material included weight and gloss measurements carried out before and after treatment. Attenuated total reflectance Fourier transform infrared spectroscopy (ATR-FTIR) was used to monitor chemical modifications. Lastly, Nuclear Magnetic Resonance Mobile Universal Surface Explorer (NMR MOUSE) was the only technique to examine the bulk material, aiding interpretation of the reversibility of the cleaning process based on the bulk diffusion of solvents from the gels into the PMMA.

#### **1.4. THESIS STRUCTURE**

Chapter 2 is a research method chapter about the scope of the design and methods for data collection, analysis and interpretation, employed in this study. The literature review and the survey method of modern materials/plastics conservators that informed the research and helped define the problem, are set forth. The discussion within this chapter maps the overall research design, including the following: the selection of PMMA and its artificial light ageing, the sample preparation and artificial dirt application methods, the selection of gels and solvents for cleaning, as well as the design of cleaning experiments and their evaluation. Lastly,

the case study cleaning application of the successful treatments on real museum objects, which validated the experimental work, is outlined.

Chapters 3 and 4 offer a framework through presentation of literature review on the development of plastics and PMMA, PMMA properties, structure and degradation, light ageing and UV exposure, chemistry and properties of gels, and gel cleaning. The literature review was crucial for the contextualisation of the current research. Chapter 3 discusses the development of plastics, the use of PMMA and its chemical and physical properties, with a particular emphasis on the initial, unaged state. Fundamentals of organic polymer chemistry and mechanical behaviour of PMMA are discussed. Degradation and its effect on the chemical and physical structure are also reviewed. Emphasis is given to the effect of solvents and UV radiation on the PMMA structure, both aspects of interest in this research and further examined.

Chapter 4 introduces the state-of-the-art conservation cleaning of plastics and PMMA, as well as cleaning with the use of gels in conservation. The chemistry and properties of gels, as well as typical gel systems commonly employed by the conservation community are reviewed. In addition, a list of assumed benefits and drawbacks of the use of gels is presented, so as to begin understanding the challenges and complications that may arise in a gel cleaning campaign of transparent and highly polished acrylic surfaces. Selection of solvents to add in the gel cleaning systems are also explained. The preliminary survey of conservators of modern materials and the data obtained regarding the most problematic types of plastic surfaces to clean and the most common types of dirt encountered on plastics in museum collections are also presented.

Chapter 5 sets forth the methodology for the light ageing regime of the PMMA used in this study and discusses sample preparation. Decisions regarding the light ageing were based on the mechanical properties and physical behaviour of PMMA, explored through tensile testing and Dynamic Mechanical Analysis (DMA) of samples in their unaged state and exponentially aged for 4, 8, 16, 32, 64 and 96 days under UV radiation. Moreover, Chapter 5 describes the selection of the type, grade and dimensions of PMMA samples, considering the needs of the cleaning experiments and the analytical studies in this research. The preparation, characterisation and standardisation of application of the artificial dirt simulating oily human fingerprints and adhesive remains from label, packaging and sticky tapes, are also discussed.

Chapter 6 offers an overview of all qualitative and quantitative methods employed for the evaluation of the cleaning experiments. Methods include both analytical and non-analytical techniques, aiming at detecting changes in the visual appearance, chemical composition and physical properties of the PMMA in its unaged, aged, untreated and treated states. In their majority, evaluation methods dealt with the surface topography, with one exception NMR

MOUSE examining the bulk material. In Chapter 7 the practical aspects of gel preparation are explained. Characterisation of the individual gel components is included as it was necessary to be able to identify residues on the treated surfaces at a later stage. The study investigating the damage that solvents could cause to PMMA after prolonged exposure is presented.

Chapter 8 consists of the preliminary experimental work. Preliminary experiments played the role of a preparatory, pilot step that was required in order to refine variables and identify the most significant factors for the cleaning of PMMA to be further scrutinised. Chapters 9 and 10 present the main experimental work of this research through comparative gel cleaning tests. They investigate in detail a variety of variables on new and artificially UV-aged material with new and artificially UV-aged surface dirt. The former chapter tests three applications of five minutes each, while the latter examines multiple applications of shorter times. All experiments were performed in successive groups aiming to find the most significant factors until optimised treatments are identified. Methods presented in previous chapters are employed for the evaluation of treatments and surface condition of samples.

Chapter 11 discusses the cleaning of three transparent and highly polished PMMA objects from a historical museum collection in Doha, Qatar. Cleaning of the three case studies was performed with the systems identified as safe and efficient at removing the artificial dirt of oily (synthetic sebum soil) or/and adhesive nature (pressure-sensitive spray adhesive), to test the treatments in real-life conditions and correlate them with laboratory experimental results.

In Chapter 12 literature review and experimental results are drawn together into one discussion. The section considers all information and data acquired throughout this study and discusses whether the use of gel systems is overall beneficial for cleaning PMMA and other plastic surfaces. Finally, the chapter summarises the important points and conclusions of this study. Areas of interest, additional factors, alternative and supplementary analysis, as well as some aspects not examined here due to limited time and resources are highlighted for future research.



## **Chapter 2. RESEARCH DESIGN & METHODS**

---

This chapter presents the research design and methods used in this study for data collection, analysis and interpretation. The study employed a mixed methods research approach for collecting data through an open-ended survey of experts opinions (primary source), literature review (secondary source), and experimental work on cleaning mock-up surfaces under laboratory conditions. To investigate the key research questions (see Chapter 1) and evaluate the cleaning experiments, this study gathered both qualitative and quantitative data for statistical analysis - obtained through visual observation, measurements and analytical techniques. A case study cleaning application on real museum objects was carried out to validate the experimental results. Choices regarding the selection and preparation of samples and artificial dirt employed in the experimental work, as well as the artificial light ageing of samples, are also discussed.

### **2.1. OPEN-ENDED SURVEY (RESEARCH METHOD I)**

The first part of this research consists of a series of open-ended questions canvassing the expert opinion of conservators of modern materials and plastics. The survey was sent via email to gather primary, qualitative data from specialists regarding the cleaning of plastics. Open-ended questions are questions where the respondent's answers are not chosen from predefined options. They are exploratory in nature and allow the respondents to give a free-form answer (Singer and Couper 2017). Open-ended questions are essential for designing research questions and are ideal for studies, such as this, with smaller populations (Singer and Couper 2017). This necessary preliminary research informed the need for cleaning in real-life conditions by identifying plastics and types of surfaces that are particularly problematic and more commonly in need to clean, as well as types of dirt commonly encountered on plastic objects in collections. Therefore, this online survey assisted in gathering information specific in nature, eliminating the potential bias and limitation of a preselected set of choices, identifying the practice-informed problems and establishing conservators' priorities in the cleaning of plastic museum objects. Overall, it rendered this research targeted and relevant to the field of modern materials conservation.

The population surveyed was based on expert conservators of modern materials and plastics, an emerging professional field, hence very small. Emails of conservators were retrieved from the list of participants of a well-attended conference on modern materials and plastics conservation, the proceedings of which form the main corpus of literature in this field. The data collection was conducted between February and March 2015. From a total of thirty-five conservators that were contacted, fifteen responded, amongst whom some offered information in the form of links or suggested people to contact. One email was answered in

Italian. For the open-ended survey and responses see Appendix B. Respondents were from the following institutions and private sectors: the Museum of Modern Art in New York, Die Neue Sammlung in Munich, Museum Tinguely in Basel, the British Museum, Victoria and Albert Museum, Tate and The Science Museum in London, Fondazione Plart in Naples, the Hamburger Kunsthalle in Hamburg, the Museum of Design in Plastics in Bournemouth and private practice in the Netherlands, Germany and Paris. The small number of answers facilitated the manual extraction and grouping of relevant information. Answers were analysed by number of counts/mentions to evidence main trends and recurring themes within the responses, and were plotted with the use of a spreadsheet software (Microsoft Excel). Results are presented and discussed in Chapter 4.

## **2.2. LITERATURE REVIEW (RESEARCH METHOD II)**

Literature review aimed to obtain an understanding of existing body of work and identify the gaps in the conservation field and its literature. Secondary (qualitative) data sources were obtained from literature regarding a very vast range of topics to offer a theoretical, contextual and methodological background to frame this research. Over 900 articles, books and reports were reviewed for this research. Reviewed sources include textbooks, conference proceedings, journals, newsletters, manuals, standards and websites about plastics conservation, cleaning in conservation, gels in conservation, polymer chemistry and science, materials science, photochemistry, polymer degradation, solvents and solubility, mechanical and chemical engineering, art and design, industrial documents, cultural history, theory of plastics consumption, statistics and chemometrics, forensics, clinical trials, dentistry and agriculture. This research is inter- and cross-disciplinary in that it used information and sources from various other fields and integrated them in its methodology of data collection and interpretation. Sources that could not be accessed online were retrieved from the UCL Main Library and UCL Science Library in London, the library at the Material Science Laboratory at the UCL Department of History of Art in London, the UCL Qatar Library in Doha, the ICCROM library in Rome and the British Library in London.

## **2.3. EXPERIMENTAL WORK (RESEARCH METHOD III)**

### **2.3.1. Selection of PMMA & artificial ageing**

The survey and literature review assisted in defining the primary concerns related to the cleaning of transparent and highly polished PMMA surfaces investigated in this research. The first step was to select the type and grade of PMMA samples to be studied. Two grades of commercially available transparent, colourless PMMA sheets were purchased, keeping in mind the wide range of different types available in the market and by extension available to artists

and designers. Their composition was unknown, as it is often considered an industrial 'secret'. One grade (1.0 mm) was described as cast with no further information provided, while the other (1.2 mm) was presumably of high purity and free from UV absorbers. It was anticipated that their behaviour would be different due to possible differing manufacturing techniques, and possible presence of additives (i.e. photo-initiators, UV absorbers) which could regulate the wavelength sensitivity and therefore the rates of degradation.

The selection of PMMA and the length of artificial light ageing, in order not to be an arbitrary decision, was based on the mechanical properties and physical behaviour of the material before and after ageing. To explore such properties tensile testing and DMA were carried out. Initially, a preliminary test was carried out to determine the experimental parameters for the tensile analysis. This aimed to establish whether the breaking loads of the samples were within the instrument tolerance, determine the relationship between sample dimensions and breaking load, and lastly, determine whether the orientation and direction of cut influenced the mechanical behaviour of the samples. Once these parameters were determined, the two grades of PMMA were cut into rectangular coupons (for cutting decisions see 2.3.2) and exposed to six levels of UV radiation. Both tensile testing and DMA had very specific requirements regarding coupon size and dimensions, therefore they were custom-built for the needs of each technique (see 5.1.1). Coupons were exponentially aged for 96 days with sampling steps at 4, 8, 16, 32 and 64 days according to standards simulating accelerated outdoor weathering conditions (see 5.1).

The purpose of testing samples of varied exposure lengths lied in the need to detect the points of load at which PMMA broke based on the amount of light absorbed. By correlating break points (i.e. at half and quarters of its initial load) with the equivalent amount of exposure, it was possible to standardise accelerated degradation based on an indication of the extent of ageing. This allowed to set forth the methodology for the light-ageing regime (see Chapter 5). Differences in the tensile behaviour between the unaged and differently aged replicates were more distinct in the 1.0 mm cast PMMA, therefore it was selected for further testing. Samples aged for 32 days showed the most mechanical change (embrittlement) in the shortest possible timeframe. Results of DMA were complementary and confirmed, through identification of relative values of  $T_g$ , that there was definite change between the 1.0 mm unaged and 32-day aged PMMA. DMA also offered information that aided understanding of PMMA's chemical behaviour in different ageing stages.

In summary, 1.0 mm cast samples were aged for 32 days under UV radiation following outdoor artificial weathering, in five batches of roughly 190 samples each ( $n=1000$  samples). Following, ATR-FTIR and pyrolysis-Gas Chromatography/Mass Spectrometry (py-GC/MS) were

employed to chemically characterise the samples. Py-GC/MS was mostly used to investigate the decomposition products.

### 2.3.2. Sample preparation & artificial dirt

Regarding the preparation of samples the following questions were raised: what was the preferred technique for cutting PMMA by industries? How did each of the techniques affect the material? Conventional sample preparation involved machining, such as mechanical or laser cutting. Machining operations not only could influence the surfaces of cut samples, but in some cases, they could alter their mechanical behaviour, cause dimensional changes, internal and tensile stress (Machining PLEXIGLAS® Guidelines for Workshop Practice-Evonik Röhm GmbH). Since experimental results were strongly dependent on all these parameters, tools and machining conditions were reviewed according to ISO 2818-1996, to ensure reproducible results.

Sample preparation as well as sample size/shape could have significant impact on the experimental outcome. Sample thickness was one of the most important parameters, because it affects the polymer degradation, as well as plays a critical role in analytical studies. It was recommended for samples to be prepared such that thickness, concentration of components, morphology, and physical-mechanical properties were uniform throughout their depth (Wypych 2013). Sample requirements impact artificial ageing too; sample size, thickness, density, weight and orientation needed to be identical throughout (Wypych 2013), to facilitate uniform irradiation. Studies showed that inhomogeneous thickness across the sample resulted in unwanted variation in properties, and on the depth of degradation. In fact, uneven thicknesses may lead to shifting of wavelength absorption. Thicker samples were seen to absorb more radiation and undergo degradation at a faster rate, but according to Adam *et al.* (1989 cited in Feller 1994) samples thicker than 21 mm were not expected to have a homogeneous distribution of absorbing groups.

In recent decades, lasers have been employed to fabricate PMMA due to the ability of multi-directional and support-free machining, automation and adaptive controlling. Even though PMMA is one of the most widely laser-cut polymers, with an excellent precision of cut (Choudhury and Shirley 2010), laser machining was not favoured. Lasers are known to heat-induce micro-defects responsible for stress concentration and acceleration of the initiation and propagation of crazes and micro-cracks in the cut edge during cyclic loading (Abar *et al.* 2015). They also tend to decompose plastics, affecting the surface quality of samples at the point of laser-plastic interaction. This happens through polymer evaporation, which forms bubbles in the vicinity of cut surfaces, resulting in a pronounced roughness (Choudhury and Shirley 2010; Abar *et al.* 2015). Laser cutting would affect the surface quality of PMMA samples, constituting an uncontrollable variable that would affect measurements and reproducibility of tests.

The challenge with mechanical cutting was the brittleness of glassy PMMA. Care was needed to limit stress generated adjacent to the machined areas and prevent fracture formation usually starting in areas with existing defects - often in the form of voids or micro cracks which lower the material strength (Subbiah and Melkote 2013). Behaviour of other materials, such as composite polymers and steel, were reviewed here, as literature on the effects of cutting PMMA was limited. In the mechanics of composite materials, effects connected with stress in the cut edge of samples are called edge effects (Polyakov and Perov 1988). These could cause problems during subsequent work steps, i.e. crazing (Javidi *et al.* 2008). Surface quality after machining could also affect the samples' mechanical behaviour (Javidi *et al.* 2008).

Another issue to consider was the intensification of the effect of cutting and machining operations after exposure (ISO877-1:2010). PMMA embrittles evidently on weathering, and occasionally delaminates at the edges if cut from a larger piece, rendering subsequent machining difficult (ISO4892-1:2016). Therefore, it was important for PMMA samples to be machined and prepared in the desirable shapes and dimensions, in which they were to be tested/analysed, before exposure to UV radiation. The choice of samples and their size had to ensure in advance that they satisfied every criterion on thickness and dimensions that each analytical technique and evaluation method imposed, so as to avoid subsequent machining following artificial ageing.

SEM imaging, ATR-FTIR and NMR MOUSE practically dictated the dimensions of samples in this study, as they required specific provisions regarding sample dimensions. SEM imaging required a maximum size of samples to be within 305 mm in diameter and up to 80 mm thick, to fit in the specimen chamber and be held on the specimen stage. The ATR crystal used in this study had no width restrictions, and was able to analyse a sample from a few microns (ca. 0.5  $\mu\text{m}$ ) to a maximum thickness of roughly 30 mm. In the case of unilateral NMR analysis, the depth of samples was of most significance: they had to be at least 2.5 mm and up to 4 mm thick for the analysis to become possible. It was favourable for samples to be roughly of similar size to the analytical window (30 x 30 mm), where placed for analysis. In an attempt to compromise between all analytical criteria and experimental needs, as well as for ease of handling, the samples were prepared as 25 x 25 mm square coupons.

PMMA square coupons were received from the company they were purchased from, with traces of residual packaging, as confirmed by ATR-FTIR analysis. Residues were expected to interfere with the surface's soiling behaviour, the cleaning experiments and their reproducibility, so pre-washing of samples was considered essential. Ultrasonic cleaning in deionised water was identified as the safest and most efficient method for residue removal.

While the examination of virgin substrates provides valuable information about the effect of cleaning on a plastic surface, real-life surfaces are rarely in pristine condition. In addition to the type of plastic, the survey of conservators of modern materials and plastics, also identified

types of dirt that are commonly encountered on plastic objects in collections. Based on the survey and literature review, this research examined two different types of 'dirt': a synthetic sebum soil formulated to mimic human oily fingerprints from handling along with deposited surface loose dust and an acrylic-based pressure-sensitive spray adhesive selected as representative of adhesive residues from labels, packaging and sticky tapes commonly remaining on objects after storage and transportation. The composition of synthetic sebum soil followed a published recipe used in forensics and cosmetics studies, closely approximating human sebum. Following common practices in conservation, carbon black pigment was incorporated to simulate encrusted grease. The adhesive was supplied as a pressurised aerosol, preferred for its ability to be standardised, enabling a uniform and repeatable deposition. The spraying process of both dirt types was standardised to eliminate inconsistencies that would affect the accuracy of cleaning data and cause variability to the results, ensure the repeatability of the experiment and enable the study to be comparative. Both types were characterised with ATR-FTIR.

### **2.3.3. Gels & solvents for cleaning**

Literature review enabled the selection of the most common gel systems used in the conservation cleaning of cultural heritage materials and the assumed safest solvents used on PMMA. Individual materials comprising the gel systems were chemically characterised with FTIR in transmittance mode as potassium bromide (KBr) pellets in their pure powder form as well as in ATR as dried hydrogels. This aimed to identify their characteristic absorption bands and be able to distinguish them if found as residue on PMMA surfaces after cleaning.

A preliminary study was carried out on the effects of solvents selected for the cleaning experiments. For its purposes, unaged samples were immersed in each of the four solvents/liquids for 30 days in order to understand the level of potential damage they could cause to PMMA when in direct contact, as some sort of 'worst case scenario'. The effects were studied through stereomicroscopy, weight measurements and ATR-FTIR analysis.

### **2.3.4. Design of cleaning experiments**

The topic in this research was explored through laboratory-based cleaning experiments on unaged and aged PMMA samples, with or without unaged and aged artificial dirt. Ageing of samples was performed under UV radiation. The two types of artificial dirt are described above. Design of experiments (DOE) was employed to organise the experiments, render them reproducible, reassure balanced and unbiased results, avoid systematic and random errors, and map the results, with the use of Minitab® 17 software. The overarching aim of the experiments was to acquire systematic data and ultimately assist in answering the research questions.

DOE enabled identification of factors with a significant effect in the cleaning process. The most critical factors were established through the literature and personal communication with conservators as Gel, Solvent, Application time, PMMA surface condition, Dirt and Dirt condition. The assessment of experiments was based on macroscopic examination, stereomicroscopic observation under raking light, SEM imaging, weight and gloss measurements, ATR-FTIR and NMR MOUSE (see 2.3.5). In addition, DOE offered information about the interactions and relationships among tested variables, and minimised the number of experimental runs and thus of replicates needed to evaluate the cleaning process. For more details see Chapter 6.6. The use of statistically-designed experiments was vital for the progressive narrowing down to the most significant liquids and gel carriers (factors), eventually leading to the optimisation of treatments, as the most suitable for cleaning PMMA. The experimental work was divided in two parts. The first was a pilot cleaning study on unaged, unsoiled surfaces which offered preliminary results, helped refine design and variables, and led to the main experiments. These were performed on unaged and aged surfaces with unaged and aged artificial dirt, controlled variables on controlled surfaces, and tested gel systems, application times and number of applications for removal of the two 'dirt' types.

### **2.3.5. Evaluation methods & data analysis**

Cleaning treatments and their effects on PMMA in this study were systematically evaluated, both qualitatively and quantitatively, for their effectiveness and safety at removing artificial dirt in the form of synthetic sebum soil and pressure-sensitive spray adhesive. Qualitative data were obtained through macroscopic examination, stereomicroscopic observation under raking light and SEM imaging. The latter two offered descriptive data, essential to the understanding of cleaning efficiency and of phenomena taking place on the surfaces post-treatment. In an attempt to quantify visual results, organise and standardise reporting of observational data, the macroscopic examination was documented through the use of a condition survey and the production of a condition score, known as the criterion anchored ranking scale (CARS), developed for this study. CARS is a method of making visual assessment of object condition and human judgement an objective process (Loehnert 2010). Descriptive terms, providing information about the treated surface condition and treatment effect, were allocated numbers (scores) that could be measured on an ordinal scale (ranked values), and therefore be ordered. This meant that the use of a ranking system turned qualitative data into quantitative, adding parametric statistical texture. This allowed data from macroscopic examination to be analysed in a similar manner with data obtained from analytical techniques. For a discussion of the limitations of doing so see Chapter 6.6.

Sample weight measurements provided a quantitative indication of changes in the material and gloss measurements provided quantitative information about surface changes. ATR-FTIR and NMR MOUSE, respectively used to monitor chemical modifications and the physical condition of samples treated with the optimised, successful treatments, also offered quantitative data. Peak height ratios were calculated for all the ATR-FTIR spectra between an internal standard and the changing peaks of interest, to (semi-quantitatively) detect relative chemical change as a result of ageing under UV irradiation, immersion in solvents (preliminary study on the effects of solvents) and cleaning.

Such numeric data were statistically analysed with the use of analysis of variance (ANOVA), which was supported by the use of DOE and run in Minitab® 17. ANOVA compared all factor levels based on the null hypothesis that all cleaning treatment levels had the same effect, therefore had no statistical significance. The significance was set at  $p = 0.05$  with a 95 % confidence. If the p-value was less than the significance level ( $p < 0.05$ ) it was established that some of the means were different. By rejecting the null hypothesis results confirmed a significant systematic difference. DOE results of ANOVA were presented in the main effects plots, which depicted examined factors and their levels. Once it was concluded that there was statistical difference between different levels, Tukey's honestly significant difference post-hoc (Tukey's HSD) test was used to locate where the significant effect occurred and which were the different levels. Data were represented in the form of line graphs, bar charts, pie charts, tables, plots, spectra, curves and 2D contour heat maps (see Chapters 8-10).

#### **2.4. CASE STUDY CLEANING APPLICATION OF MUSEUM OBJECTS**

Analysis of all qualitative and quantitative data from the preliminary and main cleaning experiments offered optimised gel treatments identified as safe for PMMA and efficient at removal of artificial dirt of oily or/and adhesive nature. To validate these laboratory experimental results obtained on model surfaces, three transparent and highly polished PMMA museum objects acted as case studies for real-life cleaning application. These case study cleaning applications offered descriptive data which confirmed that the optimised treatments for cleaning model surfaces under laboratory conditions were able to achieve equally successful results under real conditions.

This chapter presented the research design and methods used in this study for data collection, analysis and interpretation. The following chapter presents the material under study through literature review of the historical development of plastics and the use of PMMA, as well as its chemical and mechanical structure, properties and degradation.



### 3.1. BRIEF REVIEW OF PLASTICS

#### 3.1.1. Overview of historical development

The history of plastics manufacturing dates back to the first half of the 19<sup>th</sup> century (Albus *et al.* 2008). Although we consider plastics to be new materials, only semi-synthetic and synthetic plastics are modern. Development of modern plastics expanded in the first fifty years of the twentieth century, with at least fifteen new classes of polymers being synthesised (Andrady and Neal 2009). The polymers synthesised before the start of the 20<sup>th</sup> century were all based on naturally occurring polymers formed by plants, trees, insects and animals, and most had been developed into commercial materials by trial and error (Shashoua 2008). The first plastics were produced by chemical modification of natural polymers, which being less dense, more robust and available in limited colours and forms, were modified with the aim of producing physically stable, mouldable products (Shashoua 2008; Rogerson 2009). Semi-synthetic materials evolved as imitation materials to replace objects made of rarer, natural materials including ivory used in billiard balls, mother-of-pearl and tortoiseshell used in combs (Waentig 2008; Andrady and Neal 2009).

In 1839-1840, Charles Goodyear and Thomas Hancock discovered that heating natural rubber with a few per cent of sulphur (rubber vulcanisation) allowed it to remain both elastic over a wide range of temperatures and resistant to solvents. In 1870, cellulose nitrate, popularised as Celluloid, was mixed with camphor, heated under pressure and shaped (Albus *et al.* 2008; Shashoua 2008). The most important commercial application for celluloid was photographic film, which by the 1920s dominated the movie industry. Its high flammability and ability to soften on heating, led to the development of substitutes, namely casein-formaldehyde in 1899 and cellulose acetate in 1905 (Shashoua 2008).

The leap from modified natural products to the first fully synthetic polymer was made in 1907 with the introduction of phenol-formaldehyde, a thermosetting plastic known as Bakelite (Albus *et al.* 2008; Feldman 2008). Poly (vinyl chloride) was first polymerised in 1872, but patented in 1912. This long delay between synthesis and commercial development was also seen with polystyrene; synthesised long before World War II (WWII) and industrially produced in large scales in 1939, just before the outbreak of WWII (Shashoua 2008). The 1930s, was a period in which numerous new polymers were invented with the support of U.S. government investments (Rogers 2005), rather than of independent scientists as in previous decades (Shashoua 2008). Promotion through the "better things for better living through chemistry" slogan of DuPont chemical company (Finkelstein 2008) corresponded to an ever-growing technological innovation and industrial consolidation (Fisher 2008, 146). By the 1940s, people were so fascinated by plastic that "the word *cellophane* was designated the

third most beautiful word in the English language” (Freinkel 2011, 8). Cutting-edge discoveries included nylon used to make clothing and parachutes, polytetrafluoroethylene, known by its trade name Teflon, used as insulation in radios and electrical cables, and silicones, widely used for adhesion and their chemical resistance (Shashoua 2008).

Just prior to the WWII and 1940s, plastics were used as synthetic substitutes for natural resources and supplies unavailable due to wartime shortage (i.e. silk, rubber and metals) (Mason 2011). At the time, plastics had become a household material in America (Meikle 1992), and were mostly used for decorative purposes. WWII increased their demand, especially for military applications, electronics and food industries, including gas masks, protective helmets, electrical insulation and radio components (Shashoua 2008; Freinkel 2011). During the inter-war years, advances in organic chemistry (Brydson 1999; Waentig 2008) enabled the development of many new plastics (Rogerson 2009; Fricker 2016). Polyesters were among them, initially developed around 1847, and first industrially produced in 1941 (Shashoua 2008). With the U.S. entering WWII, commercial high-end plastics were pulled from the market and supplied exclusively to the military for tires (Fig.3.1c), parachutes, cockpit windows and fighter planes, linings, goggles, raincoats, waterproof tents, electrical wiring, and parts for the atom bomb (Rogers 2005; Freinkel 2011).

After WWII, production of newer plastics happened in larger quantities and lower cost. The discovery of these plastics in the first half of the 20<sup>th</sup> century resulted in many of the common plastics in use today (Fricker 2016). The end of wartime forced the focus of mass-produced plastics to shift towards household goods (Waentig 2008; Rogerson 2009). By the beginning of the 1950s, an impressive range of products could be manufactured from the new synthetic materials (Albus *et al.* 2008). They not only replaced older polymers, such as cellulose nitrate, and traditional construction materials, such as metals, wood, leather and glass, but they were being turned to ephemeral conveniences too (Shashoua 2008; Freinkel 2011). The post-war boom of plastics, such as Styrofoam picnic and coffee cups, food wrap (cling film) (Fig.3.1a, d), disposable lighters and pens (Freinkel 2011), was largely caused by massive public spending, powerful lobbying, and sophisticated public relations. During this time the notorious Tupperware party was born (Rogers 2005). The benefits of strategic marketing and creative promotion were paying off, and Tupperware helped plastic to become a symbol of healthy American family life (Fig.3.1e) (Rogers 2005). Consumers slowly realised that plastic products were more than just substitutes (Albus *et al.* 2008).



Figure 3.1. Posters in the U.S. showing the benefits of plastics.

(a: <https://www.pinterest.com/pin/14988611229390449/?lp=true>,

b: <http://www.advertisingarchives.co.uk/detail/55932/1/Magazine-Advert/Vinylite-Plastics/1940s>,

c: <https://www.pinterest.com/pin/294845106840349001/?lp=true>,

d: <https://www.pinterest.com/pin/39195459230383095/?lp=true>,

e: <https://www.smithsonianbooks.com/store/history/tupperware-promise-plastic-1950s-america/>).

In the mid-1950s and early 1960s, the development of plastics entered a second phase. Their production surpassed that of steel and aluminium in the U.S. and became one of the largest industries (Gschwind 1950). In the second half of the 20<sup>th</sup> century, chemists and engineers manufactured highly specialised plastics, such as polyurethanes and polyolefins, which were not for general use (Albus *et al.* 2008). Polycarbonate was also commercially produced during this time (1959), although it was first developed in 1953. It was most famously used for the production of CDs and DVDs, and widely replaced aluminium in household appliances by the end of the 1970s (Shashoua 2008).

The plastic availability stopped suddenly in the 1970s impacted by the oil crisis (Bensaude-Vincent 2013). This led to the acceptance that sources of petroleum are not inexhaustible, and motivated research into alternative sources for raw materials for plastics (Shashoua 2008). Up to that time, industries promoted the idea that plastics lasted forever

(Lambert 2012), a misconception that still exists even today (Lavédrine and Shashoua 2012). This was enhanced by some highly stable polymers and their residues that persist in landfill for decades without breaking down, connecting plastics to environmental pollution (Fisher 2008). Being commercial products and designed as disposable, often cheap and fashionable, plastics were not intended to last forever, but were designed to become obsolete after a number of uses. They had a specific role in consumption, driven by a desire for new, fashionable things (Bensaude-Vincent 2013). By the 1980s plastics fell out of favour due to their connotation with 'cheap' non-exclusivity and a human desire for opulence, the increasing awareness of the need to conserve resources, as well as massive volumes of rubbish in a more environmental-friendly consumer society (Shashoua 2008; Bensaude-Vincent 2013).

### 3.1.2. Application in industry, art & design

Plastics managed to play an important role in modern society, overtaking more traditional materials (Bensaude-Vincent 2013). Plastics ubiquitous nature has led to their use in many fields, and their employment in the design of everyday objects, art and fashion are no exception, reflecting daily life for more than a century (Newman 1965; Meikle 1998). Almost all aspects of daily life involve plastics in some form or the other (Andrady and Neal 2009). The history of plastics in the visual arts started towards the end of Victorian times (1837-1901), in the late 19<sup>th</sup> century. Semi-synthetic plastics were invented during that time, mostly as decorative everyday items. Vulcanised rubber and celluloid, among others, were widely used as cheap jewellery substitutes to ivory, tortoiseshell and other expensive materials. They were commonly employed in combs, dresser/vanity sets, necklaces, umbrella handles, brooches, earrings and other elaborate craft objects (Waentig 2008; Freinkel 2011).

Between the years 1910-1945 there was a boom in industrial design (Waentig 2008). The history of plastic design was influenced by the successes of material developers and the production growth of modern plastics (Albus *et al.* 2008). Among the first artists to employ plastics were the brothers Antoine Pevsner and Naum Gabo, of the Russian avant-garde, who regarded plastics as modern technological materials in the later machine age (Albus *et al.* 2008). In the late-1910s, they produced three-dimensional Cubist<sup>3</sup>-inspired forms with cellulose nitrate sheets (Albus *et al.* 2008; Shashoua 2008). The Constructivist theories<sup>4</sup> of

---

<sup>3</sup> Cubism developed a visual language of geometric planes and rejected the conventions of perspective and representation. It broke down subjects into their geometrical components and often represented them from several angles at once ([https://www.moma.org/learn/moma\\_learning/themes/cubism/](https://www.moma.org/learn/moma_learning/themes/cubism/)).

<sup>4</sup> Influenced by Cubism, and linking art with industry, technology, and the ideals of a classless society through the production of socially useful objects (<https://www.guggenheim.org/artwork/movement/constructivism/>).

artists, such as Pevsner and Gabo, and of Bauhaus<sup>5</sup> artist László Moholy-Nagy (Fernández-Villa *et al.* 2012) revolved around the idea that art and industry should share goals, introducing the notion of using industrial materials in art (Albus *et al.* 2008). Such artists introduced a new kind of synergy between art and technology, where they would collaborate technical experts and chemists from the plastics industry to master the use of these materials (Albus *et al.* 2008).

In the 1920s, plastics were also employed in fashion; Coco Chanel used them in combination with gemstones to produce jewellery (Rogerson 2009). Many fashion designers followed, utilising plastics' decorative potential (Waentig 2008). The use of plastics was also crucial in the construction of Hollywood glamour in the 1920s and 1930s, providing new shiny surfaces and effects (Kane 2015). From the 1930s and 1940s, plastics started being viewed as distinctive materials connected with distinct design ideas (Albus *et al.* 2008). The focus had shifted from fascination about the new materials and their potential usage, to their visual qualities and creating unusual, curved shapes that could not be created with other traditional materials like wood (Fricker 2016). This is when the Streamline Moderne<sup>6</sup> emerged, an Art Deco<sup>7</sup> architecture and design style expressed through electrical appliances (Albus *et al.* 2008). By the early 1940s, the car industry also began to employ plastics to construct car bodies. Ford had already made a car prototype in glass-reinforced polyester by 1941 (Shashoua 2008).

Plastic was everywhere; in decoration, furniture, fashion, utilitarian and functional everyday objects. It was considered progressive and encouraged avant-garde designers, operating according to the motto adopted in 1947 by architect Ludwig Mies van der Rohe 'less design is more design' (Astbury 2018). Plastics had become invaluable in a variety of other fields, including aerospace applications, i.e. manufacturing of spacecraft components, medical applications and other technological advances, such as computing and engineering (Kane 2015).

A transformation in design can be traced back to the second half of the 20<sup>th</sup> century (Waentig 2008). In the early 1950s, and for the first time, many designers used polyurethane soft foam; a material that not only promised comfort, as padding to seating furniture, but virtually

---

<sup>5</sup> It was influenced by the Arts and Crafts movement, Art Nouveau and its many international incarnations, including the Jugendstil and Vienna Secession, all seeking to level the distinction between the fine and applied arts, and reunite creativity and manufacturing. The Bauhaus aimed to reunite fine art and functional design, creating practical objects with the soul of artworks (<https://www.theartstory.org/movement/bauhaus/>).

<sup>6</sup> The American response to Art Deco (<https://www.theartstory.org/movement/art-deco/>). See <sup>5</sup>.

<sup>7</sup> It can be seen as successor to and a reaction against Art Nouveau. Its chief difference is the influence of Cubism, which gives Art Deco design a more fragmented, geometric character. It attempts to infuse functional objects with artistic touches, reflecting the relative newness and mass usage of machine-age technology rather than traditional crafting methods to produce many objects (<https://www.tate.org.uk/art/art-terms/a/art-deco>; <https://www.theartstory.org/movement/art-deco/>).

offered creative shaping (Albus *et al.* 2008). Around the same time, acrylic solution paints also appeared on the commercial market (Learner 2012; Kane 2015). Among the first plastic objects associated with the characteristic 1960s style were pieces of furniture, such as those by Luigi Colani, whose organic look was reminiscent of Art Nouveau's<sup>8</sup> imitations of nature, including leaves and other plant parts (Albus *et al.* 2008). Other designers who turned to plastics, were Charles and Ray Eames, Eero Saarinen and Gaetano Pesce, who used methods of mass-producing plastics to create constant replicas. Along with Pesce, many artists and designers, notably Eero Aarnio and Verner Panton (Freinkel 2011), produced more than just furniture, experimenting with inflatable furniture and acrylic light fixtures (Mandarim de Lacerda 2010).

Although plastics had been previously used by artists and designers since the beginning of the 'Plastic age', as the 20<sup>th</sup> century was characterised (Bensaude-Vincent 2013; Fricker 2016), it was not until the late 1950s and 1960s that plastics became widely employed in art-making (Kane 2015). In art galleries, plastics appeared more and more often alongside granite and wood (Albus *et al.* 2008). To give an example of how much they had been used in a steadily growing extent, it is worth mentioning that in 1964 at Documenta 3, a large-scale perennial contemporary art exhibition in Kassel, only two artists displayed works incorporating plastics. Just four years later, in 1968, the exhibition featured as many plastic works as objects made of conventional materials (i.e. bronze, stone, etc.) (Ward 2008). By the end of the 1960s, the number of plastics used by artists had increased dramatically despite the growing evidence that they were unstable and required either conservation or replacement.

Plastics offered great freedom of expression and experiment to artists (Sandino 2004). Examples of artists using them include significant painters and sculptors such as Jean Dubuffet and Niki de Saint Phalle, Duane Hanson, known for their hyper-realistic sculptures and installations, Pop artists Andy Warhol, Robert Rauschenberg, Richard Hamilton and Roy Lichtenstein, Minimal artists Donald Judd, Craig Kauffman, Carl André, Eva Hesse, and Sol Lewitt, as well as contemporary artists Paul McCarthy, Jeff Koons, Ron Mueck, Maurizio Cattelan and Damian Hirst, among others (Albus *et al.* 2008; Fernández-Villa *et al.* 2012).

In the 1970s plastic design had become so flexible that even anti-design movements emerged, with chairs from soft materials creating the illusion of hard ones, such as the polyurethane foam *Capitello* chair designed by Studio 65 resembling an ancient Greek Ionic marble column and capital, and polyurethane foam *Il Piede* by Gaetano Pesce, reminiscent of Constantine's marble foot in Rome (Albus *et al.* 2008). In the late 1990s, a movement known

---

<sup>8</sup> It was aimed at modernizing design and drew inspiration from both organic and geometric forms, uniting flowing, natural forms resembling the stems and blossoms of plants. The emphasis on linear contours took precedence over colour (<https://www.theartstory.org/movement/art-nouveau/>).

as environmental or recycled art reused discarded plastic objects from rubbish bins, dumps, beaches and streets to create collages and sculptures (Shashoua 2008).

### 3.2. DEVELOPMENT & USE OF POLY (METHYL METHACRYLATE)



*Figure 3.2. László Moholy-Nagy and his studies of light through the use of acrylics. Upper left: Vertical Black, Red, Blue (1945) (<https://www.christies.com/features/Laszlo-Moholy-Nagy-8250-1.aspx>), Lower left: Untitled (1939-1945) <https://risdmuseum.org/art-design/collection/untitled-70125>, Right: Mobile Sculpture (Space Modulator) (1943) (<https://thecityreview.com/f12simp2.html>).*

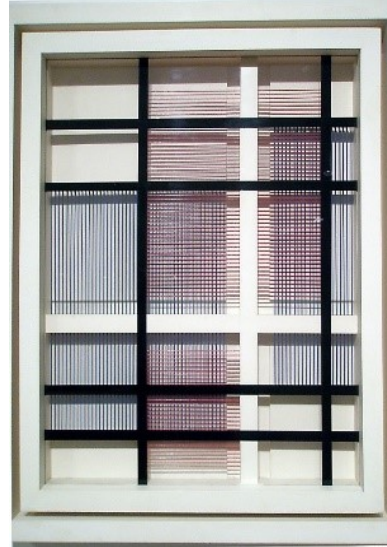
PMMA, widely known as acrylic, Perspex or Plexiglas, was developed in 1872 and commercially produced in 1933-34 (Morgan 1991b; Rogerson 2009). It was in high demand for aircraft glazing, windshields and protective screens in WWII, due to its rigidity, transparency and shatter-resistance (Sale 1993; Feldman 2008). In addition, it provided a weather-resistant alternative to glass (Shashoua 2008).

Gabo and Pevsner were the first artists to use PMMA for Constructivist sculptures (Albus *et al.* 2008). Cellulose nitrate's instability led them to replace it with the more stable PMMA; it had similar visual properties, better ageing properties, and could be worked with woodworking tools (i.e. saws, files, sandpaper, drills, etc.) (Ward 2008). In 1937, Naum Gabo was reportedly enthused about PMMA's high clarity, total internal light reflection enabling light to travel through the material (Rogerson 2009), and capacity to be softened with heat and be easily

molded into various shapes (Ward 2008; Comiotto and Egger 2009). Moholy-Nagy also extensively used PMMA in his investigations of light (Fig.3.2) (Chiantore and Rava 2012).

The first artist to use coloured acrylic sheeting in his geometric reliefs was Charles Biederman in 1938 (Fig.3.3). The following year, Rohm and Haas, the chemical manufacturing company of PMMA branded under the name Plexiglas, hosted a competition with the Museum of Modern Art in New York for Plexiglas sculptures. Winner Alexander Calder was the only participant to make further work in plastic (Taylor 2018). Sculptor Arthur Fleischmann also adopted PMMA as his favoured medium. He carved blocks as if they were transparent stones, exploring the material's similarities and differences to conventional carving materials (Rogerson 2009). In 1946, artist Alexander Archipenko selected PMMA for the production of three-dimensional sculptures symbolising time and space, due the material's capability to radiate incident light and make the sculptures appear as if they would radiate and shine from within (Ward 2008).

*Figure 3.3. Charles Biederman's geometric relief (<https://blog.dma.org/tag/charles-biederman/>).*



At the beginning of the 1960s, Arman created his PMMA trademark sculptures (Ward 2008), whereas Donald Judd, another landmark figure in the history of post-war art, commonly incorporated coloured, transparent PMMA in his installations (Mumok 2013). Leroy Lamis, a sculptor and digital artist strongly influenced by Constructivism, along with Mon Levinson and Julian Stanczak, also turned to constructions made of PMMA sheets in the 1960s (Lenz 2012). Lamis, renowned for his work in acrylic, stated that:

One advantage I have found in using plastic is the way in which it transmits light, much like glass.... Its greatest advantage is its unique optical effect. It's a beautiful thing in itself (Lenz 2012, para. 10).

De Wain Valentine and Helen Pashgian, members of the Light and Space movement<sup>9</sup>, are amongst the artists who pioneered the use of PMMA for its ability to transmit, diffuse, or refract light, allowing the viewer to “become involved with both the inside space and the

<sup>9</sup> It developed in California in parallel to the dominant Minimalist movement in New York in the early 1960. It is characterised by industrial materials, influenced by the flourishing aerospace industry, and a hard-edge, geometric aesthetic. Its signature characteristic is the creation of two- and three-dimensional works, sculptural or environmental in scale (<https://www.theartstory.org/movement/light-and-space/>).



outside space or surface - where most sculpture visually stops”, as Valentine explained in an interview with the Getty Conservation Institute (Learner *et al.* 2011; Simms 2015). Bruce Beasley, another artist based in California in the 1960s, successfully explored large-scale transparent sculptures in cast PMMA. Although experts at DuPont chemical industry and Rohm and Hass thought it was impossible, Beasley managed to cast a massive acrylic sculpture. *Apolymon* (1970) (Fig.3.4), 4 meters wide and 1 meter thick, won the competition run by the State of California against a selected group of sculptors and was installed in Sacramento (Wheeler 2015).

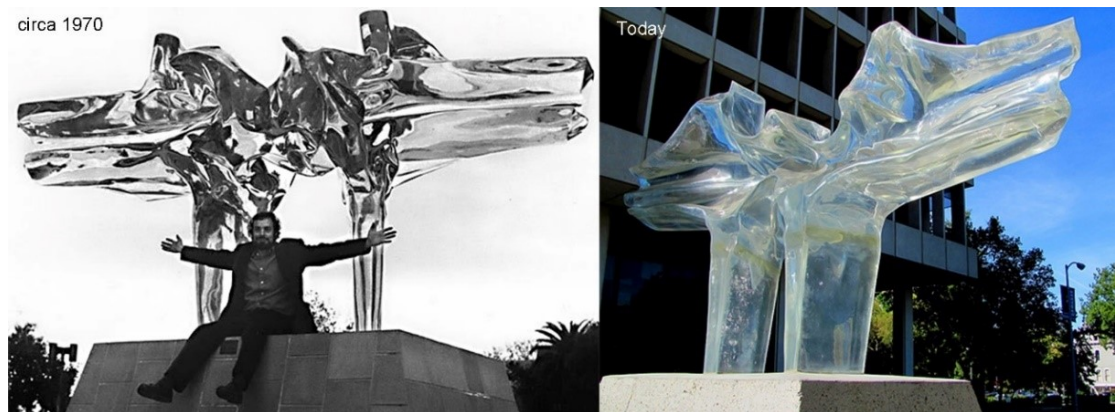


Figure 3.4. Bruce Beasley in front of *Apolymon* in Sacramento, 1970 (<http://brucebeasley.com/apolymon/>).

PMMA artworks were also created by artists Craig Kauffman (Fig.3.5), Gino Marotta (Fig.3.6b) (Laganà 2008), John Chamberlain (Fig.3.6a) and Yoko Ono, to mention a few (García Fernández-Villa *et al.* 2012). Contemporary leading design companies, such as *Kartell* (Fig.3.6c,d,e) (Freinkel 2011), symbols of Made in Italy design around the world, still today create acrylic objects ranging from household furnishings, to kitchenware and lighting. These qualities and abilities of PMMA that all the



Figure 3.5. Craig Kauffman next to his acrylic sheet (<https://www.nytimes.com/2010/05/15/arts/design/15kauffman.html>).

mentioned artists and designers cherished, to transmit light, luminosity, be smooth, opaque, clear, or coloured, be shaped, twisted, stretched and bent (Lenz 2012), were also reportedly useful to jewellers (Rogerson 2009). The importance of transparency, glossiness and reflective qualities of PMMA in regard to jewellery is extensively discussed by Rogerson (2009).

All these transparent PMMA artefacts, either sculptures, everyday objects or jewellery, were created to be immaculate. Craig Kauffman stated that “he would find any visible damage or

repair unacceptable” (2009 cited in Rivenc 2016) and repaired superficial scratches and cracks himself by sanding and polishing. John McCracken of the Light and Space movement, would also resort to polishing techniques in order to repair his highly polished sculptures (Rivenc 2016). Similar was the case with Helen Pashgian and De Wain Valentine, who would polish their high translucent and pristine monumental sculptures, to:

Allow the viewer to become involved with the Southern California landscapes of light, skies, and ocean views, where the sculpture was created (Learner *et al.* 2011).

The aforementioned statements of California-based artists of the 1960s demonstrate that a number of imperfections developed in the material due to inherent ageing phenomena and accidental damage, would change the whole perception of the work and the way it was meant to look (Learner *et al.* 2011).

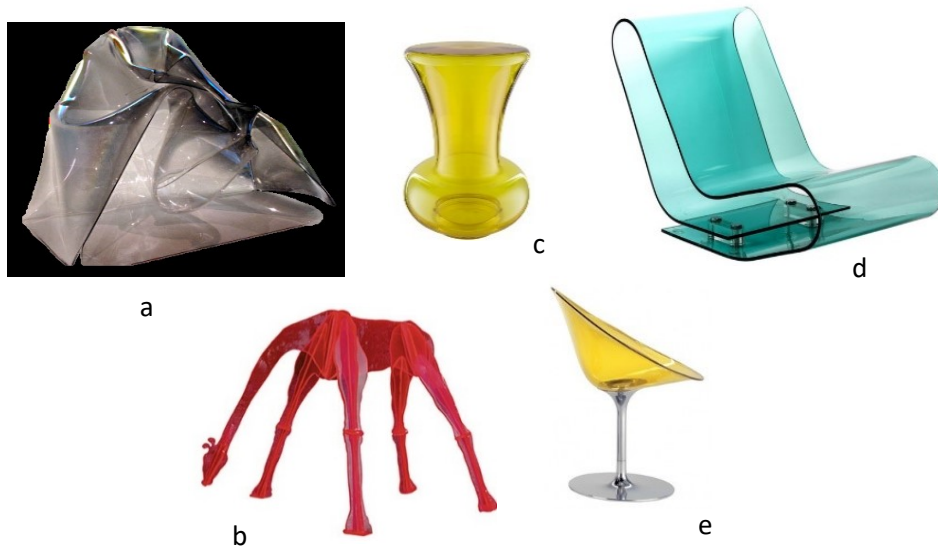


Figure 3.6. a. Heat-formed mineral-coated PMMA by Chamberlain (<https://theartstack.com/artist/john-chamberlain/luna-luna-luna-in-memory-of-elaine-chamberlain-1970-mineral-coated-synthetic-polymer-resin-photograph-by-katy-hamer-image-courtesy-of-the-guggenheim-ny>), b. Giraffa artificiale con fiore by Marotta ([https://www.vogue.it/en/people-are-talking-about/vogue-arts/2012/11/tribute-to-gino-marotta?refresh\\_ce=#ad-image234871](https://www.vogue.it/en/people-are-talking-about/vogue-arts/2012/11/tribute-to-gino-marotta?refresh_ce=#ad-image234871)), Transparent PMMA stools and chairs made by Kartell: c. <http://dapurauto.com/gaske/>, d. <https://www.pinterest.com/pin/82190761922054270/?lp=true>, e. <http://www.ideacollection.net/products/Kartell-Eros-Swivel-Chair.html>.



Figure 3.7. Helen Pashgian sanding one of her transparent sculptures at the California Institute of Technology, 1970 (<https://blogs.getty.edu/pacificstandardtime/explore-the-era/archives/i130/>).

### 3.3. POLY (METHYL METHACRYLATE): PROPERTIES, STRUCTURE & DEGRADATION

PMMA is classified as a synthetic polymer, often known as plastic. Plastics are man-made materials (Holländer 2009) of organic compounds, deriving from crude oil, coal, natural gas and others (Barker 1999). Polymers are high-molecular-weight materials that consist of repeating molecular units (monomers) reacted to form long chains. Plastics are most commonly made from compounds containing carbon and incorporating other atoms, such as hydrogen and oxygen, or inorganic chemicals, i.e. silicones (Hayden *et al.* 1967). They can be modified with additives (Lee *et al.* 2003), which can be organic or inorganic, such as plasticisers, colourants, antioxidants, light stabilisers, or talc, contributing to the polymer formation, physical and chemical properties, useful lifetime and degradation.

Polymers are produced via two reaction routes, namely addition and condensation polymerisation (Brydson 1999; Lee *et al.* 2003). Addition or chain-growth polymerisation occurs when one or more types of unsaturated monomer units become attached end-to-end to form one long continuous linear chain (Shashoua 2008). Presence of double bonds is essential for this type of polymerisation to take place, enabling the bond to break and form two new bonding sites (Fig.3.8). The presence of further reaction sites enables formation of side groups and branching, which will have further impact on the polymer properties (Hayden *et al.* 1967). It often results in the formation of thermoplastic polymers such as PMMA. These can be readily deformed as they soften with increasing temperature, while upon cooling, retain the shape into which they were molded (Hayden *et al.* 1967). Condensation or step-growth polymerisation occurs when covalently cross-linked adjacent chains link through intramolecular bonds. An increase in temperature does not enable their plastic deformation (Meijer and Govaert 2005). They are

typically shaped with one or more molecular species to form molecular chains, while excluding a small molecule, usually water (Moncrieff and Weaver 1992; Shashoua 2008), at each point of reaction. This by-product is able to further react with additional monomers to ultimately give a long-chain polymer.

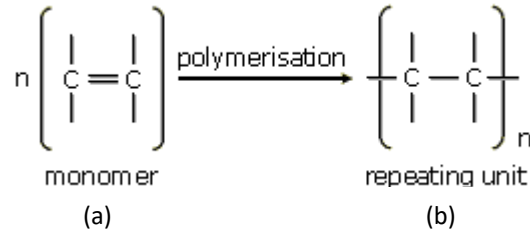


Figure 3.8. Addition polymerisation is reliant on the presence of unsaturation. The double bond between the two carbon atoms of the monomer (a) break and form two new bonding sites (b).

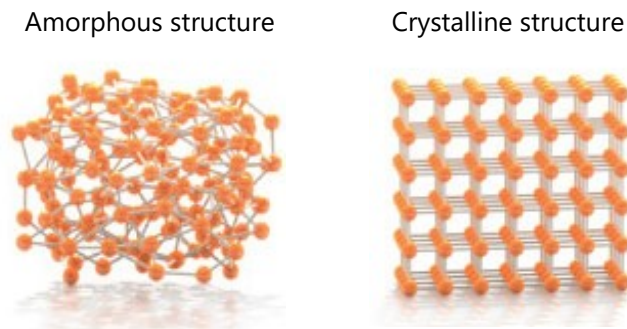


Figure 3.9. Two distinct physical structures found in polymers: amorphous and crystalline (Wager and Hoffman 2011).

Segments of polymer molecules can exist in crystalline or amorphous physical structures. Crystalline polymers, such as polyethylene or polypropylene, tend to have a regular and symmetrical chemical structure. Their chain packing produces a highly ordered atomic arrangement (Fig.3.9), which is responsible for their density being greater than in amorphous polymers (Callister and Rethwisch 2014). Their three-dimensional ordered phases (Cowie 1991) can be compared to that of a diamond (Fig.3.10) (Hayden *et al.* 1967). Highly crystalline polymers predominantly consist of small crystals (De Rosa and Auriemma 2014). On the other hand,

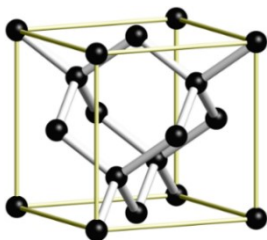


Figure 3.10. The perfect three-dimensional network of a diamond.

amorphous polymers, such as PMMA, polycarbonate and polystyrene, have an irregular structure that does not favour crystal formation. They lack order by being randomly arranged and entangled (Fig.3.9) (Shashoua 2008). The majority of polymers can exist as semi-crystalline structures possessing both crystalline and amorphous domains. These polymers take on forms known as fringed micelles, where the chains pack into ordered micelle structures and are surrounded by disordered fringes (Fig.3.11).

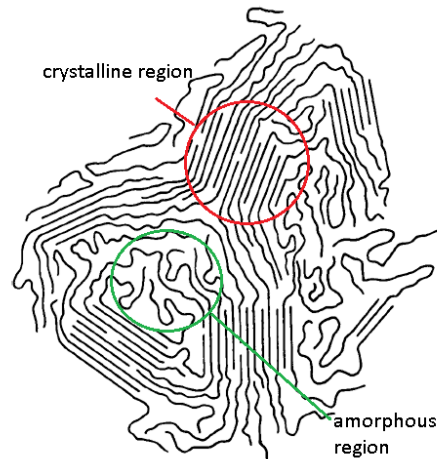


Figure 3.11. Crystalline regions of closely packed chains and amorphous regions of random tangles (Bryant 1947, p. 549).

### 3.3.1. Chemical & physical properties

<b>Poly (methyl methacrylate)</b>	
Polymer acronym	PMMA
Chemical formula	$(C_5H_8O_2)_n$
Monomer (industrial name)	Methyl methacrylate
Monomer (IUPAC name)	Methyl (2methyl propenoate)
Repeat unit structure (monomer)	$\begin{array}{c} \text{CH}_3 \\   \\ -\text{CH}_2 - \text{C} - \\   \\ \text{COOCH}_3 \end{array}$
Trade names	Plexiglas <sup>®</sup> , Perspex <sup>®</sup> , acrylic glass, Lucite <sup>®</sup> , Acrylite <sup>®</sup>

Table 3.1. Generic information about PMMA.

PMMA is a synthetic, amorphous, linear and thermoplastic homopolymer (Askeland and Fulay 2010). Its backbone consists of covalently bonded atoms of carbon, hydrogen and oxygen forming long molecular chains. Weaker secondary van der Waals bonds exist between adjacent polymer chains (Ward and Sweeney 2013). PMMA belongs to the family of acrylates and methacrylates formed on the basis of acrylic ( $\text{CH}_2 = \text{CHCOOH}$ ) and methacrylic acids ( $\text{CH}_2 = \text{C}(\text{CH}_3) \text{COOH}$ ), respectively, and their esters (Stuart 2007; Koleva 2013). Methacrylates are acrylates with an extra group attached to the alpha-carbon (Fig.3.12). The monomer of PMMA is methyl methacrylate which comprises a methylene ( $\text{CH}_2$ ) forming the backbone structure with the alpha-carbon, a methyl ( $\text{CH}_3$ ) group and an ester ( $\text{COOR}$ ) side group, both attached to the alpha-carbon (Fig.3.12). In PMMA the termination group on the ester is another methyl ( $\text{CH}_3$ ) group (Jones *et al.* 1999), which exists as a pendant on the principal chain and is also termed as a methoxycarbonyl ( $\text{COOCH}_3$ ) side group.

Addition polymerisation can be achieved via several different types of mechanism, namely free radical, bulk or suspension polymerisation (Shashoua 2008). PMMA is produced by the addition polymerisation of methyl methacrylate monomers through free radical polymerisation (Askeland and Fulay 2010; Zumdahl and Zumdahl 2010) (Fig.3.13). This is a time- and temperature-dependant process; different stages of manufacturing subject a polymer to a variety of environmental stresses and temperatures that drive the polymerisation reactions and polymer aggregates. By controlling the conditions and rate of the reactions, the degree of polymerisation can be manipulated. This is assisted by the quantity of catalyst in the polymer (Braun 2009). A typical catalyst for acrylics would be an organic peroxide, such as methyl ethyl ketone peroxide (MEKP) (Singh and Sharma 2008).

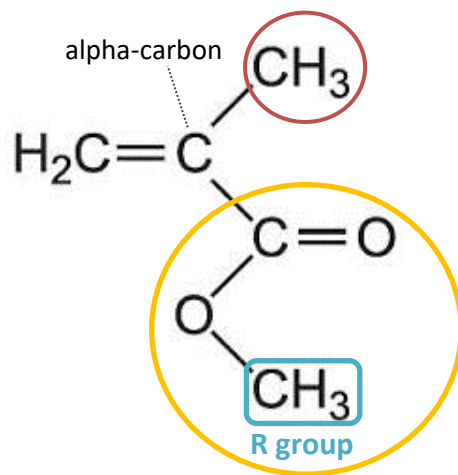


Figure 3.12. Methyl methacrylate: the monomer of PMMA. The methyl side group attached to the  $\alpha$ -carbon is highlighted in red and its ester side group (methoxycarbonyl) with a methyl as its R group (in blue) is highlighted in yellow.

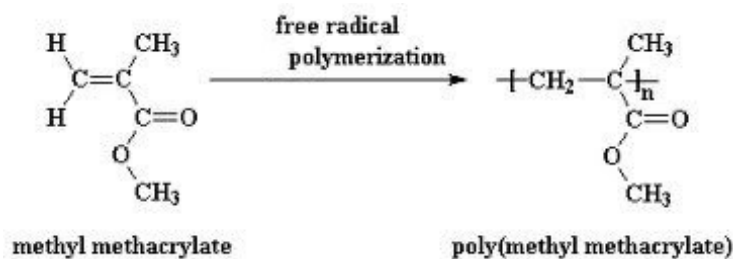


Figure 3.13. The chemical structure of PMMA monomer methyl methacrylate before (left) and after (right) free radical polymerisation (PolymerScienceLearningCenter 2019).

In the presence of catalysts, free radicals, species with an unpaired electron, are produced in an initiation reaction (Zumdahl and Zumdahl 2010, 1028). Once produced, free radicals attack the C=C double bonds present in the PMMA main chain causing them to open up (Schlenker 1969; Nicholson 2006). A new carbon radical is formed on the monomer unit, which can then go on to react with another monomer unit (Lee 2009, 57; Askeland and Fulay

2010, 501). Free radicals act as active centres for chain growth, and are continuously relocated at growing chain ends (Guerrero-Santos *et al.* 2013). The sequential auto-oxidative additions of new methyl methacrylates happen through the repetitive process of propagation.

Sometimes, free radicals can also act as inhibitors of chain growth. For the polymer to halt growing, radicals must lose their activity in chain-terminating reactions (Braun 2009). Catalysts once again play a vital role; their rate of decomposition in this process, dictated by reaction conditions, such as medium, polymer concentration, temperature etc. (Guerrero-Santos *et al.* 2013), governs the termination step. Termination (Nicholson 2006) happens when two radicals either react together to form a single bond and one reaction product (combination), or interact via hydrogen abstraction to form a saturated and an unsaturated reaction product (disproportionation) (Crighton 1988), or when two chains bond together. PMMA is known to terminate entirely by disproportionation at temperatures above 60 °C (Nicholson 2006). Termination is fundamental because it influences the degree of polymerisation and average molecular weight (Nicholson 2006, 25), and by extension, the polymer's physical properties (Cowie 1991; Ward and Sweeney 2013).

#### Amorphous regions, packing and chains

PMMA as an amorphous polymer shows no distinct structure. The distribution of chains in the PMMA matrix is primarily asystematic in the form of random coils of long chains (Fig.3.14a) (Sperling 2006). This characteristic, along with movements of single chain molecules with multiple bends, twists and kinks, presence of side groups (pendant methyls and esters) (Ionita *et al.* 2015), branching with side groups, atacticity<sup>10</sup>, and any chain disorder, all prevent PMMA from packing closely in a crystalline fashion (Peacock and Calhoun 2006; Ashby and Jones 2012; Callister and Rethwisch 2014). Amorphous polymers occasionally favour the formation of oriented batches of tangled coils. This happens when a linear polymer like PMMA is stretched (i.e. during drawing) and its chain molecules orient in the direction of the stretching, and with regards to each other, leading to an increasingly regular order, often encountered in well-oriented polycrystalline materials. This arrangement leads to a misinterpretation that relates such oriented amorphous structures of erratically interlaced chains (Fig.3.14b) with crystalline polymers (Kargin 1958).

---

<sup>10</sup> Tacticity is the stereochemical regularity or molecular conformation of the repeating units (monomers) of a polymer that has a considerable role in its properties (Huggett *et al.* 1984).

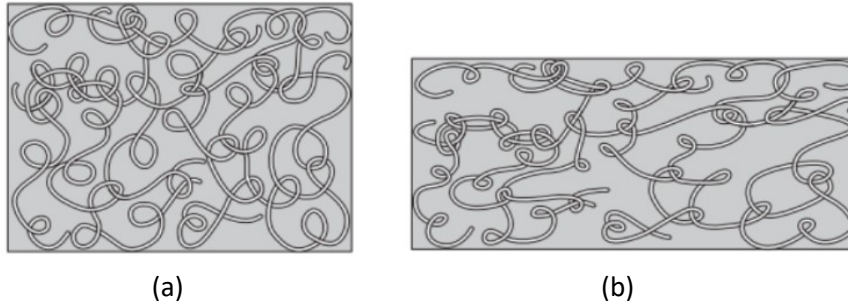


Figure 3.14. Schematic diagram of an unoriented (a) and oriented (b) amorphous polymer. (Ward and Sweeney 2013, p. 11).

The phenomenon of melting strictly occurs in crystalline structures and corresponds to the transition from solid to liquid with application of heating (Shashoua 2008, 108). The transition region is called a melting temperature ( $T_m$ ) and depends on the crystal packing, in particular the size and perfection of the crystallites (Cowie 1991, 231). Below  $T_m$  the material is solid and above  $T_m$  it shifts to a viscous liquid with a random configuration and no structure (Belfiore 2010). Equivalent to the melting temperature ( $T_m$ ) seen in crystalline polymers, is the glass transition ( $T_g$ ) in amorphous polymers (Fig.3.15). The glass transition temperature is an important thermo-physical property occurring only in amorphous viscoelastic<sup>11</sup> materials such as PMMA.  $T_g$  is the point at which the polymer experiences profound physical changes between states, corresponding to gradual transformation: at cooling one can observe a prompt increase of viscosity passing from the liquid, traversing the rubbery flow and the elasticity of glass-transition regime, to the glassy-solid state (Hayden *et al.* 1967, 130; Callister and Rethwisch 2014). PMMA as a typical viscoelastic polymer can exist in all the aforementioned states of deformation. Fig.3.16 is a typical diagram of linear-amorphous polymers and shows the relationship between the mechanical properties of PMMA and temperature. As temperature is increased from 0-200 °C the modulus falls by several orders of magnitude. In the glassy state, the modulus is large, then drops steeply in the glass-transition regime, flattening out again in the rubbery regime. Finally, in the liquid state there is a further drop in modulus. Contrary to  $T_m$ ,  $T_g$  is a function of molecular motion and not polymer structure (Cowie 1991, 257). In other words, crystalline areas melt on heating, whereas amorphous regions undergo glass transition.

<sup>11</sup> Viscoelastic materials are capable of displaying all intermediate/transitional properties between an ideal solid (Hookean elastic solid) and an ideal liquid (Newtonian viscous liquid), showing characteristics of both (Mark *et al.* 1993). This is possible due to their time- and temperature-dependent behaviour (Callister and Rethwisch 2014).



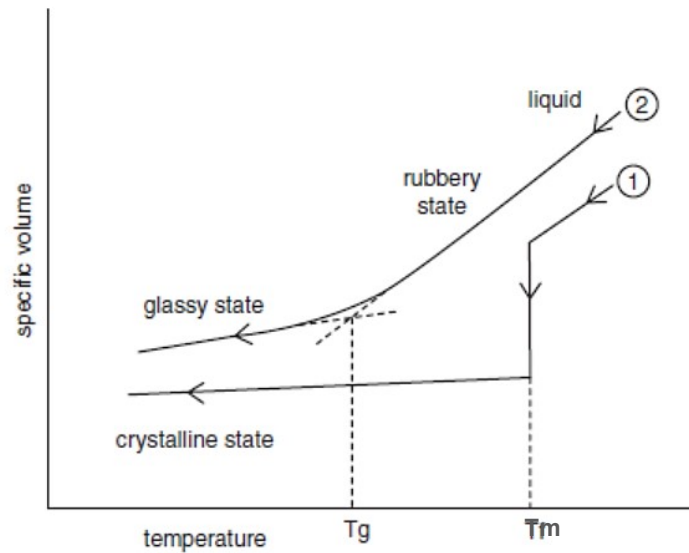


Figure 3.15. The volume of crystalline and amorphous polymers in relation to their transition regions:  $T_m$  for crystalline and  $T_g$  for amorphous (Shashoua 2008, p. 108).

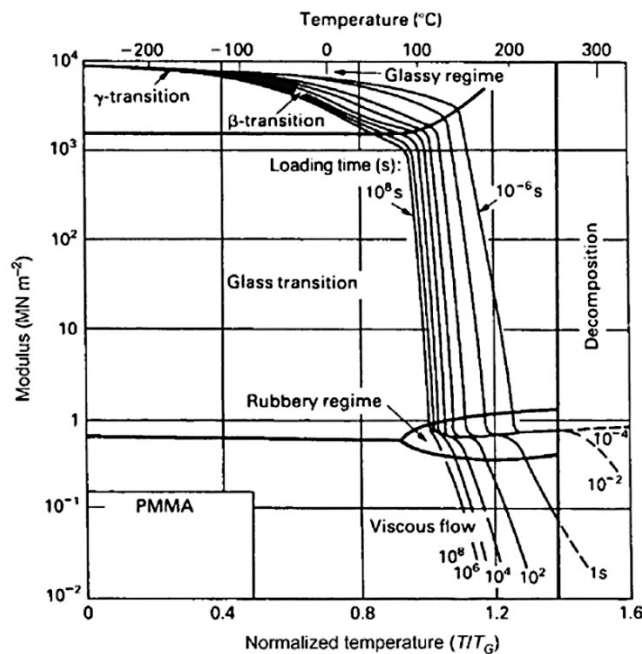


Figure 3.16. Diagram of PMMA, typical of all linear-amorphous polymers, exhibiting the distinguishable states of deformation: liquid, rubbery, elastic, glassy-solid (Ashby 2012, p. 429).

The only condition for this process is the availability of minimum molecular mobility (Martinez-Vega *et al.* 2002). Rotational movement is dependent on repeat unit structure and chemistry. The methoxycarbonyl ( $\text{COOCH}_3$ ), being a bulky side group, can restrict PMMA's chain rotation (Callister and Rethwisch 2014), which results in rising of the  $T_g$  (Read *et al.* 1990; Choudhury and Shirley 2010). The presence of side groups attached to the polymer backbone prevents the chains from rotating freely and packing closely in a crystalline fashion,

and is responsible for the tough and rigid characteristics of PMMA (Ionita *et al.* 2015). PMMA can often experience a brittle-to-ductile transition (from low to high temperatures). At the lowest temperatures in the glassy region, the material is rigid and brittle, retaining the disordered molecular structure characteristic of the liquid state (Callister and Rethwisch 2014), resembling a frozen liquid (Cowie 1991). At temperatures below  $T_g$  and upon cooling, molecular segments, requiring less energy, are confined by secondary bonding (Hayden *et al.* 1967; Ashby and Jones 2012). As temperature increases secondary bonds dissociate and entanglement points slip (Hayden *et al.* 1967). The rubbery state occurring around the  $T_g$  appears when the single covalent C—C bonds have enough energy to break intermolecular bonds and rotate enabling the chains to assume a large number of conformations without significantly disentangling (Brydson 1999). The molecules that were frozen in position below  $T_g$ , start to experience rotational and translational motions above it.

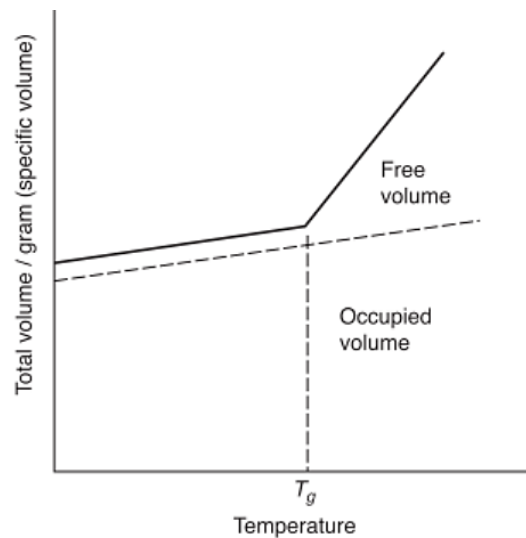


Figure 3.17. The  $T_g$  is the point of break in the slope of free volume plotted versus temperature (Ward and Sweeney 2013, p. 151).

With sufficient thermal energy, a segment is able to jump into a void within the matrix, known as free volume (Ashby and Jones 2012). A series of such jumps enables the complete polymer chain to eventually change position (Cowie 1991). It is the free volume aided by thermal energy that allows entanglement points to slip, the molecules to become free and move past one another, giving viscous flow (Hayden *et al.* 1967). Vibration of molecules causes a further increase in the free volume, resulting in accumulation of packed interlacing chains close together allowing more regions to slide (Ashby and Jones 2012). Free volume of a polymer is greatly interconnected with its  $T_g$ , and governed by molecular chains, their packing and side groups. Free volume attains a maximum value at the point of  $T_g$  (Ward and Sweeney 2013). The  $T_g$  can even be detected by plotting free volume versus temperature, and

documenting the point of break in the slope (Fig.3.17). The amount of thermal energy is also related to both the free volume and the  $T_g$ , as it activates the molecular motion of chains (Cowie 1991).

$T_g$  is not a first order transition (Cowie 1991), but a secondary, corresponding to the  $\alpha$ -relaxation. Amorphous polymers exhibit at least one or more secondary relaxations (Shaw and MacKnight 2005) denoted by the Greek letters  $\beta$ ,  $\gamma$  and  $\delta$ , in order of decreasing temperature. Comparative studies on similar polymers, using NMR and dielectric measurements, showed the  $\beta$ -relaxation to be associated with side chain motions of the ester (methoxycarbonyl) group (Read *et al.* 1990, 1205). The  $\gamma$ - and  $\delta$ -relaxations involved motion of the ester methyl group (R group) and the methyl group covalently bonded to the alpha-carbon in the main chain, respectively (Read *et al.* 1990, 1205; Ionita *et al.* 2015, 1776).

$T_g$  largely depends on the chemical nature and structural features of amorphous polymers. The main factors governing the  $T_g$  include the preparation and thermal history of the polymer, its molecular weight, tacticity, free volume, amount of thermal energy, size of side groups, bonding and additives (Brydson 1999; Belfiore 2010). Thermoplastics are commonly melt-processed by techniques that involve temperatures between 160 °C (where PMMA becomes soft) and 180 °C (where PMMA starts to flow) to ambient (Cowie 1991). This is a polymer's thermal history that affects the distribution of relaxation times and is enough to initiate physical ageing (Hutchinson 1995, 707).

The conformational characteristics of the polymer chains, such as the presence of the pendant methyl side groups, play a key role in determining PMMA's physical properties, particularly the chain stiffness,  $T_g$  and relaxation behaviour (Ionita *et al.* 2015). Understanding the  $T_g$  is vital for understanding the (thermo)physical behaviour of PMMA under study, particularly in relation to cleaning treatments. Possible risks and damage induced during cleaning (i.e. stress cracking, crazing, and diffusion of liquids) can be elucidated owing to the  $T_g$  theory presented here.

### 3.3.2. Mechanical behaviour

In this section the mechanical behaviour of linear-amorphous PMMA is presented. Mechanics are concerned with the response of a 'physical body' to external forces and determined by the relationship between applied load or force (stress) and resulting elongation or deformation (strain) (Ortíz-Rodríguez 2013; Ward and Sweeney 2013). The tensile characteristics of a polymer form one part of its mechanical behaviour and describe its response to an applied pulling force (stress). Tensile strength corresponds to the applied stress at which fracture of a polymer occurs. The difference between stress-strain and load-elongation lies in the fact that the former considers the cross-sectional area over which deformation occurs (perpendicular to the applied

force). This is beneficial because it accounts for differences in the material (i.e. composition, thickness, surface condition). This stress and its resulting strain are conventionally expressed as engineering stress and strain, defined as the ratio of the maximum applied load or magnitude of elongation to the initial cross-sectional area or length (Fig.3.18) (Peacock and Calhoun 2006, 104; Belfiore 2010, 326). From the results of a tensile test however, both a stress-strain and a load-elongation curve can be plotted.

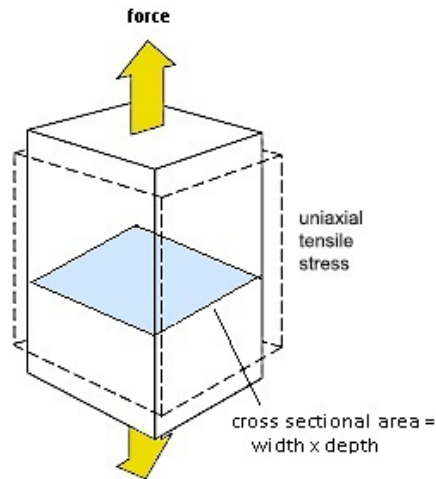


Figure 3.18. Mechanical deformation (elongation) of a solid under an applied pulling force (stress).

A perfectly elastic solid during deformation is expected to store mechanical energy obtained from external forces as elastic energy (structural memory), and upon force removal, to revert instantaneously to its original form (Chartoff *et al.* 2008). When exposing PMMA and other viscoelastic polymers to a strong and constant force, they undergo molecular rearrangement and alterations in chain conformations (Mark *et al.* 1993), in an attempt to minimise localised stresses (Foreman 1997). Viscoelastic polymers respond by breaking some of the intermolecular interactions and disentanglements, thus leaving the material weaker and more susceptible to stress (Peacock and Calhoun 2006).

### Stress and strain

Stress-strain curves are schematically presented for each of the three typically different types of mechanical behaviour found in polymers (Fig.3.19) (Chartoff *et al.* 2008). For PMMA at room temperature below  $T_g$ , curve A is relevant. The stress-strain relationship of glassy polymers is linear, which means that strain increases with increasing stress, and reaches a maximum at fracture (Hayden *et al.* 1967). Curve A illustrates the stress-strain behaviour of all amorphous materials in their glassy/solid state (Aguilar-Vega 2013), where deformation is elastic, and fracture happens without prior noticeable change in the rate of elongation. The fracture is completely brittle and happens abruptly. Some degree of non-recoverable plastic deformation may precede fracture (Bowden and Jukes 1972), but generally the extension up to the point of

failure is elastic, thus largely reversible. Elastic deformation is instantaneous, which means that total deformation occurs the instant the stress is applied, and upon release of the external stress, the deformation is totally recovered (Callister and Rethwisch 2014). The ultimate load strength coincides with the tensile strength, that is, the stress at which fracture occurs (Hayden *et al.* 1967, 3). At the glass transition region, where PMMA is rubbery, the typical stress-strain curve B shows an initial elastic behaviour, followed by plastic deformation and finally fracture, occurring at the ultimate load strength. The stress point at which the material begins to deform plastically, becomes visible due to a deviation in the curve, defined as the yield point (Hayden *et al.* 1967). In curve C the deformation is totally elastic, behaviour exhibited only by elastomers (Callister and Rethwisch 2014). Given that PMMA is viscoelastic, it can display both brittle (curve A) and plastic (curve B) behaviours (deformation) when in different temperature ranges below and at the  $T_g$  region. In other words, deformation can only take place when PMMA is in its glassy/solid or rubbery states.

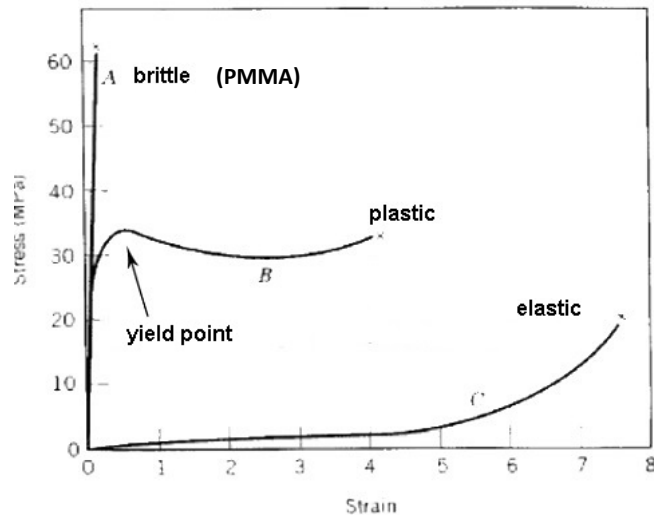
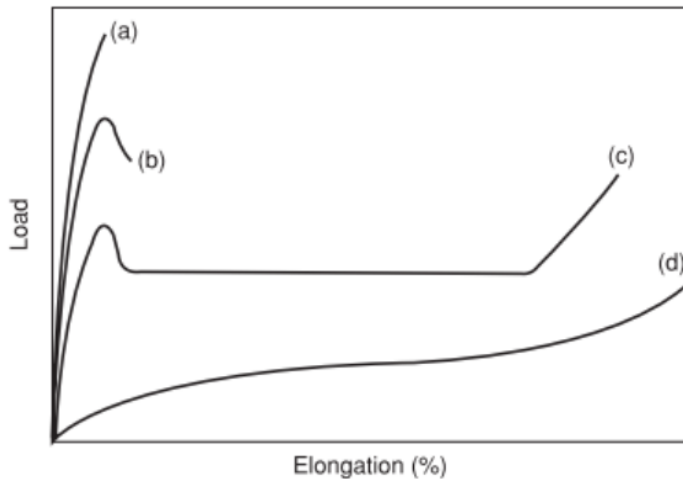


Figure 3.19. Stress-strain curves displaying three typically different types of stress-strain polymer behaviour: A. brittle, B. plastic and C. highly elastic (Callister and Rethwisch 2014, p. 571).

### Load and elongation

Load-elongation curves are schematically presented for each of the four different regions of mechanical behaviour in a thermoplastic polymer (Fig.3.20). The data was acquired at a constant strain rate with increasing temperature (Ward and Sweeney 2013). Curve (a) depicts the characteristic behaviour of polymers in their glassy/solid state. At low temperatures below  $T_g$ , the load rises linearly with increasing elongation, until it fails at its maximum load at comparatively low strains (< 10 %). In an intermediate temperature range below  $T_g$ , the load-deformation relationship characteristic of a ductile polymer is shown in curve (b). Here, there is a load maximum, which coincides with the yield point and is followed by rupture at a lower

stress (Ward and Sweeney 2013). At higher temperatures, still below  $T_g$ , curve (c) displays the conventional load-elongation curve with a similar yield point to curve (b), and a subsequent decrease in conventional stress. With a constant application of strain, the load maintains a constant level at which deformations of the order of 300-1000 % are reached. With a further increase in strain, a neck is formed and eventually, the load begins to rise again and finally fracture occurs (Ward and Sweeney 2013). At high temperatures over  $T_g$ , curve (d) displays load rising to the breaking point with a sigmoidal relationship to the elongation, and rupture occurring at very high strains.



*Figure 3.20. Load-elongation curves displaying a typical polymer mechanical behaviour at four different temperatures: (a) brittle fracture, (b) ductile failure, (c) necking and cold-drawing and (d) rubbery behaviour (Ward and Sweeney 2013, p. 380).*

### 3.3.3. Degradation

The most common mechanisms taking place during chemical degradation are crosslinking and bond cleavage/chain scission, which result in conflicting phenomena: the former links bonds of one polymer to another, thus increasing the molecular weight of the polymer, whereas the latter causes chains to break down leading to polymer reduction (Wiles 1993). These phenomena often occur simultaneously (Wypych 2013), and can either take place in the main chain (backbone) or the side groups of polymer molecules (Lister and Renshaw 2004). The main focus is on the chemical degradation and physical ageing of PMMA in relation to UV radiation and liquid environments. That is because PMMA undergoes a number of degradative reactions during its lifetime through natural ageing and during contact with liquids/gases either in the form of environmental moisture or as a result of wet cleaning (Table 3.2).

degradation of PMMA			
	factor	process	effect
chemical degradation	<i>UV radiation</i>	free radical depolymerization	weight loss
	<i>oxygen</i>	free radical depolymerization	initiation of further reactions
	<i>water</i>	hydrolysis	weight loss
	<i>high temperature</i>	depolymerization	weight loss, reduction of mechanical properties
physical ageing	<i>liquid environment</i>	absorption, diffusion	swelling, dissolution/extraction, cracking or/and crazing

*Table 3.2. Main factors (degradation agents) causing either chemical degradation or physical ageing to PMMA, their processes and chemical and physical effects.*

### 3.3.3.1. Physical ageing

Physical ageing of an organic polymer is a very slow, but continuous process of gradual reorganisation towards an equilibrium state (Ribelles and Calleja 1984; Mijović *et al.* 1994; Mittermeier *et al.* 2015). It depends on: molecular weight, molecular form and structure, intermolecular forces, free volume and presence of plasticisers, as well as external factors related to time (Muzeau *et al.* 1994), thermal changes and mechanical stresses (McGlinchey 1993). Although physical ageing is thermodynamically-driven (Wiles 1993, 106), involving readily thermo-reversible changes in the effected polymer, these are only reversible up to a certain point (Struik 1977; Hutchinson 1995). The temperature range over which physical ageing occurs can be quite broad (Wiles 1993), but is restricted to processes taking place in the glassy state of amorphous polymers below the  $T_g$  (Etienne and David 2007). Specifically, it occurs between the  $T_g$  and the next lower secondary transition defined as  $T\beta$  (Struik 1977; McGlinchey 1993). At an elevated temperature (in the rubbery state), the structure of the material, as determined by molecular conformations, is in thermodynamic equilibrium. Below  $T_g$ , and as the temperature is cooled, the conformational changes (vibrations and rotations of molecules) needed to maintain an equilibrium structure are significantly restricted by reduced mobility. There is still sufficient molecular mobility for structural changes in the glassy state, which take place towards a slow and gradual approach to equilibrium (Maxwell *et al.* 2005). This process is physical ageing expressed through changes in the material properties (Struik 1977).

Physical ageing may affect any polymer properties related to its morphology (Ward and Sweeney 2013), such as chain length (molecular weight) and flexibility, extent of molecular motion, packing (degree of crystallinity), degree of orientation, and rotational isomerism (tacticity or else distribution of chains). To give an example, the property of PMMA to lack chain orientation and have a random chain distribution allows visible radiation to be

transmitted and refracted and becomes largely responsible for the material's optical clarity (Brydson 1999; Bodurov *et al.* 2013). So, even the smallest change in the chain distribution can in theory impact on the material's transparency. In the same way, changes instigated by the viscoelastic behaviour (structural relaxations) of glassy amorphous polymers, as all temperature-dependent properties that can change abruptly at the  $T_g$ , contribute to physical ageing (Cowie 1991; Etienne and David 2007). In addition to mechanical relaxation phenomena, given that physical ageing affects the segmental mobility of molecules, it eventually affects chemical degradation too.

#### Liquid environments and solvent diffusion

Physical ageing has a direct effect on the rheological behaviour of most polymers, typically observed as changes in the free volume (Struik 1977; Zhao *et al.* 2008). The low degree of molecular packing, attributed to PMMA's amorphous nature, implies that there is empty space between PMMA molecules. This is often described as sub-microscopic cavities in its matrix, and along with its lack of order, render PMMA very vulnerable to permeability to liquids (Shashoua 2008). In fact, liquids are soluble only in amorphous areas and their polymerisation develops more freely in these cavities than in denser regions (Bobalek *et al.* 1959; Affolter 2015). Penetrant liquid molecules replace polymer-polymer with polymer-solvent interactions (McGlinchey 1993) and cause a shift in the relaxation time and  $T_g$  through plasticisation effects. During diffusion, the activation energy of small molecules, i.e. water, causes a segment of the PMMA chain to move. As earlier explained, molecule movement/vibration causes a further increase in the free volume (Ashby and Jones 2012), allowing diffusant molecules to pass (Struik 1977; Dickens *et al.* 1984).

The presence of a low-molecular-weight solvent, equal to or smaller in size than the methyl methacrylate monomer, constitutes a chemical environment that aggravates PMMA's physical properties, without the involvement of any chemical reaction, i.e. chain scission. The solvent affects PMMA's mechanical behaviour, through a characteristic viscoelastic diffusional mechanism occurring via the free volume (Bogdanova *et al.* 1986). Diffusion shows an increased rate below  $T_g$ , in the nonequilibrium glassy state (Belfiore 2010, 58). Solvent influence is perceived as changes in structure and properties of the surface layers, not so much the bulk (Bogdanova *et al.* 1986).

Several factors affect diffusion of low-molecular-weight substances through the amorphous PMMA (McGlinchey 1993; Affolter 2015). To begin with, aspects internal to the polymer: the physical state and structure of the polymer affects the extent of packing of the chains, their mobility and extent of movement between them, all of which determine the free



volume. The less restricted the polymer chain segments are, the higher the diffusion rate. The diffusing substance also plays an important role in the process: its molecular weight, shape and quantity, as well as its chemical interaction with PMMA (i.e. polarities), all affect its ability to diffuse and produce free volume in the material.

Environmental Stress Cracking

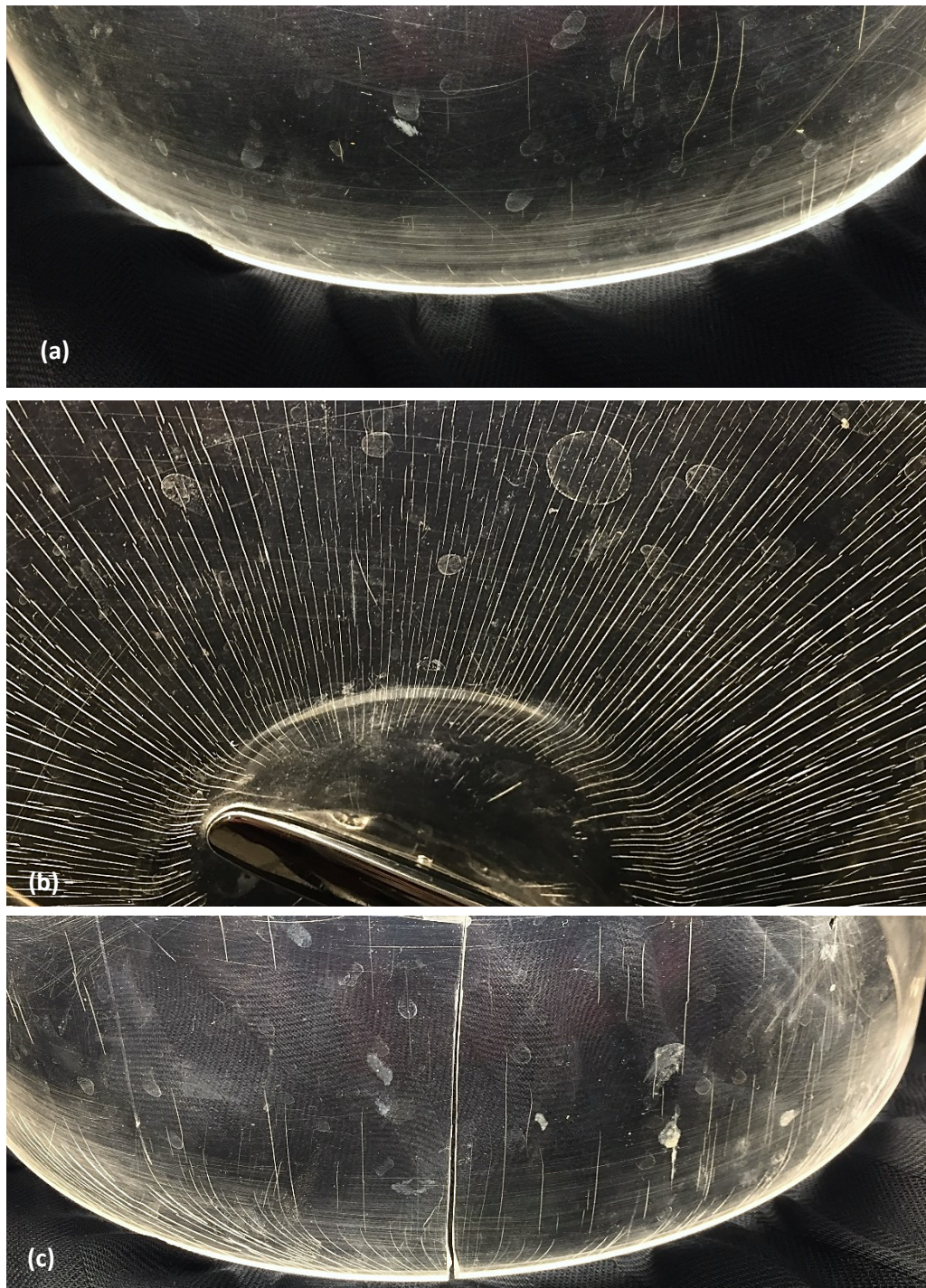


*Figure 3.21. PMMA dome-cover of cake plate with visible scratches on its surface (a), parallel microcrazes (b) and crack formation (c).*

The presence of an active liquid on amorphous polymers leads to one of the most common causes of brittle fracture (Akhurst 2008), the physical phenomenon of Environmental Stress Cracking (ESC). PMMA is particularly susceptible to ESC (Broughton *et al.* 2005) due to its relatively open structure. The more chemically compatible the liquid to the PMMA, that is the closer their solubility parameters, the more susceptible the polymer is to ESC (Arnold 1998). During ESC the diffusion of liquids, such as water, into the material causes plasticisation, a localised reduction in yield strength. This means that craze formation can happen at a much lower stress than if it would be in contact with air (Burchill and Stacewicz 1982; Malacarne-Zanon *et al.* 2009). On transparent PMMA, ESC starts with the formation of fine interconnecting crazes (Fig.3.21b). Due to them having a different refractive index, they are especially visible (Lampman 2003) and the material loses its transparency becoming opalescent (Passaglia 1987) and resembling white crystalline structures (Akhurst 2008).



*Figure 3.22. Transparent PMMA bracelet exhibiting crack formation (Laganà and van Oosten 2011, 7).*



*Figure 3.23. Transparent PMMA architectural model exhibited at the National Museum of the 21st Century Arts (MAXXI) in Rome, showing cracks.*

Crazes initiate at points of stress localisation, such as scratches on the surface (Fig.3.21a), structural defects, voids or impurities in the bulk (Michler 1989). They are fine fibrils able to take shapes (circular, shallow or equal thickness across) (Donth and Michler 1989) and initiate in the interior of the material. Crazes allow an easy diffusion path accelerated in the presence of a liquid (Arnold 1998). These structures propagate, and once parallel microcrazes form (Fig.3.21b), they lead to crack formation (Fig.3.21c, 3.22, 3.23) that ultimately causes PMMA to split (Quye and Keneghan 1999). Attention however is needed to distinguish between the phenomena of crazing and cracking (Fig.3.24), both of which can cause failure of polymeric glasses (Andrews and Bevan 1972). Cracking is always preceded by crazing, and also initiated in heterogeneities of a craze (Passaglia 1987). Environmental factors, such as moisture, induce a plasticising action to the material (Broughton *et al.* 2005), which can sometimes act favourably and others not; on one hand, moisture can, through plasticisation (softening), relieve residual stresses produced during the curing process (Maxwell *et al.* 2005). On the other hand, it can increase intermolecular free volume and lead to weakening or breaking of bonds (Levine *et al.* 1988), which accelerate the craze formation process (Broughton *et al.* 2005).

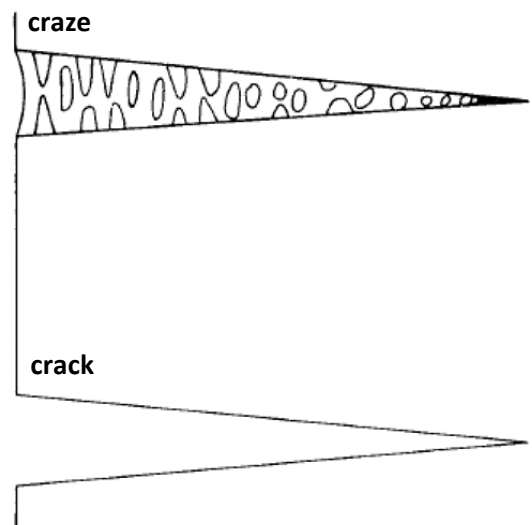


Figure 3.24. Structures of a craze and a crack in comparison (Andrews and Bevan 1972, p. 337).

### 3.3.3.2. Chemical degradation

Chemical degradation takes place mainly near the polymer surface (Dickens *et al.* 1986) and as opposed to physical ageing, it is energy-driven (Chiantore and Rava 2012). The overall chemical degradation process involves a change of the polymer properties due to a chemical reaction. It normally involves a relatively long temperature-sensitive induction period, during which little degradation can be visually detected (Feller 1994a; Broughton *et al.* 2005). Chemical degradation can be accelerated by physical ageing, which may affect the covalent bond structure

(McGlinchey 1993) and consequently the molecular weight and segmental mobility of the polymer. Such alterations can result in irreversible changes in the polymer's physical-mechanical properties (Qayyum and White 1987; Hutchinson 1995; Wypych 2013). Changes to the chemical structure can also be caused by factors external to the material, such as environmental factors. The main weathering agents initiating or promoting chemical degradation in organic polymers are sunlight, especially UV radiation, temperature, oxygen and moisture in various forms (Saunders and Kirby 2001; Nicholson 2006). Degradation can be assisted by more than one agent, in which case their synergistic effects are more severe (Feller 1994b).

### UV radiation

For PMMA the most important reaction leading to decomposition is induced by the UV portion (290-400 nm) of the radiation spectrum (Singh and Sharma 2008). The bands of absorption are characteristic of a material (Wypych and Faulkner 1999) and PMMA is capable of absorbing energy at certain particularly damaging wavelengths (further discussed in Chapter 5). UV radiation can cause changes in the physical properties of plastics, such as loss of mechanical properties, embrittlement and crack formation, as well as in the optical properties, such as loss of gloss and yellowing.

Photochemical reactions have no activation energy of their own (Wiles 1993). They are initiated by solar radiation, which results in the absorption of UV radiation by chromophores within the molecules and the activation of highly reactive species (Broughton *et al.* 2005). Chromophores are light-absorbing, colour-imparting functional groups (Schaeffer 2001; Chiantore and Rava 2012) that act as the principal initiators of degradation in acrylic polymers (Crighton 1988). They might be incorporated intentionally during manufacture, be present in additives as colourants, be part of the molecular structure of the polymer, or contained in small quantities of impurities (Cooper 2012). The most important chromophore in PMMA is its pendant ester side-group ( $\text{COOCH}_3$ ); the conjugated double bonds between the carbon and the oxygen in the methoxycarbonyl group (see Fig.3.12) (Dickens *et al.* 1984; Feller 1994a) break upon UV absorbance, producing methoxy and carbomethoxy radicals (Kambe *et al.* 1977). These radicals define the wavelength to which the material is susceptible (Peacock and Calhoun 2006).

UV absorption results in reactions related to the mechanism of reverse polymerisation (depolymerisation) (Grassie and Melville 1947), a branching chain reaction involving the formation of free radicals ( $\text{R}\bullet$ ). Radicals are highly reactive, neutral species of unpaired electrons formed by chain scission of a double bond. Free radicals tend to form more stable species and be chemically self-perpetuating in a hydrocarbon matrix (Wiles 1993). They are products of homolytical breakage of chemical bonds by energy introduced in the polymer during fabrication

or use (Wiles 1993). Depending on the bond breaking, radicals can cause crosslinking or chain shortening by forming two shorter molecules (Lister and Renshaw 2004). With the breaking of even a small fraction of the bonds per molecule, the properties might be lost, unless the scission occurs near the very ends of the chains (Wiles 1993). It is possible for the radical formed to oxidise, initiating a chain of further photooxidative reactions. The incorporation of photo-initiators and photo-accelerators can be used to regulate the wavelength sensitivity, and thus, the rates of degradation.

Initiation of the reverse polymerisation is caused by the absorption of radiation (Feller 1994a) followed by, either transfer of this energy through heat dispersion or radiation emission to another molecule, or direct scission of PMMA bonds. PMMA photodegradation can take place through direct scission of C–C or C–H bonds in the main chain or the ester side chain (Torikai *et al.* 1990; Mitsuoka *et al.* 1993). Since the atoms in its matrix are vulnerable to random scission mechanisms by radiation energy input even at room temperature, PMMA is very susceptible to photolysis (Kambe *et al.* 1977). A distinction must be made between photolytic degradation, that is breakdown in absence of oxygen, and photooxidative degradation, in the presence of oxygen (Schaeffer 2001). Photodegradation of PMMA in the absence of oxygen has been thoroughly studied by Gupta *et al.* (1980). Some reports have concluded that oxygen may have no effect or even a retarding one on PMMA. Dickens *et al.* (1984) showed that both reactions, in the presence and absence of oxygen, cause degradation of PMMA.

It has been reported that free radicals which consume oxygen, absorb the shorter wavelengths in the solar spectrum, in the region of 300-350 nm, more than the original PMMA material does (Dickens *et al.* 1986). It has been demonstrated that the more degraded PMMA specimens displayed a stronger absorption in the UV region (Dickens *et al.* 1984; Nagai *et al.* 2005). The additional absorption did not produce significant amounts of free radicals. As degradation proceeds to the bulk of the material, generation of free radicals decreases due to lack of radiation (Dickens *et al.* 1986). In such a glassy matrix of PMMA, radicals are relatively immobile, favouring termination reactions between radicals generated in the same initiation step, or their oxygenated derivatives, or with a radical derived from some low-molecular-weight impurity (Dickens *et al.* 1984).

### Water

Hydrolysis is another chemical reaction that may lead to the degradation of PMMA, during which bonds break with the addition of water molecules. Water is not as reactive as oxygen, but the PMMA ester side group is inherently susceptible to it (Wiles 1993; Holländer 2009). Hydrolytic reactions are promoted in PMMA due to the presence of the ester side group (Affolter 2015). Esters being polar groups, are inherently susceptible and prone to absorb water quantities (Van

Oosten 2002). PMMA has the capacity of absorbing this water due to being amorphous (Affolter 2015). Hydrolysis can result in a reduction in molecular weight and loss of mechanical properties (Affolter 2015). This will be further discussed in detail in Chapter 7.1.2, where empirical studies examine the immersion of PMMA in water for 30 days.

### Temperature

Decomposition due to thermal reactions follows the free radical mechanisms (depolymerisation reaction) earlier discussed. These are largely based on the presence of chromophores, which, upon heating of the polymer, are required for energy absorption and initiation of thermal degradation (Dickens *et al.* 1986). See Appendix A for primary PMMA photooxidation routes relating to the movement of free radicals. Only in this case, chain scission is initiated by thermal energy, also produced by UV radiation. Contrary to photochemical reactions that are near-surface reactions, thermal reactions may begin from the surface but can propagate throughout the polymer bulk. At elevated temperatures, addition polymers like PMMA can be easily broken down and converted to almost complete monomer units. The mechanism consists of two distinct reactions, the random scission of bonds and the scission of chain-ends of C–C bonds (unzipping). These mechanisms are known to happen simultaneously, one causing a reduction in the molecular weight and the other generating volatile products, respectively. Side group elimination of the methacrylate is also possible (Cooper 2012). Unzipping starts from one end of the chain, and is better described as the opposite of the propagation step in addition polymerisation (Peacock and Calhoun 2006; Singh and Sharma 2008).

This chapter reviewed the historical development and application of plastics and PMMA in industry and art and design, as well as the degradation of the physical and chemical structure of PMMA. It focused on its interaction with liquids and solvents, and on the effects of UV radiation. Overall, this chapter aimed to help the reader understand the material under study and prepare them to be introduced in the discourse of gel cleaning presented in the following chapter. Gel chemistry, advantages in the use of gels and complications that may arise during a treatment are examined in relation to the PMMA.

## **Chapter 4. CLEANING OF POLY (METHYL METHACRYLATE)**

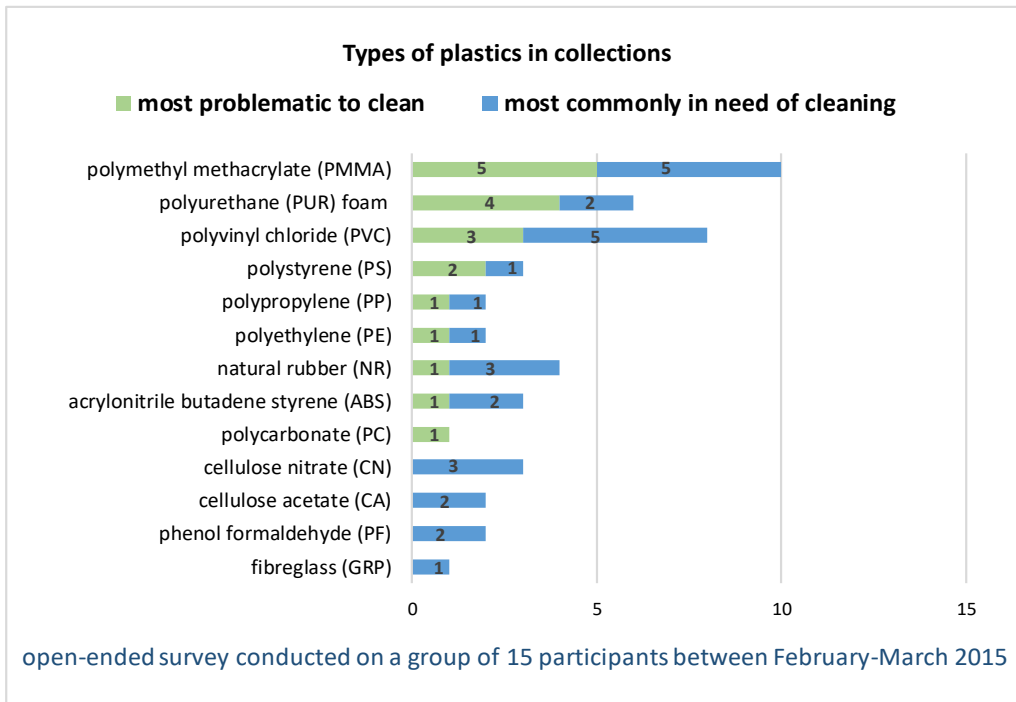
---

This chapter presents the findings of the open-ended survey canvassing the expert opinion of conservators of modern materials and plastics, that assisted in identifying the problems and establishing conservators' priorities in the cleaning of plastic museum objects. The chapter then moves on to review recent developments and current ideas in the industrial and conservation cleaning of plastics and PMMA, as well as the use of a variety of gels in the cultural heritage sector. Studies pioneering the use of gel systems for treating cultural heritage have increasingly been published, but with a very limited focus on plastics, and even more limited focus on acrylic surfaces. A large body of work has been presented and subsequently published in the recent *Gels in the Conservation of Art* conference in London in 2017, organised by Tate and International Academic Projects. Amongst seventy-five research papers, only the one presented by the author focused on cleaning three-dimensional plastics.

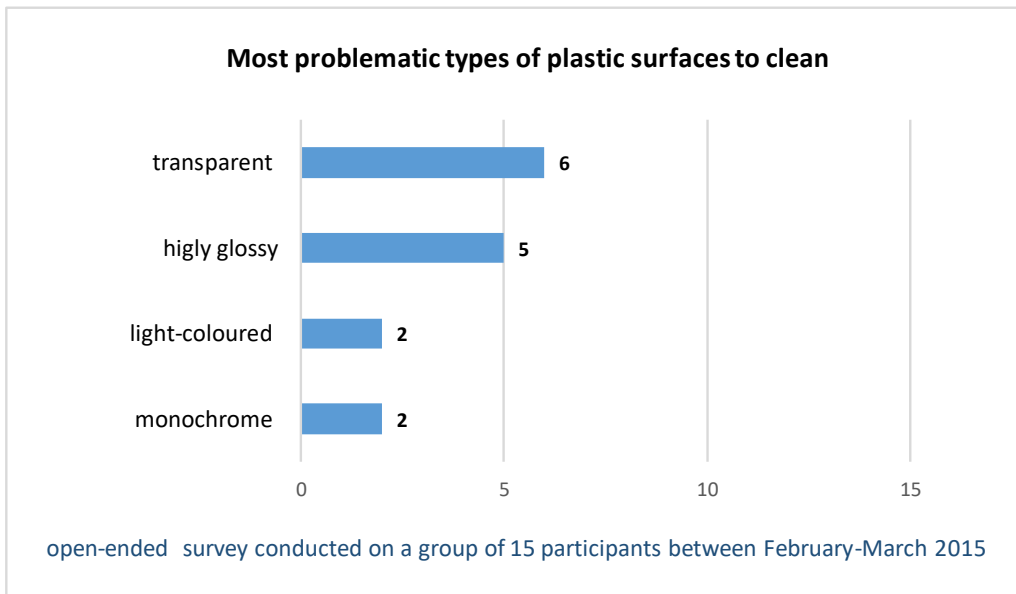
### **4.1. OPEN-ENDED SURVEY OF EXPERTS OPINIONS**

Respondents of the survey (see Chapter 2.1 for details and Appendix B for questionnaire format and answers) were asked to offer their expert opinion through a series of five open-ended questions. Questions were broad and non-limiting allowing conservators to answer freely to the extent they wished to do so. Analysis of findings was both quantitative (i.e. based on recurrent themes) and qualitative. The responses led to the formation of four main topics: i) plastics that more commonly require cleaning, ii) plastics that are more problematic/harder to clean, iii) types of plastic surfaces that are more problematic to clean and iv) types of dirt that are more commonly encountered on plastics and require removal.

Overall, twelve plastics were mentioned as more commonly in need of cleaning. Eight out of them, plus one that was not listed as commonly in need of cleaning, were cited as more problematic/harder to clean too (see Graph 4.1). PMMA and PVC were the most frequently cited as more commonly in need of cleaning, with five mentions out of fifteen each, followed by natural rubber and cellulose nitrate with three mentions out of fifteen each. PMMA, PUR foam and PVC were the most cited as more problematic to clean, with five, four and three mentions respectively. Respondents listed four types of surfaces as more problematic to clean, with transparent and highly glossy being the most frequently mentioned (six and five mentions out of fifteen respectively), followed by light-colored and monochrome surfaces (two and one mentions out of fifteen respectively) (see Graph 4.2). Regarding the most common types of dirt encountered on plastics, respondents cited more often loose dust, followed by adhesive tape/label and oily fingerprints (see Graph 4.3). Answers also included plasticizer, stains, waxy products and pencil/pen marks.

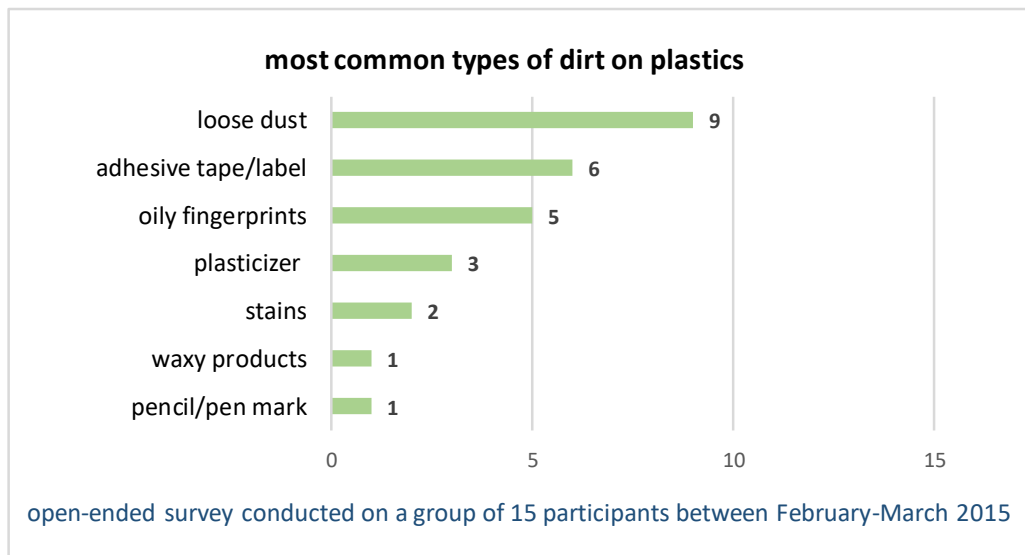


*Graph 4.1. Plastics identified as more commonly requiring cleaning (blue) and as more problematic/harder to clean (green) in an open-ended survey of conservators of modern materials and plastics.*



*Graph 4.2. Types of plastic surfaces mentioned as more problematic to clean in an open-ended survey of conservators of modern materials and plastics.*





Graph 4.3. Types of dirt mentioned as more commonly encountered on plastics in an open-ended survey of conservators of modern materials and plastics.

Findings revealed that one in three respondents identified PMMA both as more commonly in need of cleaning and more challenging to clean, among plastics in collections they have had experience with. Transparent surfaces were identified by two in five respondents as the most problematic plastic surfaces to clean, followed closely by highly polished surfaces, identified by one in three respondents. The literature supported that transparency in plastics presents an inherent difficulty in cleaning, mainly because surfaces readily show modifications (Shashoua 2012b). References also maintained the concerns of surveyed conservators about cleaning highly polished surfaces, which as stated ‘call for a very low tolerance to physical damage’ (Rivenc *et al.* 2011; Dei 2013). It was thus established that transparent or/and highly polished surfaces are almost impossible to clean without instigating visual change, and the importance of being able to clean such surfaces was highlighted.

Findings also demonstrated that three in five respondents indicated loose dust as the most common dirt type encountered on plastic surfaces in collections. Adhesive remains from use of tapes/labels and oily fingerprints followed closely, with six and five mentions out of fifteen, respectively. Following the results of the survey and discussion with conservators, it was decided to combine two of the common types of dirt, the loose dust and the oily fingerprints, and formulate a dirt of greasy and soiled nature for the cleaning experiments in this research. Synthetic sebum soil was prepared to mimic a combination of human fingerprints from inappropriate handling with deposited surface loose dust, by synthesising synthetic sebum based on natural oils and carbon black pigment. The second dirt type to use in the experiments was the second most cited response, adhesive tape/label. It was selected as

representative of adhesive residues from labels, packaging and sticky tapes commonly remaining on objects after storage and transportation.

The results of this survey, although limited in sample size, verified the existing literature and were confirmed by further consultation with conservation professionals. From archival research it became apparent that the majority of PMMA in collections is found as transparent and highly polished museum objects. Bearing all characteristics described as problematic in this survey, PMMA was identified as one of the most problematic plastics to clean.

#### **4.2. INDUSTRIAL & CONSERVATION CLEANING OF PLASTICS**

The vast range of plastics available and the fact that cleaning can cause irreversible damage, have resulted in the absence of a universal cleaning protocol or standards available for treating plastic objects (Fricker 201). Cleaning of plastics in museums has been carried out with conservation cleaning treatments commonly employed on other cultural heritage materials, and sometimes, even with industrial methods (Buys and Oakley 1993). Current guidelines available suggest the use of dry or wet treatments. Dry cleaning with cotton swabs, sponges and different types of cloths (spectacles, commercial, cotton, microfibre) is commonly advised for removal of loose surface dirt/soiling (Morales-Muñoz 2010; Balcar *et al.* 2012; Plastics Historical Society 2015). In some occasions, the use of dry cloths is avoided due to the potential of having dirt particles settled/held on the treated surface as a result of electrostatic charging during cleaning (Waentig 2008b). The Canadian Conservation Institute recommends mechanical cleaning by brushing, wiping or vacuuming, when possible (Williams 2019).

Wet cleaning is generally not encouraged when it comes to plastics (Plastics Historical Society 2015; Williams 2019), and use of solvents has been disapproved (Shashoua 2008; Plastics Historical Society 2015; Williams 2019). However, some persistent types of soiling and adhesive remains require more interventive solutions. Dampening of a cloth or cotton swab with deionised water, while strictly avoiding wetting, is acceptable for plastics that are invulnerable to hydrolysis (i.e. not cellulose esters) (Fricker 2016). In some cases, surface dirt has been removed with surfactants and detergents, and subsequently rinsed with cotton swabs dampened in deionised water (Van Oosten and Huys 2005; Morales-Muñoz 2010). A wide range of cleaning agents, including anionic and non-ionic detergents and organic solvents, such as Dehypon LS45, Orvus WA Paste, synthetic saliva and tri-ammonium citrate, are recommended in the POPART project (Balcar *et al.* 2012). Cleaning agents suggested by POPART are discussed later.

Very limited published studies have used gels for cleaning plastic works of art. Van Oosten and Huys (2005) used Carbopol 980/Ethomeen C-25 with ethanol applied for five hours

to soften and remove adhesive remains from PVC, while Bollard *et al.* (2011) found the use of Pemulen TR-2 emulsions satisfactory for cleaning PVC – discussed in more detail later. Carbopol 980/Ethomeen C-25 was applied with a spatula and removed with cotton swabs with ethanol (Van Oosten and Huys 2005).

As recognised in Chapters 1 and 3, the transparency, glossiness and reflective qualities of PMMA are crucial for the art works and objects. In some cases, compromises are inevitably made and the need for more aggressive solutions is raised to maintain the works' pristine appearance (Waentig 2008; Rivenc 2016). Statements by California-based Minimalist artists De Wain Valentine, Helen Pashgian and Craig Kauffman (see Chapter 1.2 and 3.2) indicate that small damages easily lead to the invasive sanding and polishing of art pieces. The need to respect the artists' intent that their works must at all times look pristine dictates the routine re-sanding and re-polishing of surfaces to maintain their pristine condition (Learner *et al.* 2011).

Industrial cleaning is commonly carried out using commercial polishes containing abrasive particles suspended in a solvent or a silicone polymer. The former physically smooths the scratches, whereas the latter fills them with silicone and imparts high gloss. Use of silicone polishes is irreversible thus impossible to remove/re-treat (Shashoua 2008). Commercial polishes can be applied with polishing cloths or buffer grinding wheels. Polishing and sanding can also be carried out with automobile sanding tools, such as the body fender grinder employed by De Wain Valentine (Learner *et al.* 2011). Rough sanding is typically carried out with electric tools to impart the initial shape, followed by hand polishing with different grades of sandpaper to refine the polished surface and give the final gloss (Learner *et al.* 2011; Rivenc *et al.* 2011). A subsequent dilemma remains whether this type of polishing should be carried out with technologies used in the time of the artwork's creation or with current materials and methods.

#### **4.2.1. Review of cleaning poly (methyl methacrylate)**

A lot of the cleaning tools and methods discussed in this chapter, are general, all-purpose guidelines for plastics in museum collections. However, it is important to focus on individual plastics, as the effect of treatments and agents is highly dependent on the nature of each material (Fricker 2016). Examples of current approaches to cleaning PMMA presented here, were retrieved from the limited pool of publications available regarding this topic.

The POPART project concluded that the least damaging and more efficient tools and agents for PMMA are the microfibre, synthetic spectacles and cotton cloths, anionic and non-ionic surfactants (Balcar *et al.* 2012). Fricker (2016) tested the aqueous agents recommended by POPART and confirmed that Orvus WA Paste as an anionic surfactant and Dehypon LS45 as

a non-ionic surfactant caused the least damage and successfully removed artificial soil. It is worth mentioning that the presence of residual surfactant was documented on the PMMA post-treatment (Fricker 2016). The use of cloths requires consideration, because not all cloths are equally effective with different types of dirt/soil (Balcar *et al.* 2012; Fricker 2016). Nilsen *et al.* (2002) observed scratching and pitting on PMMA after cleaning with microfibre cloths. Waentig (2008b) who investigated the cleaning of a transparent PMMA violin, removed surface dust with a microfibre cloth dampened with a non-ionic surfactant/deionised water solution and rinsed with a cloth dampened with deionised water. Nagy *et al.* (2011) mechanically removed adhesive from PMMA sheets of a Donald Judd work, using scalpels. A more detailed review of cleaning agents, with a particular focus on organic solvents, is presented in the following section.

#### **4.2.2. The use of cleaning agents on poly (methyl methacrylate)**

Solvents traditionally used for the removal of discoloured varnishes were considered for the purposes of this research, because such varnishes are of oily nature, similar to the synthetic sebum soil applied on samples in the later stages of the cleaning experiments. Systematic or published studies suggesting the use of suitable solvents for cleaning PMMA were not available at the time of this study. Some conservators totally reject the use of solvents because acrylics are highly sensitive to them (Nagy *et al.* 2011). As discussed in Chapter 3, polymer glasses such as PMMA, are especially sensitive to damage (i.e. cracking, crazing) in the presence of solvents in liquid or vapour state (Ballenger *et al.* 1997). So, solvents recurrently reported in the conservation literature (Sutherland 2001; Sutherland and Phenix 2001; Belmares *et al.* 2004) are selected and assessed in this section for their suitability on PMMA. How solvent damage is related to solvent and polymer solubility parameters is also discussed here.

According to an earlier conservation literature survey by Waentig (2008a), at room temperature PMMA was believed to be resistant to some nonpolar solvents, in particular aliphatic hydrocarbons. Aliphatic hydrocarbon solvents contain carbon and hydrogen linked in linear or branched chains and non-aromatic rings, and include petroleum-based solvents, such as hexane, cyclohexane and petroleum ether, also known as petroleum or white/mineral spirit. The same survey identified aromatic hydrocarbon solvents, such as xylene, toluene, benzene, chlorinated hydrocarbons (i.e. dichloromethane, tetrachloroethylene) and most polar solvents, such as ketones (i.e. acetone, methyl ethyl ketone, also known as butanone), as unsafe for PMMA (Waentig 2008a, 274). More recent studies agree that mainly deionised water and aliphatic, non-aromatic hydrocarbons are safe on PMMA (Sale 2011; Debik *et al.* 2013).

Aliphatic alcohols, in particular, ethyl alcohol, also known as ethanol, and isopropyl alcohol, also known as isopropanol, are characterised as the most effective in cleaning PMMA (Morgan 1991b; Waentig 2008a). Although safe, the duration of contact should be kept as short as possible. After prolonged exposure they are documented to microscopically cause a long-term crazing effect (Sale 1993; Sale 2011).

A study of PMMA stress-crazing caused by solvent after contact with an adhesive, reports that water and petroleum ether are the only two, truly harmless solvents for PMMA, commonly available and used by conservators (Sale 1993). Petroleum ether is also recommended by other scholars researching interventive treatments for PMMA used in museum objects (Lorne 1999; Laganà 2008; Waentig 2008a). The POPART project evaluated the wet mechanical cleaning of PMMA at removal of two types of synthetic soil (palmitic- and paraffin-based), through the use of aqueous and solvent media (Balcar *et al.* 2012). Their study showed that between water, ethanol, isopropanol, petroleum ether and xylene applied with cotton swabs, microfibre- and spectacle-cloths (the least damaging materials to apply solvents), ethanol was most successful. It induced the least scratching and successfully removed both oil-soil types. Petroleum ether appeared to be the least effective, but also the least damaging, even though it still managed to remove palmitic soil.

Regarding water, literature shows contradictory evidence, with some scholars verifying its safe use (Sale 1993), while others stating that it is detrimental (Turner 1982; Barrie and Platt 1963). POPART evaluated water too, and assessed its use on PMMA as unsuccessful and ineffective (Balcar *et al.* 2012). Due to a lot of conflicting results on the effect of water on PMMA, water was included in this study and its experimental work in order to be assessed. The discrepancy laid on the fact that PMMA is occasionally claimed to be penetrable by water. This is arguable because on one hand, the bulk PMMA is largely hydrophobic due to its non-polar hydrocarbon backbone, and water, although high-diffusing, due to its low viscosity and high surface tension, didn't allow wetting of hydrophobic surfaces. On the other hand, PMMA's ester side group is polar, thus inherently susceptible to water (Wolbers 2000; Van Oosten 2002; Tham *et al.* 2010). Yet, water is expected to offer the right environment for desirable processes during a cleaning treatment. Water's unique properties of being highly dielectric and a good medium for chemical reactions, namely dissociation of charged particles from one another (chelation), emulsification or detergency (Cremonesi 2010), as well as being the most accessible and commonly used solvent among conservators in removing surface dirt (Buys and Oakley 1993), supported the decision to include it in this study.

So, based on the reviewed literature, deionised water, ethanol, isopropanol, hexane and petroleum ether appeared likely candidates for the safe cleaning of PMMA. The selection

of isopropanol (C<sub>3</sub>H<sub>8</sub>O) and ethanol (C<sub>2</sub>H<sub>6</sub>O) is not only justified by their cited efficiency in cleaning PMMA, but also their acclaimed lubricating behaviour that reduces scratching (Balcar *et al.* 2012). The Hildebrand solubility parameter<sup>12</sup> was then used to provide a systemic description of the miscibility behaviour of solvents (Belmares *et al.* 2004; Burke 2008). According to this solubility theory, solvents with less than two units difference from the solubility parameter of PMMA (18.7 MPa<sup>½</sup>), are likely to dissolve the material (Sale 1993; Brydson 1999). Solubility parameters of deionised water, ethanol and isopropanol (Table 4.1) present larger units than 2 MPa<sup>½</sup>, thus appear suitable for use on PMMA (Brydson 1999).

<b>Hildebrand solubility parameters of exemplary solvents</b>		
<b>Solvent</b>	<b>Hildebrand solubility parameter (MPa<sup>½</sup>)</b>	<b>Dissolution of PMMA</b>
Hexane	14.9	No
Petroleum ether	16.1	Maybe
Cyclohexane	16.8	Yes
Xylene	18.2	Yes
Toluene	18.3	Yes
Benzene	18.7	Yes
Butanone (MEK)	19.3	Yes
Acetone	19.7	Yes
Dichloromethane	20.2	Yes
Isopropyl alcohol	24.2	No
Ethyl alcohol	26.2	No
water	48.0	No

*Table 4.1. Hildebrand solubility parameters of selected solvents appropriate for the safe cleaning of PMMA.*

As previously mentioned, the bulk PMMA is largely hydrophobic due to its non-polar hydrocarbon backbone, rendering it harder for water to access the hydrophilic, polar pendant ester group. Based on this model, and the fact that deionised water has a solubility unit of 48.0 MPa<sup>½</sup>, water is not expected to damage PMMA (Cooper *et al.* 1986). Nevertheless, studies in orthopaedics demonstrated that, although hydrophobic, when immersed in water for 24 h, PMMA absorbed up to ~2 % w/w (N'Diaye *et al.* 2012; Ayre *et al.* 2014). Other studies showed that when in water for one month PMMA gained ~1 % w/w (Arnold 1998), while when immersed for fourteen days it showed ESC caused by the propagation of a single craze that proliferated rapidly across the sample (Wypych 2013). As seen, water molecules are small

<sup>12</sup> It provides a systemic description of the relative solvency/miscibility behaviour of solvents. The solubility parameter is a numerical value derived from the cohesive energy density of the solvent, which in turn is derived from the heat of vaporisation divided by the molar volume.

enough that even though chemically incompatible, are able to diffuse between molecules (Turner 1982; Ayre *et al.* 2014). Exposure to water is documented to cause an increase to the PMMA weight (Tham *et al.* 2010; N'Diaye *et al.* 2012; Mishra and Keten 2013), attributed to water filling the overall free volume and causing swelling (Burchill and Stacewicz 1982; Turner 1982; Arnold 1998; Malacarne-Zanon *et al.* 2009). In some cases softening of the material is also observed (Gilbert *et al.* 1977; Malacarne-Zanon *et al.* 2009).

Ethanol based on its solubility unit of 26.2 MPa<sup>½</sup> is not expected to dissolve PMMA. In fact, PMMA at room temperature is insoluble in water and ethanol alone (Basavarajappa *et al.* 2016), but when mixed together (80 % volume ethanol), maxima of solubility and swelling are observed (Piccarolo and Titomanlio 1982). Controversial information was yet reported in studies indicating that ethanol caused increased leaching of MMA monomer from the polymer matrix (Bettencourt *et al.* 2002), increased dissolution (Kawagoe and Morita 1994) and even sample shape change (Zhao *et al.* 2013). Isopropanol with a solubility unit of 24.2 MPa<sup>½</sup> is also not expected to cause PMMA dissolution, yet immersion for fourteen days resulted in rapid local dissolution; Over half the sample dissolved within the first week with no noticeable swelling (Arnold 1998). Similar to water/ethanol, water/isopropanol mixtures showed increased solvation of PMMA, as opposed to water or isopropanol alone (Cowie *et al.* 1987). Studies confirm that co-solvency of water with alcohols increase the solvating power of each other (Hoogenboom *et al.* 2010; Tran *et al.* 2013), which in turn increases the PMMA dissolution rate (Cooper *et al.* 1986; Miller-Chou and Koenig 2003). According to Cowie (1987), a possible explanation is that alcohols act as carriers of water molecules in the PMMA, which gives water access to the polar pendant ester group and allows it to interact favourably with the hydrophilic carbonyl groups once near them.

A sebaceous synthetic soil added in the experiments, aimed to examine the efficiency of solvents at its removal. Addition of nonpolar, lipophilic solvents, hexane or petroleum ether, would therefore be essential in increasing the probability of dissolution of the greasy dirt. Between hexane and petroleum ether, the former is dismissed because of its claimed reduced effect at removing oil (Sutherland and Phenix 2001). Petroleum ether (C<sub>3</sub>H<sub>6</sub>O) is added to the experimental design as it has been cited for its degreasing effect (Sale 1993), and offers an additional chemical type of cleaning agent next to polar water and alcohols. Based on the solubility parameter of petroleum ether with a unit of 16.1 MPa<sup>½</sup>, it is expected to dissolve PMMA (Comiotto and Egger 2009). Overall, good solubility/compatibility is expected between amorphous non-polar PMMA and non-polar solvents (Brydson 1999), such as aliphatic hydrocarbons i.e. petroleum ether. Aliphatic hydrocarbons are a solvent class known to have low craze and crack promoting action to PMMA in short-time contact (Comiotto and Egger

2009). Other studies claim that non-polar solvents can satisfactorily moisten PMMA without dissolving it (Belokon *et al.* 1976).

The main risk with cleaning with free liquids is the redistribution of dissolved material/dirt further within the porous matrix of objects (Gorel 2010), after completion of treatments. When wetted with solvent and in solution, foreign matter (dirt) can reach an atomic scale of such fineness (Moncrieff and Weaver 1987) that, without a physical action to remove it once the solvent has evaporated, it may re-deposit on the treated area. However, clearing of the surface with a cotton swab is a disadvantage relative to the mechanical stress it induces. It must be kept in mind that solvents might also extract components from the material, dissolve it (Shashoua 2012b), or swell it after a brief penetration time, even if the likelihood of that being visible is minor. Such drawbacks (re-deposition of dissolved surface dirt and physical friction), are hoped to be eliminated with the use of gels. In theory, gels are matrices that can hold dirt, avoiding its re-deposition on the treated surface.

However, the absence of investigations make it hard to assess. This is why the present research includes gravimetric measurements before and after application of artificial dirt, and after treatment, aiming to monitor weight changes due to material dissolution and solvent absorption. Moreover, all these specific issues related to the effects of the selected solvents, are examined in detail in Chapter 7.1.2.

### **4.3. INTRODUCTION TO GEL CLEANING IN CONSERVATION OF CULTURAL HERITAGE**

Gel cleaning was first established as a conservation method for painted surfaces of more traditional materials (i.e. stone, easel paintings, wooden frames etc.). Plenty of research was available in the literature regarding the chemistry of gels, especially in the field of microbiology and microbial growth. A lot of conservation studies commonly focused on treating paper and paintings (Carretti *et al.* 2005; Carretti *et al.* 2008; Baglioni *et al.* 2009; Iannuccelli and Sotgiu 2010; Sansonetti *et al.* 2012; Cremonesi 2015), as well as painted and varnished wooden and plaster surfaces. Angelova (2013) researched the use of nanomaterials for conservation applications focusing on developing new gel matrices, such as poly (vinyl alcohol) (PVA)/borax used in this research, for cleaning paintings, wooden frames and metal objects. Most of these aqueous systems based on gel matrices (physical, chemical, enzyme etc.) were formulated to remove aged natural or synthetic resins previously used as varnishes, overpaints or coatings from polychrome surfaces (Bellucci *et al.* 1999; Cremonesi 2010). Their efficiency and success at removing older, aged resins was often attributed to their ability to soften rigid dirt layers. However, their use for cleaning plastic surfaces was quite uncharted, innovative and applied on limited types of plastics. It has even been suggested that since they are designed to remove



aged polymer resins, they are not suitable for use on plastic surfaces (Fricker 2016).

An increasing number of gel systems have been introduced to the conservation community as a means of delivering liquids to an artwork surface during cleaning treatments in a controlled and effective manner (Wolbers 2000; Carretti *et al.* 2010a; Cremonesi 2010; Domingues *et al.* 2013a). The most extensively used gel systems have been based on cellulose ethers like Klucel™ and xanthan gum, polyacrylic acid (PAA) derivatives Carbopol® and Pemulen™ TR2 and rigid gels, such as Agar and Gellan (Khandekar 2004b, 3; Casoli *et al.* 2014). In the 1980s, the use of aqueous gel cleaning methods prepared with PAA-based Carbopol and Pemulen thickeners, aimed at increasing conservators control over treatments, was proposed and marketed (Wolbers 2000). The aim was to create high-viscosity gels capable of carrying mixtures of solvents and surfactants for application on paintings and paper.

There are a large number of presumed advantages for the use of gel systems, documented by a vast number of scholars stating that they are ideal for controlled cleaning (Tsang and Erhardt 1992; Dorge 2000; Wolbers 2000; Khandekar 2004; Warda *et al.* 2007; Gorel 2010; Iannuccelli and Sotgiu 2010; Angelova 2013; Giorgi *et al.* 2013). Their action can be tailored to remove specific dirt types through the addition of buffers that can adjust the system's pH. They are assumed to hold larger solvent quantities than cotton swabs and reduce solvent volatility, offering more control, while extending the solvent retention time and enhancing solvent effect. Usually, the most important issues on the use of free liquid systems are related to penetration of the liquid into the material and to the consequent swelling of layers and component parts. Gels increase the viscosity of liquids, thus decreasing their diffusion rate and limiting the amount released. This strategy is commonly used to gradually introduce moisture, organic solvents or other agents into the treated substrate and improve surface wetting when using aqueous solutions (Casoli *et al.* 2014). As solvents begin to evaporate from the outer gel surface (Iannuccelli and Sotgiu 2010), the gel can draw out soluble dirt molecules absorbed into it due to its capillary action (Cremonesi 2010; Hawkes 2013). Absorption of dirt into the gel could be responsible for preventing dirt redistribution (Moore and Griffith 2006; Casoli *et al.* 2014). This activity could be monitored since most gels are transparent (Tsang and Erhardt 1992; Dorge 2000; Khandekar 2004a; Gorel 2010; Giorgi and Carretti 2013).

Perhaps most importantly, the use of gels is believed to reduce/limit levels of mechanical action/stress compared to continuous rolling of cotton swabs (Domingues *et al.* 2013b, Mazzuca *et al.* 2014; Sun *et al.* 2014) and provide a suitable method for cleaning vertical surfaces (Angelova 2013). Yellowing of certain gels has been observed and used to verify its cleaning action (Warda *et al.* 2007). Observation of gradual discolouration is possibly

attributed to migration of the object's water-soluble chromogenic components or acidic products (Botti *et al.* 2011) and subsequent absorption of the dissolved materials. In such cases, the gel action can be observed through swelling of the unwanted material (Cremonesi 2010). This swelling, enough to soften it and aid its removal with a gentle mechanical action, is also a verification of the gel cleaning action. One final benefit is that gel systems are less hazardous than free solvents as they minimise human exposure to toxic organic solvents and decrease the health risks associated with solvent vapours (McKibbin *et al.* 2017).

These alleged properties render gels safer and more efficient (Callister and Rethwisch 2014). Gels are seen as beneficial in that they enable an increased contact period between cleaning agent-substrate and enhance the solvent ability to dissolve a material. At the same time, they provide the conservator with better control over the cleaning process. However, in reality only a few studies have examined the solvent movement from the gels into the treated substrates. Thus, it is still not established that gelling agents actually control the diffusion of solvents (Casoli *et al.* 2014). Very few studies have addressed the issue of control over solvents, leading to questions related to retention properties and effectiveness of gels in limiting the solvent action.

Bollard *et al.* (2011) were the first to publish their systematic preliminary studies on cleaning pristine and artificially UV-aged plastics. They compared the use of free solvent applied with cotton swabs against thickened solvent in Pemulen TR-2 emulsions for cleaning transparent, plasticised PVC. Their aim, similar to this research, was to test the efficiency of the cleaning methods and safety of materials in their pure form. Different solvent concentrations and exposure times were tested. Based on their results, pure Pemulen gels caused the least surface change to PVC (Bollard *et al.* 2011), a remark that was taken into consideration in the present study. Domingues *et al.* (2013b) reported that chemical polyvinylpyrrolidone/poly (2-hydroxyethyl methacrylate) (IPN) hydrogels offered better control over swab cleaning and physical gels (i.e. polysaccharides). Mazzuca *et al.* (2014) evaluated the use of Gellan hydrogels on paper as more successful with respect to conventional cleaning (immersion), while exhibiting satisfying retention properties. Fife *et al.* (2015) combined gravimetric measurements with unilateral NMR of easel paintings to demonstrate a reduced uptake of solvent thickened in cellulose ether (Klucel) as opposed to its free application with cotton swabs.

Sansonetti *et al.* (2012) demonstrated that application of viscous fluid Agar (in sol state) for ion extraction from plaster surfaces was more successful than use of preformed rigid gels. Möller (2014) underlined that use of Gellan on sensitive materials, such as watercolour drawings, did not eliminate the risk of damage. Angelova *et al.* (2016) examined the diffusion

of water from a variety of gel systems into acrylic paint layers through unilateral NMR. Even though Agar gels released a minimal amount of water in the specific study, this was equivalent to the amount delivered from swabs during cleaning of the paint-film. PVA/borax and Pemulen gels, as opposed to what was anticipated in the study, released the largest amounts of water, rendering them ineffective in controlling solvents. Most recently Baij *et al.* (2017) employed time-dependent ATR-FTIR on model oil paint binding media to compare the kinetics of free water and ethanol against their thickened effect in Agar and Gellan gels. Results showed that solvent diffusion was not influenced by the method of application (Baij *et al.* 2017).

There are a number of issues that arise from the use of gels that could lead to problems and complications, during and after treatment. The biggest concern regards their complete removal from treated surfaces. Gelling agents are solid, non-volatile polymers, with variable degrees of adhesion, which can lead to permanence of residual materials (Casoli *et al.* 2014). For this reason, a post-treatment rinsing procedure (clearance step) has to be adopted to remove residual gelled material. It has been frequently suggested that post-treatment clearance is a crucial step and forms part of the complete gel cleaning method (Stavroudis and Blank 1989). However, the inevitable need to rinse is somewhat contrary to the whole purpose of using gels: to eliminate mechanical action and friction on sensitive surfaces of art/historical objects. It has been suggested that the most effective method to clear gel residues is to rinse with the same solvent (mixture) used in the gel formulation (Burnstock and Kieslich 1996). This clearing method uses water and solvents with cotton swabs to ensure proper removal of residues of the hydrophilic gelling agents, reproducing the problems connected to the application of free solvents and mechanical friction of swabs. The chief intent of employing a gel for cleaning is to avoid the use of free liquid and chemical interaction between solvent and plastic, as well as the additional - potentially harmful - mechanical friction (i.e. rubbing).

Nonetheless, even after proper post-treatment rinsing, the likelihood of residual gelling material remains (Casoli *et al.* 2014). Some residues may still remain deposited and 'trapped' in surface defects (i.e. cracks, holes). Adhesion of gelling materials plays a crucial role in the ease of their removal and can lead to permanence of residues on the treated surface (Casoli *et al.* 2014). In the literature, such a drawback has been reported to be avoided through the use of the so-called rigid gels, removing the need for a post-treatment rinsing (Cremonesi 2010). The introduction of rigid polysaccharide gels in 2003 came as a response to the PAA-based high-viscosity gels that tended to adhere to sensitive substrates (Cremonesi 2010). Interest in the use of rigid gels, especially Agar and Gellan, has steadily increased within the field of paper conservation. Due to their structure, rigid gels can act as molecular sponges to draw out and trap impurities (Cremonesi 2010), particles and degradation products within

them, while due to their compact nature and low adhesive strength to the substrate they leave little or no residue (Sansonetti *et al.* 2012). They are said to afford a high degree of control in a variety of treatments routinely performed on paper (Sullivan *et al.* 2017).

Numerous studies have discussed the presence of residual components from the gel network, such as surfactants, on treated surfaces (Carretti *et al.* 2004; Carretti *et al.* 2008; Cremonesi 2010; Mazzuca *et al.* 2014; deGhetaldi *et al.* 2017). Analytical studies with FTIR and GC/MS revealed that, contrary to most other gel types, only trace amounts of polysaccharides deriving from Agar were transferred into very porous objects, made of plaster and stone (Cremonesi 2010). In some cases, py-GC/MS detected trace amounts of migrated, residual galactose or Agaropectin, which would discolour over time, attributed to long application times (ca. 40 minutes) (Cremonesi and Casoli 2017). The biggest risk when having polysaccharide gel residues is that being natural and aqueous-based, they could induce microbial growth (Mazzuca *et al.* 2014). In the majority of instances, Agar gels left no residues of organic substances onto the treated substrates (Anzani *et al.* 2008; Sansonetti *et al.* 2012). FTIR analysis of various surfaces treated with Gellan though confirmed polysaccharide residues (Mazzuca *et al.* 2013).

Some research examining the residue issue of Carbopol/Ethomeen gels with py-GC/MS analysis of a treated oil painting on canvas and subsequent artificial ageing of 12 hours, showed no presence of Ethomeen surfactant. Analysis of paintings treated several years earlier also showed no detectable residues (deGhetaldi *et al.* 2017), suggesting that any residual surfactant eventually degraded into smaller, volatile molecules. However, research by Burnstock and Kieslich (1996 cited in Carretti *et al.* 2008) demonstrated that even when post-treatment rinsing with white spirits took place, PAA-based gel residues remained on painted surface (Carretti *et al.* 2008). In another study, treated paper samples with Carbopol displayed discolouration of deposited gel residues following artificial ageing (Warda *et al.* 2007). Carbopol/Ethomeen residues were identified as some complex salt formulation (Stavroudis 2017). Triethanolamine (from now on TEA) added in either Carbopol or Pemulen had a slow evaporation rate that constitutes it a potential source of residues with long-term detrimental effects (Hennen *et al.* 2017). Regarding PVA/borax gels, no detectable PVA or borax-derived residues were detected on paintings coated with aged, natural varnishes (Natali *et al.* 2011).

The abilities of a gel system to clean a surface, control the diffusion of a thickened liquid and eliminate residue deposition depend on the interactions between gel system, substrate to be treated and dirt to be removed. To better understand the challenges and complications that may arise during the gel cleaning of PMMA surfaces, the chemistry and

properties of gels, the assumed benefits and drawbacks, as well as exemplary gel systems commonly employed by conservators are further reviewed and discussed.

#### **4.3.1. Gels: chemistry & properties**

In the broadest sense, a gel is defined as a material that can be deformed under shear stress, but otherwise behaves like a solid (Angelova *et al.* 2017a). Gels are liquid formulations thickened with a natural or synthetic polymeric matrix or other high-molecular-weight material (Khandekar 2004) that act as carriers for solvents. Gels used in this study are a class of soft matter composed of polymer chains that form a network as a result of changes in temperature or pH (reversible gels) (Angelova *et al.* 2017a). At the initial stage of gel formation, polymer chains undergo the 'sol' phase, during which they are partially linked but still soluble. As the linking process continues the size of the polymer network increases, while solubility decreases, to form an infinite molecule: the gel. This transition is known as the 'sol-gel transition', or else 'gelation' (Sperling 2006). They are usually prepared from a solid, frequently powder, that is mixed with a liquid to form the basis of a gel system (Warda *et al.* 2007). To form a gel system, apart from thickeners/gelating agents, active ingredients (i.e. solvents) and additives (i.e. detergents, surfactants and buffers) may be added. Each component has a specific role; detergents increase the wetting capability improving contact with the surface and can separate a soiling material from a given substrate, surfactants increase the ability of the gel to solubilise a material, while buffers adjust/maintain the pH at the optimum level for cleaning purposes.

Gel systems can be prepared in aqueous or organic media (solvents) to form aqueous gels or organogels respectively, also known as solvent-gels (Angelova 2013). In this study, all gels were prepared in deionised water forming aqueous gels. Attention is needed when using the term 'hydrogel' and 'aqueous gel'. Khandekar (2000) in an extensive literature review of aqueous cleaning systems on painted surfaces pinpointed that a number of diverse cleaning methods are grouped together under the name 'hydrogel' without a clear explanation of the purpose of the use of water (Kronkright 2009). Mainly the difference is that some gels require water in order to gelate, therefore they are aqueous due to internal chemistry, while other gels use water as an active cleaning agent.

The term hydrogel describes three-dimensional lightly crosslinked network structures obtained from a class of natural or synthetic polymers, which can absorb and retain significant amounts of water (Gulrez *et al.* 2011). They are characterised by both hydrophilicity and insolubility in water (Sperling 2006). They have been described as effectively water-swollen polymer networks (Lai 1992; Sperling 2006). Aqueous gels are capable of absorbing substantial amounts of organic solvents, forming solvent-based gels, while still retaining essential

properties of solids (i.e. finite shear). Within the gel network, the solvent may retain many of the properties of a free liquid (Angelova *et al.* 2015).

Structural units composing the gel networks can be chemically or physically crosslinked (Angelova 2013, 11). Networks of physical (or rigid) gels are held together by molecular entanglements of either strong or weak polymer chains (Giorgi *et al.* 2013). Strong physical gels form strong physical bonds between polymer chains via primary forces (covalent or ionic bonding) and are effectively permanent. Weak physical gels have reversible links formed from temporary associations between chains through secondary forces (Van der Waal's or hydrogen bonding) and/or hydrophobic interactions. These associations break and reform continuously with time and temperature (thermoreversible), undergoing a transition from solid-like to liquid-like form at a certain characteristic temperature (Sperling 2006) and can be disrupted by changes in physical conditions or application of stress (Gulrez *et al.* 2011). Examples of strong physical gels are the commercial synthetic polymer matrices, namely the PAA-based Pemulen and Carbopol. Weak physical gels are in their majority gelling marine and plant polysaccharides, commonly used in the food industry, such as agars, carrageenans and alginates (Ross-Murphy 1987). Agar Agar, Agarose, xanthan gum and Gellan belong to this category.

Peelable PVA/Borax does not fall under the category 'gels', as it is in reality a high viscosity polymeric solution (HVPS) (Duncan *et al.* 2017). However, it is often included in research about physical gels, which can also be confusing because of its bonds within the crosslinks that offer the impression of being chemical gels. Chemical gelation involves formation of covalent bonds resulting in strong and permanent (thermoset) gels (Sperling 2006). The main chemical gelation processes include condensation, addition polymerisation and vulcanisation (Gulrez *et al.* 2011, 118). Such gels can be rheoreversible and magnetic, and are relatively new, still in their applied research stage and not widespread in the conservation of cultural heritage. Coming back to PVA/borax gels, the very low energy required to make and break the crosslinks implies that an increase in temperature can cause the gel to return to a liquid state (Angelova *et al.* 2017a). Not only large changes in temperature affect the state of the gel but as a physical gel, changes in pH equilibrium also alter its ability to form; lowering the pH hinders gel formation and increasing the pH creates a rigid gel (Angelova *et al.* 2017).

### **Agar**

The use of rigid Agar gels was introduced as a response to the PAA-based Carbopol and Pemulen gels that required post-treatment rinsing for removal of residues (Cremonesi 2010). Agar has been successfully used in the conservation of a wide range of materials, including

paintings, paper, stone, plaster, mural paintings, and wood, and has repeatedly proven to obtain the least damaging and most effective behaviour at removing dirt from sensitive, textured and pigmented art objects (Botti *et al.* 2011). Agar has not only been used for cleaning cultural heritage surfaces. Several studies have used it alternatively, such as an intermediary agent in laser cleaning of sensitive pigments from stone surfaces (Sansonetti *et al.* 2012) or for removal/reduction of tide stains on canvas resulting from water damage (Barkovic *et al.* 2017).

Agar is a natural, non-toxic, and biodegradable polysaccharide extracted from the red algae species of *Gelidium* and *Gracilariae* order composed mainly by two polymer fractions, Agarose and Agaropectin. Agarose is a carbohydrate comprised of 1, 3 linked D-galactose and 1, 4 linked 3, 6 anhydro L-galactose (Fig.4.1) (Varshosaz *et al.* 2015). Due to its high molecular weight Agarose is responsible for the gelling properties of Agar, and this is the reason why it is sometimes used in its own right as a gel carrier. It is the purest commercially available galactose-derived gelling agent, and can produce clear, more transparent gels than the clouded Agar gels (Cremonesi 2010). However, apart from being significantly cheaper than Agarose, Agar is favoured because of its slower rate of syneresis compared to Agarose. This is a macroscopic phase separation, which consists of the shrinkage of the gel matrix and the progressive expulsion of solvent (Divoux *et al.* 2014). During syneresis the expected mechanical properties of polymer gels are diminished and their structure is disrupted (Natali *et al.* 2011). This is also encountered in the literature as gel thinning, that can take place after water evaporation, and increases the risk of the gel's absorption into the material (Khandekar 2004a).

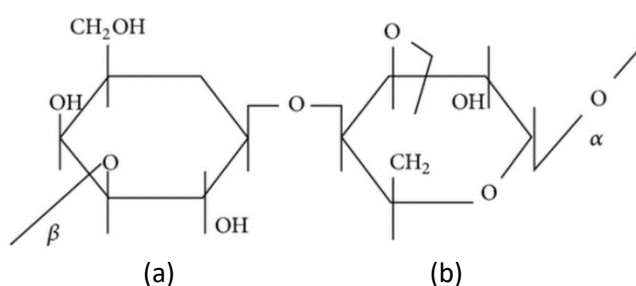


Figure 4.1. Agarose repeat unit: 1, 3 linked D-galactose (a) and 1, 4 linked 3, 6 anhydro L-galactose (b) (Varshosaz *et al.* 2015, p. 2).

Agaropectin is a sulfated polymer that is a complex mixture of low-weight saccharide molecules. In addition to D-galactose, 3, 6 anhydro L-galactose repeating units (Sansonetti *et al.* 2012) contain D-glucuronic acid and pyruvic acid (Fig.4.2) (Varshosaz *et al.* 2015). These are responsible for decreasing the pore sizes within the Agar network, thus slowing down the discharge rate of water (Cremonesi 2010). Contrary to Agarose, Agaropectin has no gelling

properties (Sansone *et al.* 2012). Its gel network contains double helices stabilised by the presence of water molecules bound inside the double helical cavity and formed from left-handed threefold helices.

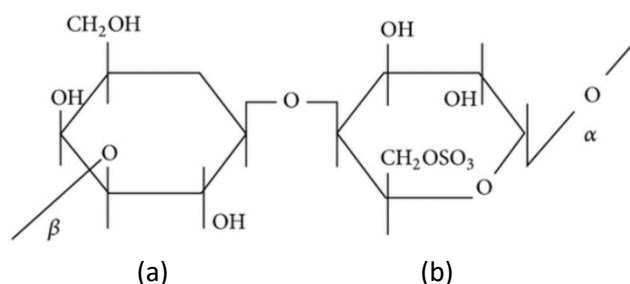


Figure 4.2. 1, 3 linked D-galactose (a) and sulfated 1, 4 linked 3, 6 anhydro L-galactose with D-glucuronic acid and pyruvic acid (b) (Varshosaz *et al.* 2015, p. 2).

Insoluble in cold water, Agar gels are prepared by dispersing the dry powder in boiling water up to about 90 °C to form a colloidal solution (sol phase). By allowing it to cool slowly at around 35 °C it thickens, forming a rigid thermoreversible gel. While cooling (sol-gel process) randomly coiled polymer chains shift to an organised three-dimensional network. Agar can be re-liquefied by heating a second time to improve homogeneity and transparency (Sansone *et al.* 2012). The gel rigidity is attributed to its macro-reticulate structure based on hydrogen bonding between the Agarose helices. While on one hand this structure is advantageous because it allows entrapment of enormous quantities of water, either bonded to the polysaccharide molecules or free (Sansone *et al.* 2012), on the other hand the same rigidity can transform into a main drawback; namely, it doesn't allow the gel to obtain good contact with (especially non-planar) surfaces, even if its thickness is decreased.

Different concentrations of Agar gels are found in published research in conservation, but always in concentrations between 2.5-5 wt.% (Cremonesi 2015). Gorel (2010), Cremonesi (2015) and Warda *et al.* (2007) preferred gels of 2 wt.%, while the latter also tried 4 wt.%. Tortajada-Hernando and Blanco-Dominguez (2013) used both 2 wt.% and 4 wt.%. Agar hydrogels can be enhanced with surfactants, chelating agents or/and polar solvents. Attention is needed with solvents because too high concentrations may cause the gel to dissociate (Scott 2012). Scott (2012) reported that the best results for workability of the gel were achieved with ethanol. Agar gels allow the conservator to select gel concentration, temperature, application time and technique (pre-formed, grated, sol state), thus offering control over cleaning; preliminary tests should address the various parameters. Different varieties of Agar performing in a very similar way are commercially available, ranging from laboratory to food additive grades (Cremonesi 2010). The melting and gel point temperatures of Agar gels vary slightly due to the natural diversity in the chemical composition of each algae.



Application times vary depending on the nature of the substrate, the condition of the surface and the composition of the dirt to be removed. For example, wooden surfaces have been treated from 1 up to 90 minutes (Gorel 2010), easel paintings for less than 1 minute (Warda *et al.* 2007), and plaster from 2 minutes to 24 hours (Tortajada-Hernando and Blanco-Dominguez 2013). Application methods can also vary; Agar can be applied while not yet gellified (sol) directly on the artwork surface (Sansonettil *et al.* 2012) or as a pre-formed rigid gel, which can be portioned by cutting and applied on the surface in pads of appropriate form. In fact, Agar gel applied as a viscous fluid forms an adherent thin film, which on complete cooling, exhibits the ability to peel off soiling after its partial solubilisation (Anzani *et al.* 2008). The advantage consists in avoiding mechanical stress of the treated surface, when considering materials that are sensitive to any kind of scrape, physical stress and highly textured with relief (Sansonettil *et al.* 2012). However, this may also be problematic when considering the porosity of a material, which may allow the sol to penetrate into it. For sensitive surfaces a brush-on application has been recommended (Cremonesi 2010), while recently (2015) a technique where Agar is grated has been published (Cremonesi 2015).

### **Gellan**

Gellan has been employed in various treatments from the removal of (paper) auxiliary supports to enzyme delivery, deacidification and reductive bleaching (Iannuccelli and Sotgiu 2010). Gellan, as a rigid gel, has a lot of similarities with Agar, hence it is often used as a substitute. It is a natural, non-toxic, and biodegradable high-molecular weight polysaccharide produced by aerobic non-pathogenic bacteria that grow on the aquatic plant *Sphingomonas elodea* or *Pseudomonas elodea*. In the conservation field, Gellan is used in its deacylated type (Fig.4.3) (Botti *et al.* 2011) consisting of four linked monosaccharides and acetyl groups forming repeated tetra-saccharide units (b-D-glucose, b-D-glucuronic acid, b-D-glucose, and b-L-rhamnose), the percent of o-acetyl substitution and the protein content including nucleic residues and other organic nitrogen sources. Gellan shares similar properties with Agar, such as being water-soluble in boiling temperatures and thermoreversible (Iannuccelli and Sotgiu 2010, 32). Like Agar, the level of water transferred to the substrate from Gellan can be modulated by the concentration of the gel. Its function is gelling, texturizing, stabilizing, suspending, film-forming and structuring. Similarly, it is supplied as a dry powder and is widely used in the industries of food, biomedicine and pharmaceuticals for its thickening/gelling properties (Botti *et al.* 2011).

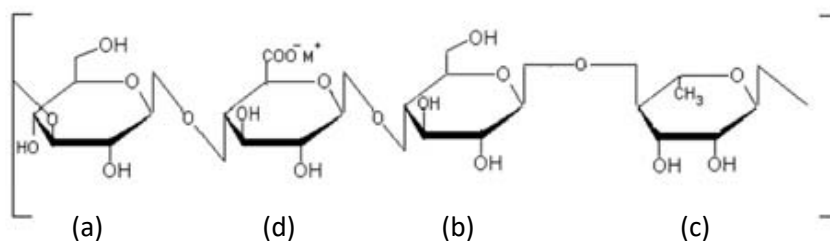


Figure 4.3. Primary chemical structure of deacetylated Gellan gel; linear anionic heteropolysaccharide made of repeating units of two molecules of  $\beta$ -D-Glucose (a,b), one molecule of  $\alpha$ -L-Rhamnose (c) and one molecule of  $\beta$ -D-Glucuronic acid (d) (ICF Consulting 2006, p. 1).

Gellan forms a hard and brittle aqueous gel; a network of long polymeric chains dispersed in water that creates one massive structure (Wolbers 2013). This ability to form one compact piece allows it to be removed without leaving residues behind. Its gellification requires heating to boiling conditions in aqueous solutions. Through heating, the molecules form a disordered coil (single chain), and in turn the structure completely hydrates and forms a homogeneous colloidal dispersion (Fig.4.4). Upon subsequent cooling at room temperature, Gellan rapidly gellifies (Iannuccelli and Sotgiu 2010) as a result of the formation of intertwining helical models (Wolbers 2017).

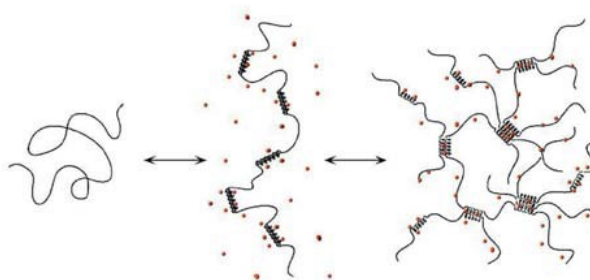


Figure 4.4. Gellan gel coil helix and its transition scheme (Iannuccelli and Sotgiu 2010, p. 31).

Typically, while a 2 wt.% is enough to form a rigid gel (Hawkes 2013), Gellan can be prepared in concentrations of 1-4 wt.% (Iannuccelli and Sotgiu 2010). Case studies and experimental work published to date have mostly used a 3 wt.% aqueous solution (Iannuccelli and Sotgiu 2010; Bonaldo 2015) or a 1-2 wt.% (Yip 2015). Casoli *et al.* (2013) and Mazzuca *et al.* (2014) used a 2 wt.% Gellan hydrogel on paper for 30 minutes and for 1 hour respectively.

### **Carbopol**

Carbopol is an acrylic acid polymer that can be prepared either directly in water or in the required blend of solvents. It is partially soluble in water, in which the tightly coiled molecule starts to unfold exposing carboxylic acid groups along the backbone due to partial dissociation of carboxyl. However, for the gel to be fully thickened and form a stable network,

neutralisation of these acid groups is required (Blüher *et al.* 1995). During neutralisation, an organic base added to the aqueous Carbopol causes removal of protons from these acid groups, partially converting the polymer to a carboxylate salt (Stavroutis 2017; Wolbers 2017). This process in effect results in the unfolding of the polymer chains forming a clear, highly viscous gel (Warda *et al.* 2007). If neutralisation is achieved through the use of an amine that also has detergent properties, such as Ethomeen C-25, very stable solvent-gels can be formed.

Ethomeen is a polyethoxylated cocoalkyl amine available as C-12 and C-25; the latter was preferred in this study because, firstly, it was the only Ethomeen to dissolve in water (Blüher *et al.* 1995), secondly it was recommended for non-polar solvents used in this study, and lastly, it was used in the majority of recipes in conservation publications (Wolbers 2000). Thickening already begins in the pH range 5.0-6.0 (Blüher *et al.* 1995), but viscosity will begin to decrease at pH above 9.0 (Wolbers 2017).

Even though Carbopol has a slight detergency effect itself, a variety of organic solvents including non-polar systems are typically added in the system. Various gel formulations can be prepared by substituting one solvent for another (Blüher *et al.* 1995). Attention is recommended when it comes to the solubility and compatibility of solvents with the gelled Carbopol, which is very sensitive to changes in pH or ionic strength (Wolbers 2017). Insolubility of Carbopol in the solvent system becomes immediately visible by precipitation out of the solution as a sticky, white, stringy residue. Generally the answer is to add more water or additional polar solvents, which make the Carbopol soluble in the solution (Stavroutis and Blank 1989). Based on empirical observation and personal experimentation with the preparation of Carbopol/Ethomeen gels, it is very easy for them to 'fail'. The advantage of this 'salt' formulation is that, like most 'salts', it tends to stay associated together in non-polar environments, so the 'salt' link is a convenient way of using the Carbopol polymer as a kind of scaffolding to hold in place the Ethomeen surfactant (Wolbers 2017).

Studies have recommended application of Carbopol gels by brush or by stirring them on the surface to be cleaned in order to solubilise materials to be removed (Casoli *et al.* 2014). Warda *et al.* (2007) employed a 2 wt.% Carbopol gel on paper for ca. 6 minutes, followed by 2-3 applications of shorter time (less than 1 minute) until adhesive was removed. Different grades of Carbopol exist and exhibit different physical and chemical properties. Carbopol/Ethomeen systems are also feasibly formed without the addition of water, as paste-like solvent/surfactant gels. Such gels can be used as soon as they settle, but often they are allowed to stand overnight for the Carbopol to fully disperse. Upon the mixing of solvents (polar and non-polar) the water-free formation turns into a milky dispersion.

In the majority of studies, Ethomeen was proven to leave residues after clearance of the Carbopol gel (Carretti *et al.* 2004), hence rinsing of the treated area is advised. Other scholars have concluded that Ethomeen degrades fairly rapidly to volatile components and eventually disappears from the treated surface (Hennen *et al.* 2017). In all cases, possible presence of non-volatile residues can be satisfactorily removed by appropriate rinsing. Studies have shown that Carbopol/surfactant gels are soluble to mineral spirits, but only when they are complexed together. Generally, post-treatment clearing methods that have appeared to be most effective at reducing residues include rolling several dry cotton swabs dampened with either relatively polar solvents or/and solvents included in the solvent mix used in the gel (Kronkright 2009). The sequence of separated washes should be followed by wiping with dry swabs (Wolbers 2000). Studies have suggested the use of a thin sheet of Japanese tissue as a barrier to prevent the deposition of Carbopol gel residues on the substrate (Warda *et al.* 2007). This would be more successful for uses where the gel was intended as a poultice, for example to soften a dirt layer, rather than a 'sponge' to pick up dirt.

### **Pemulen TR-2**

Pemulen TR-2 is a polyacrylic acid-polyacrylate ester block copolymer responsible for thickening, emulsifying, surfactant and chelating properties. The formulation of Pemulen gel involves the neutralisation of the block copolymer with an alkali (organic base) in an aqueous environment (Stavroudis 2017). In this study, TEA was used due to its frequent recommendation (Stavroudis 2014). TEA is a polar tertiary amine with three primary alcohol end groups, which provided it with a similar solvent action to alcohol solvents. As with Carbopol, when Pemulen is neutralised by an amine, the resulting species is partially dissociated in the aqueous environment and exists in both ionic and neutral form. High viscosity of the gel occurs at a pH range between 5.0-9.0 (Bollard *et al.* 2011). If present in sufficient quantities, the non-ionised free amine bases form micelle-like structures that improve the polymer ability to emulsify a non-polar phase. The non-ionised molecules not only may act as a solvent, being active in the cleaning process (Ravenel 2010), but surely offer surfactant actions during cleaning. Both Pemulen and Carbopol bring a mild chelation-like capability to the cleaning system by virtue of the carboxylate groups along the polymer (Stavroudis 2017).

Pemulen's block copolymer of hydrophilic polyacrylic acid and hydrophobic long-chain C10–C30 methacrylates allows non-water miscible liquids to be made into oil-in-water gel-emulsions. In this study, the only non-water miscible solvent used was petroleum ether, which mixed with Carbopol and Pemulen (polymeric emulsifiers) formed emulsions that improved

the consistency and physical properties of the systems. The emulsion droplets of PET (dispersed phase) are stabilised into the polymer's methacrylate portion (continuous phase) and held in a thickened aqueous gel network (Stavroudis 2017). These gel-emulsions can be considered as a gel matrix in which droplets are embedded or as two immiscible liquids (by convention described as 'oil and water'), one of which is dispersed as fine droplets uniformly throughout the other (Budai-Szűcs 2008). In a similar way, forming virtual micelles analogous to the micelles formed by surfactants, Pemulen can suspend non-polar grime into its structure without the need of an added surfactant (Bollard *et al.* 2011; Stavroudis 2017). For such reasons Pemulen and Carbopol emulsion-gels are highly recommended for removal of greasy dirt, such as soiling material of oily human sebum (fingerprints) (Wolbers 2000; Aguilar-Sánchez and Buentello-Martínez 2017).

A number of recipes and variations are available for the preparation of Pemulen gels/emulsions (Stavroudis and Blank 1989; Wolbers 2013; Stavroudis 2014), according to the needs of the surface to be cleaned and the composition of the dirt to be removed. Organic solvents can be added up to about 20 % (v/v) (Pavitt 2012). Attention is needed to avoid pH levels below 6.0, as it is probable that the gel will result in a slimy emulsion (Stavroudis and Blank 1989; Pavitt 2012). It is not recommended for porous materials.

### **80 % PVA/borax**

Poly (vinyl alcohol) (PVA) is the largest synthetic water-soluble polymer produced in the world due to its biodegradability, chemical resistance, biocompatibility and excellent physical properties (Bibire and Carja 2013). PVA is generally classified into two groups: fully hydrolysed and partially hydrolysed (Fig.4.5) (Bibire and Carja 2013). In this study an 80 % partially hydrolysed PVA was chemically crosslinked with borate ions (Fig.4.6) (from borax salt [ $\text{Na}_2\text{B}_4\text{O}_7 \cdot 10\text{H}_2\text{O}$ ]) forming aqueous dispersions with high elastic modulus, explored because their physical properties make them attractive tools for use in conservation treatments (Angelova *et al.* 2011; Natali *et al.* 2011). The 80 % represents the percentage of hydroxyl units on the polymer backbone, whereas the remainders are acetate groups. The borate ester cross-links result in very strong interactions between PVA chains. The elasticity and the rheological properties of these systems can be tuned by changing either the ratio of PVA to borax or their total concentration (Carretti *et al.* 2010b).

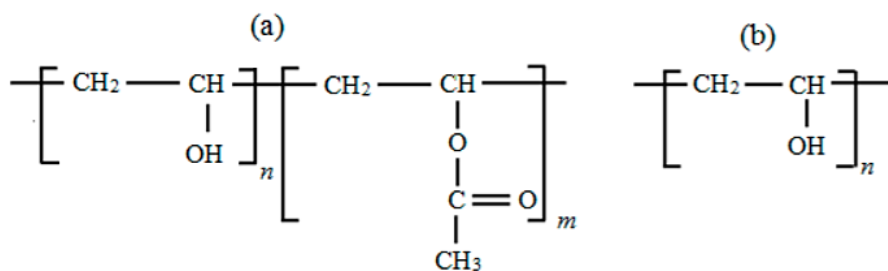


Figure 4.5. Partially hydrolysed poly(vinyl acetate) (xPVA) (a) and fully hydrolysed poly(vinyl alcohol) (PVA) (b) (Ben Halima 2016, p. 39823).

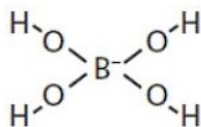


Figure 4.6. Borate ion.

The pH range of the aqueous gels is typically between 8.0-8.5. A decrease below 7.0-7.5 causes the gel to undergo syneresis and revert to a viscous liquid/solution state, whereas an increase above 9.0-10.0 causes the gel to become stiffer (Angelova *et al.* 2015). An excess of borax can disrupt the balance causing syneresis and a two-phase system (i.e. separation of a portion of the liquid from the gel), but can also result in the formation of borax crystals that appear as efflorescence on the treated substrate (Angelova *et al.* 2015). Liquid may also become visible on the gel borders and the treated surface, when the gel acts too rapidly. This in effect meant that the gel can solubilise the surface dirt layer very effectively, resulting in a layer of liquid between the gel and the substrate. Alternatively, this may denote that the surface dirt/solubilised components lower the pH of the gel system, thus causing its syneresis (Angelova *et al.* 2015).

PVA/borax cannot be dissolved in pure organic liquids due to its high polarity, but it can be used with organic solvents between 10-25 wt.% (e.g. methanol, ethanol, n-propyl and isopropyl alcohol, benzyl alcohol) to form aqueous gels (Angelova *et al.* 2015). Depending on the substrate, different application times have been used. For instance on paintings, PVA/borax gels have been usually applied for 1-4 minutes. A 15-minute application was documented as very successful, while 30 minutes over softened the substrate (Carretti *et al.* 2010). The main advantage of this system is its ability to adapt its shape to establish intimate contact with a surface to be cleaned and its very high shear elastic moduli, which allows it to be peeled off after completion of the treatment. PVA/borax gels were shown to retain the liquid well and with little lateral solvent spread, thereby providing confined cleaning for spot treatment. It has been claimed that their structure contributes to the cleaning action of the

system, and as with most thickened/gelated systems, the rate of evaporation of the solvent is said to be reduced (Carretti *et al.* 2010a; Angelova 2013; Angelova *et al.* 2015).

This chapter presented the conservator survey data, which led to an understanding of the current problems in cleaning plastic museum objects, and establishing the conservator priorities and gaps in the field of modern materials conservation. Analysis of the survey data revealed the need for research into the cleaning of transparent and highly polished PMMA. The limited literature on the cleaning of plastics and PMMA, as well as an introduction to the gel cleaning systems and their chemistry were reviewed. The following chapter discusses the selection of PMMA samples for the cleaning experiments and the design of their artificial light-ageing regime, on the basis of the material's mechanical properties. Large part of the chapter focuses on the preparation, characterisation and application of artificial dirt that simulates surface dirt on PMMA in the cleaning experiments.

## Chapter 5. ARTIFICIAL AGEING, SAMPLE PREPARATION & ARTIFICIAL DIRT

---

This chapter initially focuses on the tensile testing and DMA analysis, as well as on understanding the competitive processes of crosslinking and chain scission occurring in the PMMA in different ageing stages. These aimed to identify the amount of UV exposure at which PMMA shows the greatest change within the shortest possible exposure time and set forth the methodology for its accelerated artificial ageing. Mechanical testing also aimed to enable decisions about sample preparation (grade, shape and dimensions). A subsequent discussion draws upon all data obtained from weight measurements, tensile testing, DMA, ATR-FTIR and py-GC/MS analysis, to shed light on the mechanical and chemical behaviour of PMMA.

Next, this chapter examines the surface state of PMMA samples as received from the manufacturing company. Microscopic observation confirmed that unwanted residues from packaging materials were covering all newly-purchased samples. ATR-FTIR analysis employed to chemically characterise these residues is presented here, along with the pre-washing method identified as the safest and most efficient for their removal. Lastly, the two types of artificial surface dirt, simulating fingerprints and mimicking tape remains, used in the main cleaning experiments are also discussed here. Their standardisation along with ATR-FTIR investigation of their synthesis are further described.

### 5.1. LIGHT AGEING REGIME

Light-induced ageing is one of the most common causes of deterioration of art objects (Jakubowicz 2001, 545). For many plastics, the principal degradation route is photo-oxidation via exposure to light and the UV portion of the electromagnetic spectrum ranging between 280-400 nm (Fricker 2016). Photo-chemical changes in most materials are wavelength specific (Torikai and Hasegawa 1998; Tokiwa *et al.* 2009), with PMMA being mostly affected by the shortest ones with the highest energy (Wiles 1993; Saunders and Kirby 2001, 95; Waentig 2008a, 274). Museum lighting, comprising the visible and infrared portions, except for causing thermal activation (Haillant *et al.* 2004, 53), was proven to have no direct effect on the weathering of PMMA (Jakubowicz 2001, 546). Longer wavelengths could also be absorbed by additives or impurities in PMMA – when present, and cause damage (Torikai and Hasegawa 1998). Torikai *et al.* (1995) (quoted in Schaeffer 2001, 140) showed that light-induced deterioration of PMMA was only achieved when UV wavelengths were of 340 nm or below. Wypych (2013, 428) mentioned that the specific wavelength was a critical point for PMMA degradation, equating to midday summer sun in July. According to Kambe *et al.* (1977), PMMA degraded at wavelengths shorter than 330 nm. Other studies by Torikai *et al.* (1990) indicated 320 nm as the threshold wavelength over which no shift was observed. According to Kambe *et al.* (1977) and Dickens *et al.* (1984, 715), PMMA displayed a broad UV absorption below 300



nm, while intense absorption of the ester group was documented near 240 nm. Torikai *et al.* (1990) sustained that the number of PMMA main-chain scissions reached a maximum value when exposed to 280 nm, whereas Wypych (2013) suggested that wavelengths between 260 and 280 nm cause the most damage.

As seen, information found in the literature is inconsistent, however, there are some common lines to be drawn. PMMA shows low to no absorptivity to UV longer than ca. 300 nm and is affected by wavelengths roughly between 240 and 300 nm. Given that the more detrimental UVB range is the only region in the electromagnetic spectrum that can damage PMMA, the shorter wavelengths between 280-315 nm were particularly emphasised in this study. Another issue to consider was that photochemical damage is largely a near-surface phenomenon (Feller 1994a), which means that intensity decreases throughout the material thickness (Broughton *et al.* 2005). When considering how deep radiation might penetrate, an important aspect emerged: the rigidity of PMMA (Wypych 2013). This would affect chain photolytic scission by limiting the mobility of free radicals, while favouring their interaction leading to termination of further degradation (Dickens *et al.* 1986). This material aspect was expected to weaken the UV absorption of PMMA, limiting its light-induced damage.

Accelerated ageing has historically been employed to understand and predict the long-term behaviour of materials in shorter time spans than would be achievable via natural ageing (Quye *et al.* 2011; Fricker 2016). While, generally, in cultural heritage studies it has been used to produce mechanisms as close as possible to those causing materials to naturally degrade<sup>13</sup> (Feller 1994; Wypych 2013), the aim of current artificial ageing was different. In this research, the intention was to accelerate the chemical degradative reactions in PMMA samples and their physical consequences (ISO4892:1981), to effectively and adequately obtain aged material within a workable timespan. In addition, accelerated ageing offered control over the well-defined weathering conditions, which rendered the experiment repeatable (Feller 1996; Wypych 2013). PMMA is a rather durable plastic to ageing (Shashoua 2008) and needs a long time to show material changes. For these reasons, irradiance levels that mimic aggressive outdoor weathering conditions and would provide the highest permissible accelerating factor at the maximum rate of photolytic degradation were selected. This approach of simulating the worst-case light exposure scenario was also followed by one of the other two available studies on the conservation cleaning of PMMA (Fricker 2016).

Indoor museum conditions usually prevent collections' exposure to direct sunlight, and window glasses typically filter radiation in the UV part of the spectrum (Fricker 2016).

---

<sup>13</sup> It is worth mentioning that correlation of accelerated ageing of plastics to natural ageing is questionable (Feller 1994).

However, not all objects are stored in environmentally controlled conditions, corresponding to the recommended levels for ageing in indoor museum conditions (ISO877-2:2009) (exposure behind window glass). Some artworks designed to be displayed outdoors, such as sculptures, experience illumination levels containing damaging UV radiation. Objects in collections with a user life may have also been exposed to UV radiation before acquisition, either through outdoor exposure or artificial sources (i.e. flash photography) (Feller 1994; Fricker 2016).

A Ci3000 Atlas Weather-Ometer was employed for the accelerated artificial ageing of PMMA coupons. For details on mounting samples in the ageing chamber see Appendix C. To mimic outdoor conditions, ISO 4892-2:2013 Test method A, Cycle No.1 was followed for 'artificial weathering' and exposures using daylight filters. The exposure period of the selected test method included two phases (Table 5.1); The water spraying phase simulated the effect of precipitation, as usually material degradation results from a complex combination of variables (Feller 199). Xenon arc lamps were selected for most closely matching the spectral distribution of solar radiation in the visible and UV-wavelength range (see Fig.5.1) (ISO4892:1981; Wypych and Faulkner 1999; Wypych 2013). To improve correlation of emitted light spectra with natural sunlight conditions, exposures were performed with the use of filter sets, which allow for very specific spectra selection. Here an inner Right Light and outer Quartz daylight filter combination was indicated by Atlas, the material testing equipment company, as the most suitable to simulate outdoor conditions similar to the short UV wavelengths of midday sun exposure.

<b>Method A: Exposure using daylight filters (artificial weathering)</b>				
<b>Phase</b>	<b>Phase duration</b>	<b>Irradiance (W/m<sup>2</sup>)</b>	<b>Chamber temp (C°)</b>	<b>Rel. humidity (%)</b>
dry	102 min	60 ± 2	38 ± 3	50 ± 10
wet (water spray)	18 min	60 ± 2	-	-

*Table 5.1. ISO 4892-2:2013 Test Method A: Exposure using daylight filters (artificial weathering) selected in this study for accelerated ageing of PMMA, included two phases: one dry and one wet.*

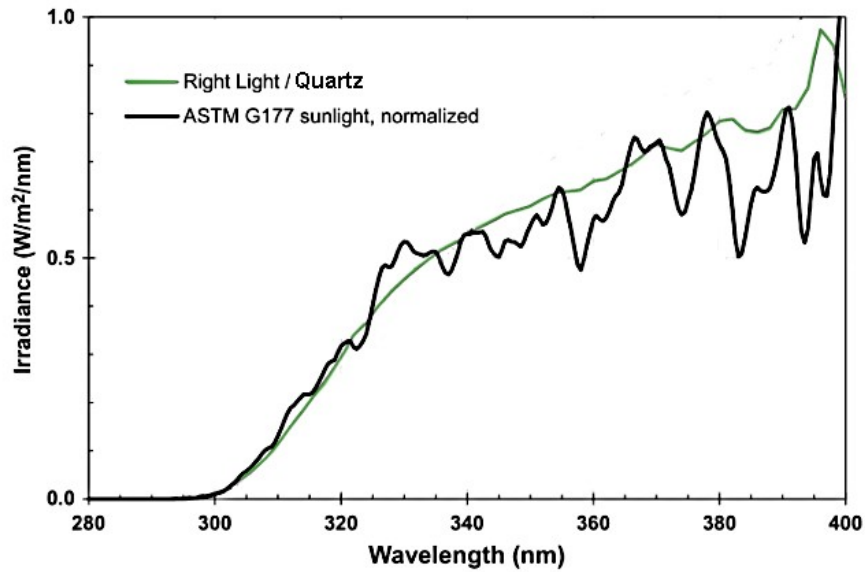


Figure 5.1. Spectral power distributions of xenon arc with Atlas Right Light/Quartz filters compared to normalised ASTM G177 sunlight (After Pickett 2018, p. 177).

### 5.1.1. MECHANICAL TESTING OF POLY (METHYL METHACRYLATE)



Figure 5.2. Instron 5944 Single Column.

Prior to starting the tensile test (Table 5.2), the grip force of the clamping system was checked to avoid premature failure of the sample at the jaws (BS2782-3:Methods 320A to 320F:1976). As the tensile stress was applied in uniaxial alignment, the force induced within the sample was recorded, until fracture occurred, and the test halted. The results were plotted as engineering stress/strain, according to convention (Bower 2002; Peacock and Calhoun 2006), so as to consider the maximum load divided by the initial cross-sectional area before elongation and account for possible inconsistencies in the sample dimensions.

Based on sample preparation information in 2.3.2, manual mechanical cutting was preferred as the least invasive to the material. Samples were cut from commercial transparent sheets by means of a circular saw, in the form of rectangular coupons, at the Institute of Making (IoM), UCL. Use of a circular saw was specified in ISO 2818-1996, and recommended by the manufacturing company Goodfellow Inc., who supplied the PMMA sheets. The company did not disclose any information related to the manufacturing or synthesis of the supplied material, claiming this was for safeguarding their industrial process and recipes. It was speculated that the supplied material was produced using injection- or compression-moulded sheets or shaped articles (ISO20753:2014). *In situ* polymerisation, extrusion or other

processing operations could also have been used to produce semi-finished products. Sample surfaces were flat and planar, and their edges were free of visible cracks, scratches, pits, production marks or other defects, when observed under magnification<sup>14</sup> (50x).

<b>Tensile loading</b>	
<b>Instrument</b>	Instron® 5944 Single Column fitted with pneumatic grips (Fig.4.1): The lower grip was fixed, while the upper was moveable to extend the sample and increase the deformation in one direction (i.e. tension).
<b>Extension rate/speed</b> (velocity of the cross-head)	Constant strain rate of 1 mm/min.
<b>Gauge length</b> (initial distance between the grips before extension)	Constant at 45.0 mm throughout all tests to enable comparisons between elongation measurements.
<b>Environmental conditions</b>	Room temperature

*Table 5.2. Experimental parameters used in tensile test.*

#### 5.1.1.1. Preliminary tensile test: fine tuning the method

Two sets of preliminary tensile tests were conducted on 1.0 mm thick PMMA samples to:

- establish whether the breaking loads of the samples were within the tolerance of the instrument.
- determine the relationship between sample width and breaking load.
- determine whether the samples' orientation and direction of cut influenced their mechanical behaviour.

These tests aimed at determining the experimental parameters and methodology for the main tensile analysis, presented in the following section. All samples regardless direction of cut, broke within the load range of the instrument, rendering the technique suitable for the purpose of this study. Results showed that sample dimensions were proportional to load, and thus load measurements could be extrapolated from the results. In addition, results showed that the direction of cut did influence the mechanical behaviour of samples and lastly that, longer samples were more suitable for tensile testing than shorter. For detailed description and results see Appendix D.

#### 5.1.1.2. Main tensile test of exponentially aged material

The mechanical testing presented here aimed to determine the appropriate ageing protocol for PMMA, by subjecting samples to varied levels of UV exposure and subsequently to tensile analysis. By accepting for instance that the unaged material broke at 700 N, it was of interest

<sup>14</sup> Leica DM 2500P optical microscope.

to locate the point at which, post-ageing, it would break at 1/3 of its initial load, then half of that at ca. 350 N, and so on and so forth. Correlating these points with the equivalent amount of UV exposure required for PMMA to break at different points of its initial load, enabled estimation of its ageing extent. This, standardised accelerated degradation and set forth the methodology for the light-ageing regime based on a quantifiable mechanical aspect of the material (Feller 1994), rather than an arbitrary decision. Such tests on ageing materials were better described by the theory of linear viscoelasticity (Martinez-Vega *et al.* 2002). The more robustly a degraded material is understood, the easier it is to make decisions relating to its durability.

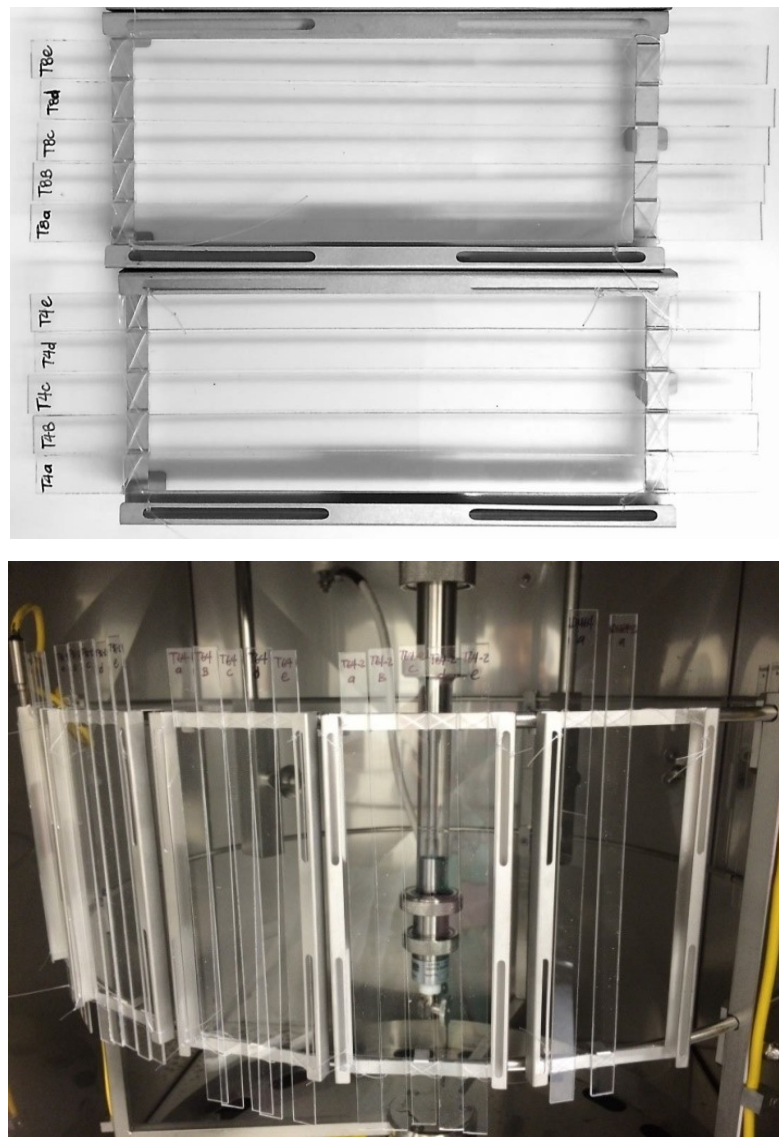
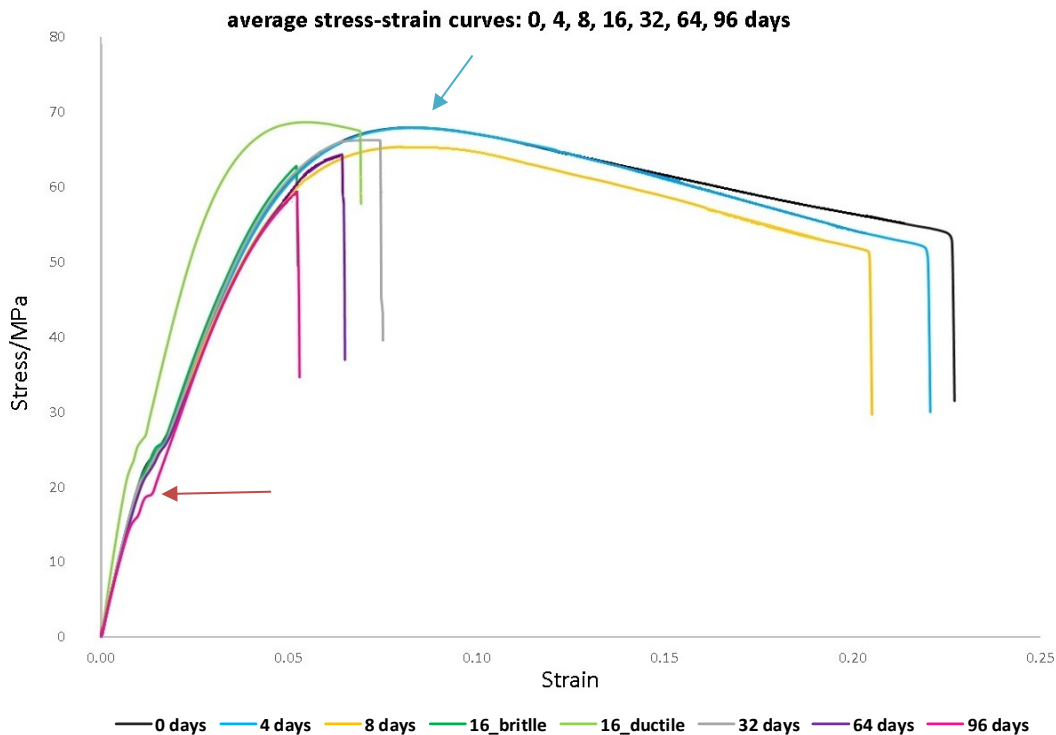


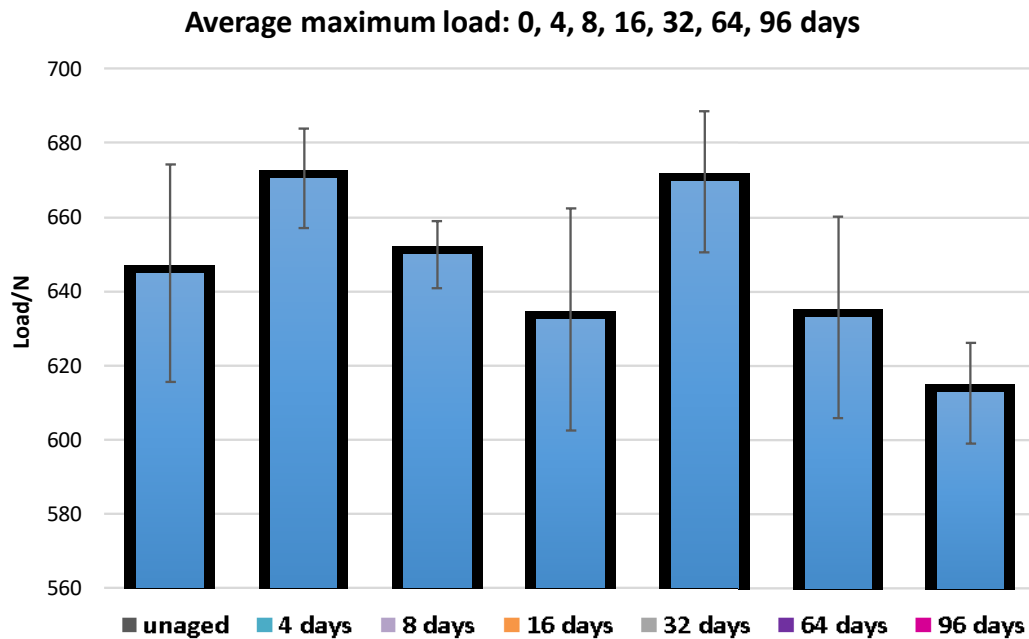
*Figure 5.3. Samples for exponential artificial ageing, cut for subsequent tensile testing, were mounted on the holders with nylon thread. Labelling used permanent marking to endure the artificial weathering.*

Tensile results of exponentially aged PMMA were examined in the form of stress-strain curves, as opposed to load-elongation used in the preliminary tensile test. Stress-strain curves considered the cross-sectional area of samples, rendering results from publications (that often employ stress-strain over load-elongation), as well as between sample sets of different compositions, thicknesses, and ageing conditions, comparable.

The preliminary tensile tests dictated the specifications regarding the size/number of samples, based on which two grades of transparent PMMA sheets (200 x 200 mm) were ordered: a 1.0 mm thick grade described as cast with no further information provided and a 1.2 mm thick of high purity and free from UV absorbers. The presence and composition of additives was unknown, as it was considered classified information. Alkyl benzyl phthalates and phosphates have commonly been added as plasticisers in acrylics (Williams 1993). Once the orientation of these two sheets was identified, following the steps described in the Orientation test (see Appendix D), samples were cut accordingly (10 mm wide x 100 mm long). A set of five replicates were artificially aged for each of the six exposures (Fig.5.3), and a further set was kept unaged as control. Exponential ageing was carried out for a total length of 96 days with sampling steps at 4, 8, 16, 32 and 64 days according to ISO 4892-2: 2013 Test method A, Cycle No.1 for 'artificial weathering', as earlier discussed (see Appendix E for mounting of samples in Atlas).

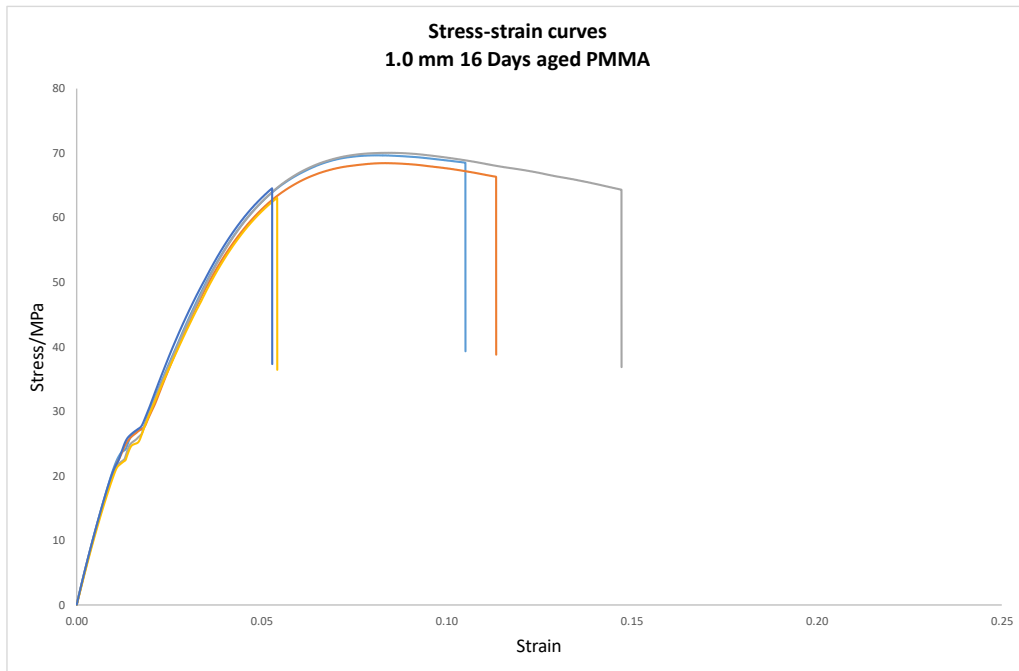


*Graph 5.1. Averaged stress-strain curves of unaged and exponentially aged 1.0 mm PMMA samples under UV radiation for 4, 8, 16, 32, 64 and 96 days. The curves are averaged from five replicates.*



*Graph 5.2. Averaged maximum load of unaged and exponentially aged 1.0 mm PMMA samples under UV radiation for 4, 8, 16, 32, 64 and 96 days - seen in Graph 5.1. plotted as curves. Error bars show the standard deviation.*

At low strains the stress-strain curves of all 1.0 mm samples (Graph 5.1) show an initial linear region, which is elastic, reversible deformation, known as the modulus of elasticity. This is defined as the tensile stress divided by the tensile strain. Above this region, at approximately 20 MPa, a break in the slope of the curves is seen (see red arrow). From observation of the averaged stress-strain curves (Graph 5.1) it is evident that the unaged material is more ductile than the aged. The averaged unaged curve (0 days) exhibits a near linear behaviour up to 50 MPa, followed by further extension up to the point of yielding where the samples are drawn, exhibited as a drop in load. The yield point coincides with the observation of a maximum load, seen as a more rounded curve (see blue arrow). This behaviour is influenced by the result of a slow extension rate, which allows the unaged material time to respond to the applied stress and relax. The composition of the 1.0 mm grade (unknown) is also held responsible for this behaviour. Based on the stress-strain curves presented in Chapter 3.3.2, the unaged PMMA exhibits an intermediate behaviour between a brittle and a linear plastic polymer; this tensile behaviour is also exhibited by samples aged for 4 and 8 days (blue and yellow respectively - Graph 5.1)

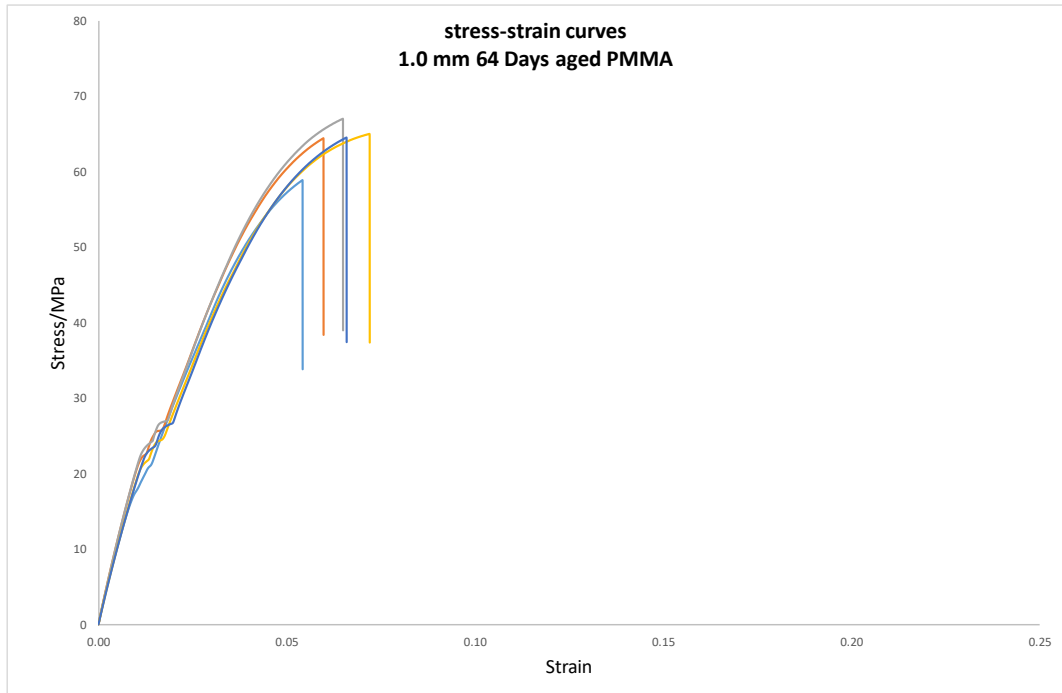


*Graph 5.3. Stress-strain curves of 1.0 mm: set of five PMMA replicates UV-aged for 16 days.*

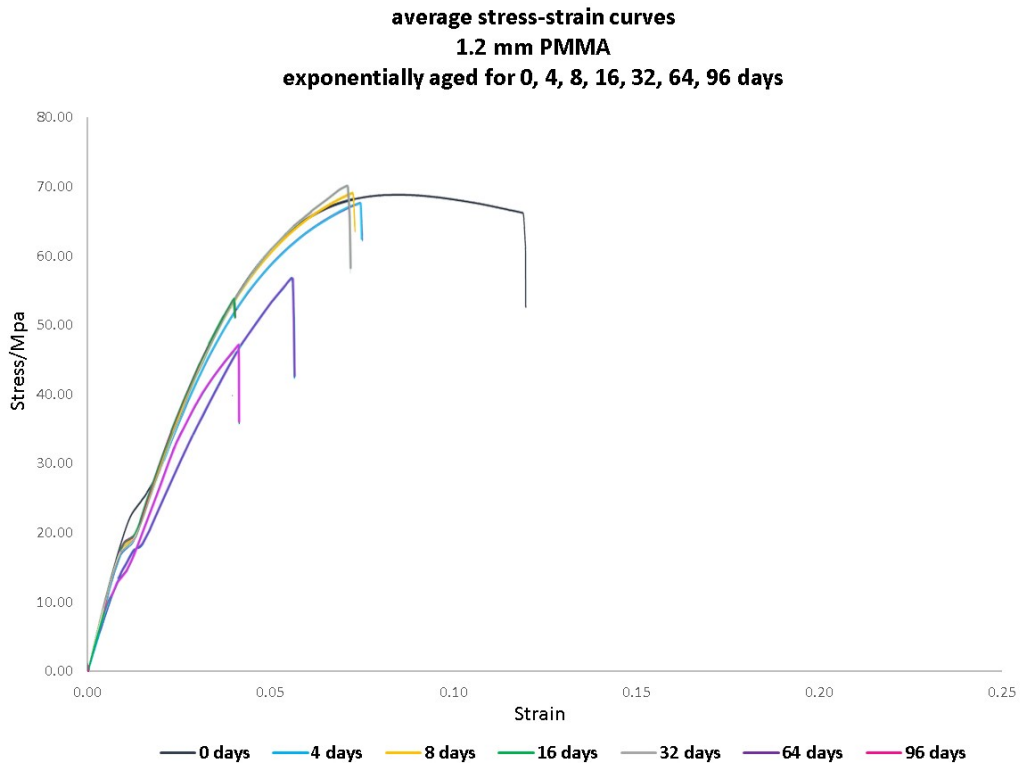
The material aged between 16 and 96 days appears less ductile and more brittle than the unaged, 4 and 8 days aged, based on the steeper curves of the samples (Graph 5.1). The curves exhibit no drawing, but a more abrupt break at the point of yield (Eve and Mohr 2010). This suggests possible crosslinking, preventing the chains from slipping past each other. Samples exposed for 16 days display two types of behaviour (lighter and darker green - Graph 5.1): three replicates show a ductile behaviour (Graph 5.3), closer to new, 4 and 8 days aged samples, whereas the remaining two replicates are more brittle (Graph 5.3), lacking the previous drawing seen in unaged PMMA and exhibiting an abrupt break, closer to samples aged for 64 and 96 days (purple and fuchsia respectively - Graph 5.1). This is confirmed by the large standard deviation in Graph 5.2. Material aged for 32 days (grey - Graph 5.1) shows steeper curves than after 16 days, with no drawing and a more abrupt break at the point of yield. After 64 days, PMMA shows very similar results to 32 days-aged samples, but with replicates displaying less variability in their breaking point. This is visible from the consistency between curves within the set (Graph 5.4). Samples aged for 96 days show the most brittle behaviour, with the fastest and most abrupt break (Graph 5.1). It is worth noting that consistency between the tensile behaviour of replicates within a set, increases with ageing. It is speculated that after longer exposures, crosslinking renders PMMA structure more homogenous as opposed to its amorphous, unstructured state when unaged (i.e. StDev of unaged replicates was 29.20, whereas after exposure of 32 days it dropped to 24.93). In fact, samples aged for 32, 64 (StDev: 25,51) and 96 days (StDev: 11,73) exhibited less variability in



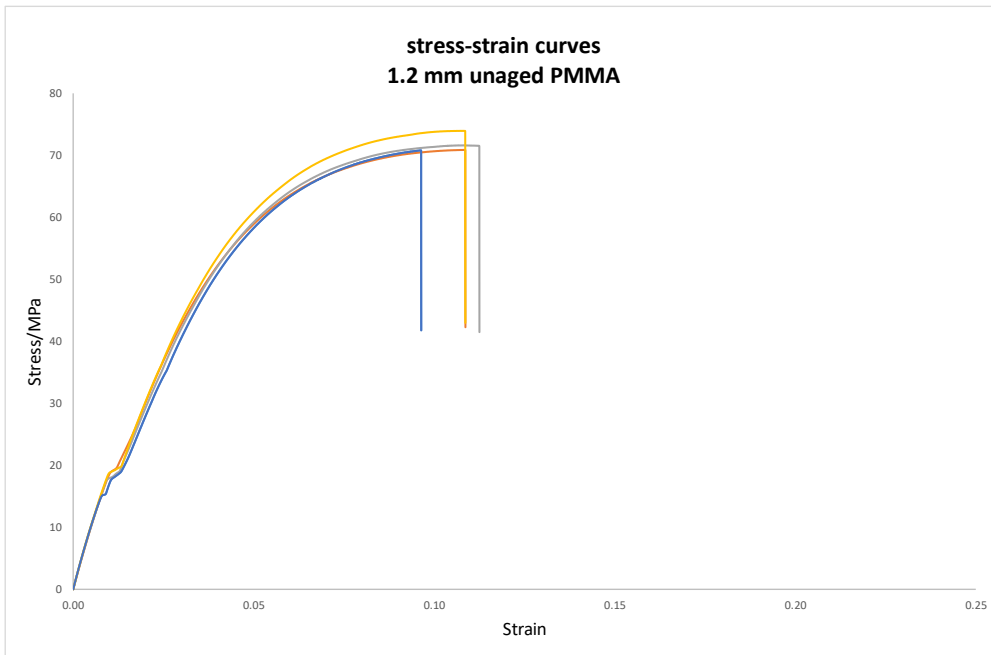
their breaking points, evident as an increase in consistency of stress-strain curves within sets (see Appendix F).



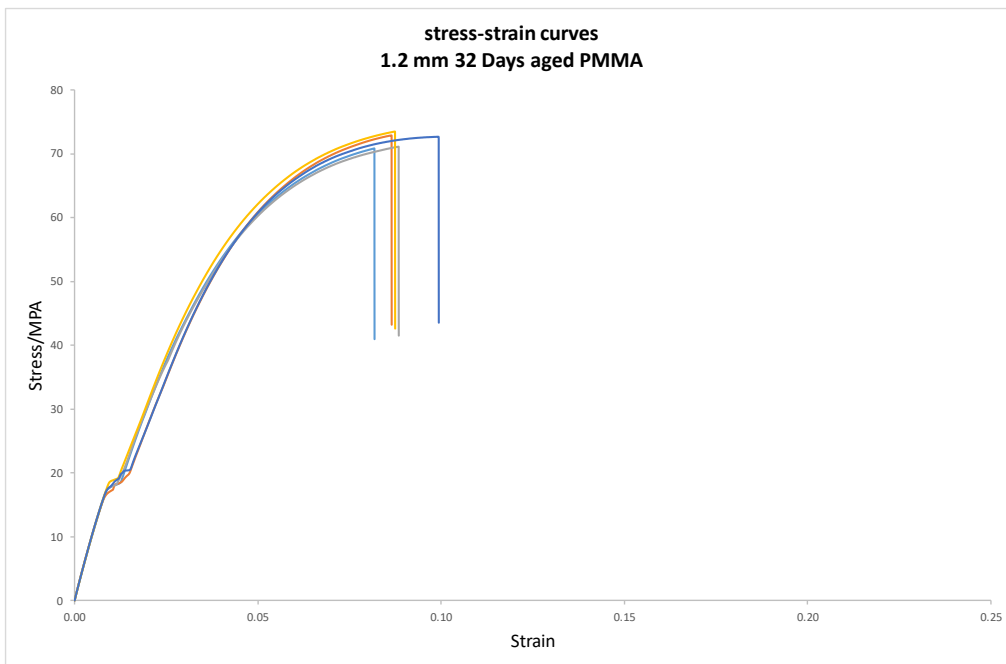
Graph 5.4. Stress-strain curves of 1.0 mm: set of five PMMA replicates UV-aged for 64 days.



Graph 5.5. Averaged stress-strain curves of unaged and exponentially aged 1.2 mm PMMA samples under UV radiation for 4, 8, 16, 32, 64 and 96 days.



Graph 5.6. Stress-strain curves of 1.2 mm: set of five unaged PMMA replicates.



Graph 5.7. Stress-strain curves of 1.2 mm: set of five PMMA replicates UV-aged for 32 days.

In the 1.2 mm grade, differences between the new and aged material are less distinct than in the 1.0 mm. The linear region at the very beginning of the curves is visible here too (Graph 5.5), whereas the break in the slope happens at a lower load than in the 1.0 mm PMMA, beginning at 15 MPa. The 1.2 mm grade appears stronger, with slightly higher load at break with respect to the 1.0 mm, and smaller apparent differences between the behaviour of new and aged replicates. This can be seen in the stress-strain curves for the unaged (Graph 5.6) and 32-days aged PMMA (Graph 5.7). The unaged material is slightly more ductile, but

overall the 1.2 mm samples are relatively brittle. This is evident by their lack of drawing, steeper curves and abrupt break at the point of yield. Given that differences between the new and aged replicates are more distinct in the 1.0 mm than in the 1.2 mm, the former is selected for further mechanical testing.

### 5.1.1.3. Dynamic Mechanical Analysis of exponentially aged material

DMA is the most commonly used technique for viscoelastic characterisation of polymers (Mark *et al.* 1993). It was performed on the 1.0 mm grade of new and exponentially aged PMMA and offered measurements of relaxation processes as a function of temperature (Duncan 2007; Dixit *et al.* 2009), as well as their  $T_g$  values. Through analysis, changes in the physical behaviour of samples due to the influence of various lengths of UV exposure (i.e. unaged and 32 days aged) enabled their comparison. Moreover, knowledge of their  $T_g$  yielded information about their mechanical properties over a wide temperature range (Ashby and Jones 2012). It was anticipated that dynamic mechanical behaviours of differently aged samples would be different. Not only did they exhibit different tensile properties, but their thermal history (Pethrick *et al.* 2011), as well as preparation (i.e. lack of consistency) (Belfiore 2010), are known to affect the value of  $T_g$ . Coupled with stress-strain curves, DMA offered complementary information that assisted in the understanding of PMMA chemical behaviour in different ageing stages.

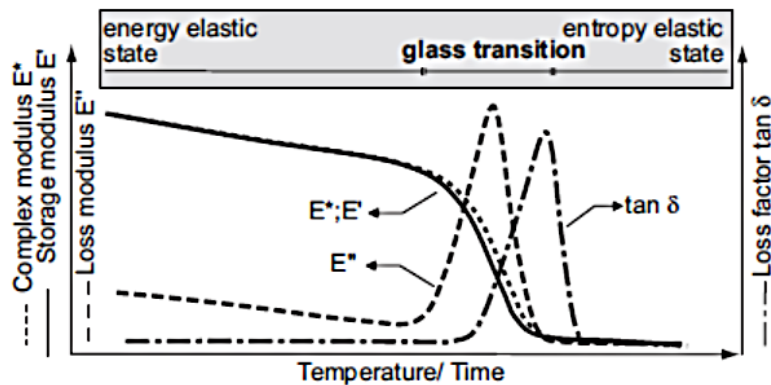


Figure 5.4. Schematic diagram of the DMA curve of the unaged PMMA sample analysed in this study (Ehrenstein *et al.* 2004, p. 239).

Viscoelastic materials, such as PMMA, consist of two components: an elastic and a viscous. DMA offers their dynamic response as modulus and tangent delta ( $\tan \delta$ ) (Xie *et al.* 2008). The modulus, also known as tangent, refers to the stiffness of a material and is divided in two phases: the elastic part expressed as storage modulus ( $E'$ ) and the viscous component expressed as loss modulus ( $E''$ ) (Duncan 2007). This energy dissipation of a material, often called damping, is measured with tan delta ( $\tan \delta$ ) (Øysæd 1990) and expressed as the ratio between loss (viscous component) and storage (elastic component) modulus ( $\tan \delta = E''/E'$ )

(Fig.5.4). Both the loss modulus and  $\tan \delta$  peaks are defined as the  $T_g$ , with the latter occurring at a higher temperature than the former (Nemat-Nasser et al. 2015).

Typical DMA curves of amorphous PMMA exhibit two relaxation processes, the  $\alpha$  and  $\beta$ , on decreasing temperatures (Fig.5.5). The  $\beta$ -relaxation has a very broad distribution of relaxation times, but is not involved in the physical ageing process as the main  $\alpha$ -relaxation (Muzeau *et al.* 1994), corresponding to the glass transition. Given that  $\alpha$ -relaxation ( $T_g$ ) is parameter dependant, the location of the two transitions on the temperature scale will shift when the heating rate of the measurement (Cowie 1991) or the parameters of the analysis are altered (i.e. temperature or rate of applied stress) (Yun *et al.* 2011).

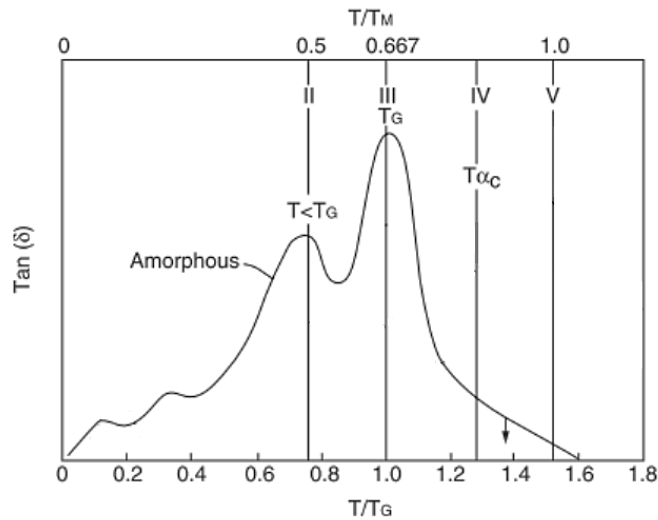


Figure 5.5. DMA curve of amorphous PMMA exhibiting two relaxation processes: the  $T_g$  ( $\alpha$ -relaxation) and  $T\beta$  (Chartoff *et al.* 2008, p. 411).

Glass transition temperature of various materials	
material	$T_g$ ( $^{\circ}\text{C}$ )
isotactic	Between 37-56
PMMA	~ 105
	Between 100-120
	Between 110-130
polycarbonate	145
polystyrene	95
Silica glass	1189
Fused quartz	~ 1200

Table 5.3. A range of exemplary  $T_g$  values of different materials and PMMA molecular arrangements/tacticities (Biroš *et al.* 1982; O'Reilly *et al.* 1982; Cowie 1991; Brydson 1999; Shaw and MacKnight 2005; Shin *et al.* 2005; Shashoua 2008; Villalobos and Debling 2013; Ionita *et al.* 2015).

DMA routinely applies a single frequency of 1 Hz for the analysis of PMMA (Wollny 2006; ASTM E1640-07; Dixit *et al.* 2009a; Dixit *et al.* 2009b). The bulk PMMA T<sub>g</sub> value is generally considered high, at approximately 100 °C. It is acknowledged that the T<sub>g</sub> occurs over a range of well-known temperature values (Table 5.3) (Shaw and MacKnight 2005; Chartoff *et al.* 2008) dependent on molecular composition, tacticity, and thermal treatments (Biroš *et al.* 1982; Pethrick *et al.* 2011; Bourhis 2014). For example, the T<sub>g</sub> of atactic and syndiotactic PMMA might display a difference of at least 20 °C (Ionita *et al.* 2015).

### Testing modes

DMA testing modes were based on the physical dimensions and properties of the polymer, which dictate the geometry needed for sample preparation (PerkinElmer 2013). For amorphous thermoplastics that are relative stiff, Ehrenstein *et al.* (2004) and Chartoff *et al.* (2008) recommend the general-purpose cantilever (single or dual) mode. McDonagh-Smith *et al.* (2001) tested three rectangular replicates of 3 mm thick PMMA copolymers in dual cantilever (McDonagh-Smith *et al.* 2001). Perkin Elmer (2011) - supplier of the DMA instrument used here - also favours single cantilever bending geometry for PMMA and also uses it for instrument calibration. Several other studies analysed PMMA in a variety of modes (Alves *et al.* 2004; Wollny 2006; Hub *et al.* 2007; Diani *et al.* 2015), but there was enough empirical work hitherto to support the decision to test current samples in single cantilever mode.

The basic principle of DMA requires a force or displacement in the form of a minor oscillation to be applied to the viscoelastic sample. The force could be a sinusoidal stress or a cyclic strain and is small enough not to alter the shape and size of the sample under analysis

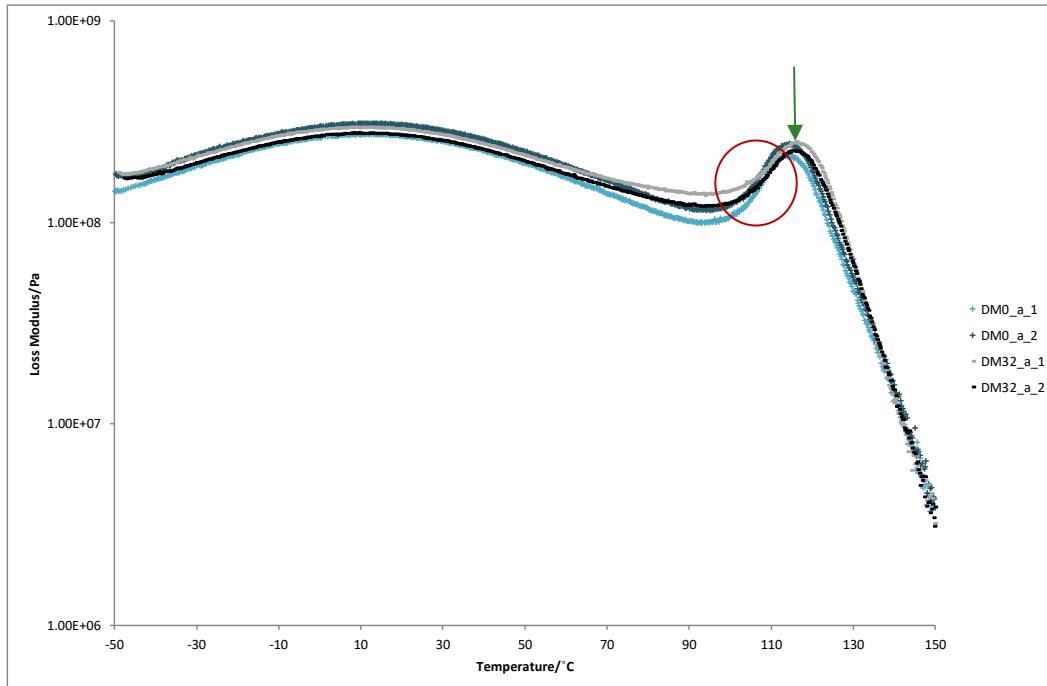


Figure 5.6. DMA 8000 Perkin Elmer.

(Dixit *et al.* 2009a). The sample is clamped between fixtures and enclosed in a thermal chamber. The appropriate frequency, amplitude, and temperature range were defined for the PMMA under scrutiny. The drive-shaft controlled the selected oscillation while slowly moving through the specified temperature range. A Perkin Elmer DMA 8000 (Fig.5.6) was employed with single cantilever bending geometry at 1 Hz with a heating rate of 2 °C/min.

Samples selected for destructive DMA were based on the tensile results presented above. The 1.0 mm unaged PMMA was selected as a reference material and the 32 days aged was selected because it embrittled in the shortest possible timeframe. Sets of two replicates were prepared following preparation dictated by the needs of the analysis. They were cut at

the IoM, UCL, from commercial transparent sheets by means of a circular saw in rectangular strips of 30 x 10 mm, before exposure to UV radiation.

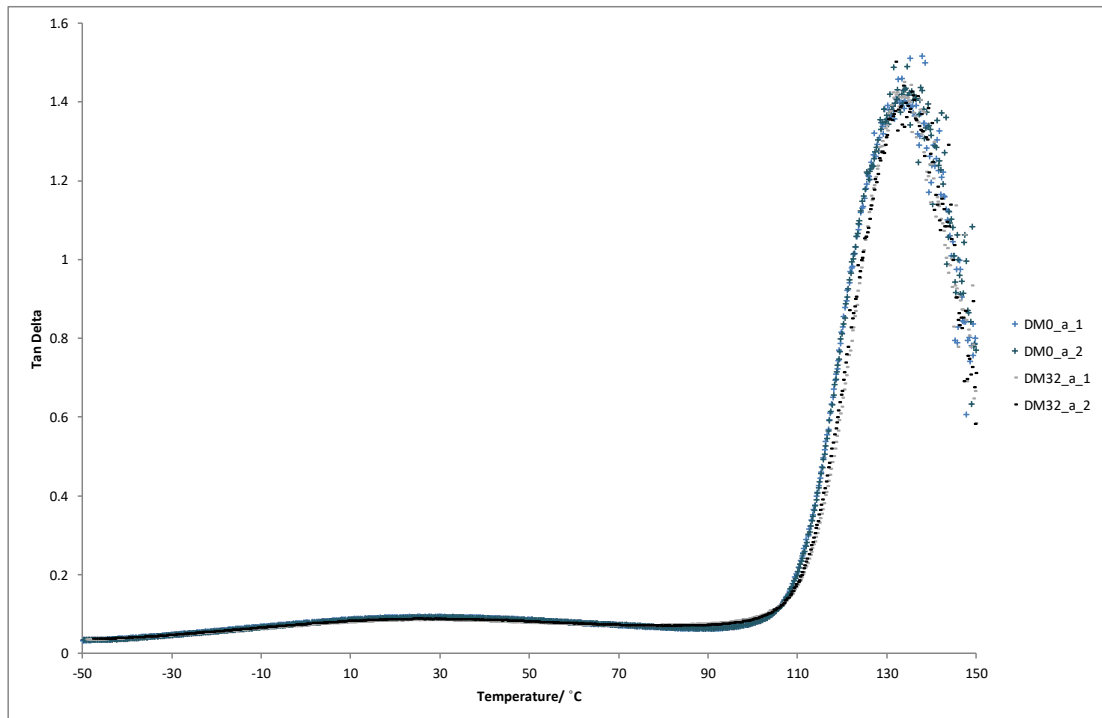


Graph 5.8. Curves of loss modulus of unaged (blue) and 32-days UV-aged (grey) PMMA of 1.0 mm as a function of temperature. The curves are averaged from two replicates.

The loss modulus curves (Graph 5.8) show the unaged (blue) and 32-days aged (grey) replicates. During heating up of viscoelastic PMMA, the elastic and the viscous components compete: the former decreases, while the latter increases. At temperatures below  $T_g$ , where PMMA is rigid and brittle, the storage modulus is high. Upon heating, the stiffness is expected to drop, along with the modulus (Ward and Sweeney 2013, 10), because less energy is required for segmental movement, denoting softening (Hayden *et al.* 1967). However, around the  $T_g$  (circled in red) an abrupt change takes place and the modulus exhibits an increase. At this point, the material shows some stiffening; a resistance to deformation caused by molecular friction and energy dissipation, until it reaches the glass transition (green arrow) and segmental motion is activated (Hayden *et al.* 1967).

The curves in Graph 5.8 are noticeably different before and after ageing. The unaged material (blue) shows a larger decrease right before forming a neck and narrower curves, whereas the aged material (grey) shows a lesser decrease before neck formation and broader curves. The altered shapes confirm that in unaged specimens, the  $T_g$  is lower than in the aged. The peak maximum of the loss modulus places the  $T_g$  values at 114 °C for the unaged and 116 °C for the 32 days aged PMMA. Changes in the  $T_g$  values are small, but the consistent nature of the heating curves indicates that the structure of the polymer has undergone photo-induced reactions. This confirms that anticipated changes in the material have taken place under UV

radiation. It needs to be underlined that  $T_g$  values are strongly dependant on the heating rate, heat treatment and processing history.

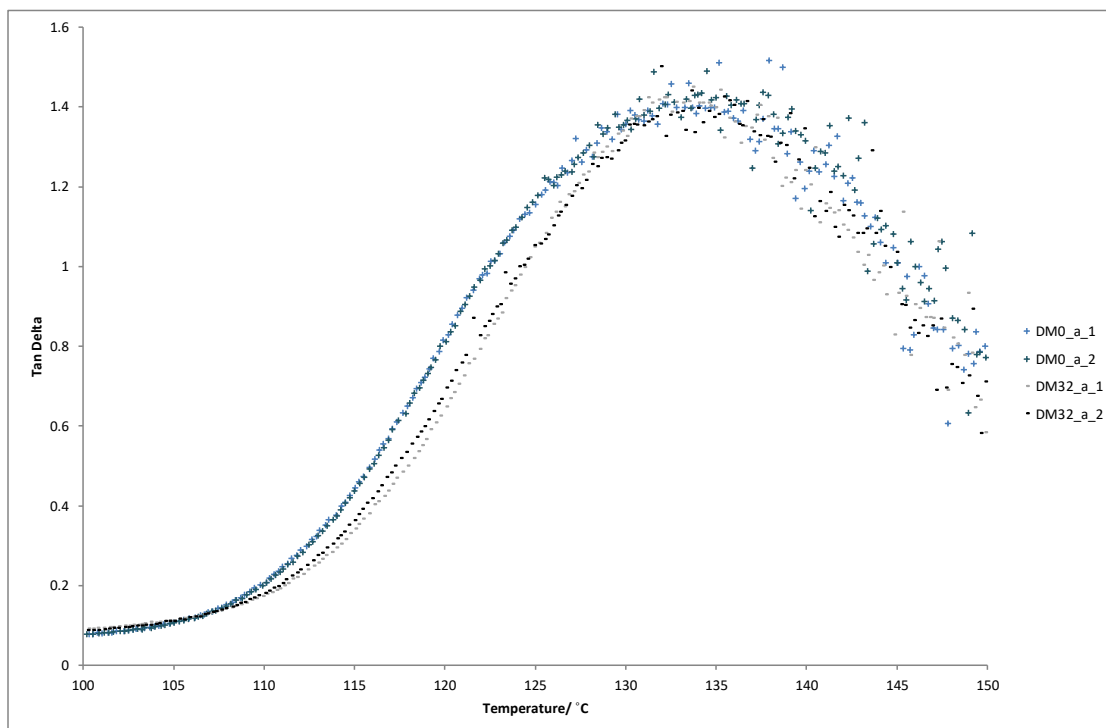


Graph 5.9. Curves of  $\tan \delta$  of unaged (blue) and 32-days UV-aged (grey) PMMA of 1.0 mm as a function of temperature. The curves are averaged from two replicates.

The curves of  $\tan \delta$  as a function of temperature (Graph 5.9) are also used to locate the  $T_g$  (Placido 2010). At the point of the highest temperature in loss modulus – where it attains sufficient heat energy to enable mobility –  $\tan \delta$  reaches a maximum (seen as a peak in the curves), identified as the  $T_g$ . The material becomes viscous due to secondary transitions causing local relaxations. Beyond this point  $\tan \delta$  consistently decreases and the material passes from viscoelastic to more viscous causing a further drop on loss modulus (Hayden *et al.* 1967; Ashby and Jones 2012).

The magnified curves of  $\tan \delta$  (Graph 5.10) show that there is a measurable difference between unaged and aged samples. The curves of replicates are superimposed in a consistent fashion, indicating that the change recorded is a real phenomenon, rather than an error. Changes observed with ageing are not dramatic, but are definite. In the unaged PMMA (blue curves), the  $T_g$  is marginally lower than in the aged, indicating that the aged samples are more brittle. Differences in the curves shapes also indicate this; the grey curves of the 32-day aged samples are sharper, narrower, and have slightly shifted, suggesting that the material is more brittle. This is attributed to crosslinking, induced by UV radiation (polymerisation), causing restraint of the segmental movement. With crosslinks, amorphous PMMA gains some form of stability that renders the structure more resistant to movement upon applied stress (Min *et al.*

2014). In the unaged material, the curves are broader and less well defined, due to the amorphous structure of untangled chains; this broader shape suggests greater inhomogeneity in molecular packing.



Graph 5.10. Close up of the  $\tan \delta$  peak ( $T_g$ ) of unaged (blue) and 32-days UV-aged (grey) PMMA of 1.0 mm seen in Graph 5.9.

## 5.1.2. CHARACTERISATION OF POLY (METHYL METHACRYLATE)

### 5.1.2.1. Attenuated total reflectance Fourier transform infrared spectroscopy

ATR-FTIR is commonly employed for chemical surface analysis, useful in the identification of the composition of polymers (Chiantore *et al.* 2003; Stuart 2004; Asensio *et al.* 2009; Ghosh 2010) and their components, i.e. additives. Coupling FTIR with ATR is considered ideal for analysis of plastics (Derrick *et al.* 1999; Asensio *et al.* 2009), especially when combined with a microscope. It has been frequently used to determine changes in the molecular structure of polymeric materials (Nagai *et al.* 2005; Miller *et al.* 2010; Troiano *et al.* 2014), particularly valuable when studying and monitoring effects of ageing and/or chemical agents (Urbaniak-Domagala 2012) and (ongoing) degradation processes (Haider and VanOosten 2009; Lazzari *et al.* 2011; Winther *et al.* 2013). Here, it was employed to characterise the selected 1.0 mm thick PMMA, in its unaged and aged state. Analysis aimed to understand the PMMA tacticity, as well as monitor structural changes caused by UV radiation. Samples here were transparent, but presence of additives, such as colorants, would change the observed ageing behaviour and thus, result in different spectra. For a detailed description of ATR-FTIR technique and analytical parameters see Chapter 6.4.



## IR spectra of new &amp; 32-days UV-aged PMMA

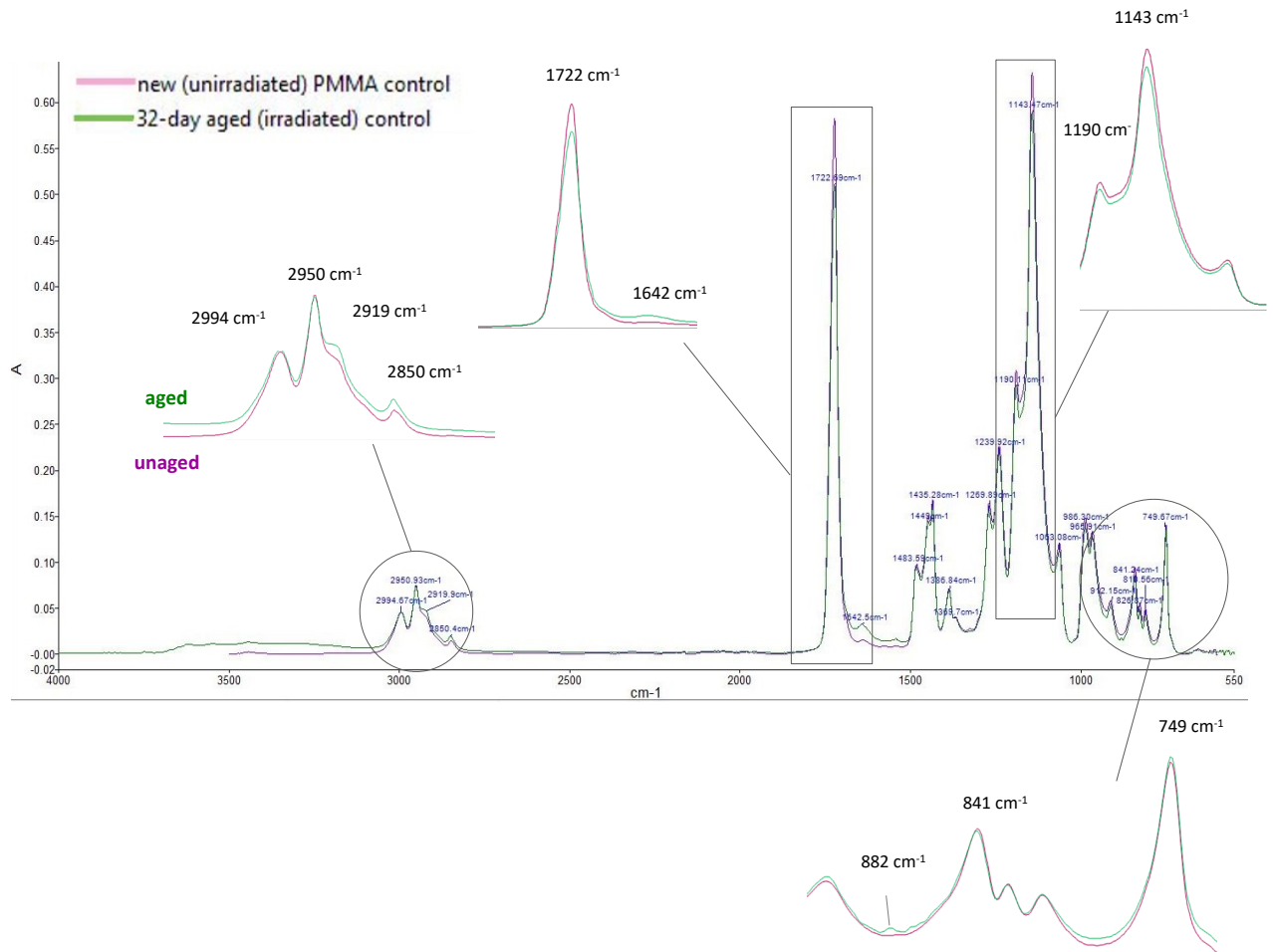


Figure 5.7. Spectra of unaged (pink line) and 32 days UV-aged (green line) reference PMMA. Peaks were enlarged and labelled inset. The spectra were averaged from three replicates.

#### 5.1.2.1.a. New poly (methyl methacrylate)

In the spectrum of unirradiated PMMA (Fig.5.7), absorption bands in the region between 3000-2800  $\text{cm}^{-1}$  are fundamental stretching vibrations of the methyl ( $\text{CH}_3$ ) in the ester side group (Nagai 1963). Two distinct peaks at 2995 and 2950  $\text{cm}^{-1}$  are characteristic of the stretching vibration of  $\text{O}-\text{CH}_3$  in the ester side group, while peaks 2920 and 2850  $\text{cm}^{-1}$  are attributed to combination bands also associated with the ester methyl ( $\text{CH}_3$ ) (Nagai 1963; Eve and Mohr 2010; Kaczmarek *et al.* 2010). The strong absorption of peak 1723  $\text{cm}^{-1}$  is characteristic of carbonyl ( $\text{C}=\text{O}$ ) stretching vibration in the ester side group. Bands 1483  $\text{cm}^{-1}$ , 1387  $\text{cm}^{-1}$  and 965  $\text{cm}^{-1}$  are attributed to the  $\alpha$ -methyl group ( $\alpha\text{-CH}_3$ ) in the main chain (Nagai 1963), whereas band 1447  $\text{cm}^{-1}$  to the methylene group ( $\text{CH}_2$ ) in the main chain. Absorption at 1435  $\text{cm}^{-1}$  is assigned to the stretching vibration of  $\text{O}-\text{CH}_3$  in the ester side group (Nagai 1963; Dybal and Krimm 1990; Kaczmarek *et al.* 2010). The weak band at 1369  $\text{cm}^{-1}$  may correspond to the amorphous band associated with vibrations of the main chain methyl ( $\alpha\text{-CH}_3$ ) (Nagai 1963). Bands between 1300-1000  $\text{cm}^{-1}$ , such as absorptions at 1270  $\text{cm}^{-1}$  and 1240  $\text{cm}^{-1}$ , are attributed to  $\text{C}-\text{C}-\text{O}$  between

the main chain and the ester side group (Nagai 1963; Kaczmarek *et al.* 2010). Strong absorptions at  $1190\text{ cm}^{-1}$ ,  $1144\text{ cm}^{-1}$  and  $986\text{ cm}^{-1}$  are assigned to C–O–C stretching in the ester side group (Nagai 1963; Liu *et al.* 2006; Kaczmarek *et al.* 2010). Peaks between  $1000\text{--}800\text{ cm}^{-1}$ , such as peak  $1063\text{ cm}^{-1}$ , are generally associated with main chain C–C stretching vibrations (vinyl absorption) of PMMA (Duan *et al.* 2008). Band  $965\text{ cm}^{-1}$  is associated with vibrations of the  $\alpha$ -methyl ( $\alpha\text{-CH}_3$ ) in the main chain (Nagai 1963) and peaks located at  $840\text{ cm}^{-1}$  (Kaczmarek *et al.* 2010) and  $749\text{ cm}^{-1}$  with vibrations of the methylene group ( $\text{CH}_2$ ), also in the main chain (Nagai 1963). For a detailed list of all absorption peaks of unaged PMMA refer to Table 5.4.

PMMA. Diagnostic IR absorptions and assignments	
Wavenumber ( $\text{cm}^{-1}$ )	Tentative band assignment
3400	–O–H stretch
2995, 2950	O–CH <sub>3</sub> (ester group)
2920, 2850	CH <sub>3</sub> (ester group)
1723	C=O (ester group)
1640	C=C (main chain)
1483, 1387	$\alpha\text{-CH}_3$ (main chain)
1447	CH <sub>2</sub> (main chain)
1435	O–CH <sub>3</sub> (ester group)
1270, 1240	C–C–O (ester group)
1190, 1144, 986	C–O–C (ester group)
1063	C–C skeletal (main chain)
965	$\alpha\text{-CH}_3$ (main chain)
882	C=CH <sub>2</sub>
840, 749	CH <sub>2</sub> skeletal (main chain)

Table 5.4. Assignments of diagnostic IR absorptions of the unaged (unirradiated) and aged (irradiated) PMMA reference analysed with ATR-FTIR. The new bands formed with ageing are circled in blue.

### 5.1.2.1.b. UV-aged/irradiated poly (methyl methacrylate)

The reported effects of UV absorption are not consistent; photo-oxidative degradation is reported to cause a number of competitive reactions and phenomena, expected to take place simultaneously. These reactions include main chain scission of C–C bonds, side group cleavage of the pendent ester (methoxycarbonyl) (COOCH<sub>3</sub>) or the methyl (CH<sub>3</sub>) in the ester group, formation of new oxidised products and free radicals, crosslinking, and direct UV-depolymerisation (unzipping) (Çaykara and Güven 1999; Kaczmarek and Chaberska 2006; Kaczmarek *et al.* 2010). During unzipping, MMA could be lost/released from the end of the polymer chain, once scission has started, while free radicals are commonly generated (Aboueiezz and Waters 1978).

ATR-FTIR chemical analysis focused on the material surface, rendering it particularly valuable for monitoring PMMA photo-oxidative reactions due to UV radiation in air (not to be confused with thermal degradation). The effect of oxygen on the degrading polymer is known to be most prominent near the exposed surface (Brown and Kashiwagi 1996). This type of photo-oxidative degradation is a free radical chain process that once initiated on the surface layers, can penetrate through surface defects and propagate into the material bulk even without light (Kaczmarek and Chaberska 2006). Cracks, holes, or openings created on the surface by MMA monomer vapor leach into the air from within the bulk (Brown and Kashiwagi 1996), allow the migration of reactive species (i.e. unbound oxygen, free radicals) out of the material leading to polymer vaporisation (gasification) (Eve and Mohr 2009).

Following UV exposure for 32 days, the IR spectrum (Fig.5.7) shows distinct changes: formation of a broad absorption centred around 3400 cm<sup>-1</sup> (between 3700-3000 cm<sup>-1</sup>), increase of shoulder peaks 2920 cm<sup>-1</sup> and 1642 cm<sup>-1</sup>, decay of bands 1723 cm<sup>-1</sup>, 1270/1240 cm<sup>-1</sup> and 1190/1144 cm<sup>-1</sup> and formation of a new, small band at 882 cm<sup>-1</sup> (see Table 5.4).

#### Formation of oxidised structures

The broad band centred around 3400 cm<sup>-1</sup> is evidence of photo-oxidation, demonstrating the presence of oxidised structures resulting from substitution of C–H bonds by hydroxyl groups (–OH bonds) (Luo *et al.* 1993; Kaczmarek *et al.* 2010). The new PMMA does not contain hydroxyl groups.

#### Main chain scission

There are no main chain scission reactions evidenced in the spectrum of the UV-aged PMMA.

#### Ester side group scission/cleavage

An increase of shoulder peak absorbance at 2920 cm<sup>-1</sup> along with an increase in the absorption and amplitude of 2850 cm<sup>-1</sup> confirm chain scission reactions in the methyl (CH<sub>3</sub>) in the ester side group. The decrease in intensity of peaks 1270 cm<sup>-1</sup> and 1240 cm<sup>-1</sup> evidences complete

side group elimination from the main chain upon UV radiation (Eve and Mohr 2010). In this case the resulting chemical structure is  $\text{CH}_2=\text{C}-\text{CH}_3$ . The presence of oxidised structures at  $3400\text{ cm}^{-1}$  also suggests separation of the  $\text{O}-\text{CH}_3$  from the carbonyl group  $\text{C}=\text{O}$  (incomplete ester separation) (Wochnowski *et al.* 2005). A decrease in the carbonyl absorption (reduction of peak  $1723\text{ cm}^{-1}$ ) is attributed to loss of the  $\text{C}=\text{O}$  bond (Kaczmarek and Chaberska 2006), seen as a result of scission of the pendant ester group (Wochnowski *et al.* 2005) from the main chain. A decrease in intensity of the peaks at  $1190\text{ cm}^{-1}$  and  $1140\text{ cm}^{-1}$  confirm ester group chain scissions (Wochnowski *et al.* 2005).

#### Formation of C=C bonds

The increase of absorption at  $1640\text{ cm}^{-1}$  is attributed to the generation of carbon double bonding (C=C bonds/vinyl unsaturation), resulting from several, often conflicting, processes.

- *Complete or incomplete ester side group cleavage*, earlier confirmed by an increase of peaks  $1270/1240\text{ cm}^{-1}$ , decrease of  $1723\text{ cm}^{-1}$  and absorption at  $3400\text{ cm}^{-1}$ , are known to lead to carbon double bonding (C=C) in the main chain (Choi *et al.* 1988; Stansbury and Dickens 2001; Wochnowski *et al.* 2005).
- *Main chain radicals* formed after complete ester side group cleavage (McNeill *et al.* 1995), may have formed crosslinks between them, leading to the generation of unsaturated C=C bonds (Rai *et al.* 2016).
- *Incorporation of oxygen (O=O)* in the main polymer chain may have caused random chain scission generating a terminal vinyl group, which would act as a weak link from which depolymerisation could initiate (Brown and Kashiwagi 1996; Holland and Hay 2001). Oxygen is also capable of causing hydrogen-abstraction, leading to the formation of hydroxyl groups (oxidised structures), confirmed here by the new broad absorption at  $3400\text{ cm}^{-1}$ . In both cases, carbon double bonds arise as a result of oxygen incorporation (Choi *et al.* 1988).

Absorptions at  $965\text{ cm}^{-1}$  and  $750\text{ cm}^{-1}$  have been reported to remain unaltered with increasing temperature (Tretinnikov and Zhbankov 1991), a phenomenon anticipated to occur in the accelerated weathering chamber during 32 days. Here, band  $965\text{ cm}^{-1}$  is associated with vibrations of the  $\alpha$ -methyl ( $\alpha\text{-CH}_3$ ) and peak  $749\text{ cm}^{-1}$  with vibrations of the methylene ( $\text{CH}_2$ ), both found in the polymer backbone (main chain), where no evidence of scission is seen in the ATR spectra. Hence, both bands have remained unaltered during the light ageing of PMMA.

The appearance of a new, small band at  $882\text{ cm}^{-1}$  (Fig.5.7) is assigned to the  $\text{C}=\text{CH}_2$  (Coates 2000) between the  $\alpha$ -carbon and the  $\alpha$ -methylene ( $\text{CH}_2$ ) comprising the polymer backbone. This double bond, absent in the new material, is a clear indication of UV ageing of PMMA, during which several processes, including side group eliminations and oxidation, gave

rise to vinyl unsaturation. Absorption at  $882\text{ cm}^{-1}$  is characteristic of the crystalline phase of PMMA (Dybal and Krimm 1990; Luo *et al.* 1993), and is typically weak or barely visible as a shoulder (Luo *et al.* 1993). It has been suggested that existence of crystalline structures at  $882\text{ cm}^{-1}$  is evidence of annealing (Luo 1994). Industrially annealed PMMA is carried out at temperatures around  $70\text{-}90\text{ }^{\circ}\text{C}$  (Comiotto and Egger 2009), near, but sufficiently below the polymer's  $T_g$  at  $114\text{ }^{\circ}\text{C}$ . However, a study has shown that any controlled thermal treatment, even conditioning of PMMA at room temperature for three months, could cause a more highly organised structure (Grohens *et al.* 2001). In this study, annealing is interpreted as the thermal/heating process that the aged samples underwent during UV exposure for a period of 32 days. The Atlas weathering chamber temperature was lower than standard annealing temperatures for PMMA but remained constant at  $38\text{ }^{\circ}\text{C}$  for 32 days. Theory dictates that the lower the temperature, the weaker the absorption, which explains the relatively small, but distinct absorption at  $882\text{ cm}^{-1}$ .

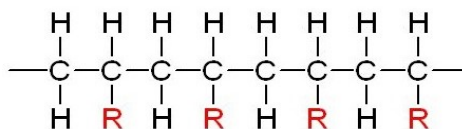
Increased signal documented in the absorption spectrum after UV radiation, indicates formation of crosslinking structures or double bonds. It has not been possible to confirm crosslinks based on the FTIR data obtained, as earlier anticipated.

#### **5.1.2.1.c. Tacticity of poly (methyl methacrylate)**

FTIR analysis has been commonly employed to monitor the crystallinity of polymer chains and identify the molecular conformation, also known as surface stereoregularity or tacticity, of polymers in their surface vicinity (Tretinnikov 1999). The two PMMA tactic forms, isotactic (*iso-*) and syndiotactic (*syn-*) (Fig.5.8), are formed from the same MMA monomer unit, which renders them chemically identical. Differences in their surface behaviour are strictly attributed to the difference in their conformational characteristics (Tretinnikov 1999). In the PMMA under study, several bands - especially those found in the  $1300\text{-}1100\text{ cm}^{-1}$  region, known to be very sensitive to tacticity (Grohens *et al.* 1998; Shin *et al.* 2002), are characteristic of *syn*-PMMA (Nagai 1963; Chuanfu *et al.* 1994). The strong bands at  $1438\text{ cm}^{-1}$ ,  $1270\text{ cm}^{-1}$  and  $1240\text{ cm}^{-1}$  (Tretinnikov 2003),  $1063\text{ cm}^{-1}$  and  $750\text{ cm}^{-1}$  (Nagai *et al.* 1962; Tretinnikov and Ohta 1998) seen in the unaged reference spectrum (pink line-Fig.5.7), are strictly encountered in *syn*-PMMA (Tretinnikov 1999).

**isotactic**

functional group R on the same side of the main polymer chain

**syndiotactic**

functional group R on alternate sides of the main polymer chain

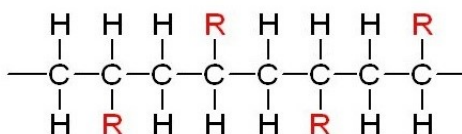


Figure 5.8. Conformational characteristics of isotactic and syndiotactic polymers (Reusch 2013).

The tacticity of a polymer can be confirmed through its T<sub>g</sub>. According to studies, isotactic PMMA is expected to display values of 45 °C, whereas syndiotactic values of 115 °C (O'Reilly and Mosher 1981). Earlier DMA performed to document differences in glass transition values between the unaged and 32-days aged PMMA grades, showed that the T<sub>g</sub> of the new is in the order of 114 °C and that of the aged 116 °C, confirming the syndiotacticity of the PMMA under study.

#### 5.1.2.2. Pyrolysis-Gas Chromatography/Mass Spectrometry

The new and 32 days aged samples (one replicate each condition) were chemically analysed with py-GC/MS, aiming to aid understanding of PMMA degradative behaviour. A Frontier Lab PY-2020D double-shot pyrolyser was used. The pyrolysis interface was maintained at 320 °C. The pyrolyser was interfaced to an Agilent Technologies 5975C inert MSD/7890A GC/MS. A Frontier Ultra ALLOY-5 capillary column was used for the separation (30 m x 0.25 mm x 0.25 μm), with helium carrier gas set to 1 ml/minute. The split injector was set to 320 °C with a split ratio of 50:1 and no solvent delay. The GC oven temperature program was 40 °C for 2 minutes, then ramped to 320 °C at 20 °C/minute, followed by a 9-minute isothermal period. Samples were placed into a 50 μl stainless steel Eco-cup fitted with an Eco-stick, and pyrolyzed using a single-shot method at 550 °C for 6 seconds. The analysis was carried out by the Getty Conservation Institute.

Results (Fig.5.9) showed different decomposition products (structural fragments) during the pyrolysis of samples. The primary products of thermal decomposition of 32 days UV-aged PMMA were 2-Methyloxirane-2-carboxylic acid, methyl ester (CAME) (Fig.5.10) and Propanoic acid, 2-oxo-, methyl ester (PAME), also reported as Methyl pyruvate (Fig.5.11), with CAME being the most abundant. These are oxidised chain scission products formed by the oxidative degradation of PMMA and correspond to the two peaks altered substantially after UV ageing. The mechanism of their formation is as follows: gas phase oxygen (atmospheric) initiated random main chain scission at weak links in the PMMA backbone (Brown and

Kashiwagi 1996) by hydrogen-abstraction and subsequent formation of reactive radicals (possibly oxy) (Peterson *et al.* 1999).

In detail, oxygen attacks the most labile hydrogen, activated by the terminal vinyl or vinylidene group ( $C=CH_2$ ), and to a lesser extent the ester groups, to form a hydroperoxide. The latter undergoes  $\beta$ -scission to produce a hydroxyl ( $-OH$ ) terminated compound and a carbonyl ( $C=O$ ) vinyl ester compound (or oxo-vinyl ester) (Brown and Kashiwagi 1996; Peterson *et al.* 1999). The final fragment generated from this radical reaction contains a weak  $C=C$  terminal group, from which depolymerisation (unzipping) is initiated. Rearrangement of radicals from the same terminal  $C=C$  group, along with hydrogen-abstraction from another neighbouring molecule, gave rise to CAME. Reaction of the oxy radicals with oxygen yields peroxy radicals, subsequently converted to different types of radicals and finally decomposition. This decomposition reaction leads to the formation of PAME (Song *et al.* 1992).

PAME appears at 3.33 minutes in the mass spectrum with a probability of 92.3 %. The mass spectrum of the compound appearing at 4.74 minutes, displays a 46.3 % probability of matching the structure of CAME. CAME has been previously identified as a major compound in the condensable volatile products of PMMA pyrolysis, and was almost exclusively found along with PAME (Song *et al.* 1992), supporting their characterisation. Other major constituents of the PMMA thermal ageing seen here, apart from the CAME and PAME oxidation products of the MMA monomer, are the free radicals produced as reactants, products or by-products from the oxidised MMA (Martin *et al.* 1987).

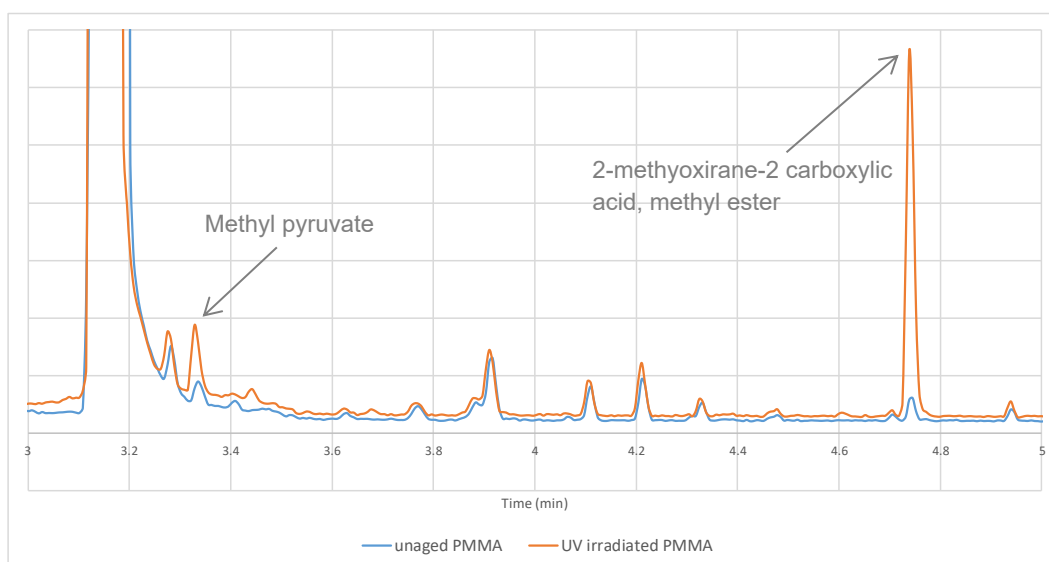


Figure 5.9. Normalised comparison between unaged and UV-aged PMMA. With ageing two peaks were altered substantially: at 3.33 minutes appearance of Methyl pyruvate (or Propanoic acid, 2-oxo-, methyl ester) and at 4.74 appearance of 2-Methoxyirane-2-carboxylic acid, methyl ester.

Chemical structures of the pyrolysis products/compounds of PMMA:

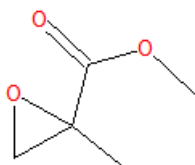


Figure 5.11.

2-Methyloxirane-2-carboxylic acid, methyl ester  
(CAME)

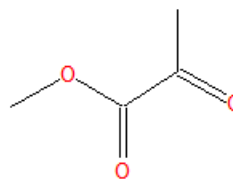


Figure 5.10.

Methyl pyruvate  
Or Propanoic acid, 2-oxo-, methyl ester  
(PAME)

Results also showed that the oxidative chain scission is the main reaction during the thermal degradation of PMMA. The decomposition of hydroperoxides formed by the free radical initiated oxidation, leading to the formation of PAME, has previously proven responsible for both chain scission and crosslinking mechanisms (Gugumus 1990). The mechanisms described here, resulting from PMMA pyrolysis, are not anticipated to be the only (nor the exact) reactions occurring during photolysis. To understand the oxidative degradation of PMMA exposed to UV radiation in a controlled environment, it is important to correlate the py-GC/MS results with the IR absorptions documented by ATR-FTIR. It proved challenging to distinguish the presence of crosslinks – if any – on the basis of FTIR (Ennis and Kaiser 2010; Kaczmarek *et al.* 2010), so additional data from gravimetric studies and previous tensile tests of the unaged reference and exponentially UV-aged samples, are also considered to investigate the possible occurrence of crosslinks in the aged material.

### 5.1.2.3. Discussion of gravimetric study, mechanical testing & chemical analysis

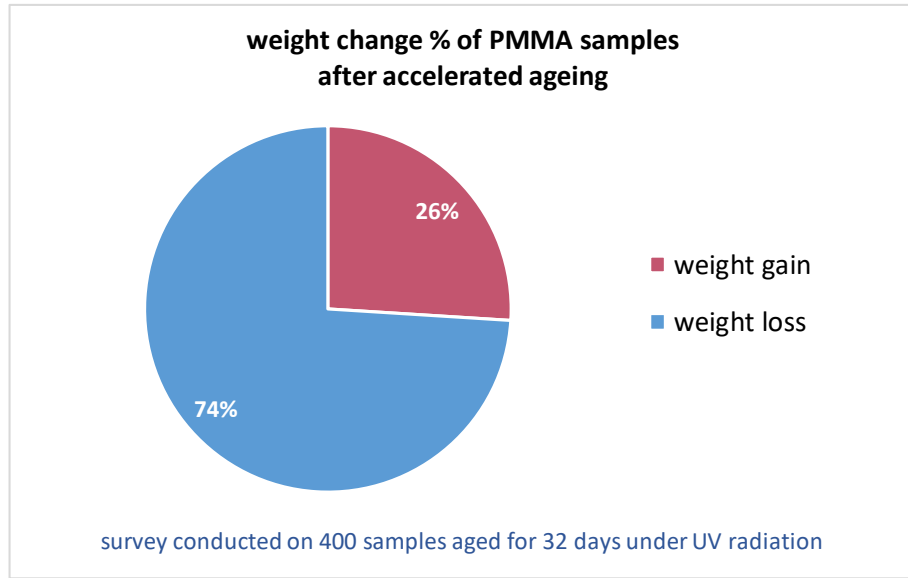
#### Weight changes

PMMA samples were aged for 32 days under UV radiation in five batches of roughly 190 samples each ( $n=1000$  samples), as described in Appendix C. Samples were prepared, handled and aged under standardised conditions. Their weight changes after exposure are measured relative to the initial, pre-ageing weight and expressed as percentage change, aiming to document gravimetric trends after ageing. The use of weight changes has been suggested as an index for the stability of acrylic polymers (Chiantore *et al.* 2000). Coupling gravimetric with tensile data, ATR-FTIR analysis and peak height ratioing offers a holistic approach to the interpretation of PMMA's ageing behaviour. Four hundred samples were randomly selected and their weight change trend was examined.

Graph 5.11 shows that the majority of aged samples lost weight after exposure, due to photodegradation and chain scission reactions (Shashoua 2008). The weight loss, however, does not exclude the simultaneous development of crosslinks. Crosslinking could cause an increase in weight (Shashoua 2008; Maitra and Shukla 2014) (also observed), but may have



occurred concurrently with the formation of volatile fragments (Eve and Mohr 2010). This means that photodegradation reactions are potentially competitive: chain scission and evaporation of products are manifest as weight loss (Çaykara and Güven 1999; Eve and Mohr 2010), whereas crosslinks as weight gain. Some loss during ageing in the chamber may also be attributed to the leaching of unreacted residual monomer from the polymerisation reaction (Gates and Grayson 1999; Ayre *et al.* 2014). Even if all three reactions were to happen simultaneously, it appears that weight loss is favoured.



*Graph 5.11. Weight change % of PMMA samples after 32 days UV ageing in the Atlas chamber. The 74 % of the aged samples (%) (blue) show weight loss and 26 % (%) (magenta) show weight gain. Weight changes are measured relative to the initial, pre-ageing weight.*

### Tensile data

Mechanical properties of polymers are directly related to their molecular weight (Eve and Mohr 2010), so a presumed reduction in properties is linked to a decrease in weight (Aboueiezz and Waters 1978). In turn, molecular weight is directly related to chemical degradation. Following PMMA degradation, tensile strength and elongation at break are expected to decrease in case of chain scission or increase in case of crosslinking (Çaykara and Güven 1999).

Revisiting the averaged maximum load of new and aged PMMA samples (Graph 5.2), discussed in section 5.1.1.2 of this chapter, it becomes clear that the tensile strength values of aged PMMA are higher (max average load 669,40 MPa) than values of unaged (max average load 644,85 MPa). This suggests crosslinking caused by UV radiation (Eve and Mohr 2010), also supported by the lack of drawing in aged samples, as crosslink formation prevents the chains from slipping past each other. This interpretation is in line with Eve and Mohr (2010), who observed that UV-exposed PMMA initially undergoes a crosslinking process accompanied by an

increase in tensile strength, and then a decrease that can be related to subsequent breaking of the polymer chains. Tensile data of the exponentially aged PMMA support this argument; UV irradiated samples after 4 days show an increase in maximum load, followed by a subsequent decrease after 8 and 16 days. The same pattern of an increase in maximum load is observed after 32 days, followed by a decrease after 64 and 96 days, associated with the higher irradiation doses causing PMMA's chain scission.

#### ATR-FTIR of exponentially UV-aged PMMA

FTIR was employed at the different stages of UV ageing to monitor chemical changes of PMMA surface layers. Spectra of samples after 4, 8 and 16 days show similar absorption bands to the unaged samples (Fig.5.12), suggesting no photo-destruction. Changes in the absorption spectra become evident after 32 and 64 days, with samples presenting similar absorptions. Spectra after 96 days show similar changes to that of 32 and 64 days, but are more prevalent.

Spectra of samples exposed for 32, 64 and 96 days, display a broad absorption around  $3400\text{ cm}^{-1}$  and a decrease of peak  $1723\text{ cm}^{-1}$ . These changes suggest a comparable quantity of oxidised products formed and loss of the carbonyl bond due to ester side group cleavage. Samples after 32 and 64 days show a comparable increase of shoulder peak  $2920\text{ cm}^{-1}$  and peak  $2850\text{ cm}^{-1}$ , while after 96 days, spectra show larger absorptions of the respective bands, indicating scission reactions in the ester methyl ( $\text{CH}_3$ ).

The intensity of peak  $1642\text{ cm}^{-1}$ , attributed to the formation of carbon double bonding is more dominant in samples exposed for 32 days. The increased formation of C=C bonds is interpreted as an increased presence of crosslinks (Rai *et al.* 2016). That is in agreement with the tensile data, where, as earlier explained, samples aged for 32 days exhibit the highest tensile strength among the exponentially aged samples attributed to crosslinking. The fact that tensile strength drops after 32 days (at 64 and 96 days), supports the conclusion that an increase in strength, denoting crosslinking, is followed by a decrease, suggesting chain scissions.

A steady and consistent decrease of bands in the  $1500\text{-}1000\text{ cm}^{-1}$  range is equally displayed in the 32, 64 and 96 days aged spectra, evidencing comparable damage to the ester side groups, including chain scissions between group bonds (Wochnowski *et al.* 2005), as well as complete elimination from the polymer chain (Eve and Mohr 2010). Spectral changes examined here confirm the photo-destruction of PMMA (Kaczmarek and Chaberska 2006).

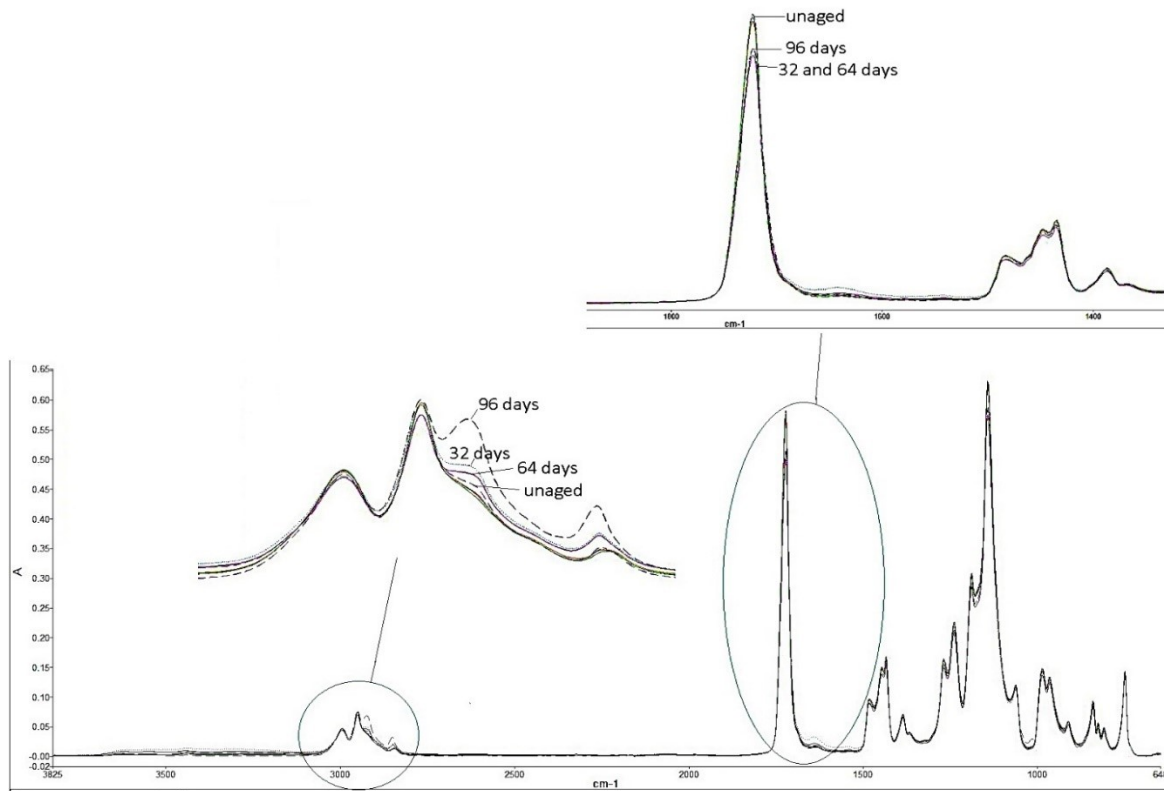
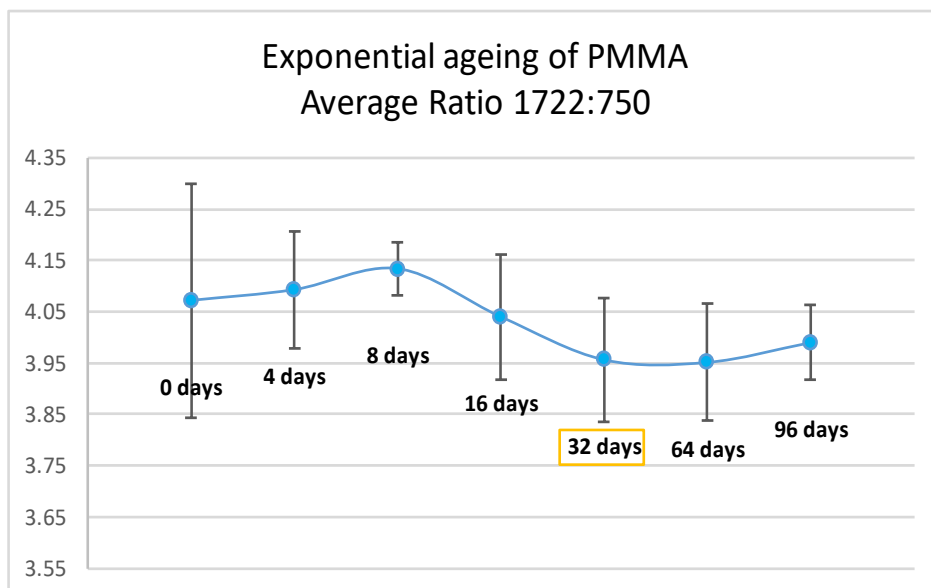


Figure 5.12. Spectra of unaged and UV-aged PMMA for 4, 8, 16, 32, 64 and 96 days. Spectra are averaged from three replicates for each stage of ageing. For absorption bands and assignments of new and exponentially UV-aged PMMA see Table 5.4.

Ratioing of peak heights at  $1723\text{ cm}^{-1}$  (C=O) and  $750\text{ cm}^{-1}$  ( $\text{CH}_2$ ) was used as a means to semi-quantify relative change in the samples, resulting from exponential photo-oxidative ageing under UV radiation. The ratios (Graph 5.12) show the progression between the relative decrease of carbonyl groups due to ester side group elimination, monitored via band  $1723\text{ cm}^{-1}$ , and the methylene ( $\text{CH}_2$ ) band at  $750\text{ cm}^{-1}$  found in the polymer backbone. The prominent carbonyl peak was chosen due to its dramatic decrease in intensity that confirms the progression of PMMA photolysis. Band  $750\text{ cm}^{-1}$  was selected as a reference spectral band (internal standard), because as earlier shown, its intensity remains constant during UV ageing of PMMA. The lack of scission in the main chain methylene was earlier confirmed through examination of spectra of new and 32 days aged PMMA, and was also reported by Tretinnikov and Zhabankov (1991). For each spectrum, the intensity of each of the two peaks was given by their maximum height measured relative to a linear baseline drawn from the valleys appearing on either side of each peak.



*Graph 5.12. Ratios between peak heights at  $1722\text{ cm}^{-1}$  and  $750\text{ cm}^{-1}$  of unaged reference PMMA and UV-aged samples for 4, 8, 16, 32, 64 and 96 days. Samples after 32 days show the greatest chemical change based on the increased loss of carbonyl bonds ( $\text{C}=\text{O}$ ) in relation to an internal standard. The ratios are expressed as the average of three scans/replicates at each stage of ageing. Error bars show the standard deviation of the ratios.*

Ratioing of peak heights confirms that samples after 4 and 8 days ageing show similar spectral response to the unaged material. After 16 days spectral changes occur. Results also confirm that PMMA aged for 32, 64 and 96 days exhibit similar relative chemical change. In light of these results, it is suggested that at 32 days greatest chemical change (spectral alterations) can be achieved within the shortest possible exposure time.

## 5.2. SAMPLE PREWASHING: RESIDUE REMOVAL



*Figure 5.13. PMMA coupons immediately after being removed from the black hard-plastic, on which they were attached when received. Transparent and black (dust) residues are visible on all the coupons.*



Figure 5.14. Ultrasonic bath cleaning of PMMA coupons in deionised water.

PMMA samples were received with traces of residual packaging from the black backing on which they were attached, transparent adhesive tape keeping them in place and transparent film protecting them (Fig.5.13). According to Fricker (2016, 134) residue from the protective film on newly acquired PMMA surface, although not visible to the naked eye, is likely to result in local changes in surface energy. This could change the surface's soiling behaviour and also have implications for the cleaning experiments and their reproducibility. Pre-washing of samples for removal of residues was considered essential to avoid interference in the experiments. Pre-washing was carried out in an ultrasonic bath of deionised water (Fig.5.14) for 1 minute. Samples were subsequently blotted with tissue and dried under compressed air. For a detailed description of all pre-washing tests, reasoning for choosing ultrasonic cleaning, as well as ATR-FTIR characterisation of the backing, adhesive tape and protective film residues, see Appendix G.

### 5.3. ARTIFICIAL DIRT: PREPARATION & APPLICATION

Cleaning treatments in this study were evaluated for their effectiveness at removing artificial dirt in the form of synthetic sebum soil and pressure-sensitive spray adhesive. The use of a published synthetic sebum recipe was advantageous because of its definite and known composition that renders the use of dirt repeatable. Moreover, Wertz (2009) reported that its composition more closely approximated human sebum than previously published formulations used in forensics and cosmetics studies. For the purposes of NANOMaterials for the REStoration of works of ART (NANOESTART) project<sup>15</sup>, Tate carried out cleaning tests, similar to the experiments in this study, on pristine PMMA mock-up sheets bearing two types of artificial soil; one of them based on the Wertz (2009) formulation simulating greasy fingerprints with carbon black pigment (Angelova *et al.* 2016b). NANOESTART, unlike this study where carbon black powder was incorporated in the formulation, sieved it on the already applied sebum soil. Tate tested a variety of solutions to find the best method to remove surface soil and clean an object from its collection; the opaque, white PMMA Op Art sculpture 'Op Structure' (1967) by artist Michael Dillon (Angelova *et al.* 2016b). They also carried out cleaning tests on mock-up stickers for removal of two pressure-sensitive adhesive (PSA) labels (Angelova *et al.* 2017b).

<sup>15</sup> A 3.5-year collaborative research project (2015-2018) (<https://www.tate.org.uk/about-us/projects/nanorestart>) aimed to develop a range of materials based on nanotechnologies to support the long-term protection and continued access to modern and contemporary cultural heritage.

### 5.3.1. Synthetic sebum soil/carbon black

The synthetic sebum consisted of 12.4 g squalene, 44.7 g triolein, 17 g oleic acid, 25 g jojoba oil and 1 g alpha-tocopherol (12.4 % squalene, 44.7 % triglyceride, 17 % fatty acid, 25 % wax monoester and 0.1 % vitamin E) (Wertz 2009). All ingredients were in liquid form. The powdered carbon black pigment was incorporated into the sebum composition and thoroughly mixed with a magnetic stirrer to eliminate pigment globules (Fig.5.15). It is common practice in conservation to add particulates such as carbon black in artificial soils to simulate encrusted grease (Scialla 2006, 158). The addition of a black pigment imparted a coloration that allowed the monitoring of residues remaining on the surfaces after treatment.

Four mixtures of sebum soil were prepared consisting of 1, 2, 3 and 4 wt.% carbon black pigment. Application of the mixtures was carried out with G222-Set Master Airbrush (TCP Global) fitted with a 0.2 mm nozzle selected for its fluid tank capacity and fine and homogenous spray pattern. To regulate the spraying consistency and amount of synthetic sebum soil, application was performed roughly 8-10 cm away from the surfaces and at 30 dpi, point at which the spraying reached steady pressure levels.

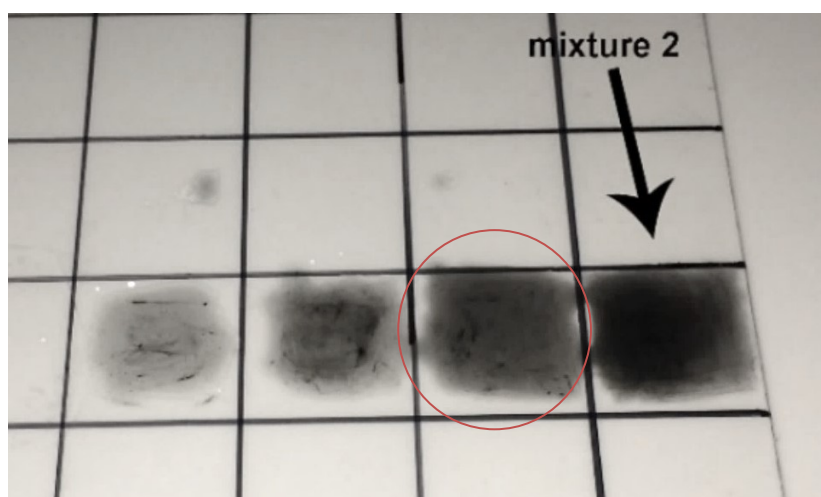


*Figure 5.15. Different mixtures of sebum oil with carbon black pigment after one application with different consistencies. The circled mixture shows pigment globules. Mixture 2 (2 % carbon black) shows the best homogeneity.*

Application was tested on transparent mock-up sheets to assess the appropriate concentration and consistency for simulation of the greasy fingerprints. In the 1 wt.% mixture, carbon pigment was not abundant to cover the transparent surface (Fig.5.16-Mixture 1). A 2 wt.% mixture exhibited improved consistency (good blend of pigment and sebum) (Fig.5.16), fineness and homogeneity of spread, satisfactory thickness of sprayed layer and desirable visual result given by the colour intensity of the soil. The 3 and 4 wt.% mixtures did not appear homogenous in texture. The black pigment separated out (flocculation) after a few hours of

application and an intense separation between oil and pigment was exhibited (Fig.5.16- Mixtures 3,4). Mixtures 3 and 4 resulted in an irregular sprayed layer, while mixture 1 produced a soft and thin layer with inadequate black shade. Mixture 2 was the most satisfactory.

Multiple spray applications of the 2 wt.% mixture were tested to determine how many repetitions were suitable for this experiment. Each consecutive application was sprayed vertically to the previous one. One application was not adequate to evenly cover the surfaces, whereas more than two applications were too thick, and possibly responsible for the formation of visible oil droplets. Therefore, two applications (one horizontal and one vertical) offered adequate visual coverage of the surface and thickness.

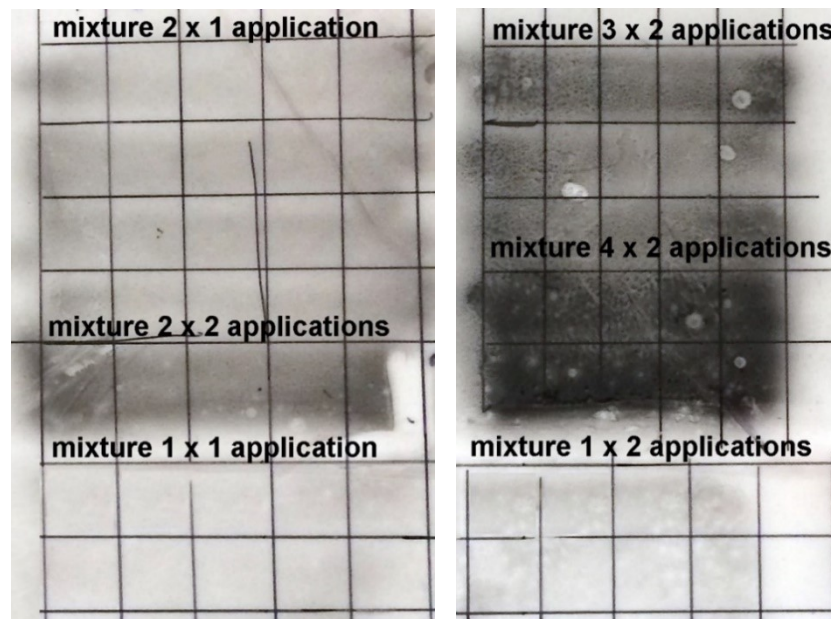


*Figure 5.16. Test applications of the four different sebum oil/carbon black mixtures with airbrush on transparent PMMA surrogate surface.*

The stability of the formulation upon application was also considered. This is a non-drying oil that remains liquid at room temperature, due to the antioxidant properties of Vitamin E (Harvey *et al.* 2010). The jojoba oil present in the formulation also contains Vitamin E as well as other antioxidants, which contribute to its general stability (Wertz 2009). Artificial human sebum exposed to the atmosphere and under conditions mimicking human skin surface (32 °C) has been reported to remain chemically stable for 28 days in the presence of Vitamin E (Stefaniak *et al.* 2010). Squalene is the only component that 'dries' progressively over time, but this only occurs in the absence of Vitamin E (Stefaniak *et al.* 2010). According to Wertz, the formulation has the capacity to remain stable for at least 48 hours at 32 °C (Wertz 2009). To confirm this, the different mixtures were visually monitored over a period of 30 days following

application, during which no apparent 'drying' was observed, except that carbon black pigment was seen to flocculate. Samples were airbrush-sprayed with two applications of 2 wt.% mixture and left in laboratory environment (ca. 21 °C and 55 % RH) for 48 hours, at which point cleaning treatments were performed.

#### Synthetic sebum soil film thickness

The thickness of sprayed soil was measured with a metal sheet thickness gauge, also known as step or comb gauge. The gauge had calibrated, numbered notches on its edges, which were placed into the sprayed film soon after application on the PMMA substrate. Contact between the end points of the gauge with the substrate enabled 'wetting' of the notches. The thickness was indicated to be between 25-50  $\mu\text{m}$ . The method was not precise, but it provided an approximation of thickness of each layer.



Figure 5.17. Step/comb gauge to measure synthetic sebum soil thickness.

#### **ATR-FTIR Characterisation**



Figure 5.18. Dried synthetic sebum soil (sebum oil and carbon black pigment) at 180 °C for 24 hours.

ATR-FTIR analysis was performed on the synthetic sebum soil with 2 wt.% carbon black pigment dried at 180 °C for 24 hours (Fig.5.18). Drying formed a solid sample of the liquid formulation aimed to ease contact with the ATR and avoid damage. The analysed sample (Fig.5.19) exhibited the characteristic IR absorption bands of the reference sebum from human skin (Table 5.5) (Brancaleon *et al.* 2000; Brancaleon *et al.* 2001). Peaks at 2920  $\text{cm}^{-1}$ , 2850  $\text{cm}^{-1}$ , 1457  $\text{cm}^{-1}$  and 1378  $\text{cm}^{-1}$  confirm the presence of lipids. The carbonyl peaks at 1740  $\text{cm}^{-1}$  and 1710  $\text{cm}^{-1}$  are the most characteristic absorption bands of sebum, with the latter assigned to the presence of free fatty acids (Brancaleon *et al.* 2000; Brancaleon *et al.* 2001). However, characteristic carbon black absorptions, such as the most intense band at 1600  $\text{cm}^{-1}$  (aromatic ring stretching) (O'Reilly and Mosher 1983; Rositani *et al.* 1987), are absent from the spectrum. The sample was re-analysed several times and, on several spots, to confirm the absorption



bands. Consistent spectra suggested that when incorporated into the proposed sebum-based formulation, carbon black was not detected.

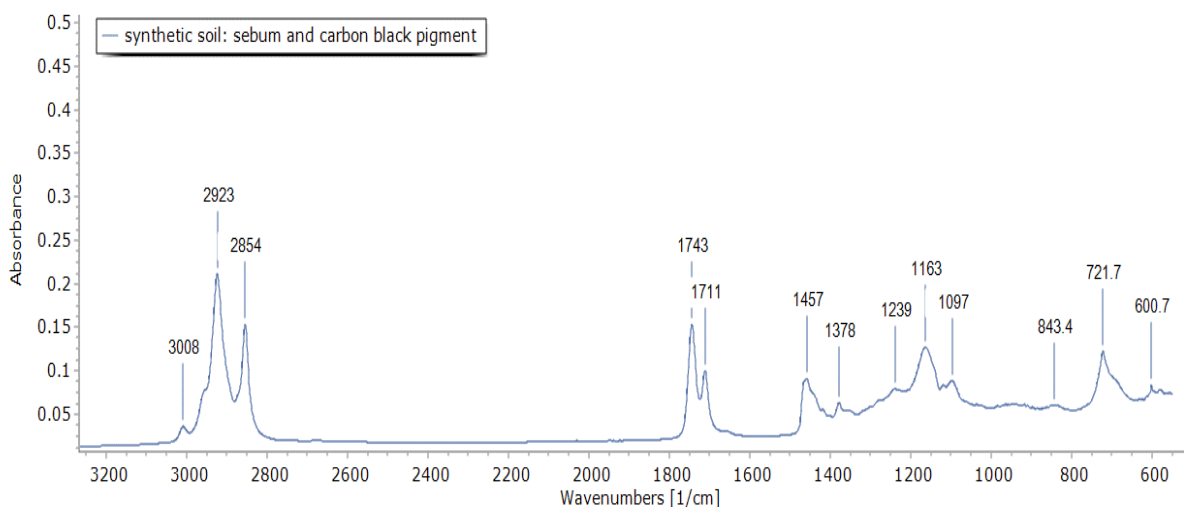


Figure 5.19. Spectrum of sebum oil and 2wt.% carbon black pigment formulation with 16 scans at ambient temperature and pressure, with a resolution of  $4\text{ cm}^{-1}$  equating to a penetration depth of  $0.5\text{--}5\ \mu\text{m}$ . Labelled absorption bands correspond to assignments in Table 5.5.

Sebum. Diagnostic IR absorptions and assignments	
Wavenumber ( $\text{cm}^{-1}$ )	Band assignment
2920	$\text{CH}_2$ stretch
2850	$\text{CH}_2$ stretch
1740	$\text{C}=\text{O}$ stretch
1710	$\text{C}=\text{O}$ stretch
1457	$\text{CH}_2$ scissoring
1378	$\text{CH}_2$ and $\text{CH}_3$ bending

Table 5.5. Assignments of diagnostic IR absorptions of reference sebum in ATR mode.

### 5.3.2. Pressure-sensitive spray adhesive

PSA is found on tapes with a multi-layered structure consisting of (starting at the back of the tape): a release coating applied to ensure ease of unwinding of the tape during application, a backing or carrier, a primer coat used between the adhesive and backing and the adhesive (Zięba-Palus 2007; Duplat *et al.* 2018). PSA tapes, such as office and packaging tapes often possess plastic backings with rubber- or acrylic-based adhesives (Gorassini *et al.* 2016). In addition to the conservators' survey, the conservation literature also indicated that PSA tapes are widely encountered on museum objects and archival materials, i.e. books, and paper-

based artworks (Duplat *et al.* 2018). As they are usually firmly bonded to substrates, it is challenging to visibly, fully remove such tapes without leaving adhesive residues behind (Czech 2006).

PSA in this study belongs to the same adhesive type described above, but was supplied as a pressurised aerosol, with the adhesive polymer dissolved in a volatile solvent. This form was preferred for its ability to be standardised, enabling a uniform and repeatable deposition. PSA found on tapes requires application of pressure for adequate adhesion, which relies on polar attraction to the substrate (Varanese 1998). This rendered their application challenging to standardise and would leave sporadic adhesive deposits, in minor quantities.

Application was carried out by spraying adhesive directly from the pressurised can from a distance of roughly 20 cm. One application was adequate to uniformly cover the sample surfaces with a homogenous PSA layer. Sprayed samples were left to sit for 72 hours prior to the cleaning treatments. The comb gauge used for thickness measurement of the synthetic sebum soil failed to measure the PSA thickness. This was possibly due to the layer being too thin to visually determine or to the PSA quickly forming an elastic, solid structure that left no residues on the small gauge indentations (notches).

#### **ATR-FTIR Characterisation**

The most widespread commercial PSAs used for tape, on the basis of their primary constituent are (natural or synthetic) rubbers or acrylates (Zięba-Palus 2007). The material data sheet supplied by 3M spray adhesive stated that it contained 7-10 % non-volatile components, 7-13 % propane, 20-30 % isobutane, 20-30 % heptane isomers and 30-40 % acetone. ATR-FTIR analysis (Table 5.6) indicated the polymer as a solvent-borne modified acrylic-based PSA. The spectrum (Fig.5.20) allows the identification of two main components: an acrylic and a petroleum-based polymer. Modified acrylic adhesives are fabricated from acrylic polymers with incorporation of additional components, such as tackifiers, found in rubber-based systems (Varanese 1998). The preferred tackifiers, compatible with the acrylic phase, are synthetic hydrocarbon resins derived from petroleum (Foreman *et al.* 2003).

Pressure-sensitive adhesive: Diagnostic IR absorptions and assignments		
	Wavenumber (cm <sup>-1</sup> )	Tentative band assignment
<b>Polyacrylate</b>	1733	C=O stretch of ester
	1650	C=C stretch
	1456	CH <sub>2</sub>
	1367	α-CH <sub>3</sub>
	1238	C–C–O of ester
	965	α-CH <sub>3</sub>
	835	CH <sub>2</sub> skeletal
<b>Terpene tackifier</b>	3445	O–H stretch
	2956, 2871	C–H stretch of (cyclo)aliphatic groups
	1738, 1651	C–H stretch of aromatic rings
	1456	C–C stretch of aromatic rings
	1382	C–H stretch of (cyclo)aliphatic groups
	835	C–H out-of-plane wagging

Table 5.6. Assignments of diagnostic IR absorptions of the PSA used in this study analysed in ATR mode. It consisted of two solid components: the acrylic adhesive and a terpene tackifier.

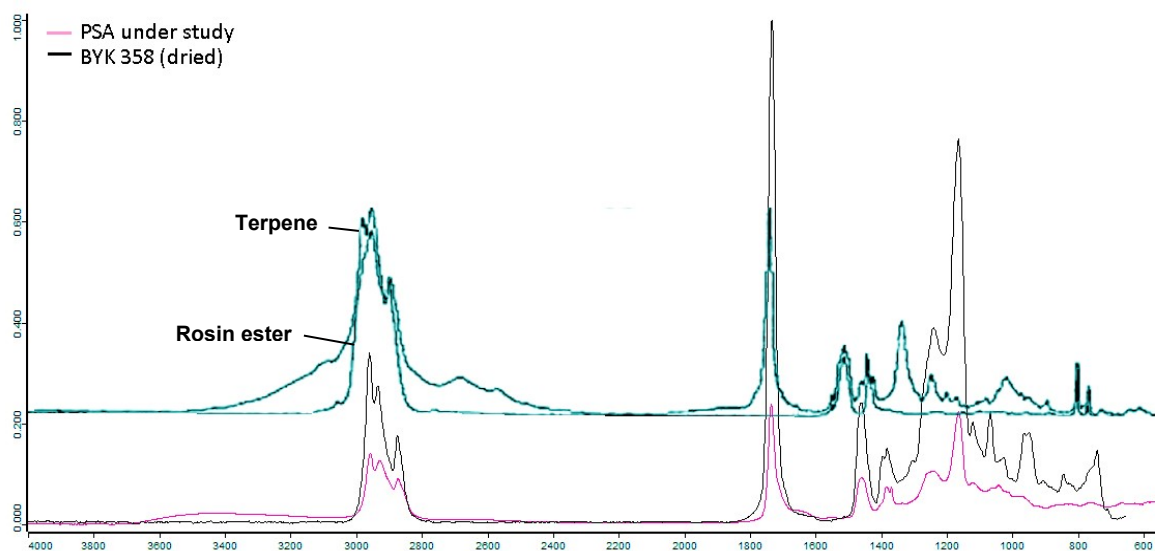


Figure 5.20. IR spectra of PSA under study (pink) in ATR mode matched with reference commercial product BYK 358 (black): a polyacrylate-based solution with 52 % solid content in naphtha, petroleum, light aromatic and isopropyl benzene. Absorption bands and assignments available in Table 5.6.

The PSA spectrum (Fig.5.20-pink) was compared to a reference database and matched to a commercial product under the name BYK 358 (Fig.5.20-black), identified as a polyacrylate-based solution with 52 % non-volatile/solid content prepared in alkylbenzenes, namely naphtha, petroleum, light aromatic and isopropyl benzene (SAFETYDATASHEET 2018). This established the PSA as an acrylic-based material, also indicated from its characteristic peaks at  $1730\text{ cm}^{-1}$ ,  $1450\text{ cm}^{-1}$  (Chung *et al.* 2015),  $1238\text{ cm}^{-1}$  and  $1161\text{ cm}^{-1}$  (Nagai 1963; Kaczmarek *et al.* 2010). For absorption assignments see Chapter 5.1.2.1.

Acrylic PSAs are predominantly manufactured by polymerisation of a wide selection of acrylic and methacrylic groups, and can be prepared either as hot melts, aqueous emulsions or solvent-borne solutions (Tobing and Klein 2001; Czech *et al.* 2007). Dissolution tests were carried out to detect the type of solvents capable of solubilising the present PSA. Cotton swabs moistened in a range of solvents (water, alcohols and petroleum-based) showed that only petroleum ether was able to dissolve the adhesive. This indicated that the PSA is solvent-borne rather than aqueous-based, and particularly a benzene-derivative solution. This was supported by the literature, suggesting that solution polymerisation of PSA polyacrylates commonly employs petroleum-based solvents, such as cyclohexane, toluene, and *n*-heptane (Wu 2014).

The solvent used for polymerisation of the PSA would readily evaporate after application, therefore it was not expected to be detectable by ATR-FTIR analysis. With this in mind, the second petroleum-based component visible in the spectrum can be attributed to a solid component. To confirm this, ATR-FTIR analysis of the PSA was repeated six months after application, allowing the complete evaporation of solvent content and reducing solvent interference. Results showed identical spectral absorptions for PSA analysed immediately after application and six months later, confirming the presence of a second, petroleum derived solid component. Based on the literature, tackifiers frequently added to acrylic PSAs were primarily crude oil derivatives: rosin ester, polyterpene and hydrocarbon (petroleum) resins (Mess *et al.* 2011; Wu 2014).

Tackifiers are added in quantities between 10-50 % (Mess *et al.* 2011). They are used to improve adhesive performance in terms of tack or peel adhesion (Tobing and Klein 2001), whilst decreasing resistance to solvents and high temperatures (Czech *et al.* 2011). Tackifiers are selected according to their compatibility to the adhesive polymer, based on degrees of polarity, softening points and molecular weight (Barrueso-Martinez *et al.* 2003). Rosin resins, similar to terpene-based resins, are obtained from trees or as by-products of wood pulp manufacture (tall oil rosin). Polyterpene resins, also known as 'universal tackifiers', are produced by polymerisation of terpenes of plant origin (citric fruits or natural turpentine from trees) (Mess *et al.* 2011). Lastly, hydrocarbon resins derive from petrochemical processes and are mixtures of aliphatic and aromatic constituents.

Spectra of rosin esters and polyterpene resins show greatest similarity to the PSA (Fig.5.20). Rosin esters contain ester groups (Barrueso-Martinez *et al.* 2003), which absorb similar wavelengths (1600-1750  $\text{cm}^{-1}$ ) to acrylic-based materials. Presence of bands around 3400  $\text{cm}^{-1}$  are attributed to the OH contribution, common for both terpene and some rosin ester resins (Silverwood *et al.* 2014). Decisive for the identification of the tackifier component was the weak peak at around 830  $\text{cm}^{-1}$ , which indicated the presence of terpenes (Silverwood *et al.* 2014). Most terpenes show their most significant absorption used to distinguish different types of aromatic ring substitution (Schulz *et al.* 2005) (CH and  $\text{CH}_2$  out-of-plane wagging vibrations) between 750-950  $\text{cm}^{-1}$ . Definitive identification of the exact nature of the tackifier is not possible with sole use of FTIR. Further analysis would require methods such as GC/MS (Silverwood *et al.* 2014). However, after examination of several spectra of tackifiers available within the literature, the most suitable match to this petroleum-based component was a terpene resin.

This chapter presented two methods of mechanical analysis obtained to set forth the artificial ageing methodology of PMMA samples. It investigated the physical behaviour of the unaged control and compared it with its behaviour after UV-ageing. It was also determined that samples should be pre-washed in a deionised water ultrasonic bath for removal of packaging residues. The process of preparing and applying artificial dirt, selected to represent dirt types commonly found on plastic museum objects, was also examined here. Spraying processes of two dirt types were standardised to eliminate inconsistencies that would affect the accuracy of cleaning data and cause variability to the results, ensure the repeatability of the experiment and enable the study to be comparative. The following chapter presents all the techniques used in this research for evaluation of the treatments' cleaning effects. The relevance of such techniques in this study are argued through the literature review of past research.

## Chapter 6. CLEANING EVALUATION & ANALYTICAL METHODS

This chapter gives an overview of the methods employed for evaluation of the cleaning experiments. These are categorised into qualitative and quantitative methods. Evaluation aimed at detecting changes in the visual appearance, chemical composition and physical properties of PMMA in its unaged and aged states, before, during and after treatment. In their majority, evaluation methods dealt with surface changes. It is the surfaces of museum objects that are the first to be cherished, and to endure the unavoidable process of soiling and weathering, affecting the chemical and physical structure and aesthetics of objects. Analysis of treated surfaces allowed evaluation of the efficiency and suitability of treatments at removing surface deposits, while preserving surface integrity. To allow statistical evaluation of the results and calculation of potential experimental errors, at least three replicates exposed in each experimental set had to be run when non-destructive tests were used, and at least five replicates for destructive tests (ISO 4892-2).

The surface response to treatments was optically assessed through macroscopic examination presented in tables, stereomicroscopic images captured under raking light and with SEM imaging. Although crucial to the understanding of the cleaning efficiency and of phenomena taking place on the surfaces after cleaning, visual observation could not be measured nor compared due to its qualitative nature. Being able to convey such information numerically was beneficial, therefore CARS was developed. This was a ranking system according to which treated surfaces were ascribed scores representative of their condition (Loehnert 2010).

Quantification of visual and physical changes was rendered possible through measurement of surface gloss and weight, before and after treatment. ATR-FTIR was used to detect surface chemical modifications, before and after treatment. NMR MOUSE was the only technique to examine the bulk material. It assisted the understanding of mechanical change, hence samples were scanned before, during and after treatment.

TECHNIQUES FOR EVALUATION OF CLEANING RESULTS	
Qualitative	Quantitative
Macroscopic evaluation	Gloss
Stereomicroscopy	Weight measurements
CARS	ATR-FTIR peak height ratio (semi-quantitative)
SEM imaging	NMR MOUSE (semi-quantitative)
ATR-FTIR raw spectra	

*Table 6.1. Qualitative and quantitative techniques, including analytical methods, performed on PMMA samples for the evaluation of cleaning experiments. Measurements and analysis were carried out on all samples before and after treatment, and sometimes during treatment.*

## 6.1. VISUAL ASSESSMENT

### 6.1.1. Macroscopic evaluation

Naked eye evaluation was documented immediately after treatment completion as a simple, overall assessment of performance based on dirt removal. Information recorded whether dirt had been removed or not according to three categories: *cleaned*, *partly cleaned* or *not cleaned* (for an example see Table 6.2).

samples with synthetic soil	
Agar EtOH	partly cleaned/cleaned
Pemulen EtOH	partly cleaned
Pemulen IPA	not cleaned
PVA PET	cleaned

Table 6.2. Example of visual macroscopic evaluation of treated samples based on the level of dirt removal.

### 6.1.2. Stereomicroscopy under raking light

Stereomicroscopy is widely used as the most straight-forward, easy and accessible technique for observation of surface topography. Raking light offered more information about the surface microstructure. It was used as a preliminary step to identify areas of interest, which were further investigated with SEM imaging.

Stereomicrographs were used for documentation purposes. Digital photography was dismissed for presenting complications in capturing the transparent and highly polished PMMA surface, while Leica M205 A 3D stereomicroscope managed to eliminate the scattering effect of light. Samples were photographed while mounted on a clip against a black background, which resulted in images appearing grey scaled (Fig.6.1). The technique demanded complete darkness with only source the raking light illuminating the surfaces at an oblique angle, almost parallel to them. The magnification used was kept at 78.1x for consistency. A polyester film (Melinex<sup>®</sup>) was cut in the dimensions of the sample (25 x 25 mm) with an opening of 24 x 24 mm allowing the surface area to be imaged. This masking method was developed to standardise the process of capturing surfaces under magnification and enabled comparison of surface condition before and after treatment.

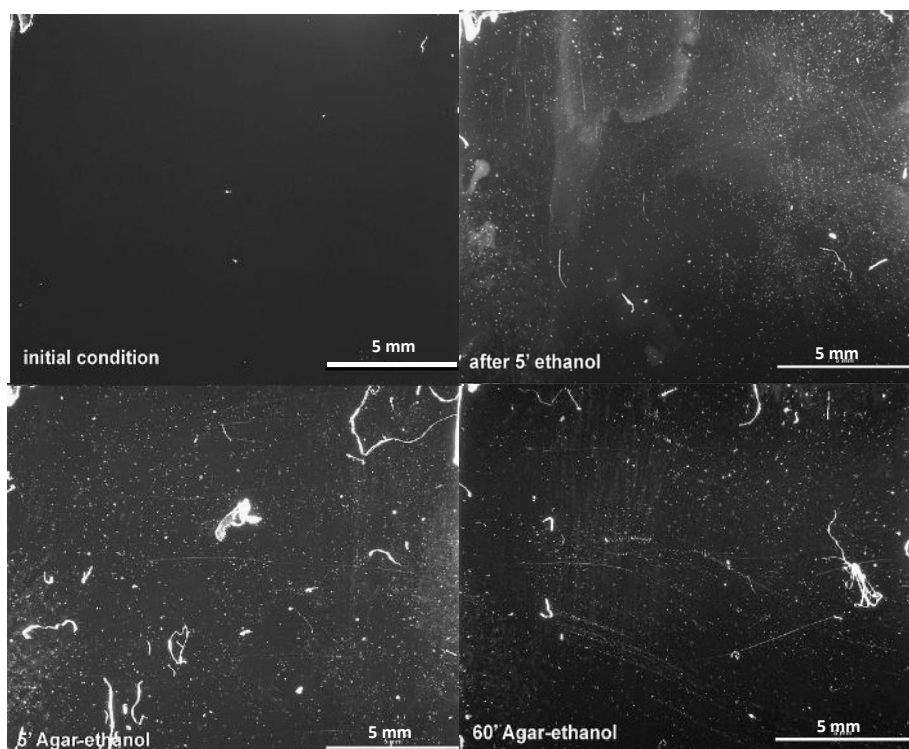


Figure 6.1. Microimages of treated PMMA samples captured under the stereomicroscope (x78.1) with raking light. Samples were mounted on a clip and a mask placed on them defined the area to image. EtOH left PMMA with large areas of non-uniform loss of transparency. Agar EtOH after 5 and 60 minutes left deposits of fine nature and imprints of post-treatment swabbing.

### 6.1.3. Scanning Electron Microscopy imaging

SEM is a microscopic technique that provides high-resolution and high-magnification topographical images. It has been used to image the structure of porous polymers (Meyers *et al.* 2011). A study used Environmental SEM for imaging bulk PMMA in low vacuum mode at 5 kV with water vapour as chamber gas, to focus on the topography degradation (Arnoult *et al.* 2012). Another study in ophthalmology and the use of intraocular contact lenses, employed SEM for imaging of PMMA at 5 kV with a maximum magnification at 500x (Spyratou *et al.* 2010). In the conservation field, SEM imaging has been employed along with other techniques (often FTIR and stereomicroscopy) for studying degradation effects. In particular, Winther *et al.* (2013) investigated degradation phenomena through identification of changes as types of damage, i.e. breakage in a micro scale.

In this study, SEM imaging was important in shedding light to the physical or chemical PMMA surface changes. Due to its ability to reach very high magnifications, it was the main tool used to describe different types of surface damage (without any dirt layer interference) resulting from contact with free solvents, hydrogels and solvent gels. The aim was to



understand the types of change: surface deposition, residue i.e. cotton fibre from the swab or gel, stain (removable or a permanent chemically-induced discolouration), or a defect in the surface microstructure (i.e. scratching, local dissolution, etc.). For this task imaging relied on the stereomicrographs to detect areas of interest, requiring detailed examination.

At a later stage of the cleaning experiments, with factors being narrowed down and added artificial dirt, SEM imaging offering a large range of magnifications (including the ones used in stereomicroscopy), was the only technique employed for surface visualisation. It was rendered valuable when studied alongside and compared against information provided by the other techniques and methods.

A JEOL JSM-6610LV SEM with attached EDS Detector Oxford Instruments X-Max was used. Untreated unaged and aged controls, one for each type of condition and dirt, were captured (Table 6.3). Different options of high and low vacuum were tested to achieve the largest magnification, while keeping the image sharp and the samples intact. Secondary electron emission signal showed satisfactory results and was used in all test conditions/modes.

SEM images of untreated PMMA controls	
Untreated, unsoiled new PMMA	Untreated, unsoiled aged PMMA
Untreated new PMMA/synth. sebum soil	Untreated aged PMMA/synth. sebum soil
Untreated new PMMA/spray adhesive	Untreated aged PMMA/spray adhesive
Untreated new PMMA/aged synth. sebum soil	Untreated aged PMMA/aged synth. sebum soil
Untreated new PMMA/aged spray adhesive	Untreated aged PMMA/aged spray adhesive

Table 6.3. List of the untreated PMMA controls, per type of condition and dirt, imaged under the SEM.

High vacuum was initially set at 10 kV. Even though the image sharpness was high and with a good resolution, the beam damaged the sample surface (see Fig.6.2). PMMA is sensitive to electron beam irradiation, with its main degradation process being radiolysis inducing mass loss due to evaporation of volatile components (Arnoult *et al.* 2012). Irradiation affects PMMA by the energy transfer between incident electron and material atoms. A large number of processes can occur, including formation of free radicals, the reaction of which can result in further chemical change (Varlot *et al.* 1999), such as deformation similar to Fig.6.2.

Next, a high vacuum mode at 1 kV was tested, appearing to be satisfactory only up to about 300x, magnification also available with the stereomicroscope. A micrograph captured at a magnification of 500x (Fig.6.3-right) was not sharp, rather blurry, rendering the 1kV mode unsatisfactory. Further experimentation was needed to adjust the settings to allow higher magnification, at around 1000x, and optimum image quality. Samples were thus observed under high vacuum at 5 kV, earlier identified as a safe mode used by other researchers. This offered good resolution and was used for this study.

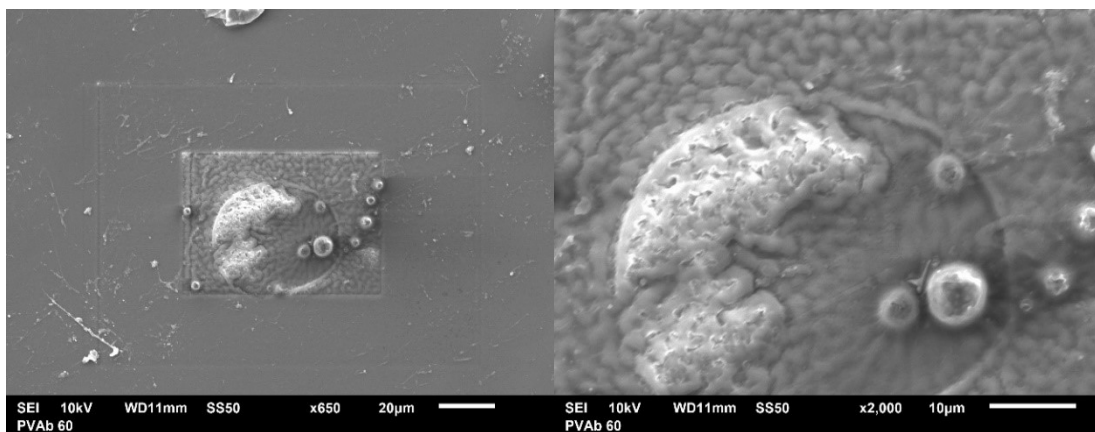


*Figure 6.2. PMMA sample observed under 10kV/high vacuum showed damage (deformation and loss of volatile components) in a squared-like shape due to irradiation of the electron beam.*

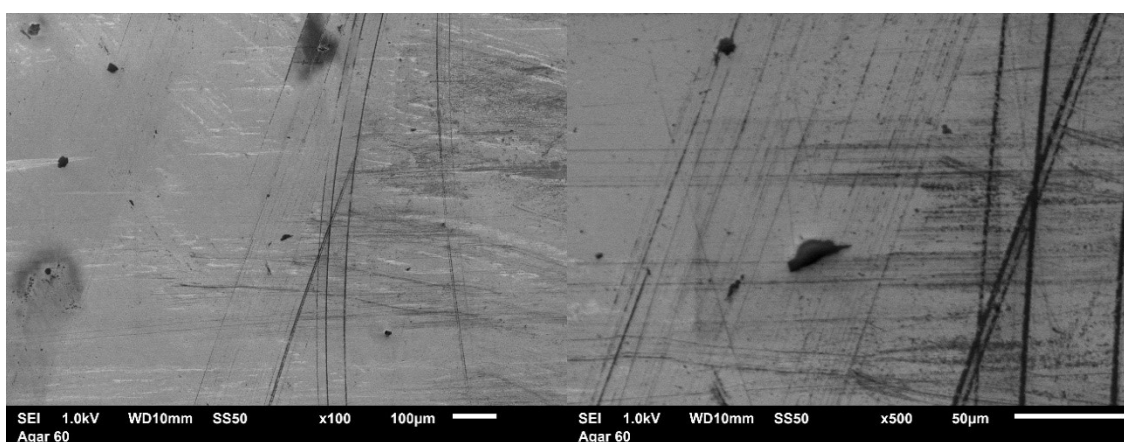


*Figure 6.3. PMMA sample after Agar hydrogel treatment at 1kV/high vacuum. SEM micrograph at a magnification of 100x appeared sharp, while at 500x was blurry.*

SEM imaging required surfaces to be electrically conductive by increasing the number of secondary electrons emitted from the sample (Pavlidou 2013). PMMA, like most plastics, is nonconductive and the electron emission was enhanced by destructively coating the samples with a thin layer of gold; a conducting element, which allowed image clarity. A drawback of the technique was that it didn't allow reanalysis of the samples after coating.

#### **6.1.4. Criterion anchored ranking system**

Macroscopic evaluation and initial observations of treated surfaces were documented in survey sheets immediately after cleaning, offering an early outcome regarding the performance of the treatments. This was particularly relevant in this study concerned with the aesthetics of objects. Condition assessment of surfaces is a subjective approach and uses scales within a personal value system (Suenson-Taylor and Sully 1996). The use of survey sheets and the production of a condition score (CARS) aimed to quantify these visual results, render evaluation uniform, easy

and rapid, minimise observer bias, increase reliability and add statistical texture to the data (Suenson-Taylor and Sully 1996).

To standardise data recording and limit the subjectivity inherent in such value assessments (Suenson-Taylor *et al.* 1999), descriptive terms were allocated numerical scores that could be measured on an ordinal scale (Suenson-Taylor and Sully 1996). The scale was formulated on a five-point basis (described in Table 6.4) expressed in a progressive ranking from 0 (worst) to 4 (best). Such ranking systems are suitable for samples that are visually graded according to relative degrees, as opposed to quantitative instrumental measurement (Reedy and Reedy 1994). To improve objectivity, samples were assessed in a random order, without prior knowledge of treatments carried out on them.

The Pass/Fail evaluation system would not have worked in this case, as it could not examine the efficiency of treatments nor allow comparison between their performances. By not being able to differentiate between better/poorest, such a system could evaluate a treatment that is better than others, but only suitable under certain conditions, as 'Fail'. The ranking system employed here, not only enabled assessment of the effects of treatments, but also provided an adequate overview of the condition of treated surfaces.

The feasibility of linking perceptual judgements, such as that of physical attributes, with rating scales has been often questioned (Ettwein *et al.* 2017). Although all evaluation was performed by the author, to test the inherent subjectivity, four different subjects (including the author) tested the ranking system and survey sheet through evaluation of randomly selected treated PMMA surfaces. The scoring was performed individually by each subject, in a random order and without knowledge of the treatments carried out on samples being evaluated. This aimed not only to refine the rating scale, but test the evaluation process with realistic surfaces. Points in need of further explanation and rephrasing were located, misleading descriptions were amended and most importantly, it was demonstrated that the three subjects were in accordance. The four 'judges' assigned similar scores, proving that the ranking system was efficient. Minor differences were documented between the lowest scores, 0 and 1, or the highest 3 and 4, but overall it was demonstrated that the criteria (condition categories) were adequately described.

Scores were based on the following criteria: *Dirt removal*, *Abrasion*, *Residues*, *Ease of use* and *Control*. Samples could score between 0 and 4 for *Dirt removal*, *Abrasion* and *Residues*, providing information about the treated surface condition and treatment effect, and 0, 2 or 4 for *Ease of use* and *Control*, referring to the practicality and ease of application/removal of treatments. Their additive relationship generated the CARS score. The lower its value, the least efficient the cleaning treatment.

<b>Dirt removal</b> Assess the amount of dirt on treated surface in relation to the untreated PMMA reference.	<b>0</b> 76-100% whole surface covered by dirt	<b>1</b> 51-75% greater part covered by dirt	<b>2</b> 26-50% Partially removed, still dirt partly visible	<b>3</b> 1-25% few/limited areas covered by dirt	<b>4</b> 0% completely removed, no dirt at all
<b>Abrasion</b> Assess the area scratched in relation to the untreated PMMA reference.	<b>0</b> 76-100% abrasions cover whole area	<b>1</b> 51-75% greater part liable to abrasions	<b>2</b> 26-50% Partially intact, with part of surface abraded	<b>3</b> 1-25% few/limited areas liable to abrasions	<b>4</b> 0% Surface intact, no abrasion at all
<b>Residues</b> Assess the amount of residues remaining upon treatment (gel, cotton fibres).	<b>0</b> 76-100% whole surface covered by residues	<b>1</b> 51-75% Greater part covered by residues	<b>2</b> 26-50% Partially free of residues, with part of surface covered	<b>3</b> 1-25% Few/limited areas covered by residues	<b>4</b> 0% Surface intact, no residues at all
<b>Ease of use</b> Handling of gels: consider the difficulty in application/removal.	<b>0</b> Difficult handling		<b>2</b> Relatively easy		<b>4</b> Very easy
<b>Control</b> Consider the control over the targeted area. Assess solvent spread and gel behaviour (i.e. shrinkage levels).	<b>0</b> No control		<b>2</b> Some control		<b>4</b> Absolute control, limited to areas applied

Table 6.4. Criterion anchored rating scale (CARS) comprised of five categories: three (highlighted in blue) concerning surface condition of treated PMMA samples and the effect of treatments and two (in white) referring to the quality/handling of gel treatments.

Different weighing factors were attributed to each of the five condition categories (Michalski and Rossi-Doria 2011). *Dirt removal* and *Abrasion* contributed a double weight in the final score, as they were considered vital to the assessment of the outcome (Table 6.5). Detection of physical modifications, such as abrasions, to which PMMA has a low tolerance due to its transparent and pristine nature, were the main drive behind this study and the investigation of the use of gel systems. Since the materiality of an object/artwork lies in its appearance and structure, it was anticipated that any optical alteration would be considered as damage. So, the ability of gel systems to clean without inducing scratches was an important criterion that required a larger weighing factor. The same applied to removal of dirt. The ability of a treatment to remove surface matter/soiling was the main purpose of cleaning, and it was granted a higher weighing factor.

	<i>Dirt removal</i>	<i>Abrasion</i>	<i>Residues</i>	<b>Score</b>
<b>weight</b>	x2	x2	x1	
Reference PMMA	4 x 2	4 x 2	4 x 1	20

*Table 6.5. Matrix showing the weighing factors used in the assessment of cleaning experiments for the condition categories describing the surfaces of samples after treatment. Criteria Ease of use and Control are missing as this is the control.*

CARS used in the assessment and statistical analysis of the cleaning experiments only included condition categories concerning the treated surface condition and treatment effect (*Dirt removal*, *Abrasion* and *Residues*). The untreated control was considered a ‘pristine’ surface with no defects, no abrasions, no dirt or residual material, scoring the maximum possible in all three categories for a total CARS 20 (Table 6.5). Samples scores could range between 0 and 20. Scores for condition categories *Ease of use* and *Control* were considered in the evaluation of the physical properties of gels (Appendix I). An example of the format of survey sheets and the assignment of scores.

SYNTHETIC SOIL										
	Dirt Removal	Abrasion	Residues	Ease of use	Control	TREATMENT	Comments	score	average	StDev.p
Weight	x2	x2	x1	x1	x1					
Sample										
<b>NEW</b>										
U250	0	4	3	2	0	Pemulen PET	solvent spread	13		
U293	1	4	4	2	0		difficulty to clear gel	16		
U327	0	4	4	2	0			14		
U279	1	4	3	2	0			15		
U282	1	4	4	2	0			16	14.8	1.17
<b>AGED</b>										
1132	4	4	2	4	4	PVA etOH	gel not well applied	26		
476	3	4	2	4	4		cotton fibre deposits	24		
742	3	4	2	4	4			24		
669	2	4	3	4	4			23		
600	2	4	3	4	4			23	24	1.10

*Table 6.6. Condition survey sheet: examples of samples assessed and scored based on CARS ranking system, immediately after treatment.*

### **Limitations of use of ANOVA with CARS data**

CARS are qualitative data in the ordinal scale, gathered via questionnaires and surveys. In statistical terms, the production of a condition score (CARS), very similar to a Likert scale (Jamieson 2004; Norman 2010; Boone and Boone 2012), allocates numbers to descriptive terms. These numbers are ranked and therefore can be ordered (Suenson-Taylor and Sully 1996). By using a CARS ranking system, qualitative data (ordinal) are transformed/converted into quantitative (interval), enabling the full spectrum of quantitative mathematical-statistical analysis (Loehnert 2010).

Assigning numerical values to observation categories, and treating them as interval has long been controversial (Jamieson 2004). Ordinal data represent verbal statements and have an inherent order, but are not truly numeric, measured along a scale and equidistant from one another, such as interval data (Jamieson 2004; Loehnert 2010). In order for data to be used with parametric statistical methods, such as ANOVA, they need to show some kind of standardisation that enables the comparable usage of statistical parameters, i.e. mean, variance, correlation and other distribution characteristics (Loehnert 2010). CARS being ordinal are expected to not be normally distributed, so parametric tests are not appropriate for their analysis (Suenson-Taylor *et al.* 1999). The danger CARS data pose is that of using scores that look like real numbers, while in fact are only ordered categories on an imprecise scale. To give an example of what this means, imagine using a 5-point scale recording descriptive terms, such as optimum, good, fair, poor, worst. There may be no reason why the difference between an object scoring '5' and another scoring '6' should be exactly the same as an object scoring '4' and the other '5'.

Although techniques designed for interval data are controversial for statistical analysis applied on ordinal data, a number of scholars (Carifio and Perla 2007; Loehnert 2010; Paltridge and Phakiti 2010; Norman 2010; Boone and Boone 2012) have described their ordinal data using statistical parameters (i.e. means and standard deviations). Their research in clinical trials of drugs and applied linguistics commonly treat ranked data with unequal variances and non-normal distributions, as interval. Some have even demonstrated that ranked scales can produce interval data (Carifio and Perla 2007). It has, thus, become common practice to assume that ranked variables constitute interval-level measurements (Jamieson 2004) and use statistical parametric tests without concern.

Although controversial, CARS data in this research were analysed with ANOVA. The reason for this choice was, first and foremost, to provide an equal comparison with the other interval data in this research, obtained through measurements and analytical techniques. Parametric tests are after all based on the assumption of normality of the distribution of means, and not of the data. It has been proven that for sample sizes greater than five, means of ordinal data are approximately normally distributed regardless of their original distribution (Norman 2010). So CARS, created by calculating a composite score and a mean of five replicates, was analysed at the interval measurement scale (Boone and Boone 2012). This choice may not be universally accepted by statisticians, but is supported by a large number of scholars conducting research in other fields.

In the conservation field, literature on statistical methods is limited (Reedy and Reedy 1988; Reedy and Reedy 1994). Chemometrics in experimental design and sampling strategies in conservation have been employed by Golfomitsou and Merkel (2004) and epidemiological

approaches to collections management questions have been proposed by Suenson-Taylor and Sully (1996) and Suenson-Taylor *et al.* (1999). So, except for the aforementioned literature, for the statistical analysis of data this research referred to texts on clinical research and chemometrics, of which research questions are similar to those of conservation treatments (Suenson-Taylor 1999).

## 6.2. GLOSS MEASUREMENTS

Gloss is an important aspect of the visual properties of objects, but it is relatively subjective. A glossmeter is capable of measuring the specular qualities of a surface by assigning a gloss unit (GU) and providing quantitative information about physical changes. Practically, it does so by shining a known quantity of light at a surface and measuring the degree of light reflectance at a specified angle (Shashoua *et al.* 2009; Ignell *et al.* 2010). This technique has been of increasing importance in the automotive industry (Ignell *et al.* 2010) and has gained popularity in the conservation field for investigation of microscopic surface damage (i.e. cracking) caused by cleaning. For example, a glossmeter was employed on a transparent and colorless PVC after cleaning with Pemulen and moistened cotton swabs (Bollard *et al.* 2011). PVC's high gloss hindered the accuracy of results and the technique was abandoned. In similar research, Shashoua *et al.* (2009) employed a glossmeter on a transparent colorless PMMA after cleaning.

The GU scale is based on a highly polished reference, a black glass standard with a defined refractive index and a specular reflectance of 100 GU. There are three angles at which measurements can be performed, 20, 60 and 85 degrees. Each angle is used for a different type of surface. Highly reflective surfaces, such as the PMMA under study, are expected to give measurements over 100 GU, and are usually measured with an incident angle at 20 degrees. On such surfaces, where measurements can be disturbed by the multiple reflections within the



Figure 6.4. Glossmeter with options of incident angles at 20°, 60° and 85°.

material bulk (Shashoua *et al.* 2009), glossmeters tend to be inaccurate (Bollard *et al.* 2011). According to Shashoua *et al.* (2009), Minolta, the manufacturer of the glossmeter used here, suggested that readings greater than 100 should be expressed as a percentage. As this study was interested in the relative change of surface gloss after treatment, percentages were not deemed appropriate and the technique was used in a comparative fashion.

### **Correlation between instrumental data and human perception**

An important issue here was to understand what level of visual change expressed by an instrumental method, such as the glossmeter, could be perceived by the naked eye. If changes were not reflected in the macroscopic observation and could not be detected by the human eye, but only on a micro- or nano-scale, then the impact of cleaning on the surface materiality was an arguable topic. Was a measured change/damage significant to the aesthetics of the PMMA surface? As there is no linear relationship between human visual perception and measured instrumental gloss data (Ettwein *et al.* 2017), CARS, an observer-based rating procedure dependent on macroscopic evaluation, was formulated and directly correlated with the gloss measurements. In this study, CARS scores appeared more applicable than measured gloss values, given they represent visual evaluation from the perspective of a human observer. This corresponds more accurately to the perception of a museum visitor, whose assessment might impact on the appreciation of art and design objects made of transparent and highly glossy PMMA.

When trying to correlate gloss values with human detection limits, it has been reported (Minolta 2017) that on a matte surface of about 5 GU, the human eye can detect a difference of roughly 3 GU. However, measuring a difference of 3 GU on a higher gloss surface (> 70 GU) would prove challenging (Minolta 2017). The higher the glossiness, the harder it is to detect changes in reflectance. According to optical technology specialists, differences of less than 15 GU are not detectable by the human naked eye (PCE Instruments 2018).

### **Background testing**

Following the methodology by Shashoua *et al.* (2009), gloss measurements in this study were performed before cleaning and within a standardised time period upon its completion. Measurements were carried out on five spots per sample and each spot measurement was repeated five times for increased consistency. Three replicates were measured and averaged for each treatment. Raw data were numeric (example in Fig.6.5), expressed in GU. Calibration against the black glass standard was carried out at the start of every period of operation and between every change of sample.

	1	2	3	4	5	6	7	8	9	10
20°	53.1	86.4	92.2	98.8	93.6	96.8	94.9	90	94.5	93.1

Figure 6.5. Example of raw gloss values expressed in gloss units (GU) at measuring angle of 20 degrees.

Given that PMMA, as a highly reflective surface, tends to display values exceeding those of the standard (100 GU), experimental set-up aimed to identify a suitable background



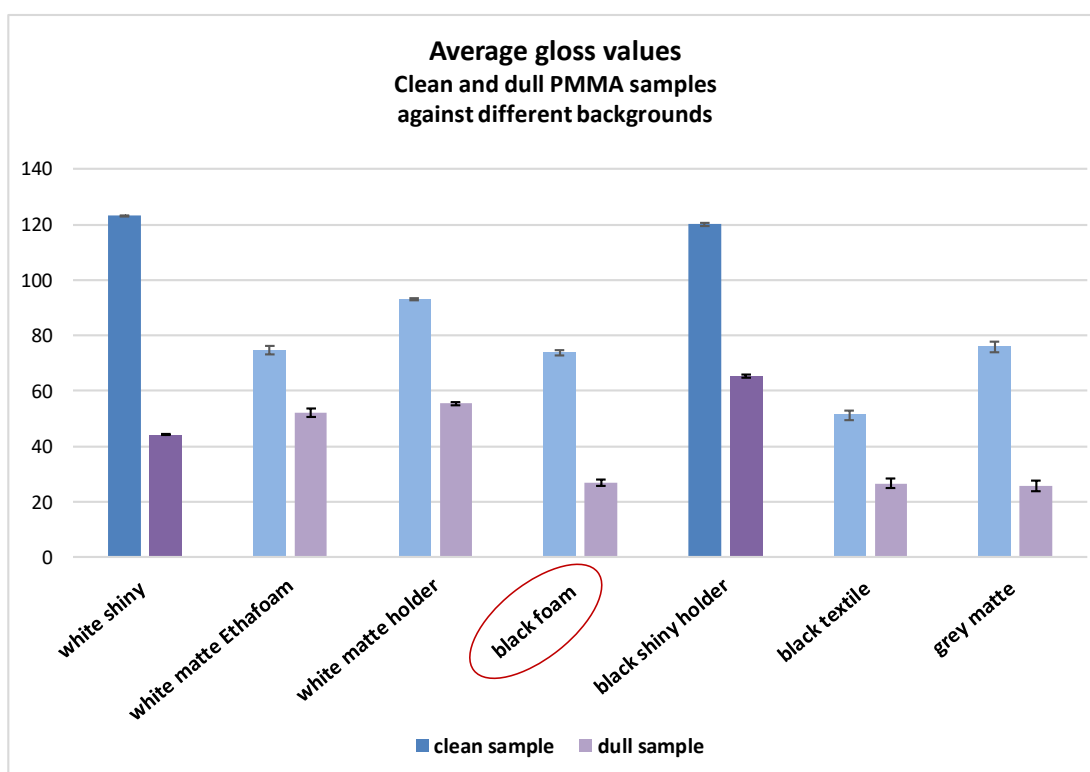
to be placed behind each transparent sample. This was with a view to reducing internal and external reflections, such as those originating from the lower surfaces. Background material that would allow the most consistency in repeated measurements was also desirable. Measurements were carried out using a Konica Minolta Multi Gloss 268 Plus meter at an incident angle of 20° on a control PMMA (labelled clean) and a solvent-treated sample that exhibited surface dullness (labelled dull). The following materials, including white and black, shiny and matte surfaces, as well as a grey matte, were tested directly under the samples:

- shiny, highly polished, white marble surface (*white shiny*)
- white Ethafoam® (*white matte Ethafoam*)
- white plastic surface (*white matte holder*)
- black Plastazote® (*black foam*)
- black plastic surface (*black shiny holder*)
- black matte textile (*black textile*)
- grey textile (*grey matte*)

sample	clean PMMA sample							dull PMMA sample						
	white shiny	white matte Ethafoam	white matte holder	black foam	black shiny holder	black textile	grey matte	white shiny	white matte Ethafoam	white matte holder	black foam	black shiny holder	black textile	grey matte
1A	157	85.50	133	63.50	127	41.10	93.07	47.30	64.27	93.78	17.98	93.15	16.73	13.29
2A	155	97.77	133	64.92	127	49.10	77.77	47.09	69.72	93.76	17.91	93.14	19.03	14.46
3A	156	99.23	133	66.54	127	51.08	80.36	47.24	71.28	93.79	18.18	93.19	20.12	14.12
4A	156	97.78	133	67.21	127	50.90	81.08	47.00	73.22	93.77	18.65	93.16	20.54	14.62
5A	155	97.38	133	61.49	127	58.20	82.90	46.70	71.91	93.79	18.79	93.13	20.89	14.25
Average A	156	96	133	65	127	50	83	47	70	94	18	93	19	14
StDev A	0.75	5.05	0.00	2.07	0.00	5.46	5.28	0.21	3.12	0.01	0.35	0.02	1.50	0.46
1 B	95.15	64.14	47.24	61.31	128	108	83.27	46.75	73.00	73.36	15.92	59.34	19.10	21.37
2 B	97.53	62.81	47.24	67.61	128	105	85.03	43.79	70.25	73.37	15.71	59.42	19.27	20.87
3 B	97.00	63.03	46.88	69.34	127	105	83.78	43.40	71.81	73.40	16.23	59.46	19.57	21.60
4 B	97.42	65.14	46.62	70.02	127	106	84.05	43.81	73.42	73.32	16.41	59.50	19.65	21.79
5 B	96.33	64.67	45.88	71.54	127	107	84.04	52.57	74.21	73.32	16.28	59.48	20.47	21.53
Average B	97	64	47	68	127	106	84	46	73	73	16	59	20	21
StDev B	0.87	0.91	0.50	3.56	0.49	1.17	0.57	3.47	1.38	0.03	0.26	0.06	0.47	0.31
1 C	133	76.12	33.71	80.27	129	59.34	61.58	51.88	42.32	32.35	23.17	28.05	38.62	13.25
2 C	135	78.03	34.82	81.98	130	55.90	61.00	51.94	41.89	32.34	24.51	28.08	43.37	13.63
3 C	132	80.79	30.43	83.41	130	57.46	62.10	50.77	41.96	32.35	24.05	27.79	45.93	14.09
4 C	132	82.41	33.67	85.25	130	58.25	62.40	49.66	42.36	32.32	25.33	27.75	47.42	14.62
5 C	133	82.82	32.28	85.79	130	61.64	61.59	50.51	42.35	32.31	24.90	27.89	48.09	14.18
Average C	133	80	33	83	130	59	62	51	42	32	24	28	45	14
StDev C	1.10	2.58	1.51	2.04	0.40	1.92	0.48	0.86	0.21	0.02	0.74	0.13	3.44	0.47
1 D	74.55	67.11	125	72.63	105	12.26	73.76	36.86	57.46	28.30	13.35	108	26.89	22.64
2 D	75.10	68.24	125	70.62	105	12.18	77.19	36.63	59.85	28.07	13.79	108	28.61	23.20
3 D	75.45	69.05	125	70.72	105	12.43	77.55	36.61	62.34	28.15	14.13	107	28.56	22.76
4 D	75.52	69.60	125	70.46	104	13.40	77.34	36.58	61.98	27.55	14.23	107	29.51	23.21
5 D	73.68	70.36	127	70.58	104	12.98	76.27	36.52	62.80	27.47	14.28	106	30.57	23.13
Average D	75	69	125	71	105	13	76	37	61	28	14	107	29	23
StDev D	0.68	1.12	0.80	0.82	0.49	0.47	1.40	0.12	1.99	0.33	0.35	0.75	1.22	0.24
1 E	157	64.36	128	81.08	109	26.21	73.03	40.90	15.28	50.10	59.02	38.80	18.06	55.46
2 E	157	67.45	127	82.20	112	27.42	73.28	40.24	15.11	49.69	60.72	38.92	19.96	54.63
3 E	157	65.84	127	81.89	112	29.42	73.22	40.67	15.02	50.14	61.18	38.96	20.75	55.21
4 E	156	65.57	127	81.43	113	31.98	73.82	40.65	15.07	50.15	63.00	38.96	21.05	55.75
5 E	155	65.05	127	82.29	113	28.45	74.24	40.59	15.67	50.03	62.23	38.97	21.45	56.55
Average E	156	66	127	82	112	29	74	41	15	50	61	39	20	56
StDev E	0.80	1.03	0.40	0.46	1.47	1.96	0.45	0.21	0.24	0.17	1.36	0.06	1.20	0.63
average	123	75	93	74	120	51	76	44	52	55	27	65	27	26
StDev	0.14	1.58	0.50	1.09	0.48	1.72	1.86	1.27	1.10	0.13	0.41	0.27	1.00	0.14

Table 6.7. Raw gloss data of an untreated-clean and a solvent-treated/dull PMMA sample measured at an incident angle of 20° against a variety of backgrounds. Table includes averages and standard deviations of five measurements repeated for each of the five spots per sample.

Clean PMMA samples tended to exhibit higher gloss values (Graph 6.1 - blue bars), regardless of the background. Shiny backgrounds of both white and black (*white shiny* and *black shiny holder*) caused an increase in the gloss values, especially in combination with the clean sample, thus were considered inappropriate. As standard methods for testing gloss of plastics recommended the use of a black matte backing (D2457-13), further examination focused on the darker matte backgrounds (Table 6.8). The *black textile* caused large deviations to all samples. The *grey matte* performed well behind the *dull* PMMA, but did not offer consistency of measurements to the *clean* PMMA. The *black foam* resulted in average gloss values lower than 100 GU and satisfactory standard deviations (highlighted in Table 6.8), rendering it the most suitable background for this study.



Graph 6.1. Bar chart of average gloss values of an untreated-clean (blue) and a solvent-treated/dull (purple) PMMA sample against a variety of backgrounds. Gloss measurements were carried out at an incident angle of 20° on five spots repeated five times. Error bars represent the standard deviation.

	clean PMMA samples			dull PMMA samples		
sample	black foam	black textile	grey matte	black foam	black textile	grey matte
Average A	65	50	83	18	19	14
StDev A	2.07	5.46	5.28	0.35	1.50	0.46
Average B	68	106	84	16	20	21
StDev B	3.56	1.17	0.57	0.26	0.47	0.31
Average C	83	59	62	24	45	14
StDev C	2.04	1.92	0.48	0.74	3.44	0.47
Average D	71	13	76	14	29	23
StDev D	0.82	0.47	1.40	0.35	1.22	0.24
Average E	82	29	74	61	20	56
StDev E	0.46	1.96	0.45	1.36	1.20	0.63
<b>average</b>	<b>74</b>	<b>51</b>	<b>76</b>	<b>27</b>	<b>27</b>	<b>26</b>
<b>StDev</b>	<b>1.09</b>	<b>1.72</b>	<b>1.86</b>	<b>0.41</b>	<b>1.00</b>	<b>0.14</b>

Table 6.8. Raw gloss data of the averages and standard deviations of the untreated-clean and the solvent-treated/dull PMMA samples measured at an incident angle of 20° against the darker matte backgrounds: black foam, black textile and grey matte. Total average and standard deviation are calculated from the five spot measurements per sample.

### 6.3. WEIGHT CHANGE MEASUREMENTS

Gravimetric studies, or else weight change measurements, provide a quantitative indication of changes in a material. They are based on percentage change and comprise one of the most popular methods of monitoring polymer degradation (Wypych 2013), mainly due to their simplicity and wide adaptability (Troiano *et al.* 2014). Fife *et al.* (2014) carried out comparative analysis of paintings cleaned with different solvent-based treatments and used percentages of mass changes as an indication of treatment effect. Weight changes were examined in combination with the relaxation data acquired from NMR MOUSE, proving complimentary techniques for monitoring underlying physical change.

Measurements offered quantitative evidence of the changes taking place in samples as a result of cleaning. Solvent gels were expected to cause immediate changes to weight. Chapter 7.1.2, discussing the effect of solvents on PMMA after immersion for 30 days, demonstrated that liquid absorption, polymer extraction and dissolution (Quye and Keneghan 1999; Shashoua 2012) were directly attributed to the solvent nature and the PMMA solubility (Troiano *et al.* 2014). Caution was needed when interpreting these weight changes that could be influenced by a number of competing processes related to chemical reactions, probably occurring concurrently. Gravimetric studies overlook the possibility of simultaneous extraction and diffusion of components; Weight loss may denote depolymerisation during degradation, but also dissolution, extraction and subsequent evaporation of (volatile) components. Weight gain might result from solvent absorption and diffusion in the sample, swelling, and/or dissociation of the gel leaving residues. It becomes evident that it is important to combine

weight measurements with other techniques. Based on studies that used weight measurements alongside unilateral NMR (Ulrich *et al.* 2011; Fife *et al.* 2014), this study coupled weight changes % with NMR MOUSE and py-GC/MS (see Chapter 7.1.2 for discussion of results), for understanding of the behaviour of PMMA.

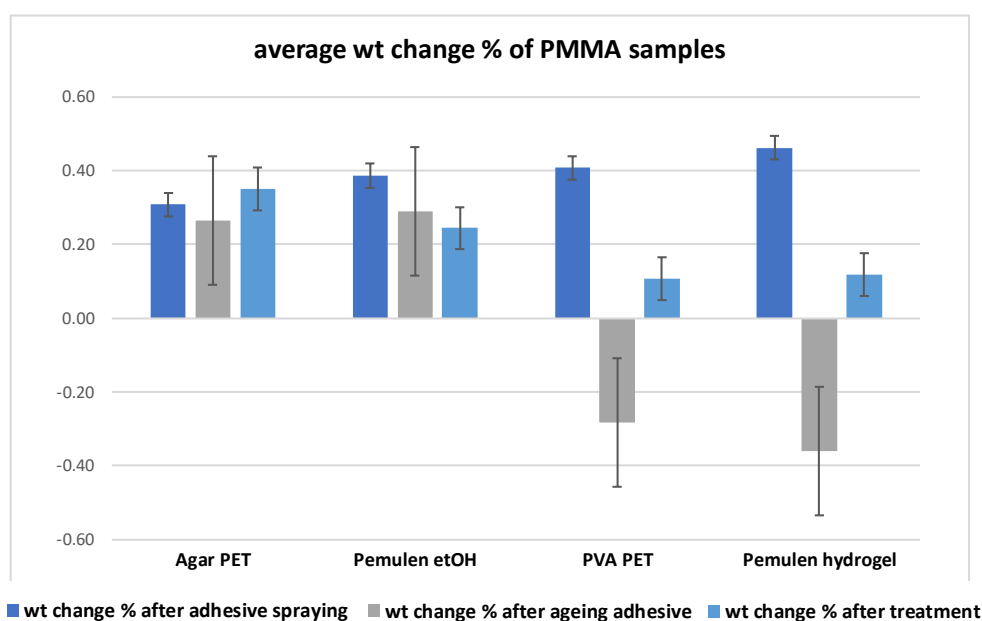
Weight measurements were performed using a Sartorius MSE225S-000-DU Cubis Semi-Micro Balance. The accuracy of the balance was 0.01 mg. Changes were calculated as percentages from the weight measurements before and after cleaning according to the following formula:

$$\text{wt change \%} = \left( \frac{\text{wt after treatment} - \text{initial wt}}{\text{wt after treatment}} \right) * 100$$

In the preliminary experiments (Chapter 8) weight change % is calculated after application of synthetic sebum soil (from now on synthetic soil)/PSA and after cleaning. As cleaning experiments proceeded, and more factors were added to the design (Chapters 9 and 10) weight changes % were calculated after application of synthetic soil/PSA, ageing of samples with synthetic soil/PSA and cleaning. For statistical analysis and graphic representation, changes % were averaged for the five replicates per treatment. Their standard deviation was represented to show the dispersion of values within data sets. For examples of how measurements and % change were documented, calculated and plotted see Table 6.9 and Graph 6.2.

sample	treatment	initial weight	weight after dirt	wt % after dirt	ave change % after dirt	stdev change % after dirt	weight after ageing dirt	wt % after ageing dirt	ave change % after	change % after ageing dirt	weight after treatment	wt % after treatment	ave change % after	change % after treatment
U397	Agar PET	0.71615	0.71880	0.36867			0.71860	0.34094			0.71924	0.42962		
U399	Agar PET	0.71905	0.72147	0.33543			0.72104	0.27599			0.72177	0.37685		
U406	Agar PET	0.71719	0.71928	0.29057			0.71876	0.21843			0.71933	0.29750		
U429	Agar PET	0.71670	0.71856	0.25885			0.71834	0.22830			0.71897	0.31573		
U431	Agar PET	0.73597	0.73806	0.28317	0.30734	0.04	0.73790	0.26155	0.26504	0.04	0.73845	0.33584	0.35111	0.05
U410	Pemulen etOH	0.69452	0.69673	0.31720			0.69654	0.29000			0.69632	0.25850		
U416	Pemulen etOH	0.72639	0.72863	0.30743			0.72844	0.28142			0.72785	0.20059		
U419	Pemulen etOH	0.67642	0.67900	0.37997			0.67872	0.33887			0.67822	0.26540		
U420	Pemulen etOH	0.70528	0.70777	0.35181			0.70722	0.27431			0.70692	0.23199		
U425	Pemulen etOH	0.73513	0.73938	0.57481	0.38624	0.10	0.73708	0.26456	0.28983	0.03	0.73707	0.26320	0.24394	0.02
340	Agar PET	0.77090	0.77478	0.50079			0.77186	-0.37831			0.77280	0.12164		
440	Agar PET	0.82111	0.82386	0.33379			0.82267	-0.14465			0.82349	0.09958		
523	Agar PET	0.76107	0.76524	0.54493			0.76209	-0.41334			0.76291	0.10748		
977	Agar PET	0.71603	0.71846	0.33822			0.71657	-0.26376			0.71731	0.10316		
1068	Agar PET	0.73126	0.73360	0.31897	0.40734	0.10	0.73200	-0.21858	-0.28373	0.10	0.73275	0.10235	0.10684	0.01
506	Pemulen etOH	0.76110	0.76435	0.42559			0.76222	-0.27945			0.76298	0.09961		
693	Pemulen etOH	0.80701	0.81300	0.73678			0.80773	-0.65245			0.80869	0.11871		
768	Pemulen etOH	0.75177	0.75474	0.39351			0.75250	-0.29767			0.75352	0.13536		
997	Pemulen etOH	0.74859	0.75163	0.40445			0.74930	-0.31096			0.75020	0.11997		
1127	Pemulen etOH	0.72195	0.72447	0.34784	0.46164	0.14	0.72256	-0.26434	-0.36097	0.15	0.72342	0.11888	0.11851	0.01

Table 6.9. Example of weight measurements on new and aged PMMA samples treated with solvent gels. Weight changes % were calculated according to the above formula. Averages and standard deviation of changes % were also estimated.



Graph 6.2. Example of a bar chart displaying the averaged weight changes % from Table 6.9. Changes % were averaged from five replicates after spraying of PSA (blue), ageing of samples with PSA (grey) and cleaning (light blue). Changes % are normalised to the starting/initial weight. Error bars show the standard deviation.

#### 6.4. ATTENUATED TOTAL REFLECTANCE FOURIER TRANSFORM INFRARED SPECTROSCOPY

In conservation, ATR-FTIR has been regularly employed as the main analytical technique for identification of plastics (Ploeger *et al.* 2009; DeGroot *et al.* 2011; Toja *et al.* 2011a; Toja *et al.* 2011b; Laganà *et al.* 2013; Toja *et al.* 2013) found as objects in museum collections or as conservation materials. Bollard *et al.* (2013) employed ATR-FTIR and correlated spectra with colour measurements to investigate chemical changes in plasticised PVC and identify the component responsible for yellowing. The spectra of unaged and aged PVC samples showed no significant difference rendering identification impossible (Bollard *et al.* 2013). Winther *et al.* (2013) employed ATR-FTIR among several techniques, to assess the effect of adhesives on plastics. Asensio *et al.* (2009) used it for identification of polymers used in the conservation of artworks (Asensio *et al.* 2009).

ATR-FTIR is an analytical method that provided information on the PMMA surface chemistry, scrutinising only a few microns of the sample surface. This was desirable in this study, fundamentally interested in the changes taking place on surfaces after gel treatment. The main interest was to assess the effect of different solvent gels in the PMMA molecular structure. The primary advantage of ATR was that it could be readily used, requiring neither sampling nor sample preparation. This opposes to the traditional FTIR by transmission, where the sample must be diluted or pressed into a pellet or thin film prior to analysis. Transmission was not selected here, because PMMA was capable of total IR absorption at shorter wavelengths leading to a flat spectrum with no peaks/bands at the group frequency region (Zolotarev *et al.* 2006). Instead,

ATR received signal from the surface and utilised the phenomenon of total internal reflection. However, the quality of the resultant spectrum depended on the intimate contact between the ATR crystal and the sample. The IR light had to penetrate the interface and into the sample upon reflection inside the ATR crystal (Salzer 2013), and this was only possible when contact between them was good. The samples remained intact after ATR analysis, although it is not ideal for real museum objects due to applied pressure and difficulty to adjust non-planar surfaces to be in contact with the ATR crystal. This was not of concern in this study as the analysed materials were planar mock-up substrates.

Analysis was performed with 32 scan accumulation at ambient temperature and pressure with a zinc selenide (ZnSe)/diamond Universal ATR Sampling Accessory (Perkin Elmer FT-IR/NIR Frontier) between 4000 and 600  $\text{cm}^{-1}$  (mid-IR region), with a resolution of 4  $\text{cm}^{-1}$  and a maximum penetration depth of the IR beam into the samples between 0.5-5  $\mu\text{m}$ . The region of the mid-IR, called the 'fingerprint' region, was the most adequate for analysis and identification of materials, as it was dominated by strong bands. The resulting spectra were characteristic and unique for each compound (Bacci 2000). Reference spectra were acquired from the new and aged controls, the hydrogel polymer networks, the synthetic soil and PSA. Its purpose was to identify all peaks attributed to PMMA, the gels and dirt individually, and enable the detection of alterations to the treated surfaces (spectral changes by comparison of initial spectra to post-treated ones). Solid materials comprising the gels were initially prepared as potassium bromide (KBr) pellets and analysed in transmittance mode. Hydrogels were heated, dried and analysed in ATR.

FTIR has not always been recommended for diagnosing the chemical degradation of PMMA (Miller *et al.* 2010). The material shows no strong indication for chain scission, or else, peaks related to by-products and new species emerging after ageing. This was partially due to the fact that all PMMA prominent peaks were associated with the ester and methyl groups, which depleted simultaneously. Nevertheless, even though no new peaks may occur, depletion may manifest itself as a decrease of intensity throughout the spectra. Therefore, this would provide adequate proof of change in the material after cleaning. Moreover, it was anticipated that some functional groups resulting from gel residues would be visible in the treated PMMA spectra. Since the main aim of this study was to detect relative change, the technique was used qualitatively and was coupled with other techniques presented in this chapter. ATR-FTIR has been often combined with SEM imaging and py-GC/MS used here too, in order to evaluate treatments (Winther *et al.* 2013).

## Spectra

Identification of the characteristic PMMA functional groups present, took place via direct comparison to reference spectra (Fig.6.6) (Shashoua 2008) and correlation to absorption bands with specific chemical bonds. Interpretation was generally based directly on visual inspection. Both the presence and absence of characteristic group frequency bands may be useful for detection of changes in the molecular structure. Perkin Elmer Spectrum version 10.5.1 (2015) software connected to the ATR-FTIR instrument was used to obtain the ATR spectra and calculate peak height ratios, while softwares *Spectragryph* and *Essential FTIR* were used for processing and manipulation of data.

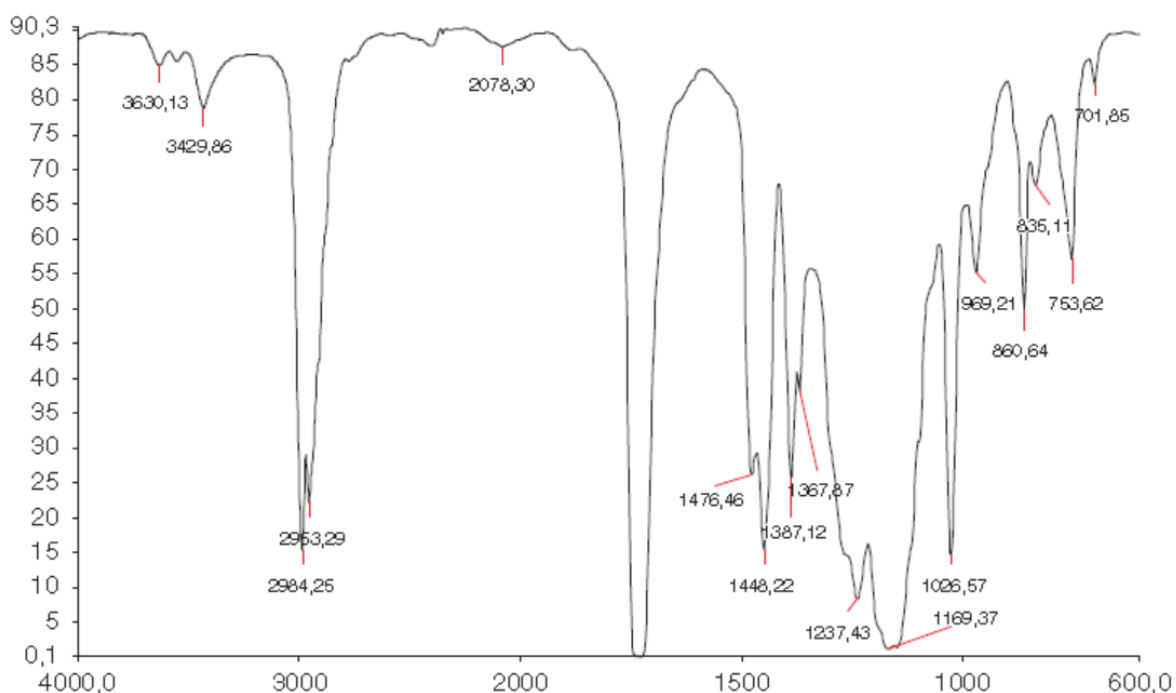


Figure 6.6. ATR-FTIR reference spectrum of PMMA (Shashoua 2008, 264).

Caution was needed when interpreting spectra, as several aspects influenced the results. Primarily, it was important to understand that analysis was performed on the first few microns of material that was in contact with the ATR crystal. The penetration depth of analysis, here up to 0.5-5  $\mu\text{m}$ , was proportional to specific wavelengths, meaning that relative band intensities would change in different regions according to pressure of the crystal during analysis (Diz and Spragg 2010). In addition, the high refractive index of PMMA would result in peak distortion, skewed baselines, and shifts in both peak positions and peak intensity (Shimadzu 2019). Such differences were caused by changes of the material in a physical level, and not a chemical, and in order to account for them, peak height ratios were generated.

The method involved using an internal standard (band  $750\text{ cm}^{-1}$ ) to eliminate variation and guarantee that any changes present were chemical (due to depletion) and not just

differences in path length. Internal standards are bands that are chemically constant during analysis and accord for any intensity variations due to sampling depths. Peak height ratios were calculated for all spectra between internal standard and the changing peaks of interest, in order to confirm relative change in the samples based on peak fluctuation. Measurement of peak height was a manual procedure. A linear baseline correction was applied on all spectra and for each peak of interest between the beginning to the end of the valleys appearing around them. The peak height was the distance between the baseline and the apex of the peak (a vertical line showing the maximum height measured relative to the linear baseline).

The method was possible on PMMA surfaces being treated without the addition of surface dirt. A layer of surface dirt complicated interpretation of FTIR spectra, especially in the case of PSA that was of similar acrylic nature to PMMA itself. Gel treatments added an additional challenging factor, the presence of gel residues, also of organic polymeric nature. Contribution of peaks from PMMA, PSA and gel with similar absorptions would be very challenging to interpret. Therefore, ratioing of peak heights at  $1723\text{ cm}^{-1}$  and  $750\text{ cm}^{-1}$  was used to detect (semi-quantitatively) relative chemical change in samples as a result of: exponential photooxidative ageing under UV irradiation earlier presented (Chapter 5), immersion in liquid environments and hence solvent-induced damage (discussed in Chapter 7) and lastly, cleaning with free solvents, hydrogels and solvent gels (see Chapter 8).

Band  $750\text{ cm}^{-1}$  was selected as the internal standard. As reported by Tretinnikov and Zhbankov (1991), the intensity of this band remained constant/invariant during UV ageing, providing a reference spectral band for the assessment of photo-oxidation in PMMA. Peak  $750\text{ cm}^{-1}$  was attributed to vibrations of C–H bonds in the methylene group ( $\text{CH}_2$ ) of the main chain (Nagai 1963). The very prominent carbonyl vibration band at  $1723\text{ cm}^{-1}$  was chosen to be ratioed against peak  $750\text{ cm}^{-1}$  as it showed the most dramatic changes in intensity. The progression of changes was based on the decrease of peak  $1723\text{ cm}^{-1}$ , indicating chain scission confirmed by the loss of carbonyl C=O and subsequent shortening of polymer chains evidenced as detachment/loss of the ester side group. Calculation of ratios offered a comparative/relative assessment of surface changes. For exponentially UV-aged samples smaller ratios confirmed the progression of PMMA photodegradation, for 32 days liquid-immersed samples smaller ratios denoted solvent-induced damage and for treated samples chemical changes could be attributed either to solvent damage or gel residues (hindering absorption of PMMA resulting in decrease of absorption or overlapping peaks resulting in increase of absorption).

## 6.5. NUCLEAR MAGNETIC RESONANCE MOBILE UNIVERSAL SURFACE EXPLORER

Unilateral (or single-sided) NMR is a non-invasive diagnostic tool able to probe layers tens of microns thick in the bulk of organic materials and monitor the presence and relaxation



properties of proton spins (hydrogen), known as unilateral relaxometry. The only requirements for analysis are presence of hydrogen, materials being free of magnetic parts and non-electrically conducting (Blümich *et al.* 2010). The MOUSE can practically trace the presence of water, moisture or any liquid containing hydrogen (Oligschläger *et al.* 2014), assisting in the understanding of mechanical change (Del Federico *et al.* 2010). The higher the hydrogen content is, the stronger the NMR signal that can be acquired in shorter times (Blümich *et al.* 2010). Information is obtained in the form of a depth profile and includes relaxation times as a function of depth, and signal intensity as a function of hydrogen density i.e. concentration of liquid within a given volume (Bortolotti *et al.* 2006).

Most notably it is used in the field of geophysics, food industry, biomedical diagnostics in organic tissues i.e. skin and tendon (Del Federico *et al.* 2010), and soft matter (i.e. rubber in car tires). In industrial applications it offers a rapid and inexpensive polymer screening. This is useful for the development of new polymer parts and identification of potentially defective components (Chinn *et al.* 2006). Gazi and Mitchell (2012) used it to determine the wetting characteristics (ability to absorb liquid contamination) of a coating for protection of military equipment surfaces against chemical warfare agents.

In the cultural heritage sector, it has been extensively employed for non-destructive analysis of objects and examination of their composition, degradation and condition (Capitani *et al.* 2013; Fife *et al.* 2014). The technique permits shallow penetration depths to be reached with a resolution of tens of micrometres permitting a profile of the samples and their underlying matrix. A common application example in conservation is uncovering the stratigraphy of easel paintings by producing a depth profile through two-dimensional (2D) mapping of the composite layers and their relative thicknesses (i.e. paint and primer) (Blümich *et al.* 2010; Anselmi *et al.* 2011; Capitani *et al.* 2012) without removing a physical cross-section. Capitani *et al.* (2012) obtained NMR depth profiles of an Egyptian mummy, identifying the stratigraphy of various anatomical layers in both wet and dry tissues. Depth profiles have also been employed to discriminate between textile wrapping from tissue and bone (Rühli *et al.* 2007).

The MOUSE has been used to monitor degradation of bulk materials (Guthausen *et al.* 1998; Blümich *et al.* 2003; Kehlet 2013). An example of this application was the investigation of the effect of UV radiation on crosslinked natural rubber (Goga *et al.* 2008). Kehlet *et al.* (2013) employed NMR MOUSE to investigate the extent of molecular change in (semi) synthetic polymers, including PMMA. They were able to map degradation by scanning plastics from the surface into the material. Comparison of a naturally aged latex museum object to a new sample showed the latter having a constant relaxation time throughout, as opposed to the former that relaxed faster at the surface than in the bulk, showing changes in the structure. It has also been

widely employed to study the porosity of materials (Bortolotti *et al.* 2006), water/moisture mobility and monitor its content/levels in the conservation of stone, wall paintings, mosaics, paintings and wood (Bortolotti *et al.* 2006, Capitani *et al.* 2012), assess the presence of salt efflorescence and detachment of paint (Del Federico *et al.* 2010; Oligschläger *et al.* 2014) and determine the nature of stains on paper (Del Federico *et al.* 2010).

Its ability to quantify material relaxation properties, makes the MOUSE ideal for evaluation of interventive treatments and monitoring of their progress (Del Federico *et al.* 2010). This becomes possible through non-invasive comparison of different depth profiles of treated and untreated samples. Capitani *et al.* (2012) employed it to study treatments and their effect on the sound quality of wooden *Stradivari* violins. Chiantore *et al.* (2003) and Ulrich *et al.* (2011) studied the influence of surfactants in acrylic paint films during aqueous cleaning, in regard to absorption and diffusion of water with different salt concentrations. Fife *et al.* (2014) used it on easel paintings before and after free solvents applied with cotton swabs or thickened in gels. They demonstrated that the thickened application allowed less solvent to penetrate the sample. Moreover, they stressed that the way solvents penetrate materials based on their different application methods is very critical, but yet insufficiently studied. This remark is of significance to the present research and will be further explored on treated PMMA. Fife *et al.* (2014) demonstrated that the effect of different solvent treatments can be successfully explored with NMR profilometry, rendering it highly applicable to this study.

Angelova *et al.* (2015) contributed to the importance of undertaking systematic studies on the ability of different types of gel systems to control or limit solvent action. In their study, unilateral NMR was employed to explore how far water from cleaning treatments, had penetrated new and light-aged paint layers. They investigated the rate of diffusion and quantified the water amount swelling the paint. Treatments included Agar, methylcellulose, Pemulen and Velvicol Plus emulsion-gels, and PVA-borax against water-moistened cotton swabs. Results showed that aged samples were less prone to absorbing large quantities of water during cleaning. Most importantly, they showed that moistened swabs did not release more water than gels (Angelova *et al.* 2016a). Doherty *et al.* (2014) used depth profiles to evaluate gel treatments and their interaction with paint layers on paper substrates, in particular application of methylcellulose and gelatine film. The study showed that methylcellulose would penetrate into the paper, whereas excess water from the gelatine film was absorbed by the paper.

NMR MOUSE was employed in this study to evaluate how different gel systems influence liquid movement/diffusion into the PMMA. The main interest was in relative values and changes in solvent distributions before and after treatment, rather than the distributions themselves or their absolute values. Proton density and relaxation data were used in a

comparative manner to determine physical differences before and after treatment. NMR scanning aimed to detect whether thickened solvents penetrated PMMA, trace how profound they infiltrated sample thickness, document how long it took them to do so and whether they followed a preferential path (Blümich *et al.* 2010). By keeping experimental parameters constant throughout all NMR experiments, detection of the rate, behaviour and extent of solvent spread, along with information about the PMMA molecular mobility at various depths (Kehlet *et al.* 2013), allowed understanding of the effect and reversibility of different solvent gel cleaning processes.

The value of this technique has already been demonstrated, but what was most beneficial was that samples were directly monitored during treatment (Anselmi *et al.* 2011), gaining information on their real-time behaviour. Of particular interest was detection of wetting, swelling and dissolution/evaporation. As discussed in 3.3.3.2, solvents of similar solubility parameters as PMMA, are expected to penetrate its free volume causing elongation of polymer chains (Kwamen 2014). The rate of these phenomena was hoped to be understood.

The technique combines an open magnet and a radio-frequency coil. The former generates a homogenous magnetic field, external to the magnet where hydrogen protons align with the magnetisation and the NMR signal is generated and detected (DiTullio *et al.* 2017). The coil introduces an electromagnetic pulse perpendicular to the magnetic field, inducing an instantaneous rotation of the magnetisation, causing the protons to rotate. The time taken for the protons to realign within the magnetic field is taken as a measure of mobility and is known as longitudinal relaxation, spin-lattice relaxation, or  $T_1$  relaxation (Del Federico *et al.* 2010).

The magnetic field is applied to one side of the object non-destructively allowing measurement of the transverse  $^1\text{H}$  relaxation decay of protons using a pulse program sequence, the Carr–Purcell–Meiboom–Gill (CPMG) (Kehlet *et al.* 2013). The transverse  $^1\text{H}$  relaxation time constant ( $T_{2\text{eff}}$ ) of the signal decay reflects the molecular mobility of the material (Rühli *et al.* 2007). CPMG echo experiments performed at each sample depth can determine signal intensities (amplitude  $A$ ) and relaxation times ( $T_{2\text{eff}}$ ) (Sun 2012). Signal intensities correspond to the proton  $^1\text{H}$  density through the scan depth and are used for acquisition of depth profiles, offering information on the molecular mobility at various depths (Rühli *et al.* 2007). Relaxation times are numeric values denoting material stiffness (Fife *et al.* 2014).

Rigid materials, such as PMMA, with low mobility atoms are known as short components. They have a fast relaxation (Blümich *et al.* 2010; Del Federico *et al.* 2010; Ulrich *et al.* 2011), which translates in reduced  $T_{2\text{eff}}$  relaxation times (Fig.6.7) (Del Federico *et al.*

2010). Liquid presence acts as a plasticiser, corresponding to enhanced molecular mobility (Guthausen *et al.* 1998). So, solvents as long components, were expected to initially cause an increase of  $T_{2\text{eff}}$  by diffusion in PMMA, and then a decrease upon evaporation (Oligschläger *et al.* 2014). In order for the  $T_{2\text{eff}}$  values to be calculated, the resulting CPMG echo decay curve required fitting to a component model (Oligschläger *et al.* 2014). Here, it was fitted with a single exponential model decay function.

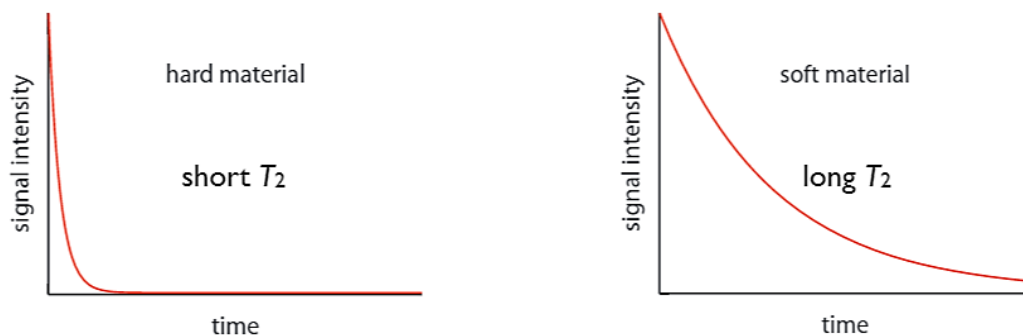


Figure 6.7. Relaxation times ( $T_{2\text{eff}}$ ) of rigid and soft materials, as obtained by unilateral NMR. The harder the material, the shorter the relaxation (Meldrum 2013).

### **Set up & experimental parameters**

NMR relaxation studies were carried out using a PM-5 Profile  $^1\text{H}$  NMR MOUSE (Magritek, Aachen, Germany) with a field strength of approximately 0.5 T (ca. 19 MHz proton frequency). The magnet was mounted on a precision lift controlling its horizontal position. Profile scans were recorded by collecting CPMG echo radiofrequency pulse sequences, obtained at 50  $\mu\text{m}$  depth increments. A 2.0 mm spacer adjusted the sampling depth (working distance) from an initial 5250  $\mu\text{m}$  to 3250  $\mu\text{m}$ . Scans were performed on duplicates *before* treatment, immediately after (*dynamic experiment*) and 24 hours after. NMR experiments simulated the cleaning protocol used in the final experiments (Chapter 10): three consecutive gel applications of 3 minutes each, cleared in between with three moistened cotton swabs. Samples were the same size as the analytical window, therefore they were placed on a microscope glass slide to properly position them.

*Dynamic* experiments, performed immediately after treatment, included running 10 consecutive profile scans through the samples' depth to capture possible solvent movement. The result was to create depth profiles of the volume of solvents penetrating from the gel to the PMMA surface into its bulk. Fluctuations in molecular mobility were expected to go hand-in-hand with associated changes in the relaxation time. Post-treatment scanning aligned with the decision to obtain all weight and gloss measurements 24 h after treatment completion. It was anticipated that this was enough time for residual solvent from treatments to evaporate.

### **Parameter optimisation**

It was important to ensure that experimental parameters were appropriately set for PMMA, because the NMR response (signal intensity and relaxation time) is parameter-dependent (Fife *et al.* 2014). Parameters were set after exhaustive testing of the sampling depth, number of scans and echoes, echo and repetition time, providing the optimum signal-to-noise ratio. It was equally important to define the physical boundaries of the material(s) being scanned, as different components produce different signal amplitude in profile scanning. All scans were performed on free standing PMMA samples (1000  $\mu\text{m}$  thick) with aged synthetic soil or PSA, placed on a microscope glass slide (600  $\mu\text{m}$  thick) (see Fig.6.8). The synthetic soil and PSA couldn't be detected during parameter optimisation. Although the smallest sampling size tested at 30  $\mu\text{m}$  produced very noisy scans, there was no discernible signal from the two dirt types, suggesting that neither layer was thicker than 30 microns. Attempts to isolate and measure the artificial dirt layers were discontinued, as the profiling aim was to detect solvent movement. After all, removal of artificial dirt was visually evident with other methods used in this study.

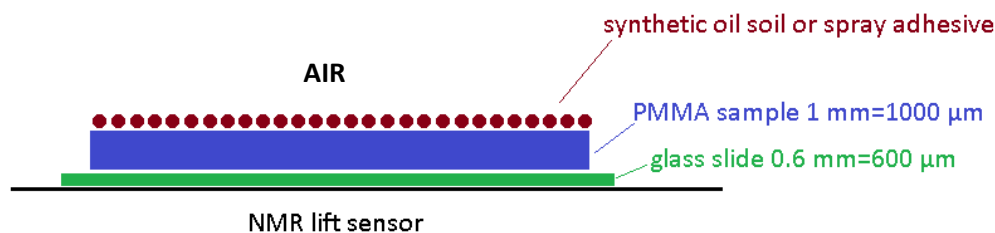


Figure 6.8. Sketch of experimental set up of PMMA sample on the NMR MOUSE lift ready for scanning.

### **Data processing**

Data were acquired using Prospa software (Magritek Aachen, Germany) and processed with OriginPro 2016 Software. The data is visualised as 2D contour heat maps created for each sample *before*, right after (*dynamic*) and 24 hours *after* treatment. An example is shown in Fig.6.9 with a 2D map of aged PMMA with aged synthetic soil before treatment, with the x-axis representing the CPMG echo decay and the y-axis the sample depth (step number in microns). Each horizontal segment 'slice' through the thickness of the sample represented a step of 50  $\mu\text{m}$ , while each vertical segment 'slice' (from echo 1 to 16) represented the signal through the sample depth. The profile scan/sequence localises the boundaries of the air-sample and sample-glass slide interface (yellow dotted lines).

The most intense signal was recorded in the first 2 echoes (between 0.06 – 0.08 on the colour scale). The first vertical slice (far left) through the map on the x-axis displays the proton density through the depth of the scanned sample. The 1<sup>st</sup> echo represented the highest intensity

throughout the whole sample depth. The material had fully relaxed by the 6<sup>th</sup> echo both before and 24 hours after treatment. From the 7<sup>th</sup> up to roughly the 10<sup>th</sup> echo the signal had weakened, from which point onwards there was none – denoted by a background of blue tones (below 0.03 on the colour scale).

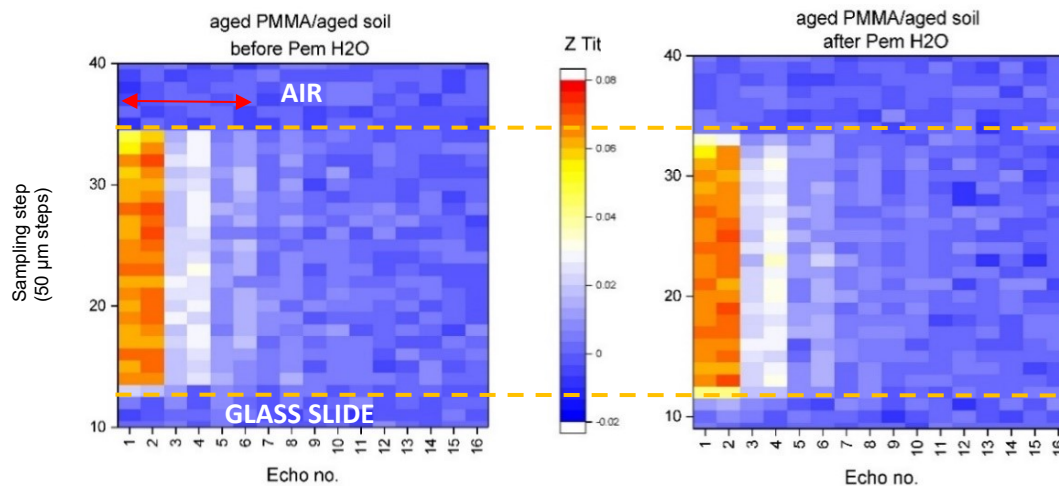


Figure 6.9. 2D colour-intensity contour heat map of the aged PMMA with aged synthetic soil before (left) and 24 h after (right) treatment. The first 2 echoes (between 0.06 – 0.08) showed the highest proton density. The material has fully relaxed by the 6<sup>th</sup> echo.

The need to capture the signal moving through the sample required optimisation of the dynamic experiment, which due to the large time scale needed for complete relaxation of the samples at each depth, was not possible. It was decided to focus on the first two echoes, which as seen, effectively represented the proton density. The 2D maps of the dynamic experiments (Fig.6.10) showed no solvent movement into any of the samples, either because penetration happened so fast that it was difficult to detect, or because no liquid penetrated in the given timeframe. If there would be liquid present in the sample, in such optimised profile scans, they would have been differentiated and visualised as two components.

It was possible that due to the hardness of PMMA, no significant penetration took place into its bulk. However, this would be challenging to detect due to difficulties in interpreting signal in the 2D maps (Fig.6.9-6.10). Additional visual representation was decided to ease the interpretation of results, and the sum of the signal amplitude of the 1<sup>st</sup> and 6<sup>th</sup> echoes were plotted against depth as line graphs. The 6<sup>th</sup> echo was selected because all PMMA samples, regardless surface condition and treatment, had fully relaxed by then. So, if a treated sample would show relaxation past the 6<sup>th</sup> echo, it would mean that solvent gel treatment altered its bulk behaviour. Plotting the 1<sup>st</sup> and 6<sup>th</sup> echoes of the *before* and *24 hours after* scans in the same graph would show changes in signal intensity and therefore relaxation behaviour.

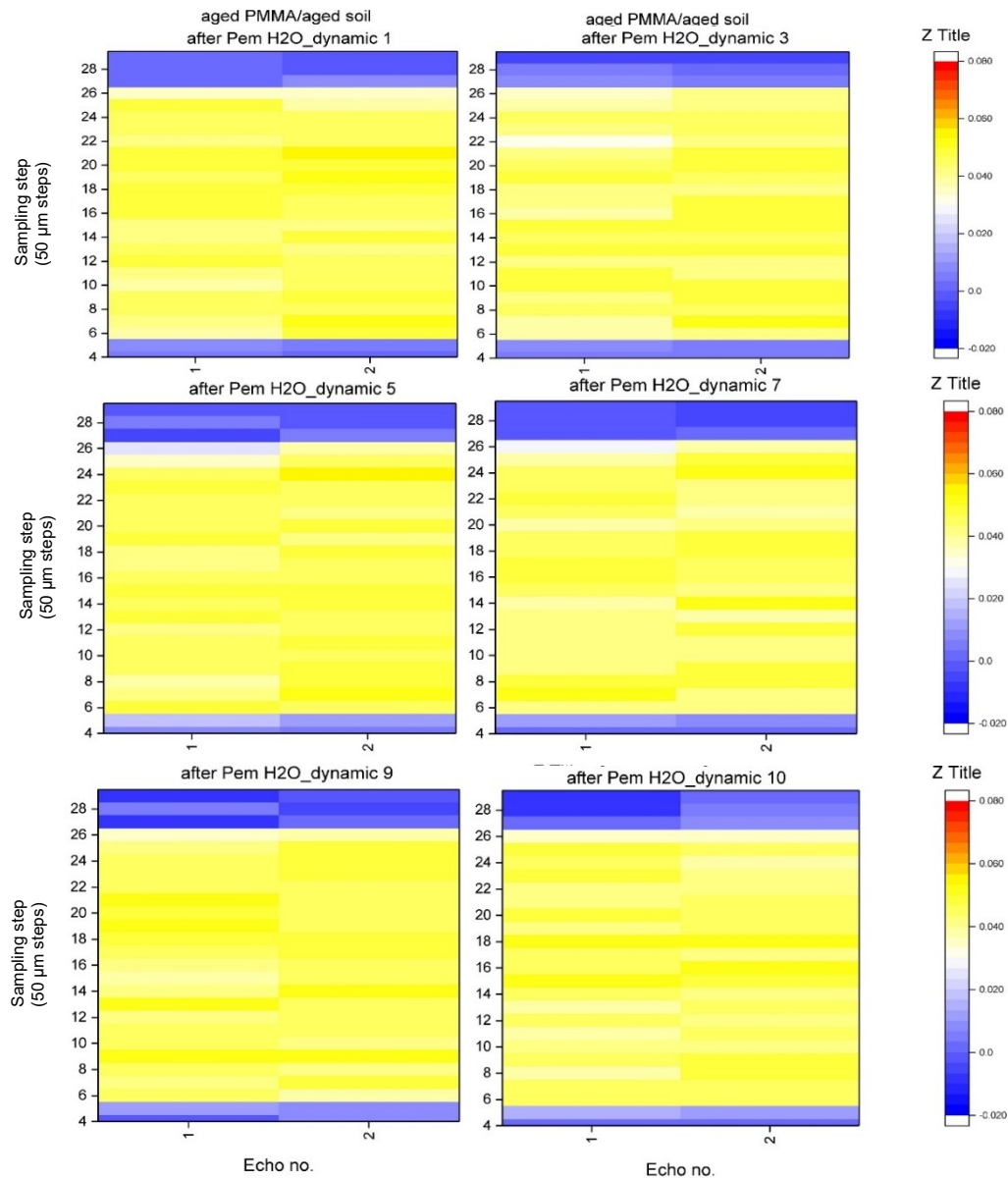
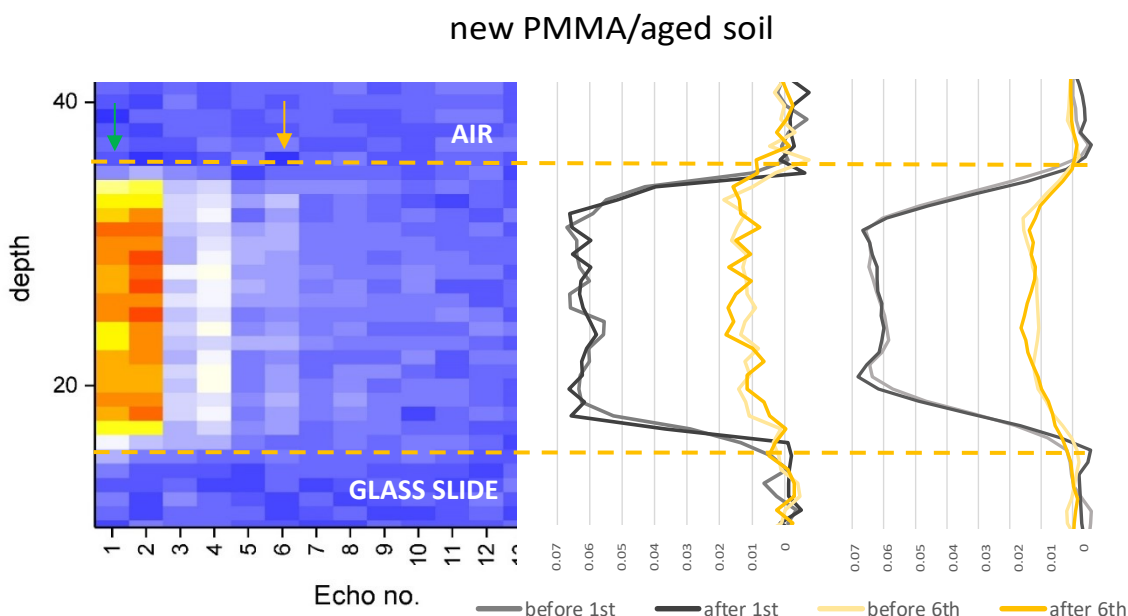


Figure 6.10. 2D colour-intensity contour heat maps of the dynamic scans of aged PMMA with aged synthetic soil immediately after treatment. The scans were acquired only for the first 2 echoes. Each increment (sampling depth) equates to 50  $\mu\text{m}$ .

Although the data were optimised by increasing the number of scans, interference was still present as background noise (Graph 6.3), hindering the detection of changes in the graphs. Given that it was already hard to detect liquid movement in the samples due to their stiffness, visual data were further enhanced by using Savitzky-Golay filtering with a 9-point convolute (window) to smooth the sum of the signal amplitude (Richardson *et al.* 2017) (for details see Appendix J). Attention was needed to normalise the line graphs to the back of the samples, the reason being that the back (bottom surface of scanned samples) was always constant regardless sample thickness, surface condition or gel treatment. Only by aligning the graph lines to start from the constant back could any real change in the front of the samples be established.



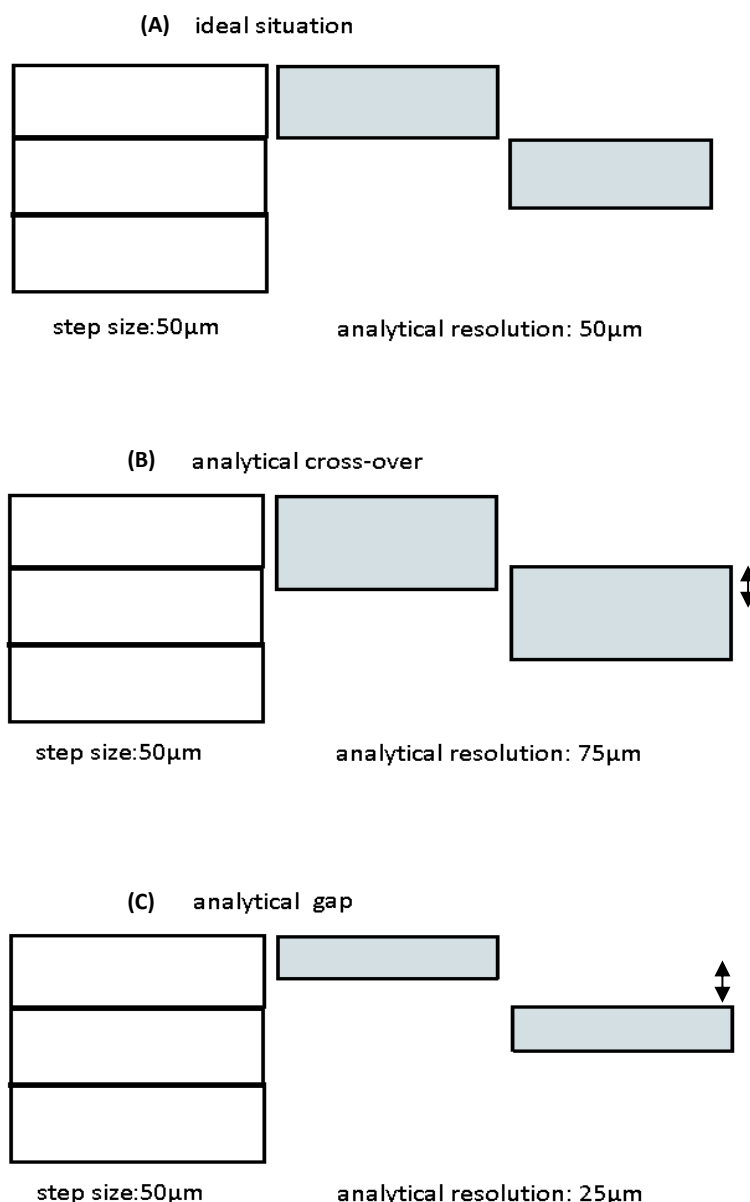
Graph 6.3. An example of the 2D colour-intensity contour heat map (left) obtained for a new PMMA sample with aged synthetic soil. A vertical slice through the 2D data at the 1<sup>st</sup> (green arrow) and 6<sup>th</sup> (yellow arrow) echo yields a profile of the proton density through the scan depth (1<sup>st</sup> echo: black line, 6<sup>th</sup> echo: yellow line). The central line graph is before smoothing and the one on the right is after smoothing using Savitzky-Golay filtering with a 9-point convolute.

After thorough testing, the number of scans was increased to 1024 acquisitions at each depth to reduce noise. The whole sample scan was repeated 10 consecutive times, lasting approximately 6 hours, to determine whether there was a change with time. Line graphs of the dynamic scans of the 1<sup>st</sup> and 2<sup>nd</sup> echoes showed no detectable difference between the 10 consecutive scans, suggesting that the focus should be turned to the *before* and *after* scans. PMMA before and 24 hours after had fully relaxed by the 6<sup>th</sup> echo, as earlier shown, but some signal was still faintly visible up to the 10<sup>th</sup> echo. Since the aim was to detect a possible increase of relaxation after treatment, and throughout the whole sample thickness, these scans were further optimised. Scanning was set to 16 echoes, number of scans was increased to 1536 acquisitions at each depth and lasted approximately 5 hours. The CPMG parameters for each Profile scan are listed in Table 6.10.

Profile scan	Repetition time (ms)	No. scans	No. echoes	Echo time ( $\mu$ s)	Pulse length ( $\mu$ s)	Step size ( $\mu$ m)	No. experiments
Before treatment	250	1536	16	50.2	3.8	50	1
Dynamic	80	1024	2	50.2	3.8	50	10
24 h After treatment	250	1536	16	50.2	3.8	50	1

Table 6.10. Analytical set up for NMR MOUSE scanning experiments of PMMA samples. Before and after treatment scans were longer and more optimised, while dynamic scans were shorter consisting of 10 experiments.



**Resolution versus step size**

*Figure 6.11. Issues arising from analytical depth resolution not representing signal and set step size. (A) depicts the ideal situation, while (B) and (C) instances where resolution is bigger or smaller than the step size.*

The step size in unilateral NMR profile scanning is of great significance. As earlier mentioned, NMR relaxometry is dependent on the experimental parameters. In the same way, the depth of the excitation region above the magnet i.e. sampling resolution, in particular the pulse length and acquisition time, are dependent on the experimental parameters. Therefore, although the precision lift controlling the magnet might be set to 50  $\mu$ m (sampling step) this does not actually mean that the excitation resolution is 50  $\mu$ m (Fig.6.11 A). However, if the resolution slice would be greater than the step size, then the data acquired would cross-over

and regions of the sample would be sampled twice (Fig.6.11 B). An example of this would be segment 7 (highlighted in Fig.6.12), positioned 350  $\mu\text{m}$  into the aged PMMA with aged PSA and a signal amplitude of ca. 0.05. Based on the phenomenon described here, this may be attributed to the aged PSA layer on its surface or to signal overlapping from different segments, i.e. air and sample, resulting in a distorted amplitude not corresponding to reality. The resolution may also be smaller than the step size, in which case the sampling region would be smaller than initially intended, leading to an analytical gap (Fig.6.11 C). In both cases information may be lost, or false signal may be documented.

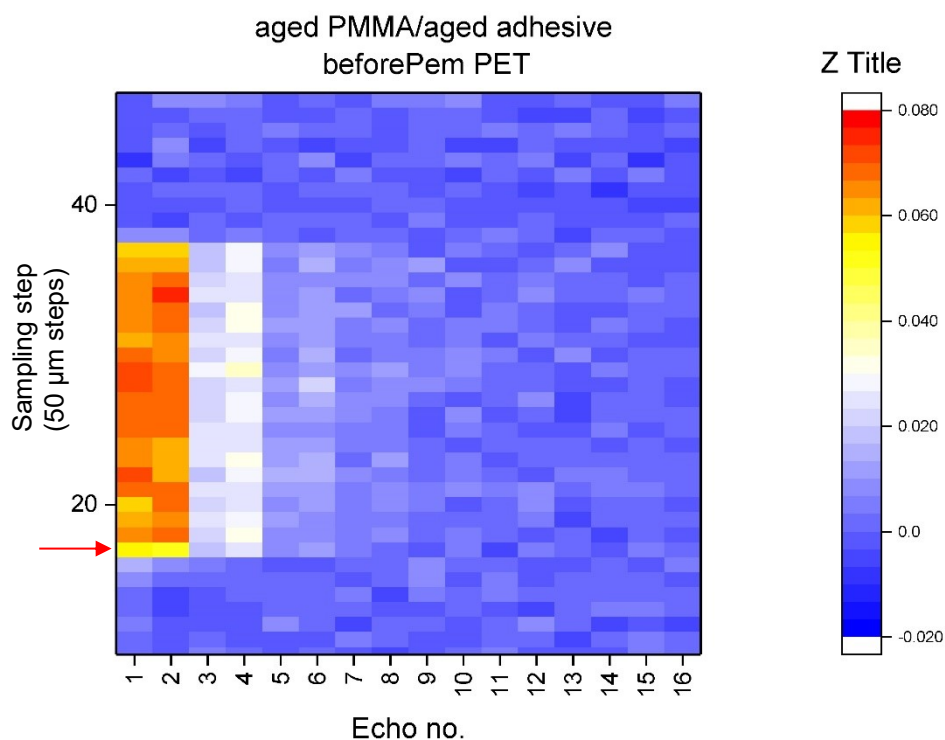


Figure 6.12. The 7<sup>th</sup> segment (highlighted with a red arrow) is 350  $\mu\text{m}$  from the sample surface and shows signal of approximately 0.05 based on the colour intensity scale.

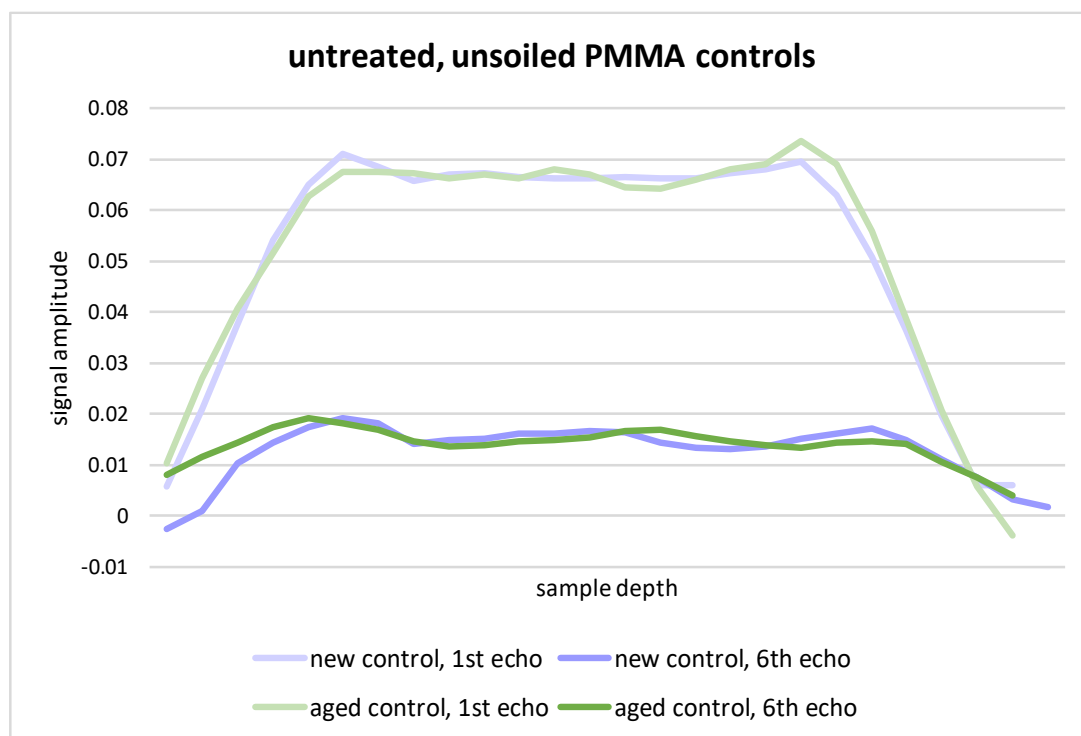
### **Controls**

PMMA controls did not show significant changes between the new and aged conditions. The surface pattern showed the edges of both samples having an increased signal compared to their bulk (over 0.07 at the edges and ca. 0.065 at the bulk) (Graph 6.4). This was clearly the case for the 1<sup>st</sup> echo, less visible for the 6<sup>th</sup>. PMMA controls have almost fully relaxed by the 6<sup>th</sup> echo with signal ca. 0.015 for the bulk and ca. 0.02 for the edges.

### **Immersion in liquids**

New, unsoiled and untreated samples were immersed in each of the liquids used in the experiments: deionised water ( $\text{H}_2\text{O}$ ), ethanol ( $\text{EtOH}$ ), isopropanol (IPA) and petroleum ether

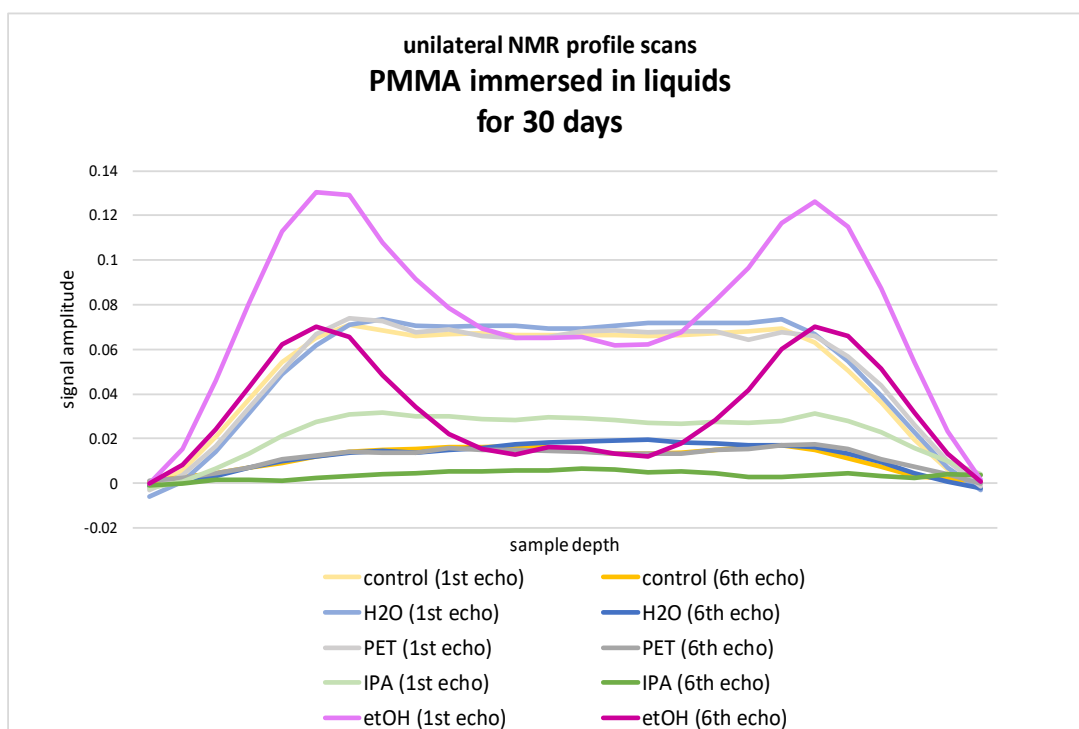
(PET). Samples were removed from their baths 30 days later and were left for 24 hours in lab environment to allow excess solvent evaporation. NMR profiles would act as comparative measurements for assessing the ‘extreme’ damage that these solvents, later thickened in gel systems, were capable of inducing to PMMA. Samples immersed in H<sub>2</sub>O and PET displayed profile scans similar to the controls, suggesting no physical change to the material. Samples immersed in EtOH and IPA caused significant change. The behaviour of PMMA was different in the two solvents.



*Graph 6.4. Smoothed line graphs of NMR profile scans of 1<sup>st</sup> and 6<sup>th</sup> echoes: unaged PMMA control (purple tones) and aged PMMA control (green tones). Control samples are unsoiled and untreated.*

A very interesting phenomenon was encountered in PMMA after 1 month in EtOH (Graph 6.5 – pink): the two edges of the sample appeared to have an increased signal – almost double that of the controls – for both 1<sup>st</sup> and 6<sup>th</sup> echoes examined here. However, the centre of the material and its bulk behaved differently, showing relaxation similar to the controls, with no change at all. This surface effect of PMMA immersed in EtOH, while magnified, was consistent with the surface pattern seen on the new and aged PMMA controls, where their edges also exhibited an increased signal compared to their bulk. The augmented signal amplitude in EtOH-immersed PMMA may be attributed to solvent trapped in the upper layers of the sample surface edges. This may translate into difficulty of the solvent to move through the PMMA surface and penetrate the bulk, or alternatively, it may suggest the exact opposite: sensitivity of the PMMA upper surface layers. Having established that this effect was consistent – in different magnitudes,

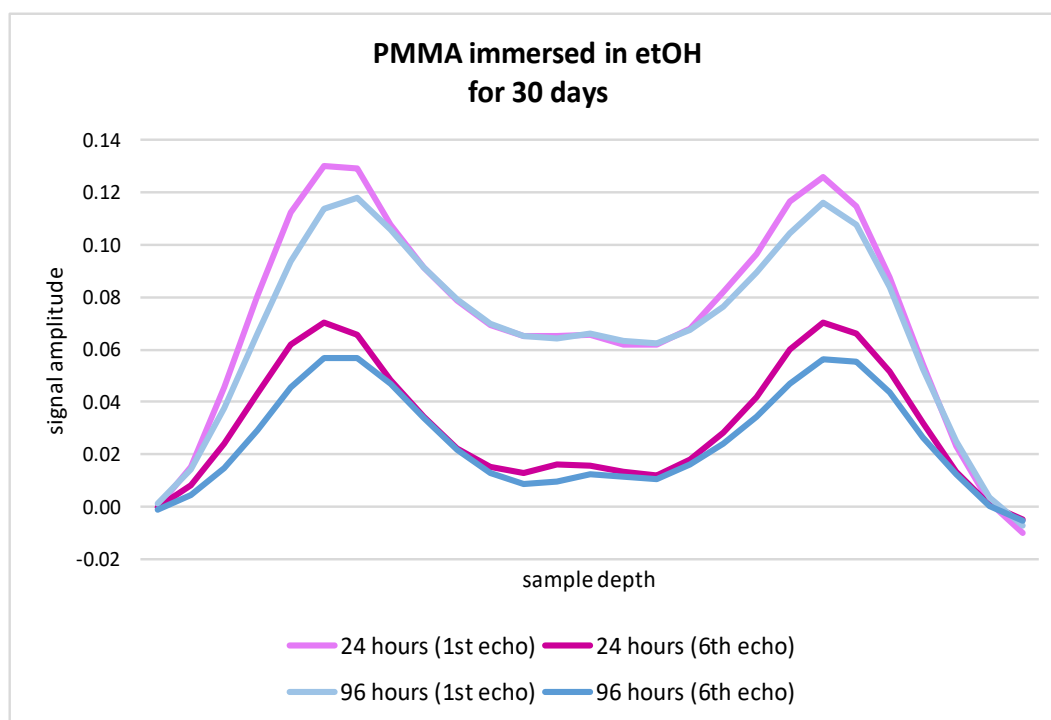
in all samples, treated and controls regardless surface condition, denoted that it may have been innate to the material. This effect may be the result of industrial surface treatment of the specific manufactured PMMA sheet or of cutting it into samples.



*Graph 6.5. Smoothed line graphs of NMR profile scans of PMMA samples immersed in H<sub>2</sub>O, EtOH, IPA or PET for 30 days. Samples were scanned 24 h after to allow liquid evaporation. The scans represent the extreme damage these liquids are capable of inducing - when applied free-standing..*

The sample removed from EtOH was left in the lab environment for 72 more hours to allow any remaining solvent residues to evaporate and was rescanned to understand how that influenced the relaxation behaviour. Results showed the same pattern after 24 and 96 h upon removal of PMMA from the EtOH bath (Graph 6.6), with the latter showing a small decrease in signal (ca. 0.02), both after the 1<sup>st</sup> and 6<sup>th</sup> echoes. This decrease of 0.02 was within error, determined as  $\pm 0.03$ , thus not allowing confirmation that with time, some sort of PMMA plastic deformation (possibly swelling) is being restored and that the material can recover its initial shape/size.

The signal of the 1<sup>st</sup> echo of IPA-immersed PMMA was reduced to almost half (ca. 0.03) compared to ca. 0.07 seen in controls (Graph 6.5 – green). By the 6<sup>th</sup> echo, PMMA signal after 30 days in IPA was almost zero. This suggested that IPA caused hardening of the material, which enabled it to relax faster than before. Faster relaxation may mean chain scission (Guthausen *et al.* 1998) or even material dissolution (extraction in solution) that created free volume/empty space for fast solvent movement.



Graph 6.6. Smoothed line graphs of NMR profile scans of the PMMA sample immersed in EtOH for 30 days: 1<sup>st</sup> and 6<sup>th</sup> echoes 24 h after (pink tones) and 96 h after (blue tones) standing in lab environment.

## 6.6. EXPERIMENTAL DESIGN & ANALYSIS OF VARIANCE

ANOVA was performed on the numeric data from the evaluation methods and analytical techniques (CARS scores, gloss measurements, weight change %, FTIR peak height ratios) used to assess the experimental results. This process was supported by the use of designed experiments in Minitab® 17.

### Statistically designed experiments

The pharmaceutical industry was the first to introduce and implement DOE for clinical trials (Nekkanti *et al.* 2015). Nowadays, DOE has become a necessity that adds validity to any scientific study (Dellaportas *et al.* 2014). This systematic and cost-effective method has been used to extract useful information about the interactions and relationships among tested variables and thus can be used for product yield optimisation (DeLoach 2010; Weissman and Anderson 2014; Nekkanti *et al.* 2015). Quantitative description of trends of a population may be provided by studying a sample of that population. From results, the researcher generalises or draws inferences/conclusions to the population.

DOE allowed the simultaneous analysis of a number of possible effects of multiple factors (input variables) and their interactions on several responses (output variables) for the cleaning of PMMA. Factor interactions are difficult to detect when experimenting with one factor at a time and this was an important motivation for using DOE. It enabled the identification of main and interaction effects, that is the influence of each variable on the

outcome and of variables on each other (Edmonds and Kennedy 2017), requiring only a limited number of experiments (Nekkanti *et al.* 2015; Praticò *et al.* 2016). Experiments consisted of a series of runs, at the end of which data were systematically collected. The experimental groups of samples were measured before and after treatment and their change was compared with the control group (Reedy and Reedy 1994).

Factorial experiments were favoured because they minimised the number of experimental runs (Domagalski *et al.* 2015), and thus of replicates needed to evaluate the cleaning process. This was possible by detecting factors with a significant effect, which reduced the total experimental time required for generating useful data (Golfomitsou and Merkel 2004; Weissman and Anderson 2014). Minitab offered a structured approach to scientific investigations; It assisted in the organisation of the experiments, in mapping the results and avoiding systematic and random errors. Apart from reassuring balanced and unbiased results, the software offered presentational options, i.e. plots and graphs, to aid understanding of results.

Samples were randomly allocated to the treatments and tested in random order, to ensure that the only systematic source of variation resulted from differences between the data groups (Suenson-Taylor *et al.* 1999). Randomisation of experiments was essential for multiple reasons, including creation of homogeneous treatment groups that eliminated bias, prevention of mistaken interpretation by spreading instrument effects among treatment groups (Reedy and Reedy 1994) and minimisation of the risk of systematic errors (Morgan 1991a). This increased credibility of the statistical analysis and ensured the integrity of the significance performed (Creswell 2014). In short, randomisation rendered the significance tests valid (Andersson 2012). The experiments were carried out in a controlled environment which in principle had controlled temperature and relative humidity conditions. Still, it was impossible to carry out all experimental runs under exactly the same conditions. Given that experimental runs were performed throughout a period of time, runs of different days may have been conducted under potentially different environmental conditions, which could have affected the response values. For such reasons, environmental conditions were monitored throughout the experiment and DOE used the randomised block design, which allowed ANOVA to separate the variation due to treatments, blocks and residual error (Morgan 1991a, 53).

### **ANOVA**

ANOVA was employed to statistically analyse DOE and was run in Minitab. It compared all factor levels based on the null hypothesis that all cleaning treatment levels were equal (had the same effect), therefore had no statistical significance. The way analysis worked was by pairing all possible sample responses (i.e. CARS scores, weight change %, etc.), comparing their mean values and using variation in their responses to decide if treatment effects were

significant (Andersson 2012). The significance (probability level) was set at  $p = 0.05$  (5 %) with a 95 % confidence (Morgan 1991a). By rejecting the null hypothesis results confirmed a significant systematic difference in the sample means, which in turn confirmed high probability of a statistical difference between treatments. If the  $p$ -value was less than the significance level ( $p < 0.05$ ) it was established that some of the means were different.

Results of ANOVA were presented in the main effects plot, which depicted examined factors and their levels as lines connecting points/dots. An example of this is seen in Fig.6.13 displaying levels Pemulen H<sub>2</sub>O, Pemulen EtOH, Pemulen PET and PVA PET of factor *Treatment* and levels new and aged of factor *Condition* in relation to CARS scores (response variable). Main effects were the difference in the mean response between two levels of a factor and their plots were only available in factorial designs – used in this study. Each point represented the mean value for all runs per factorial level, i.e. mean value of CARS scores for all five new and five aged replicates treated with the four solvent gels in Fig.6.13. The horizontal dotted line pointed out the mean value of all replicates (factorial runs) in the experiment. It was possible to distinguish from the plot the statistically significant paired levels as steeper lines: the bigger the significance of the level the steeper the line, as seen between levels Pemulen H<sub>2</sub>O and Pemulen EtOH.

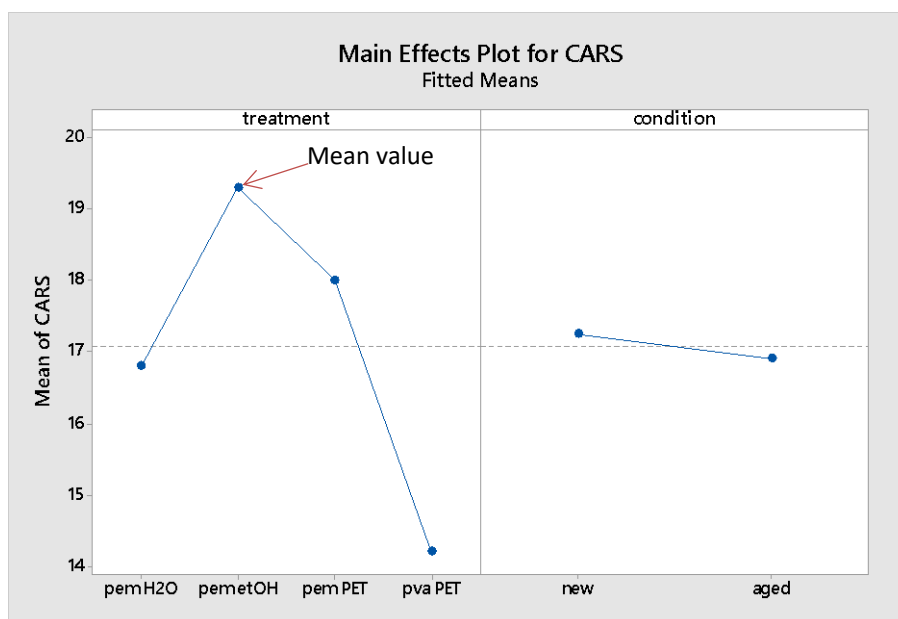


Figure 6.13. The main effects plot of new and aged PMMA samples on CARS scores. Points represented the mean values for all runs per factorial level. Horizontal dotted line represented the mean value of all factorial runs in the experiment.

### Tukey's honestly significant difference post-hoc test

ANOVA didn't indicate which pair of factorial levels (i.e. Agar or Pemulen) was significantly different. Once it was concluded that there was statistical difference between different levels, the next step was to locate where the significant effect occurred. Multiple comparison tests, or

post-hoc tests, were run to confirm which were the different levels. Such tests could only take place after an overall statistically significant difference in group means had been demonstrated. Such a test was Tukey's HSD post-hoc test, selected for being sensitive to pairwise comparisons, comparing two conditions at a time. Tukey's HSD allowed comparisons of all possible pairs of factorial levels at the same time (simultaneous pairwise comparisons), to test whether their difference was significant or not. It did that by examining the random variation between any pair of means (standard error or HSD) and using it to compare all pairs against it (Hinton 2004). If a difference in means was greater than HSD then the difference was significant (Morgan 1991a; Hinton 2004). The problem with multiple comparisons was that the more the comparisons with the same data sets the greater the risk of accepting a false positive, that is, accepting a result as significant when in reality it occurred by chance (Type I error). Tukey's method overcomes this risk by setting an overall level of significance.

Tukey's method presented significance of results by attributing letters to the compared factorial levels. When means were identified as significantly different, they were assigned a unique letter that was not shared with other means. In Tukey's HSD of the factor *Treatment*, where ANOVA established statistical difference between its levels, Pemulen EtOH, Pemulen H<sub>2</sub>O and PVA PET did not share a letter with any other level. This signified that these three treatments had a statistically significant effect on the CARS scores, hence on the macroscopic evaluation of the samples. The next step was to examine if their effect was positive, by comparing the mean value of each level's CARS score from the main effect plot. In this example, Pemulen EtOH offered the highest CARS hence having a positive effect on cleaning, whereas PVA PET induced the worst CARS having a negative effect.

**Tukey Pairwise Comparisons**

**Grouping Information Using the Tukey Method and 95% Confidence**

<u>treatment</u>	<u>N</u>	<u>Mean</u>	<u>Grouping</u>
pem etOH	10	19.300	A
pem PET	10	18.000	A B
pem H2O	10	16.800	B
pva PET	10	14.200	C

*Means that do not share a letter are significantly different.*

The evaluation methods presented in this chapter are employed in previous Chapter 5 dedicated to the chemical characterisation of the artificial dirt types used in the cleaning experiments, as well as Chapter 7 dedicated to the individual components of the gel systems, and the study of solvent effects and the extent of their damage on PMMA. Cleaning experiments in Chapters 8, 9 and 10 could not have been possible without the methods presented here.



## Chapter 7. CLEANING: MATERIALS & PROTOCOLS

This section presents the practical aspects of preparing the gel systems, any difficulties encountered during their making, and the ATR characterisation of their components separately and in gel formulations. In addition, a study on the 30-day immersion of samples in the solvents used in the cleaning experiments, investigates the potential damage that they can cause to PMMA. The samples' behaviour and monitoring of their change is investigated through visual observation, weight change measurements and ATR-FTIR analysis.

### 7.1. CLEANING MATERIALS

#### 7.1.1. Synthesis of gels



*Figure 7.1. Glass jars with lids for storage of Carbopol/Ethomeen, Pemulen/TEA and PVA/borax hydro- and solvent-gels.*

Aqueous gel systems in this study were prepared both as hydrogels and solvent-gels - in some cases thickened dispersions were technically emulsions<sup>15</sup> (see Chapter 4.3.1). As discussed earlier, all gels were prepared in H<sub>2</sub>O, essential for the gelling process. Hydrogels used H<sub>2</sub>O as a cleaning agent and their effect was examined in the preliminary experiments. Solvent-gels were H<sub>2</sub>O-based too, but also loaded with amines and bases for neutralisation or cross-linkers for gel formation, as well as organic solvents (EtOH, IPA or PET) for their cleaning action. H<sub>2</sub>O conductivity was regularly measured at 1  $\mu$ S with Hanna HI9033 Multi-range Portable Conductivity Meter, verifying the low salt concentration.

After a long period of experimentation with the gel formulations, Carbopol gels were prepared with Ethomeen C-25 (Fig.7.3). This was preferred over TEA due to its compatibility with higher ratios of solvent to H<sub>2</sub>O (Stavroudis and Blank 1989). This formulation is available in a variety of recipes (Wolbers 2000), which were frequently tailored to specific case studies

<sup>15</sup> An emulsion is a mixture of two or more liquids that are normally immiscible, where one liquid contains a dispersion of the other liquids. Two liquids, such as water and oil, can form different types of emulsions, i.e. an oil-in-water emulsion where the oil droplets are dispersed in water, or a water-in-oil emulsion with water dispersed in oil.

and artwork surfaces. For recipes used in this study see Appendix K. For NMR MOUSE profiles of the gels see Appendix L. The challenge with this formulation was insolubility of Carbopol in the desired solvent quantities. Precipitation would take place as a sticky, white and stringy residue. Carbopol is also known to react and precipitate with calcium salts in hard water, therefore strict use of distilled water is recommended (Stavroutis and Blank 1989). Considering all these complications, preparation of Carbopol/Ethomeen C-25 was challenging.



Figure 7.2. Physical, solid Agar and Gellan hydrogels and solvent-gels prepared as rectangular pieces ready to be used. Gels were refrigerated in resealable polyethylene zip lock bags.

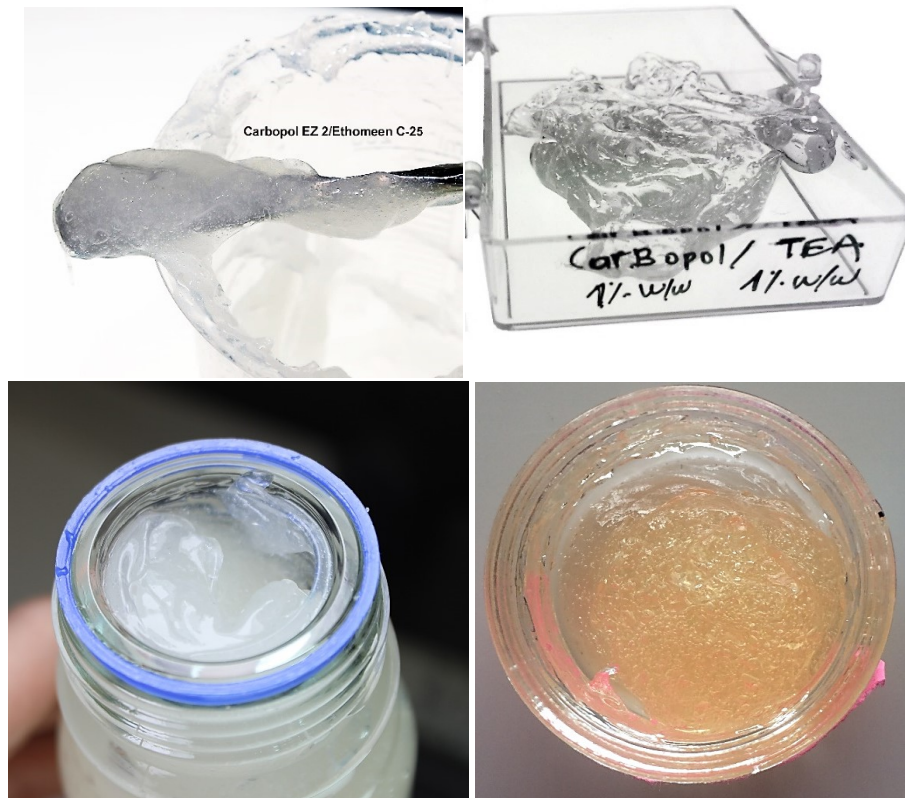


*Figure 7.3. Carbopol/Ethomeen C-25 hydrogels and solvent-gels prepared and stored in glass jars with lids.*



*Figure 7.4. Pemulen/TEA hydrogels and solvent-gels prepared and stored in glass jars with lids.*

Agar and Gellan gels were easy to formulate (Fig.7.2). They showed an inability to contain PET, however, its introduction did not prevent gel thickening. This inability was attributed to mixing water with a non-water miscible solvent. This is better explained as a macroscopic phase separation (syneresis), where extraction or expulsion of liquid takes place through the gel surface. Pemulen with TEA was prepared following many different recipes, all of which led to a similar texture and consistency (Fig.7.4) (Stavroudis and Blank 1989; Pavitt 2012; Stavroudis 2012). PVA/borax dispersions would readily form (Fig.7.5), nevertheless it

was crucial to, firstly, allow PVA to sit undisturbed for the time instructed, and secondly, stir vigorously once borax was added.

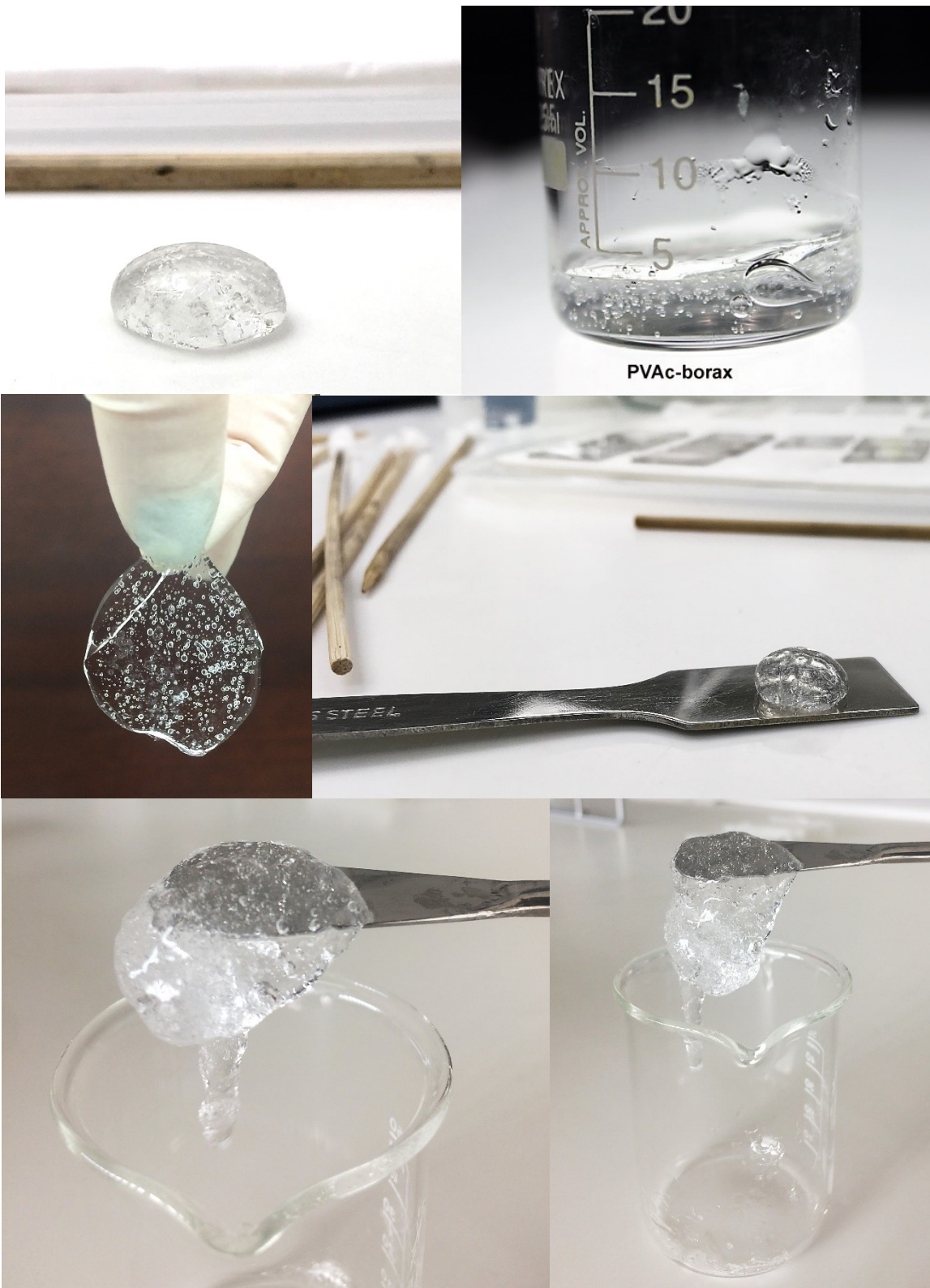


*Figure 7.5. PVA/borax hydrogels and solvent-gels prepared and stored in glass jars with lids or flat plastic containers allowing them to spread in pre-formed sheets.*

### 7.1.1.1. Fourier Transform Infrared Spectroscopy characterisation of gels

It was important to chemically characterise the individual materials comprising the gel systems and identify their characteristic absorption bands, in order to distinguish them if found as residue on PMMA surfaces. The materials were analysed in transmittance mode as potassium bromide (KBr) pellets and ATR as dried hydrogels. Agar, Gellan, Carbopol, Pemulen, PVA and borax were analysed in their pure powder form as KBr pellets. Gel and PMMA bands were expected to overlap due to wavelength proximity and absorptions of similar functional moieties. Overlapping of two neighbouring peaks corresponding to different materials, i.e. to a gel component and PMMA, may lead to masking of peaks and incorrect interpretation of spectra.

Gels were prepared as hydrogels, dried at 80 °C and analysed with ATR. Although drying of the materials at high temperatures may have altered their chemical structure and thus IR absorption, this was deemed necessary. Except Agar and Gellan that formed solid gels, in their non-dried forms Carbopol/Ethomeen and Pemulen/TEA were paste-like, and PVA/borax putty-like. Drying aimed to transform their viscoelastic nature into a more solid, analysable state, and possibly avoid deposition of - hard to clear - residues and damage to the crystal. Analysing dried gel systems also aimed at documenting potential shifts and changes in bands resulting from gel formation. The resulting gel was expected to give rise to new bands or cause shifts attributed to crosslinking or bonding. Knowledge of these bands would enable distinguishing them from PMMA absorptions, and in particular, tracing PMMA chemical alterations versus residual gel.

To avoid any ambiguous interpretation of spectra obtained upon heating from dried samples, these are presented alongside spectra obtained from KBr pellets, wherever applicable (see Gellan). In cases where no spectral differences were identified between the dried hydrogels and pellets of raw materials (see Agar), the least noisy spectrum is presented. Spectra of Agar (Fig.7.6) and Gellan (Fig.7.7) exhibit comparable IR band absorptions.

#### IR spectra of gel systems

##### **FTIR spectrum of Agar (KBr pellet – transmittance)**

In the FTIR spectrum of Agar analysed as a KBr pellet in transmittance mode, the characteristic absorption band at 3435  $\text{cm}^{-1}$  is associated with hydroxyl groups ( $-\text{OH}$  stretching), while the peak at 2900  $\text{cm}^{-1}$  is attributed to C–H stretch of methoxyl groups. The peaks at 1643  $\text{cm}^{-1}$  and 1439  $\text{cm}^{-1}$  are due to the asymmetrical and symmetrical carbonyl absorption (C=O stretching) of carboxylate ions ( $\text{COO}^-$ ) (Samiey and Ashoori 2012; Cao *et al.* 2014). Band 1375  $\text{cm}^{-1}$  is due to the presence of ester sulfate groups, attributed to the variation of Agar and its method of extraction. Sulfates are not visible in the chemical structure of Agar (Fig.7.6) due to their low

content (< 2 %) (Armisen and Galatas 1987). Characteristic bands of agarose at  $1159\text{ cm}^{-1}$ ,  $1075\text{ cm}^{-1}$  and  $930\text{ cm}^{-1}$  (Fig.7.6) are associated with the C–O–C stretching vibration of 3,6-anhydro-galactose bridges (El-Hefian *et al.* 2012; Trivedi and Kumar 2014), which represent the glycosidic bond between monosaccharide units and ester groups (Praiboon *et al.* 2006; Rossi *et al.* 2011; Bertasa *et al.* 2017). The characteristic band at  $890\text{ cm}^{-1}$  corresponds to the C–H of residual carbons of  $\beta$ -galactose (Freile-Pelegri *et al.* 2007), while characteristic bands  $770\text{ cm}^{-1}$  and  $740\text{ cm}^{-1}$  are attributed to skeletal bending of galactose ring (Pereira *et al.* 2003).

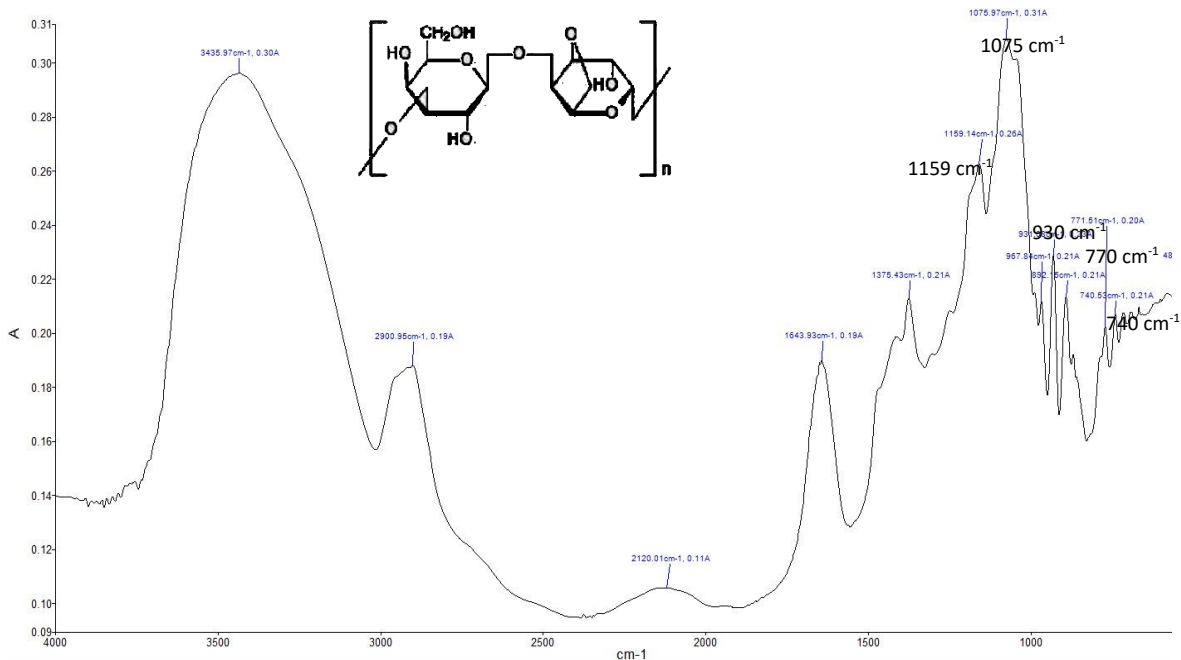


Figure 7.6. IR spectrum of Agar analysed as a KBr pellet in transmittance mode. Absorption bands and assignments available in Table 7.1. Monomer chemical structure inset.

#### AGAR. Diagnostic IR absorptions and assignments

Wavenumber ( $\text{cm}^{-1}$ )	Band assignment
3435	–O–H stretch
2900	C–H stretch
1643, 1439	C=O stretch
1375	ester sulfate vibration (possibly S=O)
1159, 1075, 930	C–O–C stretch of 3,6-anhydro-galactose bridge
890	C–H stretch of $\beta$ -galactose
770, 740	galactose ring vibration

Table 7.1. Assignments of diagnostic IR absorptions of raw Agar analysed as a KBr pellet in transmittance mode.

Both Agar and 32-days aged PMMA exhibit peaks attributed to hydroxyl moieties. These contributions from the two different materials, when both present, may result in a broader and more intense absorption band at  $3400\text{ cm}^{-1}$ . Agar absorptions at around  $2920\text{ cm}^{-1}$  due to methoxyl groups and  $1640\text{ cm}^{-1}$  due to carboxylate ions may overlap aged PMMA peaks that indicate formation of carbon double bonding. Lastly, the characteristic C–O–C stretching vibration of 3,6-anhydro-galactose bridges of Agar at  $1075\text{ cm}^{-1}$  and the C–C skeletal bands of PMMA may also overlap (Chapter 5, Fig.5.7, Table 5.4). See Fig.7.12 for overlay.

#### FTIR spectra of Gellan (KBr pellet – transmittance and dried hydrogel – ATR)

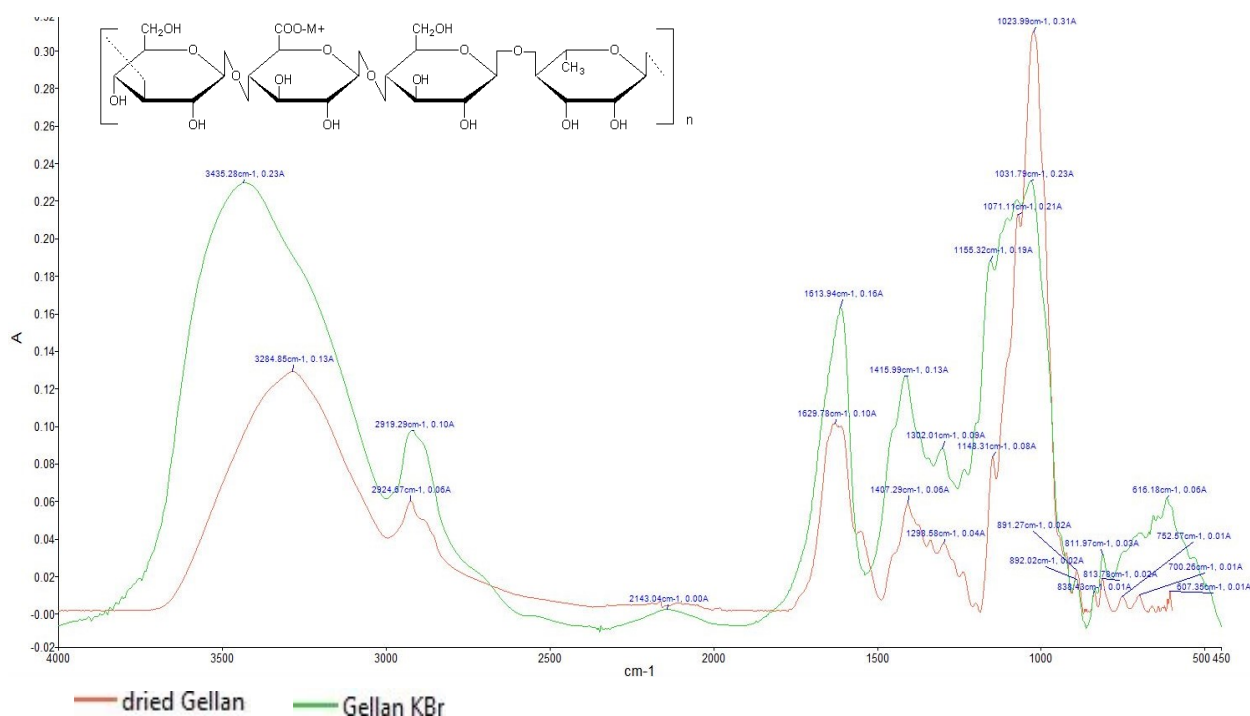


Figure 7.7. IR spectra of Gellan analysed as KBr pellet in transmittance mode (green) and dried hydrogel in ATR mode (red). Absorption bands and assignments available in Table 7.2. Monomer chemical structure inset.

Spectra of Gellan are presented here in both the KBr pellet and dried form, because not all peaks are legible in the two spectra. Gellan displays absorption bands at  $3427\text{ cm}^{-1}$  due to the presence of  $-\text{OH}$  group of the glycopyranose ring and  $2927\text{ cm}^{-1}$  due to the stretching vibrations of  $-\text{CH}_2$  groups. Bands at  $1629\text{ cm}^{-1}$  and  $1409\text{ cm}^{-1}$  are due to asymmetric and symmetric stretching of carboxylate group, while those appearing at  $1153\text{ cm}^{-1}$  and  $1024\text{ cm}^{-1}$  are assigned to etheral and hydroxylic C–O stretching (Verma and Pandit 2011).

As seen with Agar and aged PMMA, bands of Gellan at  $3400\text{ cm}^{-1}$  and  $2920\text{ cm}^{-1}$  coincided with PMMA moieties evidencing photolysis; particularly formation of hydroxyl groups and main chain scission reactions (Chapter 5, Fig.5.7, Table 5.4). The region between

1640-1630  $\text{cm}^{-1}$  shows an overlap of carboxylate groups in Gellan and carbon double bonds in aged PMMA. Finally, the Gellan band at 1150  $\text{cm}^{-1}$  overlaps with the C–O–C stretch of PMMA (see Fig.7.12 for overlay).

GELLAN. Diagnostic IR absorptions and assignments		
Wavenumber ( $\text{cm}^{-1}$ )	Band assignment	Sampling technique
3427	–O–H stretch	KBr
2927	C–H stretch	ATR
1629, 1409	asymmetric and symmetric COO–M stretch	ATR
1153	ethereal C–O stretch	KBr
1024	hydroxylic C–O stretch	ATR

Table 7.2. Assignments of diagnostic IR absorptions of Gellan analysed as a KBr pellet (raw form) in transmittance mode and as a dried gel in ATR mode.

#### FTIR spectrum of Carbopol EZZ/Ethomeen C-25 (dried hydrogel – ATR)

Carbopol/Ethomeen was analysed as a hydrogel (in its dried state) to capture the chemical structure of the gel formulation containing both components. The spectrum (Fig.7.8) shows a broad absorption band centred around 3430  $\text{cm}^{-1}$  attributed to free hydroxyl groups (–OH bonds) (Chalal *et al.* 2014). The bands at 2929  $\text{cm}^{-1}$  and 2855  $\text{cm}^{-1}$  are assigned to carboxylic groups (COOH) resulting from hydroxyl bonding with carbonyl (Todica *et al.* 2015). As a dried (anhydrous) gel, Carbopol/Ethomeen exhibits two different carbonyl stretching vibrations (C=O) of the monomer carboxylic group: a sharp band at 1722  $\text{cm}^{-1}$  indicative of free carbonyl groups and a band at 1652  $\text{cm}^{-1}$  related to the hydrogen bonded carboxyl group. The carbonyl bands of solvent-gels are expected to appear at different energy levels than the dried gel presented here (Islam *et al.* 2004).

Absorption bands at 1560  $\text{cm}^{-1}$  and 1397  $\text{cm}^{-1}$  are characteristic of the symmetric and asymmetric stretching frequencies of the carboxylate ion ( $\text{COO}^-$ ). The Ethomeen added to the system, neutralises the residual Carbopol acid groups remaining in the gel during formation (Todica *et al.* 2015), with a process known as acid-base neutralisation reaction. This neutralisation results from the formation of an amine salt between the carboxylic groups in Carbopol and the free base (Ethomeen), and appears as an ionised carboxylic band absorbing at 1560  $\text{cm}^{-1}$  (Islam *et al.* 2004). Absorption at 1452  $\text{cm}^{-1}$  is due to  $\text{CH}_2$  stretching and 1248  $\text{cm}^{-1}$  to C–O–C stretch (Kirwan *et al.* 2003), while bands at 838  $\text{cm}^{-1}$  and 804  $\text{cm}^{-1}$  are assigned to out of plane bending of =C–H (Sahoo *et al.* 2012) in the Carbopol.



The band located at  $1349\text{ cm}^{-1}$  could not be attributed to any moiety found in pure Carbopol, nor as a result of the Carbopol/Ethomeen formulation. Observation of the pure Ethomeen C-25 reference spectrum (Fig.7.9) revealed a peak at  $1351\text{ cm}^{-1}$ , which led to the speculation that the  $1349\text{ cm}^{-1}$  absorption in the Carbopol/Ethomeen spectrum is due to the presence of free (non-reacted) Ethomeen C-25 in the dried gel formulation.

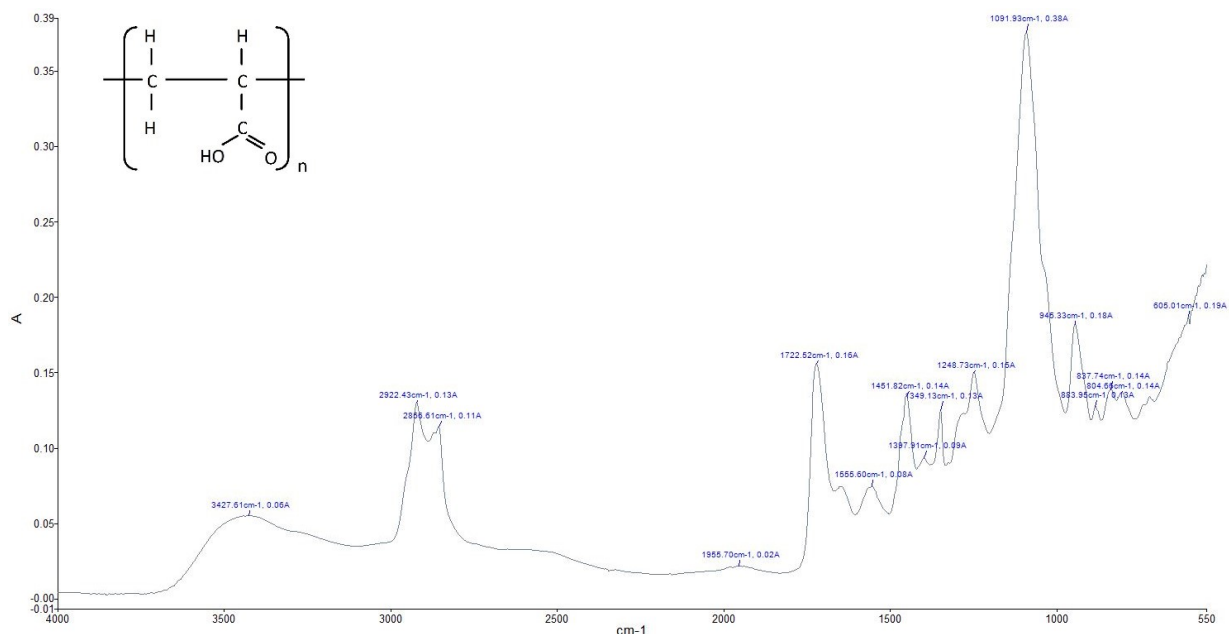


Figure 7.8. IR spectrum of Carbopol/Ethomeen hydrogel system analysed in dried state in ATR mode. Absorption bands and assignments available in Table 7.3. Carbopol EZ2 chemical structure inset.

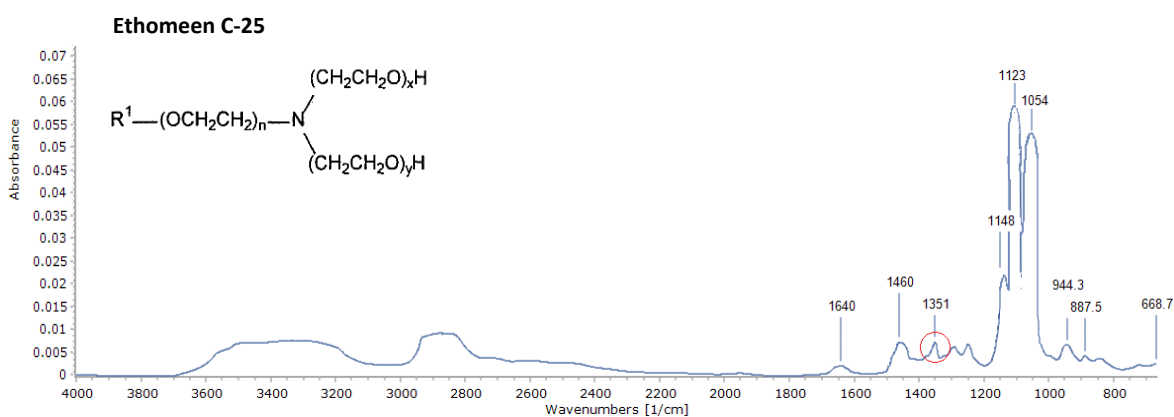


Figure 7.9. IR spectrum of pure Ethomeen C-25 prepared as a KBr pellet and analysed in transmittance mode. Ethomeen C-25 chemical structure inset.

Carbopol and PMMA exhibited a number of overlapping bands due to their shared acrylic nature. Both materials display absorptions at around  $3400\text{ cm}^{-1}$ ,  $2920\text{ cm}^{-1}$  and  $2850\text{ cm}^{-1}$  due to hydroxyl and carboxyl oxidation groups, at  $1722\text{ cm}^{-1}$  due to their characteristic carbonyl bonding and finally in the region of  $1640\text{--}1630\text{ cm}^{-1}$  due to formation of carbon double bonds. In the aged PMMA, carbon double bonding is evidence of chain scission and

other photooxidation reactions, while in Carbopol/Ethomeen hydrogel it may have been the result of desiccation during heating at 80 °C (see Fig.7.12 for overlay).

CARBOPOL E22/ETHOMEEN C-25. Diagnostic IR absorptions and assignments	
Wavenumber (cm <sup>-1</sup> )	Band assignment
3430	–O–H stretch
2929, 2855	COOH stretch
1722, 1652	C=O stretch
1643	C=C stretch
1560, 1397	symmetric and asymmetric COO <sup>-</sup> stretch
1452	C–H stretch
1248	C–O–C stretch
838, 804	=C–H stretch

Table 7.3. Assignments of diagnostic IR absorptions of Carbopol E22-Ethomeen C-25 system analysed in its dried state in ATR mode.

### Spectrum of Pemulen TR-2/Triethanolamine (dried hydrogel – ATR)

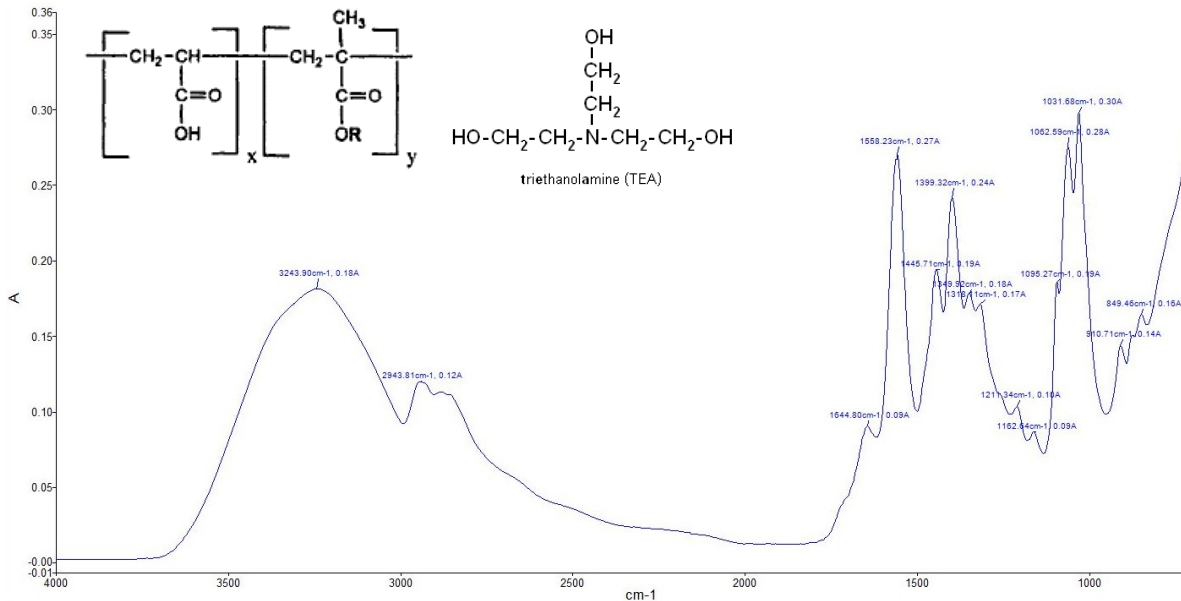


Figure 7.10. IR spectrum of Pemulen TR-2/TEA hydrogel system analysed in dried state in ATR mode. Absorption bands and assignments available in Table 7.4. Chemical structures of Pemulen and TEA monomers inset.

Pemulen/TEA is presented in its dried hydrogel formulation. The structure of Pemulen is similar to that of Carbopol (Ravenel 2010) – as they are both based on poly (acrylic acid). However, due to the addition of different bases the resulting gel systems exhibit different IR spectra. Absorption bands in the 2980-2850  $\text{cm}^{-1}$  region are attributed to the C-H stretch of TEA (Khan *et al.* 2004). Similarly to Ethomeen in Carbopol, TEA is added to the system to neutralise the Pemulen acid groups. When the ammonia group of TEA interacts with the acid sites of Pemulen (carbonyl bands), it disrupts the interchain hydrogen bonds. As a result, the vibrations of the carboxylic groups are affected by this reaction, shifting the band of pure Pemulen (similar to pure Carbopol) from 1714  $\text{cm}^{-1}$  to 1644  $\text{cm}^{-1}$  in the neutralised gel. The final neutralised gel should display a carboxylate ( $\text{COO}^-$ ) peak at around 1570  $\text{cm}^{-1}$  (Patel *et al.* 2003), however, as more TEA is added, the peak increases and shifts to 1558  $\text{cm}^{-1}$  (typically to a lower frequency up to 1530  $\text{cm}^{-1}$ ) (Pudney *et al.* 2009). The band at 1445  $\text{cm}^{-1}$  and 1031  $\text{cm}^{-1}$  indicates stretching of the C-N groups (Negm *et al.* 2003; Khan *et al.* 2004).

<b>PEMULEN TR-2/TRIETHANOLAMINE. Diagnostic IR absorptions and assignments</b>	
<b>Wavenumber (<math>\text{cm}^{-1}</math>)</b>	<b>Band assignment</b>
3243	–O–H stretch
2943	C–H stretch
1644	COOH stretch
1558, 1399	symmetric and asymmetric $\text{COO}^-$ stretch
1445	C–N stretch

*Table 7.4. Assignments of diagnostic IR absorptions of Pemulen TR-2/TEA system analysed in its dried state in ATR mode.*

There are a large number of peaks that overlap between the spectra of PMMA and Pemulen/TEA hydrogel. Absorptions denoting chain scission reactions in the 2980-2850  $\text{cm}^{-1}$  region of PMMA overlap with the C-H stretch of TEA. The PMMA band at 1640  $\text{cm}^{-1}$ , evidencing formation of carbon double bonds as a result of UV irradiation, is found in the proximity of the 1644  $\text{cm}^{-1}$  peak attributed to carboxylic absorption of the neutralised Pemulen hydrogel. A peak at 1642  $\text{cm}^{-1}$  is also visible in the spectrum of pure TEA (Todica *et al.* 2015). This would only be evident in the rare case that TEA be found unbound in the hydrogel and subsequently deposited on PMMA. Additionally, C–H stretches in PMMA appear to vibrate in the same IR region as the C–N stretches of the Pemulen/TEA system at around 1445  $\text{cm}^{-1}$  (see Fig.7.12 for overlay).

## Spectrum of PVA/borax (dried hydrogel – ATR)

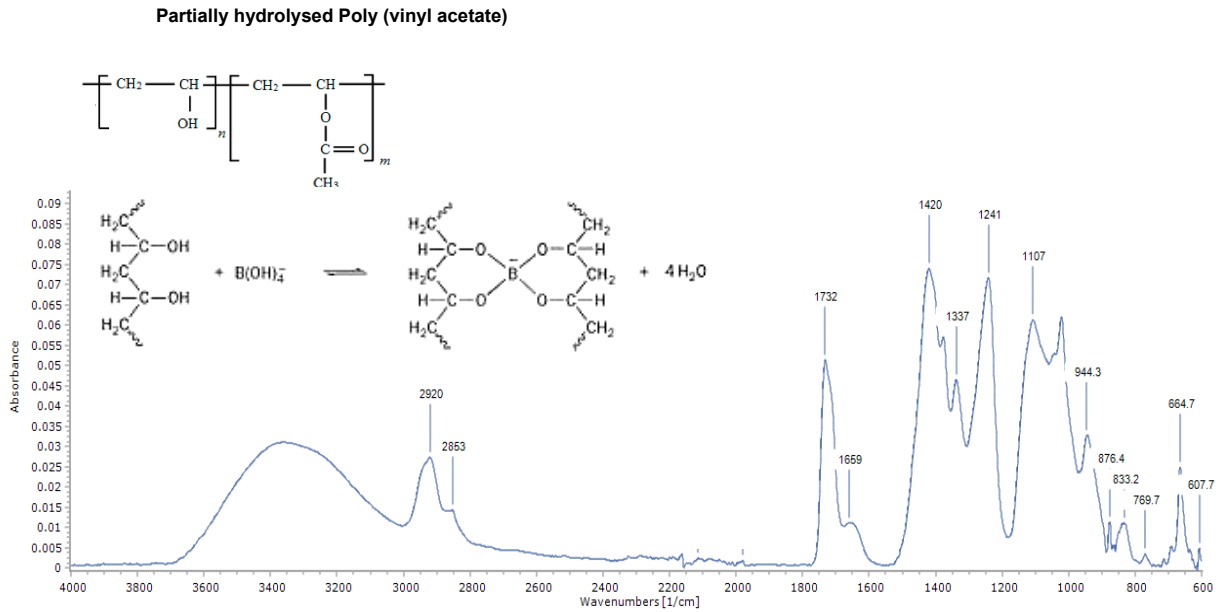


Figure 7.11. IR spectrum of PVA/borax hydrogel system analysed in dried state in ATR mode. Absorption bands and assignments available in Table 7.5. Chemical structures of PVA and crosslinked PVA/borax network inset.

**PVA/BORAX. Diagnostic IR absorptions and assignments**

Wavenumber (cm <sup>-1</sup> )	Band assignment
3400	–O–H stretch
2920, 2840	symmetric and asymmetric C–H stretch
1659, 1376	symmetric and asymmetric COO <sup>-</sup> stretch
1420, 1337	asymmetric B–O–C stretch
1107	C–O stretch
944	–O–H stretch
880, 650	B–O stretch

Table 7.5. Assignments of diagnostic IR absorptions of PVA/borax system analysed in dried state in ATR mode.

FTIR analysis was performed on the dried PVA/borax hydrogel to capture the chemical structure of the gel formulation upon interaction of the two components. The IR spectrum reveals a large peak at 3400 cm<sup>-1</sup> attributed to the presence of hydroxyl groups (–OH bonds) that form crosslinks with the borate ions (borax) and other groups that participate in intermolecular hydrogen bonding (Spoljaric *et al.* 2014). The peaks observed at 2920 cm<sup>-1</sup> and 2840 cm<sup>-1</sup> are respectively attributed to the symmetric and asymmetric C–H stretching of CH<sub>2</sub> groups in PVA (Awada and Daneault 2015). Peaks at 1659 cm<sup>-1</sup> and 1376 cm<sup>-1</sup> are attributed to

the symmetric and asymmetric stretching of carboxylate anion ( $\text{COO}^-$ ) in PVA (Labidi and Djebaili 2008). Peak  $1107\text{ cm}^{-1}$ , assigned to the C–O stretching vibration, corresponds to the characteristic absorption band of –C–OH groups of PVA (Jiang *et al.* 2016).

The presence of crosslinked borax in the system is confirmed by absorption at  $1420\text{ cm}^{-1}$  and  $1337\text{ cm}^{-1}$ , assigned to asymmetric stretching relaxation of B–O–C (Spoljaric *et al.* 2014). Even though these two bands indicate the crosslinking of borate with PVA, not all the borate ions present in the gel participate in crosslinks. A large fraction of boron tends to remain unbound, in the form of free boric acid and borate ions (Angelova *et al.* 2015). Absorption at  $944\text{ cm}^{-1}$  possibly results from a deformation of the borate O–H bond (Labidi and Djebaili 2008). The bands at about  $880\text{ cm}^{-1}$  and  $650\text{ cm}^{-1}$  are respectively attributed to the B–O stretching of residual  $\text{B(OH)}_4$  (tetrahydroxyborate acid) and the B–O–B bending of linkages within the borate networks. These bands not only confirm the crosslinking of borax with the PVA network, but also the presence of a borate network and a small amount of residual  $\text{B(OH)}_4$  in the hydrogel system (Spoljaric *et al.* 2014). In PVA/borax hydrogel and PMMA, few absorptions overlap. Bands at  $3400\text{ cm}^{-1}$ ,  $2920\text{ cm}^{-1}$  and  $2850\text{ cm}^{-1}$  evidencing formation of oxidised products (hydroxyl and carboxyl) in PMMA coincide with the hydroxyl groups and the C–H stretches in the hydrogel. The characteristic PMMA band at  $1640\text{ cm}^{-1}$ , evidencing formation of carbon double bonds as a result of UV irradiation, overlap the neighbouring peak of the PVA/borax gel system at  $1659\text{ cm}^{-1}$  assigned to carboxylate ions ( $\text{COO}^-$ ) (see Fig.7.12 for overlay).

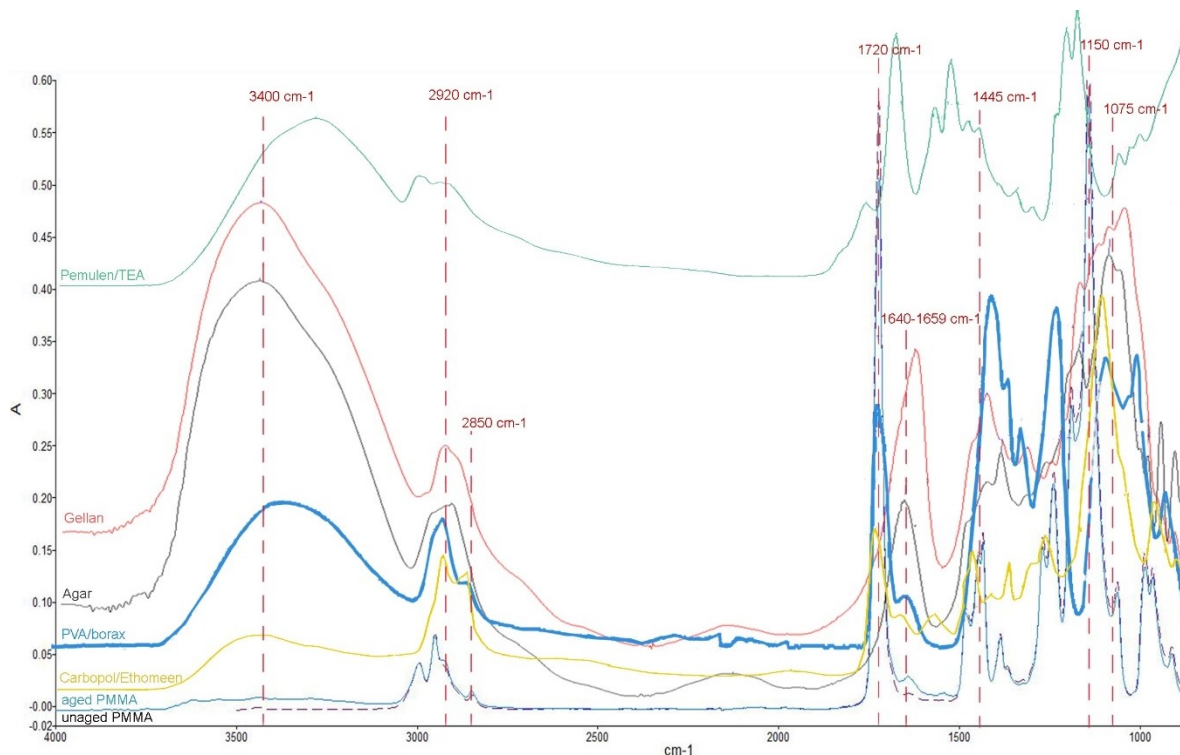


Figure 7.12. Overlay of spectra of unaged and aged PMMA and all hydrogel systems (Agar, Gellan, Carbopol/Ethomeen, Pemulen/TEA, PVA/borax). Spectral overlap/similarities are highlighted with a dotted line in red and absorptions are labelled.

### 7.1.2. Solvent effects: immersion study

The diffusion of pure organic solvents into a polymer is a complex process and may cause detrimental effects, such as swelling, cracking, softening and solubilisation/leaching of components (Carretti *et al.* 2010; Chuang *et al.* 2016). As discussed in Chapter 3, PMMA contains free volume, voids of channels and sub-microscopic cavities within its matrix responsible for permitting liquid to penetrate and diffuse (Struik 1977). During diffusion of molecules into the polymer matrix, the distance between polymer chains increases and thus more free volume becomes available for molecular movement. As a consequence liquids may swell the polymer and plasticise it forming a gel-like swollen layer between PMMA-gel layer, and gel layer-solvent. Papanu *et al.* (1989) showed that after immersion in ketones the degree of PMMA swelling was minimal. Analytical results showed that the thickness of the swollen gel layer was approx. 80 nm, with almost half (36 nm) corresponding to PMMA swelling. After an induction time, the plastic dissolves, while further penetration of the solvent increases the swollen surface layer (Papanu *et al.* 1989; Miller-Chou and Koenig 2003).

The plasticising effect of liquids, and especially H<sub>2</sub>O, may also lower the PMMA T<sub>g</sub> (Tham *et al.* 2010). Although H<sub>2</sub>O and PMMA have limited chemical compatibility, PMMA's side-chain ester bonds are polar, thus inherently susceptible to H<sub>2</sub>O (Van Oosten 2002). These polar groups increase the water sorptive capacity of PMMA (Barrie and Platt 1963, 311; Turner 1982, 198). Studies show that at higher water content, the T<sub>g</sub> can decrease to room temperature and PMMA undergo glassy-to-rubbery transition causing significant changes in its properties, such as increased reactivity and reduced chemical stability (Szakonyi and Zelkó 2012).

In some cases it is possible that polymer dissolution occurs through cracking without formation of a swollen gel layer nor an induction time (Ouano and Carothers 1980; Papanu *et al.* 1989). Cracking is also known as solvent-induced crazing or ESC, discussed in Chapter 3.3.3.1. ESC is related to the capability of a liquid to dissolve the polymer and appears as surface cracks (Basavarajappa *et al.* 2016). The closer the solubility parameters of the liquid to that of the polymer, the greater the dissolution and susceptibility to ESC (Arnold 1998). These cracks enhance penetration rates as they provide a suitable pathway for further solvent penetration (Papanu *et al.* 1989). Studies of immersion of rectangular PMMA samples in H<sub>2</sub>O showed that ESC is caused by propagation of a single craze that proliferates rapidly across the sample (Arnold 1998, 5201; Wypych 2013, 429). In the same study, PMMA samples in IPA rapidly dissolved within the first week with no noticeable swelling (Arnold 1998, 5195).

### Immersion of PMMA in liquid environments

The effects of the cleaning agents employed in the cleaning experiments (H<sub>2</sub>O, EtOH, IPA and PET) were examined in isolation in relation to PMMA. During this study, unaged, untreated 1.0 mm PMMA samples were immersed in each pure liquid (10 mL) in airtight vials for 30 days. Samples were kept at constant laboratory conditions (21 °C, 60 % ±5 % RH). The aim was to understand the level of damage these liquid agents would cause when in direct contact with PMMA, as a means of determining a 'worst case scenario'. The effects were studied through stereomicroscopy to examine changes on the surface topography, weight measurements to detect changes in the physical structure and ATR-FTIR to monitor chemical alterations.

#### Stereomicroscopy

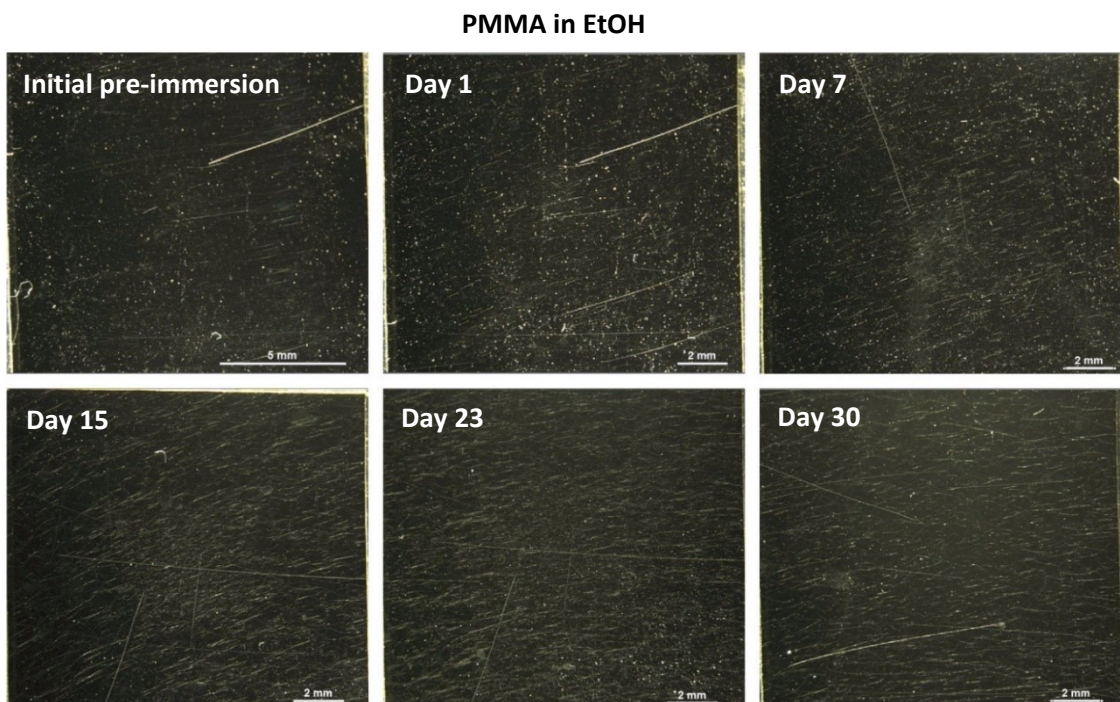


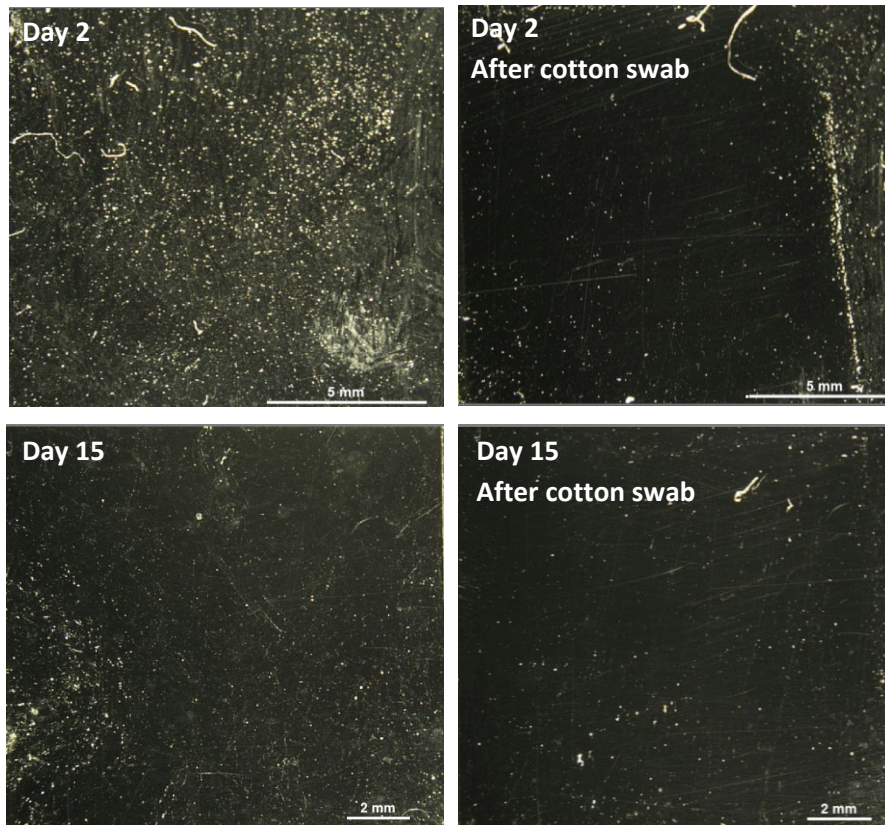
Figure 7.13. Microimages under the Leica M205 A 3D stereomicroscope (x78.1) showing the PMMA sample immersed in EtOH at different time intervals. At Day 7 a network of cracks was visible.



Figure 7.14. Microimages under Leica DM 2500P optical microscope showing the PMMA sample immersed in EtOH for a month, at different magnifications. The organised network of cracks showed fine fibrils.

Microscopic observation of immersed samples took place at different time intervals throughout the 30 days. Samples in EtOH show the most damage (Fig.7.13) and greatest deformation due to plasticisation of the PMMA matrix by the solvent. EtOH is known to cause ESC to PMMA (Higuchi 2015), confirmed under the stereomicroscope. After 7 days of immersion, samples start to form a network of cracks visible under the stereomicroscope (Fig.7.13). By day 15, the cracks are fully formed across the whole sample surface and visible to the naked eye. According to solubility theory, PMMA dissolution commonly manifests itself through cracking (Kawagoe and Morita 1994), confirming dissolution caused by EtOH. Detailed images of the cracking (Fig.7.14) under a number of magnifications, clearly show fine fibrils illustrating the formation of an organised crack network. Visual examination confirmed that, in terms of physical damage, EtOH is the most aggressive organic solvent among the liquids studied here.

#### PMMA in PET



*Figure 7.15. Microimages under the stereomicroscope (x78.1) showing PMMA sample after 2 and 15 days: 5 h after removal from PET and after moistened cotton swab clearance of the surface. Images after immersion showed dust-like residues, which were removed after use of swabs. The longer PMMA stayed in the liquid environment, the less the residues.*

Samples removed from all four liquids macroscopically display fine surface deposits that, under the microscope, resemble dust-like residues (Fig.7.15). Prior to microscopic observation samples were left for 5 hours in laboratory environment to allow solvent



evaporation. These deposits were removed with a H<sub>2</sub>O-moistened cotton swab. Fig.7.15 shows the successful removal of these deposits from PMMA after 2 and 15 days in PET.

After the first few days of immersion in all liquids, the effect of these dust-like residues was intensified. However, by Day 15, they were significantly reduced and trivial residues were visible under magnification. This could indicate that precipitation of non-volatile PMMA components extracted during surface dissolution, and redeposition after solvent evaporation took place in the first 15 days. These residues could also be attributed to contaminants found on the PMMA surface. Alternatively, in the case where substrates were clean and theoretically insoluble to the solution (i.e. PET), residues may be solvent impurities (even when 99 % pure). In addition, it was observed that after all immersions, surfaces were more susceptible to abrasion compared to the control sample. Immersed surfaces cleared with cotton swabs were more sensitive to mechanical damage and formation of abrasions than control PMMA. Scratches were particularly visible on PMMA immersed in EtOH and IPA, and less in H<sub>2</sub>O.

#### Weight measurements

Samples were weighed before immersion (initial weight) and then daily at specific time intervals, for a period of one month (excluding weekends). They were removed from the vials every 24 hours and weighed 5 hours after standing in laboratory environment, to allow solvent evaporation. A control PMMA was kept in an airtight vial with no liquid, to determine whether the changes were true, solvent-induced alterations and independent of external factors (i.e. environment). Two further sample sets were immersed in each liquid following the same methodology and weighed twice a week for one month, to statistically confirm the results.

Weight change was calculated as a percentage of change from the initial mass and the daily weight of samples. The control PMMA remained unaltered throughout the 30 days (average change <0.0001 %, considered negligible) (Fig.7.16). H<sub>2</sub>O caused a steady weight increase in the first 24 hours (+0.004 %), indicating H<sub>2</sub>O absorption soon after immersion. This was anticipated based on the literature (Chapter 3) indicating the tendency of water to fill the overall PMMA free volume. Following a 1-month immersion PMMA displayed an increase in mass of 0.007 % (Fig.7.16). The daily absorption rate was very consistent.

The PMMA sample immersed in EtOH displays the most interesting behaviour amongst the immersed samples (Fig.7.16). In the first 10 days, EtOH induced a weight decrease. In fact, during the first 24 hours, which are potentially of most interest here, given the timeframe of the cleaning treatments (5 minutes) and all subsequent measurements carried out 24 hours later, the sample displayed the greatest weight loss (average -0.003 %) across the entire month. This loss remained constant for 72 hours. In the following 12-14 days, EtOH caused the

opposite effect, showing a weight gain of ca. 0.002 %. In the remaining 15 days, the sample weight increased exponentially, going from an average of 0.002 % to septuple that (0.014 %) in the last 4 days. IPA induced weight loss within the first 24 hours and maintains this behaviour throughout the month with negligible weight fluctuations and an average loss of 0.003 %. Petroleum ether (PET) shows similar behaviour to the control sample, with a monthly average change of <math><0.00002\%</math>, indicating a high degree of stability of PMMA in PET (Fig.7.16).

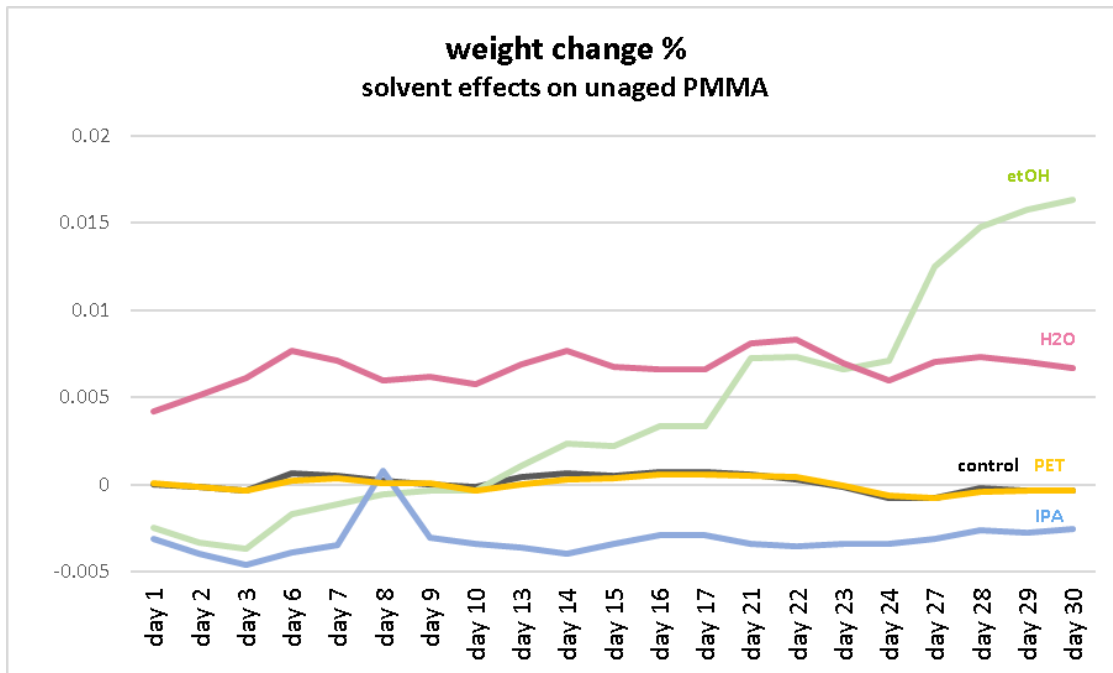


Figure 7.16. Weight change % of untreated control PMMA (black) and samples immersed in liquid environments: EtOH (green), H<sub>2</sub>O (pink), IPA (blue) and PET (yellow) for 30 days. Changes % are relative to the initial weight (pre-immersion) set at zero.

### FTIR spectra

ATR-FTIR was employed to detect chemical changes induced by the immersion of PMMA in three organic solvents and a H<sub>2</sub>O environment.

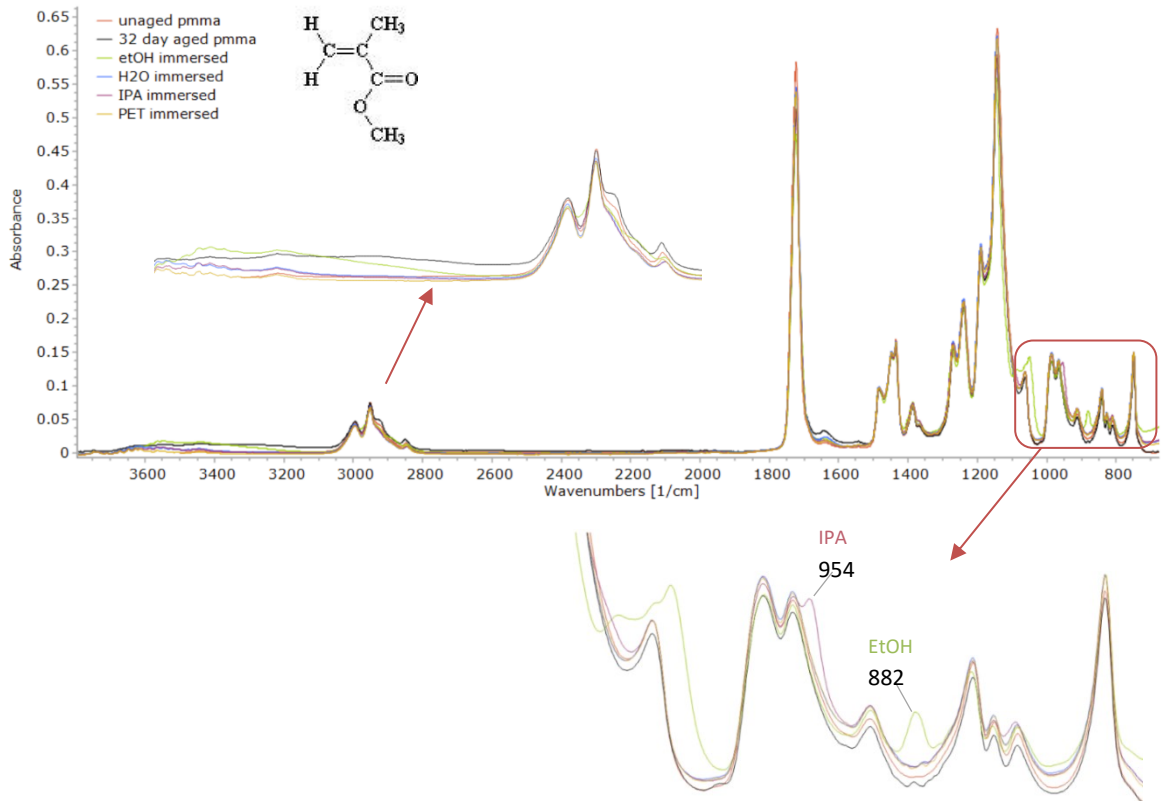


Figure 7.17. Spectra of PMMA samples: unaged control (orange), 32-days UV-aged control (grey) and 30-days immersed samples in EtOH (green), H<sub>2</sub>O (blue), IPA (pink) and PET (yellow). Regions 3700-2800 cm<sup>-1</sup> and 1000-700 cm<sup>-1</sup> were enlarged and presented in detail. MMA monomer chemical structure inset.

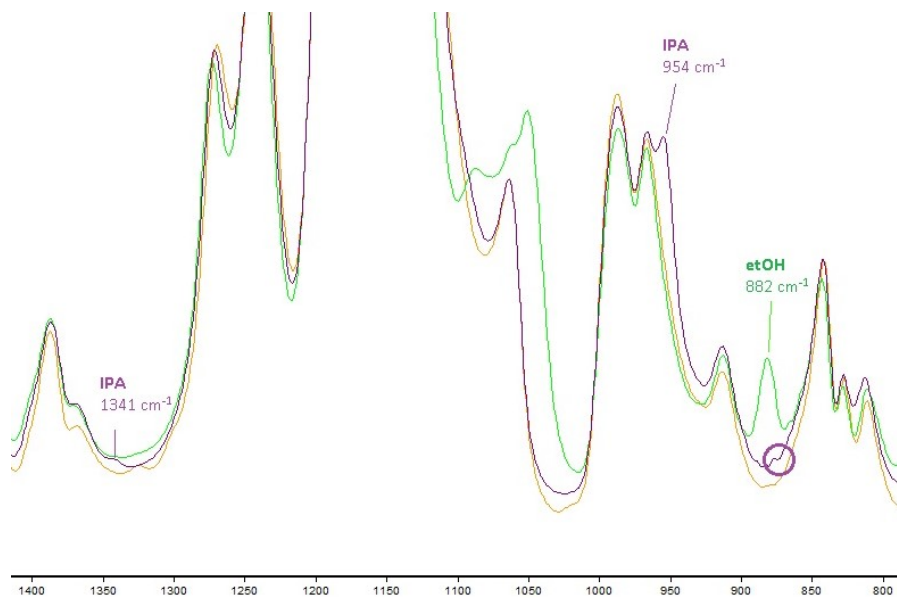
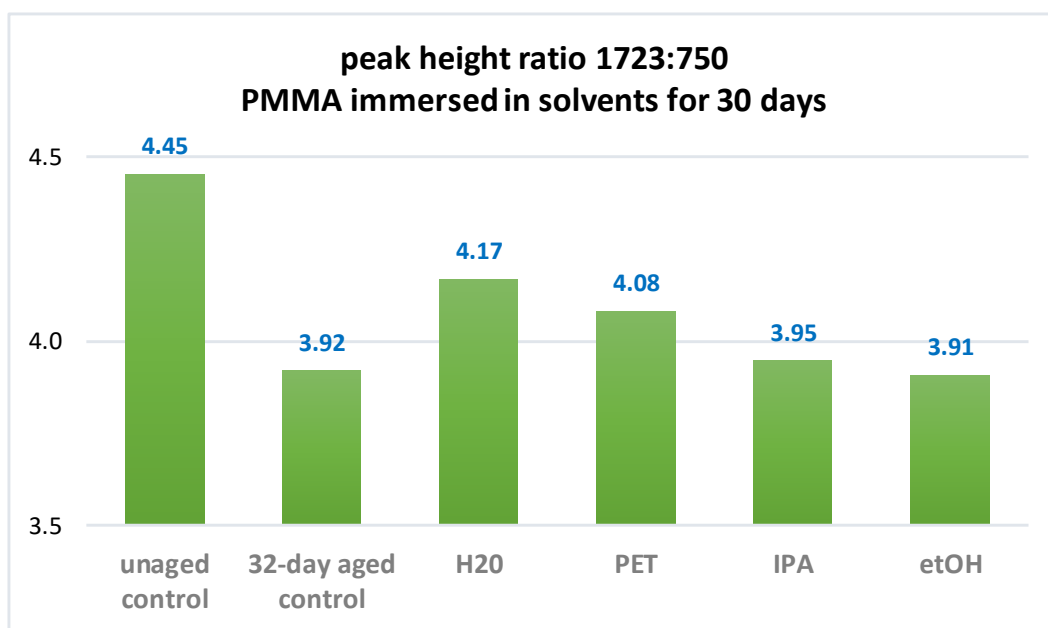


Figure 7.18. Detail of spectra of PMMA samples with the new peaks formed after immersion in EtOH (green) and IPA (purple) for 30 days.

Diagnostic IR absorptions and assignments	
PMMA immersed in ethanol, isopropanol, petroleum ether and deionized water.	
Wavenumber (cm <sup>-1</sup> )	Tentative band assignment
3400	–O–H (ethanol)
2995, 2950	O–CH <sub>3</sub> (ester group)
2920, 2850	CH <sub>3</sub> (ester group)
1723	C=O (ester group)
1640	C=C (main chain)
1483, 1387	α-CH <sub>3</sub> (main chain)
1447	CH <sub>2</sub> (main chain)
1435	O–CH <sub>3</sub> (ester group)
1341	(isopropanol)
1270, 1240	C–C–O (ester group)
1190, 1144, 986	C–O–C (ester group)
1063	C–C skeletal (main chain)
965	α-CH <sub>3</sub> (main chain)
954	α-CH <sub>3</sub> (isopropanol)
882	C=CH <sub>2</sub> (ethanol)
840, 749	CH <sub>2</sub> skeletal (main chain)

Table 7.6. Assignments of diagnostic IR absorptions of PMMA samples immersed in EtOH, H<sub>2</sub>O, IPA and PET environments for 30 days.



Graph 7.1. Ratios between the peak heights at  $1723\text{ cm}^{-1}$  and  $750\text{ cm}^{-1}$  of new and aged untreated PMMA controls and PMMA samples immersed in H<sub>2</sub>O, PET, IPA and EtOH for 30 days. Ratios were based on the loss of carbonyl bands (C=O) in relation to a constant peak. The smaller the ratio, the bigger the chemical change.

#### Deionised water & petroleum ether

PMMA immersed in H<sub>2</sub>O and PET for 30 days presents similar spectra to the unaged control PMMA, with negligible changes in absorption (Fig.7.17). For absorption assignments of control PMMA (see Chapter 5.1.2-Table 5.4) and for PMMA immersed in H<sub>2</sub>O and PET refer to Table 7.6 (Nagai 1963; Kaczmarek *et al.* 2010).

#### Isopropanol

PMMA immersed in IPA for 30 days exhibits a similar ratio to the 32-day aged PMMA (Graph 7.1). The aged PMMA shows reduced carbonyl (C=O) and reduction of peak  $1723\text{ cm}^{-1}$  due to photoirradiation that caused scission of the pendant ester group from the main chain (see Chapter 5.1.2-Table 5.4). Changes in the absorption spectrum of PMMA in IPA include the formation of a minor peak at  $1341\text{ cm}^{-1}$ , and a new, distinct shoulder peak at  $954\text{ cm}^{-1}$ . Band  $1341\text{ cm}^{-1}$  is described as characteristic of the crystalline phase of stereoregular PMMA, mostly in reference to isotactic forms (Liu *et al.* 2006). Regrettably, no reference to the band assignment was found. It is reported that PMMA polymers with different tacticities (i.e. isotactic and syndiotactic) often showed similar, slightly shifted absorptions. Therefore, even though here the PMMA is syndiotactic, appearance of a peak at  $1341\text{ cm}^{-1}$  is potentially due to the transition from amorphous to partially crystalline states and from unordered to ordered, regardless of difference in the PMMA tacticity (Dybal *et al.* 1983). It is reported that

crystallisation of amorphous PMMA of any tacticity is extremely slow, rendering the study of its process hard, but also justifying the negligible, yet clear, initial formation.

Band  $954\text{ cm}^{-1}$  is a doublet with  $965\text{ cm}^{-1}$  and is assigned to the  $\alpha$ -methyl ( $\alpha\text{-CH}_3$ ) attached to the main chain (Nagai 1963; Dybal *et al.* 1983; Bensaid *et al.* 2014). These two peaks, both assigned to the backbone conformation of PMMA, are also reported to relate to polymer crystallinity. More specifically,  $954\text{ cm}^{-1}$  has been shown to increase, while  $965\text{ cm}^{-1}$  to decrease during the process of crystallisation (Liu *et al.* 2006). Simultaneous occurrence of the two new bands at  $1341\text{ cm}^{-1}$  and  $954\text{ cm}^{-1}$  in the spectrum of PMMA after prolonged contact with free organic solvent, present sufficient evidence to support that IPA was able to induce crystallisation of PMMA.

### Ethanol

According to the ratioing of peaks (Graph 7.1), a 30-day immersion in EtOH induces a comparable carbonyl degradation to the 32-day UV-aged PMMA, similar to IPA. The FTIR spectrum of PMMA exhibits a similar formation of two new bands at  $3400\text{ cm}^{-1}$  and  $882\text{ cm}^{-1}$ . The broad absorption centred around  $3400\text{ cm}^{-1}$  is assigned to the formation of oxidised structures resulting from substitution of C–H bonds by hydroxyl groups (–OH bonds). Peak  $882\text{ cm}^{-1}$ , assigned to the  $\text{C}=\text{CH}_2$  (Coates 2000) between the  $\alpha$ -carbon and the methylene in the main chain, is characteristic of the crystalline phase of isotactic PMMA (Luo *et al.* 1993). The same absorption was observed on the surface of UV-aged PMMA samples (Chapter 5.1.2.1.b) and attributed to the thermal/heating process they underwent in the weathering chamber (Dybal and Krimm 1990; Luo *et al.* 1993). The band visible here is distinct and more pronounced than in the aged PMMA spectrum. In the literature syndiotactic PMMA is documented to have a strong tendency to form ordered aggregated structure (crystalline phase) via solvent treatment (Luo 1994). Therefore, the formation of this peak here is attributed to prolonged PMMA contact with a free organic solvent, which led to crystallisation.

The progression of chemical changes was based on the known decrease of peak  $1723\text{ cm}^{-1}$ , accompanying loss of carbonyl (C=O) and the subsequent detachment/loss of the ester side group. To account for variations in sampling depths across the sample set, the peak height of the  $1723\text{ cm}^{-1}$  vibration was normalised to an internal standard vibration at  $750\text{ cm}^{-1}$ , which corresponds to a main chain vibration and not known to alter in the presence of solvents. Ratios show (Graph 7.1) that samples immersed in all four liquid environments show loss of carbonyls relative to the unaged/untreated control PMMA (the smaller the ratio the greater the change).  $\text{H}_2\text{O}$  appears to cause the least chemical change, followed by PET.

### Discussion of results

Weight change percentages provided a quantitative indication of changes in the material. They have been widely used by scholars as an indication of the effect of solvent-based cleaning treatments on a variety of materials, with changes attributed to extraction of volatile constituents, presence of residues and non-volatile compounds, or liquid absorption (Ulrich *et al.* 2011; Wypych 2013; Fife *et al.* 2014). Care however was needed when interpreting these potential changes. Weight measurements simply offered numerical values, which, could be influenced by a number of different chemical and physical processes that may be occurring concurrently. For instance, they overlooked the possibility of simultaneous extraction and diffusion of components, rendering interpretation complicated.

Since interpretation of the data obtained from gravimetry was challenging in isolation, additional analysis was undertaken. Py-GC/MS of the PMMA under investigation (discussed in Chapter 5.1.2.2), identified the presence of volatile components (oxidation products), allowing attribution of the partial weight loss to their dissolution and extraction. Combining the weight measurements with py-GC/MS, microscopic observation, FTIR analysis and NMR MOUSE relaxation data, will enable interpretation of the cleaning results.

Solvents investigated here for their effect on PMMA were expected to cause immediate changes to weight. Low-molecular-weight liquids, including EtOH and IPA, are known to aggravate the mechanical behaviour of the polymer they are in contact with, initiating changes in the surface layers structure and properties (Bogdanova *et al.* 1986). Loss of weight upon solvent exposure indicated dissolution, extraction and subsequent evaporation of (volatile) polymer components, while weight gain was attributed to absorption/penetration and diffusion of liquid in the material, with possible associated softening or swelling (Quye and Keneghan 1999; Shashoua 2012). In the presence of a gel carrier, dissociation of the gel (i.e. due to syneresis) and deposition of residues on the treated substrate also contributed to the weight gain. Such phenomena are directly connected to the nature of the solvent and solubility of PMMA (Troiano *et al.* 2014).

Ideally for a cleaning treatment to be considered successful, the treatment should induce weight loss equivalent to the unwanted/foreign surface matter (dirt). This is rarely a realistic scenario. In this study, treatments are considered successful when surface matter, synthetic sebum soil or adhesive, are visually removed. However, examination of other factors is also performed because it is considered important to document the occurrence and pattern of extreme weight changes (see Chapters 8-10). When the effect of co-solvents added in gels appeared to be more controlled compared to extreme weight changes caused by free co-solvents alone, this was considered a positive result for the treatment quality. Other factors were

also considered, including the presence of gel residues, detected by mass gain and confirmed by visual methods.

At this stage, the aim of this immersion study was to understand the individual effect of solvents on PMMA, so as to understand their combined action with water at a later stage. Based on the results of visual observation, weight changes and chemical surface analysis (ATR-FTIR), PMMA samples exposed to H<sub>2</sub>O increased in mass, while samples exposed to EtOH and IPA decreased. Samples were not affected by contact with PET. PMMA absorbed H<sub>2</sub>O, which caused a weight gain of 0.007 % in the first 24 hours, the largest gain amongst immersed samples. Samples in PET – on the other hand, showed no changes in mass and the smallest chemical change; the closest surface chemistry to the untreated control.

Samples in EtOH and IPA showed similar weight losses, 0.003 % and 0.004 % respectively, the greatest negative change amongst the immersed samples in the first 24 hours. This was attributed to dissolution of the material in each solvent. The EtOH environment was visually the most aggressive with macroscopic ESC visible to the naked eye. EtOH also induced the greatest chemical change, comparable to the 32-day UV-aged PMMA in regard to the surface chemistry and the semi-quantitative peak height ratios, followed by samples in IPA. Both EtOH and IPA caused the formation of IR bands characteristic of the crystalline phase, suggesting that the damage caused by alcohols altered the surface structure of PMMA.

## **7.2. CLEANING PROTOCOL**

### **Application & removal of gels**

This section describes how treatments in the cleaning experiments (Chapters 8-10) were applied and removed. The free solvents were applied as three drops via a micropipette directly on the sample surfaces. Application and removal of rigid Agar and Gellan gels was carried out with a flexible and soft Teflon spatula. A glass weight was placed on top to increase the contact between the gel and the PMMA surface. Paste-like Carbopol/Ethomeen and Pemulen/TEA gels and gel-emulsions were applied with a Teflon spatula and flattened by pressing a glass slide on top of them (Fig.7.19). After treatment completion they were wiped with the Teflon spatula. Putty-like PVA/borax gels were initially flattened between two glass slides, and then pressed on the samples with the spatula, to cover their surfaces. A glass weight was placed on top of the glass slides to increase contact between the cleaning system and the treated surface. Due to their flexibility they were easily removed by peeling them from the PMMA surfaces. Gel systems covered the whole surface area of the PMMA samples under treatment. All gels weighed approximately 2 g and, except the rigid Agar and Gellan gels that were pre-formed, were applied as 2 mm thick layers. This was an arbitrary decision based on ease of application of the gels.



Samples were protected with a plastic cover to avoid drying of gels and limit the evaporation rate of solvents.

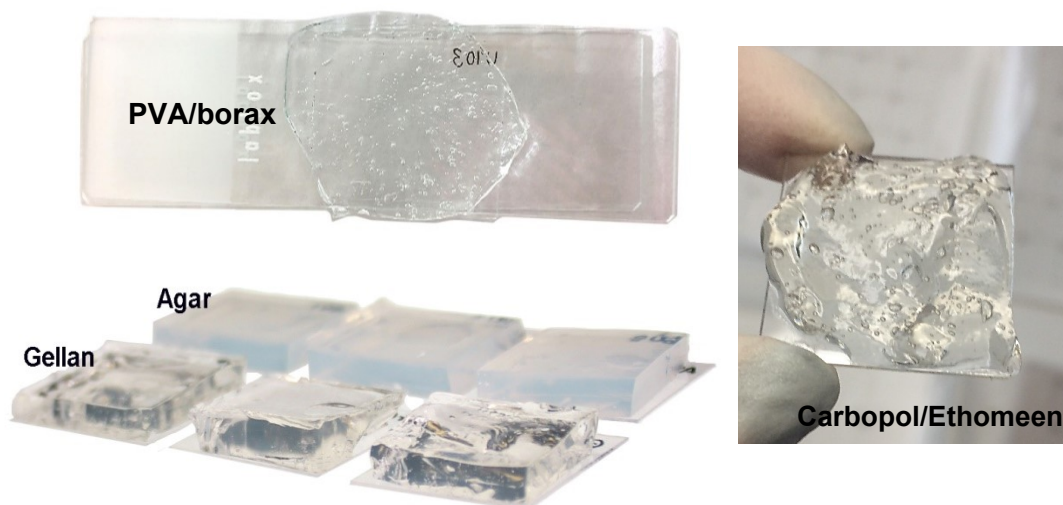


Figure 7.19. PMMA sample surfaces during cleaning treatments: putty PVA/borax gel and paste Carbopol/Ethomeen flattened with a glass slide, rigid Agar and Gellan gels placed with a Teflon spatula.

Use of Teflon spatula was decided based on a study that aimed to standardise the safe removal of gels and solvents from PMMA surfaces. Wiping of a Teflon spatula versus rolling dry cotton swabs directly on PMMA were tested, to initiate a mechanical force on the treated surfaces as recommended in the literature (Warda *et al.* 2007; Cremonesi 2010). Microscopic observation shows that the spatula produces significantly less to non-existent scratches compared to cotton swabs. In addition to producing significant scratching, dry cotton swabs tend to leave microscopic residues of cotton fibres (Fig. 7.20).

#### **Post-treatment clearance step**

Removal of gel systems was followed by a post-treatment clearance step. This was necessary to remove any gel residues, or eliminate the formation of solvent tidelines. Blotting with dry tissue/filter and rolling moistened cotton swabs directly on PMMA were tested, and by comparison, the latter was visually less damaging. Research demonstrated that rolling in linear motions in one direction along the surface was visually less damaging and more effective at removing dirt from plastic surfaces compared to other motions, such as circular, which produced scratches. This was in line with the work published by Shashoua *et al.* (2009). Hence, the post-treatment clearance in this study consisted of three separate wet washes with moistened cotton swabs in H<sub>2</sub>O, carried out by gently and linearly rolling in one direction. The extra moisture of the cotton swabs was blotted using tissue/filter paper.

This chapter dealt with the ATR characterisation of the individual gel components and the documentation of the effect of solvents when in direct and prolonged contact with PMMA.

Current studies presented here along with previous chapters have offered a comprehensive and methodical study of the PMMA material, the individual gel components and the formulated gel systems. This research has to-date presented studies and protocols for the sample preparation, the artificial light ageing, the artificial dirt application and the cleaning protocols. What follows in the next three chapters is the experimental cleaning study, where all these established protocols will be implemented.

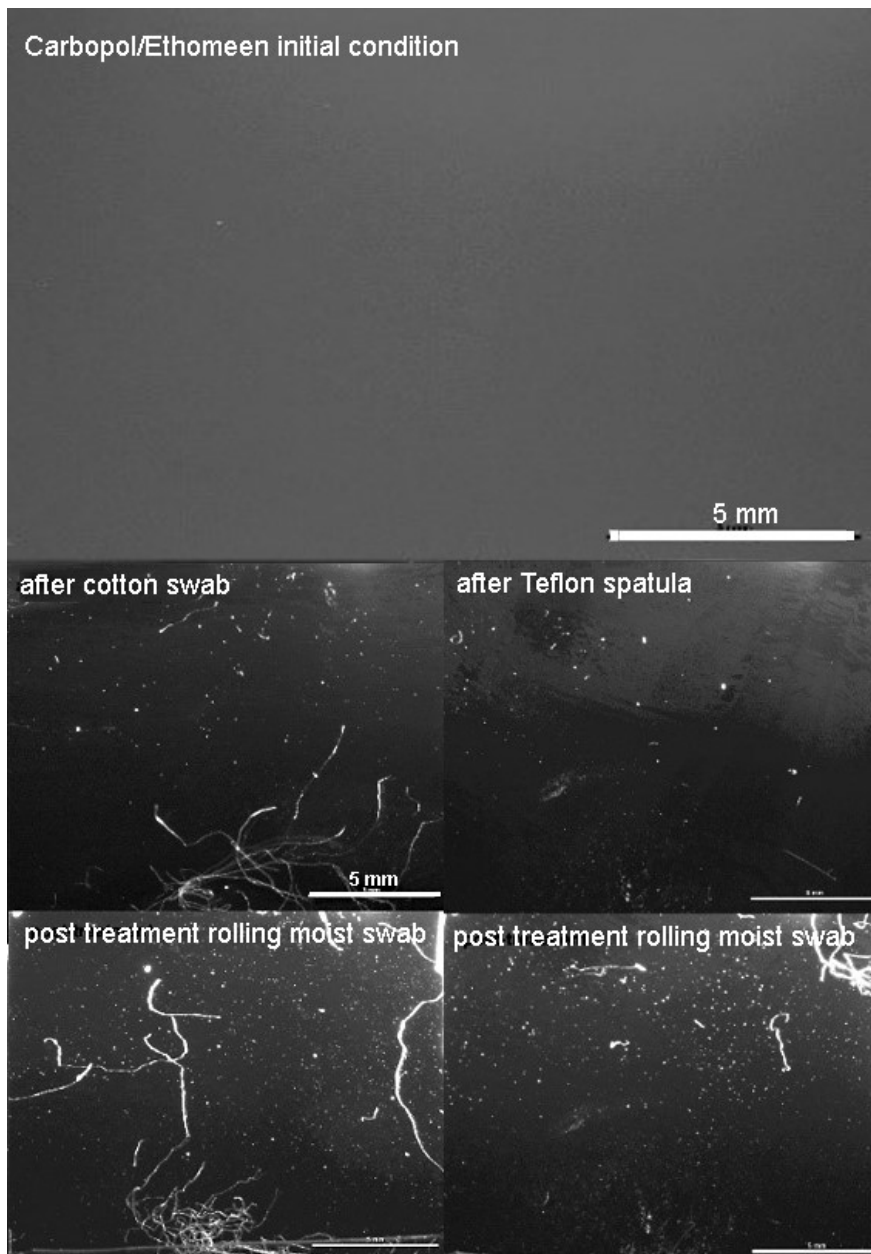


*Figure 7.20. Comparing wiping of a Teflon spatula against rolling dry cotton swabs to standardise the safe removal of gels and solvents from treated PMMA surfaces. Teflon spatula produced significantly less to non-existent scratches compared to cotton swabs.*

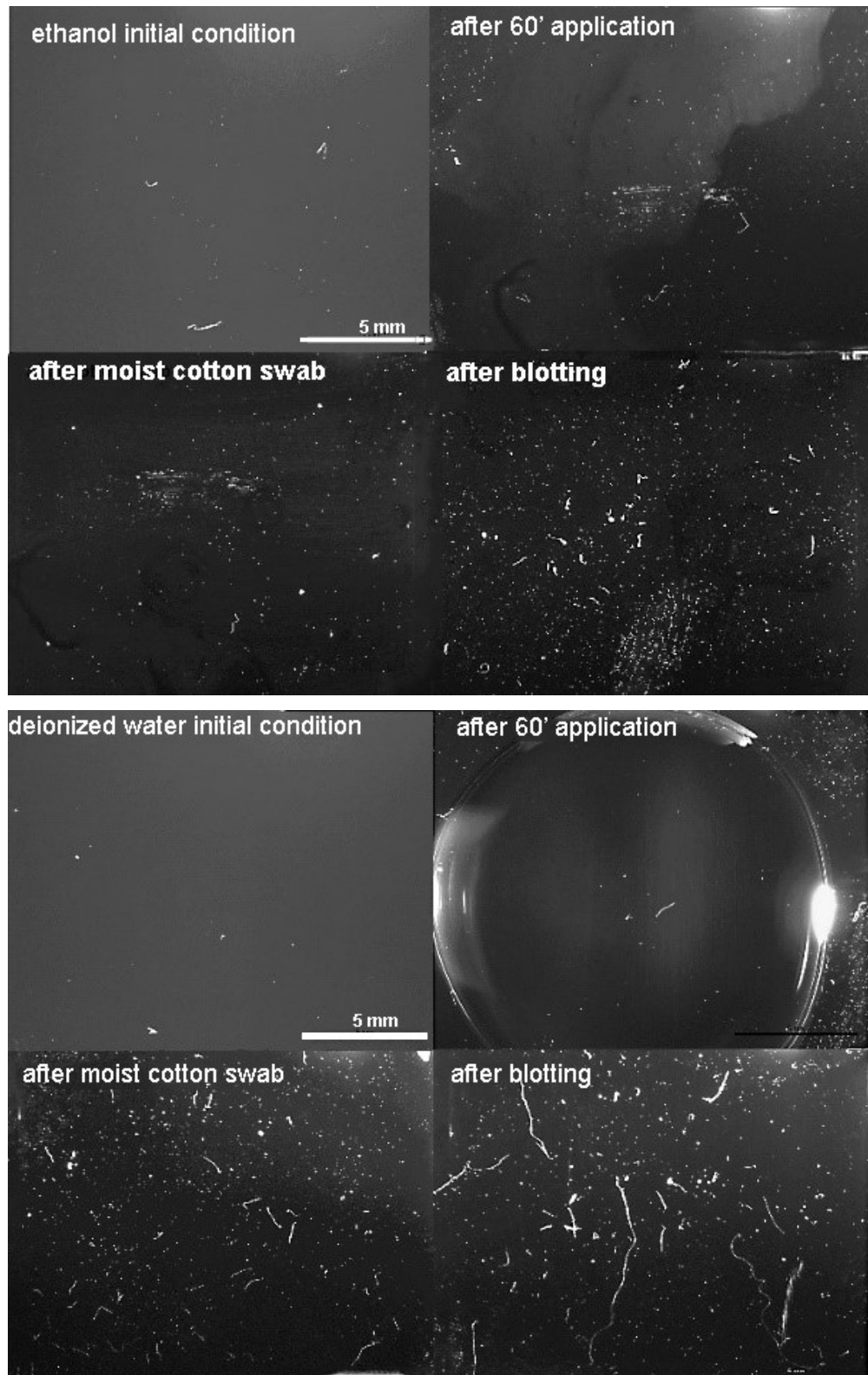


*Figure 7.21. Comparing rolling moistened cotton swabs against blotting with dry filter paper for post-treatment clearance of gel and solvent residues from the treated PMMA. Rolling moistened swabs in linear motions towards one direction was less damaging and more effective at removing dirt for the transparent surface.*

## Chapter 8. PRELIMINARY EXPERIMENTS

---

Experimental work has been divided into two sections, the preliminary work presented here and the main experiments (Chapters 9-10). This chapter contains the bulk of the preliminary experimental work consisting of testing factors and their levels by small scale cleaning trials. The aim being to understand materials (gel carriers and solvents) and methods, as well as the broader parameters affecting experimental processes, such as application time, and to refine and optimise methods that lead to the main experimental design. A series of cleaning experiments were performed on unsoiled surfaces with a number of factors established through the open-ended survey and the literature and as the most critical in the cleaning of PMMA. Their evaluation identified the most important of these. When factors and factorial levels were statistically significant to the process, they were further scrutinised in the next experiment. If a factor showed no significant impact on the cleaning process, it was discarded from the experimental design.

### 8.1. UNAGED, UNSOILED POLY (METHYL METHACRYLATE)

The preliminary cleaning experiments carried out on unaged PMMA samples (Fig.8.1) aimed to assess the damage potential, rather than the effectiveness, of the individual gel cleaning methods encountered in the literature. Samples were studied in their unaged condition to collect control data. Implications of degradation were examined in later experiments. Since the interaction between variables was expected, understanding the effect of single factors, before proceeding to more complicated experimental designs was necessary.

#### 8.1.1. Experimental design

The factors initially considered critical for cleaning PMMA were type of gel, solvent and application time. Two-factorial experiments were studied at multiple levels (general two-factorial design) (see Table 8.1) generating three smaller scale experiments:

- Effect of hydrogels Agar, Gellan, Carbopol/Ethomeen (from now on Carbopol), Pemulen/TEA (from now on Pemulen) and PVA/borax (from now on PVA) and their interaction with application times (5 and 60 minutes) - run in triplicate.
- Effect of free solvents H<sub>2</sub>O, EtOH, IPA and PET, in relation to application times (5 and 60 minutes) - run in triplicate.
- Interaction of Gels and Solvents, previously examined in isolation, combined as solvent-based gel systems - run in duplicate.

### Preliminary Experiment on unaged, unsoiled PMMA: 2 and 3 replicates

Experimental Variables			
Factor	A. Gels	B. Solvents	C. Application time
Levels	1. Agar	1. Deionised water (H <sub>2</sub> O)	1. 5 minutes
	2. Gellan	2. Ethanol (EtOH)	2. 60 minutes
	3. Carbopol®+Ethomeen	3. Isopropanol (IPA)	
	4. Pemulen™ TR2+TEA	4. Petroleum ether (PET)	
	5. PVA/Borax		

Table 8.1. Experimental variables in the two-factorial design used for the preliminary cleaning experiments of unaged and unsoiled PMMA.

For description of the sample preparation and detailed results see Appendix M.

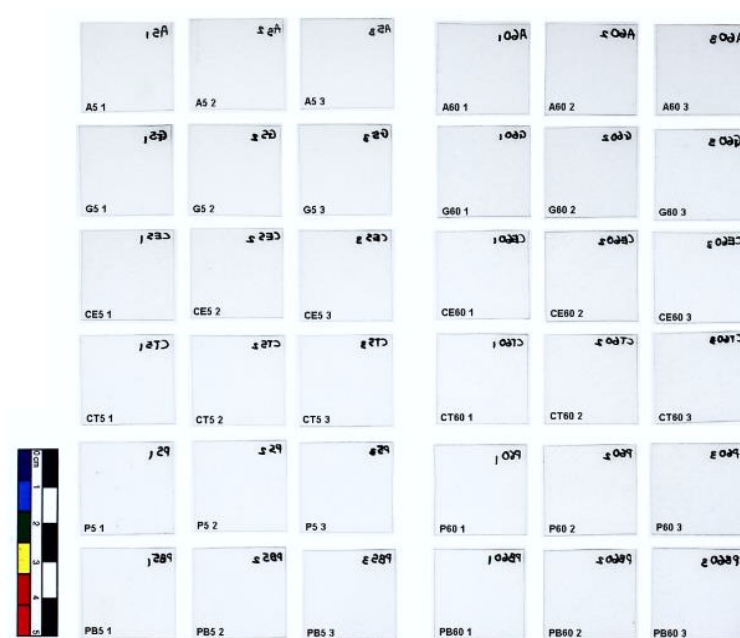


Figure 8.1. Unaged and unsoiled PMMA samples before treatment with hydrogels, free solvents or solvent-gels for 5 or 60 minutes. The samples were labelled at the back.

#### 8.1.2. Discussion of results

The three small-scale experiments carried out here helped to understand gaps in methodology and execution of this type of cleaning experiment. The results, even if somewhat inconsistent, led to the understanding that duplicates and triplicates were insufficient to draw definite conclusions and trends in relation to the cleaning methods and materials. This outcome was imperative to identify at an early stage of the research. More replicates would be essential to showcase the general trend of the treated samples' behaviour and identify outliers.

The presence of gel thickeners was shown to influence the action of solvents, in some cases by exhibiting a satisfactory performance and in others by increasing the surface damage and residue deposition. For example, the damaging effect of free EtOH and IPA (loss of transparency) was reduced when the solvents were coupled with Agar and Gellan gels. This indicated that the solvent action was more controlled when thickened rather than when applied with cotton swabs. By comparison, when the same solvents were added to Carbopol and Pemulen gels, cleaning was less efficient comparing to their application with cotton swabs. Some of these preliminary results showed a positive influence of gels on the effect of cleaning, indicating that the solvent-gel systems were promising compared to other application methods. One observation was that generally no swelling was macroscopically visible in any of the treated samples. Changes in the optical and physical properties of the treated PMMA surfaces were further scrutinised in the following experiments.

Ideally there would be no weight changes after treatment, especially in the current experiment where there was no foreign surface matter/dirt. This would be an indication that the solvent-gel action had no effect to the original material. Later experiments explored whether more than one process might occur concurrently, as bulk gravimetric analysis overlooks the possibility of simultaneous extraction and deposition of material. Results of py-GC/MS (discussed in Chapter 4) were used to support interpretation of the chemical behaviour of PMMA.

## **8.2. REPLICATION OF TREATMENTS**

Examination of interaction between factors was crucial to understand the effectiveness of treatments. Additionally, it was important to compare the use of solvent-gels to the application of the (respective) free solvents with cotton swabs. Results of the previous experiment indicated that experimental work required increase of replicates followed by duplication. In addition to the factors Gel, Solvent and Application time, Surface Condition was also examined as a factor.

All procedures and actions, from how to prepare and condition the samples pre-treatment, how and when to weigh them before and after treatment, as well as protocols for cleaning (such as application and removal of the treatments), were previously tested and established prior to carrying out this experiment (see Chapter 7.2 and Appendices G and H). This established methodology aimed at reducing consistent and random errors and increasing homogeneity across experiments.

### 8.2.1. Experimental design

A multilevel full-factorial experimental design was adopted to simultaneously examine the effect of each factor in isolation, as well as their interactions. The replicates were increased to 5 and the new cleaning experiment followed a similar approach to the previous, but with both new and 32 days UV-aged 25 x 25 mm square coupons. To enable comparison of solvent-gels to cotton swabs, the level 'no gel' was added as a variable. This allowed the examination of the individual and combined effect of Free solvents with Application time and Surface condition, in the same experimental design as Gels. The experiment was designed in quintuple with 240 new and 240 aged unsoiled samples (n=480 samples).

Preliminary experiment with replication of treatments				
Experimental Variables				
Factor	A. Gels	B. Solvents	C. Application time	D. Surface condition
Levels	1. no gel	1. H <sub>2</sub> O	1. 5 minutes	1. new
	2. Agar	2. EtOH	2. 60 minutes	2. aged
	2. Gellan	3. IPA		
	3. Carbopol	4. PET		
	4. Pemulen			
	5. PVA			

*Table 8.2. Experimental variables in the multilevel full-factorial design used for the preliminary cleaning experiment with replication of treatments on new and aged unsoiled PMMA with 5 replicates. Number of levels: 6, 4, 2, 2.*

### Multilevel Factorial Design

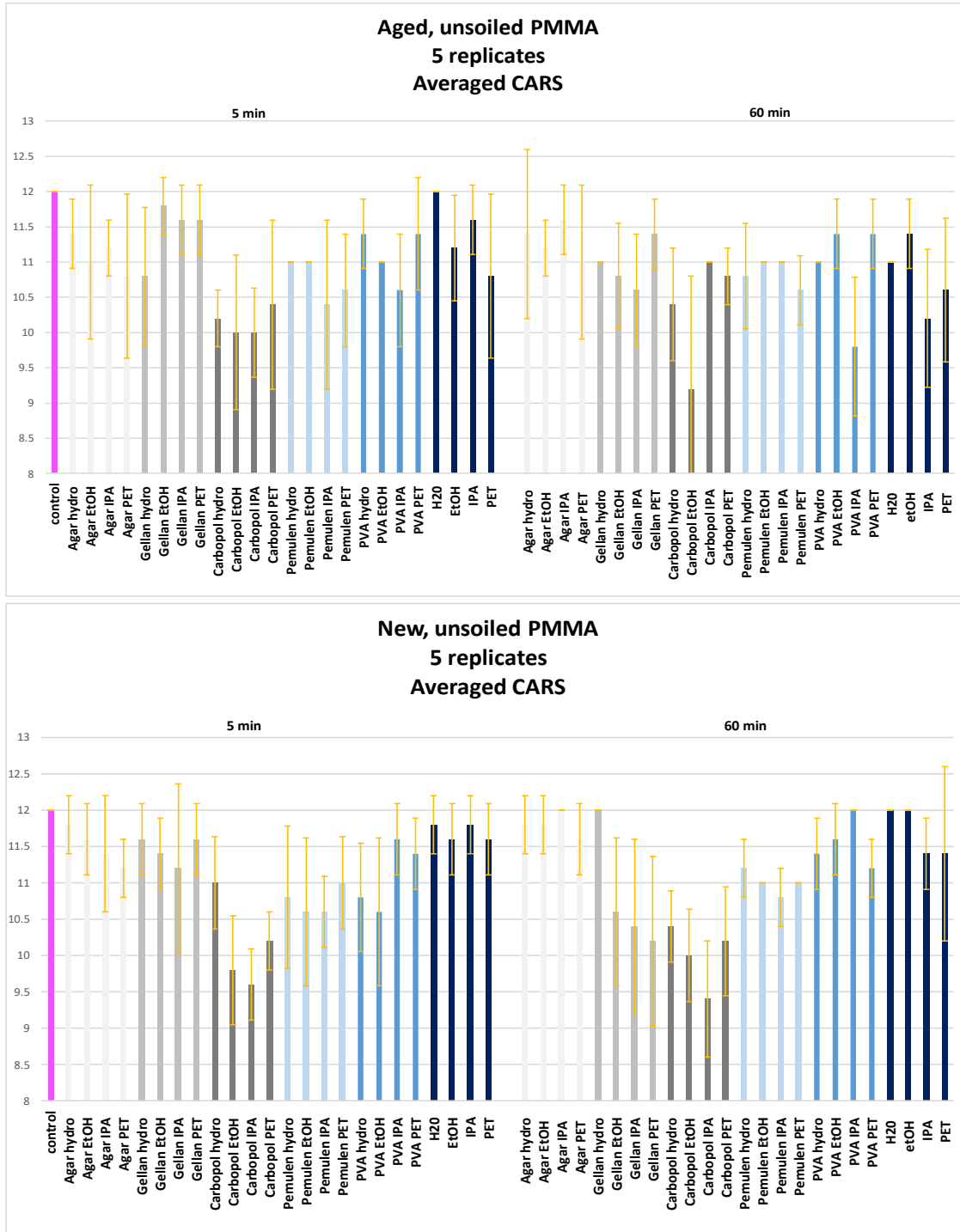
Factors:	4	Replicates:	5
Base runs:	96	Total runs:	480

### 8.2.2. Results & interpretation

The results of the cleaning experiment are presented here as follows: values and measurements of CARS, gloss, weight change % and FTIR peak height ratios. Microscopic images, as well as ATR-FTIR spectra are also presented to help with visualisation. A statistical interpretation of the significance of these findings was undertaken via ANOVA at the  $p = 0.05$  probability level (Morgan 1991). This aimed to identify whether different factors influence cleaning of PMMA independently and in combination. Once the nature of the impact of factors on the cleaning outcome was understood, and the effectiveness of treatment evaluated, these were considered for the design of the next cleaning experiment.

**VISUAL OBSERVATIONS**

**CARS scores**



Graph 8.1. CARS scores of the unsoiled, new and aged PMMA samples. Scores are based on a five-point progressive ranking from 0 (worst) to 4 (best). The scores, expressed as a bar chart, are averaged from 5 replicates for each treatment. The untreated PMMA controls scored the highest possible CARS 12 in categories 'Abrasion' and 'Gel residue'. Error bars show the standard deviation.

All treatments visually affected the surface transparency of PMMA. Graph 8.1 shows the averaged CARS scores of 5 replicates of unsoiled PMMA samples after treatment with free



solvents, hydrogels and solvent-gels. Although aged surfaces were left in a slightly worse condition than new, according to human perception, all samples followed similar patterns of CARS fluctuation. Gellan solvent-gels, along with Agar solvent-gels and free solvents left new PMMA in the best surface condition after 5 minutes (scored highest CARS) (Graph 8.1). Carbopol solvent-gels offered the worst visual result across all samples, regardless of application time. Equally poor for both aged and new surfaces was the effect of the 60-minute application of Gellan solvent-gels. Their application after 5 minutes offered improved results, rendering it the only treatment significantly affected by application time. Overall, application time showed similar pattern for both values tested (5 and 60 minutes), on new and aged samples.

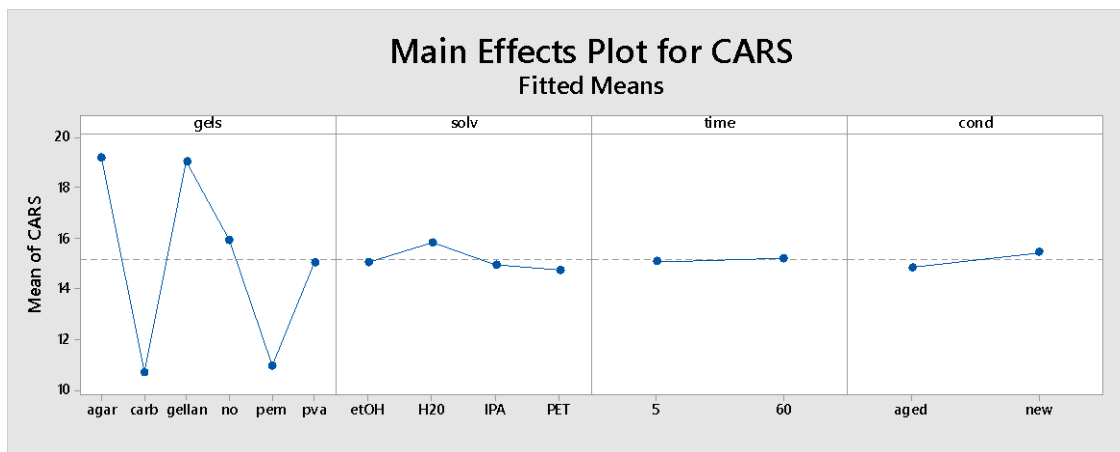
### **ANOVA CARS**

ANOVA of the CARS showed that Gels had a statistically significant impact on the effectiveness of cleaning PMMA. Tukey's HSD compared types of gel and determined which were significantly different from the other treatments by allocating them a unique letter. Agar-Gellan and Pemulen-Carbopol were paired as significantly similar, meaning that they offered similar visual results. Agar and Gellan offered the best results according to the naked eye, whereas Pemulen and Carbopol left surfaces in a poor condition. The only treatments that did not share a letter were free solvents (see 'no' with B) and PVA (C), indicating that they significantly affected the visual condition of treated PMMA samples. According to the main effects plot (Graph 8.2) free solvents scored medium CARS (above the mean value) affecting the cleaning outcome in a positive manner, whereas PVA scored below the mean CARS value thus affecting PMMA in a negative manner.

### **Grouping Information Using the Tukey Method and 95% Confidence**

<u>gels</u>	<u>N</u>	<u>Mean</u>	<u>Grouping</u>
agar	80	19.188	A
gellan	80	19.038	A
no	80	15.938	B
pva	80	15.038	C
pem	80	10.975	D
carb	80	10.725	D

*Means that do not share a letter are significantly different.*



Graph 8.2. The mean CARS scores of free solvents (no) are above the mean value, while that of PVA below the mean value, indicating they affected cleaning of PMMA in a positive and a negative manner, respectively.

### **Stereomicroscopy under raking light**

Free solvents left aged PMMA in a slightly worse condition to new samples, as previously displayed across all gel treatments. Water tended to leave surfaces in a satisfactory condition, whereas organic solvents less so. Especially EtOH and IPA, which often left surfaces with large areas of non-uniform loss of surface transparency, resembling stains (Fig.8.2). PET left the majority of treated aged samples appearing greasy. Samples were then visually examined under the higher magnification of SEM to understand the types of damage encountered.

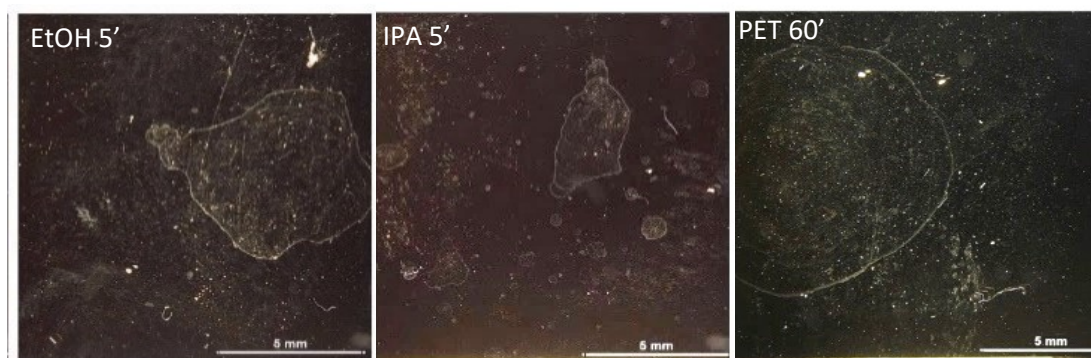
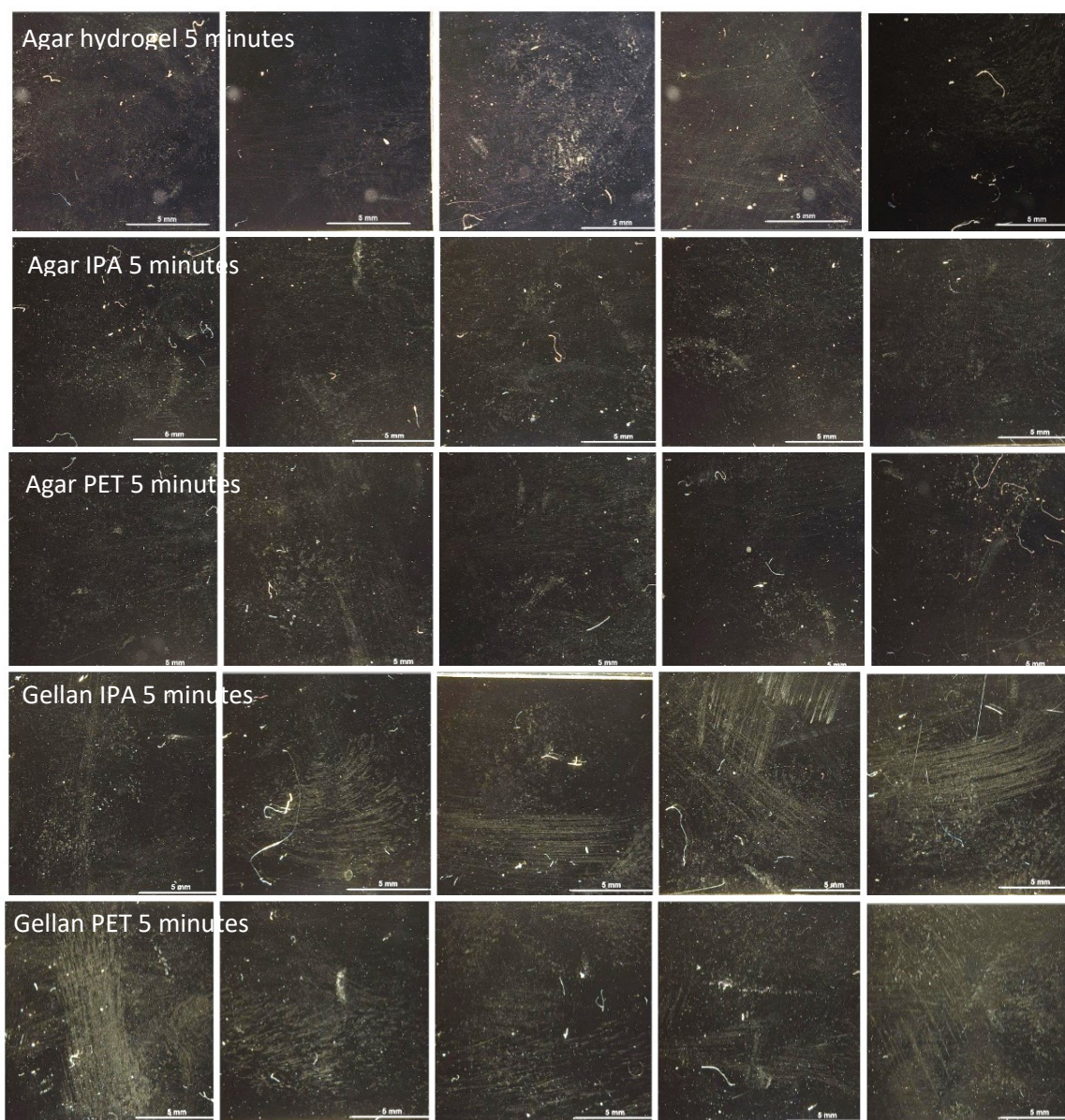


Figure 8.2. Microimages under the stereomicroscope (x78.1) with raking light. Aged PMMA samples treated with organic solvents (EtOH, IPA or PET) for 5 minutes, display comparable damage: few deposits, discolouration and intense stains.

All solvent-gels (except for Carbopol, discussed later) behaved similarly, leaving PMMA surfaces in a comparable visual condition, regardless of application time. New samples appeared in a better condition than the aged, observation which was in agreement with the CARS results. Solvent-gels (except for Carbopol) left new PMMA with recurrent types of surface damage (Fig.8.3): deposits of fine nature, and often imprints of a rolling movement. This was possibly the result of post-treatment clearance of surfaces with 3 separate H<sub>2</sub>O-

moistened swabs rolled over the samples, which instead of clearing the gel remains, spread them across the surface. Solvent-gels left aged PMMA with recurrent types of surface damage too (Fig.8.4): fine deposits and residues, discolouration, staining and imprints of post-treatment swabbing. Here only samples treated with Agar and Gellan solvent-gels are displayed as they exhibited damage also seen after Pemulen and PVA solvent-gels.

#### PMMA samples



*Figure 8.3. Microimages under the stereomicroscope (x78.1) with raking light. All five replicates for each treatment are presented. Agar and Gellan gels coupled with water, IPA or PET, for 5 minutes, induced similar types of surface damage to new PMMA samples: deposits and intense surface imprints of swabbing. Gellan caused more intense damage.*

Carbopol solvent-gels left all samples in an inferior visual condition, with a lot of deposits, residues, discolouration and extensive smudges resulting from post-treatment clearance, caused by the large amount of gel remains (Fig.8.5). These visibly entrapped cotton

threads from the swabs. Additionally, abrasions, induced by none of the other treatments, became evident after treatment with Carbopol. The extensive gel residue documented was partly attributed to Ethomeen. Previous research showed that Ethomeen was still present after clearance with swab rolls and clearing solvents (Carretti *et al.* 2010).

### Aged PMMA samples

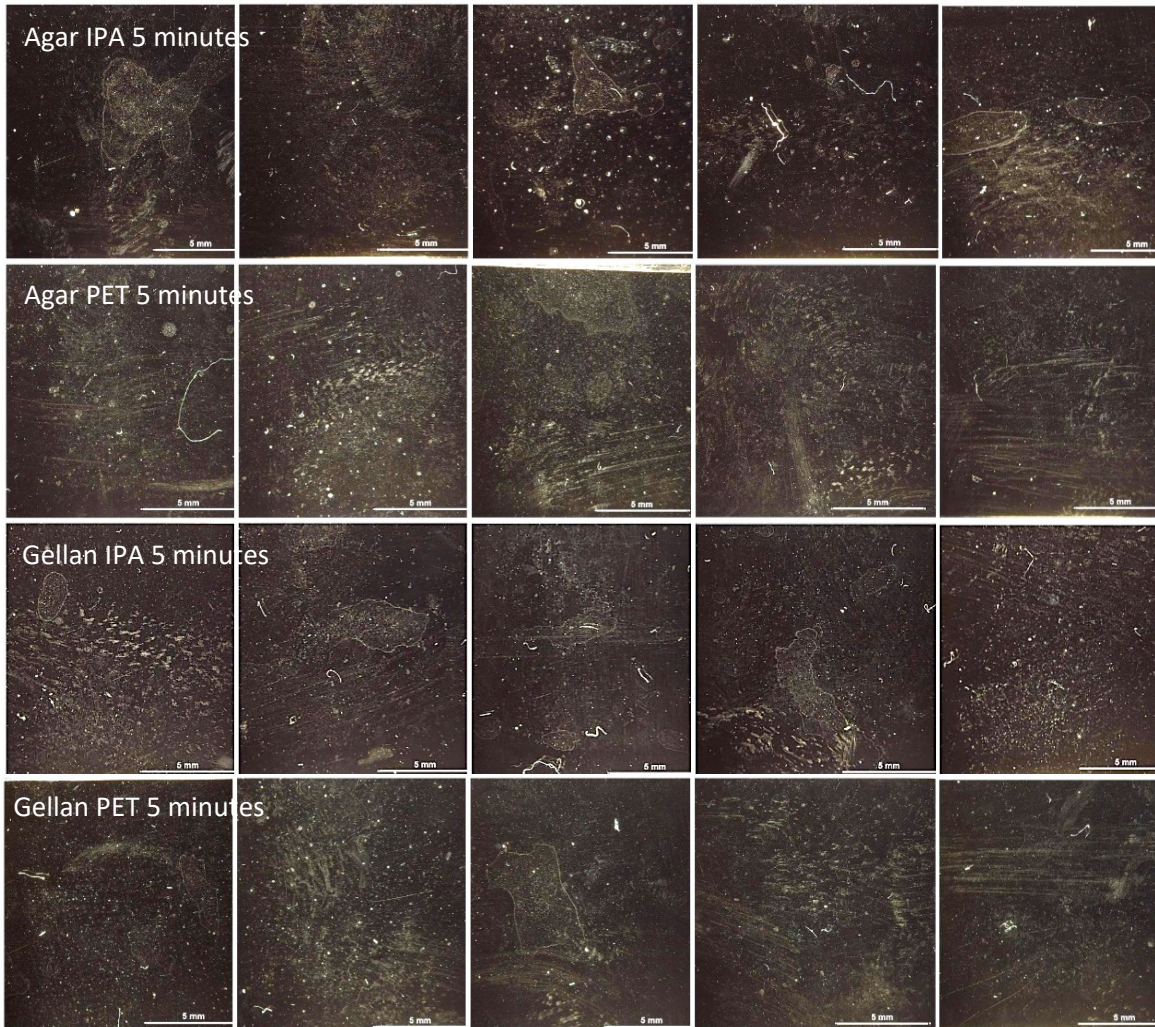


*Figure 8.4. Microimages under the stereomicroscope (x78.1) with raking light. All five replicates for each treatment are presented. Agar and Gellan gels coupled with IPA or PET, for 5 minutes induced comparable damage to aged PMMA samples: a lot of deposits and residues, discoloration and surface imprints of swabbing.*

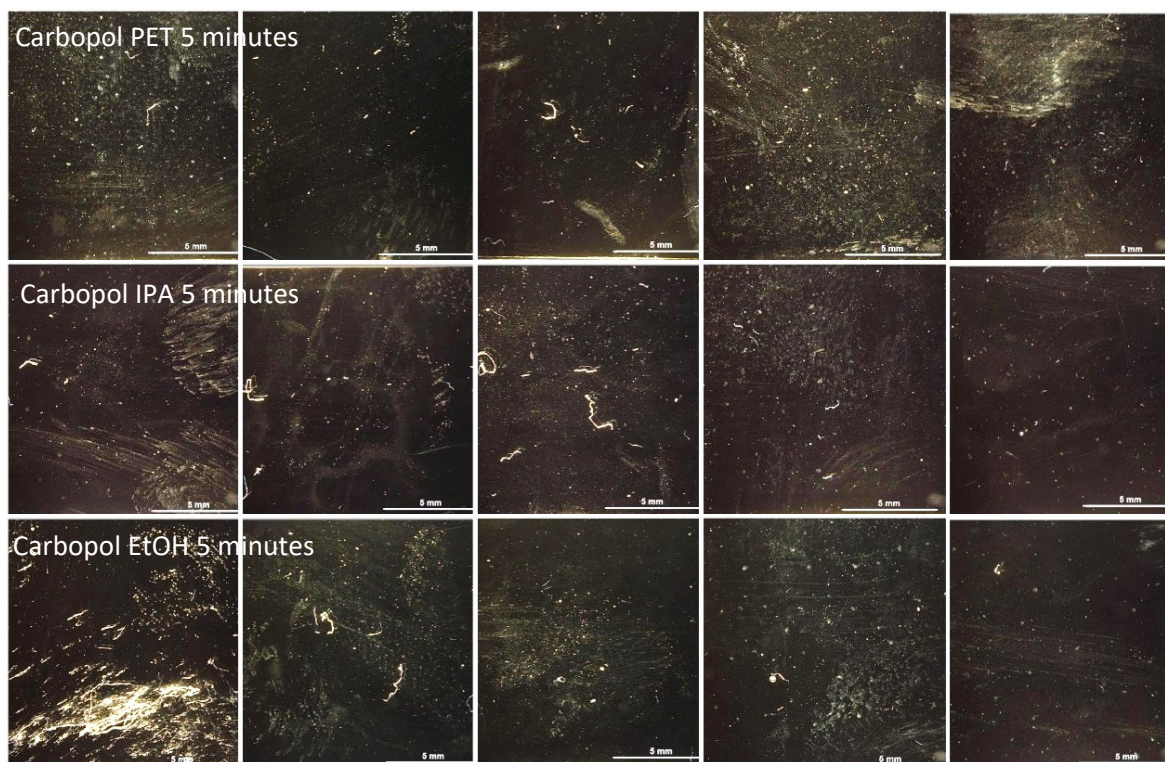


*Figure 8.5. Microimages under the stereomicroscope (x78.1) with raking light. All five replicates for each treatment are presented. Carbopol solvent-gels for 5 minutes left aged PMMA samples in a very poor visual condition: deposits and residues, discoloration and surface imprints of swabbing.*

### **SEM imaging**

SEM imaging was used to observe the surfaces of treated samples under high magnification. Stereomicroscopic observations with raking light were used as a guide for the SEM observations. ANOVA of CARS scores, gloss measurements and peak height ratio (to follow) indicated that application time had no statistically significant effect on the cleaning outcome. As it would be inconsequential and time consuming to further continue with both application times when having no (positive or negative) effect, only samples treated for 5 minutes are examined here.

Under the SEM, new control surfaces were found in pristine condition (Fig.8.6), while aged control surfaces bared minute residues of unknown nature and small areas of discoloration (Fig.8.7). These may have been remains of PSA from the protective film covering the industrially supplied PMMA coupons, which were subsequently exposed to UV and subjected to wet cycles with spraying water. All samples were pre-treated and pre-washed under the same conditions following identical procedures, to assure homogeneity of surfaces. Differentiation was introduced when the aged samples underwent ageing for 32 days in the weathering chamber. This may have caused previously transparent, minute PSA remains (possibly film-form) from the protective film to break down and conglomerate on the surface.

Aged samples were handled a lot more than the new ones so these residues may have just been dust particles.

#### Unaged (unsoiled) PMMA control

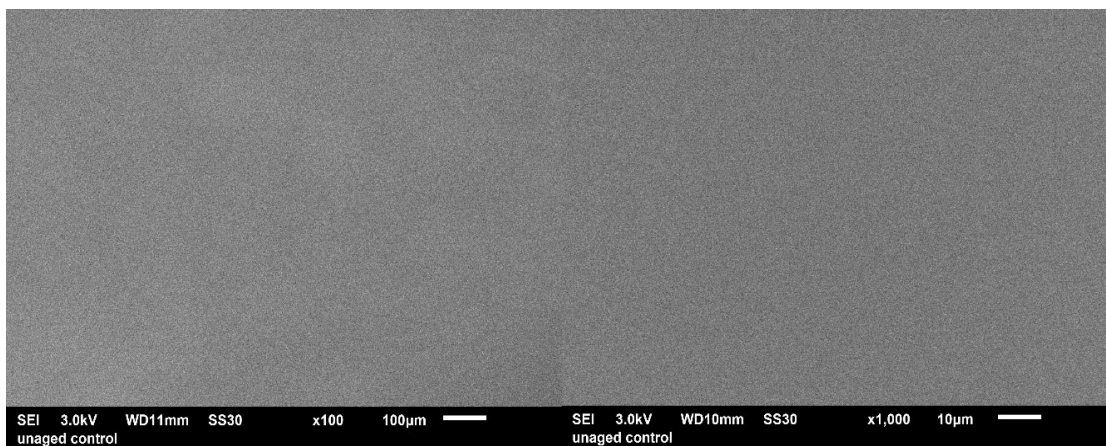


*Figure 8.6. SEM micrographs: Unaged, unsoiled PMMA control under magnification x100 (left) and x1000 (right).*

#### Aged (unsoiled) PMMA control

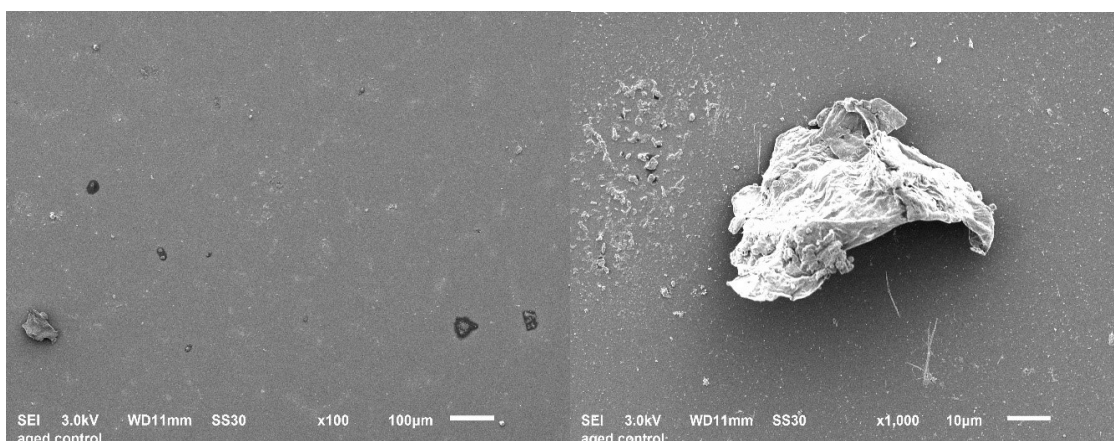


*Figure 8.7. SEM micrographs: Aged, unsoiled PMMA control under magnification x100 (left) and x1000 (right).*

Areas of interest identified under the stereomicroscope, namely gel residues, fine deposits, areas of non-uniform loss of surface transparency resembling stains, imprints of a rolling movement, as well as abrasions and opacity of the surface, were examined. Surface alterations/damage caused by solvents thickened in gels or applied free, appeared similar on all samples independent of their surface condition. SEM imaging was aimed at understanding their occurrence and elucidate patterns of formation and manifestation.

Intense smudges attributed to post-treatment clearance, were observed under the SEM. Fig.8.9 F-G showed signs of PVA gel spread across the surface, which was attributed to the post-treatment rolling of cotton swabs over the surface. Gel residues were commonly

deposited either as three-dimensional matter or thin films. It was noted that discoloration would often accompany gel residues, as a halo/stain (see Agar hydrogel and Carbopol IPA residues, Fig.8.8). At higher magnification, two types of phenomena were identified; loss of transparency and the presence of fine deposits (Fig.8.9 A-D). These would often occur concurrently contributing to one macroscopically visible phenomenon, that of discoloration of the treated surface, as previously described.

Surface opacity possibly resulted from solvents (thickened in the gels) penetrating the upper micron layers of PMMA, becoming entrapped and rendering the material cloudy. Free solvents on PMMA surfaces may cause the formation of a network of cracks, which resemble a 'frosted' material to the naked eye (Akhurst 2008, 161). However this was not observed in any of the samples treated in this experiment.

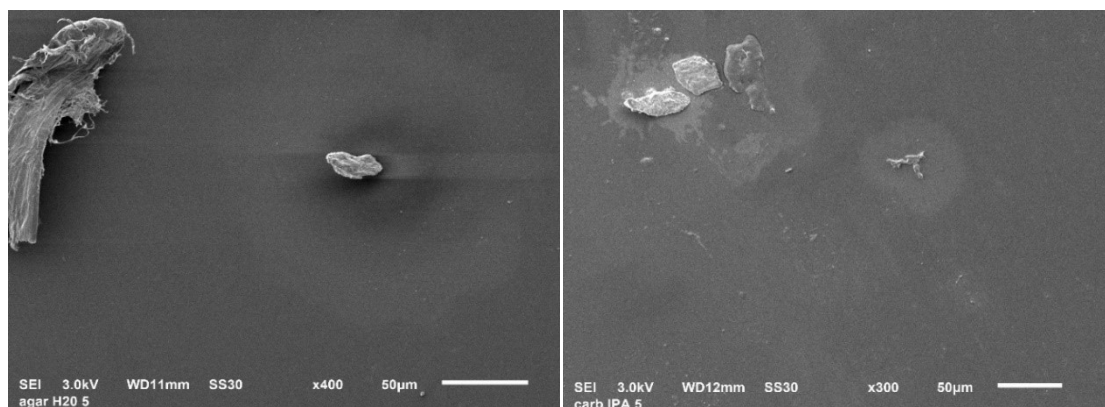


*Figure 8.8. SEM micrographs of unaged, treated PMMA. Left: Agar H<sub>2</sub>O for 5 minutes rarely left minute gel residues and surface discoloration around them. Right: Carbopol solvent-gels left a large amount of gel residues and surface discoloration.*

The presence of fine matter on the treated surfaces may be explained through the 'coffee stain effect', more commonly known as the evaporation of droplets (Shahidzadeh *et al.* 2015). Evaporation is fastest near the edge of a drop, such as a solvent drop either coming from the gel or applied as free solvent. The solvent/liquid lost by evaporation around the edge is replaced/replenished, causing fluid to flow from the interior of the droplet to the edge. This carries along solutes that are subsequently deposited at the edge, once the liquid has evaporated. These solutes and their uncontrolled distribution are generally responsible for the formation of ring-like stains (Shahidzadeh *et al.* 2015) with strong perimeter concentrations (Deegan *et al.* 2000).

Solutes here are derived from the gels, which in their raw form are powder materials suspended in water. For instance, PVA used here contained powdered borax (in its raw form) as a buffering agent. Studies of PVA/borax gels showed that some fraction of borax does not crosslink with the polymer gel upon formation, remaining free as a salt in the gel (Angelova

2013). This can then be deposited in the form of dried droplets on treated surfaces. Similarly, Carbopol gels formulated with Ethomeen, which once added in the system forms a salt, may be deposited on the treated surface after removal of the gel.

This phenomenon was also noted after treatment with rigid, intact Agar and Gellan gels, as seen in Fig.8.9, although they did not tend to dissociate nor leave gel residues behind (Sansonetti *et al.* 2012). Other scholars observed a similar 'edge effect' or tideline created around the applied Gellan gels after treatment of paper (Miller *et al.* 2017; Sullivan *et al.* 2017). The literature suggests greater residue depositions along the edges of Gellan gels (Sullivan *et al.* 2017) indicating that they leach water more readily than agarose-based gels (Miller *et al.* 2017). This reinforces the 'coffee stain effect' theory where gel solutes are carried in droplets onto the plastic surface from inside the gel. Another hypothesis was that this fine surface matter may derive from the PMMA, as a result of dissolution of non-volatile components extracted and deposited on the surface. This proposition is supported by the fact that the phenomenon of ring-like stains, explained by the 'coffee stain effect' theory, was also exhibited on surfaces treated with free organic solvents (Fig.8.10).

Solutes found on samples not treated with gels were attributed to the initial cleaning or/and the solvents used. Fine, dust-like residues visible on samples after solvent treatment were attributed to precipitation of non-volatile PMMA components dissolved during exposure to the solvent and extracted onto the plastic surface (see Chapter 7.1.2). They could also be attributed to contaminants found on the pre-treated surface. Solvents, even when 99 % pure are known to leave some residues behind, which may become visible under high magnification.

As discussed previously, free solvent treatment caused cloudiness of PMMA surfaces. This was clearly visible under SEM magnification as a diffuse surface that was impossible to zoom in (Fig.8.10 B-C). The surfaces were being monitored with SEM for some time in an attempt to sharpen the image, while it was changing in real time; any liquid remaining on the treated samples was evaporating under high vacuum. All four cleaning agents used (H<sub>2</sub>O, EtOH, IPA and PET) caused the same phenomenon to the majority of samples. This real time evaporation may have been instigated by the beam of secondary electrons heating the sample surfaces. However, treated samples had been conditioned in a controlled environment for at least 48 hours prior to SEM imaging. It is therefore reasonable to assume that solvents penetrated the upper micron layers retarding evaporation and rendering the transparent material visibly hazy.



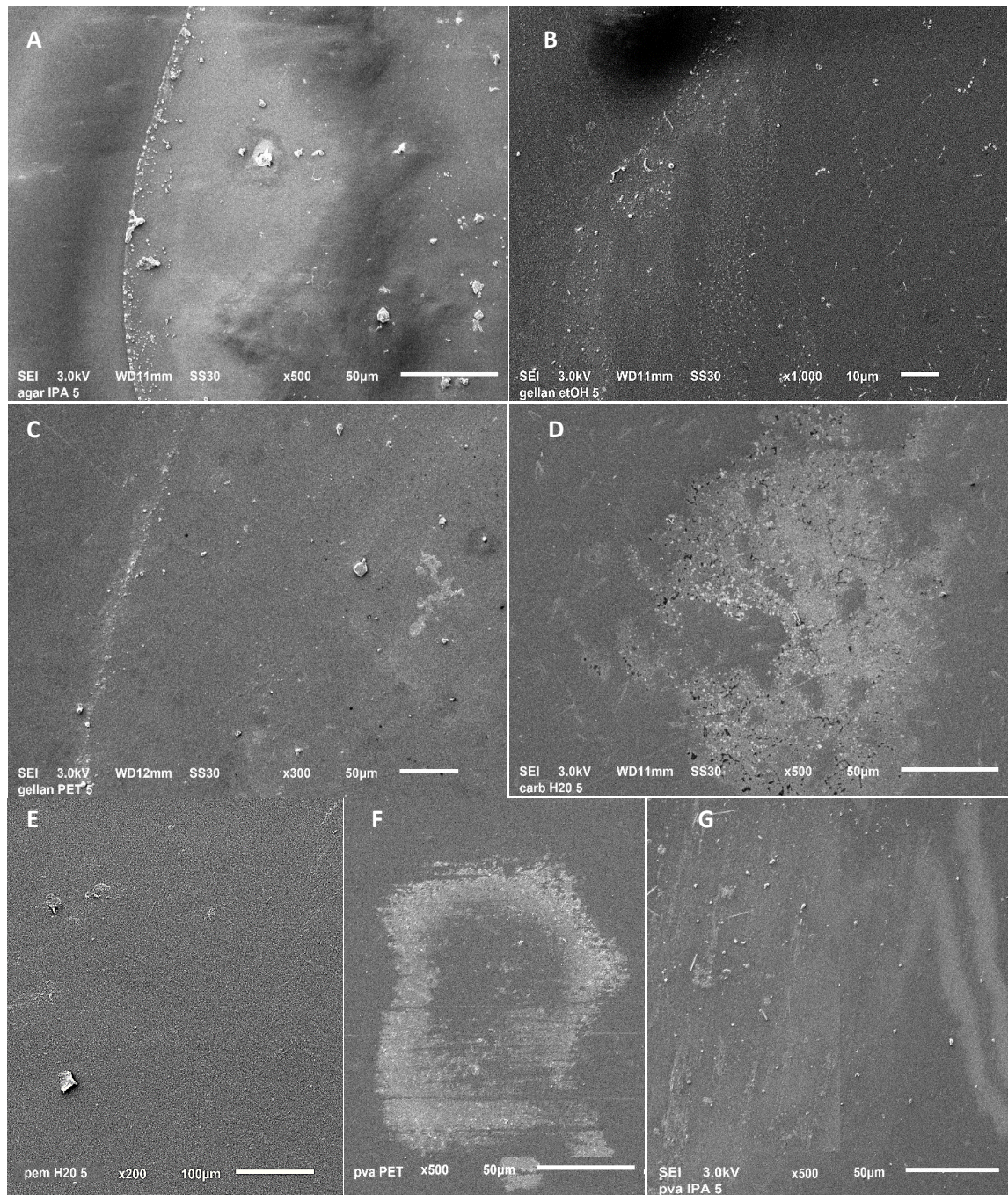


*Figure 8.9. SEM micrographs of aged, treated PMMA. A-C: PMMA surfaces that were left with ring-like stains because of gel treatment leaving behind liquid that upon evaporation left solutes, visible as fine matter; both after Agar and Gellan solvent-gels. D-E: Carbopol and Pemulen solvent-gels left large amounts of gel. F-G: Samples after PVA appeared to bare thin layers of gel giving the impression they were swabbed or spread around the surface, possibly during the post-treatment clearance. Some solvents such as IPA in PVA caused cloudiness of the transparent surface due to entrapment of solvent.*

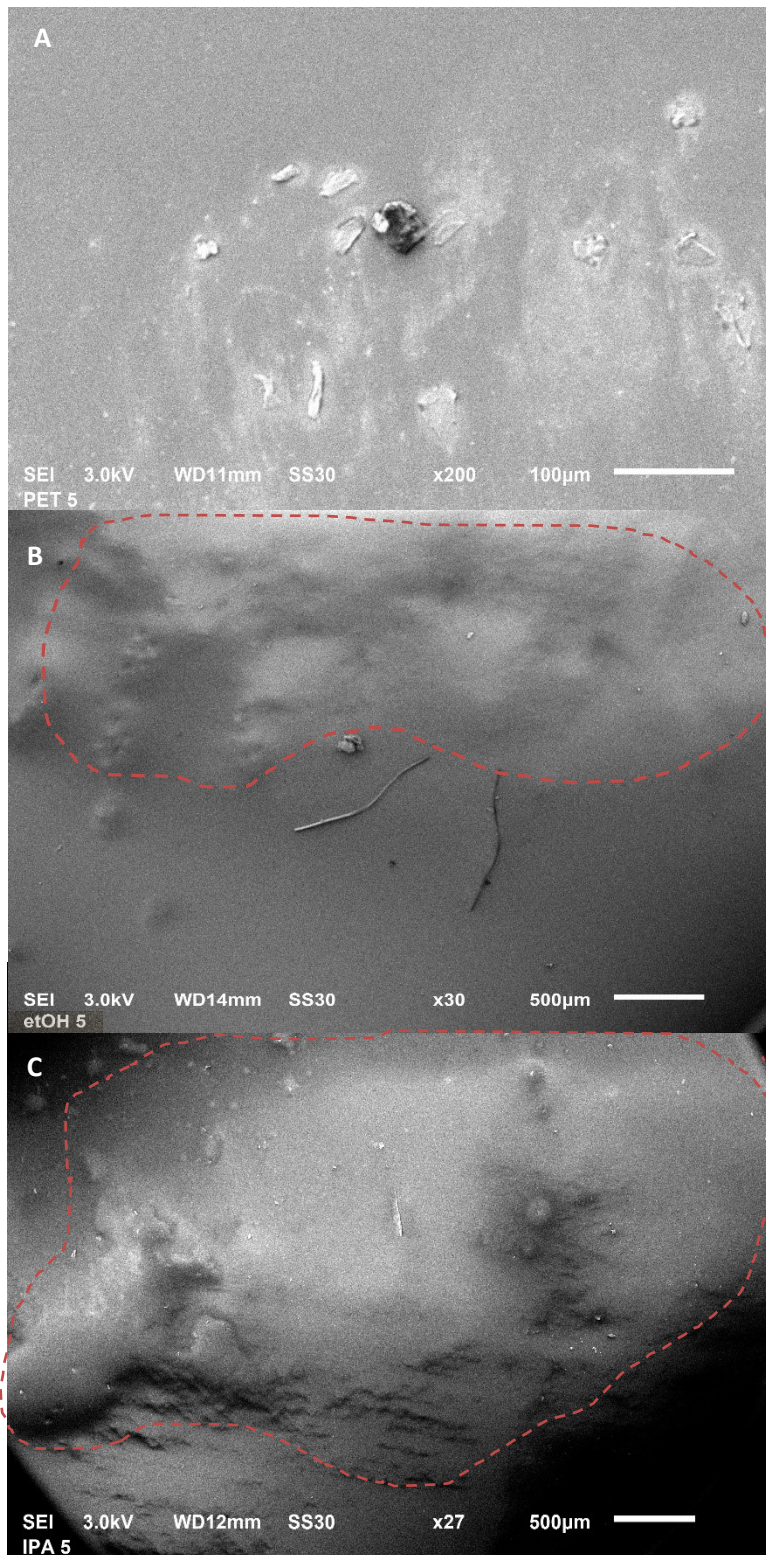
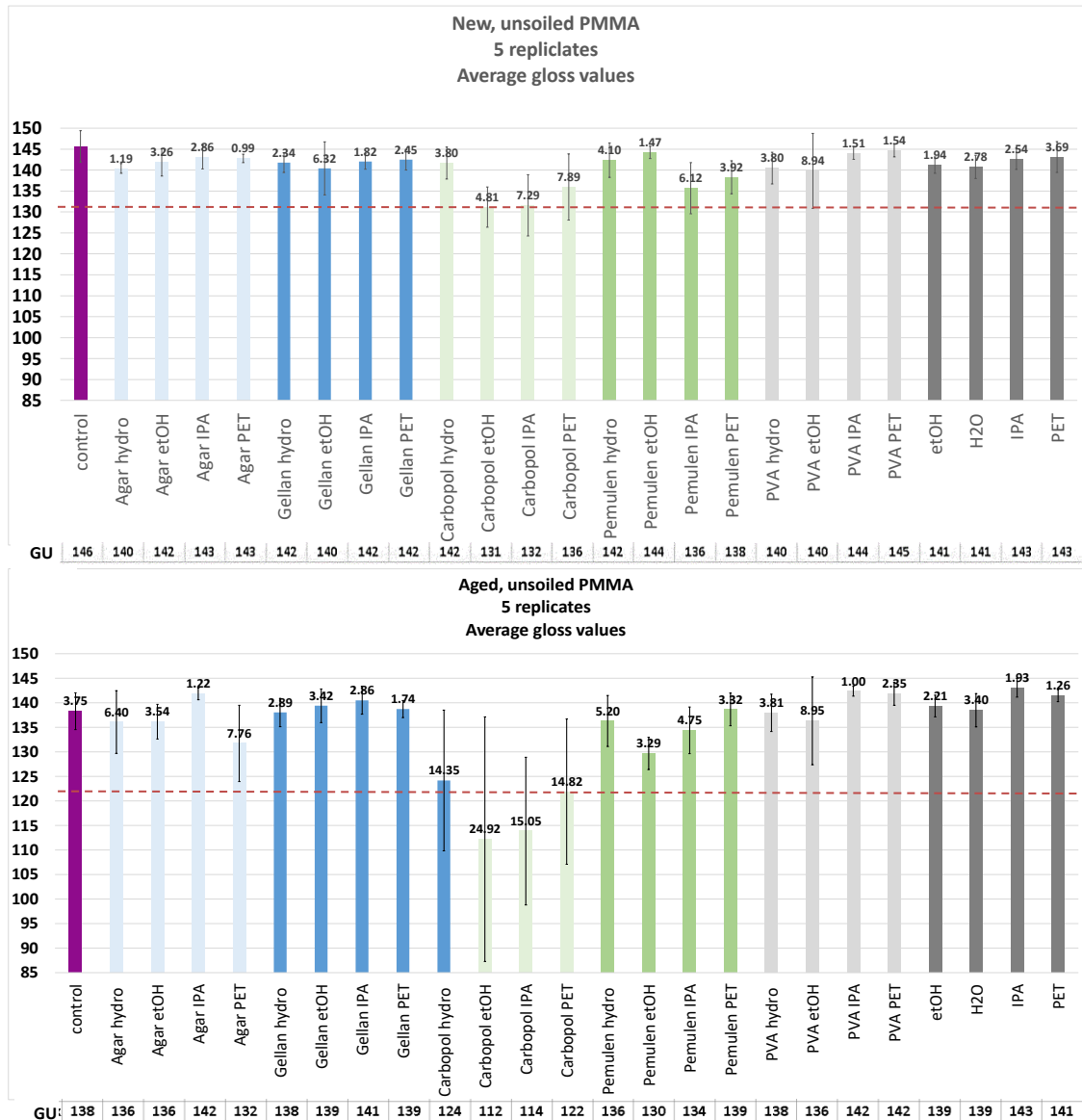


*Figure 8.10. SEM micrographs of treated PMMA with organic solvents. A: PET left surfaces with deposited material, either precipitates of non-volatile PMMA components or contaminants found on the pre-treated surface. B-C: New PMMA surfaces treated with EtOH and IPA appeared very cloudy due to real time evaporation of solvents (see red arrow) under the SEM beam.*

**GLOSS**

**Gloss measurements**



Graph 8.3. Gloss measurements of new and aged PMMA samples treated for 5 minutes, plotted as bar charts. Gloss units (GU) are averaged from 3 repetitions of 3 spot measurements on 5 replicates. Differences < 15 GU are non-detectable by the human eye. The PMMA controls are highly glossy with a value of 146 GU for the unaged and 138 GU for the aged. Red lines show below which point change is visible. Error bars show the standard deviation.

The untreated PMMA controls had the highest gloss and represented the ‘pristine’ PMMA surface. Although the new control showed a higher gloss value by 8 GU (Graph 8.3), this numerical difference might not be easily perceived by the human eye. This was based on the information that difference of less than 15 GU is not visually detectable (PCE Instruments 2018). All treatments - except for Carbopol solvent-gels - left PMMA with a high specular reflectance. Carbopol solvent-gels caused a drop in gloss greater than 15 GU from other

samples, suggesting a macroscopically noticeable change. Carbopol treatments primarily impacted the aged surfaces (see red line in Graph 8.4).

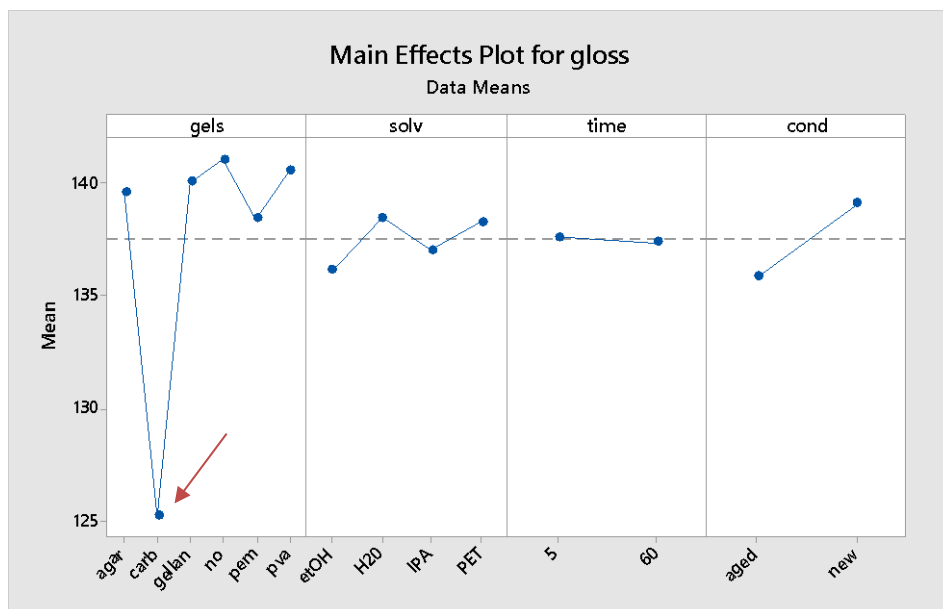
**ANOVA gloss**

ANOVA of the gloss measurements showed that Carbopol solvent-gels negatively influenced the treated samples in a statistically significant manner, leaving them with the greatest reduction in gloss. Tukey’s HSD pinpointed types of gel that were significantly different from the other treatments, by allocating them a unique letter. The only gel that did not share a letter was Carbopol (B). The main effects plot (Graph 8.4) confirms the previously discussed gloss measurements in so far as it shows Carbopol inducing the lowest gloss (see red arrow). As such it was concluded that it significantly affected the cleaning outcome in a negative manner.

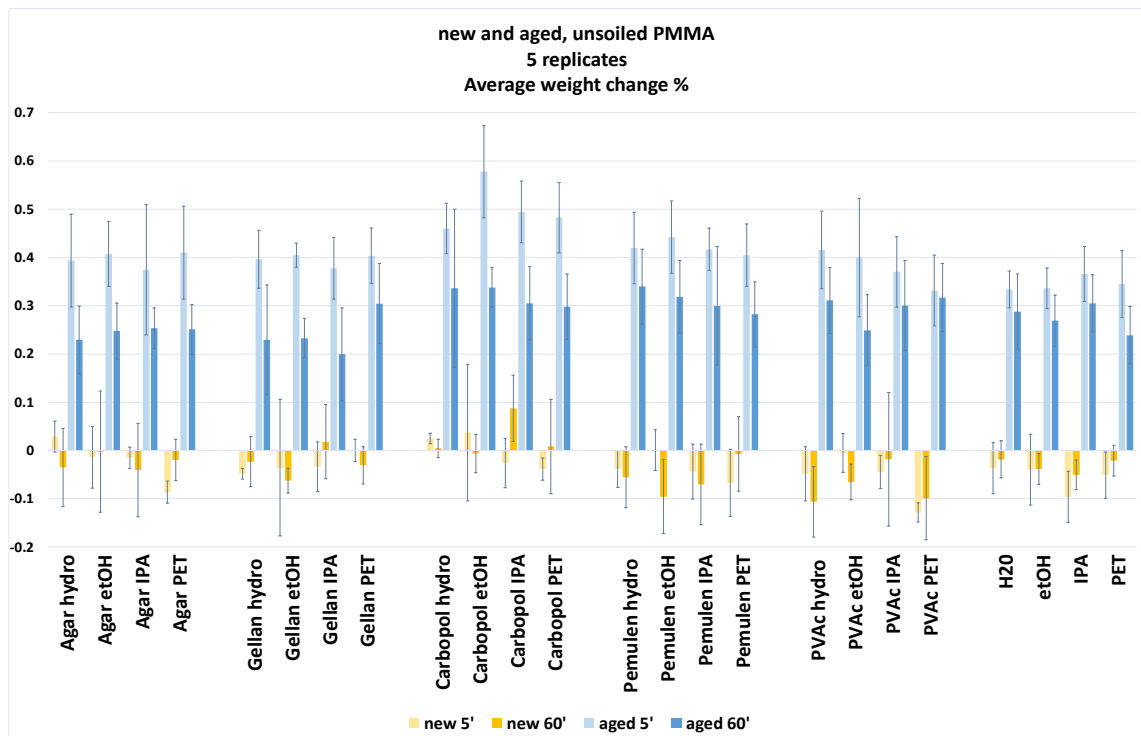
**Grouping Information Using the Tukey Method and 95% Confidence**

gels	N	Mean	Grouping
no	80	141.029	A
pva	80	140.520	A
gellan	80	140.035	A
agar	80	139.550	A
pem	80	138.403	A
carb	80	125.24	B

*Means that do not share a letter are significantly different.*



*Graph 8.4. The mean gloss scores of Carbopol are the lowest indicating it affected cleaning of PMMA in a negative manner.*

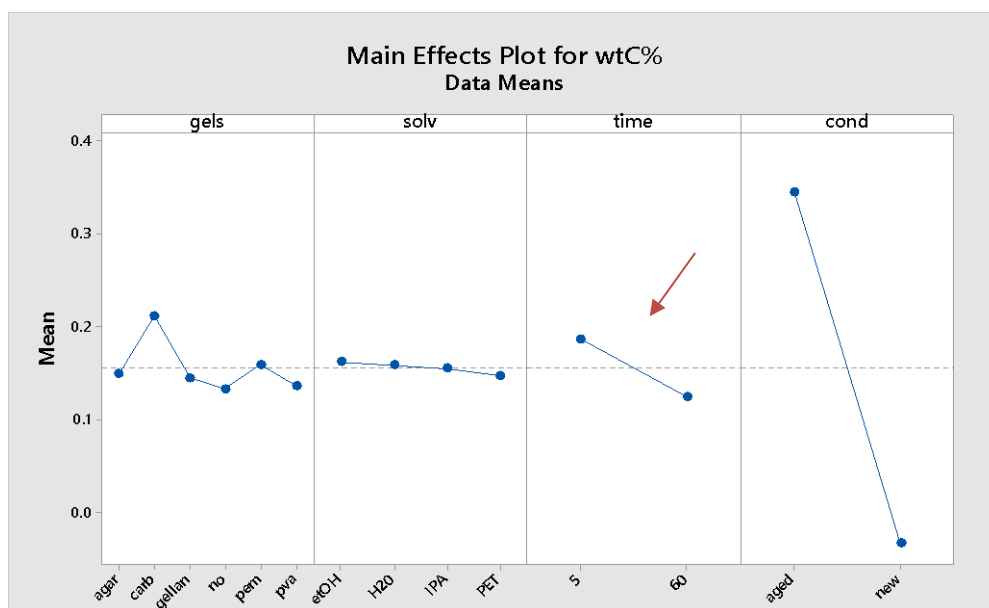
**Weight changes %**

*Graph 8.5. Average weight change % of new and aged, unsoiled PMMA – averaged from five replicates – after cleaning treatment with free solvents and solvent-gels for 5 and 60 minutes (yellow tones for new and blue tones for aged samples). Changes % are normalised to the starting/initial weight. Error bars show the standard deviation.*

All treatments caused aged samples to consistently gain weight (ca. up to 0.4 %), whereas new samples less consistently lost weight (ca. up to 0.1 %) (Graph 8.5). Contact of new PMMA with wet treatments and especially organic solvents was likely to cause dissolution, extraction and evaporation of polymer components, manifested as weight loss (Quye and Keneghan 1999). Weight gain in aged PMMA was attributed to small amounts of liquid penetrating through voids formed during UV ageing by the extraction of volatile PMMA components (Shashoua 2008; Ayre *et al.* 2014). Carbopol solvent-gels caused the greatest weight gain (up to ca. 0.6 %) to aged PMMA and the most inconsistent behaviour of both weight gain and loss to new PMMA. These were attributed to the extensive gel residue deposited during cleaning.

**ANOVA weight change %**

ANOVA of the weight change % of treated PMMA samples indicated Condition as a significant factor. Tukey's HSD comparison test confirmed that new and aged samples were significantly different.



Graph 8.6. The surface condition of PMMA aged samples significantly impacted cleaning of PMMA. Application time was another significant factor in the cleaning process.

### ATR-FTIR

Treatments of 5 and 60 minutes caused similar changes to PMMA samples, indicating the insignificance of application time. Agar, Gellan, Pemulen (except for the hydrogel) and PVA (except for EtOH) solvent-gels left samples with no change: spectra were identical to the PMMA control sample. Most treatments caused comparable absorption regardless solvent, although treatments with EtOH were expected to show changes (see Chapter 7.1.2). Only spectra of gels with EtOH are graphically displayed here because they show similar, but distinct changes.

Carbopol solvent-gels, Pemulen hydrogel and PVA EtOH caused the following changes on new samples (see Fig.8.11): formation of a broad band peak at around  $3400\text{ cm}^{-1}$  and an increase in absorption at  $1565\text{ cm}^{-1}$ . These spectra were identical to the (dried) Carbopol/Ethomeen hydrogel (Fig.8.12). The peak at  $3400\text{ cm}^{-1}$  demonstrated the formation of oxidised structures, in particular hydroxyl groups ( $-\text{OH}$  bonds) – especially visible in the aged samples. The peak at  $1565\text{ cm}^{-1}$  was repeatedly found in spectra of PMMA treated with polyacrylics, Carbopol and Pemulen (see Chapter 7.1.1.1.), and less often with PVA and Agar. This band confirmed the successful acid-base neutralisation of Carbopol and Pemulen upon the addition of Ethomeen and TEA, respectively (Patel *et al.* 2003; Todica *et al.* 2015). The same band in Agar and PVA was observed mostly when gels were coupled with alcohols, EtOH and IPA. It was postulated that this vibrational band may be the result of solvent cleavage of some chemical fractions in Agar and PVA gels. So, treatments causing absorption at  $1560\text{ cm}^{-1}$  denoted surface gel residues.

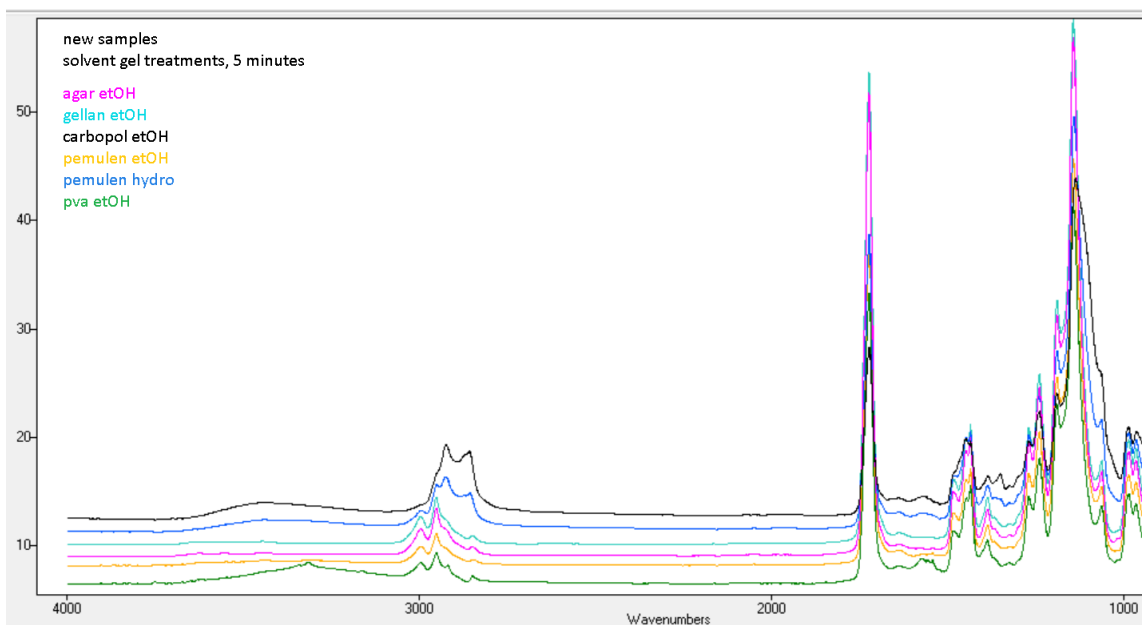


Figure 8.11. Spectra of new PMMA samples after gel treatments with EtOH (and Pemulen hydrogel). The spectra are averaged from 3 replicates for each treatment. Each replicate is averaged from 3 spot ATR analyses.

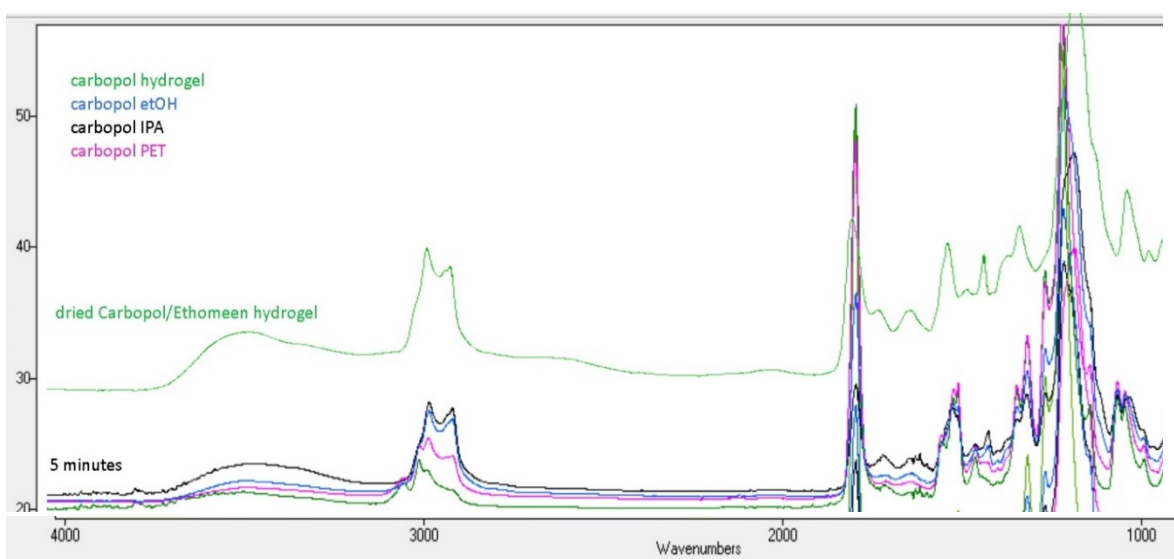


Figure 8.12. Spectra of aged PMMA samples after Carbopol gel treatments. Spectra are averaged from 3 replicates for each treatment. Each replicate is averaged from 3 spot ATR analyses. The spectrum of Carbopol hydrogel (analysed in dried state in ATR mode) is included for comparison. Carbopol left such extensive gel residue that FTIR analysis was unable to absorb PMMA peaks and detected only Carbopol peaks.

### **FTIR peak height ratio**

The peak height ratio was representative of the chemical changes taking place on the PMMA surface after treatment with solvent-gels and free solvents and cannot be taken as an absolute value. Their calculation offered a comparative/relative assessment of treatment-induced surface change. Height ratio absorption bands at  $1723\text{ cm}^{-1}$  and  $750\text{ cm}^{-1}$  were plotted and compared against the unaged and 32-day UV-aged controls as reference points for relative chemical changes (Graph 8.7). The progression of change was based on the decrease of  $1723$

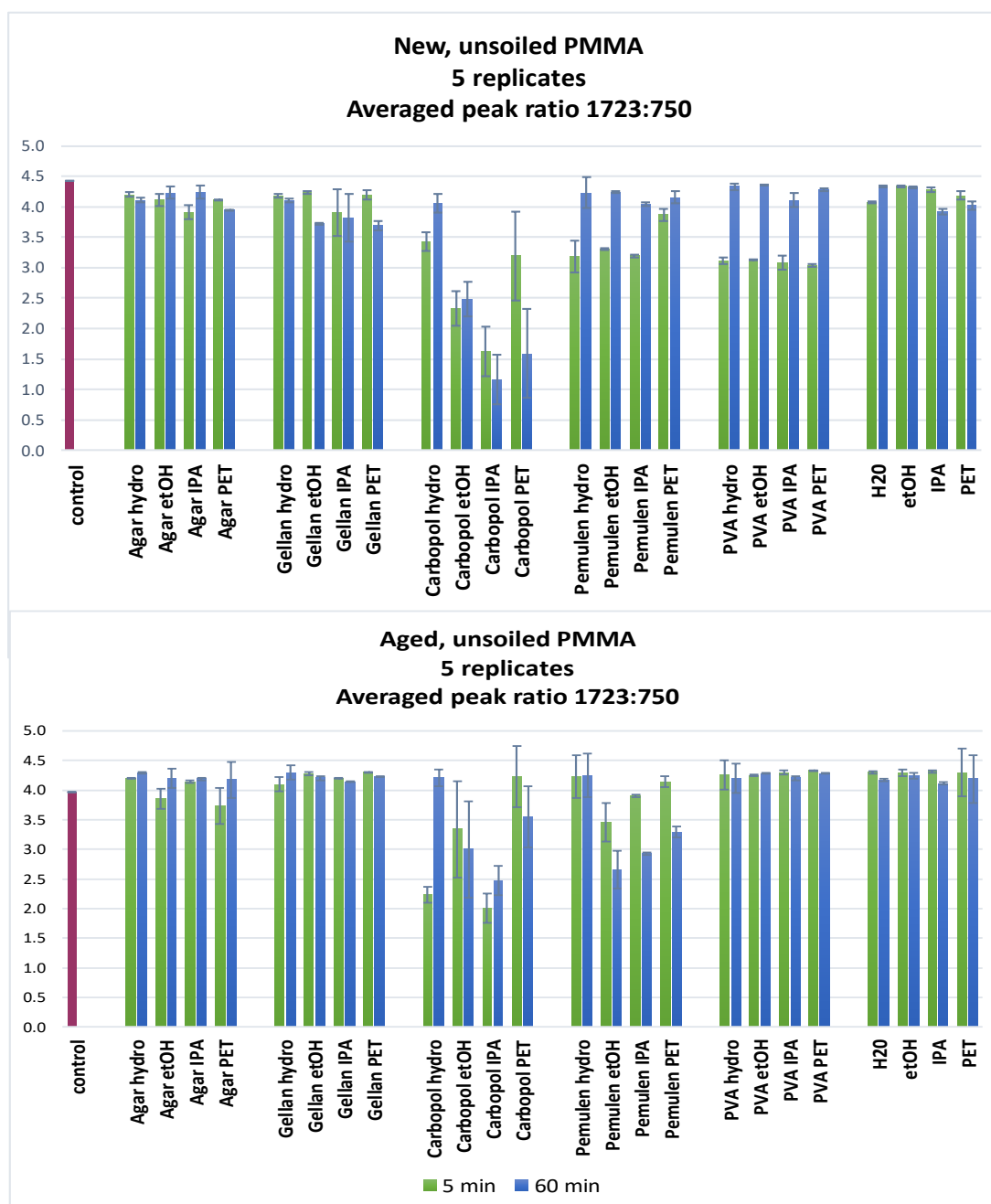
$\text{cm}^{-1}$  band, which would indicate loss of carbonyl ( $\text{C}=\text{O}$ ) and subsequently detachment/loss of the ester side group. This was compared with an internal standard, taken as the constant peak at  $750\text{ cm}^{-1}$ . The lower the ratio and the greatest difference from the control, the bigger the assumed chemical alteration on the sample surface; This is attributed to solvent-induced chain scission, thus PMMA destruction. Between the new and aged PMMA control samples, the latter indicated a larger chemical alteration. This was anticipated, as presented in Chapter 4.3, UV exposure proved to have caused ester side group elimination.

Agar and Gellan solvent-gels and free solvents caused negligible to no relative change (Graph 8.7). Pemulen and PVA solvent-gels caused comparable patterns of change to new surfaces. Spectra of samples after Pemulen indicated dissociation of the gel and residue deposition. Pemulen solvent-gels on aged surfaces behaved more like Carbopol solvent-gels (with the exception of hydrogel): They induced the largest chemical change. PVA solvent-gels caused no significant change to aged surfaces.

Carbopol solvent-gels displayed the smallest ratio and therefore greatest chemical change to all samples. However, visual observation of the samples showed that Carbopol treatments left extensive gel residue. This was vital for interpretation, as it indicated that the decrease in ratio may not be caused by chemical damage but gel residue hindering the analysis. As discussed earlier, ATR-FTIR is a surface technique and even thin layers/remains of other materials (i.e. other organic polymers) are capable of interfering with absorption and reducing contact with the PMMA substrate. This demonstrates how complicated interpretation of peak height ratios can become, when absorptions of more than one materials (here PMMA substrate and gel residues) overlap.

According to the peak height ratios new PMMA more frequently showed larger chemical changes after treatment (with Carbopol, Pemulen and PVA). This was attributed to the fact that young surfaces hadn't previously undergone processes, such as ageing under UV exposure in the weathering chamber, leading to photo-chemical alterations resulting in component extraction. The ageing of PMMA as seen in Chapter 4.3.3. may have favoured a simultaneous development of crosslinks (evidenced from an increase in tensile strength) and chain scissions (attributed to the overall weight loss of aged samples). On one hand crosslinking renders surfaces more compact, thus more durable to solvent penetration. On the other hand, chain scission and voids formed during UV ageing renders PMMA's upper micron layers more penetrable by solvents.





Graph 8.7. Ratios between the peak heights at  $1723\text{ cm}^{-1}$  and  $750\text{ cm}^{-1}$  of new and aged: untreated PMMA controls (in fuchsia) and treated PMMA samples for 5 (green) and 60 (blue) minutes. Ratios are based on the loss of carbonyl bands ( $\text{C}=\text{O}$ ) in relation to a constant peak ( $750\text{ cm}^{-1}$ ). The lower the ratio, the bigger the chemical change. Error bars show the standard deviation.

### ANOVA peak height ratio

ANOVA of the peak height ratios of treated PMMA samples indicated the Gels and Condition as significant factors. Tukey's HSD comparison test detected Carbopol as having a significantly different impact on the cleaning of PMMA. Examination of the peak height ratios showed that Carbopol gels induced the most extensive reduction, therefore negatively influencing the solvent-gel treatment of PMMA samples.

Grouping Information Using the Tukey Method and 95% Confidence			
gels	N	Mean	Grouping
no	48	4.1953	A
agar	48	4.0790	A
gellan	48	4.0593	A
pva	48	3.9253	A B
pem	48	3.6549	B
carb	48	2.848	C

*Means that do not share a letter are significantly different.*

### 8.2.3. Discussion of results

#### Experiment, design & methods

In these preliminary experiments, a number of variables and their interactions were examined. The replicates were increased to five and surface condition was introduced as an additional factor, to understand how aged surfaces behave compared to new. Factor effects were examined based on different analytical methods, enabling the next experiments to focus on the most significant factors.

#### Cleaning evaluation

Visual effect	Description/interpretation
Smudges	Imprint of gel spread across the surface during post-treatment rinsing with cotton swabs rolled over the surface.
Discolouration (as halo/stain)	Combination of two phenomena often accompanying gel residue and happening concurrently: loss of transparency and fine deposits.
Loss of transparency	Penetration and entrapment of solvent in upper micron layers. It renders the material hazy/cloudy.
Fine deposits	Evaporation of solvent droplets and deposition of gel solutes or non-volatile PMMA components carried along in the droplets. Known as 'coffee stain effect' or 'edge effect'.

*Table 8.3. Areas of interest identified under the stereomicroscope (visual effects) are understood and described under the SEM (description/interpretation).*

It was essential at this early stage of research to employ multiple methods of visual evaluation, to recognise what change was visibly detectable and to what degree. SEM imaging was guided by the stereomicroscopic observation to highlight areas of interest and when combined they enabled the description of types of damage, alteration and deposits after gel treatment. Given that all treatments used in the following experiments were evaluated with two microscopic methods in this chapter, it was anticipated that any damage possibly encountered on PMMA had already been documented and described (Table 8.3). Since these microscopic techniques offered

comparable data and SEM offered a large range of magnifications, including those achievable by stereomicroscopy, SEM was favoured for the documentation of visual changes from this point onward.

#### Weight changes

Cleaning caused the majority of new samples to lose negligible weight (ca. 0.03 %), whereas aged samples to gain the equivalent weight (ca. 0.3 %).

#### FTIR peak height ratio

This method was only used during these cleaning experiments due to the lack of surface dirt on PMMA samples enabling the interpretation of cleaning results. The method was discontinued in subsequent experiments owing to the increase in complexity with added variables co-existing on the same sample surface. Peak height ratios of treated PMMA with remains of: (i) surface dirt, particularly an PSA of acrylic nature similar to the PMMA itself, and (ii) residue of a variety of polymer gels, would prove challenging to interpret.

#### Discarded factors

Treatment with Carbopol solvent-gels consistently offered the worst cleaning results to PMMA. Macroscopically, Carbopol resulted in the poorest visual condition according to naked eye as evident by the lowest CARS scores, and it caused the highest loss of surface gloss. Statistical analysis of the gloss values indicated that Carbopol treatments had a negative effect on the cleaning of PMMA. Microscopic observation showed that samples were left with extensive gel residue, smudges of gel with entrapped cotton threads, and even abrasions, absent from all other treatments. Samples displayed the most erratic behaviour with both inconsistent gain and loss of the material. In cases of gain, this was the largest documented among all treated samples. Peak height ratio data suggested that Carbopol caused the largest chemical damage, attributed to the extensive residue deposition, also confirmed by SEM. Statistical analysis of the ratios confirmed Carbopol's negative influence. The effect of Carbopol repeatedly had a negative impact on the treatments, thus it was removed from following experiments.

The present experiment showed that in most cases, Agar and Gellan gel treatments offered similar cleaning results. Starting with the statistical analysis of CARS scores, Tukey's HSD paired Agar and Gellan solvent-gels as significantly similar (highlighted in red below). This meant that these two treatments offered similar visual results. This was in agreement with Tukey's HSD comparison test of gloss measurements, indicating that these gels offered the same surface gloss. Microscopic observation showed that, although Agar and Gellan gels left the majority of surfaces in a comparable, satisfactory visual condition, Gellan occasionally left

PMMA in an inferior condition. Examination of peak height ratios showed that, although some Gellan solvent-gels induced no chemical change, when coupled with IPA and PET a ratio decrease was observed. This was not the case with samples after Agar treatment, showing no relative change. Regarding weight changes, samples displayed similar values and followed an identical pattern of fluctuation.

### Grouping Information Using the Tukey Method and 95% Confidence

gels	N	Mean	Grouping
agar	80	19.188	A
gellan	80	19.038	A
no	80	15.938	B
pva	80	15.038	C
pem	80	10.975	D
carb	80	10.725	D

*Means that do not share a letter are significantly different.*

Agar and Gellan solvent-gels share similarities. They belong to the same category of gelling marine and plant polysaccharides and share a range of properties, such as being water-soluble in boiling temperatures and thermoreversible. A microbiological study (Shungu *et al.* 1983) that evaluated the suitability of Gellan as an Agar substitute, showed their biochemical differences to be insignificant. Bearing in mind that the aim of identifying and assessing factors with significant effect in the cleaning process, was to narrow down the variables for optimisation of the next experimental design, and given that Agar and Gellan behaved similarly, it was decided that one of the two gels could be removed. With Agar gels performing somewhat more favourably, Gellan gels were discarded.

It was established from the results of this experiment on new and aged PMMA that Application time did not influence the treatments, neither in a consistent nor a statistically significant manner. Treatments lasting 5 and 60 minutes had no statistically significant effect to the naked eye observation (CARS scores). This was confirmed by microscopic observation, where samples displayed similar types of damage to a comparable degree. Additionally, all treated samples showed similar surface gloss and comparable fluctuation patterns. Statistical analysis of gloss values, weight changes and peak height ratios confirmed that application time of treatments had no significance to the cleaning outcome. Prior to discarding application time as a factor, additional tests were undertaken in the following section on soiled surfaces.

### 8.3. APPLICATION TIME: 5 MINUTES VERSUS 60 MINUTES

Before eliminating Application time from the experimental design, additional preliminary studies were carried out. The aim was to test the impact of time on the cleaning outcome when surface dirt was present.

### 8.3.1. Experimental design

**Preliminary experiment on Application time: 5 versus 60 minutes**

Experimental Variables			
Factor	A. Gels	B. Solvents	C. Application time
<b>Levels</b>	1. no gel	1. H <sub>2</sub> O	1. 5 min
	2. Agar	2. EtOH	2. 60 min
	2. Gellan	3. IPA	
	3. Carbopol	4. PET	
	4. Pemulen		
	5. PVA		

*Table 8.4. Experimental variables in the multilevel full-factorial design used for the preliminary cleaning experiment on new PMMA with synthetic soil.*

To make an informed decision regarding application time, all gel treatments discussed in the previous experiment were carried out on new samples with synthetic soil for 5 and 60 minutes to test their efficiency. Treatments were followed by a clearance step of three separate cotton swabs moistened with H<sub>2</sub>O. Synthetic soil/carbon black was applied by means of airbrush spraying (described in Chapter 5.2). The experiment was designed without replication on 20 samples cleaned for 5 minutes and 20 samples for 60 minutes (n=40 samples).

### 8.3.2. Results & discussion

Macroscopic examination (see Appendix N) revealed no visual difference between samples treated for 5 and 60 minutes. Surfaces did not display any characteristic patterns and visually appeared to perform similarly. In some cases, gels after 60 minutes (i.e. Carbopol and Pemulen) were less effective at removing synthetic soil. This assessment was enabled by black residues of carbon-oil visible on the (often colourless and transparent) gels removed after cleaning. This supplementary test confirmed the insignificance of application time, allowing it to be discarded from future experiments. Given that 60 minute-treatments were longer, and occasionally, macroscopically appeared to leave surfaces in worst condition (i.e. removed less synthetic soil) than samples after 5 minutes, all following treatments were performed for 5 minutes.

### 8.4. 5 MINUTES: REPEATED APPLICATIONS

Upon confirmation of the statistically insignificant influence of Application time in the gel cleaning process of PMMA and its elimination from the experimental design, additional

preliminary tests were carried out with Carbopol and Agar hydrogels and solvent-gels to test the efficiency of repeated gel applications of 5 minutes.

**8.4.1. Experimental design**

Samples were treated with up to three repeated applications of 5 minutes each, in order to test if an increase in gel applications was more efficient at removing synthetic soil. The experiment was designed without replication on new samples with synthetic sebum oil/carbon black: 8 runs x 1 application, 8 runs x 2 applications and 8 runs x 3 applications all tested for 5 minutes, for a total of 24 samples. Treatments were followed by a clearance step of three separate cotton swabs moistened with H<sub>2</sub>O.

**Preliminary experiment on 5 Minutes: repeated applications**

Experimental Variables			
Factor	A. Gels	B. Solvents	C. No. of Applications
<b>Levels</b>	1. Agar	1. H <sub>2</sub> O	1. 1 application
	2. Carbopol	2. EtOH	2. 2 applications
		3. IPA	3. 3 applications
		4. PET	

*Table 8.5. Experimental variables in the multilevel full-factorial design used for the preliminary cleaning experiment on new PMMA with synthetic soil.*

**8.4.2. Results & discussion**

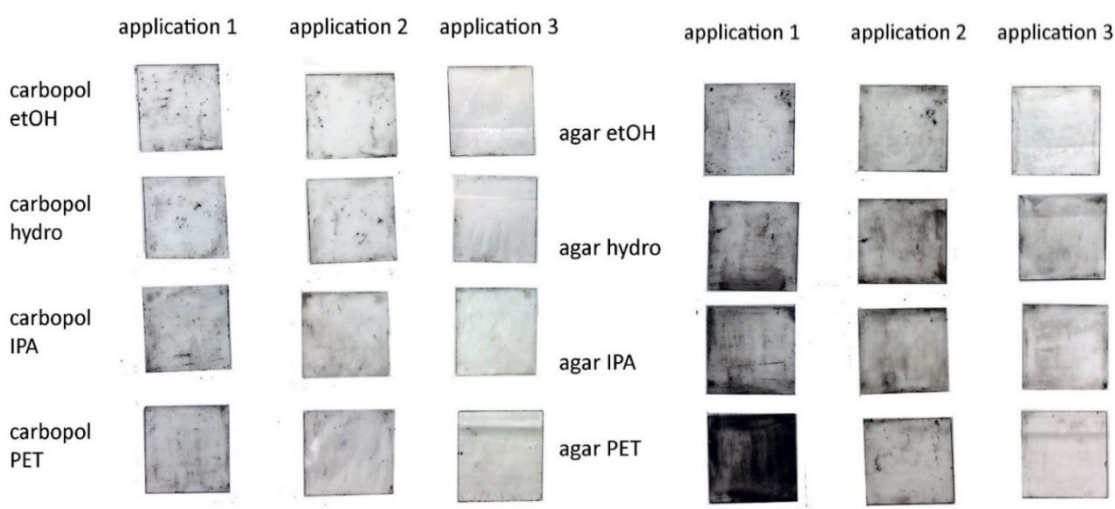


*Figure 8.13. New PMMA samples with synthetic soil treated with Agar and Carbopol solvent-gels (12 samples per gel type). Sets of 4 samples are treated with one, two and three repetitions of 5-minute applications. Three applications left samples cleaner.*

Macroscopic examination (Fig.8.13) revealed that repeated gel applications did affect the efficiency of the cleaning treatments in removing synthetic soil. Samples after two applications visually appeared cleaner than samples treated only once, and samples after three applications appeared cleaner than the ones treated once or twice.

### 8.5. PRELIMINARY SOLVENT TESTING

It was essential to confirm that the remaining solvents were truly effective at removing unaged synthetic dirt and safe for use on PMMA. To test that, further trials were performed on new, PMMA samples bearing either synthetic soil or PSA, to simulate the main experimental cleaning conditions and assess the free solvents' effectiveness at removing the two types of unaged 'dirt'. None of the solvents (H<sub>2</sub>O, EtOH, IPA and PET) had been discarded up to this point, so they were applied both with cotton swabs and thickened in the remaining gels (Agar, Pemulen and PVA). Results showed that with the exception of H<sub>2</sub>O, all solvents were effective at removing synthetic soil and PSA. H<sub>2</sub>O was removed from the main experimental design.

This study adopted a sequential approach to experimental investigation by carrying out experimental runs in successive groups, allowing to narrow down variables, keep the truly significant and proceed to their comprehensive study. Current preliminary testing was a necessary step that enabled identification of variables with no effect on the cleaning process of PMMA surfaces and their elimination, prior to moving to the more complex main experimental work. Cleaning trials on (unsoiled) new and aged PMMA surfaces examined the effect, safety and time-dependent action of solvents, hydrogels and solvent-gels. Based on the evaluation of the results Gellan, Carbopol, 60-minute application time and H<sub>2</sub>O were excluded from the forthcoming experiments either because they were shown to be insignificant to the cleaning process, unable to remove synthetic soil or PSA, or unfit for safe use on PMMA. Information gained from this preliminary stage indicated the gels and solvents to be examined in the following main experiments:

Factor	Gels	Solvents
Levels	1. Agar	1. EtOH
	2. Pemulen/TEA	2. IPA
	3. PVA/Borax	3. PET

## CHAPTER 9. MAIN EXPERIMENTS: UNAGED & AGED DIRT

This chapter presents the main cleaning experiments on new and aged PMMA samples with surface dirt. These are designed with the truly significant variables and materials safe for direct use on PMMA as narrowed down in the preliminary experiments. Application of surface 'dirt' is the newly added factor to this experiment; samples were sprayed with synthetic soil/carbon black or acrylic PSA as described in Chapter 5.2. The first part of this chapter aims to identify gel treatments able to remove unaged synthetic soil and PSA. Once assessed, in the second part of this chapter, the successful treatments are tested on aged dirt (exposed to UV radiation for 32 days). These experiments aim to assess the ability of treatments, earlier assessed as successful, at removing aged synthetic soil and PSA. All experiments are carried out on transparent coupons (25 x 25 x 1.0 mm) of two surface conditions, new and 32 days UV-aged. Due to removal of Application time from the list of factors in the previous chapter, treatments are performed for 5 minutes from this point onward.

### 9.1. POLY (METHYL METHACRYLATE) WITH UNAGED DIRT

#### 9.1.1. Experimental design

A multilevel full-factorial experimental design was adopted to simultaneously examine the effects of Gels, Solvents, Dirt and Surface condition in isolation, and combined. The experiment was designed in quintuple with 90 new and 90 aged soiled samples (n= 180 samples). Half the batch (45 samples) of each condition (new/aged) was sprayed with synthetic soil and the other half with PSA.

**Main experiment on new and aged PMMA with dirt: 5 replicates**

Experimental Variables				
Factor	A. Gels	B. Solvents	C. Dirt	D. Surface condition
Levels	1. Agar	1. EtOH	1. synthetic soil	1. new
	2. Pemulen/TEA	2. IPA	2. adhesive	2. aged
	3. PVA/Borax	3. PET		

*Table 9.1. Experimental variables in the multilevel full-factorial design used for the main cleaning experiment on new and aged PMMA with synthetic soil or PSA and 5 replicates. Number of levels: 3, 3, 2, 2.*

#### Multilevel Factorial Design

Factors: 4      Replicates: 5  
Base runs: 36      Total runs: 180



### 9.1.2. Results & interpretation

#### 9.1.2.a. Synthetic soil

#### VISUAL OBSERVATIONS

##### Macroscopic evaluation

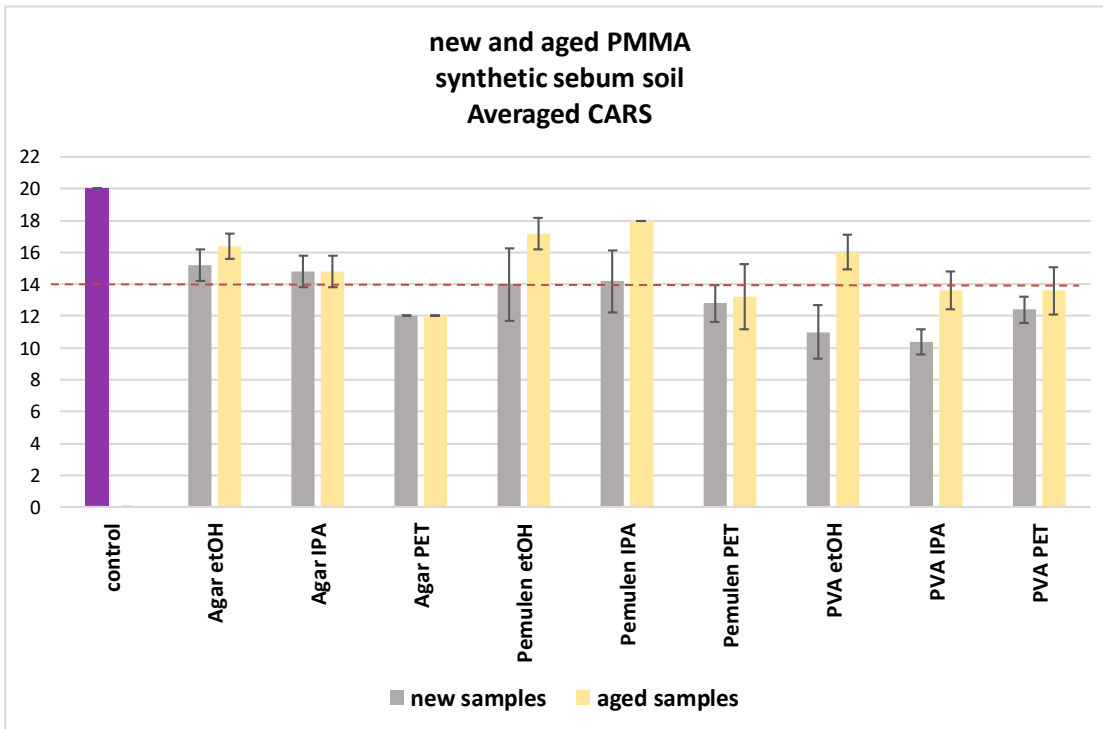
Agar and Pemulen PET failed to remove synthetic soil. Agar IPA, PVA IPA and PVA PET showed limited to no removal at all. Agar, Pemulen and PVA with EtOH and Pemulen IPA were the most successful at removing synthetic soil. Results suggest that it was easier to clean aged than new PMMA from synthetic soil.

samples with synthetic soil		
	new PMMA	aged PMMA
Agar etOH	partly cleaned/cleaned	cleaned
Agar IPA	partly cleaned/not cleaned	partly cleaned
Agar PET	not cleaned	not cleaned
Pemulen etOH	partly cleaned	cleaned
Pemulen IPA	partly cleaned	cleaned
Pemulen PET	not cleaned	not cleaned
PVA etOH	partly cleaned/cleaned	cleaned
PVA IPA	partly cleaned/not cleaned	not cleaned
PVA PET	partly cleaned/not cleaned	partly cleaned/not cleaned

*Table 9.2. Macroscopic observation of the overall impression of unaged synthetic soil removal from new and aged PMMA after treatment.*

##### CARS scores

Treatments performed better on aged surfaces than new, in agreement with Table 9.2. Agar and Pemulen with alcohols removed the most synthetic soil. Agar with alcohols left new surfaces the cleanest, while Pemulen with alcohols left aged surfaces the cleanest, according to human perception (Graph 9.1). Treatments with PET performed poorly on all surfaces. In fact, Agar PET left aged PMMA in the worst condition (scored lowest CARS) (Graph 9.1). PVA with alcohols left new PMMA with the lowest CARS. PVA with IPA performed equally poorly on aged PMMA, but with EtOH it was among treatments removing the most synthetic soil. Combination of CARS scores with Table 9.2 suggested that treatments scoring below 14 (see line in Graph 9.1) failed to remove soil.



Graph 9.1. CARS scores of treated new and aged PMMA samples with unaged synthetic soil. Scores are based on a five-point progressive ranking from 0 (worst) to 4 (best). Scores, expressed as a bar chart, are averaged from 5 replicates for each treatment. Untreated new and aged PMMA controls scored the highest possible CARS 20 in categories 'Dirt residue', 'Abrasion' and 'Gel residue'. Red line shows below which point treatments failed to remove synthetic soil. Error bars show the standard deviation.

### **ANOVA CARS**

ANOVA of CARS showed that Gels, Solvents and Condition had a statistically significant impact on the effectiveness of cleaning PMMA with synthetic soil. It also showed that the interaction effects of gels with solvents and condition were statistically significant. This means that the impact of one factor depended on the level of the other. The interaction plot (Graph 9.2) indicates that when Pemulen was coupled with IPA and Agar with EtOH they offered the highest CARS. Agar with PET and PVA with IPA offered the worst gloss. The interaction plot (Graph 9.3) indicates that Agar and PVA offered the lowest CARS on aged surfaces.

Tukey's HSD compared variables to determine the significantly different by allocating them a unique letter. Pemulen, PVA and PET were allocated unique letters indicating that they significantly affected the visual condition of samples. According to the main effects plot (Graph 9.4) Pemulen scored the highest CARS positively impacting the cleaning outcome. PVA and PET scored below the means CARS value having a negative impact on PMMA. Aged surfaces scored significantly higher than new surfaces indicating that treatments performed better on aged PMMA.

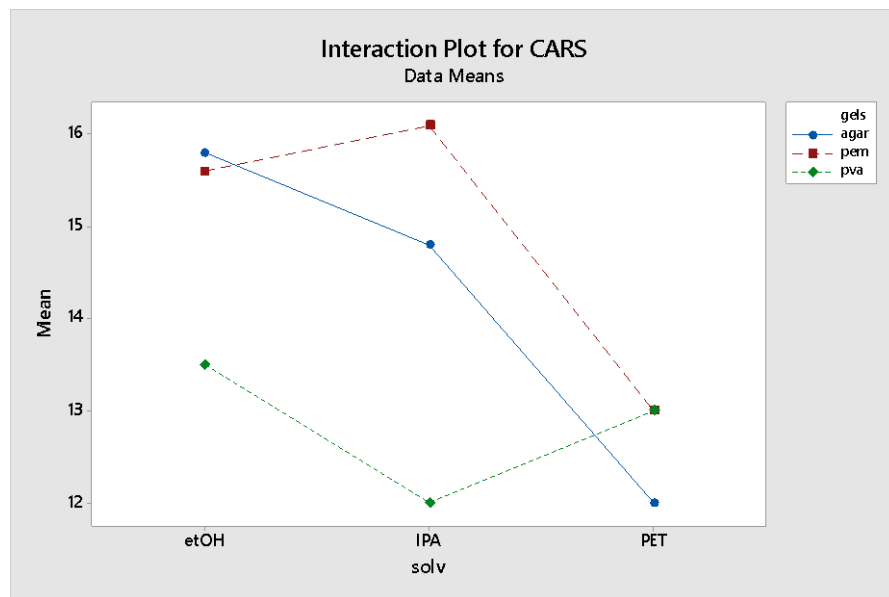
## Grouping Information Using the Tukey Method and 95% Confidence

<u>gels</u>	<u>N</u>	<u>Mean</u>	<u>Grouping</u>
pem	30	14.900	A
agar	30	14.200	A B
pva	30	12.833	B

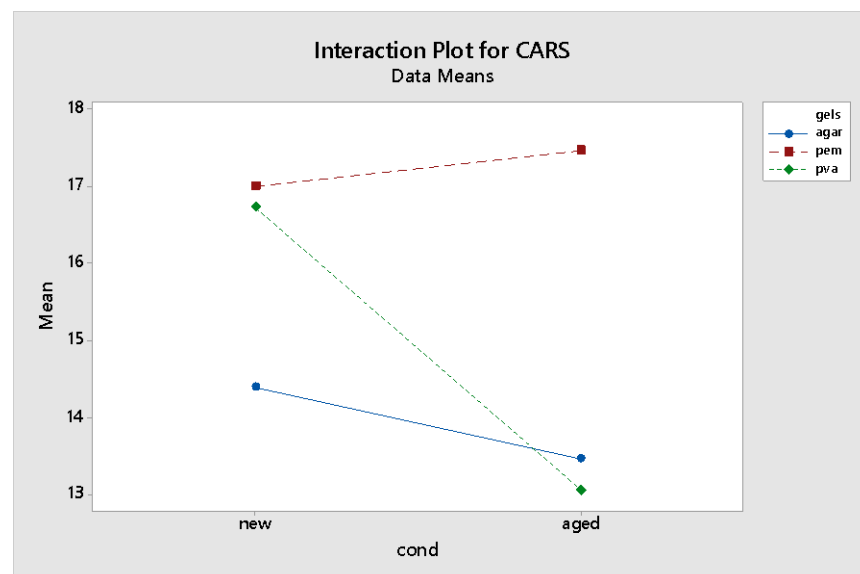
  

<u>solv</u>	<u>N</u>	<u>Mean</u>	<u>Grouping</u>
etOH	30	14.967	A
IPA	30	14.300	A
PET	30	12.667	B

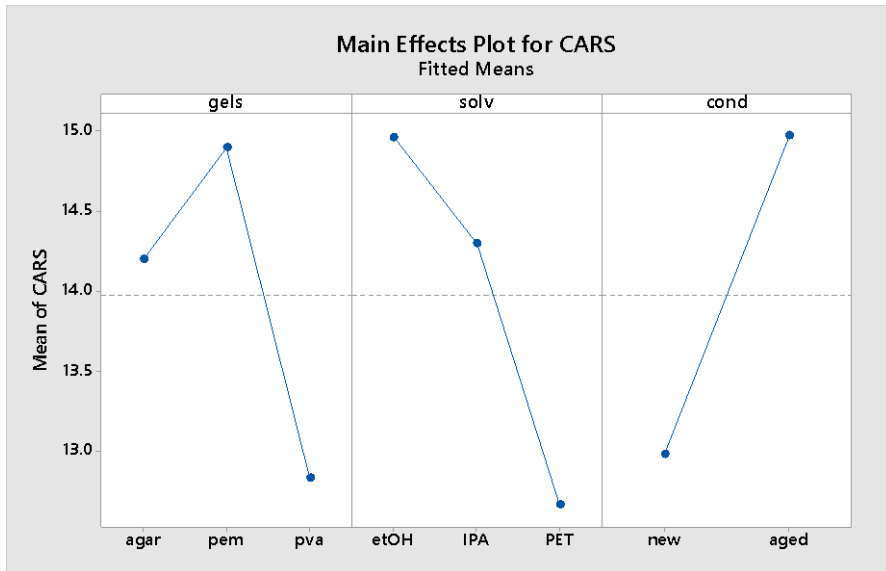
Means that do not share a letter are significantly different.



Graph 9.2. Interaction plot showing the significant interactions between gels and solvents on PMMA CARS.



Graph 9.3. Interaction plot showing the significant interactions between gels and condition on PMMA CARS.



Graph 9.4. The mean CARS scores of Pemulen are the highest, while that of PVA the lowest, indicating they affected cleaning of PMMA with PSA in a positive and a negative manner, respectively. PET scored below the means CARS value having a negative impact on PMMA.

**SEM imaging**

Under high magnification, unaged and aged PMMA controls with synthetic soil appeared indistinguishable (Fig. 9.1), regardless of surface condition. Both controls were covered with a dense and uniform soil layer with some air bubbles. These were the result of stirring the sebum oil-carbon black mixture.

**Control PMMA with synthetic soil**

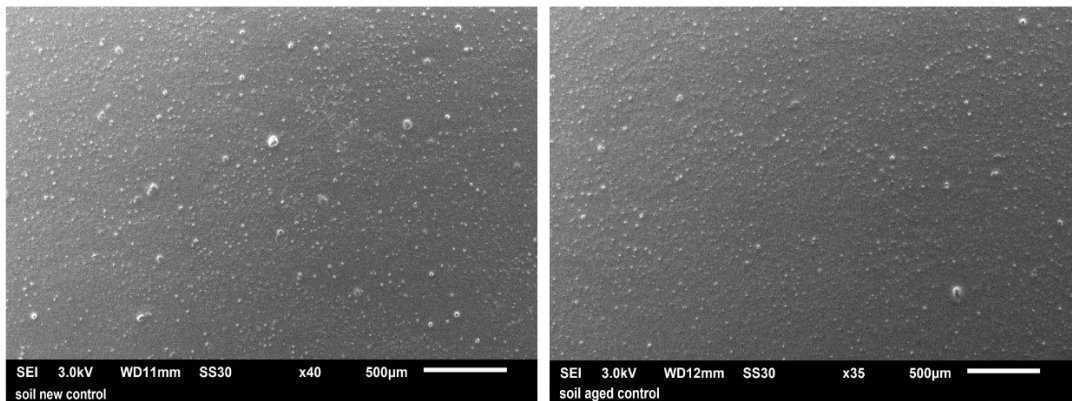


Figure 9.1. SEM micrographs: Unaged PMMA control with synthetic soil under magnification x40 (left) and aged PMMA control under magnification x35 (right).

**New PMMA samples with synthetic soil:**

<b>New PMMA samples after treatment</b>				
Treatment	Synthetic soil	Gel residue	Comments	Figure no.
<b>Agar EtOH</b>	cleaned	limited	good surface condition	9.2 A, B
<b>Agar IPA</b>	not cleaned	limited	soil smeared across, residual cotton swab threads	9.2 E, F
<b>Agar PET</b>	partly cleaned	limited		9.3 A, B
<b>Pemulen EtOH</b>		extensive*		9.3 D
<b>Pemulen IPA</b>	not cleaned	extensive		9.3 F, G
<b>Pemulen PET</b>	not cleaned	extensive		9.4 B
<b>PVA EtOH</b>	not cleaned	limited		9.4 E
<b>PVA IPA</b>	not cleaned	limited		9.4 G
<b>PVA PET</b>	not cleaned	limited		9.4 I

*Table 9.3. Evaluation based on SEM imaging of treated new PMMA samples with synthetic soil.*

\* Pemulen EtOH left new surfaces with extensive gel residue. This interpretation was based on the haziness of the images, which was attributed to real time evaporation of liquid content (mostly H<sub>2</sub>O) in the gel remains probably instigated by the SEM beam heating up the sample. By rendering the images blurry, it hindered the observation of the PMMA surfaces.

**Aged PMMA samples with synthetic soil:**

<b>Aged PMMA samples after treatment</b>				
Treatment	Synthetic soil	Gel residue	Comments	Figure no.
<b>Agar EtOH</b>	cleaned	limited	Similar impact on new PMMA	9.2 C, D
<b>Agar IPA</b>	not cleaned	limited	Similar impact on new PMMA	9.2 G, H
<b>Agar PET</b>	not cleaned	no		9.3 C
<b>Pemulen EtOH</b>	cleaned	limited	Discolouration to the naked eye	9.3 E
<b>Pemulen IPA</b>	cleaned	limited	Discolouration to the naked eye**	9.3 H, 9.4 A
<b>Pemulen PET</b>	partly cleaned	extensive		9.4 C, D
<b>PVA EtOH</b>	cleaned	limited	good surface condition	9.4 F
<b>PVA IPA</b>	not cleaned	extensive		9.4 H
<b>PVA PET</b>	not cleaned	extensive		9.4 V

*Table 9.4. Evaluation based on SEM imaging of treated aged PMMA samples with synthetic soil.*

\*\* In accordance with SEM, Pemulen IPA left aged PMMA in the best surface condition; samples scored the highest CARS and showed the least gloss change.

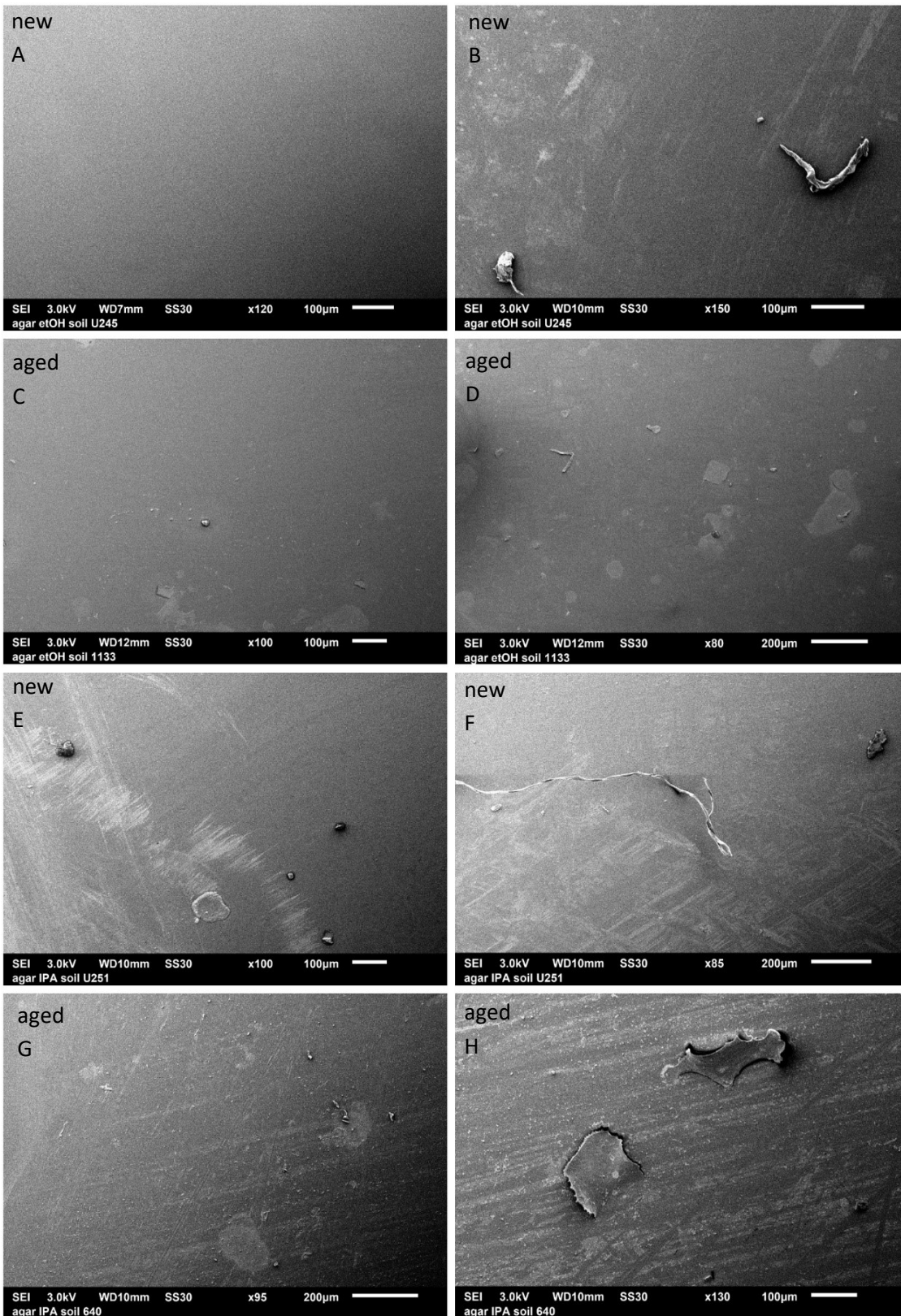


Figure 9.2. SEM micrographs: A-D: Agar EtOH left all PMMA clean with limited gel residue. E-H: Agar IPA failed to remove synthetic soil from PMMA and deposited cotton threads and gel residue.

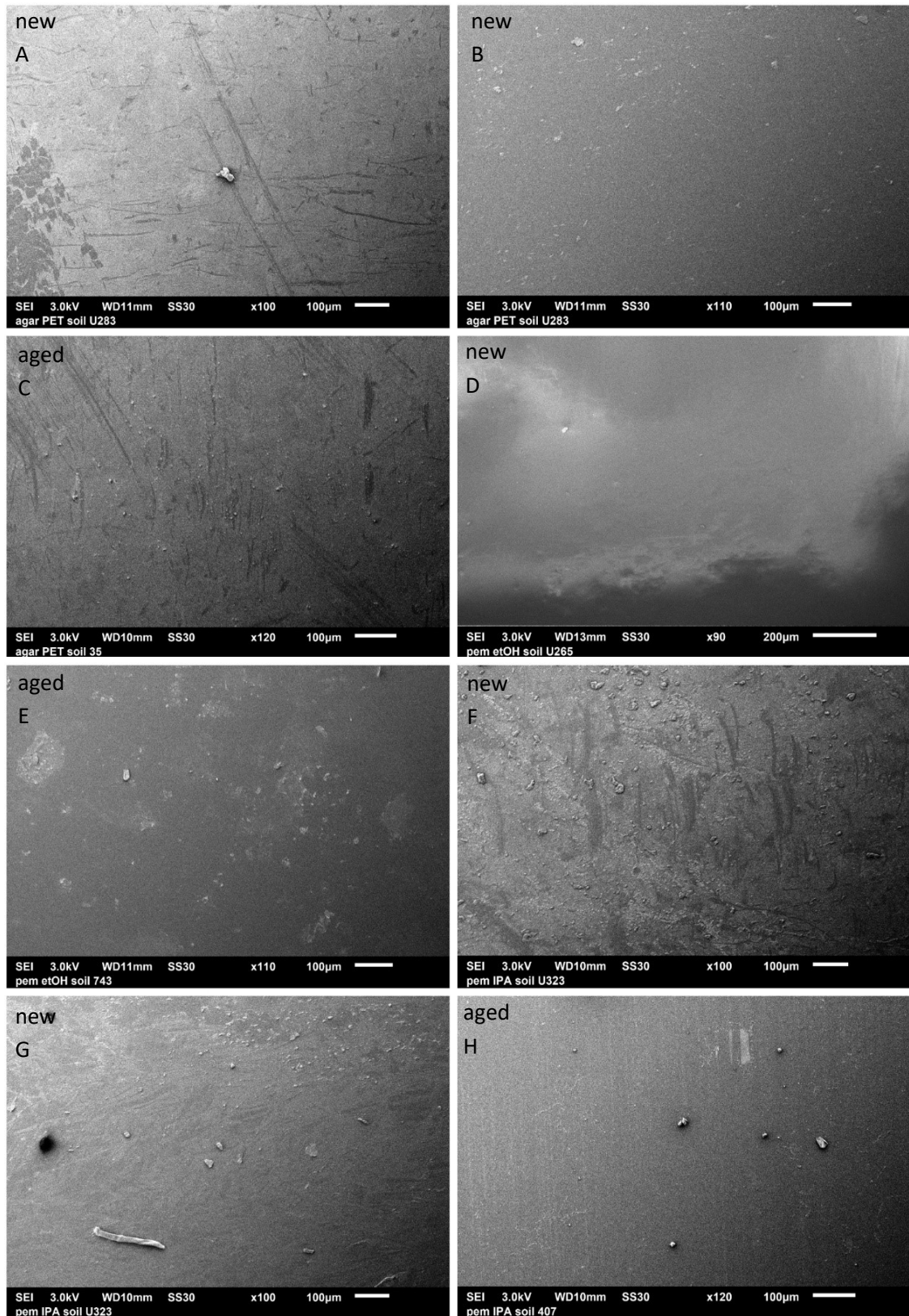
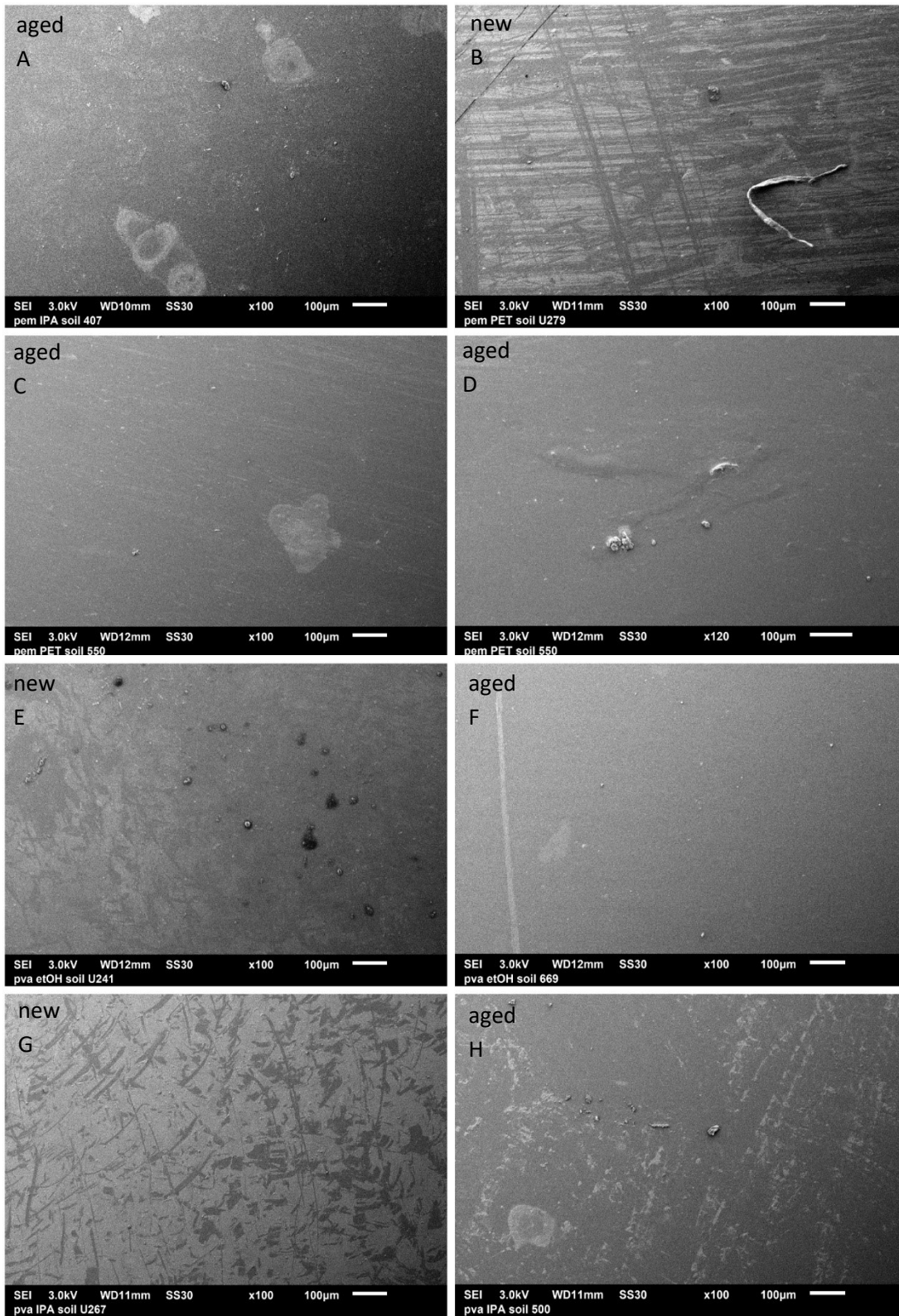


Figure 9.3. SEM micrographs: A-B: Agar PET failed to clean synthetic soil from new PMMA and deposited tiny gel residue. C: Agar PET cleaned aged PMMA depositing minute gel residue. D: Pemulen EtOH deposited extensive residue leaving new surfaces hazy. E: Pemulen EtOH cleaned aged PMMA depositing limited gel residue. F, G: Pemulen IPA failed to clean new PMMA and deposited extensive gel residue. H: Pemulen IPA cleaned aged PMMA with limited gel residue.





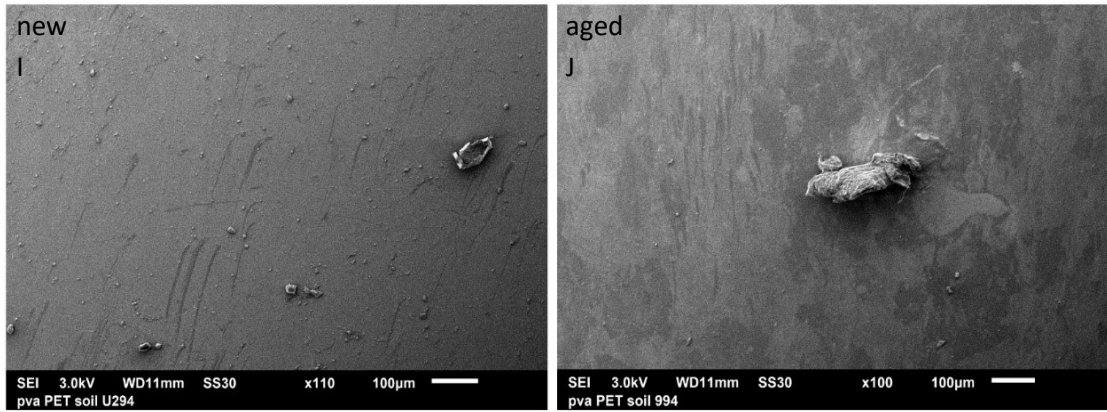
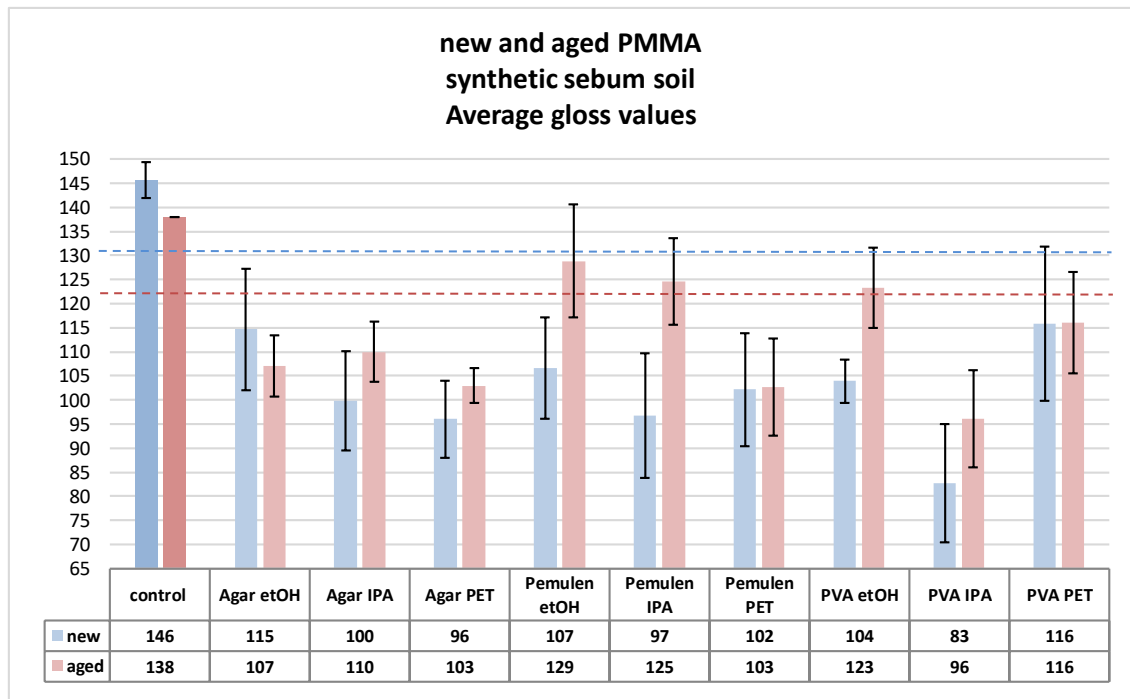


Figure 9.4. SEM micrographs: A: Minute Pemulen IPA gel residue macroscopically seen as discolouration. B: Pemulen PET failed to clean new PMMA and deposited gel residue. C: Pemulen PET cleaned aged PMMA. D: Pemulen PET gel residue on aged PMMA. E, G, I: PVA with EtOH, IPA and PET all failed to remove synthetic soil from new PMMA. F: PVA EtOH cleaned aged PMMA. H, J: PVA with IPA and PET failed to clean aged PMMA and deposited extensive gel residue.

**GLOSS**

**Gloss measurements**



Graph 9.5. Gloss measurements of new and aged PMMA with synthetic soil after treatment, plotted as bar charts. Gloss units (GU) are averaged from 3 repetitions of 3 spot measurements on 5 replicates. Differences < 15 GU are non-detectable by the human eye. The PMMA controls are highly glossy with a value of 146 GU for the unaged and 138 GU for the aged. Red line shows below which point change is visible for aged PMMA and blue line does the same for new PMMA. Error bars show the standard deviation.

All treatments visibly altered the surface gloss of new and aged samples with an average gloss difference of 38 GU, indicating their inability to remove soil. Aged samples exhibited higher gloss than new, in agreement with visual observation. None of the treatments left new PMMA in a good visual condition. Pemulen EtOH left aged surfaces with the highest gloss, with a difference of 17 GU from the control - close enough to the cut-off threshold above which surfaces macroscopically appear equally glossy. PVA IPA and Agar PET caused the biggest drop in gloss. Pemulen PET also left aged PMMA in the worst visual condition.

### **ANOVA gloss**

ANOVA of gloss measurements showed that Solvents and Condition had a statistically significant impact on the treated samples with synthetic soil. It also showed that the interaction effects of gels and solvents were statistically significant. The interaction plot (Graph 9.6) indicates that when Pemulen and Agar were coupled with EtOH, and PVA with PET they offered the highest gloss. PVA IPA and Pemulen and Agar with PET offered the worst gloss.

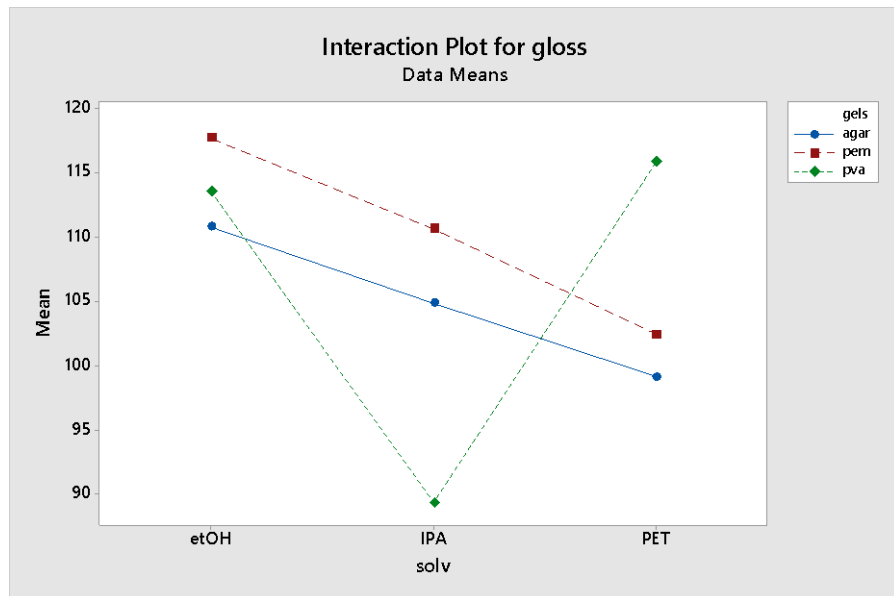
Tukey's HSD allocated unique letters to EtOH and IPA indicating that they significantly affected the gloss. In the main effects plot (Graph 9.7) EtOH induced the highest gloss and IPA the lowest. However, the difference in mean GU between samples treated with EtOH (114 GU) and IPA (101 GU) was within 15 GU, thus not visually detectable. Treatments positively impacted cleaning of aged surfaces, inducing higher gloss than on new samples.

#### **Grouping Information Using the Tukey Method and 95% Confidence**

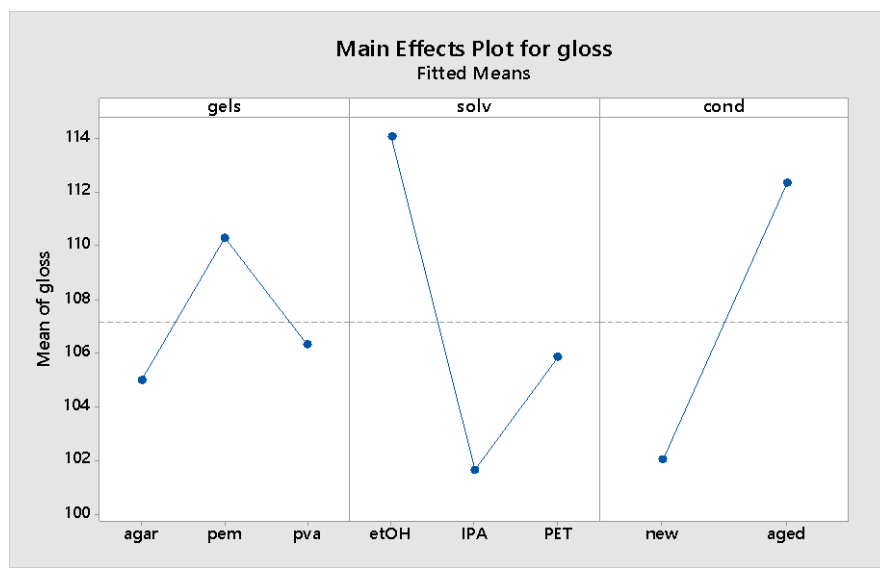
<u>solv</u>	<u>N</u>	<u>Mean</u>	<u>Grouping</u>
etOH	30	114.06	A
PET	30	105.84	A B
IPA	30	101.64	B

<u>cond</u>	<u>N</u>	<u>Mean</u>	<u>Grouping</u>
aged	45	112.34	A
new	45	102.02	B

*Means that do not share a letter are significantly different.*



Graph 9.6. Interaction plot showing the significant interactions between gels and solvents on PMMA gloss.



Graph 9.7. The mean gloss scores of EtOH are the highest, while that of IPA the lowest, indicating they affected cleaning of PMMA with PSA in a positive and a negative manner, respectively.

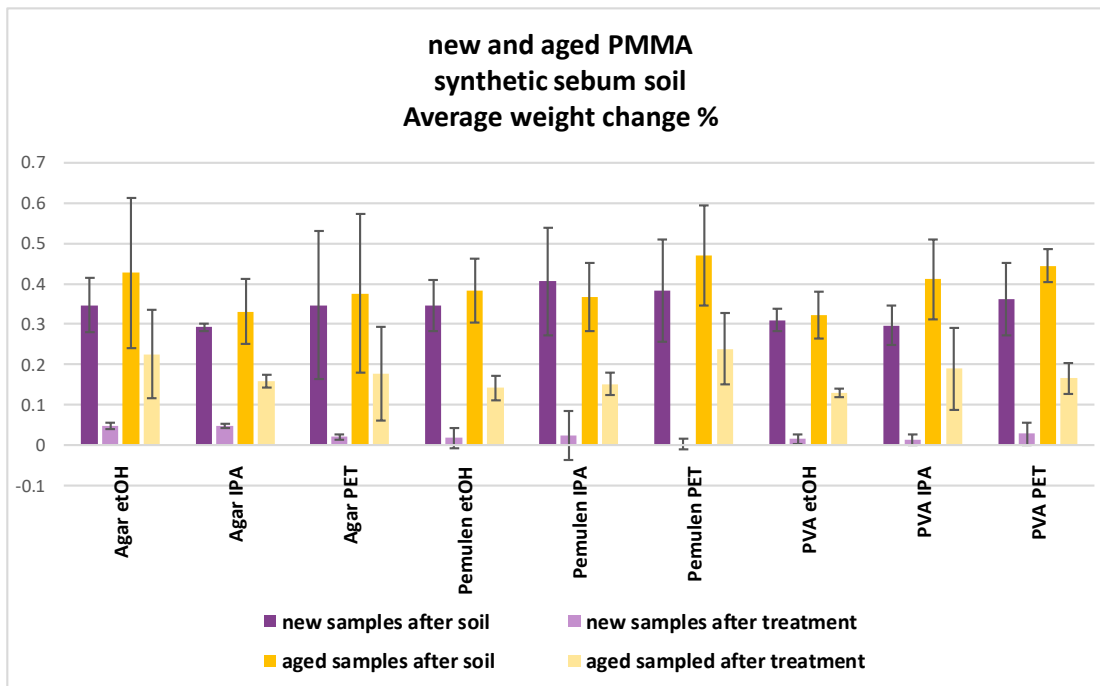
## WEIGHT MEASUREMENTS

### Weight changes %

After synthetic soil application, all samples gained weight in a very similar fashion, roughly between 0.3-0.4 % (relative to the initial weight set at zero) (Graph 9.8). The small level of fluctuation is attributed to the human factor (manual application of synthetic soil). Visual evaluation indicated that only Agar EtOH removed synthetic soil leaving new surfaces in a satisfactory condition, also reflected in the weight lost. Agar IPA, all three Pemulen treatments

and PVA EtOH failed to remove soil. Pemulen deposited extensive gel residue detected under the SEM. As previously described, H<sub>2</sub>O/alcohol mixtures in contact with new PMMA are likely to penetrate the upper micron layers and cause dissolution and evaporation of components (i.e. residual unreacted polymer). This scenario was possible in the 24 h that samples were left to stand prior to weighing. The immersion study (7.1.2) indicated PMMA dissolution in EtOH- and IPA-H<sub>2</sub>O mixtures. Here, the presence of extensive Pemulen gel residue on new PMMA delayed even further evaporation of solvent mixtures.

Visual evaluation of aged samples indicated that they were more successfully cleaned than new and most treatments completely removed synthetic soil. Interestingly, new samples lost most of the weight gained from synthetic soil application, while aged samples lost roughly half. In this case, weight change is indicative of other chemical phenomena simultaneously occurring in the aged samples. As previously described, voids formed in PMMA during UV ageing allow liquid penetration that causes weight gain. Further evaluation with ATR-FTIR will be carried out to understand what chemical reactions occur on aged surfaces in relation to new.



*Graph 9.8. Average weight change % of new and aged PMMA - averaged from five replicates - after application of synthetic soil and after cleaning (purple tones: new - yellow tones: aged samples). Changes % are normalised to the starting/initial weight. Error bars show the standard deviation.*

### **ANOVA weight change %**

ANOVA of weight change % showed that none of the treatments influenced the weight fluctuation of samples in a statistically significant manner. Comparing this to the analysis of visual evaluation suggests that data from bulk gravimetric analysis are not significant to the

assessment of treatments at this point. Condition on the other hand resulted as a statistically significant factor in weight change %, as well as in the analysis of visual evaluation.

### ATR-FTIR

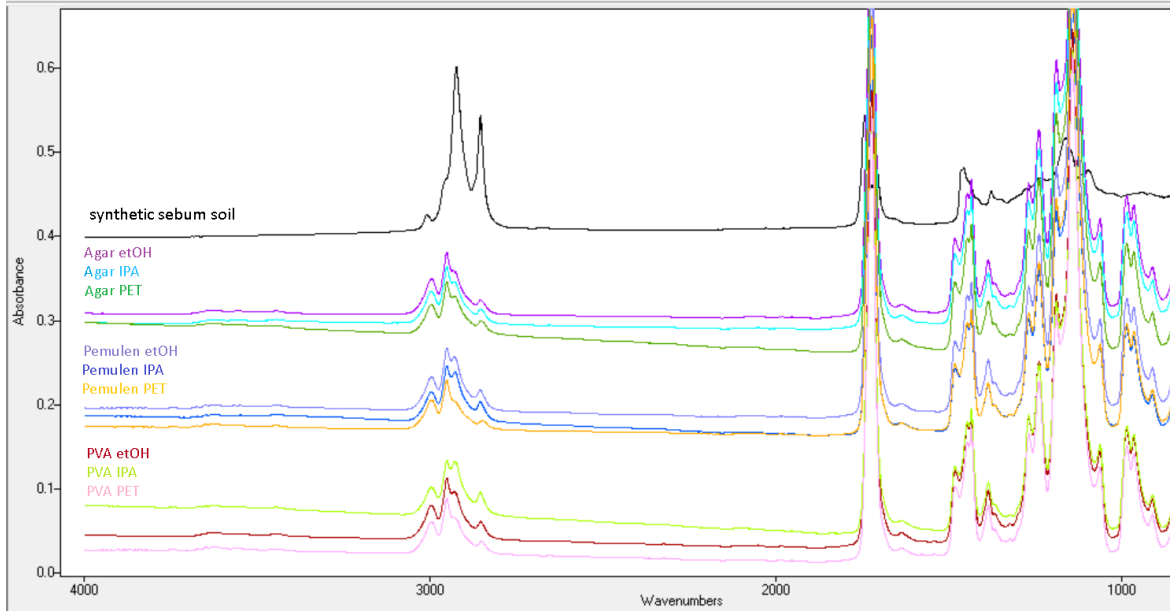


*Figure 9.5. Spectra of new PMMA samples with synthetic soil after gel treatment. The spectra are averaged from 3 replicates for each treatment. Each replicate is averaged from 3 spot ATR analyses. The spectrum of synthetic soil is included for comparison.*

Agar treatments as well as Pemulen and PVA with PET left new and aged samples with no change (Fig. 9.5). This alone would indicate that treatments did not alter the surface chemistry of PMMA. However, when looking at the visual examination and gloss data, these treatments performed poorly failing to remove synthetic soil, while only Agar EtOH offered the best outcome. This shows that ATR-FTIR was not precise to assess surface gel treatments, possibly because of being a spot analysis. Pemulen and PVA gels with EtOH and IPA caused an increase in peaks  $2919\text{ cm}^{-1}$  and  $2850\text{ cm}^{-1}$  on all samples. These peaks could be attributed to the C–H stretching vibrations (Fig. 9.5) of either the synthetic soil or the treatments, which according to visual observation left extensive gel residue.

#### 9.1.2.b. PSA

##### VISUAL OBSERVATIONS

##### Macroscopic observations

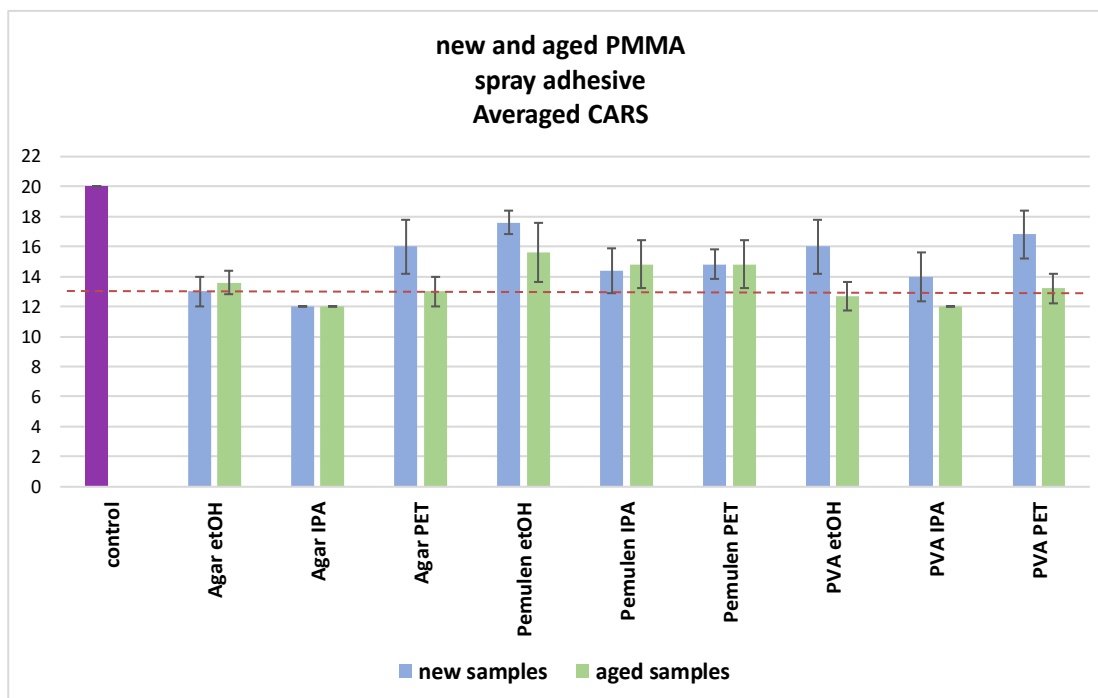
Pemulen gels were the most successful at removing PSA from all samples. Agar EtOH and PET and PVA PET managed to remove (sometimes partly) PSA, mostly from new surfaces. PVA with alcohols performed the worst, partly removing PSA from new surfaces and failing to do so

from aged. Agar IPA was the only treatment that failed to remove any PSA. Results suggest that contrary to synthetic soil, it was easier to clean new than aged PMMA from PSA.

samples with adhesive		
	new PMMA	aged PMMA
Agar etOH	partly cleaned	partly cleaned/not cleaned
Agar IPA	not cleaned	not cleaned
Agar PET	cleaned	partly cleaned/not cleaned
Pemulen etOH	cleaned	cleaned
Pemulen IPA	partly cleaned	partly cleaned
Pemulen PET	cleaned	cleaned
PVA etOH	partly cleaned	not cleaned
PVA IPA	partly cleaned	not cleaned
PVA PET	cleaned	partly cleaned

Table 9.5. Macroscopic observation of the overall impression of unaged PSA removal from new and aged PMMA after treatment.

### CARS scores



Graph 9.9. CARS scores of new and aged PMMA samples with unaged PSA. Scores are based on a five-point progressive ranking from 0 (worst) to 4 (best). Scores, expressed as a bar chart, are averaged from 5 replicates for each treatment. Untreated new and aged PMMA controls scored the highest possible CARS 20 in categories 'Dirt residue', 'Abrasion' and 'Gel residue'. Red line shows below which point treatments failed to remove PSA. Error bars show the standard deviation.

Treatments performed better on new surfaces than aged, in agreement with Table 9.5. Pemulen EtOH left all surfaces in the best visual condition, scoring 17.6 (new) and 15.6 (aged). Agar PET and PVA with EtOH and PET left new surfaces equally clean, according to human perception (Graph 9.9). The same treatments performed poorly on aged PMMA. Pemulen with IPA and PET performed similarly on all surfaces (around 14). Agar with alcohols left all surfaces in the worst visual condition (13 and 12 respectively). Combination of CARS scores with Table 9.5 suggested that treatments scoring below 13 (see line in Graph 9.9) failed to remove PSA.

### **ANOVA CARS**

ANOVA of CARS indicated that Gels, Solvents and Condition had a statistically significant impact on the cleaning of PMMA with PSA. It also showed that the interaction effects of gels with condition were statistically significant. The interaction plot (Graph 9.10) indicates that the effect of PVA was worst when treating aged PMMA, offering lower CARS. Tukey's HSD compared variables and showed that Pemulen was significantly different from the other gels. Pemulen treatments consistently scored the highest CARS (see Graph 9.11) improving the samples visual condition. Tukey's HSD also showed that IPA was significantly different from the other solvents. By scoring the lowest CARS (Graph 9.11), IPA negatively impacted cleaning. New surfaces scored significantly higher than aged surfaces indicating that treatments performed better on new PMMA.

#### **Grouping Information Using the Tukey Method and 95% Confidence**

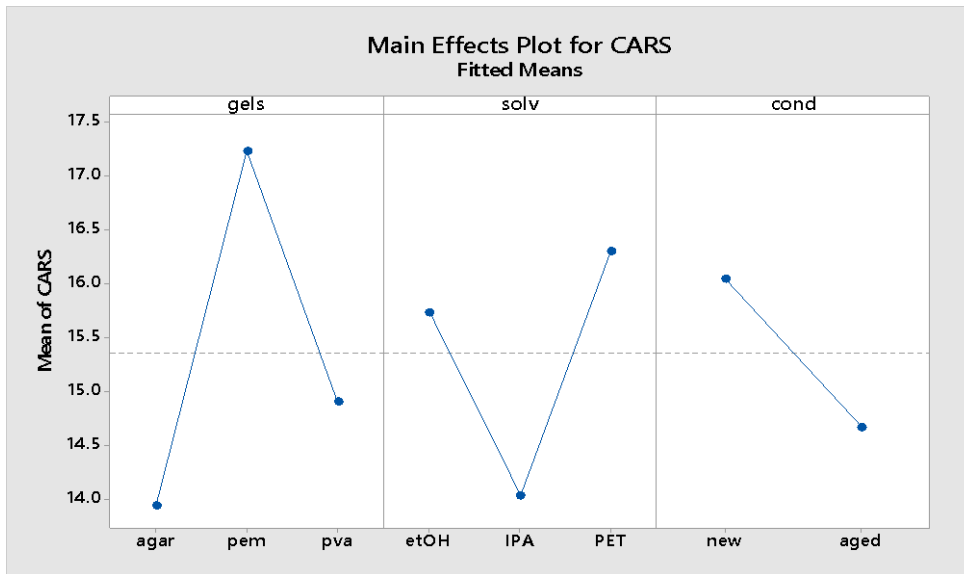
<u>gels</u>	<u>N</u>	<u>Mean</u>	<u>Grouping</u>
pem	30	17.233	A
pva	30	14.900	B
agar	30	13.933	B

<u>solv</u>	<u>N</u>	<u>Mean</u>	<u>Grouping</u>
PET	30	16.300	A
etOH	30	15.733	A
IPA	30	14.033	B

*Means that do not share a letter are significantly different.*



Graph 9.10. Interaction plot showing the significant interactions between gels and condition on PMMA gloss.



Graph 9.11. The mean CARS scores of Pemulen are the highest, while that of IPA the lowest, indicating they affected cleaning of PMMA with PSA in a positive and a negative manner, respectively. PET scored below the means CARS value having a negative impact on PMMA.

**SEM observation**

Under high magnification, the unaged and aged PMMA controls with PSA appeared indistinguishable (Fig. 9.6), regardless of surface condition. Both controls were covered with a compact PSA layer containing air bubbles. Due to the thick/dense PSA nature, the sprayed layer visibly appeared to be uneven forming areas of cluttered PSA.



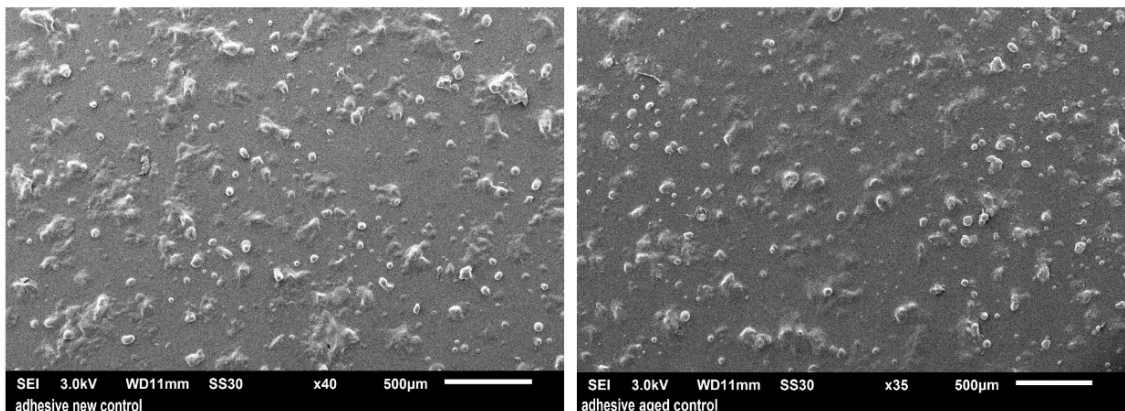
**Control PMMA with PSA**

Figure 9.6. SEM micrographs: Unaged PMMA control with PSA under magnification x40 (left) and aged PMMA control under magnification x35 (right).

**New PMMA samples with PSA:**

New PMMA samples after treatment				
Treatment	PSA	Gel residue	Comments	Figure no.
<b>Agar EtOH</b>	not cleaned	no		9.7 A
<b>Agar IPA</b>	not cleaned	no		9.7 D
<b>Agar PET</b>	cleaned	limited		9.7 F
<b>Pemulen EtOH</b>	cleaned	no	good surface condition	9.8 A
<b>Pemulen IPA</b>	partly cleaned	extensive		9.8 C, D
<b>Pemulen PET</b>	cleaned	no	scratches	9.8 G, H
<b>PVA EtOH</b>	cleaned	no		9.9 B, C
<b>PVA IPA</b>	partly cleaned	extensive	solutes from droplet evaporation	9.9 F, G, H
<b>PVA PET</b>	partly cleaned	limited		9.10 D, E

**Aged PMMA samples with PSA:**

Aged PMMA samples after treatment				
Treatment	PSA	Gel residue	Comments	Figure no.
<b>Agar EtOH</b>	partly cleaned	extensive	gel residue entrapped on PSA remains	9.7 B, C
<b>Agar IPA</b>	not cleaned	no		9.7 E
<b>Agar PET</b>	not cleaned	limited		9.7 G, H
<b>Pemulen EtOH</b>	cleaned	no	some discolouration	9.8 B
<b>Pemulen IPA</b>	partly cleaned	extensive	gel residue entrapped on PSA remains	9.8 E, F
<b>Pemulen PET</b>	cleaned	no		9.9 A
<b>PVA EtOH</b>	not cleaned	extensive		9.9 D, E
<b>PVA IPA</b>	not cleaned	extensive	solutes from droplet evaporation	9.10 A, B, C
<b>PVA PET</b>	partly cleaned	extensive	gel residue entrapped on PSA remains	9.10 F

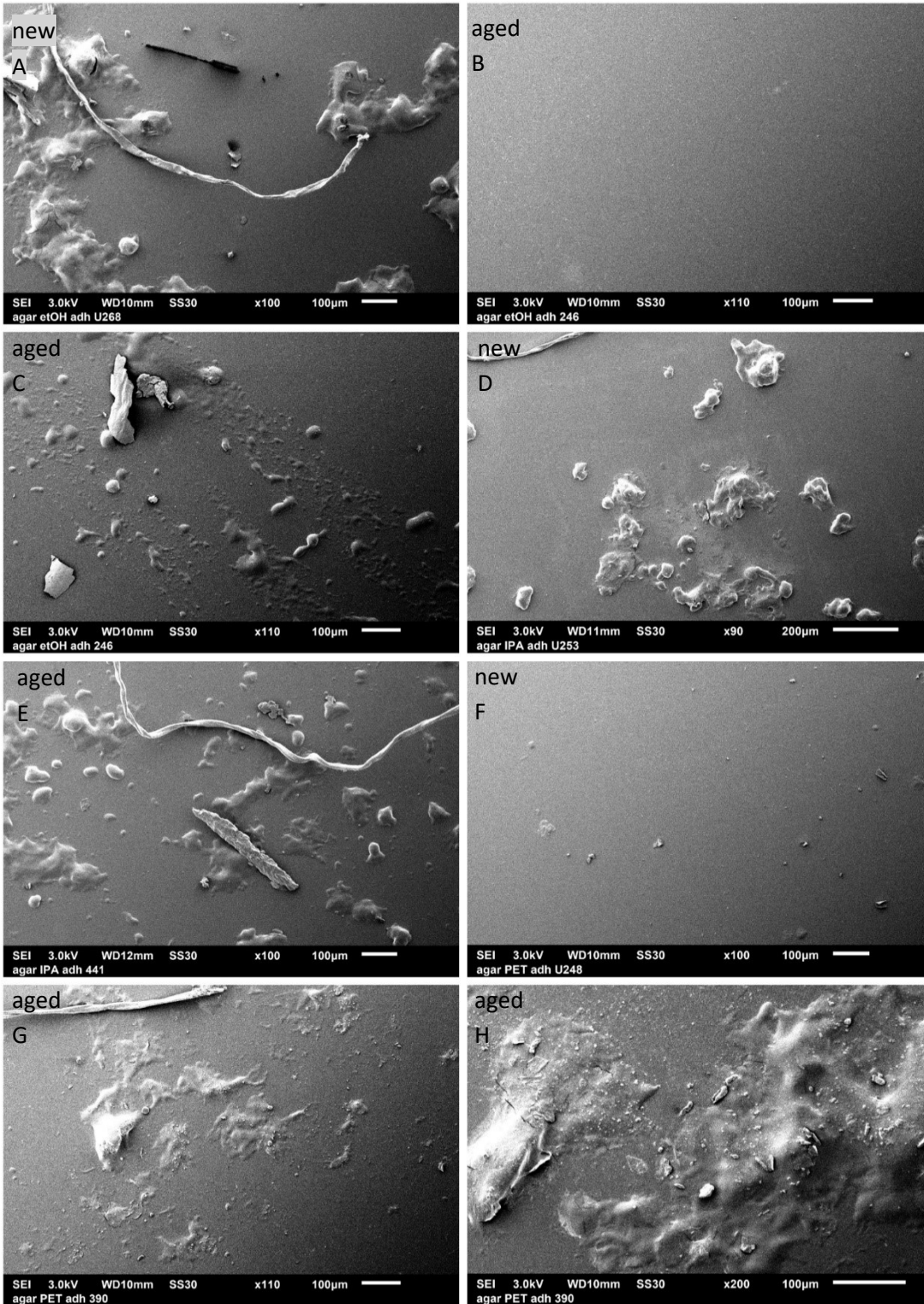
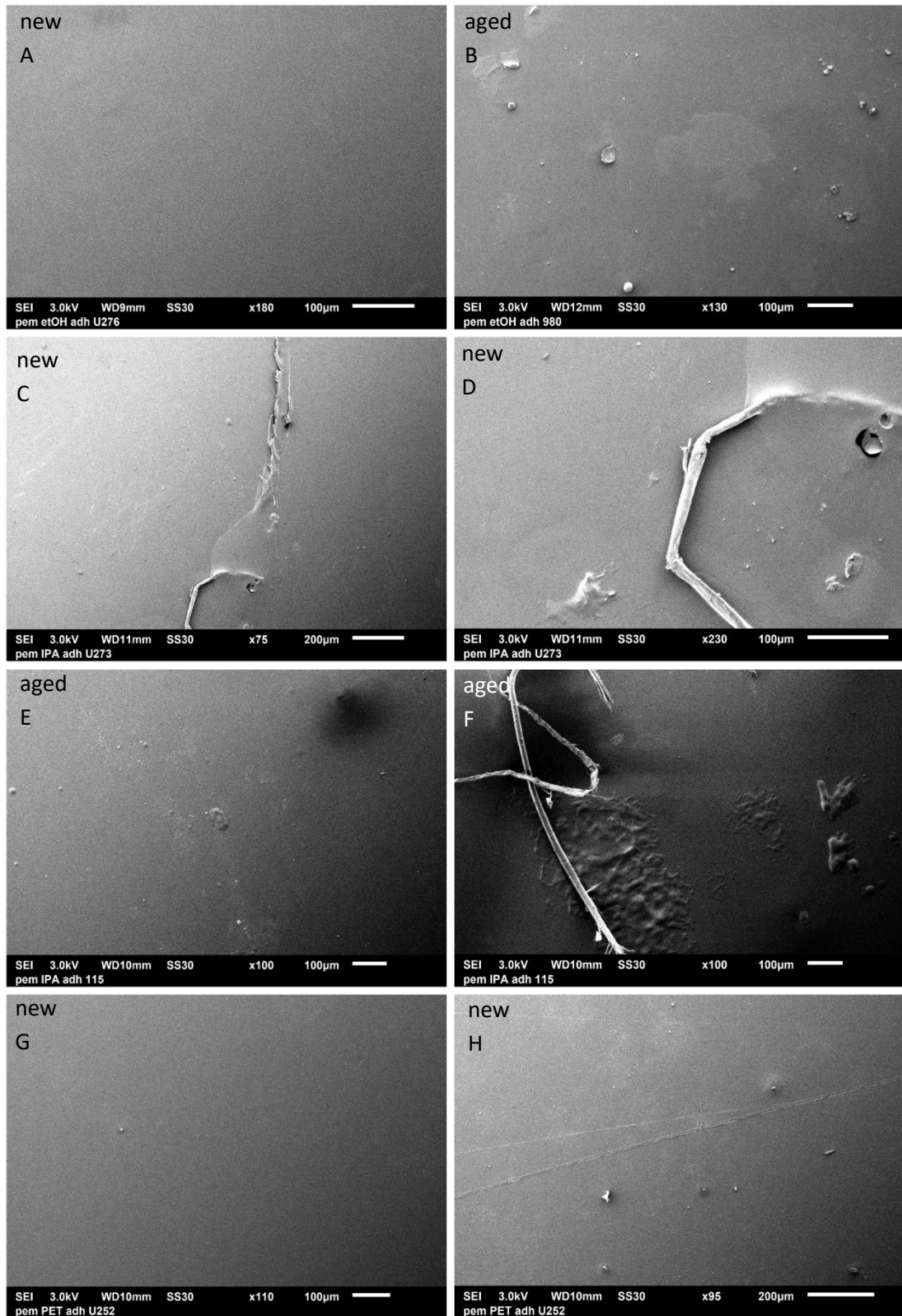


Figure 9.7 A, D: Agar with EtOH and IPA failed to removed PSA from new PMMA. B: Agar EtOH left aged PMMA partly clean. C: Agar EtOH gel residue entrapped on PSA. E, G, H: Agar with IPA and PET failed to remove PSA from aged PMMA.



*Figure 9.8. A-B: Pemulen EtOH left new and aged PMMA clean, the latter with limited discolouration. C-D: Pemulen IPA deposited extensive gel residue on new and aged PMMA. E: Pemulen IPA left aged PMMA partly clean and F: other areas with gel residue entrapped on PSA remains. G: Pemulen PET left new PMMA clean, but H: with some scratches.*

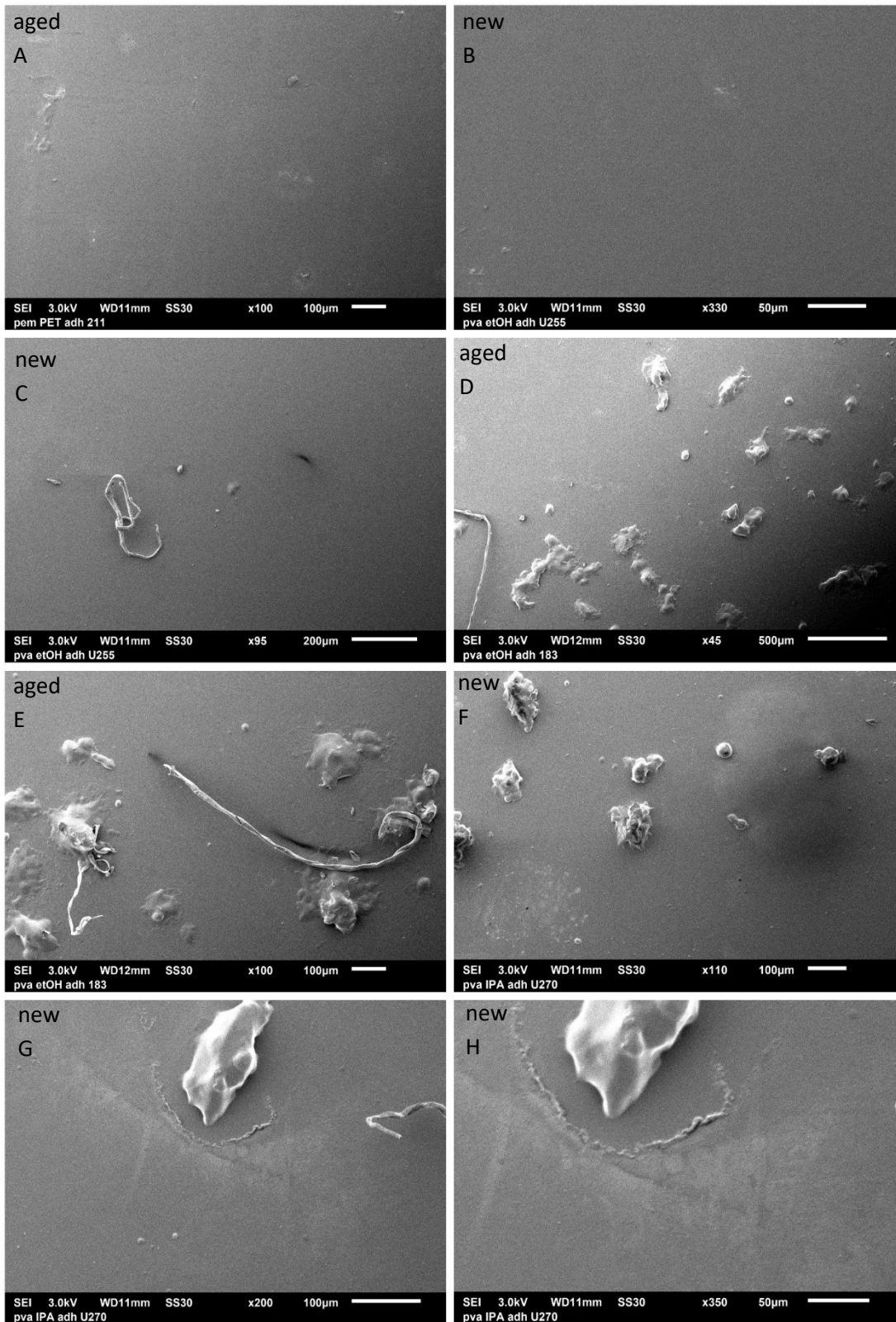
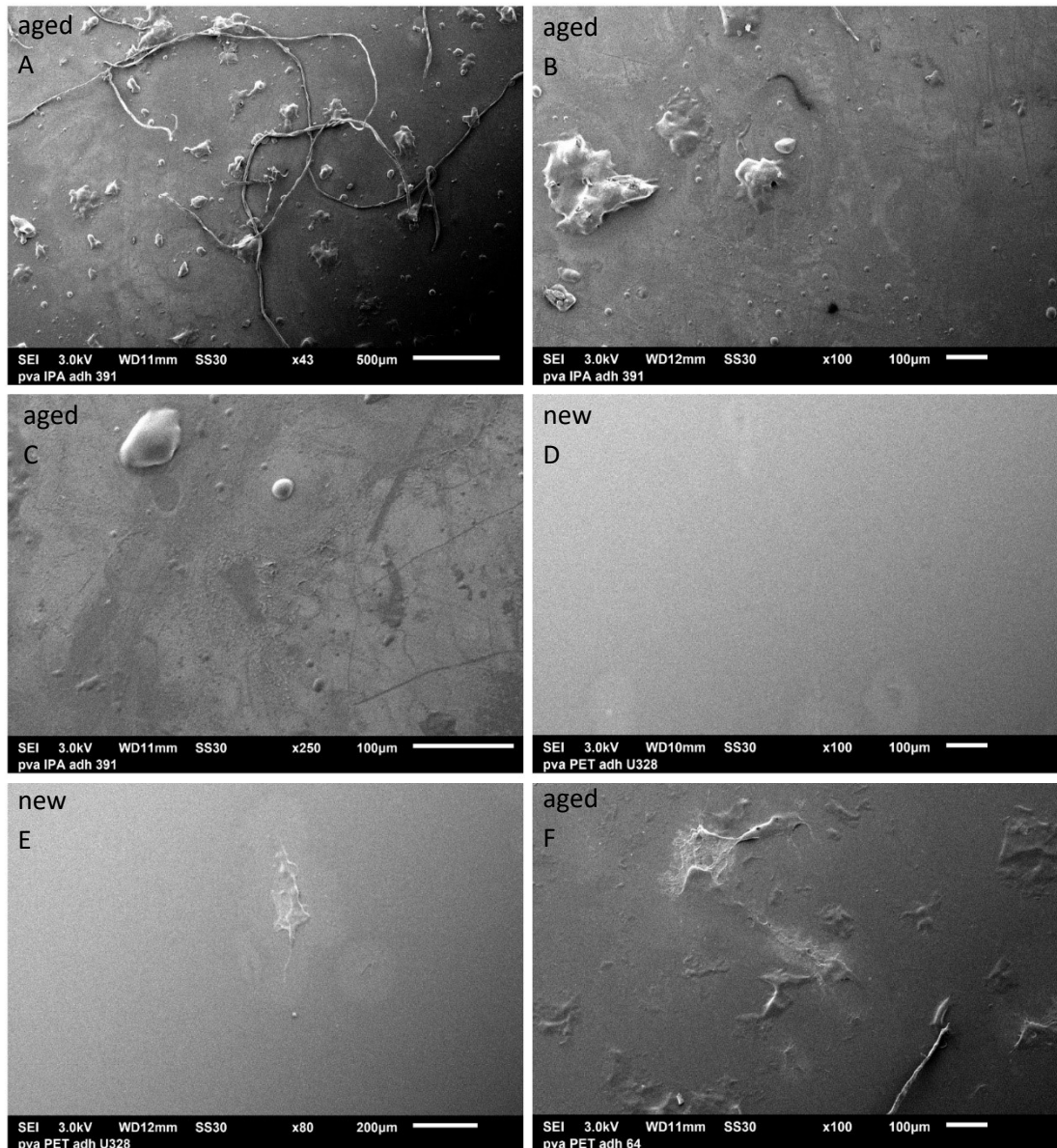


Figure 9.9. Pemulen PET left aged PMMA clean. B-C: PVA EtOH removed PSA from new PMMA. D-E: PVA EtOH left extensive gel residue on aged PMMA. F: PVA IPA left PSA remains on new PMMA and G-H: extensive gel residue and solute deposits from droplet evaporation.

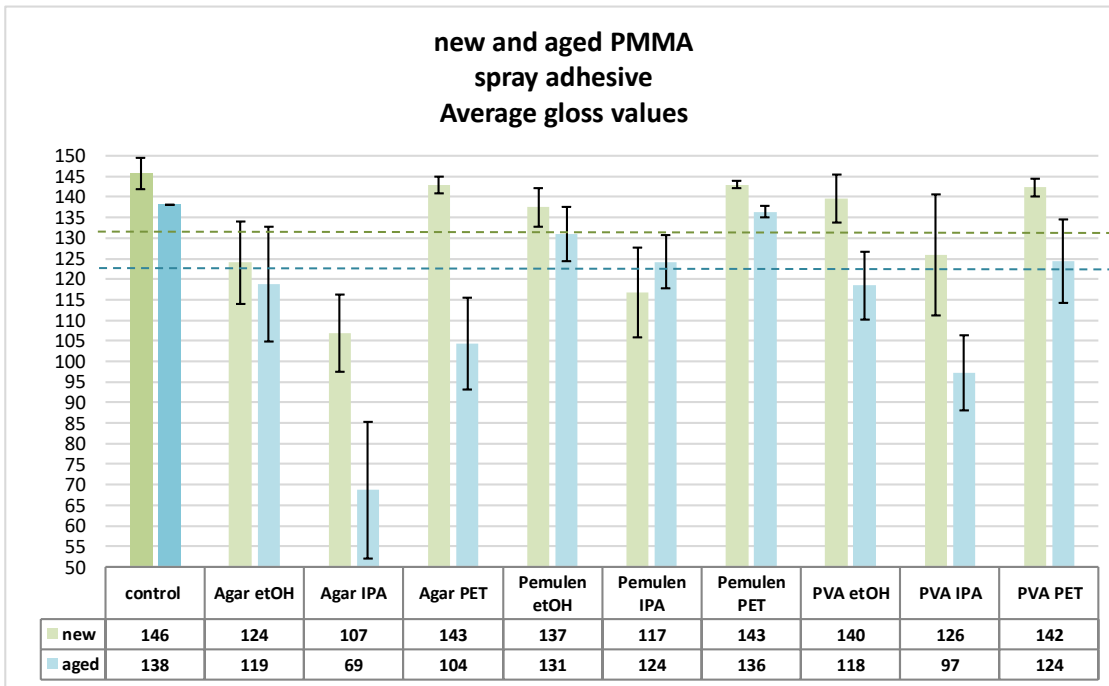


*Figure 9.10. A-C: PVA IPA failed to remove PSA leaving extensive gel residue. D: PVA PET left new PMMA clean and E: with limited gel residue. F: PVA PET partly removed PSA from aged PMMA, leaving gel residue entrapped on PSA remains.*

## GLOSS

### Gloss measurements

New samples exhibited higher gloss than aged, in agreement with visual observation. Pemulen EtOH, Pemulen PET and PVA PET left all surfaces in the best visual condition with gloss values within 15 GU from the controls. This rendered treated surfaces equally glossy to the control. Agar EtOH, Agar IPA, Pemulen IPA and PVA IPA induced the lowest gloss, attributed to their inability to remove PSA, as confirmed by visual evaluation. Agar PET and PVA EtOH left new PMMA in the best visual condition, but aged PMMA with a big drop in gloss.



Graph 9.12. Gloss measurements of new and aged PMMA with PSA after treatment, plotted as bar charts. Gloss units (GU) are averaged from 3 repetitions of 3 spot measurements on 5 replicates. Differences < 15 GU are non-detectable by the human eye. PMMA controls are highly glossy with a value of 146 GU for the unaged and 138 GU for the aged. Blue line shows below which point change is visible for aged PMMA and green line for new PMMA. Error bars show the standard deviation.

**ANOVA gloss**

ANOVA of gloss measurements showed that Gels, Solvents and Condition had a statistically significant impact on the cleaning of PMMA with PSA. Tukey’s HSD allocated unique letters to Agar and IPA indicating that they significantly affected the gloss. In the main effects plot (Graph 9.13) both Agar and IPA induced the lowest gloss indicating that they negatively impacted cleaning. Treatments positively impacted cleaning of aged surfaces, inducing higher gloss than on new samples. New surfaces scored significantly higher than aged surfaces indicating that treatments performed better on new PMMA.

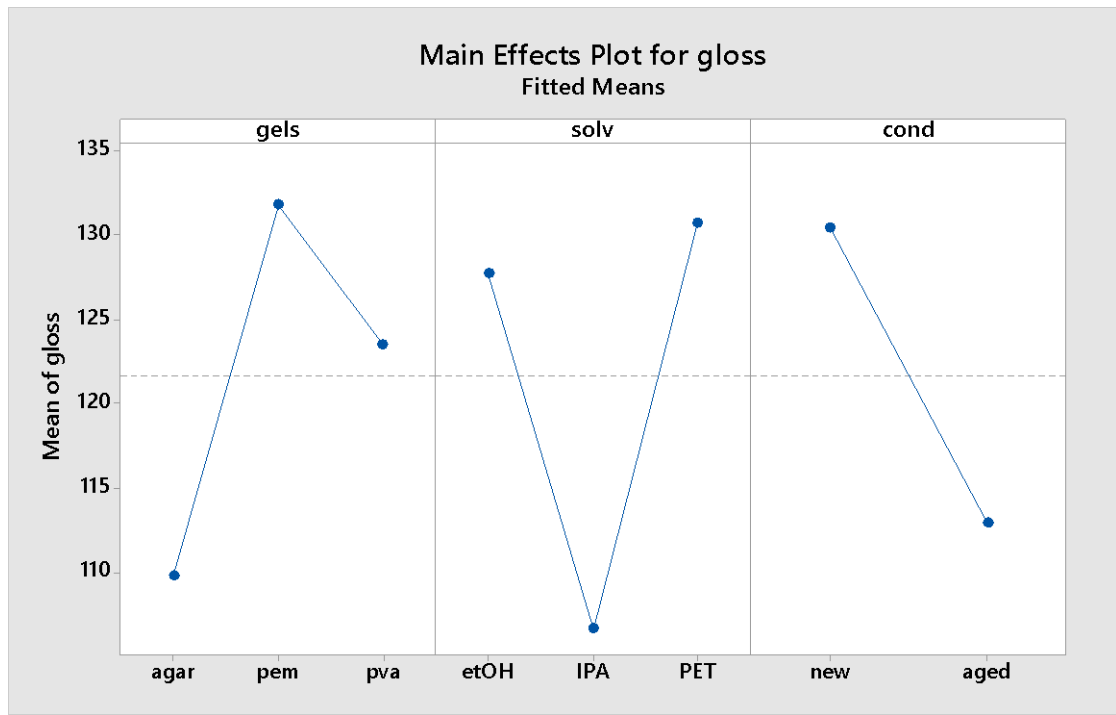
**Grouping Information Using the Tukey Method and 95% Confidence**

gels	N	Mean	Grouping
pem	30	131.77	A
pva	30	123.49	A
agar	30	109.75	B

solv	N	Mean	Grouping
PET	30	130.72	A
etOH	30	127.70	A
IPA	30	106.60	B

Means that do not share a letter are significantly different.



Graph 9.13. The mean gloss scores of Agar and IPA are the lowest indicating they affected cleaning of PMMA with PSA in a negative manner.

## WEIGHT MEASUREMENTS

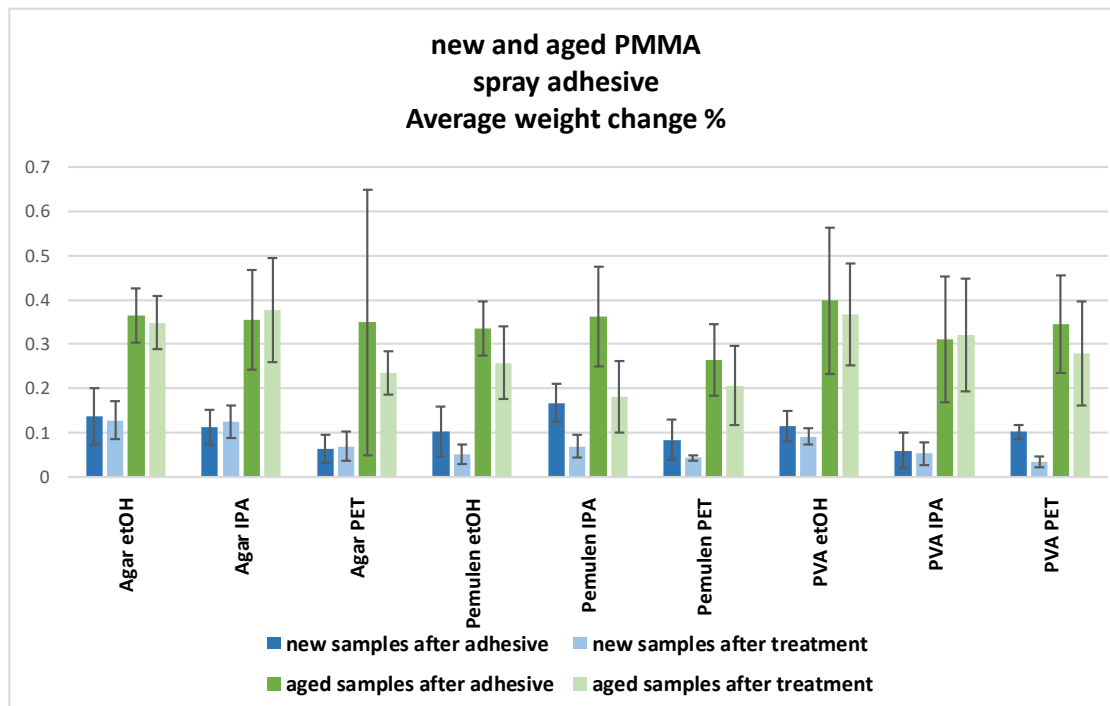
### Weight changes %

After PSA application, aged surfaces gained three times more weight compared to new (Graph 9.14 - ca. 0.3 % versus 0.1 % for new samples, relative to the initial weight set at zero). This additional weight increase in aged samples was attributed to PSA penetration in voids formed during UV ageing. New PMMA bearing a denser network with less free volume, did not allow PSA to diffuse in its bulk.

Pemulen with alcohols removed roughly half the weight gained from PSA application from surfaces of both conditions. Visual evaluation under SEM confirmed the successful PSA removal after treatment with Pemulen EtOH and PET. This was not the case for Pemulen IPA, which not only failed to remove PSA, but deposited extensive gel residue too. As discussed previously, H<sub>2</sub>O/alcohol mixtures can penetrate the PMMA upper micron layers and cause dissolution/evaporation of components. The presence of extensive Pemulen gel residue may even draw in dissolved PMMA components.

Agar PET caused no change to new samples, however, visual evaluation determined their successfully cleaning. PVA PET caused equal weight loss (0.07 %) to all PMMA surfaces, although visual evaluation indicated PSA removal only from new samples. The lack of weight change in a treatment that visually appears successful, or weight change in a treatment that visually failed to clean, are indicative of other phenomena occurring simultaneously. In the

case of Agar PET, given that microscopic evaluation did not reveal deposition of gel residue, this lack of weight change could be explained as PSA removal with simultaneous penetration of H<sub>2</sub>O from the gel. Agar and PVA with alcohols did not cause any weight change, indicating their complete inability to remove PSA, confirmed by visual evaluation.



Graph 9.14. Average weight change % of new and aged PMMA - averaged from five replicates - after application of PSA and after cleaning treatment (blue tones: new - green tones: aged samples). Changes % are normalised to the starting/initial weight. Error bars show the standard deviation.

### **ANOVA weight change %**

ANOVA of weight change % showed that none of the treatments influenced the weight of samples in a statistically significant manner. Comparing this to the analysis of visual evaluation suggests that data from bulk gravimetric analysis are not significant to the assessment of treatments at this point.

### **ATR-FTIR**

Agar PET, all three Pemulen treatments and PVA PET left samples with no change indicating that none of them altered the PMMA surface chemistry. Visual evaluation confirmed that these treatments successfully remove PSA. Samples treated with Agar and PVA with alcohols displayed spectra identical to the PSA spectrum (Fig. 9.11 - black) (see Chapter 5.2.2 for band assignments) indicating that PSA was not removed, in agreement with visual evaluation.

ATR-FTIR analysis was used to monitor gel residue deposition, but with no success. Although it was evident under the SEM that treatments such as Pemulen with alcohols and PVA



IPA deposited extensive gel residue, this was not detected by ATR-FTIR. Characteristic IR absorptions of different materials co-existing on the same sample surface, namely PMMA, remains of acrylic-based PSA and polymer gel, possibly overlapped contributing to broader/more intense absorptions. Similar absorptions do not permit clear interpretation or assignment of peaks, and so ATR-FTIR was not suitable to assess surface gel treatments.

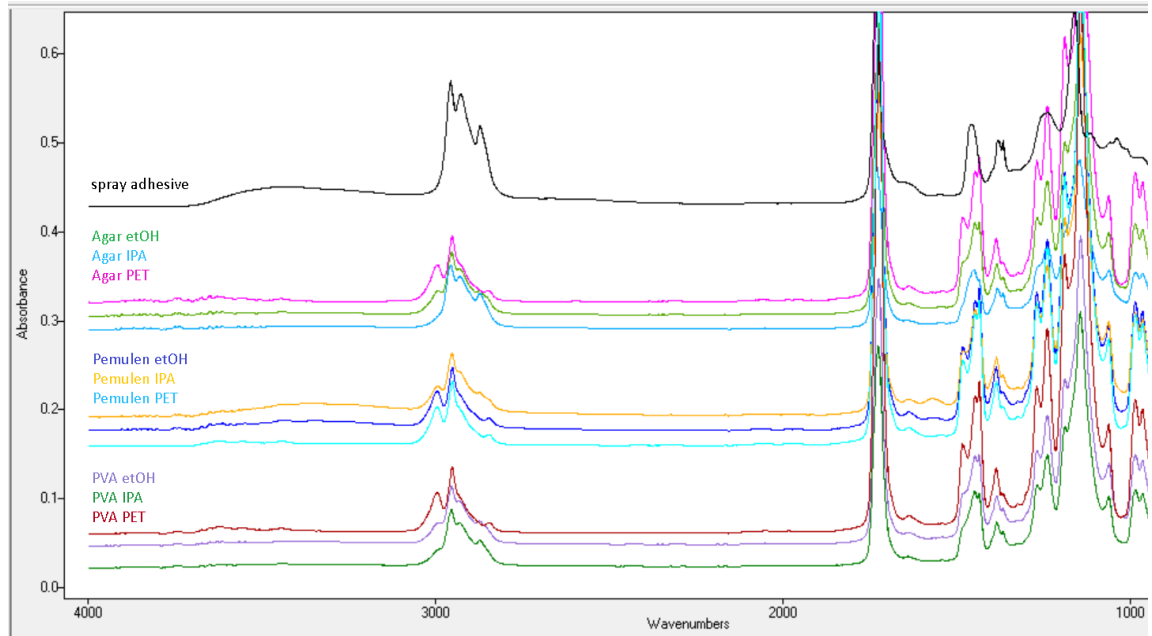


*Figure 9.11. Spectra of new PMMA samples with PSA after solvent-gel treatment. The spectra are averaged from 3 replicates for each treatment. Each replicate is averaged from 3 spot ATR analyses. The spectrum of PSA is included for comparison.*

### 9.1.3. Conclusion

#### PMMA samples with synthetic soil

All treatments caused samples to lose most of the weight gained upon application of synthetic soil. It was interesting to see that new samples, partly cleaned and with extensive gel deposition, lost more weight than aged, left free from synthetic soil and residue. Discrepancies between visual evaluation and weight changes indicated that other chemical phenomena occurred concurrently. It was argued that H<sub>2</sub>O from gels penetrating the voids formed during UV ageing caused a weight increase. Weight loss of new samples was attributed to solvent-induced dissolution of volatile components.

Agar EtOH proved to be the most successful at removing synthetic soil from all surfaces. All other treatments performed poorly on new surfaces, failing to remove synthetic soil and frequently depositing extensive gel residue. Aged PMMA was successfully cleaned by gels with EtOH (Agar, Pemulen and PVA) and Pemulen IPA. In fact, statistical analysis of CARS and gloss established the positive effect of both EtOH and Pemulen. IPA and PVA negatively

impacted cleaning whenever present in a gel formulation. Exceptions to that were Pemulen IPA and PVA EtOH that performed satisfactorily due to the positive presence of the gel in the former and the solvent in the latter case. Gels with PET failed to remove synthetic soil and performed poorly on all PMMA.

Pemulen gels performed very well during cleaning, especially in regard to their clearance from aged surfaces. During post-treatment rinsing, swabs rolled on the treated surfaces lifted Pemulen residue, which in turn peeled-off synthetic soil remains. The soil's black hue rendered its detection possible. This was not the case with new PMMA, where rinsing of the extensive Pemulen residue failed.

After treatment all samples were left in a poor visual condition, even when synthetic soil was completely removed. Although synthetic soil consisted of a fatty ingredient (sebum oil), which being inherently shiny was expected to increase the glossiness levels, all samples showed a decrease in surface gloss. Perhaps treatments removed the sebum oil responsible for high gloss, but left carbon black soil remains spread across surfaces. Its black hue on the colorless, transparent surfaces was held responsible for the reduced visual condition.

#### PMMA samples with PSA

The majority of treatments caused no weight change. In some cases, treatments that according to visual evaluation successfully removed PSA, such as Agar, Pemulen and PVA with PET, caused samples to gain weight. High magnification ruled out the possibility of gel residue. Therefore PSA removal occurred concurrently with liquid penetration from the gels. Immersion studies (Chapter 7.1.2) showed that H<sub>2</sub>O was the only solvent (among tested) to cause a steady weight gain, and was the only constant in all treatments, leading to the conclusion that H<sub>2</sub>O had penetrated PMMA during treatment.

Pemulen gels appeared to be the most effective at removing PSA from all surfaces. In fact, samples after Pemulen treatments scored among the best in the visual evaluation and gloss measurements. Statistical analysis of CARS and gloss measurements established the positive effect of Pemulen treatments. Agar performed poorly and negatively impacted the visual condition of surfaces, mostly due to their inability to remove PSA. IPA also negatively impacted cleaning, and therefore when coupled with Agar, offered the worst results: failure to remove PSA and worst visual condition. PVA gels also performed poorly, failing to remove PSA and depositing extensive gel residue, as indicated from visual evaluation and ATR-FTIR spectra of samples exhibiting characteristic PSA absorption bands. The only exceptions were Agar with PET and PVA with PET, both of which performed satisfactorily due to the positive presence of the solvent.

## 9.2. POLY (METHYL METHACRYLATE) WITH AGED DIRT

Dirt and adhesives removed from museum objects are typically found in deteriorated states, therefore it was important to test the solvent-gel treatments on aged synthetic soil and PSA. Before proceeding to the subsequent main experiment and prior to permanently eliminating treatments for being ineffective, further cleaning trials were carried out. These intended to confirm whether treatments, previously unable to remove synthetic soil or PSA, would still fail to remove them when degraded. H<sub>2</sub>O previously discarded was also re-tested both with cotton swabs and thickened in Agar as a hydrogel. Trials were performed in duplicate, on new and aged samples bearing aged synthetic soil or PSA. Table 9.6 lists all re-tested treatments and their results based on macroscopic observation.

Cleaning trials on unaged synthetic soil showed that Agar PET, Pemulen PET, PVA PET and PVA IPA performed poorly and negatively impacted cleaning. These were tested for their potential to remove aged synthetic soil after UV exposure of 32 days. Results were consistent with those of unaged soil, with the exception of Pemulen PET that was able to partly clean PMMA. This was confirmed by the black soil on the Pemulen gel after treatment and the cotton swabs used for post-treatment rinsing. Consequently, Pemulen PET was re-introduced. Cleaning trials on unaged PSA showed that Agar EtOH, Agar IPA, PVA EtOH and PVA IPA performed poorly and negatively impacted cleaning. These were tested for their potential to remove aged PSA after UV exposure of 32 days. Results were consistent with those of unaged PSA, so these treatments were discarded. Cleaning trials also confirmed that H<sub>2</sub>O in both forms tested was inefficient, thus it remained excluded from the next experimental phases.

Aged synthetic sebum soil	Observations
Agar PET	No removal
Pemulen PET	Removal
PVA PET	No removal
PVA IPA	Minimal dissolution, no removal
H <sub>2</sub> O (3 rolls and Agar hydrogel)	No removal
Aged spray adhesive	
Agar EtOH	No removal
Agar IPA	No removal
PVA EtOH	No removal
PVA IPA	No removal

*Table 9.6. Cleaning trials testing treatments - previously discarded as ineffective on PMMA with unaged synthetic soil and PSA - on their ability to remove aged synthetic soil and aged PSA.*

### 9.2.1. Experimental design

A multilevel full-factorial experiment was adopted for each type of aged 'dirt' to simultaneously examine the effects of Treatments and PMMA Surface condition in isolation, as

well as combined. The aim was to test treatments indicated as successful in previous experiments for their removal of aged surface 'dirt'. Experiments were designed in quintuple (n=110 samples). New and aged samples were sprayed with either synthetic soil (n=60 samples) or PSA (n=50 samples) (see Chapter 5.2) and aged for 32 days.

<b>Main experiment on new and aged PMMA with aged synthetic sebum soil</b>		
<b>Experimental Variables</b>		
<b>Factor</b>	<b>A. Treatment</b>	<b>B. PMMA surface condition</b>
<b>Levels</b>	1. Pemulen EtOH	1. new
	2. Pemulen IPA	2. aged
	3. Pemulen PET	
	4. Agar EtOH	
	5. Agar IPA	
	6. PVA EtOH	

*Table 9.7. Experimental variables in the multilevel two-factorial design used for the main cleaning experiment on new and aged PMMA with aged synthetic soil (5 replicates). Number of levels: 6, 2.*

### Multilevel Factorial Design

Factors: 2      Replicates: 5  
Base runs: 12      Total runs: 60

<b>Main experiment on new and aged PMMA with aged spray adhesive</b>		
<b>Experimental Variables</b>		
<b>Factor</b>	<b>A. Treatment</b>	<b>B. PMMA surface condition</b>
<b>Levels</b>	1. Pemulen EtOH	1. new
	2. Pemulen IPA	2. aged
	3. Pemulen PET	
	4. Agar PET	
	5. PVA PET	

*Table 9.8. Experimental variables in the multilevel two-factorial design used for the main cleaning experiment on new and aged PMMA with aged PSA (5 replicates). Number of levels: 5, 2.*

### Multilevel Factorial Design

Factors: 2      Replicates: 5  
Base runs: 10      Total runs: 50

**9.2.2. Results & interpretation**

**9.2.2.a. Aged synthetic soil**

**VISUAL OBSERVATIONS**

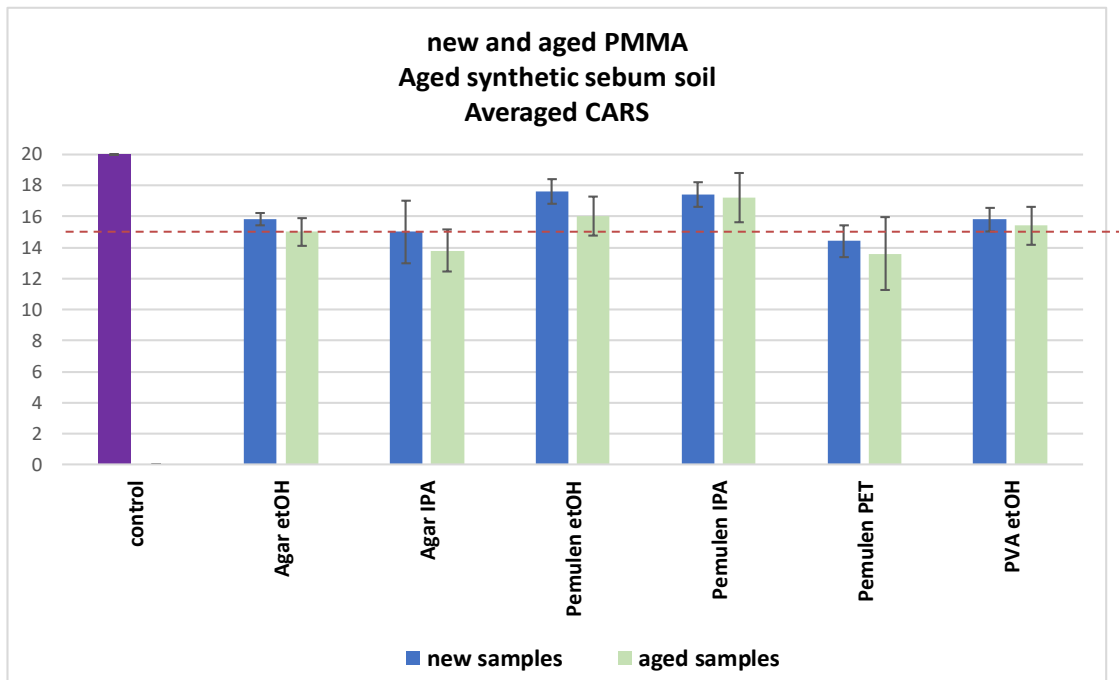
**Macroscopic evaluation**

Agar IPA and Pemulen PET failed to remove aged synthetic soil. Pemulen with EtOH and IPA, as well as PVA EtOH were the most successful at removing aged synthetic soil from all surfaces. Agar EtOH failed to clean aged PMMA, but performed better on new surfaces.

samples with aged synthetic soil		
	new	aged
Agar EtOH	partly cleaned/cleaned	not cleaned
Agar IPA	not cleaned	not cleaned
Pemulen EtOH	cleaned	partly cleaned
Pemulen IPA	partly cleaned/cleaned	cleaned
Pemulen PET	not cleaned	partly cleaned/not cleaned
PVA EtOH	partly cleaned	partly cleaned/cleaned

*Table 9.9. Macroscopic observation of the overall impression of aged synthetic soil removal from new and aged PMMA after treatment.*

**CARS scores**



*Graph 9.15. CARS scores of treated new and aged PMMA samples with aged synthetic soil. Scores are based on a five-point progressive ranking from 0 (worst) to 4 (best). Scores, expressed as a bar chart, are averaged from 5 replicates for each treatment. Untreated new and aged PMMA controls scored the highest possible CARS 20 in all categories ‘Dirt residue’, ‘Abrasion’ and ‘Gel residue’. Red line shows below which point treatments failed to remove synthetic soil. Error bars show the standard deviation.*

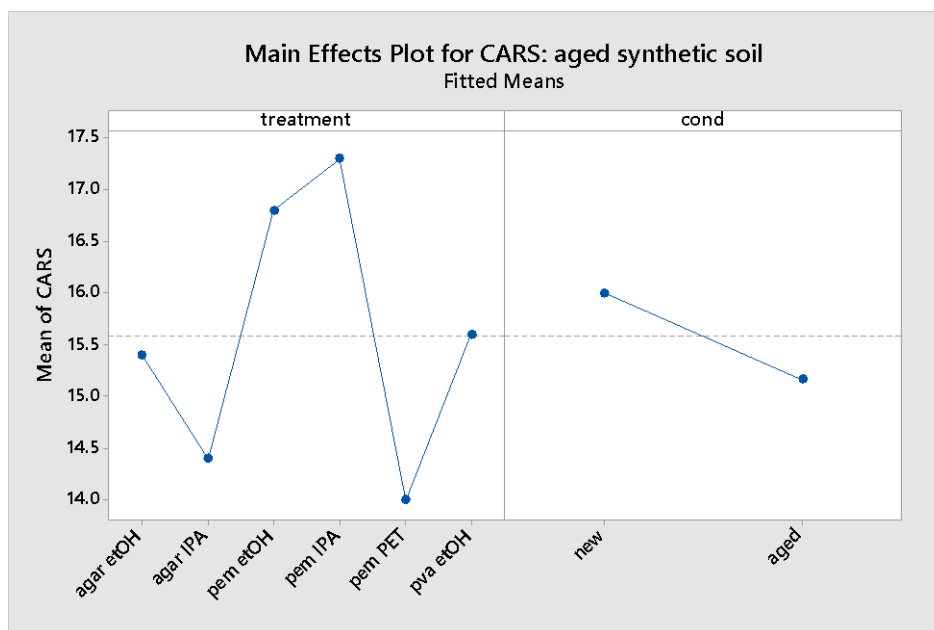
Pemulen EtOH and IPA left surfaces the cleanest, according to human perception (Graph 9.15). PVA EtOH also successfully removed aged synthetic soil. Agar EtOH failed to clean aged PMMA, but performed better on new surfaces. Pemulen PET and Agar IPA performed poorly on all surfaces, leaving PMMA in the worst condition (scored lowest CARS) (Graph 9.15). Combination of CARS scores with observations in Table 9.9 suggested that treatments scoring below 15 (see line in Graph 9.15) failed to remove aged synthetic soil.

### **ANOVA CARS**

ANOVA of CARS showed that Treatments had a statistically significant impact on the cleaning of PMMA with aged synthetic soil. Tukey's HSD determined that Pemulen EtOH with Pemulen IPA and Agar IPA with Pemulen PET performed similarly in a statistically significant manner. So, these pairs of treatments offered similar visual results. According to the main effects plot (Graph 9.16) Pemulen with alcohols scored the highest CARS positively impacting cleaning. By comparison, Agar IPA and Pemulen PET scored the lowest CARS having a negative impact on PMMA.

Grouping Information Using the Tukey Method and 95% Confidence			
treatment	N	Mean	Grouping
pem IPA	10	17.300	A
pem etOH	10	16.800	A
pva etOH	10	15.600	A B
agar etOH	10	15.400	A B
agar IPA	10	14.400	B
pem PET	10	14.000	B

*Means that do not share a letter are significantly different.*



Graph 9.16. The mean CARS scores of Pemulen EtOH and Pemulen IPA are the highest, while that of Agar IPA and Pemulen PET the lowest, indicating they affected cleaning of PMMA with aged synthetic soil in a positive and a negative manner, respectively.

**SEM imaging**

Under high magnification, new and aged PMMA controls with aged synthetic soil appeared similar (Fig. 9.12), regardless of surface condition. Before ageing, synthetic soil on both controls formed dense and uniform layers while after ageing these became less compact and inconsistent; A possible explanation could be due to accelerated ageing which includes wet cycles that could have washed off some of the soil, leaving PMMA areas partially exposed. The air bubbles, earlier seen, were still entrapped and visible in the sebum oil-carbon black mixture.

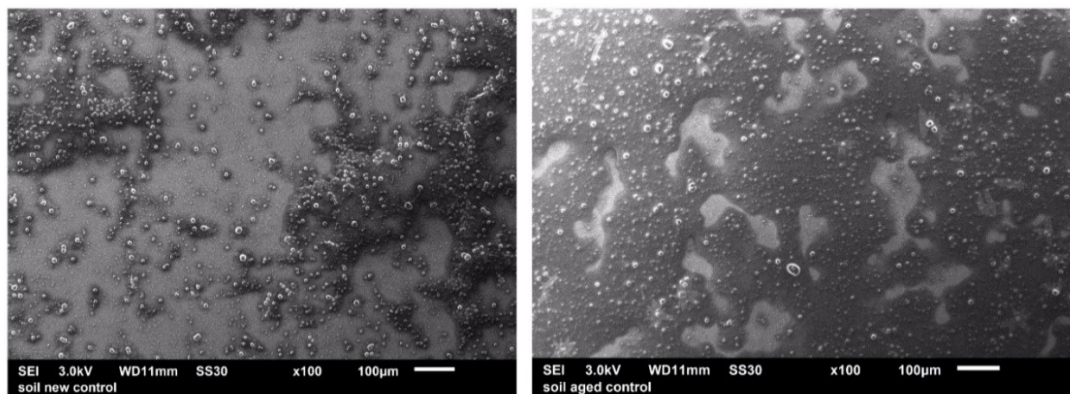
**Control PMMA with aged synthetic soil**

Figure 9.12. SEM micrographs: Unaged (left) and aged (right) PMMA control with aged synthetic soil under magnification x100.

**New PMMA samples with aged synthetic soil:**

New PMMA samples after treatment				
Treatment	Aged synthetic soil	Gel residue	Comments	Figure no.
<b>Agar EtOH</b>	not cleaned	limited		9.13 A
<b>Agar IPA</b>	not cleaned	limited		9.13 C
<b>Pemulen EtOH</b>	not cleaned	extensive	limited scratches	9.13 E
<b>Pemulen IPA</b>	cleaned	limited		9.13 H
<b>Pemulen PET</b>	partly cleaned	extensive		9.14 C, D
<b>PVA EtOH</b>	partly cleaned	extensive	a lot of scratches	9.14 E, F

Table 9.10. Evaluation based on SEM imaging of treated new PMMA samples with aged synthetic soil.

**Aged PMMA samples with aged synthetic soil:**

Aged PMMA samples after treatment				
Treatment	Aged synthetic soil	Gel residue	Comments	Figure no.
<b>Agar EtOH</b>	not cleaned	no		9.13 B, D
<b>Agar IPA</b>	not cleaned	no		9.13 C
<b>Pemulen EtOH</b>	partly cleaned	extensive		9.13 F, G
<b>Pemulen IPA</b>	cleaned	no		9.14 A
<b>Pemulen PET</b>	not cleaned	extensive		9.14 B
<b>PVA EtOH</b>	partly cleaned	extensive	gel residue as thin layers or 3D matter, scratches	9.14 G, H

Table 9.11. Evaluation based on SEM imaging of treated aged PMMA samples with aged synthetic soil.

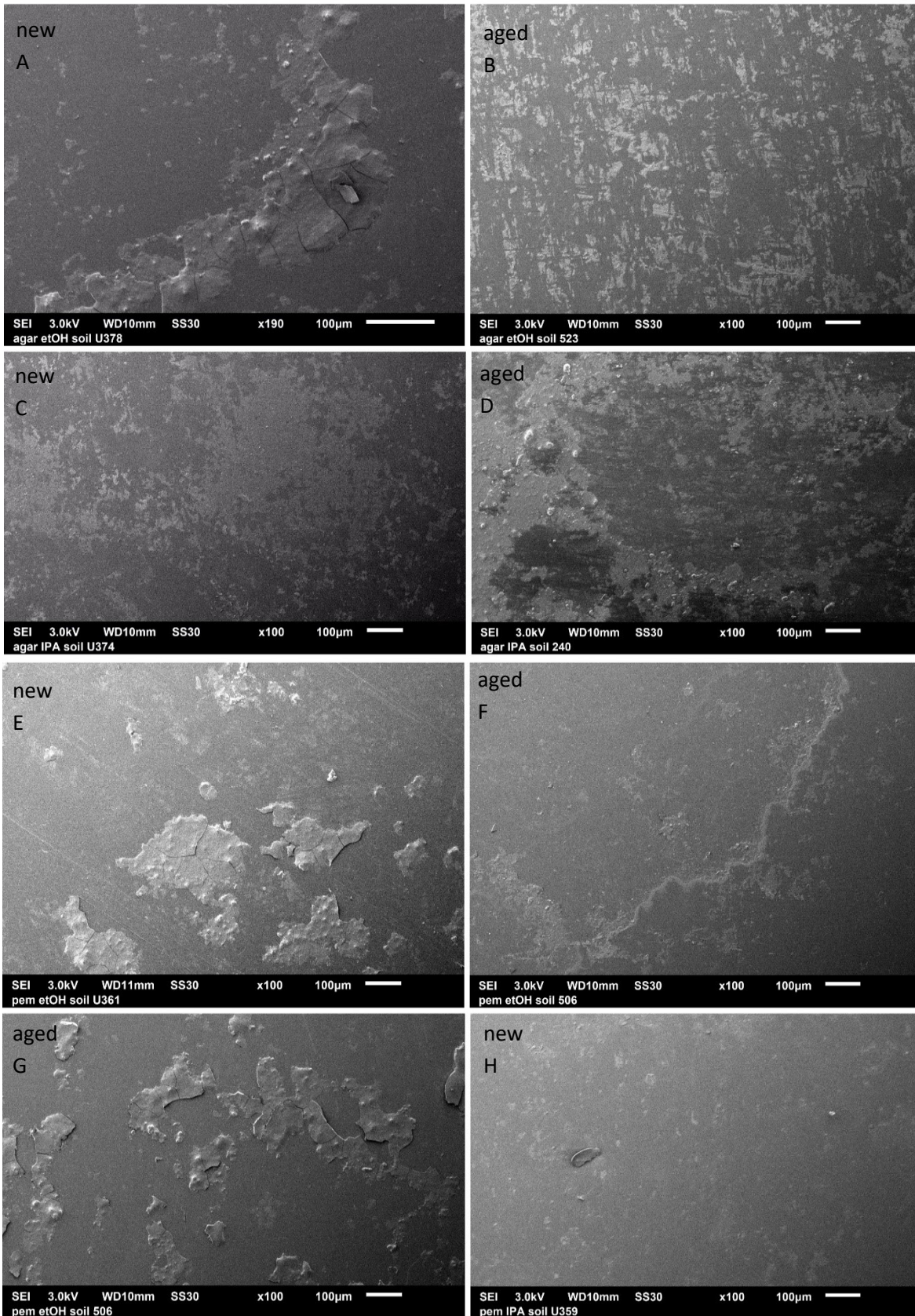
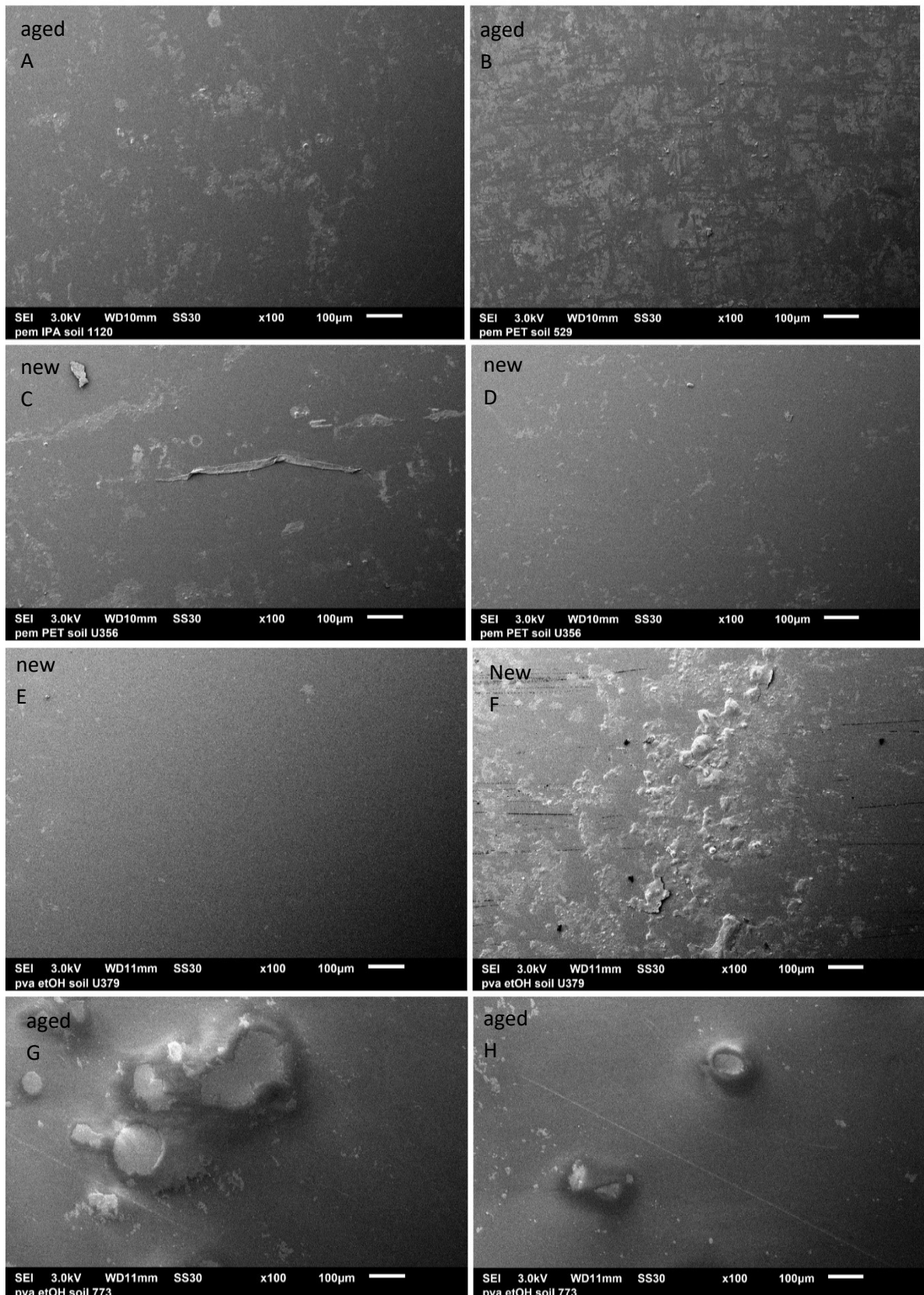


Figure 9.13. SEM micrographs: A-D: Agar with EtOH and IPA failed to clean PMMA. E: Pemulen EtOH left new surfaces covered with layers of gel residue and scratches. F: Pemulen EtOH left some areas clean. G: Pemulen EtOH left new surfaces covered in gel. H: Pemulen IPA cleaned new PMMA.



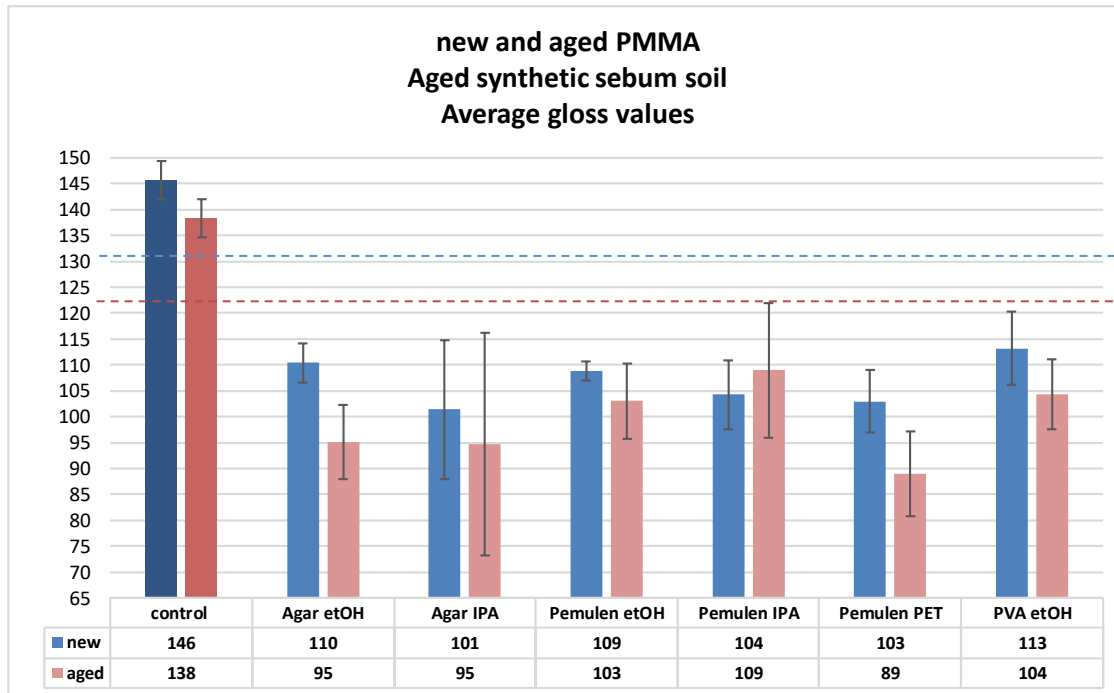


*Figure 9.14. SEM micrographs: A: Pemulen IPA cleaned aged samples. B: Pemulen PET failed to clean aged PMMA. C-D: Pemulen PET partly cleaned new PMMA and deposited extensive gel residue. E: PVA EtOH cleaned new PMMA and F: deposited extensive gel residue and scratches. G-H: PVA EtOH performed equally on aged PMMA with extensive gel residue and scratches.*

## GLOSS

### Gloss measurements

All treatments visibly altered the surface gloss of new and aged samples with an average gloss difference of 39 GU after removal of aged synthetic soil. All treatments left surfaces of the same condition macroscopically appearing equally glossy, as their differences were smaller than 15 GU.



*Graph 9.17. Gloss measurements of new and aged PMMA samples with aged synthetic soil after treatment, plotted as bar charts. Gloss units (GU) are averaged from 3 repetitions of 3 spot measurements on 3 replicates. Differences < 15 GU are non-detectable by the human eye. The PMMA controls are highly glossy with a value of 146 GU for the unaged and 138 GU for the aged. Red line shows below which point change is visible for aged PMMA and blue line does the same for new PMMA. Error bars show the standard deviation.*

### ANOVA gloss

ANOVA of gloss measurements showed that none of the treatments had a statistically significant impact on the numerical gloss of treated samples with aged synthetic soil.

## WEIGHT MEASUREMENTS

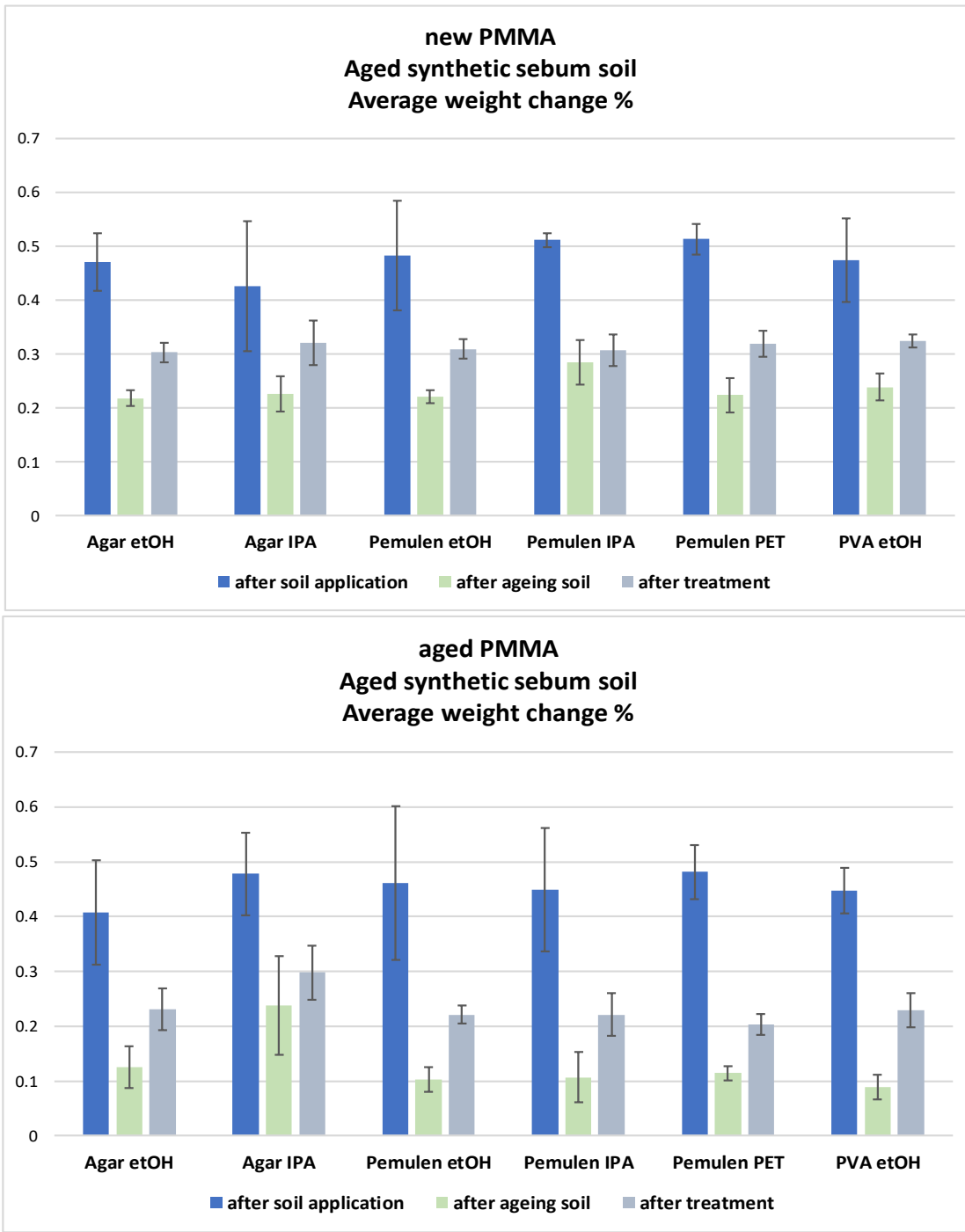
### Weight changes %

After synthetic soil application (Graph 9.18 - blue bar), all samples gained weight in a consistent manner, confirming that systematic errors were avoided due to the efficacious standardised application performed in a randomised order. After 32 days of ageing in the chamber (green bar) all samples lost weight. This loss was attributed to component loss from both synthetic soil and the PMMA or/and to the wet cycles of the accelerated ageing which

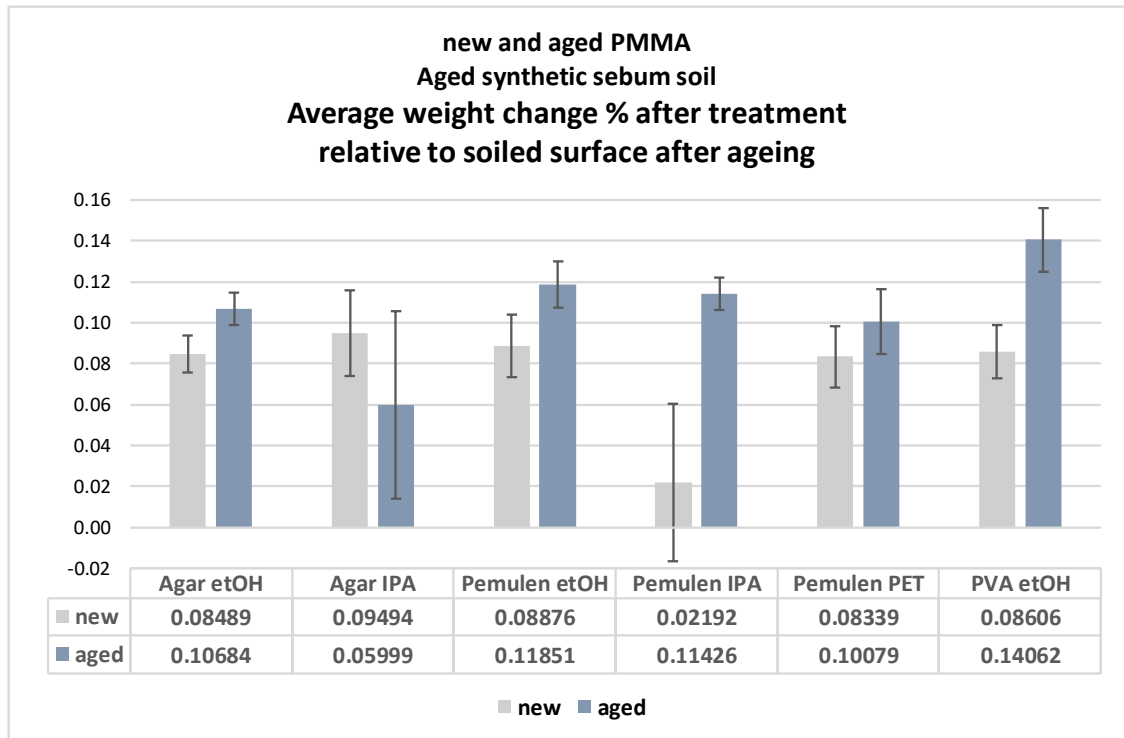
could have washed off some of the soil. Aged samples inconsistently lost on average 0.08 % more than new samples. New samples after ageing, were expected to undergo chain scissions responsible for the documented weight loss, but also competitive crosslinking reactions that counterbalance the loss by causing weight increase.

Aged samples, upon application of synthetic soil, were further aged for 32 days, reaching a total of 64 days under UV radiation. According to the ATR-FTIR analysis in Chapter 4.3.3, PMMA aged for 64 days showed a similar level of chemical degradation to samples after 32 days. The main difference being that only chain scission had taken place. Chain scission manifests itself as weight loss, and this may partly explain how aged samples with aged synthetic soil showed greater loss than new. This interpretation would only be possible if UV radiation penetrated the synthetic soil layer and reached the PMMA sample. Knowing that the synthetic soil layer was roughly around 25-30  $\mu\text{m}$  according to combined information obtained from the comb gauge and the NMR, UV radiation was expected to have moved through it and reached the PMMA surface. Especially since observation under high magnification (Fig. 9.12) showed that part of the soil was lost to evaporation under UV radiation and washed off during the wet cycles, leaving areas of the PMMA surfaces exposed. As discussed previously, UV photodegradation initiates at the surface but can penetrate the bulk via surface defects.

Studies of natural and artificial fingerprints of similar composition to the synthetic soil used here, showed that their decomposition occurred more rapidly in the presence of light, especially UV (Johnston and Rogers 2017). This is particularly expected for the unsaturated compounds, squalene and oleic acid, in the formulation (Archer *et al.* 2005; Croxton *et al.* 2010; Cadd *et al.* 2015). Degradation due to increased temperature resulted to the formation of lower molecular weight compounds with subsequent volatilisation (Girod *et al.* 2015). This loss of volatile compounds along with significant decrease of squalene and oleic acid concentration generally led to mass decrease over time (Archer *et al.* 2005). A fingerprint was seen to lose nearly 98 % of its original weight within 72 hours of deposition in ambient environment (Cadd *et al.* 2015). Therefore, synthetic soil in this study was primarily held responsible for the weight loss of samples after 32 days UV ageing.



Graph 9.18. Average weight change % of new (upper) and aged (bottom) PMMA - averaged from five replicates - after application of synthetic soil (blue), ageing of the soil (green) and cleaning treatment (grey). Changes % are normalised to the starting/initial weight. Error bars show the standard deviation.



*Graph 9.19. Average weight change % of new and aged PMMA with aged synthetic soil after the cleaning treatments - averaged from five replicates. Changes % are calculated as the change between the soiled surface after ageing and the surface after treatment. Error bars show the standard deviation.*

All treatments caused samples to gain weight (Graph 9.19). New samples consistently gained on average 0.087 % (calculated as the change between the soiled surface after ageing and after treatment), except for Pemulen IPA that gained the least (0.02 %). Visual evaluation of samples treated with Pemulen IPA indicated removal of aged synthetic soil and high magnification confirmed negligible gel residue. Therefore, the negligible weight gain was attributed to absorption of small quantity of H<sub>2</sub>O from the gel. Pemulen EtOH, Pemulen PET and PVA EtOH deposited extensive gel residue, which explains the weight gained by treated samples. Agar treatments were also seen to deposit residues on top of the aged synthetic soil they failed to remove.

Aged samples consistently gained on average 0.11 % (relative to the soiled surface after ageing), except for samples after PVA EtOH that gained the largest weight (0.14 %) and Agar IPA that gained the least (0.05 %). Agar IPA failed to remove any aged synthetic soil and deposited the least residues compared to Pemulen and PVA gels, owing to its rigidity and well-defined shape. The small weight gain was attributed to these gel residues. PVA EtOH deposited extensive gel residue across the aged PMMA surfaces, as revealed under the SEM, explaining the increased weight gain. Pemulen IPA successfully cleaned aged PMMA and left no gel residue. Pemulen with EtOH and PET were less successful at removing aged synthetic soil and deposited extensive gel residue. Yet, all three treatments caused a comparable 0.10 % weight

gain to PMMA. A possible explanation is that cleaned PMMA surfaces came in direct contact with Pemulen IPA and the free H<sub>2</sub>O expelled from it during treatment. This H<sub>2</sub>O penetrated the voids formed during ageing, causing an increase in weight. H<sub>2</sub>O release is dependent on the gel network and its interaction with surface components to be cleaned. In this gel system, H<sub>2</sub>O/IPA mixture was expected to have slowly evaporated from the gel.

### **ANOVA weight change %**

ANOVA of the weight change % showed that none of the treatments influenced the weight fluctuation in a statistically significant manner. Comparing this to the analysis of visual evaluation suggests that data from bulk gravimetric analysis are not significant to the assessment of treatments at this point.

### **ATR-FTIR**

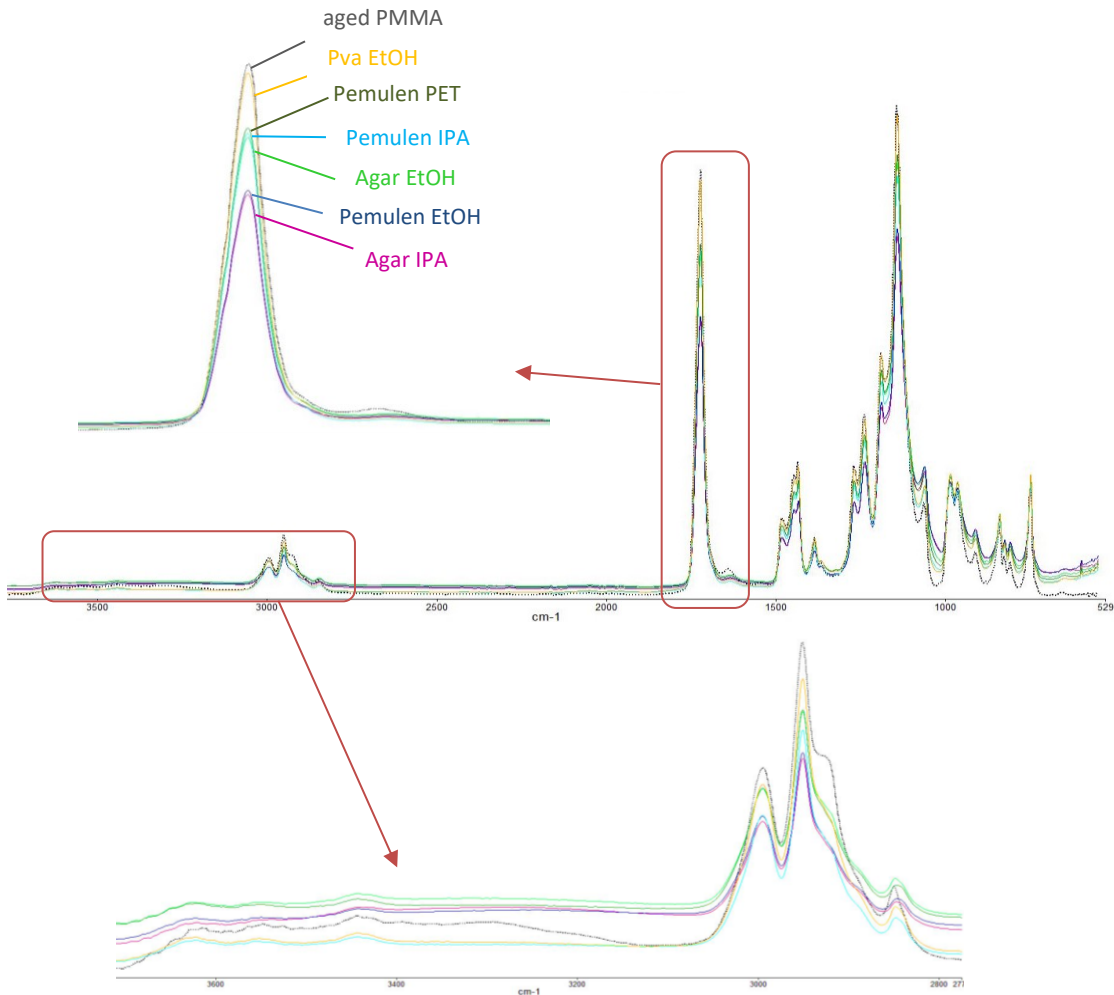


*Figure 9.15. Spectra of new PMMA samples with aged synthetic soil after gel treatment. The spectra are averaged from 3 replicates for each treatment. Each replicate is averaged from 3 spot ATR analyses. Peaks are enlarged and labelled. The spectrum of 32-days aged control (untreated, unsoiled) is included for comparison.*

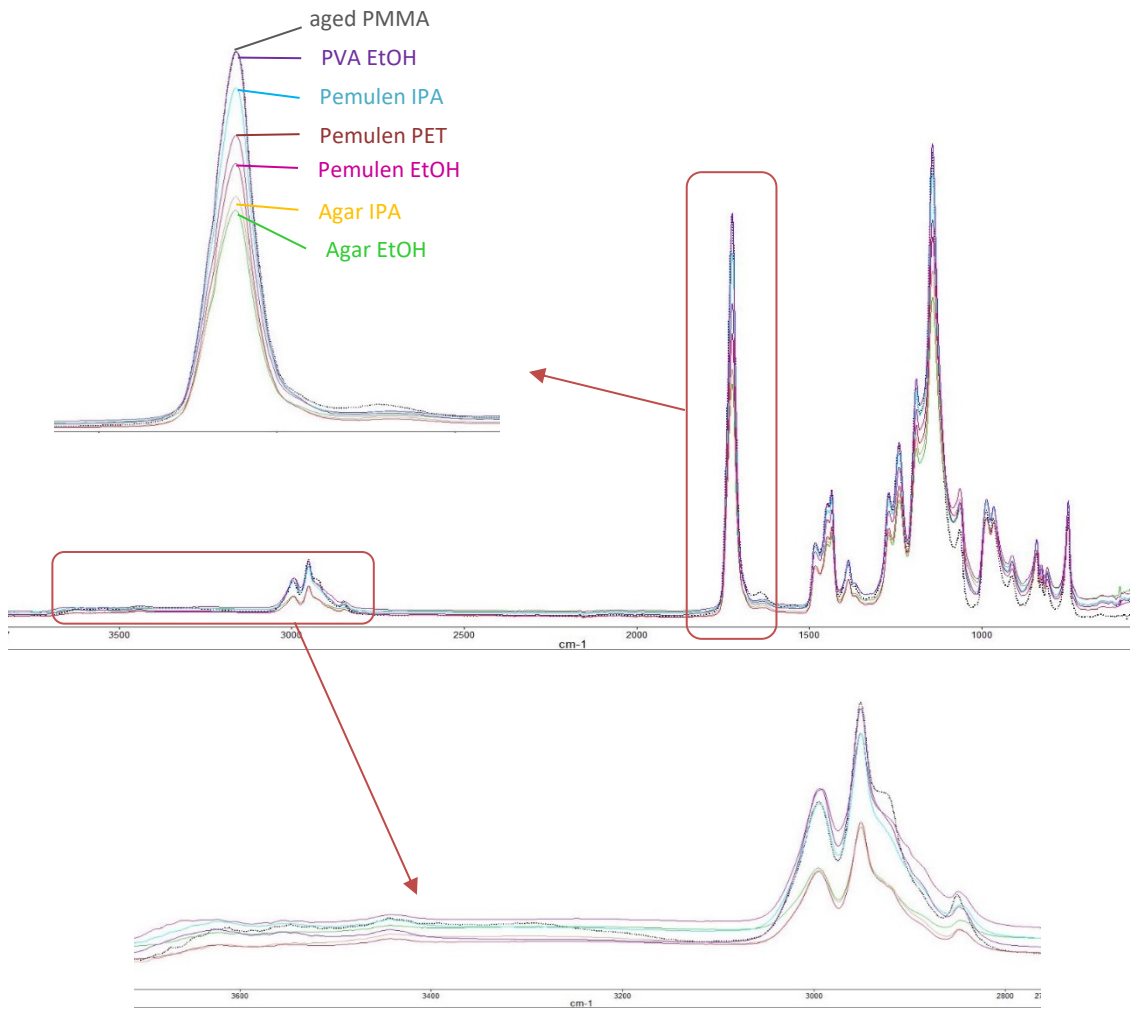


Figure 9.16. Spectra of aged PMMA samples with aged synthetic soil after solvent-gel treatment. The spectra are averaged from 3 replicates for each treatment. Each replicate is averaged from 3 spot ATR analyses. Peaks are enlarged and labelled. The spectrum of 32-days aged control (untreated, unsoiled) is included for comparison.

After treatment all samples exhibited characteristic absorption bands of the 32-day UV-aged PMMA (control) (see Chapter 4.3.1 Table 4.4), indicating that all treatments altered the surface chemistry of PMMA (Fig. 9.15-9.16). PVA EtOH caused the least change among treatments. Agar with EtOH and IPA caused the greatest decrease of peaks (loss of carbonyls), indicating the greatest surface change. Agar EtOH caused to all PMMA the formation of a new, small band at  $882\text{ cm}^{-1}$ . This peak has been previously attributed to surface crystallisation after prolonged PMMA contact with free EtOH (see Chapter 7.1.2). This change was only induced by EtOH thickened in Agar, suggesting that the gel allowed more contact between the free liquid and the PMMA surface than Pemulen and PVA gels.

9.2.2.b. Aged PSA

VISUAL OBSERVATIONS

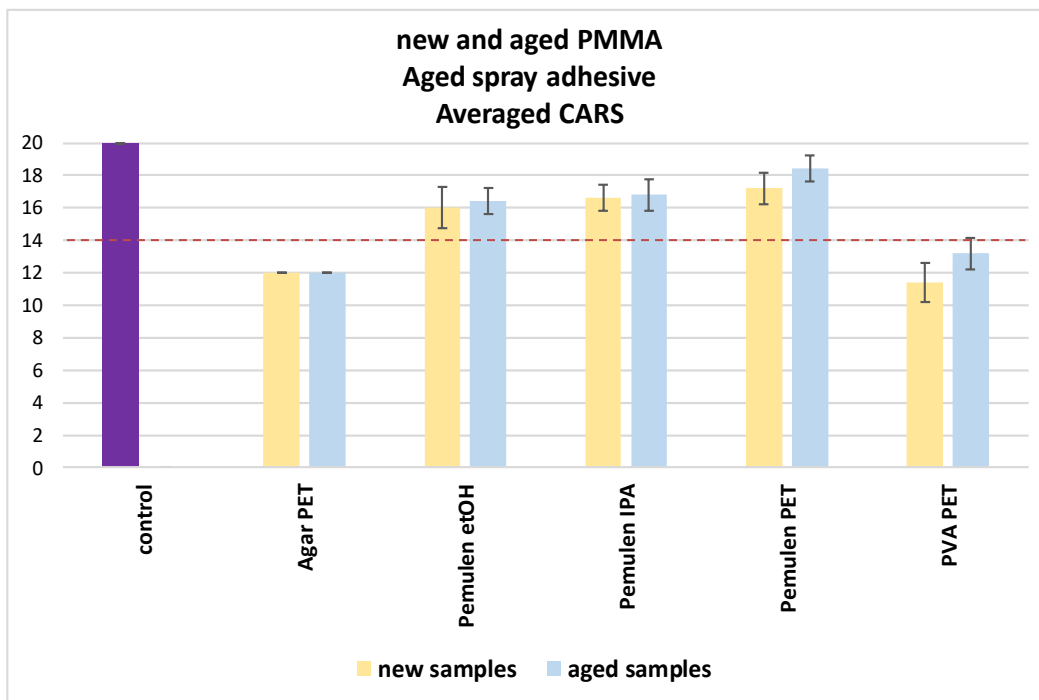
Macroscopic evaluation

Agar and PVA with PET failed to remove aged PSA. Pemulen solvent-gels, particularly with PET, were the most successful at removing aged PSA from all PMMA surfaces.

samples with aged adhesive		
	new	aged
Agar PET	not cleaned	not cleaned
Pemulen EtOH	partly cleaned	cleaned
Pemulen IPA	partly cleaned	cleaned
Pemulen PET	cleaned	cleaned
PVA PET	not cleaned	not cleaned

Table 9.12. Macroscopic observation of the overall impression of the aged PSA removal from new and aged PMMA after treatment.

CARS scores



Graph 9.20. CARS scores of treated new and aged PMMA samples with aged PSA. Scores are based on a five-point progressive ranking from 0 (worst) to 4 (best). Scores, expressed as a bar chart, are averaged from 5 replicates for each treatment. Untreated new and aged PMMA controls scored the highest possible CARS 20 in all categories ‘Dirt residue’, ‘Abrasion’ and ‘Gel residue’. Red line shows below which point treatments failed to remove PSA. Error bars show the standard deviation.

All Pemulen treatments, with EtOH, IPA and PET, left PMMA surfaces the cleanest, according to human perception (Graph 9.20). Pemulen with EtOH and IPA left surfaces in a very similar visual



condition. Agar and PVA with PET performed poorly on all surfaces, leaving PMMA in the worst surface condition (scored lowest CARS). According to Table 9.12 the latter two treatments failed to remove PSA. Combination of CARS scores with the overall impression in Table 9.12 suggested that treatments scoring below 14 (see line in Graph 9.20) failed to remove aged PSA.

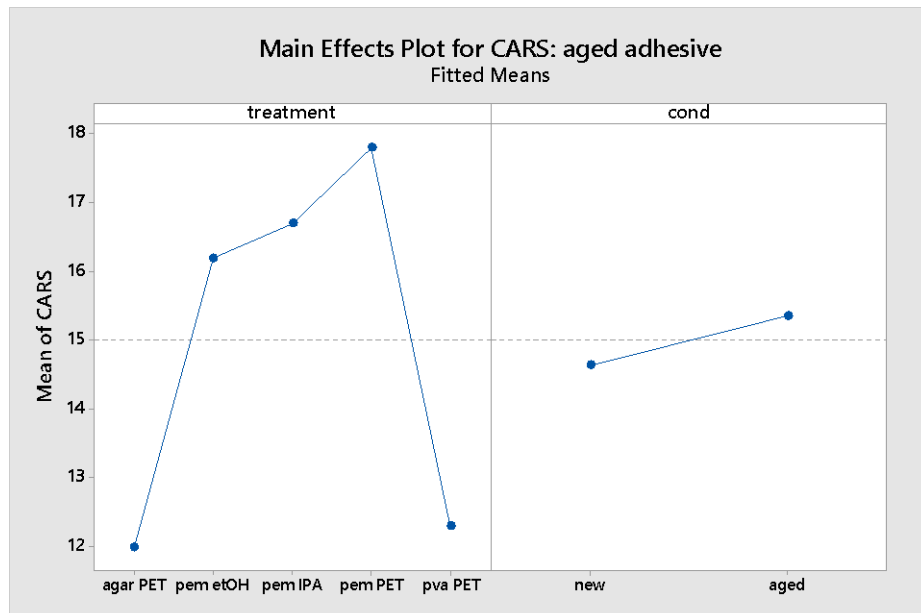
**ANOVA CARS**

ANOVA of the CARS showed that Treatments had a statistically significant impact on the effectiveness of cleaning PMMA with aged PSA. Tukey’s HSD compared variables and determined that Agar PET with PVA PET performed similarly in a statistically significant manner, so were paired together. Pemulen PET and Pemulen EtOH were allocated unique letters indicating that they also significantly affected the visual condition of treated samples. According to the main effects plot (Graph 9.21) Agar and PVA with PET scored the lowest CARS negatively impacting the cleaning outcome. Pemulen with PET and EtOH scored the highest CARS (above the mean value), having a positive impact on PMMA.

**Grouping Information Using the Tukey Method and 95% Confidence**

treatment	N	Mean	Grouping
pem PET	10	17.800	A
pem IPA	10	16.700	A B
pem etOH	10	16.200	B
pva PET	10	12.300	C
agar PET	10	12.00	C

*Means that do not share a letter are significantly different.*



Graph 9.21. The mean CARS scores of Pemulen PET and Pemulen EtOH are the highest, while that of Agar PET and PVA PET the lowest, indicating they affected cleaning of PMMA with aged PSA in a positive and a negative manner, respectively.

**SEM imaging**

Under high magnification, the PMMA controls with aged PSA appeared similar (Fig. 9.17), regardless of surface condition of PMMA. Before ageing, PSA on both new and aged controls formed an uneven layer with clots of PSA and air bubbles. After ageing these layers became slightly more sporadic; A possible explanation for this could be due to the accelerated ageing which includes wet cycles that could have washed off some of the PSA, leaving areas of the PMMA surfaces partially exposed. The air bubbles, earlier seen, were also diminished, but still visible.

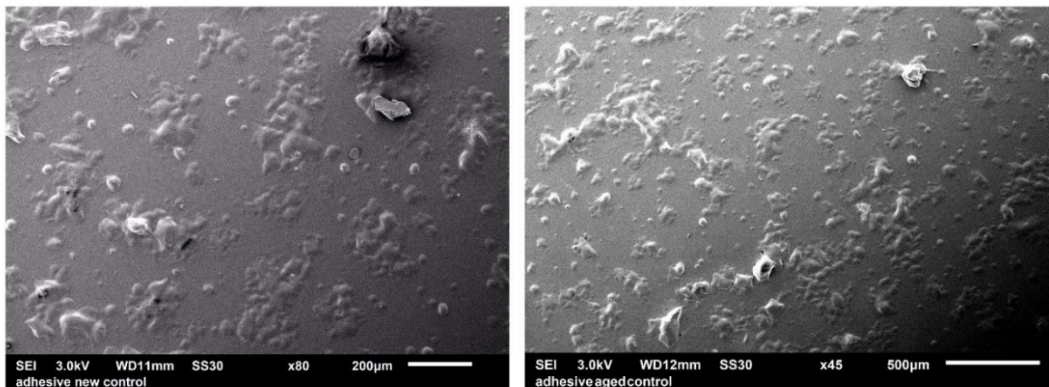
**Control PMMA with aged PSA**

Figure 9.17. SEM micrographs: PMMA controls with aged PSA: Unaged under magnification x80 (left) and aged under magnification x45 (right).

**New PMMA samples with aged PSA:**

New PMMA samples after treatment				
Treatment	Aged PSA	Gel residue	Comments	Figure no.
Agar PET	not cleaned	limited	residual cotton swab threads	9.18 A
Pemulen EtOH	partly cleaned	extensive		9.18 C, D
Pemulen IPA	partly cleaned	extensive	scratches	9.18 G
Pemulen PET	cleaned	no	solute deposition from drying droplets	9.19 A, B
PVA PET	not cleaned	extensive	Discolouration to the naked eye*	9.19 E, F

Table 9.13. Evaluation based on SEM imaging of treated new PMMA samples with aged PSA.

\* This phenomenon was explained earlier as a combination of loss of transparency and fine deposits, often accompanying gel residue.

**Aged PMMA samples with aged spray PSA:**

<b>Aged PMMA samples after treatment</b>				
Treatment	Aged PSA	Gel residue	Comments	Figure no.
<b>Agar PET</b>	not cleaned	extensive		9.18 B
<b>Pemulen EtOH</b>	partly cleaned	extensive	some scratches	9.18 E, F
<b>Pemulen IPA</b>	cleaned	extensive**		9.18 H
<b>Pemulen PET</b>	cleaned	limited	Discolouration to the naked eye*	9.19 C, D
<b>PVA PET</b>	not cleaned	extensive	some scratches, discolouration	9.19 G, H

*Table 9.14. Evaluation based on SEM imaging of treated aged PMMA samples with aged PSA.*

\*\* Pemulen IPA left aged surfaces with extensive gel residue, revealed from the haziness of the images (discussed earlier at 9.1.2.a.)

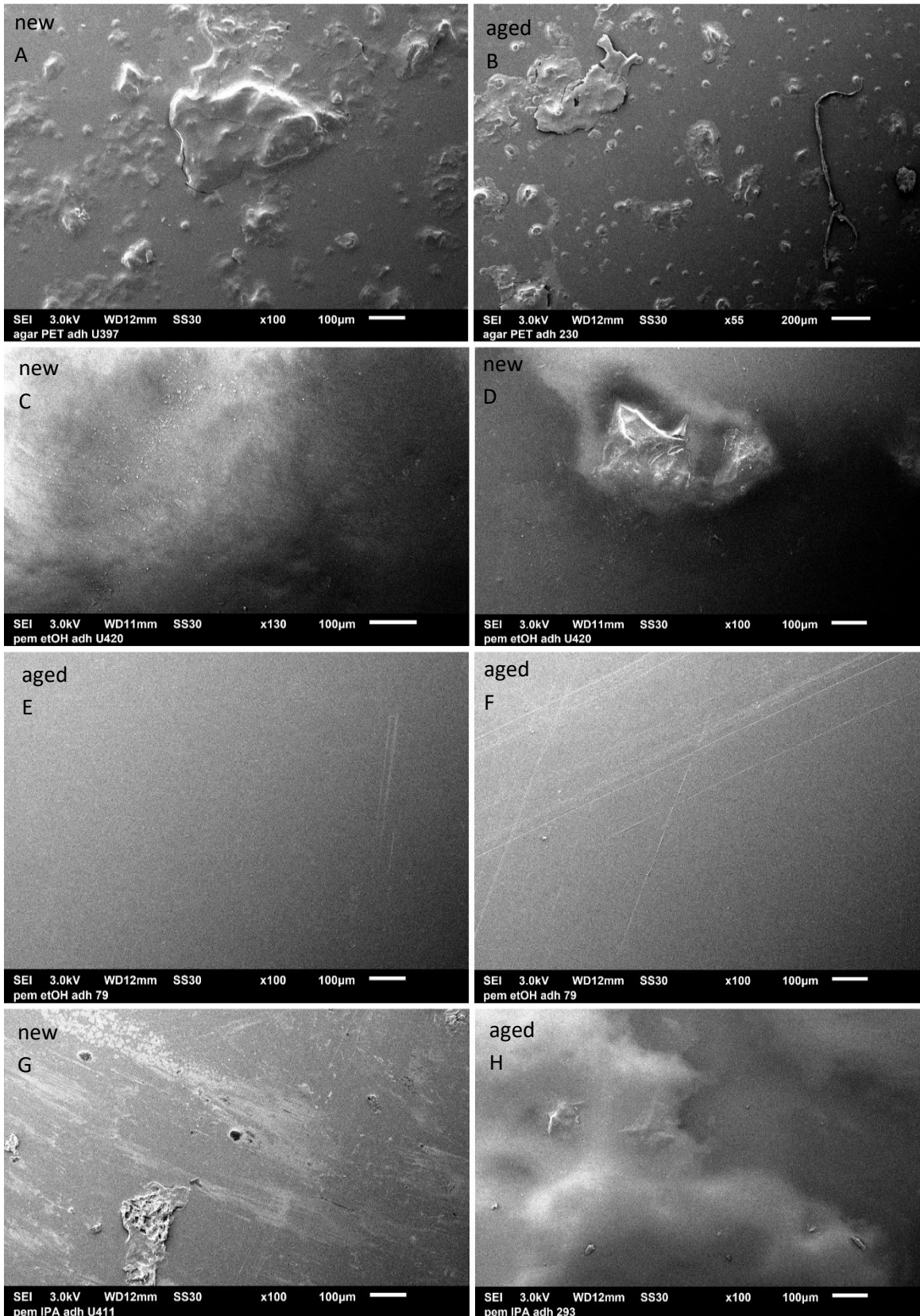


Figure 9.18. SEM micrographs: A, B: Agar PET failed to clean PMMA and deposited gel residue. C, D: Pemulen EtOH residues on new PMMA causing the haziness of images. E: Pemulen IPA left aged PMMA clean and F: with limited scratches. G: Pemulen IPA deposited gel residue and caused scratches to new PMMA. H: Pemulen IPA residues on aged PMMA causing the haziness of images.

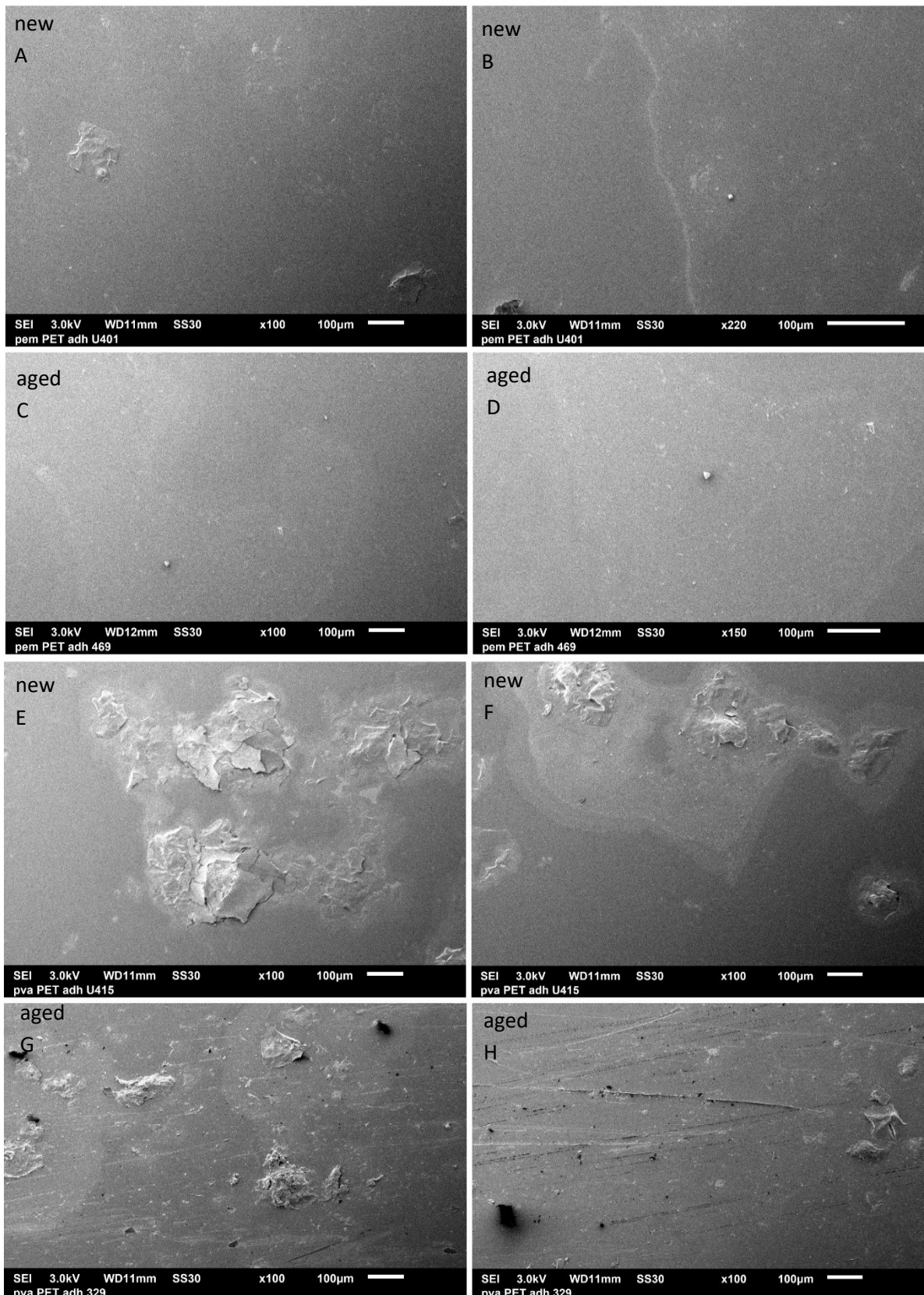
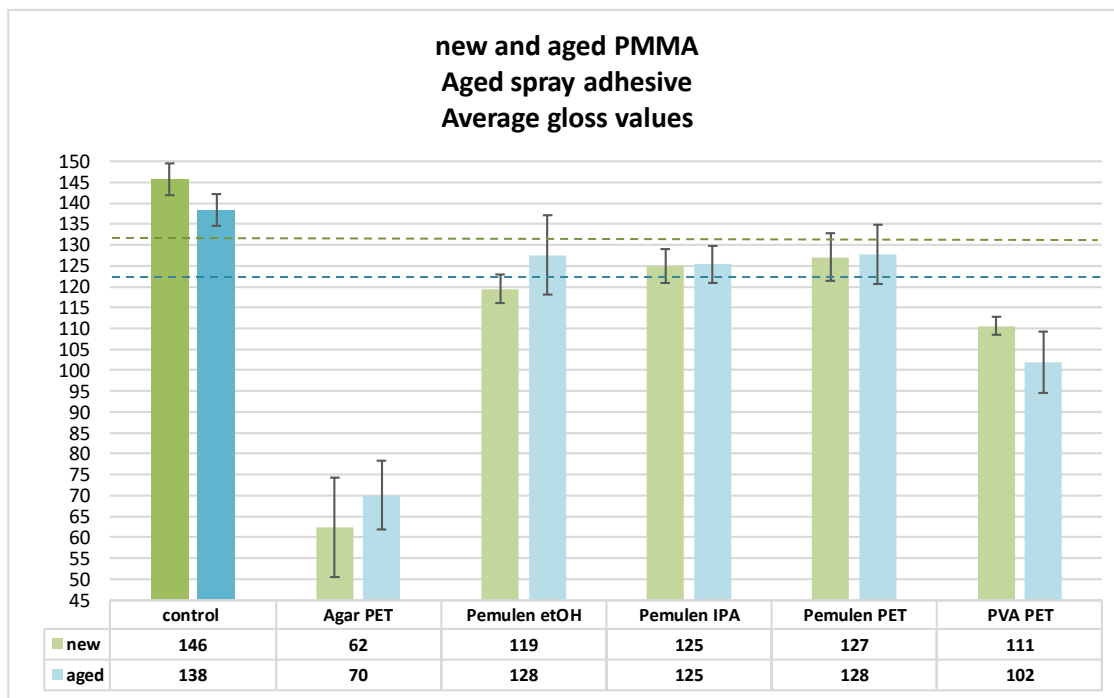


Figure 9.19. SEM micrographs: A: Pemulen PET left new PMMA clean with limited gel residue. B: Clean new PMMA with solute deposition from droplet evaporation. C, D: Pemulen PET cleaned aged PMMA and induced some discolouration. E, F: PVA PET failed to remove PSA and caused discolouration around gel residues. G: PVA PET caused discolouration around gel deposits on aged PMMA and H: induced scratches.

## GLOSS

### Gloss measurements

Aged samples exhibited higher gloss than new samples (Graph 9.22). Pemulen with EtOH, IPA and PET left aged surfaces in the best visual condition with gloss difference less than 15 GU from the controls. This rendered treated surfaces equally glossy to the control. All treatments caused a drop in gloss to new PMMA greater than 15 GU from the control, indicating a macroscopically noticeable change. PVA PET and Agar PET left all surfaces with the biggest drop in gloss, justified by their complete inability to remove aged PSA, in agreement with visual observation.

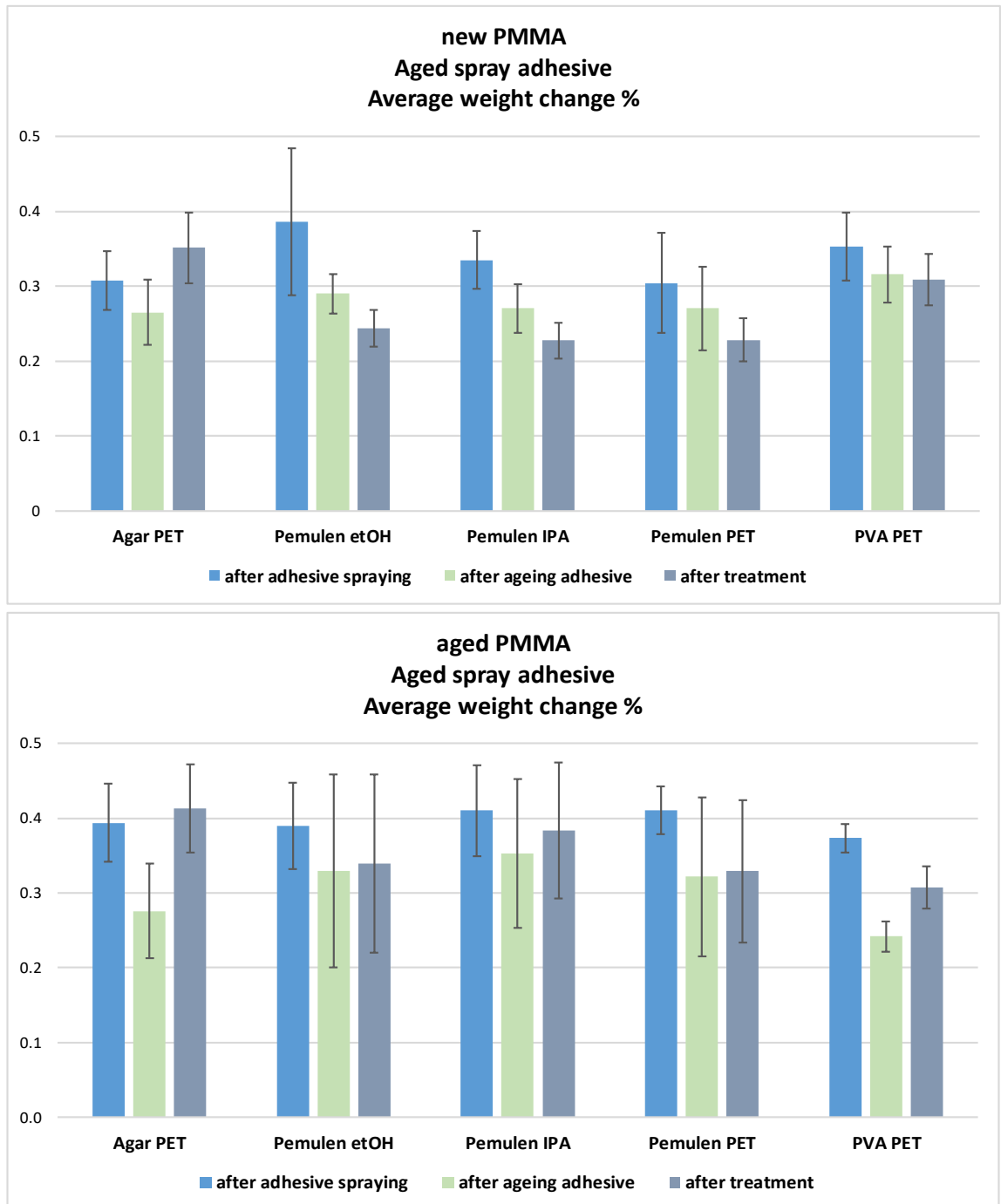


*Graph 9.22. Gloss measurements of new and aged PMMA samples with aged PSA after treatment, plotted as bar charts. Gloss units (GU) are averaged from 3 repetitions of 3 spot measurements on 3 replicates. Differences < 15 GU are non-detectable by the human eye. The PMMA controls are highly glossy with a value of 146 GU for the unaged and 138 GU for the aged. Blue line shows below which point change is visible for aged PMMA and green line does the same for new PMMA. Error bars show the standard deviation.*

### ANOVA gloss

ANOVA of the gloss measurements showed that none of the treatments influenced the numerical gloss of samples in a statistically significant manner.

## WEIGHT MEASUREMENTS

Weight changes %

Graph 9.23. Average weight change % of new (upper) and aged (bottom) PMMA - averaged from five replicates - after application of PSA (blue), ageing of the PSA (green) and cleaning treatment (grey). Changes % are normalised to the starting/initial weight. Error bars show the standard deviation.

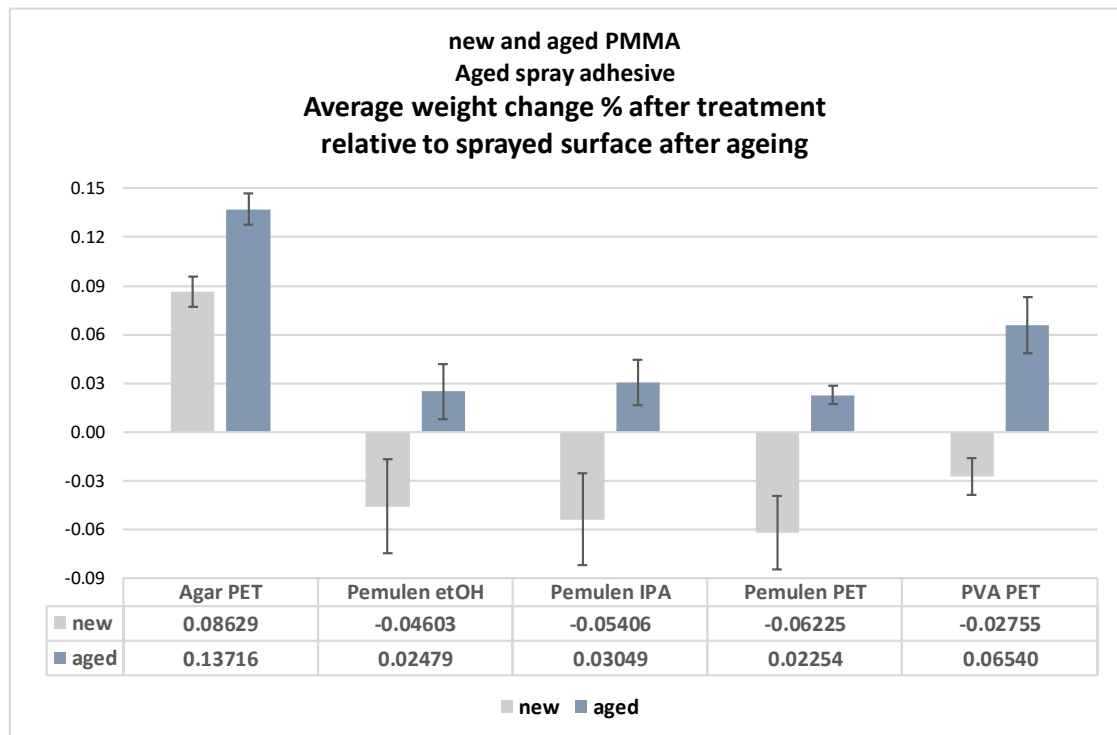
After application of PSA (Graph 9.23 - blue bar), all samples consistently gained weight, confirming that standardised application was efficiently performed. Aged samples gained on average 0.15 % more compared to new. This additional weight increase in aged samples was attributed to penetration of PSA in the voids formed during UV ageing. New PMMA did not

allow PSA to diffuse in its bulk due to its denser network with a lower free volume. In addition, once in contact with the solvent present in PSA, new surfaces were likely to undergo solvent-induced dissolution/extraction leading to loss of volatile polymer components and solvent penetration through surface defects and amorphous regions.

After 32 days of ageing (Graph 9.23 - green bar) all samples lost weight. This was attributed to component loss from both PSA and PMMA or/and to the wet cycles of accelerated ageing which could have washed off some of the PSA. Aged samples inconsistently lost on average 0.04 % more than new. New surfaces after 32 days ageing were expected to undergo competitive reactions of crosslinking and chain scission, resulting in both weight gain and loss. Aged samples, upon application of PSA, were further aged for 32 days, reaching a total of 64 days under UV radiation. At this point only chain scission took place leading to weight loss (see Chapter 4.3.3), explaining how aged samples showed greater loss than new. Regarding the acrylic PSA, it was anticipated that it would follow similar degradation pathways as PMMA, confirmed by py-GC/MS studies indicating side and main chain scission (Czech *et al.* 2009). Ageing of PSA led to formation of lower molecular weight compounds, which tend to be subsequently volatilised, resulting in loss of weight.

After treatment, all Pemulen gels caused new samples to lose on average 0.19 % (Graph 9.24) (calculated as the change between the sprayed surface after ageing and after treatment). Visual evaluation confirmed the removal of aged PSA justifying weight loss. However, Pemulen with alcohols left extensive gel residue, and yet induced weight loss. As discussed earlier, alcohol mixtures with H<sub>2</sub>O may penetrate the samples' bulk and cause dissolution and evaporation of polymer components, during the 24 hours left to stand prior to weighing. This would lead to additional weight decrease. PVA PET caused negligible weight loss (0.02 %) to new PMMA, as it failed to remove PSA. By comparison, Pemulen gels caused aged samples to negligibly gain on average 0.02 % (Graph 9.24), in comparable amounts. Treatments left surfaces clean and with no residual gel, so weight gain is attributed to H<sub>2</sub>O penetration in the voids of the 64-day aged PMMA. PVA PET failed to remove PSA from aged surfaces and deposited extensive gel residue, which explains the weight gain (0.06 %). Agar PET caused the greatest gain to new (0.08 %) and aged samples (0.14 %), attributed to the extensive gel residue deposited on the PSA it failed to remove.





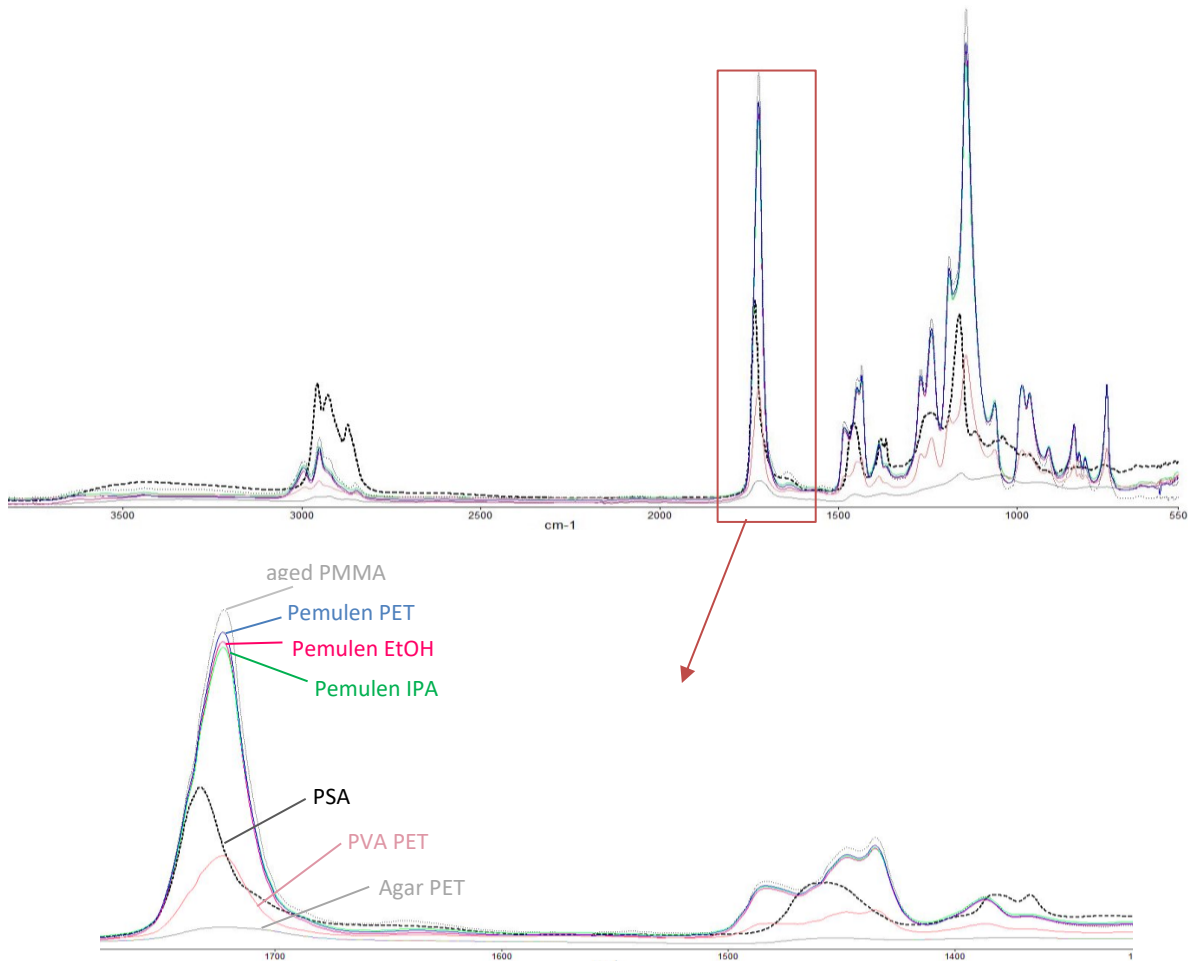
*Graph 9.24. Average weight change % of new and aged PMMA with aged PSA after the cleaning treatments - averaged from five replicates. Changes % are calculated as the change between the sprayed surface after ageing and the surface after treatment. Error bars show the standard deviation.*

### **ANOVA weight change %**

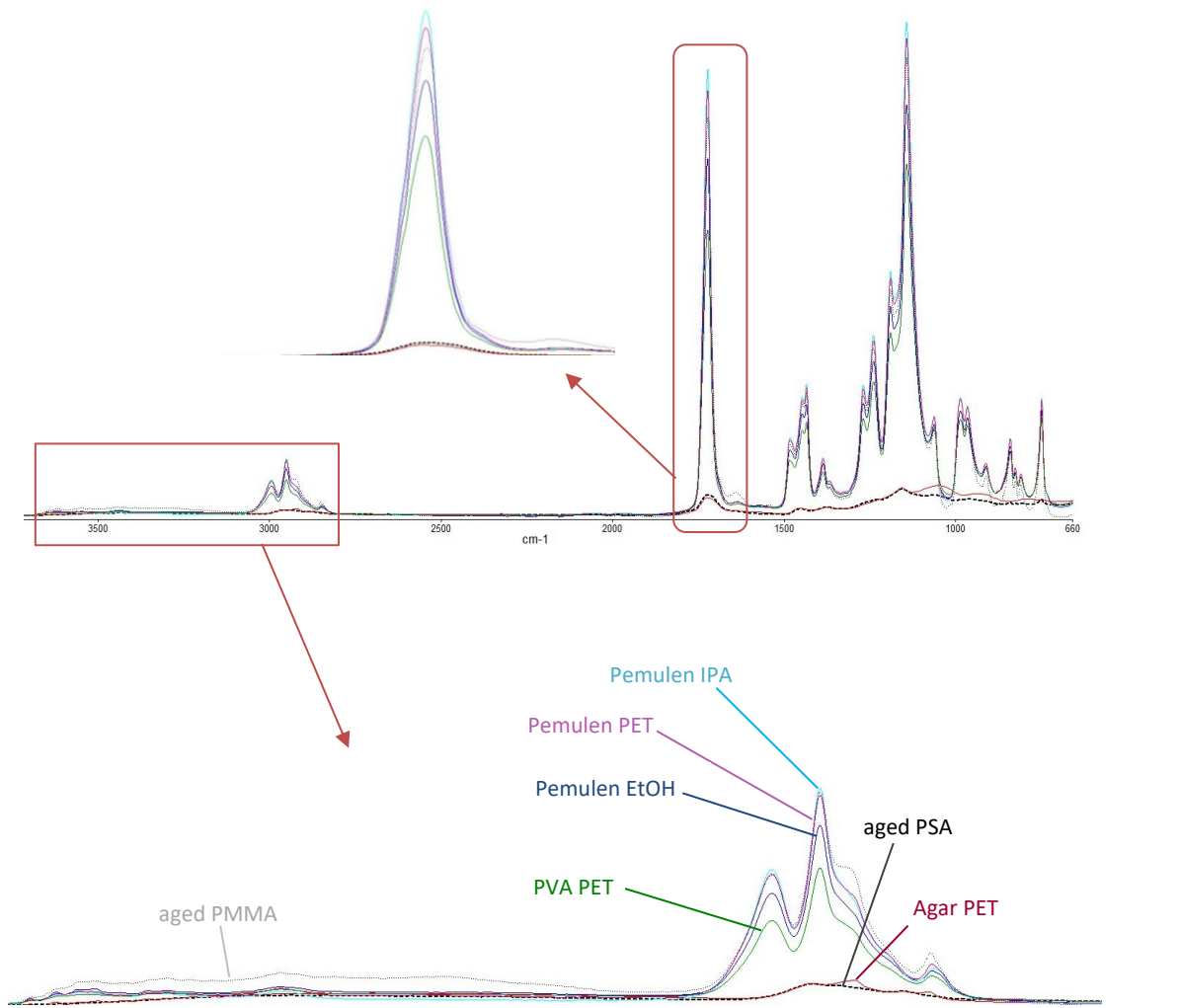
ANOVA of weight change % showed that none of the treatments influenced the weight fluctuation in a statistically significant manner.

### **ATR-FTIR**

After treatment with Pemulen all samples exhibited characteristic absorption bands of the 32-day aged PMMA control (see Chapter 4.3.1 Table 4.4), indicating that these treatments altered the PMMA surface chemistry. Visual evaluation confirmed removal of aged PSA, but revealed extensive gel residue. The IR bands of Pemulen overlap those of PMMA (see Chapter 7.1.1.1), explaining the increased absorption. After Agar PET and PVA PET (except on aged PMMA) samples exhibited characteristic absorption bands of aged PSA (Graph 9.25-9.26) indicating their inability to remove it.



Graph 9.25. Spectra of new PMMA samples with aged PSA after gel treatment. The spectra are averaged from 3 replicates for each treatment. Each replicate is averaged from 3 spot ATR analyses. Peaks are enlarged and labelled. The spectra of 32-days aged control (untreated, unsoiled) and 32-days aged PSA on PMMA are included for comparison.



Graph 9.26. Spectra of aged PMMA samples with aged PSA after gel treatment. The spectra are averaged from 3 replicates for each treatment. Each replicate is averaged from 3 spot ATR analyses. Peaks are enlarged and labelled. The spectra of 32-days aged control (untreated, unsoiled) and 32-days aged PSA on PMMA are included for comparison.

### 9.2.3. Conclusion

#### PMMA samples with aged synthetic soil

All samples with aged synthetic soil exhibited weight gain after cleaning, regardless of whether treatments succeeded at removing the soil. Agar with EtOH and IPA, and Pemulen PET failed to remove synthetic soil and deposited gel residues, justifying the weight gain. Statistical analysis of CARS scores confirmed the negative effect of Agar IPA and Pemulen PET on cleaning PMMA. PVA EtOH partly removed aged synthetic soil, deposited extensive gel residue and induced numerous scratches. Pemulen EtOH also induced scratches. Linking back to Chapter 7.1.2, PMMA in direct contact with EtOH became more susceptible to scratches, instigated by the gentle post-treatment rinsing with cotton swabs. Agar with alcohols and Pemulen PET failed to remove any aged synthetic soil.

Pemulen with EtOH and IPA were the most successful at removing aged synthetic soil from all surfaces. Statistical analysis of CARS scores confirmed the positive impact of both treatments. This was justified by the emulsifying properties of Pemulen and the surfactant properties of TEA (Söderman and Stilbs 1994), both of which increased the gel's ability to solubilise synthetic soil (Cremonesi 2010). Alcohols as polar solvents, and TEA as a polar amine, were essential for the removal of aged synthetic soil, the polarity of which increased with ageing (Stavroudis and Blank 1989; Umney and Rivers 2003). Tukey's HSD paired the two Pemulen/alcohol treatments for offering equally satisfactory visual results. Pemulen EtOH though, offered less consistency between the aged surfaces. Under high SEM magnification, it was revealed that Pemulen EtOH deposited extensive gel residue compared to Pemulen IPA that left surfaces residue-free. Given that Pemulen with IPA and EtOH behaved similarly with the former performing somewhat more favourably, Pemulen EtOH was discarded.

#### PMMA samples with aged PSA

Results showed that Pemulen gels were the most successful at removing aged PSA from all surfaces. This was explained as the result of good bonding between the basic TEA in the gel formulation and a more acidic PSA, as a result of ageing (Stavroudis and Blank 1989). All three Pemulen treatments were paired by Tukey's HSD for offering equally satisfactory visual results. However, statistical analysis of CARS scores indicated that only Pemulen with PET and EtOH positively impacted cleaning. Therefore Pemulen IPA was removed from following experiments. Agar PET and PVA PET failed to remove aged. Statistical analysis of CARS scores and gloss measurements indicated their negative effect on cleaning PMMA. Observation under high magnification revealed that they both deposited extensive gel residue, induced scratches and formation of drying droplets, which caused surfaces to appear opaque.

## Chapter 10. MAIN EXPERIMENTS: REPEATED APPLICATIONS

---

This chapter presents the main cleaning experiments on new and aged PMMA samples with aged surface dirt. This is the final experiment designed with treatments that in previous experiments were evaluated as successful and safe at removal of aged synthetic soil and aged PSA. The aim of this chapter is to optimise the application of the successful treatments. This takes place through identification of the optimum number and duration of repeated gel applications. At this final stage of experimental work, unilateral NMR MOUSE is employed among the evaluation methods, to monitor the physical condition of samples treated with the optimised, successful treatments. This analysis intended to confirm the cleaning efficiency, and more importantly, the safety of the optimised gel treatments on new and aged PMMA.

In a realistic cleaning campaign, conservators are more likely to carry out multiple applications of wet cleaning to remove unwanted, foreign surface matter. This was especially true for paintings (Bellucci *et al.* 1999; Casoli *et al.* 2014; Angelova *et al.* 2015), for which gels were tailored to clean in the first place. Repeated applications on the same surface area were sometimes seen as necessary (Warda *et al.* 2007; Iannuccelli and Sotgiu 2010), and were expected to offer improved results. Therefore, before proceeding to the final cleaning experiment and prior to permanently eliminating treatments for being ineffective, further cleaning trials were carried out. These intended to confirm whether treatments, previously unable to remove unaged or aged surface dirt, would still fail to clean PMMA after optimised repeated application.

### 10.1. POLY (METHYL METHACRYLATE) WITH AGED DIRT

Cleaning trials were performed on new and aged PMMA with gel treatments that were previously unable to remove unaged and aged dirt after one 5-minute application. The aim was to assess the effectiveness of repeated gel applications. Unsafe treatments for use on PMMA (i.e. inducing scratches, depositing extensive gel residue) were not considered. Results are illustrated in tables with colour-coded cells; green represents satisfactory results (complete or almost complete removal), while red denotes no removal or some dissolution.

#### 5 minutes x 3 applications

Trials were carried out in duplicate with three repeated 5-minute applications (see Table 10.1 for tested treatments). Pemulen hydrogel represented H<sub>2</sub>O-based treatments, absent from previous experiments due to their inability to remove synthetic soil or PSA. Pemulen was selected as the most satisfactory gel carrier at cleaning PMMA in this study.

Treatments unable to remove (un)aged dirt after one 5-minute application	
synthetic sebum soil	spray adhesive
Agar IPA	Agar EtOH
Agar PET	Agar IPA
PVA IPA	Agar PET
PVA PET	PVA EtOH
Pemulen H <sub>2</sub> O	PVA IPA
Pemulen PET	PVA PET
	Pemulen H <sub>2</sub> O

Table 10.1. Treatments unable to remove unaged or aged synthetic soil and PSA from PMMA after one 5-minute application, were tested with three repeated 5-minute applications.

### Results of aged synthetic soil (Table 10.2)

Agar IPA and Agar PET were tested on a third replicate due to inconsistent results, and having two successful removals of aged synthetic soil against one failed, they were re-introduced into the final experimental design along with Pemulen H<sub>2</sub>O and Pemulen PET.

### Results of aged PSA (Table 10.3)

PVA PET and Pemulen H<sub>2</sub>O were re-introduced into the final experimental design. The rest failed to remove aged PSA.

aged synthetic sebum soil 5 minutes x 3 applications			
Replicate A	1st application	2nd application	3rd application
Agar IPA	SD	PR	CR
Agar PET	SD	SD	PR
PVA IPA	SD	N	N
PVA PET	N	N	N
Pemulen PET	SD	SD	PR
Pemulen H <sub>2</sub> O	PR	PR - CR	CR
Replicate B	1st application	2nd application	3rd application
Agar IPA	SD	N	N
Agar PET	SD	N	N
PVA IPA	SD	N	N
PVA PET	N	N	N
Pemulen PET	PR	PR	PR
Pemulen H <sub>2</sub> O	PR	PR - CR	CR

**N = no removal**                      **PR = partial removal**  
**SD = some dissolution**           **CR = complete removal**

Table 10.2. Duplicate trials with three repeated 5-minute applications on PMMA with aged synthetic soil.

aged spray adhesive 5 minutes x 3 applications			
Replicate A	1st application	2nd application	3rd application
Agar etOH	N	N	N
Agar IPA	N	N	N
Agar PET	N	N	N
PVA etOH	N	N	N
PVA IPA	N	N	N
PVA PET	SD	PR - CR	CR
Pemulen H2O	PR - CR	CR	CR
Replicate B	1st application	2nd application	3rd application
Agar etOH	N	N	N
Agar IPA	N	N	N
Agar PET	N	N	N
PVA etOH	N	N	N
PVA IPA	N	N	N
PVA PET	N	PR	PR - CR
Pemulen H2O	PR	PR - CR	CR

**N = no removal**                      **PR = partial removal**  
**SD = some dissolution**           **CR = complete removal**

Table 10.3. Duplicate trials with three repeated 5-minute applications on PMMA with aged PSA.

#### 1 minute versus 3 minutes x 3 applications

Comparison of three repeated applications of 1 and 3 minutes with some of the successful treatments, showed the following results:

- 3-minute treatments systematically offered better results, even after the first application.
- In some occasions, three applications of 1-minute and 3-minute treatments offered similar results: see PVA EtOH on aged synthetic soil (Table 10.4) and Pemulen EtOH on aged PSA (Table 10.5).
- Applications continued until aged dirt was fully removed showed that approximately five 1-minute applications were required, as opposed to only three 3-minute applications.
- Since 1-minute treatments were unsatisfactory, shorter application times were not examined.

aged synthetic sebum						
1 minute vs 3 minutes x 3 applications						
Replicate A	1st application		2nd application		3rd application	
	1 min	3 min	1 min	3 min	1 min	3 min
Pemulen IPA	SD	PR	SD	CR	SD	CR
PVA etOH	PR	ACR	CR	CR	CR	CR
Agar PET	SD	PR	PR	PR	CR	CR
Replicate B	1st application		2nd application		3rd application	
	1 min	3 min	1 min	3 min	1 min	3 min
Pemulen IPA	PR	ACR	PR	CR	ACR	CR
PVA etOH	PR	PR	PR	ACR	CR	CR
Agar PET	SD	PR	SD	ACR	PR	CR

Table 10.4. Duplicate cleaning trials tested three repeated applications of 1 and 3 minutes on PMMA with aged synthetic soil.

aged spray adhesive						
1 minute vs 3 minutes x 3 applications						
Replicate A	1st application		2nd application		3rd application	
	1 min	3 min	1 min	3 min	1 min	3 min
Pemulen etOH	PR	PR	CR	CR	CR	CR
PVA PET	N	SD	SD	PR	PR	PR
Replicate B	1st application		2nd application		3rd application	
	1 min	3 min	1 min	3 min	1 min	3 min
Pemulen etOH	PR	ACR	CR	CR	CR	CR
PVA PET	N	SD	N	PR	PR	ACR

N = no removal

ACR = almost complete removal

SD = some dissolution

CR = complete removal

PR = partial removal

Table 10.5. Duplicate cleaning trials tested three repeated applications of 1 and 3 minutes on PMMA with aged PSA.

### 3 minutes versus 5 minutes x 3 applications

Owing to the success of 3 minutes x three applications, an increase of repetitions was considered unnecessary. Comparison of three consecutive applications of 3 minutes versus 5 minutes with some of the successful treatments, offered the same visual results. So the longer 5-minute treatments were discarded.

aged synthetic sebum soil						
3 minutes vs 5 minutes x 3 applications						
Replicate A	1st application		2nd application		3rd application	
	3 min	5 min	3 min	5 min	3 min	5 min
PVA etOH	PR	PR	CR	CR	CR	CR
Agar PET	SD	SD	SD	SD	PR	PR
Replicate B	1st application		2nd application		3rd application	
	3 min	5 min	3 min	5 min	3 min	5 min
PVA etOH	PR	PR	CR	CR	CR	CR
Agar PET	SD	SD	SD	SD	PR	PR

Table 10.6. Duplicate cleaning trials tested three repeated applications of 3 and 5 minutes on PMMA with aged synthetic soil.



aged spray adhesive 3 minutes vs 5 minutes x 3 applications						
Replicate A	1st application		2nd application		3rd application	
	3 min	5 min	3 min	5 min	3 min	5 min
Pemulen etOH	ACR	ACR	CR	CR	CR	CR
PVA PET	SD	SD	ACR	ACR	CR	CR
Replicate B	1st application		2nd application		3rd application	
	3 min	5 min	3 min	5 min	3 min	5 min
Pemulen etOH	ACR	ACR	CR	CR	CR	CR
PVA PET	SD	SD	ACR	ACR	CR	CR

SD = some dissolution      ACR = almost complete removal  
PR = partial removal      CR = complete removal

Table 10.7. Duplicate cleaning trials tested three repeated applications of 3 and 5 minutes on PMMA with aged PSA.

### 10.1.1. Experimental design

The successful treatments employed in the final experimental design are listed in Table 10.8. A two-level full-factorial experiment was adopted for each type of aged 'dirt' to simultaneously examine the effects of Treatments and PMMA Surface condition in isolation, as well as their interactions. The aim was to test the impact of treatments indicated as successful by previous experiments after repeated gel applications. The experiments were designed in quintuple for a total of 100 samples and carried out with three repeated applications of 3 minutes each. New and aged PMMA samples were sprayed with either synthetic soil (n=60 samples) or PSA (n=40 samples) and were aged in the Atlas chamber for 32 days.

Successful treatments for final experiment	
aged synthetic sebum soil	aged spray adhesive
Pemulen H <sub>2</sub> O*	Pemulen H <sub>2</sub> O*
Pemulen IPA	Pemulen EtOH
Pemulen PET*	Pemulen PET
Agar IPA*	PVA PET*
Agar PET*	
PVA EtOH	

Table 10.8. Successful treatments at removing aged synthetic soil and PSA from PMMA tested in the final cleaning experiment. Marked treatments with \* are reinserted after cleaning trials.

**New and aged PMMA with aged synthetic sebum soil**  
**3 minutes x 3 applications**

Experimental Variables		
Factor	A. Treatment	B. PMMA condition
<b>Levels</b>	1. Agar IPA	1. new
	2. Agar PET	2. aged
	3. Pemulen H <sub>2</sub> O	
	4. Pemulen IPA	
	5. Pemulen PET	
	6. PVA EtOH	

*Table 10.9. Experimental variables in the multilevel two-factorial design used for the main cleaning experiment on new and aged PMMA with aged synthetic soil (5 replicates). Number of levels: 6, 2.*

### Multilevel Factorial Design

Factors:            2            Replicates:        5  
 Base runs:        12            Total runs:        60

**New and aged PMMA with aged spray adhesive**  
**3 minutes x 3 applications**

Experimental Variables		
Factor	A. Treatment	B. PMMA condition
<b>Levels</b>	1. Pemulen H <sub>2</sub> O	1. new
	2. Pemulen EtOH	2. aged
	3. Pemulen PET	
	4. PVA PET	

*Table 10.10. Experimental variables in the multilevel two-factorial design used for the main cleaning experiment on new and aged PMMA with aged PSA (5 replicates). Number of levels: 4, 2.*

### Multilevel Factorial Design

Factors:            2            Replicates:        5  
 Base runs:        8            Total runs:        40

## 10.1.2. Results & interpretation

### 10.1.2.a. Aged synthetic soil

#### VISUAL OBSERVATIONS

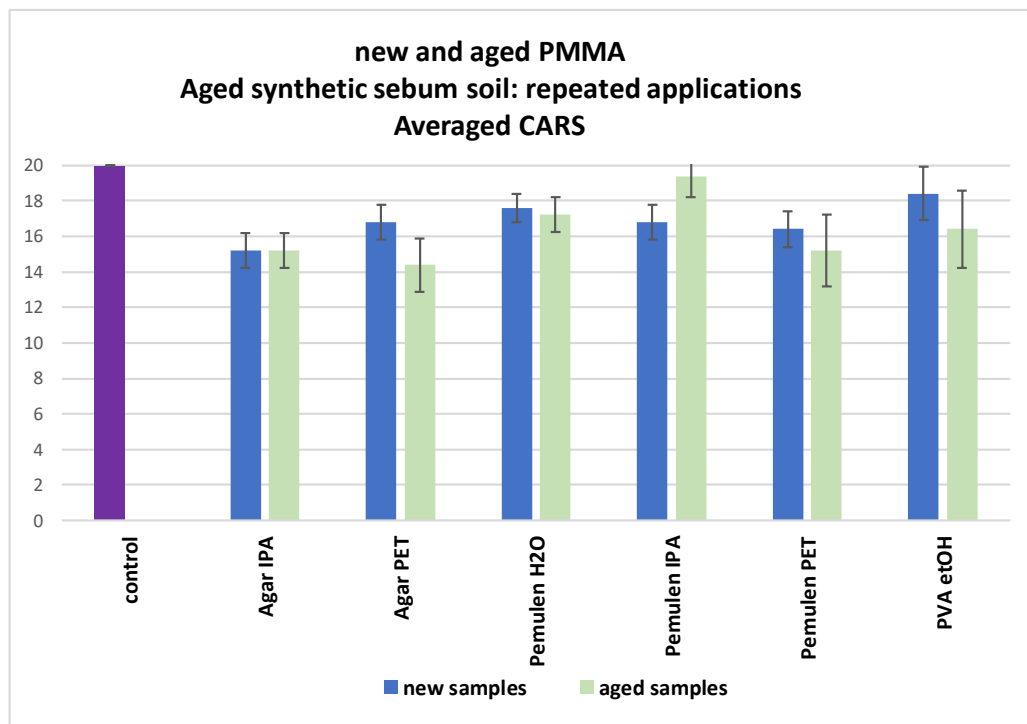
##### Macroscopic evaluation

All treatments partly or completely cleaned PMMA from aged synthetic soil. Pemulen H<sub>2</sub>O, Pemulen IPA and PVA EtOH were the most successful at removing aged synthetic soil. Agar IPA, Agar PET and Pemulen PET partly removed aged synthetic soil from all PMMA surfaces.

samples with aged synthetic soil		
	new	aged
Agar IPA	partly cleaned	partly cleaned
Agar PET	partly cleaned	partly cleaned
Pemulen H <sub>2</sub> O	partly cleaned/cleaned	partly cleaned/cleaned
Pemulen IPA	partly cleaned/cleaned	cleaned
Pemulen PET	partly cleaned	partly cleaned
PVA EtOH	partly cleaned/cleaned	partly cleaned/cleaned

Table 10.11. Macroscopic observation of the overall impression of aged synthetic soil removal from new and aged PMMA after three treatment applications of three minutes each.

#### CARS scores



Graph 10.1. CARS scores of treated new and aged PMMA samples with aged synthetic soil. Scores are based on a five-point progressive ranking from 0 (worst) to 4 (best). Scores, expressed as a bar chart, are averaged from 5 replicates for each treatment. Untreated new and aged PMMA controls scored the highest possible CARS 20 in all categories 'Dirt residue', 'Abrasion' and 'Gel residue'. Error bars show the standard deviation.

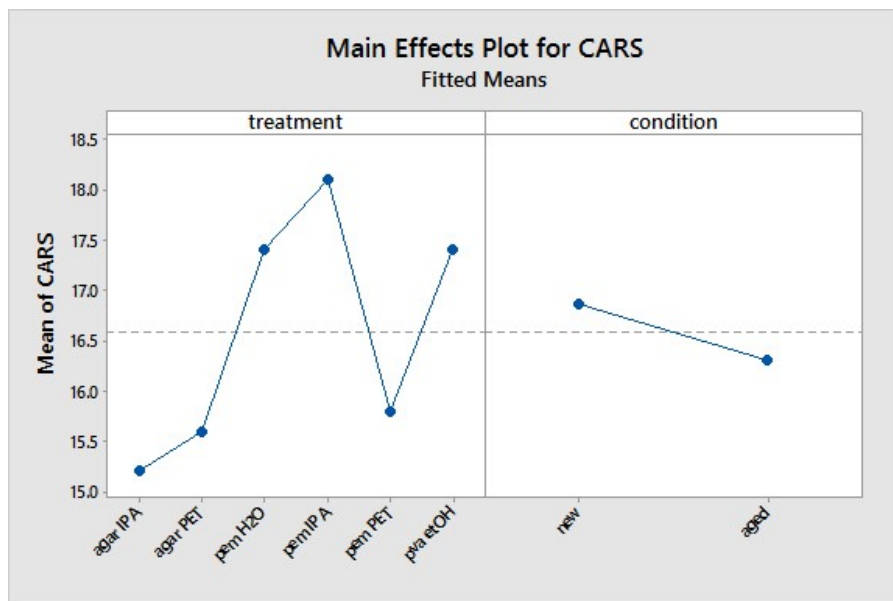
PVA EtOH left new surfaces the cleanest, while Agar IPA in the worst surface condition (scored lowest CARS), according to human perception (Graph 10.1). Agar PET, Pemulen IPA and Pemulen PET performed similarly leaving surfaces in a similar surface condition. Pemulen IPA left aged samples in the best condition (scored highest scores), while Agar PET in the worst surface condition (scored lowest CARS). Pemulen H<sub>2</sub>O left all surfaces in an equally good visual.

### **ANOVA CARS**

ANOVA of the CARS showed that Treatments had a statistically significant impact on the effectiveness of cleaning PMMA with aged synthetic soil. Tukey's HSD compared variables and determined that Pemulen IPA significantly affected the visual condition of treated PMMA samples. Tukey's HSD also paired Pemulen PET with Agar PET and Agar IPA indicating that they performed similarly in a statistically significant manner. According to the main effects plot (Graph 10.2) Pemulen IPA scored the highest CARS (above the mean value) impacting the cleaning outcome positively. The three grouped treatments scored below the means CARS value negatively impacting PMMA.

### **Grouping Information Using the Tukey Method and 95% Confidence**

<u>treatment</u>	<u>N</u>	<u>Mean</u>	<u>Grouping</u>
pem IPA	10	18.100	A
pva etOH	10	17.400	A B
pem H <sub>2</sub> O	10	17.400	A B
pem PET	10	15.800	B
agar PET	10	15.600	B
agar IPA	10	15.200	B



*Graph 10.2. The mean CARS scores of Pemulen IPA is the highest, while that of Agar IPA, Agar PET and Pemulen PET the lowest, indicating they affected cleaning of PMMA with aged synthetic soil in a positive and a negative manner, respectively.*

**SEM imaging**

For PMMA controls with aged synthetic soil see Chapter 9.2.2.a.

**New PMMA samples with aged synthetic soil:**

<b>New PMMA samples after treatment</b>				
Treatment	Aged synthetic soil	Gel residue	Comments	Figure no.
<b>Agar IPA</b>	not cleaned	no		10.1 A, B
<b>Agar PET</b>	not cleaned	no		10.1 E, F
<b>Pemulen H<sub>2</sub>O</b>	cleaned	limited	limited scratches	10.1 H, 10.2 A
<b>Pemulen IPA</b>	partly cleaned	limited	scratches	10.2 C, D
<b>Pemulen PET</b>	partly cleaned	no	solute deposition from drying droplets	10.2 F, G
<b>PVA EtOH</b>	cleaned	extensive		10.3 C

**Aged PMMA samples with aged synthetic soil:**

<b>Aged PMMA samples after treatment</b>				
Treatment	Aged synthetic soil	Gel residue	Comments	Figure no.
<b>Agar IPA</b>	not cleaned	extensive		10.1 C, D
<b>Agar PET</b>	not cleaned	extensive		10.1 G
<b>Pemulen H<sub>2</sub>O</b>	partly cleaned	no		10.2 B
<b>Pemulen IPA</b>	cleaned	no		10.2 E
<b>Pemulen PET</b>	partly cleaned	no	solute deposition from drying droplets	10.2 H, 10.3 A, B
<b>PVA EtOH</b>	cleaned	no		10.3 D

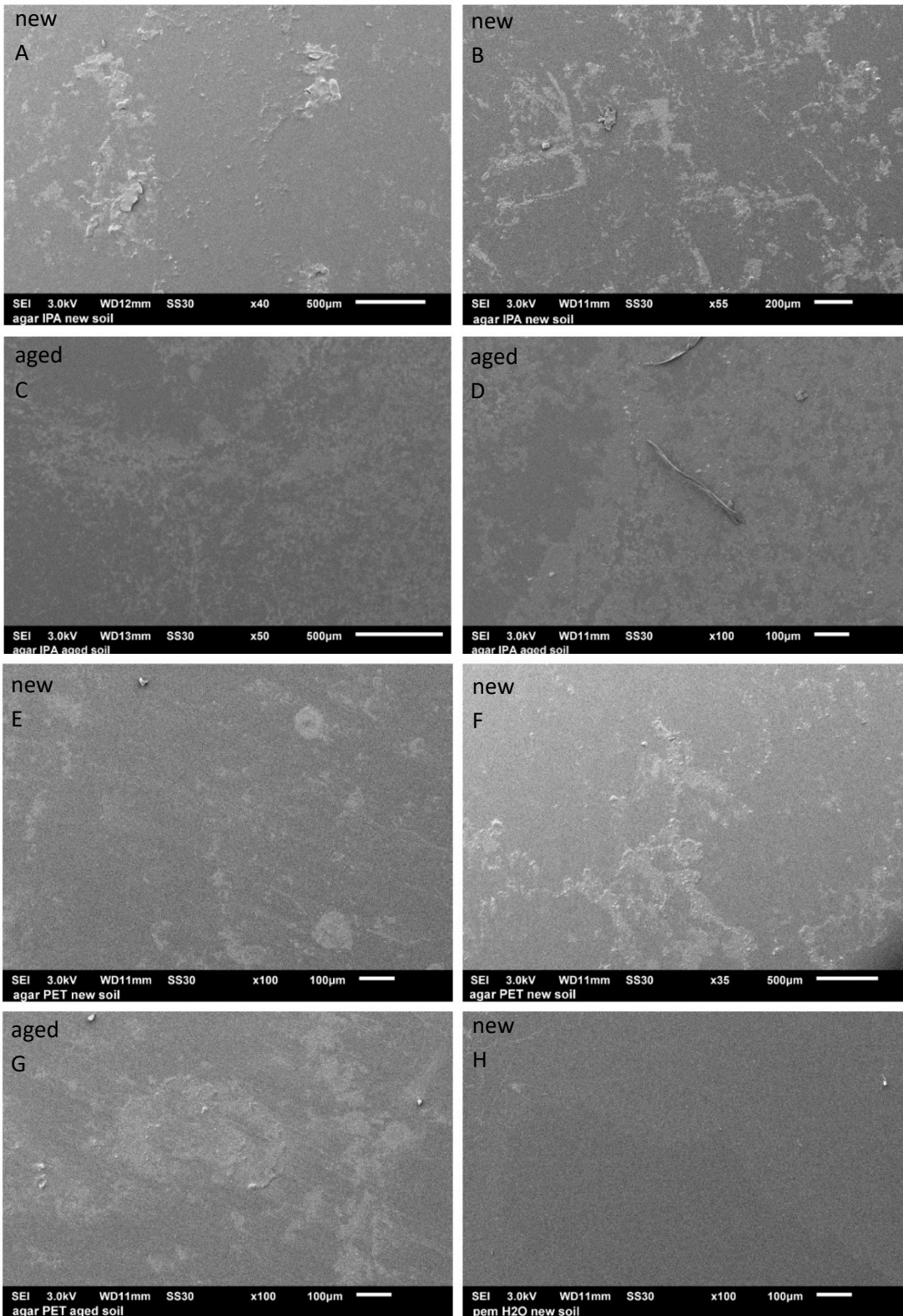


Figure 10.1. SEM micrographs: A-D: Agar IPA failed to remove synthetic soil from all PMMA surfaces. E-G: Agar PET failed to remove synthetic soil from all PMMA surfaces. H: Pemulen H<sub>2</sub>O left new PMMA surfaces clean.

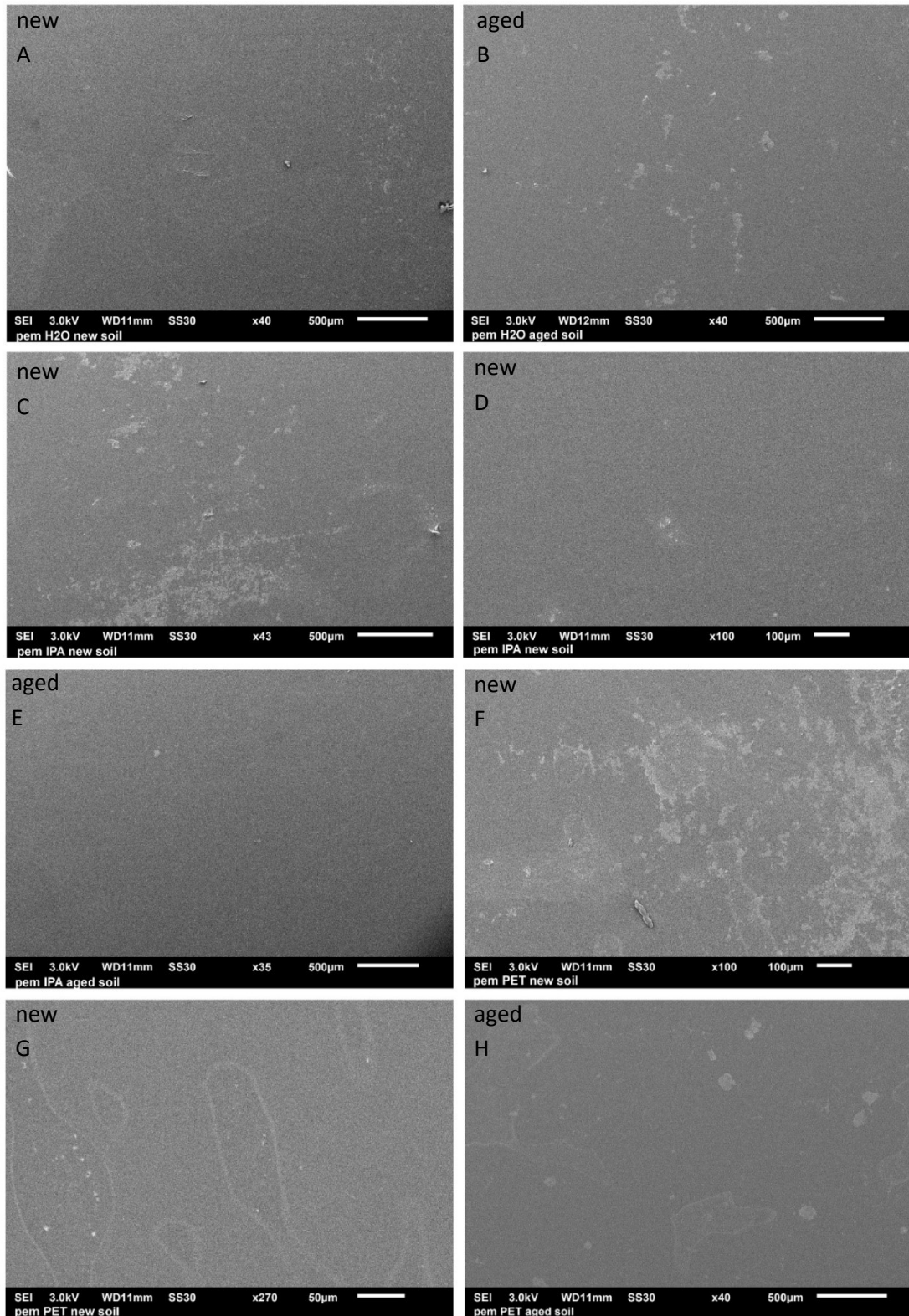
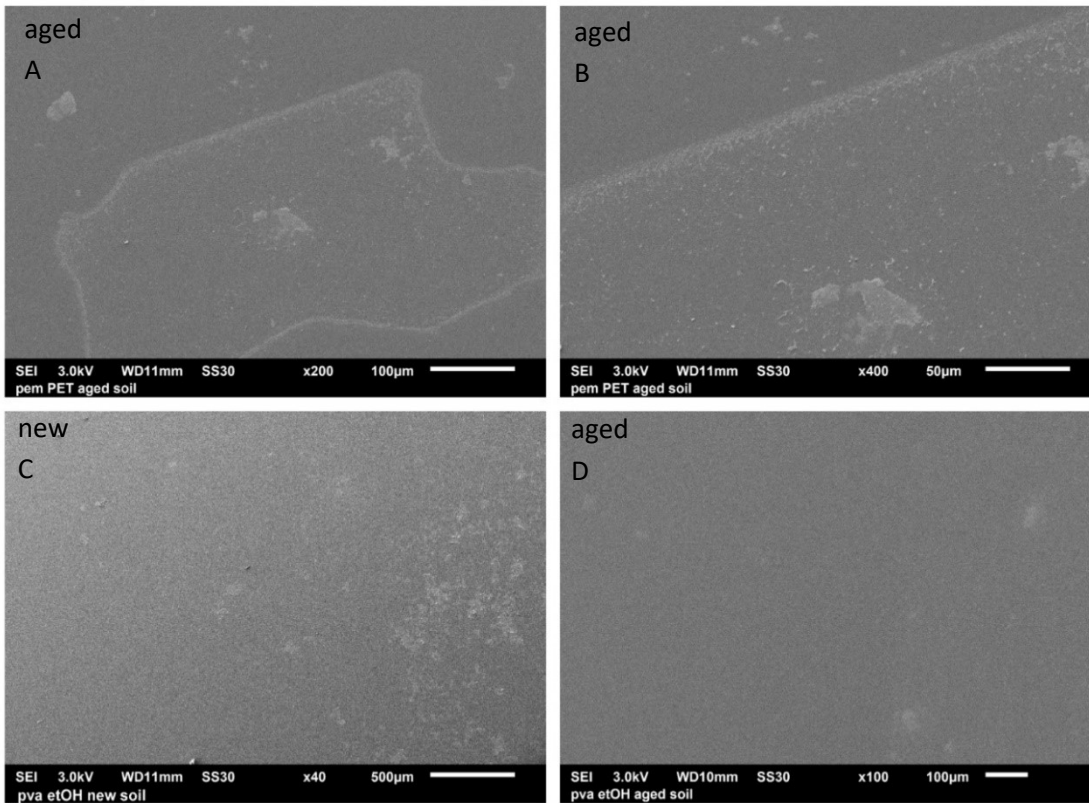


Figure 10.2. SEM micrographs: A: Tiny Pemulen H<sub>2</sub>O residues on cleaned new surfaces. B: Pemulen H<sub>2</sub>O left aged PMMA surfaces clean with limited synthetic soil remains. C: Pemulen IPA left new PMMA with some soil remains but also D: clean areas. E: Pemulen IPA left aged samples clean. F: Pemulen PET left new PMMA with some soil remains. G: Pemulen PET caused solute deposition from droplet evaporation on clean areas of new and aged PMMA. This resembled stains to the naked eye.



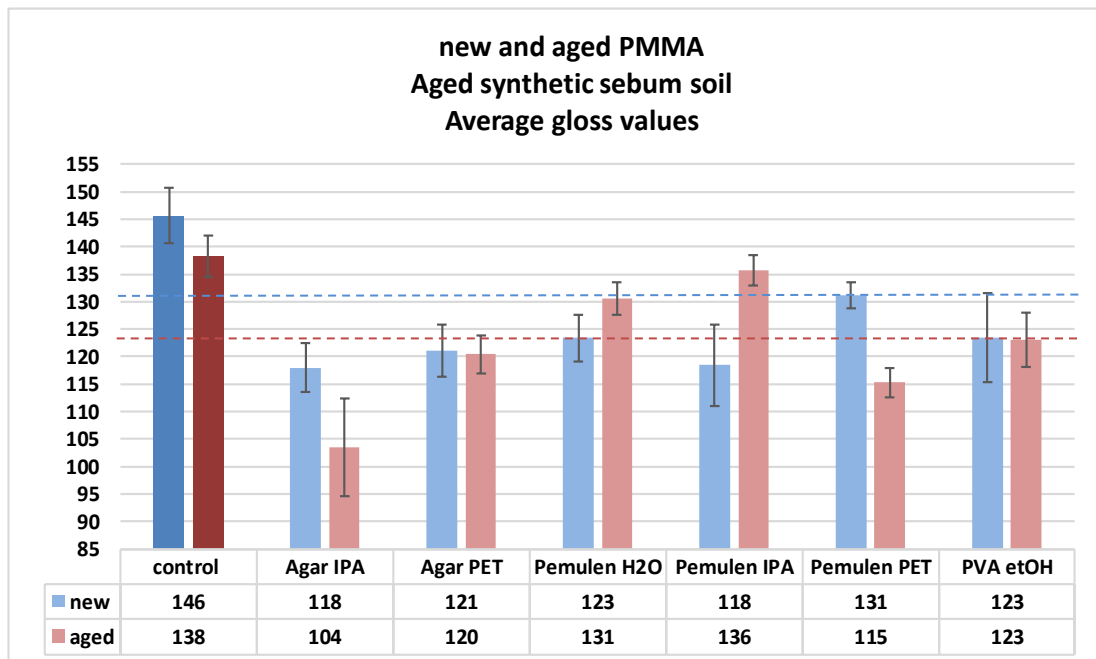
*Figure 10.3 SEM micrographs: A, B: Stains formed after Pemulen PET identified as minute gel residues and solute deposition from droplet evaporation. C: PVA EtOH left new surfaces clean with limited synthetic soil remains. D: PVA EtOH left aged PMMA clean.*

## GLOSS

### Gloss measurements

Most treatments visibly altered the surface gloss of new and aged PMMA samples after removal of aged synthetic soil. Treatments on new surfaces induced gloss differences smaller than 15 GU, rendering them equally glossy to the naked eye. Pemulen PET was the only treatment that left new surfaces with the highest gloss and equally glossy to the control. Pemulen hydrogel, Pemulen IPA and PVA EtOH left aged surfaces with the highest gloss and equally glossy to the control. Agar IPA left all PMMA in the worst visual condition.





*Graph 10.3. Gloss measurements of new and aged PMMA samples with aged synthetic soil after treatment, plotted as bar charts. Gloss units (GU) are averaged from 3 repetitions of 3 spot measurements on 3 replicates. Differences < 15 GU are non-detectable by the human eye. The PMMA controls are highly glossy with a value of 146 GU for the unaged and 138 GU for the aged. Red line shows below which point change is visible for aged PMMA and blue line does the same for new PMMA. Error bars show the standard deviation.*

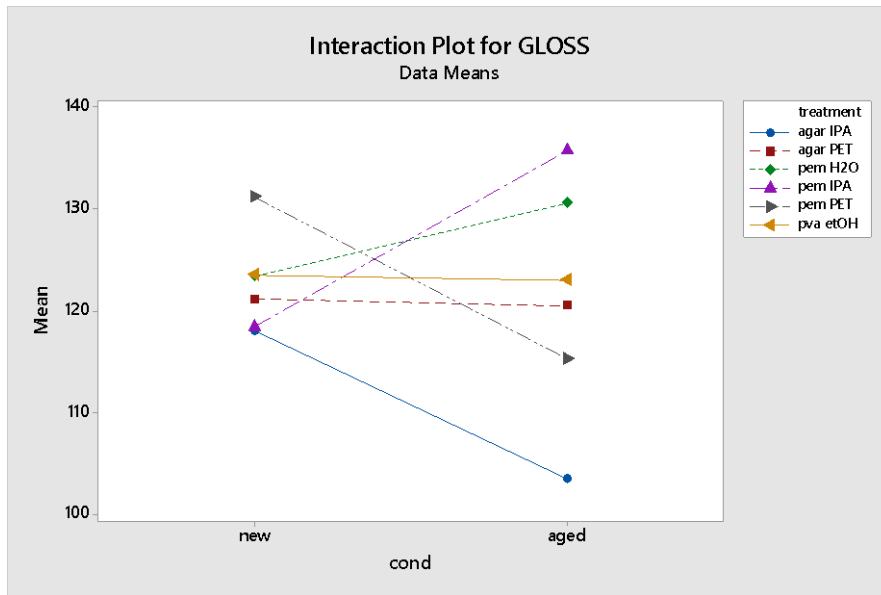
### **ANOVA gloss**

ANOVA of the gloss measurements showed that Treatments had a statistically significant impact on the numerical gloss of the treated PMMA samples with aged synthetic soil. It also showed that the interaction effects of treatments with condition were statistically significant. This means that the impact of one factor depended on the level of the other. The interaction plot (Graph 10.4) indicates that all three Pemulen treatments behaved differently depending on the surface condition of PMMA. Pemulen with H<sub>2</sub>O and IPA offered higher gloss to aged surfaces, while Pemulen PET to new surfaces. Tukey's HSD allocated unique letters to Agar IPA and paired Pemulen H<sub>2</sub>O with Pemulen IPA indicating that they significantly impacted the gloss. In the main effects plot (Graph 10.5) the paired treatments induced the highest gloss and Agar IPA the lowest, indicating the former two having a significantly positive, while the latter a negative impact to cleaning PMMA.

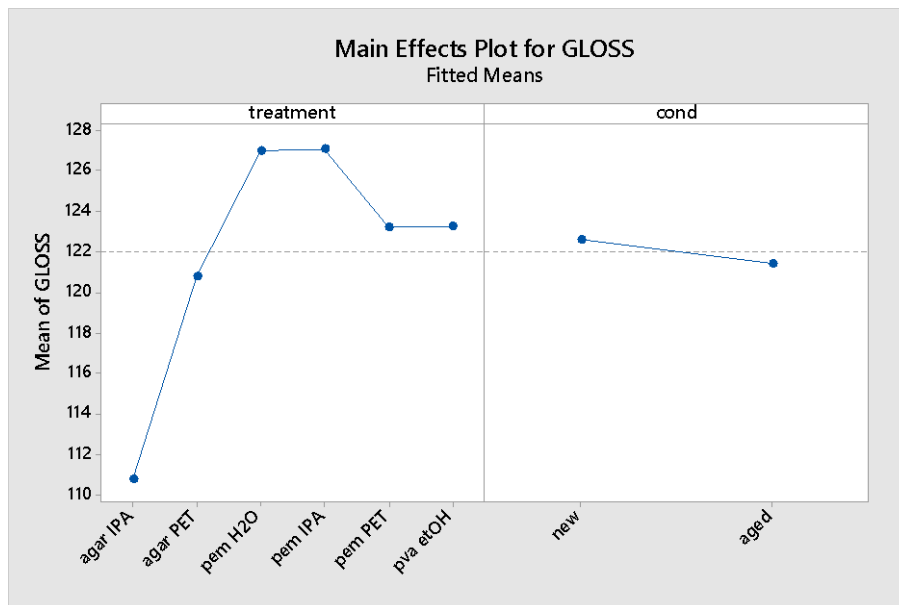
### Grouping Information Using the Tukey Method and 95% Confidence

treatment	N	Mean	Grouping
pem IPA	6	127.06	A
pem H2O	6	126.98	A
pva etOH	6	123.24	A B
pem PET	6	123.22	A B
agar PET	6	120.79	A B
agar IPA	6	110.76	B

Means that do not share a letter are significantly different.



Graph 10.4. Interaction plot showing the significant interactions between treatments and condition on PMMA gloss.



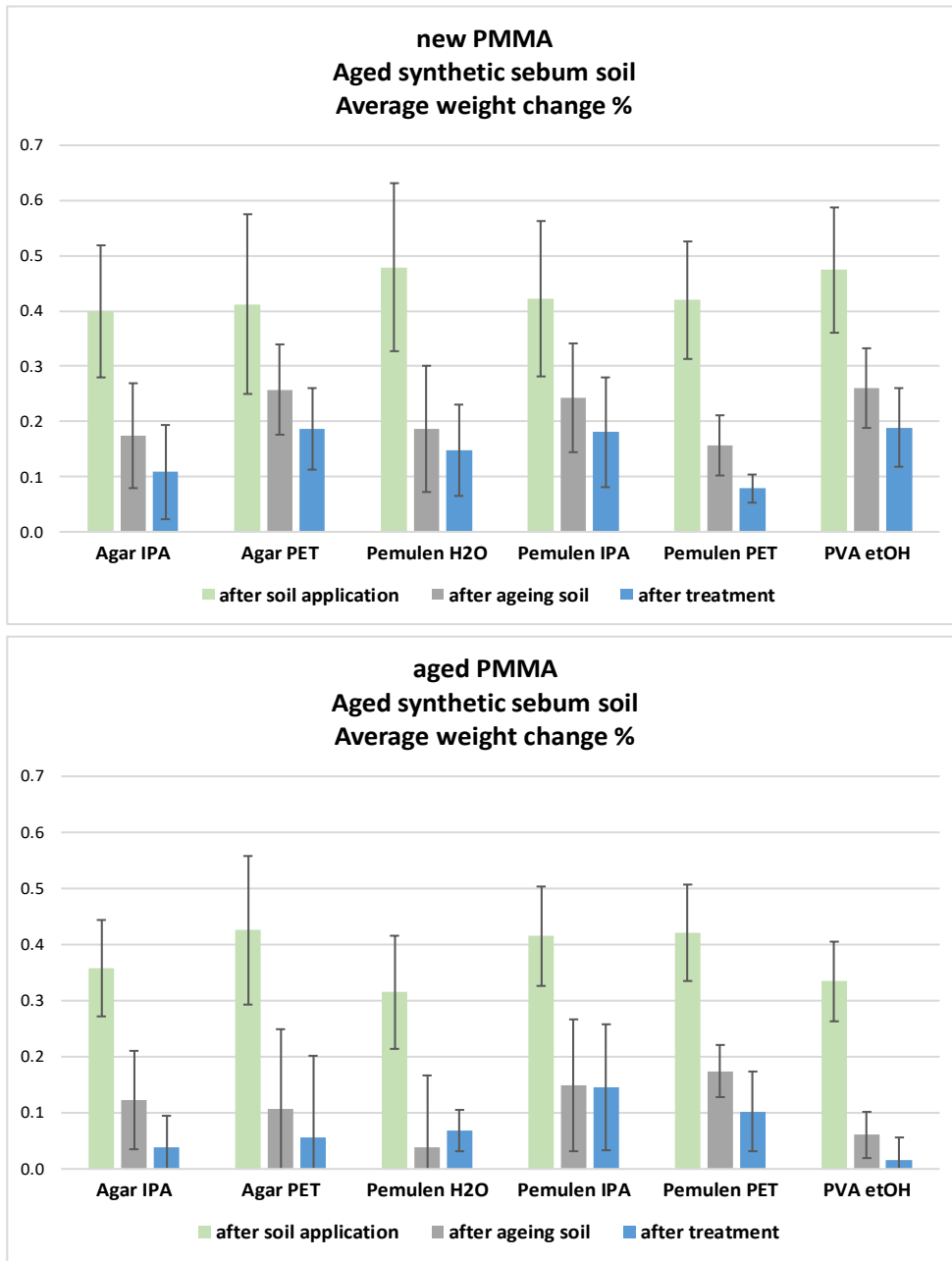
Graph 10.5. The mean CARS scores of Pemulen H<sub>2</sub>O and Pemulen IPA is the highest, while that of Agar IPA the lowest, indicating they affected cleaning of PMMA with aged synthetic soil in a positive and a negative manner, respectively.

## WEIGHT MEASUREMENTS

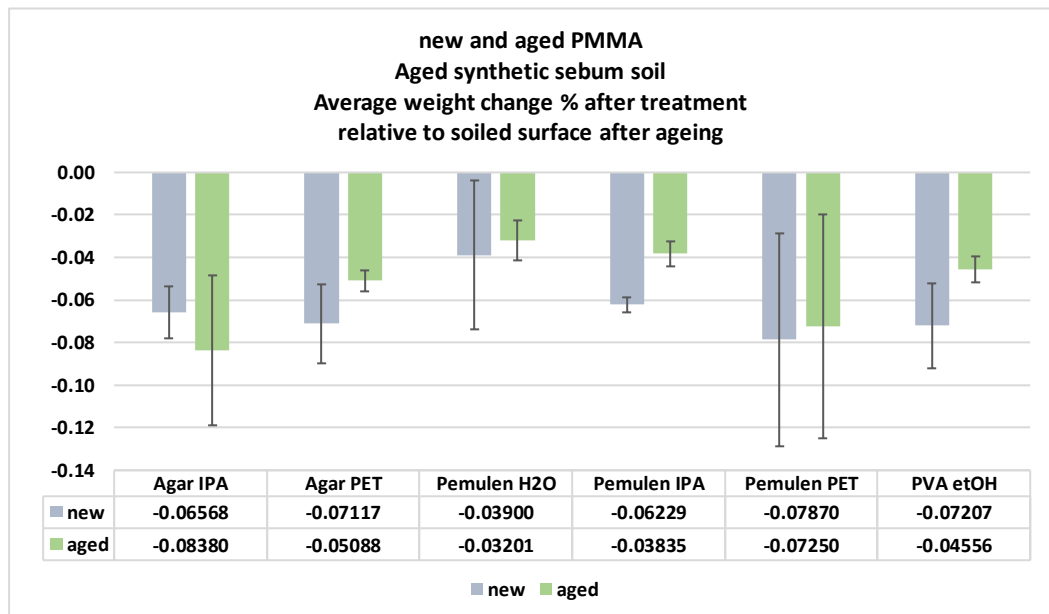
### Weight changes %

After synthetic soil application (Graph 10.6 - green bar), all samples gained weight in a consistent manner, confirming the successfully standardised application performed in a randomised order. New samples systematically gained on average 0.06 % more than aged samples. After 32 days of ageing in the chamber (Graph 10.6 - grey bar) all samples lost weight. Aged samples inconsistently lost on average 0.1 % more than new samples. This phenomenon was discussed earlier in 9.2.2.a. In short, weight loss of all samples was attributed to component loss from both synthetic soil and the PMMA. Aged samples underwent chain scission only, whereas new samples both chain scission and crosslinking.

All treatments caused samples to lose weight (Graph 10.7). All samples lost comparable weight, on average 0.06 % for new and aged. Pemulen hydrogel induced the smallest weight loss to all PMMA (ca. 0.03-0.04 %) attributed to partial removal of the aged soil. Visual evaluation of all samples after Agar with IPA and PET indicated that they failed to remove aged soil, yet they induced among the greatest weight loss (Graph 10.7). PVA EtOH was the only treatment to deposit extensive gel residue on new surfaces, and yet caused comparable loss to the successful treatments. Pemulen PET also induced great weight loss to aged samples, even though it only partly removed synthetic soil according to visual evaluation. Weight loss after Agar IPA and PVA EtOH was attributed to penetration of alcohol/H<sub>2</sub>O mixtures causing dissolution and evaporation of polymer components, as discussed earlier. PET had no effect on the weight of PMMA (see Chapter 7.1.2), so material extraction/dissolution was excluded. This, the lack of gel residue, as well as the acclaimed degreasing effect of PET (Sale 1993) and its ability to dissolve lipophilic materials, indicated that Agar PET and Pemulen PET treatments were able to remove part of the synthetic soil. It also indicated that both treatments left surfaces in a poor visual condition, as cleaning was visually hindered by black synthetic soil remains spread across the surface.



Graph 10.6. Average weight change % of new (upper) and aged (bottom) PMMA - averaged from five replicates - after application of synthetic soil (green), ageing of the soil (grey) and cleaning treatment (blue). Changes % are normalised to the starting/initial weight. Error bars show the standard deviation.



Graph 10.7. Average weight change % of new and aged PMMA with aged synthetic soil after the cleaning treatments - averaged from five replicates. Changes % are calculated as the change between the soiled surface after ageing and the surface after treatment. Error bars show the standard deviation.

#### **ANOVA weight change %**

Anova of the weight change % showed that none of the treatments influenced the weight fluctuation in a statistically significant manner.

#### **ATR-FTIR**

After treatment all samples exhibited characteristic absorption bands of the 32-day UV-aged PMMA (control) (see Chapter 4.3.1 Table 4.4), indicating that treatments altered the surface chemistry of PMMA (Fig. 10.4). Agar PET caused the biggest decrease in peaks of new PMMA, particularly loss of carbonyls attributed to its failure to remove synthetic soil, as indicated by visual assessment. Pemulen hydrogel caused the biggest decrease in peaks of aged PMMA, as well as the formation of a broad peak at  $1570\text{ cm}^{-1}$  and a small shoulder peak around  $1035\text{ cm}^{-1}$ . The peak at  $1570\text{ cm}^{-1}$  was evidence of the successful acid-base neutralisation of Pemulen upon the addition of TEA (Patel *et al.* 2003; Todica *et al.* 2015) and at  $1035\text{ cm}^{-1}$  was characteristic of Pemulen chemical moieties (C–N stretch). Both peaks indicated the presence of gel residue, which was confirmed under high magnification. PVA EtOH caused the formation of a new peak at  $880\text{ cm}^{-1}$ . This was earlier encountered in samples immersed in EtOH for 30 days, and was attributed to the crystallization of the PMMA surface. This suggested that PVA allowed sufficient free EtOH to contact PMMA within the short timeframe of the treatment, resulting in unsolicited surface chemical alteration. Agar IPA caused the least change to aged surfaces, although it failed to remove any synthetic soil. Characteristic sebum oil peaks overlapped PMMA peaks (see Chapter 5.2.1), contributing to broader/more intense absorptions.

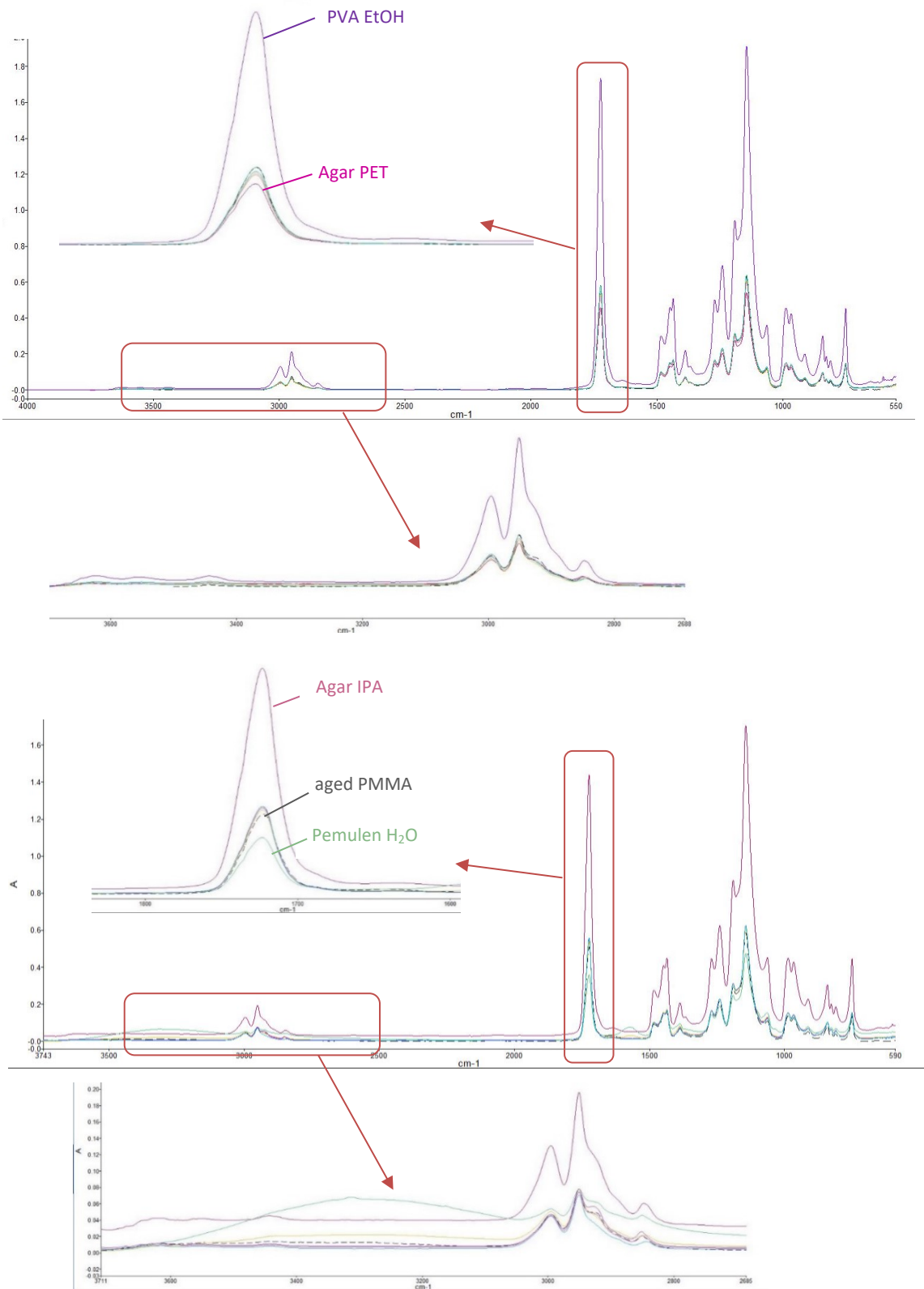


Figure 10.4. Spectra of new (upper) and aged (bottom) PMMA samples with aged synthetic soil after treatment. The spectra are averaged from 3 replicates for each treatment. Each replicate is averaged from 3 spot ATR analyses. Peaks are enlarged and labelled. The spectrum of 32-days aged control (untreated, unsoiled) is included for comparison.

### 10.1.2.b. Aged PSA

#### VISUAL OBSERVATIONS

##### Macroscopic evaluation

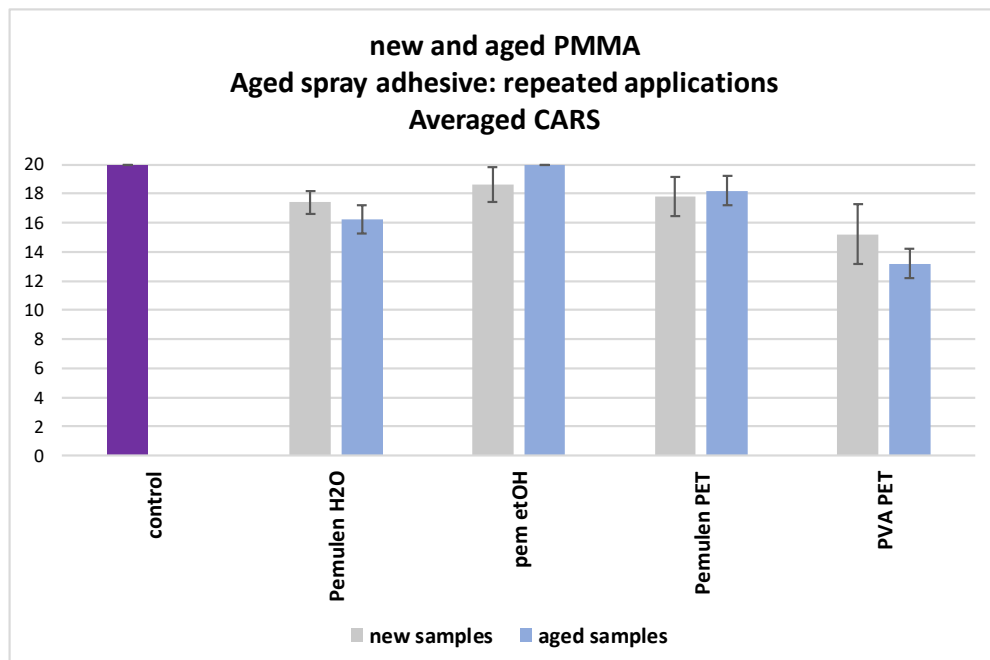
Pemulen gels with H<sub>2</sub>O, EtOH and PET offered the best results with partial or complete removal of PSA. PVA PET was less successful at removal of aged PSA from PMMA.

samples with aged adhesive		
	new	aged
Pemulen H <sub>2</sub> O	partly cleaned/cleaned	cleaned
Pemulen EtOH	cleaned	cleaned
Pemulen PET	partly cleaned/cleaned	cleaned
PVA PET	partly cleaned	partly cleaned/not cleaned

Table 10.12. Macroscopic observation of the overall impression of aged PSA removal from new and aged PMMA after treatment.

##### CARS scores

Treatments performed comparably on new and aged surfaces. All Pemulen treatments left PMMA in a good condition, according to human perception (Graph 10.8). Particularly Pemulen EtOH left surfaces in the best condition, with the aged samples scoring the highest possible and resembling the control. PVA PET was less successful at removing aged synthetic soil, offering the lowest CARS to all samples.



Graph 10.8. CARS scores of new and aged PMMA samples with aged PSA. Scores are based on a five-point progressive ranking from 0 (worst) to 4 (best). Scores, expressed as a bar chart, are averaged from 5 replicates for each treatment. Untreated new and aged PMMA controls scored the highest possible CARS 20 in categories 'Dirt residue', 'Abrasion' and 'Gel residue'. Error bars show the standard deviation.

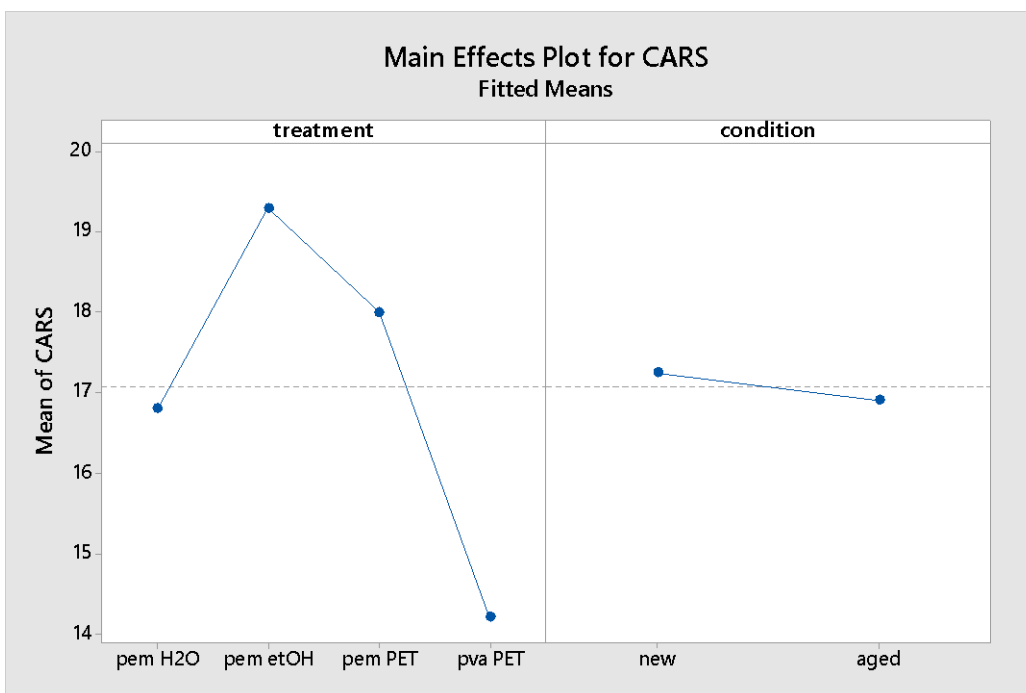
**ANOVA CARS**

ANOVA of the CARS showed that Treatments had a statistically significant impact on the effectiveness of cleaning PMMA with aged synthetic soil. Tukey's HSD determined that Pemulen EtOH, Pemulen hydrogel and PVA PET had a significantly different impact on the visual condition of treated PMMA samples. According to the main effects plot (Graph 10.9) Pemulen EtOH induced the highest CARS (above the mean value) impacting the cleaning outcome positively. Samples after Pemulen hydrogel scored negligibly lower than the overall mean CARS with 16.8. The treatment's performance was considered satisfactory, therefore Pemulen hydrogel impacted the cleaning outcome positively. PVA PET left treated surfaces in the worst condition with the lowest CARS, having a negative effect on PMMA cleaning.

**Grouping Information Using the Tukey Method and 95% Confidence**

treatment	N	Mean	Grouping
pem etOH	10	19.300	A
pem PET	10	18.000	A B
pem H <sub>2</sub> O	10	16.800	B
pva PET	10	14.200	C

*Means that do not share a letter are significantly different.*



*Graph 10.9. The mean CARS scores of Pemulen EtOH is the highest, while that of Pemulen H<sub>2</sub>O and PVA PET the lowest, indicating they affected cleaning of PMMA with aged PSA in a positive and a negative manner, respectively.*



**SEM imaging**

For PMMA controls with aged PSA see Chapter 9.2.2.b.

**New PMMA samples with aged PSA:**

<b>New PMMA samples after treatment</b>				
Treatment	Aged PSA	Gel residue	Comments	Figure no.
<b>Pemulen H<sub>2</sub>O</b>	partly cleaned	no	salt-like structures*	10.5 A, B
<b>Pemulen EtOH</b>	partly cleaned	extensive**		10.5 E
<b>Pemulen PET</b>	cleaned	no		10.5 H
<b>PVA PET</b>	not cleaned	extensive	Discolouration to the naked eye, solute deposition from drying droplets	10.6 C, D, E, F

\* Identified possibly due to chemical interactions between the PSA and the gel system.

\*\* Pemulen EtOH left aged surfaces with extensive gel residue, revealed from the haziness of the images (discussed earlier at 9.1.2.a.).

**Aged PMMA samples with aged PSA:**

<b>Aged PMMA samples after treatment</b>				
Treatment	Aged PSA	Gel residue	Comments	Figure no.
<b>Pemulen H<sub>2</sub>O</b>	cleaned	no	Discolouration to the naked eye, solute deposition from drying droplets	10.5 C, D
<b>Pemulen EtOH</b>	cleaned	no	possibly solvent penetration***	10.5 F, G
<b>Pemulen PET</b>	cleaned	no	Discolouration to the naked eye, solute deposition from drying droplets	10.6 A, B
<b>PVA PET</b>	not cleaned	no		10.6 F

\*\*\* Limited aged PSA remains formed cracks possibly due to UV ageing.

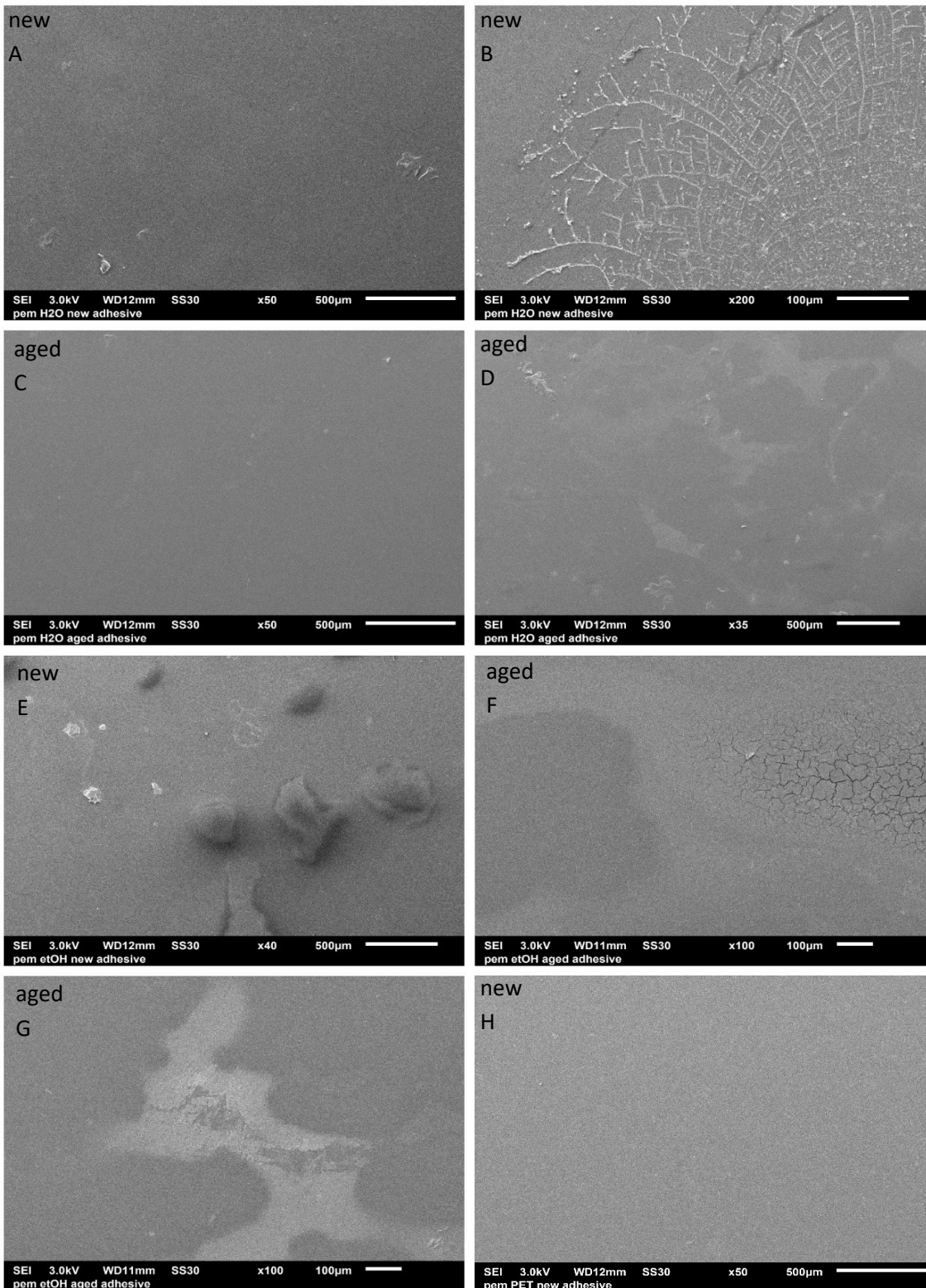


Figure 10.5. SEM micrographs: A: Pemulen H<sub>2</sub>O left PSA remains. B: Salt-like structures after Pemulen H<sub>2</sub>O. C: Pemulen H<sub>2</sub>O cleaned aged PMMA. D: Areas of discoloration identified as tiny specks of PSA remains. E: Pemulen EtOH residue on clean new PMMA. F: Formation of a network of cracks on aged PSA remains on aged PMMA. G: Solvent penetrating upper micron PMMA layers resembling stain/discolouration. H: Pemulen PET cleaned new PMMA.

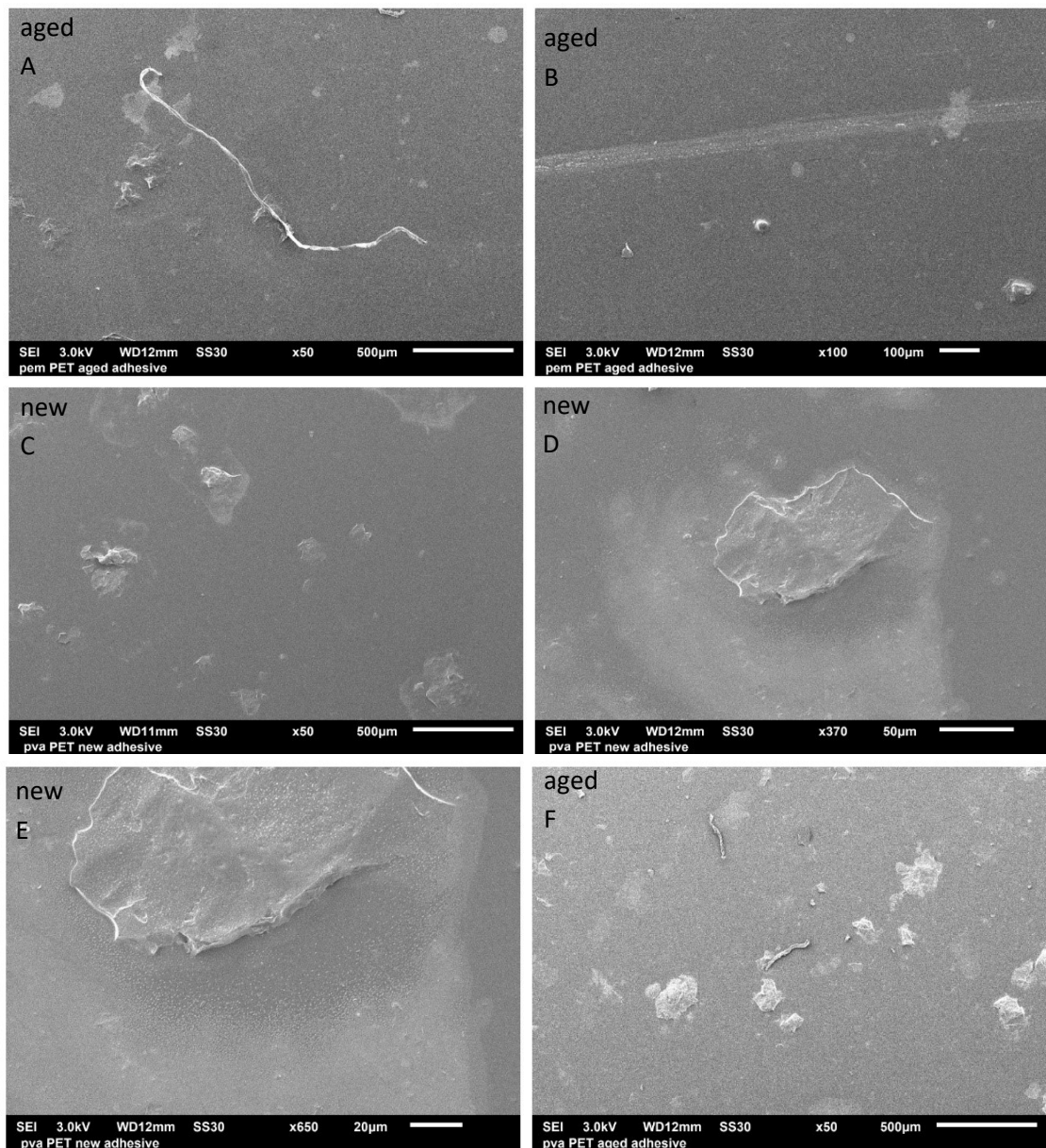
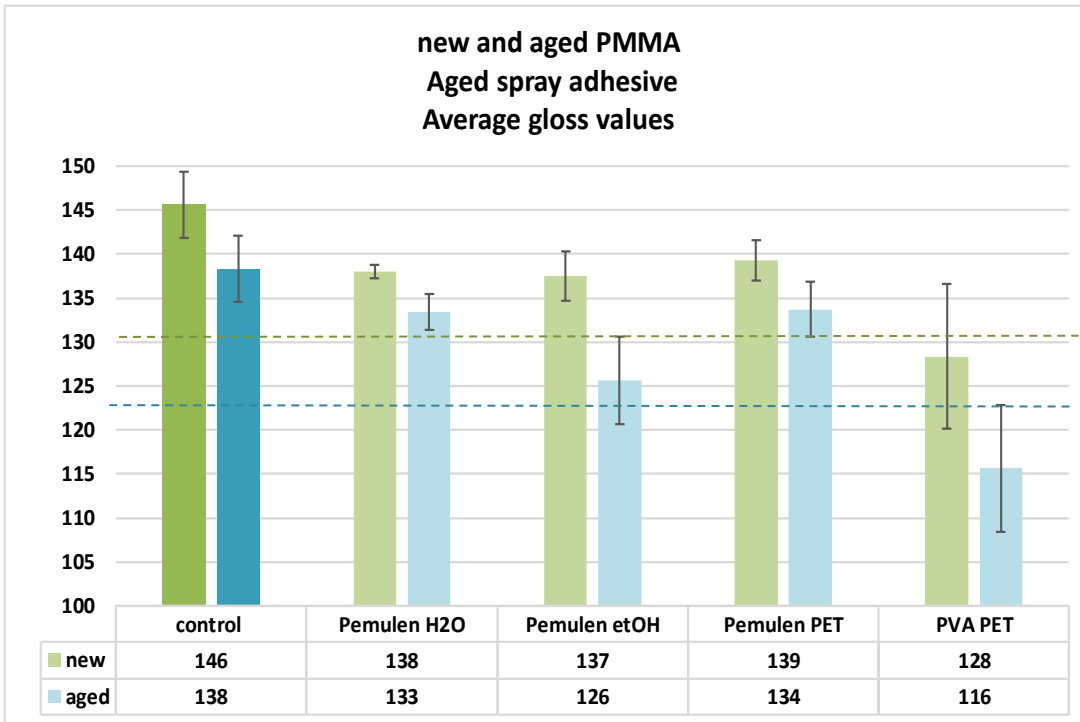


Figure 10.6. SEM micrographs: A, B: Pemulen PET left aged PMMA clean with limited PSA remains. C: PVA PET failed to remove PSA from new PMMA. D, E: Stains to the naked eye around remaining PSA after PVA PET, identified as solutes and minute gel residues. F: PVA PET failed to remove PSA from aged PMMA.

## GLOSS

### Gloss measurements

All treatments, with the exception of PVA PET, left surfaces within 15 GU from the respective new and aged controls. So, none of the Pemulen treatments visibly altered the surface gloss of new and aged PMMA samples. PVA PET left PMMA surfaces the biggest, noticeable drop in gloss.



Graph 10.10. Gloss measurements of new and aged PMMA with aged PSA after treatment, plotted as bar charts. Gloss units (GU) are averaged from 3 repetitions of 3 spot measurements on 5 replicates. Differences < 15 GU are non-detectable by the human eye. The PMMA controls are highly glossy with a value of 146 GU for the unaged and 138 GU for the aged. Blue line shows below which point change is visible for aged PMMA and green line does the same for new PMMA. Error bars show the standard deviation.

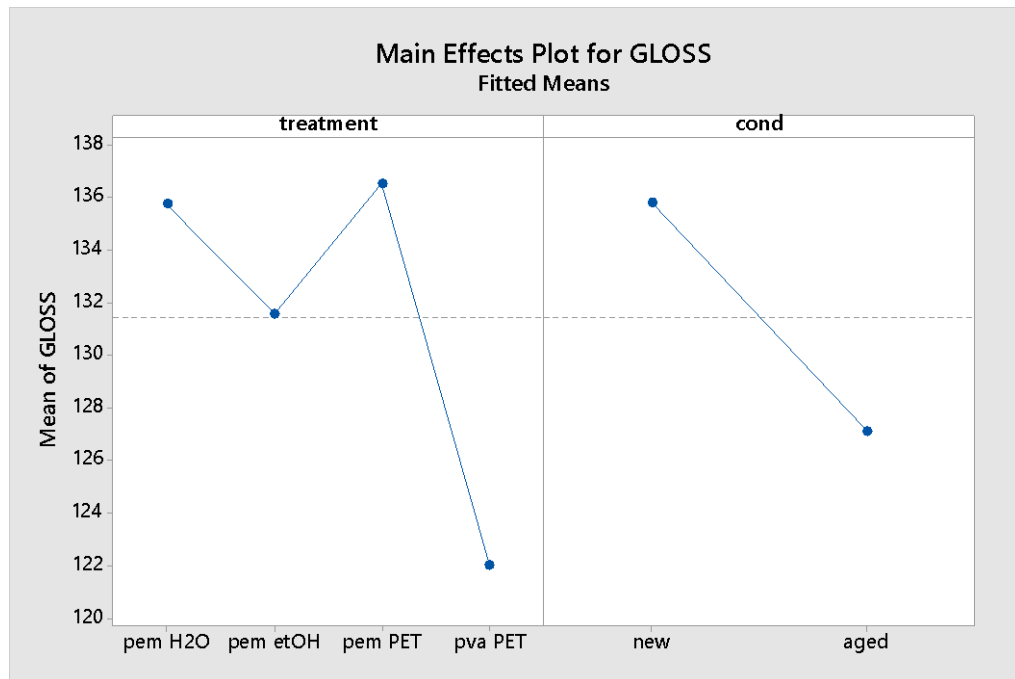
**ANOVA gloss**

ANOVA of the gloss measurements showed that Treatments had a statistically significant impact on the numerical gloss of the treated PMMA samples with aged PSA. Tukey’s HSD determined that Pemulen hydrogel with Pemulen PET performed similarly in a statistically significant manner, so it paired them together. PVA PET was allocated a different letter for being significantly different. In the main effects plot (Graph 10.11) the paired treatments induced the highest gloss and PVA PET the lowest. This indicated that the two Pemulen treatments had a significantly positive impact on the PMMA, unlike PVA PET that negatively affected the outcome.

**Grouping Information Using the Tukey Method and 95% Confidence**

treatment	N	Mean	Grouping
pem PET	6	136.50	A
pem H2O	6	135.72	A
pem etOH	6	131.56	A B
pva PET	6	122.00	B

Means that do not share a letter are significantly different.



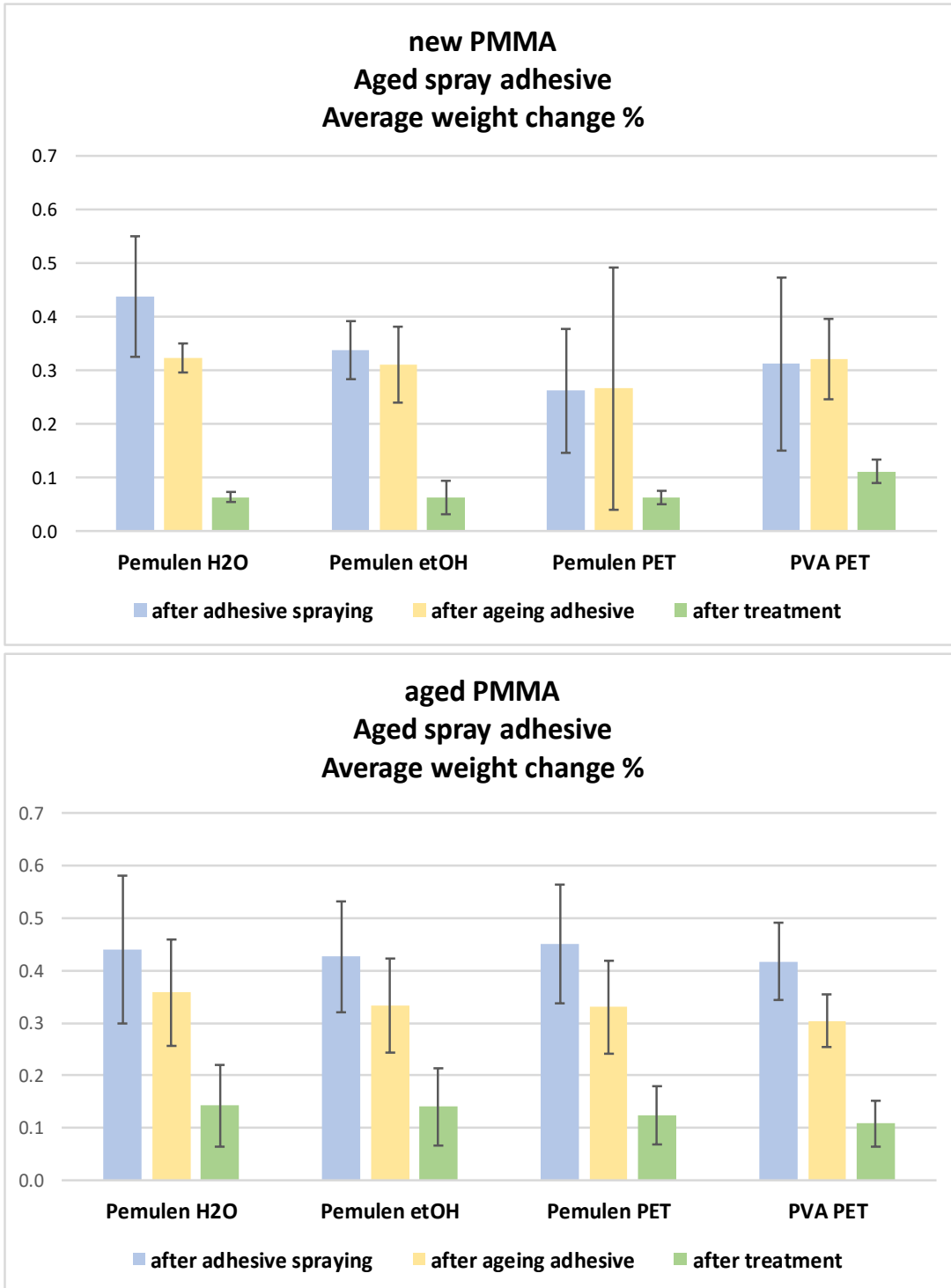
Graph 10.11. The mean CARS scores of Pemulen hydrogel and Pemulen PET are the highest, while that of PVA PET the lowest, indicating they affected cleaning of PMMA with aged PSA in a positive and a negative manner, respectively.

## WEIGHT MEASUREMENTS

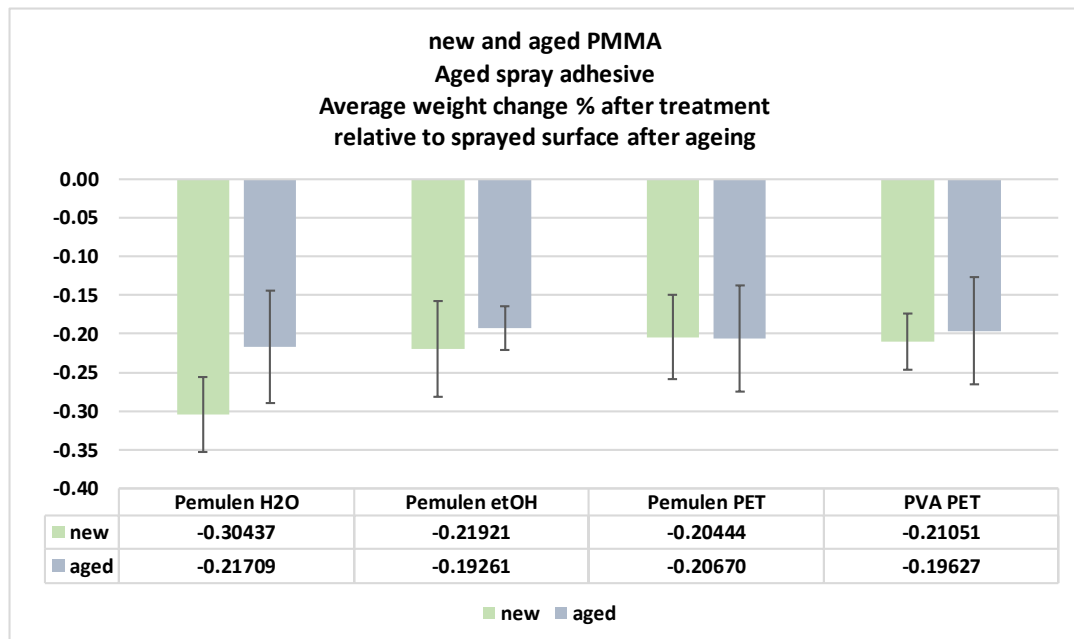
### Weight changes %

After application of PSA (Graph 10.12 - blue bar), all samples consistently gained weight. Aged samples gained on average 0.1 % more than new samples, and in a more consistent manner, as seen and explained in previous experiment (see 9.2.2.b). After 32 days of ageing in the chamber (Graph 10.12 - yellow bar) all samples comparably lost on average 0.3 % due to component loss from PSA and PMMA or/and the wet cycles during ageing, washing off some of the PSA (see 9.2.2.b for explanation of ageing phenomena).

After treatment both new and aged samples lost on average 0.2 % (Graph 10.13). Visual evaluation of samples treated with the Pemulen gels confirmed the removal of aged PSA justifying the weight loss. Although PVA PET failed to remove PSA from all PMMA and deposited extensive gel residue on new samples, it caused comparable amounts of weight loss as successful treatments. As discussed earlier, extraction/dissolution of PMMA resulting from contact with PET was excluded. Considering the ability of PET to dissolve synthetic soil, the weight loss must have been the result of removal of part of the soil, which was visually hindered by black synthetic soil remains spread across the surface. Pemulen EtOH left extensive gel residue on new surfaces, and yet induced weight loss comparable to successful treatments with no residual gel. This was attributed to penetration of alcohol/H<sub>2</sub>O mixtures causing dissolution and evaporation of polymer components, as discussed earlier.



Graph 10.12. Average weight change % of new (upper) and aged (bottom) PMMA - averaged from five replicates - after application of PSA (blue), ageing of the PSA (yellow) and cleaning treatment (green). Changes % are normalised to the starting/initial weight. Error bars show the standard deviation.



*Graph 10.13. Average weight change % of new and aged PMMA with aged PSA after the cleaning treatments - averaged from five replicates. Changes % are calculated as the change between the sprayed surface after ageing and the surface after treatment. Error bars show the standard deviation.*

### **ANOVA weight change %**

ANOVA of the weight change % showed that none of the treatments influenced the weight fluctuation in a statistically significant manner.

### **ATR-FTIR**

After treatment all samples exhibited characteristic absorption bands of the 32-day UV-aged PMMA (control) (see Chapter 4.3.1 Table 4.4), indicating that treatments altered the surface chemistry of PMMA (Fig. 10.7). PVA PET caused the biggest change to both new and aged PMMA, which according to visual evaluation was attributed to its failure to remove PSA. A layer of PSA on the PMMA surface hinders absorption of characteristic PMMA bands, falsely attributing the low intensity to a large chemical change.

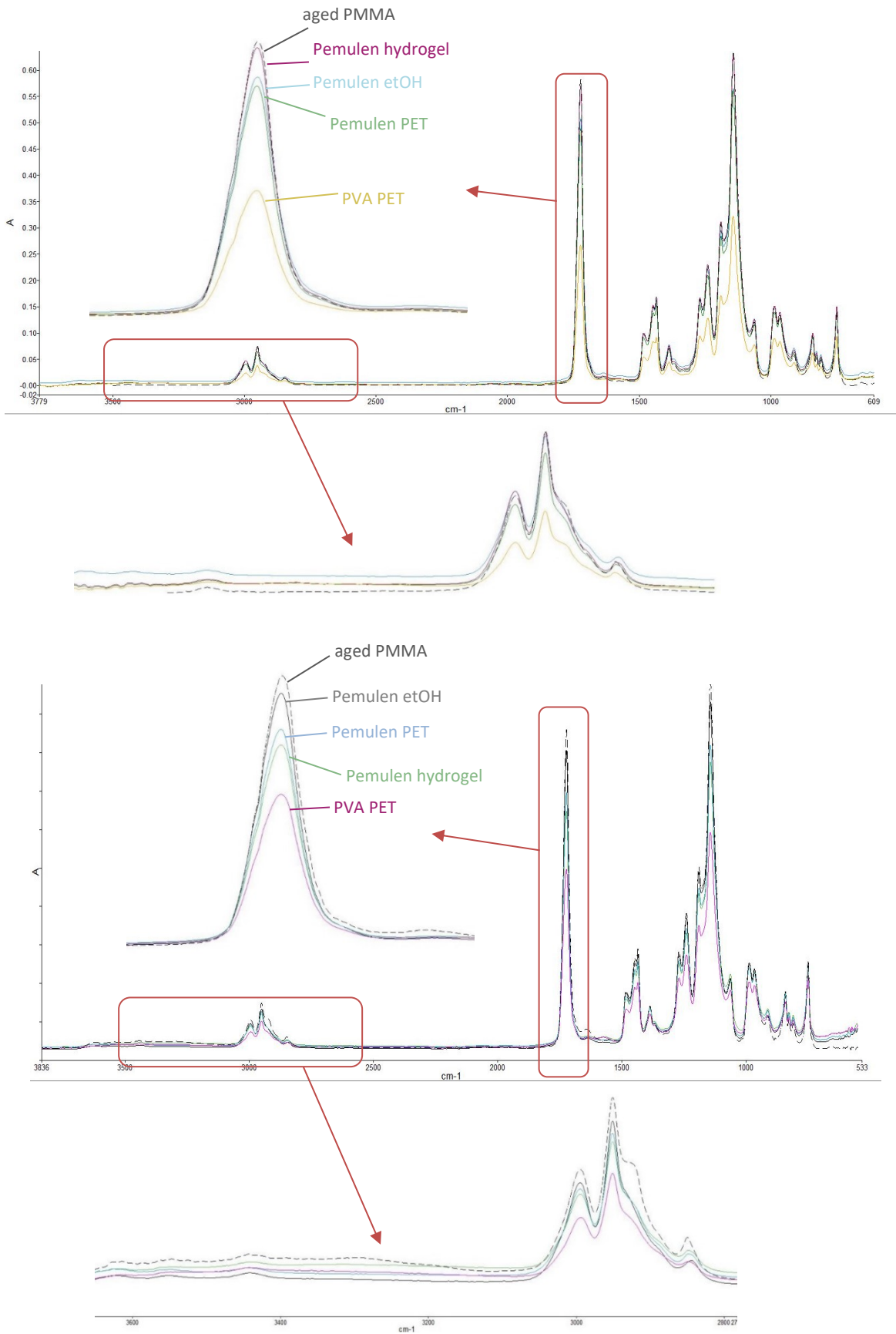


Figure 10.7. Spectra of new (upper) and aged (bottom) PMMA samples with aged PSA after gel treatment. The spectra are averaged from 3 replicates for each treatment. Each replicate is averaged from 3 spot ATR analyses. Peaks are enlarged and labelled. The spectra of 32-days aged control (untreated, unsoiled) are included for comparison.



### 10.1.3. Conclusion

#### PMMA samples with aged synthetic soil

All treatments caused samples to lose weight, even in cases where surface synthetic soil was not removed. Such examples are Agar IPA, Agar PET and Pemulen PET that failed to remove aged synthetic soil, while Agar IPA also deposited gel residues. Statistical analysis of the CARS scores and the gloss measurements indicated that all three treatments left samples in a similarly poor condition, confirming their negative impact on PMMA. Based on these reasons, these three treatments were considered unfit for cleaning PMMA and were discarded.

Pemulen hydrogel, Pemulen IPA and PVA EtOH were the most successful at removing aged synthetic soil from all surfaces. Statistical analysis of the CARS scores indicated that based on human perception, only Pemulen IPA had a positive impact on the cleaning process. Statistical analysis of the gloss measurements showed that both Pemulen IPA and Pemulen hydrogel impacted positively the surface reflectance of treated PMMA. Under high magnification of SEM, PVA EtOH was seen to deposit extensive gel residue. In addition, it induced a small level of surface PMMA crystallisation, according to the ATR-FTIR spectrum.

#### PMMA samples with aged PSA

Results showed that Pemulen gels were the most successful at removing aged PSA from PMMA surfaces. The PSA became acidic as a result of ageing and therefore responded well to the alkaline TEA added in the Pemulen gels/emulsions (Stavroudis and Blank 1989). All three Pemulen treatments (with EtOH, H<sub>2</sub>O and PET) offered the best visual condition. Pemulen EtOH occasionally left extensive gel residue revealed by the haziness of the images during observation under the SEM. This was attributed to evaporation of H<sub>2</sub>O from the gel remains. Nevertheless, statistical analysis of the CARS scores and gloss measurements indicated that Pemulen with EtOH and H<sub>2</sub>O had a positive impact on the cleaning process.

PVA PET was the only treatment that failed to remove aged PSA, leaving PMMA in the worst visual condition. PVA PET induced the deposition of solutes from drying droplets and of minute gel residue, which to the naked eye looked like stain formation or surface discolouration forming around PSA remains. This was confirmed by statistical analysis indicating that the treatment negatively impacted the surface gloss of PMMA. Although it failed to clean PMMA, the treatment caused an unjustified weight loss to the material, showing unwanted chemical reactions. Based on these reasons, PVA PET was considered unfit for cleaning PMMA and was discarded.

#### 10.1.4. Nuclear Magnetic Resonance Mobile Universal Surface Explorer

Unilateral NMR MOUSE was employed to monitor the physical condition of samples and confirm the safety of the optimised gel treatments:

PMMA with aged synthetic soil	PMMA with aged PSA
✓ Pemulen hydrogel	✓ Pemulen hydrogel
✓ Pemulen IPA	✓ Pemulen EtOH
✓ PVA EtOH	✓ Pemulen PET

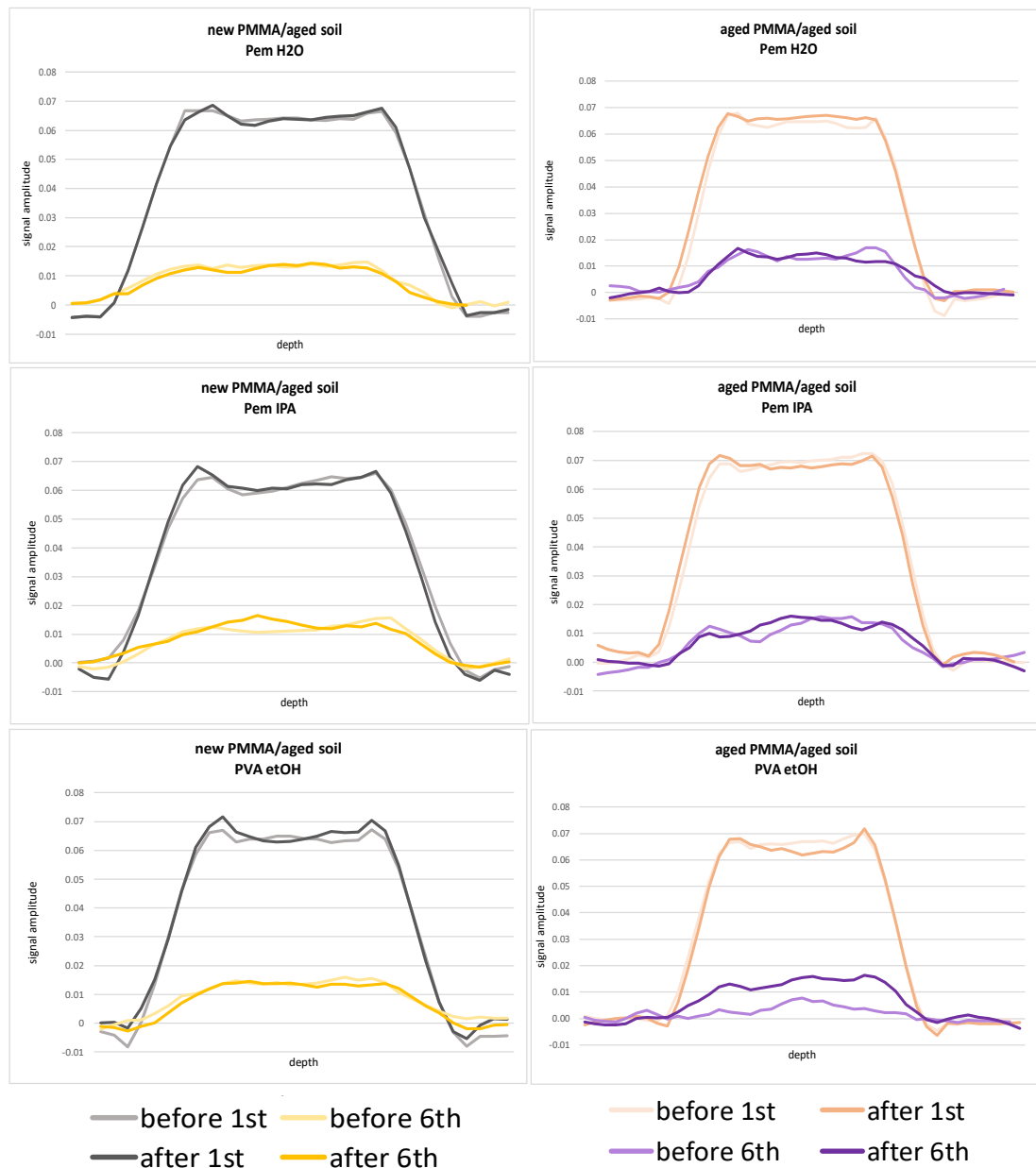
Scans were expected to non-invasively capture solvent possibly penetrated in the material (solvent uptake and movement) *24 hours after* the three 3-minute repeated gel applications ('drying' state). These scans were expected to show whether absorbed solvents were trapped in the material or evaporated, as well as any non-recoverable mechanical deformations due to solvent diffusion in PMMA bulk. For comparison purposes all treated samples were scanned *before* treatment to obtain their 'normal' relaxation state. The following smoothed line plots are practically vertical slices through the 2D heat map plots, in other words, through the samples' depth. One slice at the 1<sup>st</sup> and one at the 6<sup>th</sup> echo yielded profiles of the proton density (signal amplitude) of new and aged PMMA samples.

The analysis was designed in duplicate for a total of 48 scans (before and 24 hours after treatment) of new and aged PMMA samples with aged synthetic soil (n=12 samples) and aged PSA (n=12 samples). Data were consistent in both sets of replicates for all treatments, therefore one replicate is presented here. For all graphs see Appendix O. Graph 10.14 and 10.15 shows samples with aged synthetic soil and aged PSA, respectively, before and after treatment.

All samples, regardless of dirt type, surface condition and treatment, showed similar profiles before and after treatment. This indicated that all treatments performed similarly (in the vast majority of cases difference in amplitude never exceeds  $\pm 0.005$ ). PMMA samples exhibited almost indistinguishable 1<sup>st</sup> and 6<sup>th</sup> echoes, before and after treatment, suggesting that no significant or detectable structural changes took place as a result of solvent-gel cleaning.

NMR MOUSE showed that after optimisation of the treatments there was no liquid/solvent penetration into the PMMA. This was witnessed as a lack of change in the signal amplitude of the 10 consecutive dynamic scans of all analysed samples. These scans monitored treated samples for 6 consecutive hours, starting immediately after completion of treatments. The scans that monitored samples 24 hours after treatment, during which solvents were allowed to evaporate, indicated the same relaxation as before treatment. This lack of

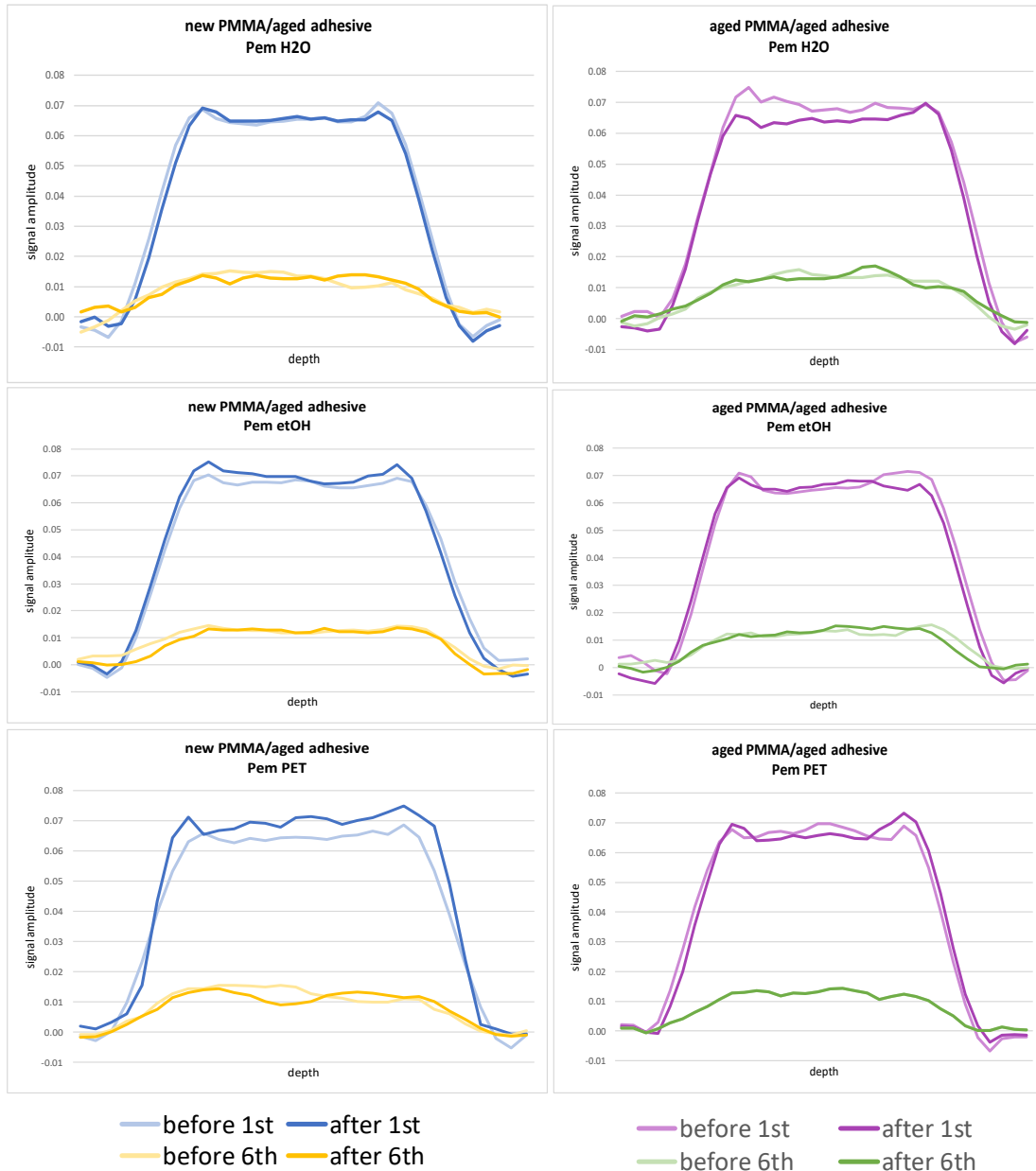
structural change in the bulk material confirmed the safety of these optimised treatments at removing synthetic soil and PSA.



Graph 10.14. Smoothed line graphs of NMR profile scans of PMMA with aged synthetic soil before and 24 hours after treatment with Pemulen hydrogel, Pemulen IPA and PVA EtOH. Profile scans of new samples (left) in black (1<sup>st</sup> echo) and yellow (6<sup>th</sup> echo) tones and of aged samples (right) in orange (1<sup>st</sup> echo) and purple (6<sup>th</sup> echo) tones.

It should be kept in mind that any increase in treatment application time or prolonged contact with solvents expelled from gels, may result in chemical and physical damage. This is particularly true for EtOH, which when expelled from gels with H<sub>2</sub>O (used to thicken the gel) is known to cause maxima of PMMA solubility and swelling (Basavarajappa *et al.* 2016). The chemical alteration of surface PMMA was, after all, seen only after the short timeframe of cleaning with Agar and PVA coupled with EtOH. FTIR analysis of samples treated with these

two gels, showed peak formation characteristic of PMMA crystallisation due to contact with solvent (Luo 1994). Likewise, the NMR profiles of samples immersed in EtOH (Chapter 7.1.2) documented changes in the material. The edge effect of PMMA, shown to have an augmented signal amplitude after immersion in EtOH for 30 days, was the result of mechanical deformation, possibly swelling of the sample edges. Furthermore, contact with an EtOH-containing treatment may lead to the surface opacity of PMMA, resulting from solvent penetration in the surface micron layers.



Graph 10.15. Smoothed line graphs of NMR profile scans of PMMA samples with aged PSA before and 24 hours after gel treatment with Pemulen H<sub>2</sub>O, Pemulen EtOH and Pemulen PET. Profile scans of new samples (left) in blue (1<sup>st</sup> echo) and yellow (6<sup>th</sup> echo) tones and aged samples (right) in purple (1<sup>st</sup> echo) and green (6<sup>th</sup> echo) tones.

## **Chapter 11. CASE STUDY: CLEANING OF MUSEUM OBJECTS**

---

This chapter presents the cleaning application of the successful experimental findings on three objects from the Msheireb Art Centre collection in Doha, Qatar. Objects selected for this purpose fulfil two requirements: they are transparent and made of PMMA. Application of the successful treatments on real objects aimed to test the validity of the lab-based results obtained on model surfaces and compare the ease of application with real-life conditions.

Pemulen/TEA treatments with H<sub>2</sub>O and IPA, as well as PVA/borax EtOH, were identified as the most successful and safe at removing (aged) dirt from PMMA surfaces. Treatments lasted 3 minutes and were repeated 3 times, followed by clearance with multiple cotton swabs moistened with H<sub>2</sub>O, linearly rolled towards one direction. The dirt tested closely simulates real-life surface dirt based on a mixture of dust and human fingerprints from handling. The case studies selected are a half meter long Arabic letter belonging to a shop sign and two smaller identical lighting lamp shades, which resemble in shape the creations of László Moholy-Nagy in Chapter 1 (Fig.1.2) and Chapter 3.2 (Fig.3.2). Given that the successful treatments for cleaning surface dirt were three, each object was treated with one solvent-gel. The shop sign is quite large and its surfaces flat, so each side was treated with a different gel for comparison of the gels' physical properties. This study also tested cleaning of (aged) PSA. Luckily, one of the lamp shades displayed tapes and residual adhesive on its surface. Experimental results indicated Pemulen/TEA treatments with H<sub>2</sub>O, EtOH and PET as the most efficient and safe at removing the type of adhesive commonly used in Scotch™ tapes, resembling the ones found on the lamp shade. Each one of the three tapes were removed and cleaned with one of the Pemulen/TEA hydro/solvent-gels, allowing comparison of the treatments and their efficiency based on thickened solvent.

### **11.1. CASE STUDIES**

The objects were retrieved from the Msheireb Arts Centre in Doha (see Appendix P) and brought into the UCL Qatar Conservation laboratories. All three of them were heavily soiled, externally and internally, displaying increased dust and dirt deposits, which due to their transparency rendered them visually darkened. The neon lamp was particularly soiled internally, with dust accessing the tube from its broken and missing parts. The internal sides of the two lamp shades visibly bared more dirt and dust. The first step was to assign them UCL Qatar Conservation accession numbers that acted as their identification. Before proceeding to condition assessment and treatment, ATR-FTIR was employed for their analysis; Confirmation of their acrylic nature was of principal importance to assessing the treatments (see Appendix Q for ATR-FTIR analysis and Appendix R for treatment reports).

11.1.1. Neon shop sign C550

Before Treatment Photo Documentation C550

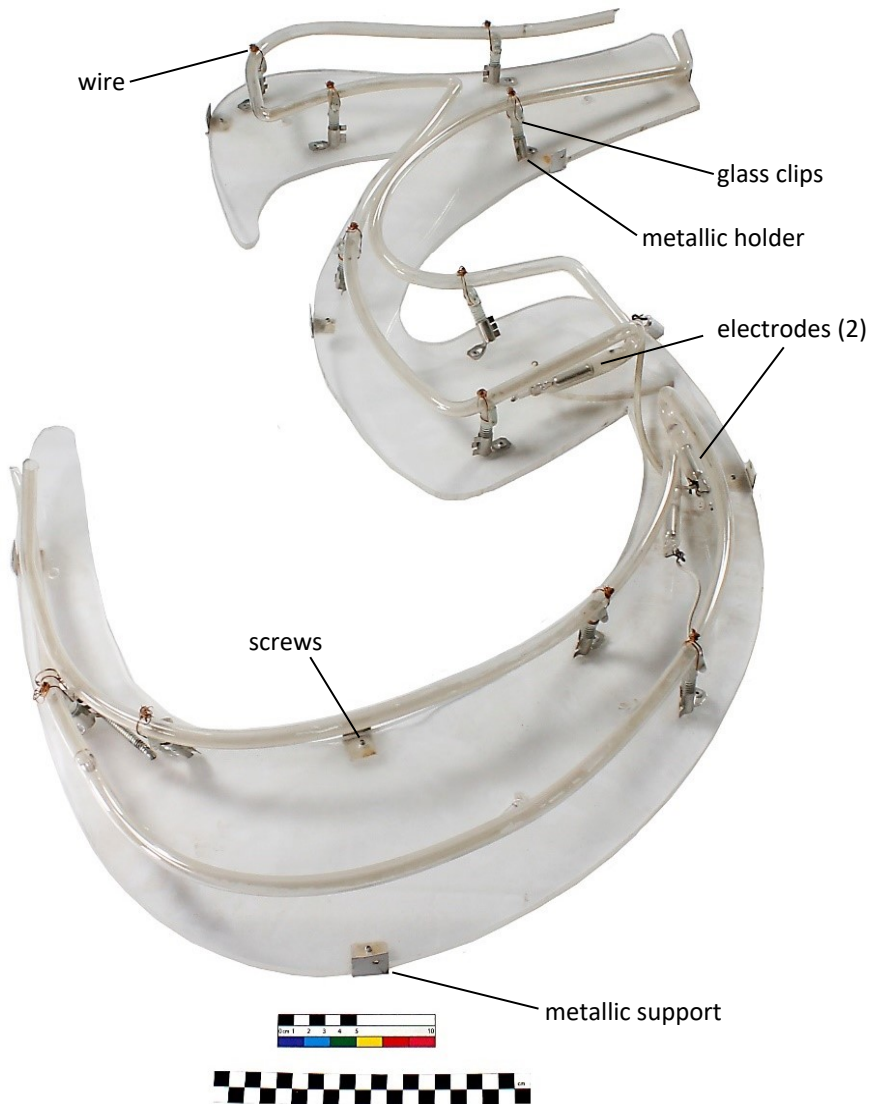


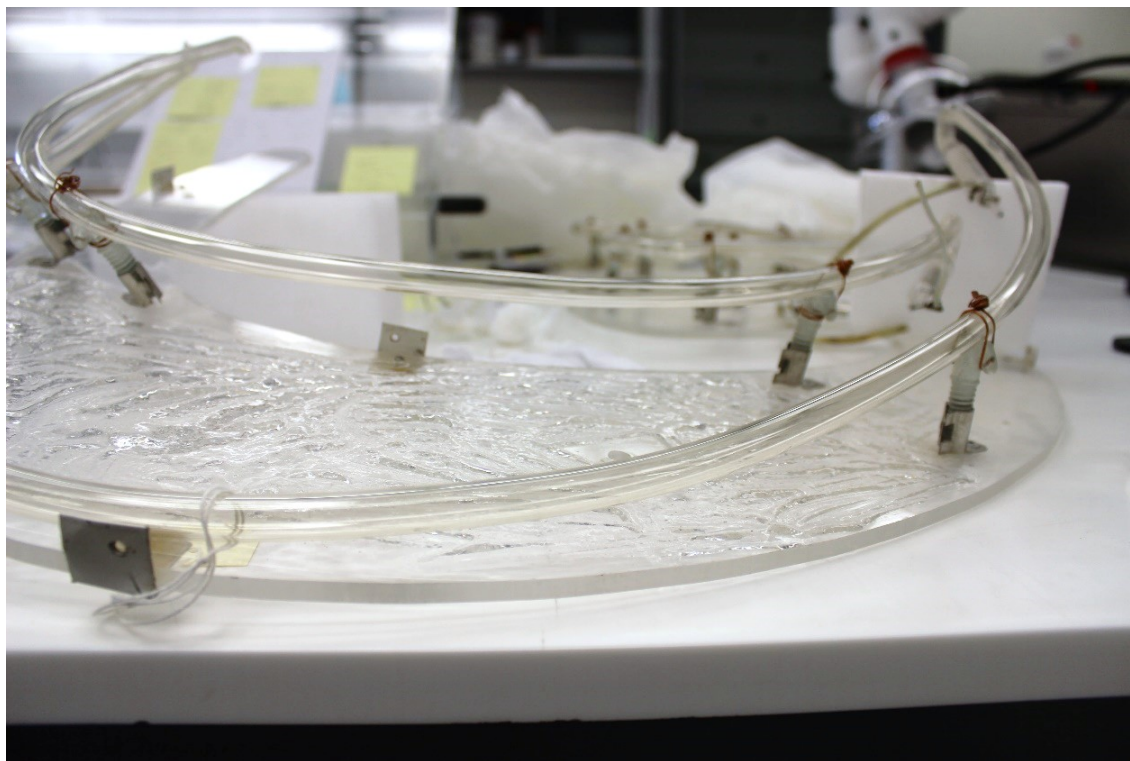
Figure 11.1. Neon shop sign C550 (front side) before treatment.



Figure 11.2. Neon shop sign C550 (back side) before treatment.

### **Treatment C550**

The two sides of the sign were treated differently to allow for direct comparisons and assess the physical properties of the gels as well as their impact on cleaning. One side was treated with 1 % Pemulen:5 % TEA hydrogel, and the other side with 80 % PVA/borax (5%:1%) with EtOH/H<sub>2</sub>O (20/80 wt.%).



*Figure 11.3. During treatment of C550 with Pemulen/TEA hydrogel.*

Pemulen/TEA hydrogel was applied in large surface areas (ca. 200 x 60 mm) (Fig.11.11) with a soft Teflon spatula and removed by soft wiping (Fig.11.12 b). Use of Pemulen/TEA, although messy and problematic to clear off due to its paste consistency, was very successful at cleaning even after the first application. Clearance of the treated surface with swab rolling was remarkable, because all the dirt was visibly picked up along with the Pemulen/TEA residue (Fig.11.13 a). The majority of dirt was successfully removed after two applications. After the third application, the hydrogel removed after treatment completion was clear, without visible soil.



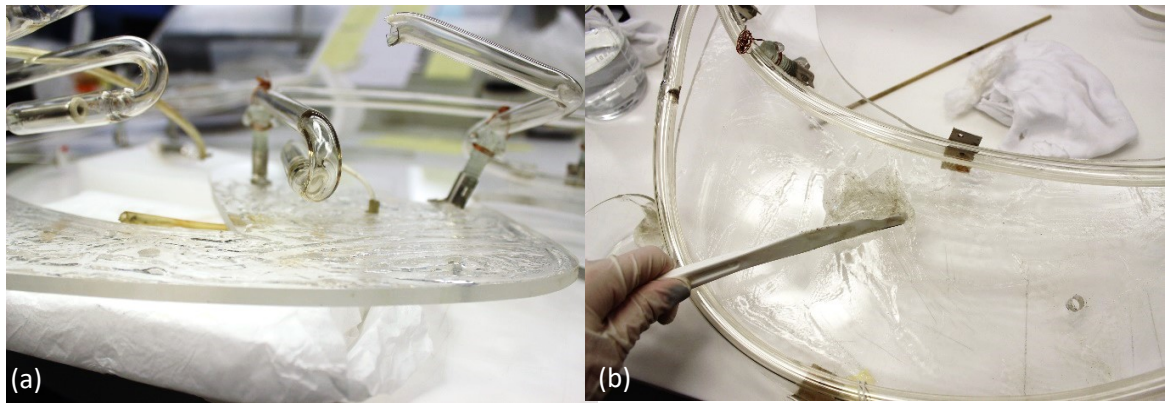


Figure 11.4. During treatment of C550 with Pemulen/TEA hydrogel  
(a). Removal of the gel with Teflon spatula (b).

PVA/borax with EtOH was applied in sheets of roughly 200 x 150 mm. The gel was prepared and stored in flat containers that allowed its putty-like and self-healing structure to spread in a flattened position (Fig.11.14 a-b). This was helpful in applying large pieces on the flat sign surface (Fig.11.14 c-d). The gel visibly darkened after removal from the treated area (Fig.11.13 b), confirming the removal of dirt. The advantage of this formulation in being a smart material that ‘repairs’ itself, is that it is able to retract/rearrange to maintain its shape. This allowed PVA/borax to entrap dirt particles in its matrix and be safely reusable, without the risk of dirt re-deposition. The treated area was not as successfully cleaned after the first application as with Pemulen/TEA.

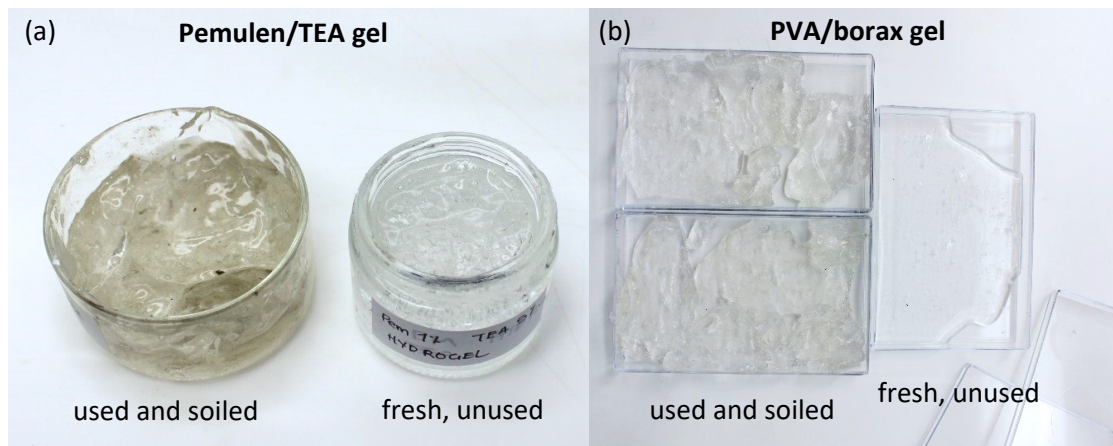


Figure 11.5. Visibly darkened Pemulen gels after use on the shop sign C550 with entrapped dirt compared to fresh, unused gel: Pemulen/TEA (a) and PVA/borax (b).

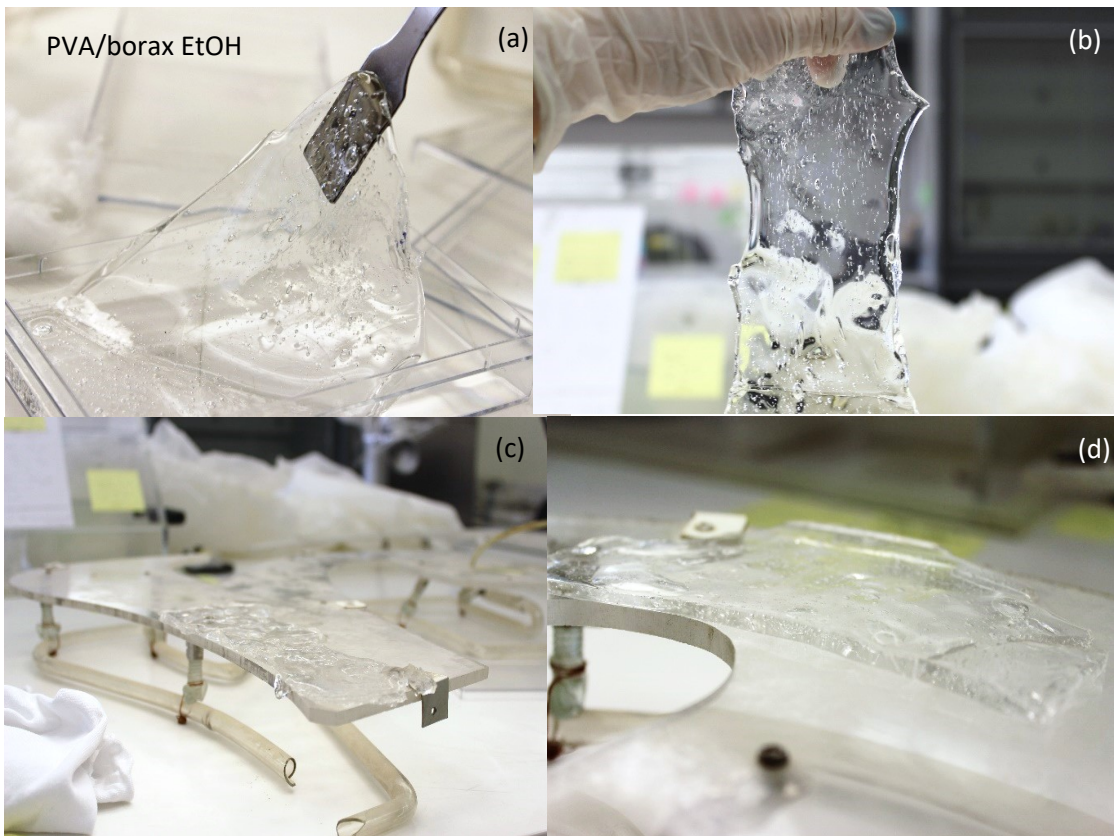


Figure 11.6. PVA/borax EtOH before application (a-b). Gel during treatment of the shop sign C550 (c-d).

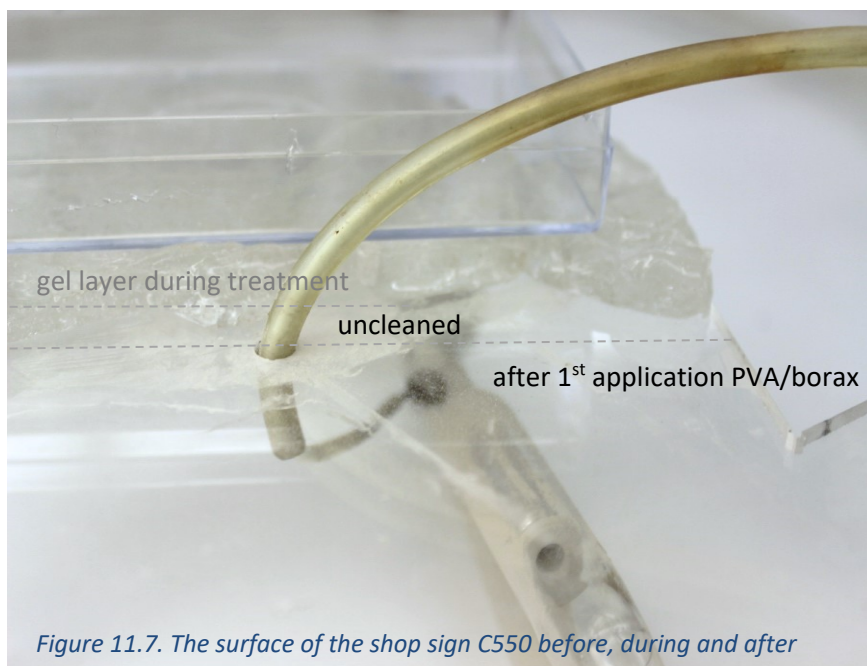


Figure 11.7. The surface of the shop sign C550 before, during and after

The use of PVA/borax was very practical, especially on large surfaces such as the one being treated here. Treatment with PVA/borax EtOH required more applications and more moistened cotton swabs to fully clean PMMA.

Pemulen/TEA's paste consistency allowed it to be easily and uniformly applied, but also rendered it uncontrollable and harder to remove. Unlike PVA/borax, Pemulen/TEA required wiping with Teflon spatula for its removal. This is both an advantage and a disadvantage, as this mechanical action gave it a head start (in successfully removing surface soil after the first application), but also involved unwanted friction on the transparent PMMA surface.

After Treatment Photo Documentation C550



*Figure 11.8. Neon shop sign C550 (front side) after treatment.*



*Figure 11.9. Neon shop sign C550 (back side) after treatment.*

11.1.2. Lamp shade C553

Before Treatment Photo Documentation C553



*Figure 11.10. Light shade C553 (internally) before treatment.*

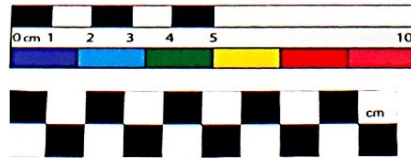


*Figure 11.11. Light shade C553 (externally) before treatment.*

**Treatment C553**

Cleaning of the light shade was carried out with 1 % Pemulen:5 % TEA hydrogel. Removal of each of the three tapes were removed with different Pemulen/TEA solvent-gels. The Pemulen/TEA hydrogel was applied with a soft Teflon spatula in large areas (blocks) (Fig.11.22 a-b). Similar to the shop sign, removal of Pemulen/TEA was carried out with soft wiping and moistened cotton swabs. The removed gels, after the first two applications were too dirty to be reused, with visible dark, soil particles. This meant that the gels were successful at removing all the (loose) soil. As previously seen, clearance of the treated surface with swab rolling visibly picked up dirt along with the Pemulen/TEA residue. The majority of the dirt was successfully removed after two applications (Fig.11.22 c). After the third application, the hydrogel removed after treatment completion was clear, without visible soil.

Results presented in Chapter 10 indicated that Pemulen/TEA gels with H<sub>2</sub>O, EtOH and PET were the most satisfactory at removal of aged PSA, so each solvent-gel was used on each one of the three tapes. The gels were 1 % Pemulen:5 % TEA with 20/80 wt.% solvent/H<sub>2</sub>O. The hydrogel failed to remove the tape (Fig.11.22 f). Pemulen/TEA EtOH was tested next, without succeeding in the complete removal of the tape either. After the first application of Pemulen/TEA PET (Fig.11.22 g), the tape was successfully removed at once. After completion of the treatment (3 applications x 3 minutes) both tape and adhesive were completely removed.

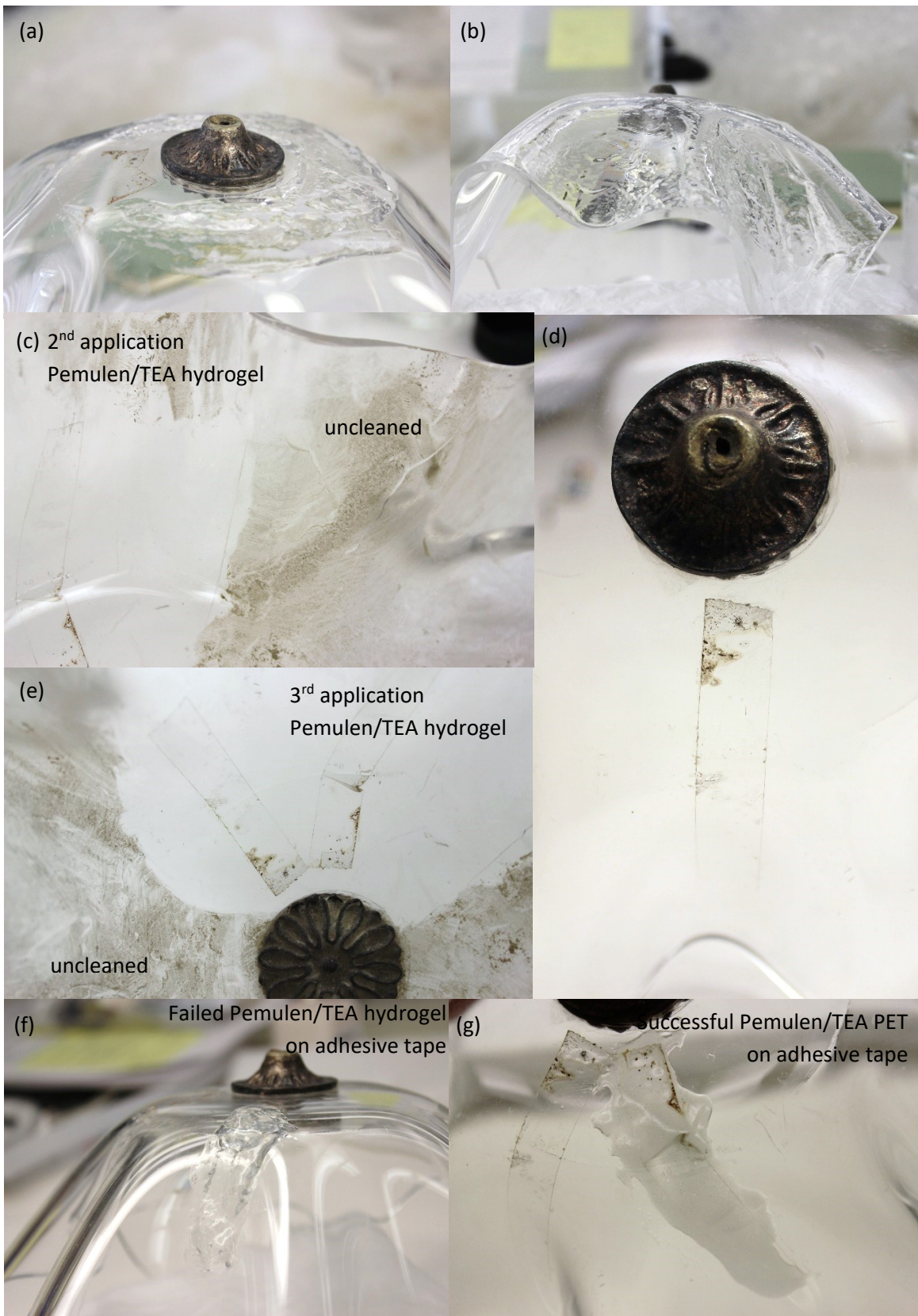


Figure 11.12. During treatment of C553 with Pemulen/TEA hydrogel (a-b). Before and after treatment with Pemulen/TEA hydrogel (c). Transparent adhesive tape (d-e). Treatment of adhesive tape with Pemulen/TEA hydrogel (f) and Pemulen/TEA PET (g).



After Treatment Photo Documentation C553



*Figure 11.13. Light shade C553 (internally) after treatment.*



*Figure 11.14. Light shade C553 (externally) after treatment.*

11.1.3. Lamp shade C554

Before Treatment Photo Documentation C554



Figure 11.15. Light shade C554 (internally) before treatment.



Figure 11.16. Light shade C554 (externally) before treatment.

**Treatment C554**

Cleaning was carried out with 1 % Pemulen:5 % TEA with IPA/H<sub>2</sub>O (20/80 wt.%) (Fig.11.29 a-b). After two applications, the removed gels were too dirty to be reused (Fig.11.30 a), indicating that the gel was successful at removing all (loose) soil. Clearance with swab rolling was remarkable, as seen in all previously treated objects with Pemulen/TEA. The majority of the dirt was successfully removed after two applications (Fig.11.29 c). The same result was seen on lamp shade C553 treated with Pemulen/TEA hydrogel. After the third application, Pemulen/TEA was clear, without visible soil.



Figure 11.17. During treatment of C554 with Pemulen/TEA IPA (a-b). Before and after treatment with Pemulen/TEA IPA (c).



Figure 11.18. Dirt removed from object C554 and entrapped in used Pemulen/TEA (a). Cotton swabs used for clearance after treatment (b). PVA/borax before use on the metallic element (c).

#### After Treatment Photo Documentation C554



Figure 11.19. Light shade C554 internally after treatment.



*Figure 11.20. Light shade C554 externally after treatment.*

## 11.2. CONCLUSIONS

Three PMMA objects from the Msheireb Art Centre in Doha were treated with the successful solvent-gel treatments indicated from the experimental findings. One neon shop sign and two lamp shades, all transparent, were heavily soiled. Each one of the three gel treatments available for removal of organic soil was used on each of the objects. Treatments included Pemulen/TEA gel with H<sub>2</sub>O or IPA and PVA/borax with EtOH. The ability to test two different gel types, a more fluid, paste-like Pemulen/TEA and a highly viscous, elastic PVA/borax was advantageous in that it allowed assessment of their efficiency at cleaning and comparison of their physical properties perceived as ease of application/removal.

Pemulen/TEA with H<sub>2</sub>O and IPA performed comparably by satisfactorily removing surface dirt after the second application. The treated surfaces were left in a transparent clean state after the third application, confirmed by gels being clear after removal. PVA/borax EtOH was less successful because it required more than three applications and extra cotton swabs to completely clean the soiled objects. The success of the Pemulen/TEA gels was attributed to their physical properties and not the solubility action of the thickened solvents. This is also supported by experimental work that showed free IPA and EtOH behaving rather similarly and having, in the past, offered comparable results when cleaning PMMA. Since the two alcohols have that same cleaning action on PMMA, it was argued that the nature of the gel carrier was what influenced the treatments.

Each of the three tapes found on one of the lamp shades were treated with either Pemulen/TEA H<sub>2</sub>O, EtOH or PET. These were the most successful gel treatments from the experimental results at removing PSA, commonly employed in transparent tapes like the ones found here. Pemulen/TEA with H<sub>2</sub>O and EtOH were not as effective as Pemulen/TEA with PET, which successfully removed the tapes and residual adhesive after only one application.

The treatments evaluated in the experimental work as successful and safe for cleaning model surfaces under lab conditions, demonstrated that are able to achieve equally successful results under realistic conditions. Treatments applied here on three-dimensional objects performed satisfactorily. Evaluation of the treated objects was not carried out with visual methods and analytical techniques, as for samples in the experiments. The reason for that was that cleaning here aimed to test the efficiency of the gel treatments in real-life conditions, typically used by conservators, and particularly assess the ease of application on three-dimensional naturally aged and soiled objects.

As a conservator, I was pleased by the performance of the aforementioned gel treatments and I would recommend their use to conservation practitioners in museums and other cultural heritage institutions. They managed to successfully, completely clean dirt and adhesive in satisfactory timeframes. They did not cause any visible change or damage to the treated surfaces. Observation of the treated objects under a magnifying glass confirmed the lack of scratches and residual gel. The ease of their application on larger surface areas renders them ideal for the cleaning of larger objects. The range of different gels tested and suggested in this study have the advantage that they can be used on a case-by-case basis. Considering the variety of object shapes and surface textures found in plastics in art and design collections, gel formulations can be selected based on the required physical properties to match the needs of the object to be treated.

### 12.1. DISCUSSION OF EXPERIMENTAL RESULTS

#### 12.1.1. The effects of free liquids, hydrogels & solvent-gels on pristine PMMA

The first step in this study was to identify gels and solvents that are safe for use on PMMA, and document their visual, chemical and physical effects. Among solvents, direct contact of isopropanol and ethanol caused the biggest damage to PMMA, witnessed as loss of transparency and gloss. This was in agreement with studies indicating the increased, rapid PMMA dissolution after contact with both alcohols (Kawagoe and Morita 1994; Arnold 1998; Bettencourt *et al.* 2002), but in disagreement with the theory of solubility, where neither ethanol nor isopropanol were expected to solubilise PMMA (Brydson 1999; Basavarajappa *et al.* 2016). The former studies also suggested that PMMA solubility increases in alcohol/deionised water mixtures; accounts that were verified here. PMMA lost weight after direct contact with alcohol/deionised water, attributed to volatile component extraction (Quye and Keneghan 1999; Shashoua 2012). NMR MOUSE analysis showed that prolonged contact of PMMA with free ethanol resulted in swelling (see Section 7.1.2.). This effect, although extreme (measured after immersion in the solvent for 30 days) and absent in the cleaning timeframe of this study, confirmed the potential risk of solvent penetration in PMMA's surface micron layers.

After direct contact with alcohol/deionised water, PMMA macroscopically showed surface opaqueness, tidelines and ring-like stains. Microscopic observation revealed the presence of fine particulate matter, which has not been documented or discussed in any previous study examining solvents in relation to the conservation of plastics. The phenomenon is linked to liquid droplets forming on PMMA during treatment and causing the dissolution and local loss of polymer components. During evaporation, a mechanism of fluid flow from the interior of the droplets allows extracted and precipitated non-volatile PMMA components to be carried along and be deposited at the droplets' edges (Deegan *et al.* 2000; Shahidzadeh *et al.* 2015). Simple cotton swab cleaning removed these solutes without any damage.

The use of deionised water was contradictory; Sometimes PMMA has been described as hydrophobic because of its non-polar hydrocarbon backbone and other times as inherently susceptible to water due to its polar ester side group (Wolbers 2000; Van Oosten 2002; Tham *et al.* 2010; N'Diaye *et al.* 2012; Ayre *et al.* 2014). Even though based on the solubility parameters water was not expected to damage PMMA, this study showed the opposite: water caused an increase in PMMA's weight, which was attributed to its penetration. Interestingly, petroleum ether expected to dissolve PMMA according to the solubility theory, was the only solvent to not have any effect. This was in fact sustained in other studies recommending its use for cleaning PMMA museum objects (Sale 1993; Lorne 1999; Laganà 2008). This research has shown that the solubility theory regarding PMMA's behaviour in contact with organic polar and nonpolar



solvents as well as the universal solvent, water, is not reliable. It is advised to consult this theory with caution, especially when planning a cleaning campaign based on the solubility parameters of plastics and solvents.

The immersion study in Section 7.1.2. showed that PMMA samples absorbed free standing deionised water soon after immersion. The literature confirmed water's tendency to fill PMMA's free volume when in direct and prolonged contact (Arnold 1998; Wolbers 2000; Van Oosten 2002; Tham *et al.* 2010; N'Diaye *et al.* 2012; Ayre *et al.* 2014). Treatment with hydrogels in this study also allowed water to penetrate PMMA and cause a weight increase. While this happened in very small amounts, it was very consistent, proving that deionised water could potentially pose a risk to PMMA - particularly with treatments longer than the 5-minute timeframe used in this immersion study.

A number of studies assessing the success of Agar on plaster (Sansonetti *et al.* 2012), acrylic paint (Angelova *et al.* 2016) and oil paint (Baij *et al.* 2017) demonstrated that the gels did not manage to control the solvent diffusion and eliminate the risk of damaging the treated surfaces, as it has been widely proposed in the literature. This was contradicted in this study with the application of Agar and Gellan solvent-gels; they displayed improved PMMA surface wetting and offered more control over solvents, witnessed as a reduction of their deleterious visual effects, especially in the case of ethanol and isopropanol. These abilities of Agar and chemically-similar rigid gels were supported by numerous other studies recommending them for their ability to reduce solvent uptake, and gradually introduce moisture/organic solvents into the treated substrate (Domingues *et al.* 2013a; Mazzuca *et al.* 2014; Fife *et al.* 2015).

The only available published systematic study that closely compares to the current one in its aims and methods, is the one undertaken on young and artificially UV-aged transparent plasticised PVC (Bollard *et al.* 2011). The study compared swab cleaning to Pemulen/triethanolamine emulsions, found to be the safest causing the least surface change to PVC. Direct application of Pemulen/triethanolamine systems on pristine PMMA here was not as safe and successful. The hydrogels left samples visually appearing greasy, opaque, with some scratches and gel residues. The solvent-gels performed better by improving the damaging effects of organic solvents. Carbopol/Ethomeen C-25 gels had the lowest viscosity among tested gels that led to the expulsion of liquid from the gel network during treatment. This undesirable aspect reproduced problems that the use of gels intended to avoid: presence of free liquid and chemical interaction between solvent-plastic. Carbopol systems consistently performed poorly, inducing scratches and depositing numerous gel residues. Although such detrimental effects were equally induced by Pemulen/triethanolamine hydrogels and Carbopol/Ethomeen solvent-gels, only the latter had a statistically negative impact on PMMA. Given all these reasons, Carbopol/Ethomeen

was considered unsafe and is not recommended for use on transparent and high gloss plastic surfaces.

Lastly, PVA/borax systems caused a more controlled action when coupled with organic solvents rather than deionised water. This was supported by a study on acrylic paint where PVA/borax failed to control water diffusion. The study paralleled the amounts of water released from PVA/borax to that delivered from swab cleaning (Angelova *et al.* 2016). The thickening of ethanol and isopropanol in PVA/borax offered improved cleaning; It reduced the visual and physical damage induced to PMMA by free alcohols (see surface opaqueness, ring-like stains, component extraction/dissolution, deposition etc.). This was sustained by several other studies (Carretti *et al.* 2010; Angelova 2013; Angelova *et al.* 2015).

What emerged as most important in relation to the gel thickening of solvents, is that the damaging effect of free-standing alcohols is indeed regulated by the presence of gels. The intense PMMA surface opaqueness caused by free ethanol and isopropanol was absent from all the solvent-gel-treated samples. This demonstrates that gels do offer control over the solvent action, as claimed by numerous scholars (Wolbers 2000; Carretti *et al.* 2010, 751; Cremonesi 2010, 179; Domingues *et al.* 2013, 2746; Sullivan *et al.* 2017). It is worth mentioning that the effects of ethanol and isopropanol on PMMA in this experimental study, as well as of deionised water and petroleum ether, were comparable. This was confirmed by statistical analysis showing that the two pairs caused similar visual effects in a statistically significant manner. The two pairs also induced similar chemical changes; the alcohols caused comparable surface crystallisation (see 7.1.2), whereas deionised water and petroleum ether showed no surface change.

An important outcome of these cleaning experiments is that application time had no impact on cleaning pristine PMMA surfaces. Treatments of 5 and 60 minutes had no significantly different effects on optical properties and surface chemistry. Another equally important outcome concerns Agar and Gellan gels. These are chemically similar and have been used interchangeably not only in conservation applications, but also in other fields as chemical/biological substitutes of one another (Shungu *et al.* 1983). Evaluation of the two gels in this study showed that they performed similarly, leaving samples in a good condition. Gellan occasionally caused some minor chemical change, whereas Agar showed no alteration to the substrate. As statistical analysis confirmed literature accounts that the two gels offer comparable results, Agar was preferred for superior performance compared to its substitute Gellan.

### 12.1.2. Removal of synthetic sebum soil & pressure-sensitive spray adhesive

The findings from Chapters 9 and 10 are summarised in Table 12.1.

unaged synthetic sebum soil		aged synthetic sebum soil	
successful gel systems	failed gel systems	successful gel systems	failed gel systems
5-minute application	5-minute application	5-minute application	5-minute application
Agar ethanol	Agar isopropanol	Pemulen/TEA ethanol	Agar ethanol
Pemulen/TEA ethanol	Agar petroleum ether	Pemulen/TEA isopropanol	
Pemulen/TEA isopropanol	Pemulen/TEA petroleum ether	PVA-borax ethanol	
PVA-borax ethanol	PVA-borax isopropanol		
	PVA-borax petroleum ether	3-minute applications x 3	3-minute applications x 3
	Carbopol/Ethomeen C-25	Pemulen/TEA hydrogel	Pemulen/TEA ethanol
	Hydrogels	Pemulen/TEA isopropanol	
		PVA-borax ethanol	

unaged pressure-sensitive adhesive		aged pressure sensitive-adhesive	
successful gel systems	failed gel systems	successful gel systems	failed gel systems
5-minute application	5-minute application	5-minute application	5-minute application
Agar petroleum ether	Agar ethanol	Pemulen/TEA ethanol	Agar petroleum ether
Pemulen/TEA ethanol	Agar isopropanol	Pemulen/TEA isopropanol	PVA-borax petroleum ether
Pemulen/TEA isopropanol	PVA-borax ethanol	Pemulen/TEA petroleum ether	
Pemulen/TEA petroleum ether	PVA-borax isopropanol		
PVA-borax petroleum ether	Carbopol/Ethomeen C-25	3-minute applications x 3	3-minute applications x 3
	Hydrogels	Pemulen/TEA hydrogel	Pemulen/TEA isopropanol
		Pemulen/TEA ethanol	
		Pemulen/TEA petroleum ether	

Table 12.1. Summary of results of cleaning experiments on unaged and aged (32 days under UV) PMMA with unaged and aged (32 days under UV) synthetic sebum soil or pressure-sensitive spray adhesive.

The gels and solvents deemed safe for direct use on PMMA were tested for their cleaning efficiency on unaged and 32 days UV-aged samples bearing synthetic sebum soil/carbon black or acrylic-based pressure-sensitive spray adhesive. Based on gel theory and chemistry, it was anticipated that Pemulen/triethanolamine gels would be the most successful at removing synthetic sebum soil due to their ability to form aggregations, much like micelles formed in surfactants. These aggregations allow Pemulen to suspend non-polar grime into its structure, such as the synthetic soil formulated in this study to simulate fingerprints of human sebum (Wolbers 2000; Bollard *et al.* 2011; Aguilar-Sánchez and Buentello-Martínez 2017; Stavroudis 2017). This theory was confirmed in this study, where synthetic sebum soil was successfully removed by Pemulen-based treatments. POPART indicated ethanol as the most successful solvent for removal of oil-based dirt and petroleum ether as the least effective (Balcar *et al.* 2012), despite a study recommending it for its degreasing effect (Sale 1993). Results in this research were consistent with both POPART remarks. Gels containing ethanol successfully removed synthetic sebum soil, while gels with petroleum ether failed to do so. PVA/borax-based treatments also failed to remove synthetic sebum soil. This was unforeseen as PVA/borax's highly viscous structure with transient crosslinks was expected to positively contribute to the cleaning action by its ability to reform/retract and conform to surfaces (Carretti *et al.* 2010; Angelova 2013; Angelova *et al.* 2015).

Gels with petroleum ether were very successful at removing acrylic-based pressure-sensitive adhesive. ATR-FTIR analysis of the adhesive identified two main components, an acrylic and a petroleum-based polymer (Varanese 1998; Foreman *et al.* 2003). The adhesive was likely prepared/polymerised in petroleum-based solvents (Wu 2014). So, based on the general principle of solubility 'like dissolves like', petroleum ether rightfully dissolved a petroleum-based adhesive. Equally successful were Pemulen/triethanolamine gels with alcohols. Their success was attributed to the ability of alcohol/deionised water mixtures to dissolve both volatile and non-volatile acrylic components (as previously discussed for PMMA) present in the adhesive. The successful treatments left surfaces in a very good condition.

Treatments were then tested for their efficiency at removing the two types of artificial dirt, after 32 days of UV-ageing. Although certain treatments, such as Agar ethanol, were able to completely remove synthetic sebum soil, they failed to do so when aged. The gel's inability to remove the soil when aged was attributed to Agar's physical properties and concentration %, both of which are known to affect liquid diffusion (Bertasa *et al.* 2017). In fact, at the low concentration of 2 wt.% prepared in this study, Agar was likely to have larger pores (than stiffer gels formed by higher concentrations) (Angelova *et al.* 2016), allowing sufficient amounts of ethanol/deionised water to be released and subsequently diffused. ATR-FTIR of the treated PMMA indicated minor crystallisation resulting from direct contact with ethanol (Luo 1994), confirming the presence of free ethanol/deionised water. This phenomenon was documented only when ethanol was thickened in Agar, and no other gels. Earlier (12.2.1), Agar applied on unsoiled PMMA showed improved surface wetting, reduced solvent uptake and gradual introduction of organic solvents into the substrate. Here, it appears that the soil's acidity, which increased with ageing, interfered with the gel's pH causing syneresis (separation of a portion of the liquid from the gel). In other circumstances, Agar's capillary action was supposed to allow the gel to act as a molecular sponge. In theory, as solvent begins to slowly evaporate from the outer gel surface, on the other side the gel draws out soluble dirt particles, absorbing/trapping them within its matrix (Sansonetti *et al.* 2012). But, as sufficient free solvent was released at once from Agar's large pores, this stopped being a feasible scenario and conditions for the 'sponge' mechanism stopped existing.

Pemulen/triethanolamine with alcohols very successful removed aged synthetic sebum soil and left surfaces in the best condition. The treatments' success was attributed to Pemulen's and triethanolamine's emulsifying properties, as well as ethanol's and isopropanol's polarity. As earlier discussed, Pemulen behaves much like a surfactant (Bollard *et al.* 2011; Stavroudis 2017) and triethanolamine, being a surfactant containing both a hydrophobic and a hydrophilic part (Söderman and Stilbs 1994), increased the treatment's ability to solubilise a lipophilic material

such as sebum soil (Cremonesi 2010). Lastly, the increase in polarity of synthetic soil with ageing (oxidation) required more polar solvents for its dissolution (Umney and Rivers 2003). Consequently, all components were critical to the treatments' success (Stavroudis and Blank 1989). Between the two treatments that performed comparably with a statistically similar impact on PMMA, Pemulen/triethanolamine with ethanol deposited gel residues so was deemed less safe than with isopropanol.

Although PVA/borax ethanol was also very successful at removing aged synthetic sebum soil, it caused scratches and deposited large amounts of gel residue. PVA/borax, a high viscosity polymeric solution, is capable of easily returning to a liquid state when changes in its pH take place (Angelova *et al.* 2017). Such a change was likely to have occurred upon contact with the aged synthetic sebum soil, which turned more acidic with ageing. The soil's acidity interfered with the chemical gelation of PVA/borax (Angelova *et al.* 2017) leading to dissociation and gel deposition. Dissociation enabled contact between free ethanol/deionised water and PMMA, and rendered surfaces vulnerable to scratches induced by swab cleaning during post-treatment rinsing.

Pemulen/triethanolamine petroleum ether performed the best at removal of aged acrylic-based adhesive in terms of cleaning efficiency, visual condition of treated PMMA and safety. It is worth mentioning that petroleum ether in other gels (Agar, PVA/borax) failed to even dissolve aged adhesive. This is attributed to the inability of gels that do not form emulsions or use surfactants, to mix water (polar-phase) necessary for their gelation with a non-water miscible solvent (petroleum ether). Inability to fully form, led such gels to deposit large amounts of residue. It is assumed then that the success of Pemulen/triethanolamine with petroleum ether is not due to the solvent, although it was earlier anticipated to be the most suitable to dissolve the adhesive - as another petroleum-based material. What becomes crucial in this case, is the formation of an oil-in-water gel-emulsion (petroleum ether in water). This appears to have increased the solvating action of the formulation, resembling almost a chelating agent (Stavroudis 2017) by its magnified ability to sequester the hydrophobic, acrylic 'dirt'. Moreover, and most importantly, the presence of the alkaline triethanolamine in the formulation is predominantly held responsible for the removal of aged adhesive (Stavroudis and Blank 1989). During light-ageing, the adhesive became weakly acidic as a result of oxidation, enabling it to bond with a basic triethanolamine and thus be removed along with the gel-emulsion (Stavroudis and Blank 1989).

### 12.1.3. Optimisation of treatments with three consecutive 3-minute gel applications

After having established which treatments were safe and efficient for use on PMMA, further testing was performed with multiple applications of arbitrary time lengths of 1, 3 and 5 minutes. The idea to test multiple applications originated from case studies of gel cleaning paintings consulted in this study, which showed that conservators are more prone to use repeated applications of shorter times than one longer application (Bellucci *et al.* 1999; Warda *et al.* 2007; Casoli *et al.* 2014; Angelova *et al.* 2015). Results demonstrated that the optimum cleaning effect on pristine PMMA is reached after three consecutive gel applications of three minutes each, with a post-treatment clearing method (rinsing) after each application. At this point, it was decided to confirm whether previously discarded treatments for failing to clean PMMA after one gel application, would still fail after 3 applications x 3 minutes. Pemulen/triethanolamine hydrogel, PVA/borax ethanol and PVA/borax petroleum ether, earlier failed to remove synthetic sebum soil (former two) and aged adhesive (latter), proved to be effective after following the optimised, repeated application method. This was proof that the method is in fact beneficial to the cleaning process of PMMA.

The optimised cleaning tests showed that Pemulen/triethanolamine hydrogel, Pemulen/triethanolamine isopropanol and PVA/borax ethanol were the most successful at removing aged synthetic sebum soil. After the three 3-minute applications PVA/borax ethanol improved, in that it didn't cause scratches, nor deposited gel residue, seen after the 5-minute application. The disadvantage of the two Pemulen-based treatments was that they deposited some gel residue detected by ATR-FTIR, whereas PVA/borax ethanol caused minor surface crystallisation (seen also after Agar ethanol). Despite these issues, these three cleaning treatments offered a good balance between sufficient safety for use on new and aged PMMA surfaces and efficiency at fully removing dirt of oily nature - with the application method and within the timeframe established here. This evaluation resulted from a combination of visual and chemical assessments. To validate the results, unilateral NMR monitoring was employed to investigate the effect of the three treatments on the physical structure of PMMA, and it established the lack of solvent penetration and liquid movement in the treated samples. It also confirmed that no mechanical, structural change occurred in the bulk after contact with the gels.

Furthermore, the optimised cleaning tests showed that Pemulen/triethanolamine gels containing ethanol, isopropanol and petroleum ether were the most successful at removing aged adhesive. Unilateral NMR monitoring confirmed the lack of solvent penetration and mechanical damage. NMR results validated the experimental outcome that these treatments have indeed been optimised to provide the safest cleaning of transparent and high gloss PMMA surfaces and the most efficient removal of synthetic sebum soil and pressure-sensitive adhesive.

Cleaning treatments, despite being optimised, need to be used with caution. Possible risks are always likely to arise. As earlier discussed, Pemulen/triethanolamine hydrogel may expel free water which can then penetrate PMMA, while unwanted gel residue is always likely to be left behind. These risks are considered acceptable in this study, as long as water quantities are low enough not to alter PMMA's physical structure. The slow evaporation rate of triethanolamine in Pemulen gels could have long-term detrimental effects (Hennen *et al.* 2017). Given the absence of more studies on the effects of gel residues on treated surfaces, this will require further attention and future investigation. Attention is also needed when using PVA/borax ethanol, as ethanol is capable of causing the formation of an ordered aggregated structure (crystallisation) on the PMMA surface. In practice this means that, within the short timeframe of the treatment, PVA/borax can allow sufficient free ethanol to contact PMMA leading to unsolicited surface chemical alterations. This constitutes a problem as a cumulative process which can, in the long-term, cause optical and structural changes (loss of transparency, cloudiness, development of a crack network).

Overall, new PMMA samples tended to steadily lose small amounts of weight regardless treatment. Since new PMMA did not undergo any prior accelerated chemical alterations, like in the case of aged samples, contact with wet treatments and especially organic solvents was likely to cause dissolution/extraction/evaporation of components, manifested as weight loss (Quye and Keneghan 1999; Shashoua 2012). Volatile components, such as unreacted residual methyl methacrylate monomer from incomplete free radical polymerisation reactions could readily evaporate (Gates and Grayson 1999; Ayre *et al.* 2014). In this study low-molecular-weight liquids, particularly alcohols, often caused the dissolution of PMMA, starting from the surface layers (Bogdanova *et al.* 1986). A very positive aspect of the optimised treatments here is that, although they dissolved PMMA components, these were only a small/negligible fraction of the sample. Most importantly, optimised treatments did not induce crazing or cracking; This is a very notable result, as it has been previously thoroughly documented that PMMA dissolution commonly manifests itself through cracking (see Chapter 7) (Ouano and Carothers 1980; Papanu *et al.* 1989; Kawagoe and Morita 1994; Basavarajappa *et al.* 2016).

In aged samples the opposite phenomenon was observed: aged PMMA tended to steadily gain weight after treatment. This was attributed to small amounts of liquid penetrating the bulk through voids (Bogdanova *et al.* 1986; Shashoua 2008; Affolter 2015) formed during UV ageing by the extraction of volatile PMMA components (Gates and Grayson 1999; Ayre *et al.* 2014). These observed trends of aged PMMA to show minor gain and new PMMA minor loss after gel cleaning are consistent throughout this study.

## 12.2. REVIEW OF CLEANING EVALUATION METHODS

This study employed several methods for the visual evaluation of treated surfaces. A system of ranked values (CARS scores) was designed to quantify surface condition based on naked eye observation. CARS was vital to this research dealing with the aesthetics of museum objects at large, because it offered a realistic - macroscopic - assessment of transparent surfaces from the human observer point of view. Moreover, it offered an evaluation of the cleaning treatments immediately after their completion. Stereomicroscopy was chosen for surface documentation, as it managed to eliminate the scattering effect of light from transparent and highly polished surfaces, while offering standardised images. SEM imaging offered higher-resolution and -magnification topographical images of areas of interest identified under the stereomicroscope, in an attempt to describe them. Gloss measurements were used as an underpinning method of surface visual assessment expressed as quantitative information. Correlating the relative numerical gloss change with macroscopic evaluation through CARS was a valuable means of rendering visual evaluation more reliable and less subjective.

CARS took into consideration scratches induced to the treated surfaces and scores were assigned based on how visible these were to the naked eye. Overall the optimised gel cleaning treatments under study did not induce macroscopically visible abrasions. All samples were left in a satisfactory condition with the vast majority scoring 4, corresponding to intact surfaces with 0 % abrasions. SEM imaging confirmed these results, with few exceptions samples treated with Pemulen/triethanolamine and PVA/borax systems, mostly coupled with ethanol. These treatments induced scratches only visible under SEM high magnification (ca. x100). This study demonstrated that cleaning with both Pemulen/triethanolamine and PVA/borax resulted in release/expulsion of ethanol and that PMMA in direct contact with it became more susceptible to scratches, instigated by the gentle post-treatment rinsing with cotton swabs. In other words, contact between free ethanol-PMMA, although brief (long as the treatments timeframe) was sufficient to increase surface sensitivity.

Scratches were also occasionally attributed to the use of soft Teflon spatula for the removal of Pemulen/triethanolamine, and less often PVA/borax. The paste-like and sometimes emulsifying consistency of the former required a soft swiping away movement to be removed. PVA/borax when mixed with deionised water or petroleum ether formed less consistent networks, unable to be removed intact. In these cases a Teflon spatula was also used directly on surfaces to swipe the gel away via gentle mechanical friction.

It is important to understand that all surfaces, even the ones seemingly intact to the naked eye, appeared rather poor and somewhat damaged when magnified. However pristine the surface condition of a material, in a micro-level this always displays some level of damage.



This led to several questions: how well did the microscale of an image correlate with the macroscopic human perception? What if changes documented under high magnification, were not reflected on macroscopic observation? Microscopy acted more as a supporting method and was employed to understand the nature of damages. Yet, human observation, even if subjective, remains a real-life approach; it corresponded more suitably to the needs of this study questioning at large the impact of cleaning on the surface aesthetics of transparent and high gloss plastics.

ATR-FTIR analysis was employed for the chemical evaluation of treated samples with the optimised treatments, some of which induced minor crystallisation of PMMA surface structure. Optimised treatments were lastly evaluated with unilateral NMR, which showed that no changes occurred in the bulk of the samples and their mechanical behaviour. Optimisation of treatments proved to be essential for the preservation of PMMA's optical qualities - critical for the appreciation of translucent pristine objects found in museum collections.

All procedures regarding preparation, conditioning, weighing and cleaning of samples followed systematic and carefully planned protocols. These were established to reduce repeated and random errors during experimental work and proved successful in doing so. Following established methodologies enabled samples to be equally handled and treated, in turn allowing data to be representative and comparable. The success of standardising methods was demonstrated in the main experiments, where clear behavioural patterns and tendencies of treatments were observed. This was something that was missing from the preliminary experiments carried out prior to the establishment of protocols. Aged samples displayed extremely consistent weight changes and comparable values, regardless treatment, whereas new samples behaved rather unpredictably/more erratically. This occurrence indicated that aged surfaces had been homogenised as a result of being subjected to controlled ageing cycles under identical conditions.

### **12.3. CASE STUDIES: CLEANING OF THREE-DIMENSIONAL MUSEUM OBJECTS**

To validate the optimised treatments obtained on model surfaces in laboratory conditions, and test whether they are safe, efficient, and user-friendly in real-life conditions, treatments were applied on three case studies. The transparent PMMA objects from Msheireb Art Centre (Doha) were heavily soiled with surface dust and dirt deposits simulated in this study with synthetic sebum soil/carbon black. Each of the three optimised treatments was used for cleaning one of the objects, which being located in the same storage and exposed to the same conditions, enabled the direct comparison between treatments.

The shop sign shaped as an Arabic word was cleaned with two different treatments, Pemulen/triethanolamine hydrogel and PVA/borax ethanol, one for each side in an attempt to compare their adaptability and level of handling ease in a realistic cleaning scenario. The two identical flower-shaped lamp shades were treated either with Pemulen/triethanolamine hydrogel or isopropanol. One of the lamp shades bared three pieces of pressure-sensitive adhesive tape and residual adhesive, of unknown composition. However, as most commercially widespread pressure-sensitive adhesives used in tapes are rubber- or acrylic-based (Zięba-Palus 2007), it was likely that this adhesive was similar to the one studied here. This was an ideal situation as it allowed testing of the three optimised Pemulen/triethanolamine treatments with water, ethanol and isopropanol, for removal of adhesive.

Use of Pemulen/triethanolamine was quite messy, both on the large flat surface of the shop sign and the curved lamp shade. Due to its paste-like consistency, removal with Teflon spatula was challenging, especially around the folds of the flower-shaped lamp shade. This unfavourable feature of Pemulen gels/emulsions had been previously recognised during the experiments. It was nevertheless rectified by their remarkable ability to completely clean PMMA, even after one application. Outstanding was also their ability to pick up and peel off residual surface soiling, especially during the post-treatment rinsing step. Rolling of moistened cotton swabs lifted any deposited residual Pemulen/triethanolamine, which in turn picked up soiling remains.

The advantage of PVA/borax was connected to its physical properties of being putty-like, malleable and self-healing. These enabled its application as pre-formed, flattened pieces on the large, flat surface of the shop sign. Moreover, its ability to constantly reform and retract was beneficial for entrapping dirt particles in its matrix, avoiding dirt re-deposition/distribution. While PVA/borax transient crosslinks were practical for cleaning large flat surfaces, they became problematic when treating non-horizontal, non-flat surfaces (i.e. lamp shade). The reason for this was that PVA/borax systems' self-healing property required some barrier during treatment, to stop them from retracting and losing contact with the substrate.

Pemulen/triethanolamine with water and isopropanol performed comparably by almost completely removing surface soiling from PMMA after the first application. PVA/borax required more than three applications and additional cotton swabs to completely clean the object. Pemulen was more uncontrollable and required wiping with a spatula to be removed. This mechanical action produced by wiping is what gave the treatment a head start in its cleaning efficiency from the first application. Although use of a spatula increased the risk of scratching, visual observation confirmed the lack of scratches. The tape and its residual adhesive were successfully removed with the Pemulen/triethanolamine petroleum ether gel-emulsion after

only one application. Gels with water and ethanol were not as effective. This outcome was in alignment with the experimental results that identified the gel-emulsion as the best treatment for removal of pressure-sensitive acrylic-based adhesive.

The case studies highlighted that different objects have different needs due to their shape, size and geometry. It was also understood that having a choice between different gel types with a range of physical properties is important. In this cleaning study of real objects, the nature and physical properties of gel systems were the most significant factors influencing the cleaning efficiency.

#### **12.4. EXPERIMENTAL CRITIQUE & LIMITATIONS**

The potential limitations of this study are addressed here. The survey consulted for the selection of plastic type to investigate was based on a limited access to practitioners of modern materials and plastics conservation. The reason for this was that the number of professionals specialising in this field and actively working as plastics conservators is small. Despite this limitation, their answers reflected the current needs of conservation practice, which were fed right into this study. The survey highlighted the problematic of cleaning transparent and highly polished surfaces, and listed PMMA among the plastics commonly in need of cleaning. These findings were cross-referenced to the conservation literature. Another factor driving the success, or otherwise, of the treatments is the swab cleaning protocol. The post-treatment clearing step for rinsing the gel systems consisted of three separate wet washes with moistened cotton swabs. These were gently rolled in strictly linear motions towards one direction along the PMMA surface. While this may be an ideal method to swab clean according to various tests carried out in this study and the literature (Shashoua *et al.* 2009), it may not reflect the routinely employed swabbing of practicing conservators. Performing the rinsing step differently, for instance in circular motions or rubbing the surface, would possibly maximise the amount of scratches on pristine PMMA. Conservators are therefore advised to employ a rolling motion when clearing residual gel from surfaces. Lastly, this study recognises that it employed 'simple'/core gel recipes with the essential components to form a gel, without testing a range of additives (i.e. surfactants). These may have offered different sets of physical properties and solvencies. The conclusions drawn based on the cleaning experiments with the specific gel formulations are not definite. Certain gel treatments that have been identified as unsafe or poor in this study, could be improved with the use of additives - not tested here. This limitation is important to acknowledge as it identifies new gaps in the field and the need for further development in the area of study.

## 12.5. CONCLUSION & FURTHER RESEARCH

This study contributes to a recently established conservation field, that of modern materials, by offering treatment solutions non-existent to date, appropriate for use on pristine acrylic surfaces. For a field that lacks established treatments and methods for cleaning these types of surfaces, with limited research publications and case studies for conservators to consult, this research provides a methodical and practical approach for the conservation of PMMA. It was important to primarily consider the experience and expert opinions of conservators of modern materials and plastics, who face these problems first-hand in real-life conditions. A conservators' survey informed the research by identifying problems in the cleaning of plastic museum objects. The analysis of findings led to the identification of transparent and/or highly polished surfaces as particularly difficult to clean, placing them in conservators' top priorities. PMMA was indicated both as more commonly in need of cleaning and more challenging to clean. Archival research and further consultation with conservators showed that PMMA in a range of collections from modern and contemporary art, industrial design and decorative arts to social history, science and technology, is recurrently found as transparent and highly polished. Thus, such pristine museum objects were selected as the focus of this study.

Research on cleaning of plastics, and more specifically of pristine types of surfaces, is very limited in the field of conservation. The topic lacked established cleaning methods and well-defined treatments, recommendations for the use of safe materials and evaluation of possible risks. This absence of studies led to contradictory evidence about the use of several cleaning agents on PMMA, even concerning the routine use of water. Limited studies carried out preliminary evaluations on cleaning materials and techniques for certain types of plastics, yet without drawing definite conclusions. A team of scholars collaborated in the POPART project, to explore the use of materials and methods on six commercial plastics, including PMMA. POPART's cleaning protocols and preliminary results formed a solid starting point, however time didn't allow thorough investigation and definite conclusions.

The inherent problem with cleaning pristine plastics is that having a low tolerance to physical damage, scratches and other surface modifications are readily visible (Rivenc *et al.* 2011; Shashoua 2012b; Dei 2013). Presence of surface deposits, as well as cleaning as an operation, can both impact the nature of the material, causing visual and chemical alterations. There is a large number of artists and designers that have attributed their choice of using transparent and highly polished PMMA to its optical qualities of high clarity and interaction with light (Rogerson 2009; Chiantore and Rava 2012; Lenz 2012). Therefore, pristine PMMA objects/artworks found in museum collections, ranging from sculptures and everyday objects to pieces of furniture or jewellery, draw their aesthetic/artistic value from their aesthetic properties and

phenomenological characteristics (Shashoua 2012). It may well be argued that a number of imperfections developed on such objects would change their whole perception and the way they were meant to look (Learner *et al.* 2011).

A very important outcome of the POPART project was the observation that prolonged exposure to solvents rendered cleaning of plastic substrates easier. This remark led to the idea of employing gel systems. A large number of conservators and conservation scientists have explored gels in other conservation fields, with a particular emphasis on easel and wall paintings. The current study builds upon these already formulated gel systems, in that it 'borrowed' and appropriated them for use on acrylic surfaces, investigating their cleaning potential.

Simple mechanical cleaning can introduce abrasions and in turn, decrease the light reflective properties by reducing gloss. Other challenges relate to the amorphous nature of PMMA; Wet cleaning, routinely employed during a conservation campaign, can enable penetration of liquids in the bulk and cause swelling, component extraction and dissolution, crazing and cracking (McGlinchey 1993; Quye and Keneghan 1999; Shashoua 1999; Akhurst 2008; Chuang *et al.* 2016). This vulnerability of PMMA to cleaning and the possibility of instigating damage, was expected to be reduced through the use of gels. The assumption was that gels were likely to optimise treatments due to their ability to thicken and immobilise solvents, increase contact time between gels-treated substrate, and offer more control over cleaning (Carretti *et al.* 2008; Gorel 2010; Baglioni *et al.* 2013; Sun *et al.* 2014; Angelova *et al.* 2015). Another important advantage, intriguing for this study, was the gels' ability to limit, and even eliminate, mechanical stress, compared to the friction induced by routine cotton swab cleaning (Callister and Rethwisch 2014). The promising use of gels in relation to plastics was understudied, and often unexplored, alongside the general lack of research on cleaning of plastics.

The present study methodically addressed this deficient topic, according to the needs and priorities of expert conservators. The systematic research leading to this thesis was conducted on pristine transparent and highly polished PMMA surfaces through statistically designed laboratory-based cleaning experiments on unaged, recently manufactured and artificially UV-aged coupons. Light ageing was carried out in an Atlas weathering chamber following standards simulating accelerated outdoor weathering conditions, as a worst-case scenario light exposure. These aggressive conditions of the more detrimental UVB range were selected because, firstly, they are the only wavelengths in the electromagnetic spectrum that can damage PMMA, a rather durable plastic to ageing (Shashoua 2008). Additionally, accelerating the degradation process, and effectively/adequately obtaining degraded material within a workable timespan, was important for the progress of the study.

One critical aspect was establishing a methodology for efficiently removing surface dirt identified in the conservators' survey as the most commonly found on plastics in museum collections: one of greasy and soiled nature simulating human fingerprints from inappropriate handling with deposited surface loose dust - combining the two most common dirt types, and a pressure-sensitive acrylic-based spray adhesive representing adhesive remains from labels, packaging and sticky tapes. Use of statistically-designed experiments was vital for the progressive narrowing down to the most significant cleaning liquids and gel carriers (factors), eventually leading to the optimisation of treatments, as the most suitable for cleaning PMMA.

The main research questions firstly regarded the efficiency and safety of gel cleaning systems at removing surface 'dirt' of oily and adhesive nature from PMMA surfaces. Secondly, the study focused on developing a methodology for use of gel cleaning systems on plastic substrates. The third objective was to evaluate potential changes and risks on the PMMA on a macro- and microscopic level, and lastly, to identify changes in PMMA's chemical and mechanical properties following gel cleaning. The successful experimental results obtained on modelled surfaces were finally applied on three, three-dimensional transparent and naturally soiled PMMA objects from a historical museum collection, to shed light on the performance of the optimised treatments and their effects, under realistic conditions.

This research employed a cutting-edge scientific approach and took into consideration the state-of-the-art knowledge of treating plastics and conservation ethics. As a result, a range of materials and methods for safely cleaning transparent and highly polished PMMA and removing surface dirt of oily nature or acrylic-based adhesive, were identified and suggested. It optimised treatments and established a cleaning methodology with detailed information on the preparation of the successful gels, their application, removal and post-treatment rinsing (clearing step). It evaluated the visual, chemical and physical effects of treatments, and quantified them. Additionally, it thoroughly documented the potential risks and damage that may be caused by the individual and combined use of the cleaning liquids and gel carriers. Throughout this research, the following became evident:

- Cleaning efficiency of a treatment is primarily dependent on the chemical interactions between gel system-type of dirt.
- Equally important for the treatment success is the chemistry between gel matrices-thickened solvents.
- PMMA-solvent interaction is what defines a treatment's safety.
- Dirt removal is often reliant on the physical properties of the formulated gel. These properties are directly responsible for the gels' adhesiveness on the treated substrate and, in turn, the presence of residues left behind.

- No treatment is completely safe, even if the damage instigated is minimal. A threshold of the acceptable damage needs to be set on a case-by-case basis, according to the material requirements.
- It is important to bear in mind that not all damage induced, takes place visibly: chemical and physical phenomena occur concurrently in the PMMA during gel treatment.
- Pristine surfaces examined here had a very low tolerance that rendered them easy to scratch and readily show it.
- The rigidity and well-defined shape of polysaccharidic Agar and Gellan is advantageous in that the gels deposit little to no residues.
- Carbopol/Ethomeen is uncontrollable and hard to remove without the mechanical action of a soft spatula. Carbopol's low viscosity renders it hard to remove and likely to deposit residues. Perhaps the post-treatment clearance step proposed in this study with three moistened cotton swabs is not sufficient for clearing off Carbopol/Ethomeen and its residues.
- Pemulen TR-2, although of similar chemical consistency to Carbopol, forms malleable gels with better retention properties. This allows their intact removal. This improvement in physical properties was evident when Pemulen formed emulsions with petroleum ether, which due to their higher viscosity are easily peelable in one piece.
- PVA/borax with ethanol and isopropanol form the most consistent networks, attributed to their self-healing/retracting property (Riedo *et al.* 2015; Angelova *et al.* 2016). Their malleability and elasticity offer great contact with the PMMA surface as well as intact removal.

In conclusion, this research answered questions about the efficiency and safety of gel cleaning of pristine PMMA surfaces, confirming accounts of past studies (Carretti *et al.* 2010; Cremonesi 2010; Sansonetti *et al.* 2012; Domingues *et al.* 2013b) that certain gel formulations actually optimise cleaning and eliminate surface mechanical stress and abrasions. This was witnessed as an ability of the gels to thicken and immobilise water and organic solvents, limit their diffusion in PMMA, while increasing their contact time. Moreover it was demonstrated that gels were able to limit, particularly in cases of ethanol and isopropanol, the (aggressive) solvent effects on PMMA, thus reducing mechanical stress, abrasions and appearance, compared to the free-standing solvents. Overall, certain gels investigated in this study, in particular Pemulen/triethanolamine, managed to offer more control over cleaning. Other gels, such as Carbopol/Ethomeen, performed poorly, were inefficient at dirt removal and unsafe for use on transparent and highly glossy PMMA.

### 12.5.1. Recommendations for future research

The field of plastics conservation has been recently established and the use of gels for their cleaning has had limited application/research. Therefore, there are still gaps in the knowledge base that need to be filled. The following suggestions include ideas for further analysis, mostly surrounding the topic of residual gel deposition, which was beyond the scope of this study. The topic was explored via visual observation with SEM imaging. Surface deposits were observed in the SEM images, but it was difficult to firmly identify them as gel residue rather than adhesive remains. In some cases, ATR-FTIR surface analysis was able to confirm their presence on the treated PMMA, while a ranking system was used to describe their relative amount by assigning scores between 0 (covered in residues) and 4 (no residues) to treated surfaces, according to macroscopic assessment. This issue could be addressed via the use of fluorescent tracers/dyes to tag/label the individual gel components, which would then be easily detectable on sample surfaces due to fluorescence. This will be helpful for the evaluation of the treatments' long-term safety. Another idea that will assist in the residual gel and additive deposition question is to employ py-GC/MS for characterisation of the treated samples. This will enable identification of residual gel, as well as degradation components, in relation to the different gel systems used for cleaning.

Another interesting area to further explore that emerged from the evaluation of the established cleaning protocol, is to test post-treatment rinsing with more/different liquids, i.e. organic solvents, than just deionised water, and re-examine the presence of residual gel. This will assist in further improving the treatments' rinsing and safety. Moreover, it will be appealing to investigate the thermomechanical behaviour of the gels used in this study with DMA. Information obtained will elucidate their physical properties, such as viscosity, adhesion and rheology, in an attempt to understand the physicochemical interaction between gels and PMMA surface. These properties are responsible for gel residue deposition, directly depended on the gel adhesiveness on the treated substrate. Lastly, what seems promising is to re-treat the same samples with the same gel treatments in the future, and re-assess their post-treatment visual, gravimetric, gloss, chemical and mechanical properties. This way we will be able to view the effects of cleaning treatments as a cumulative and repetitive process, rather than an individual event.



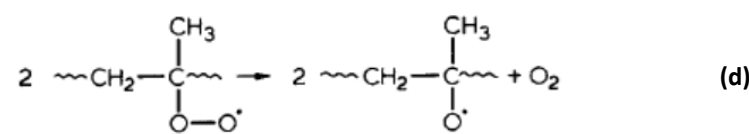
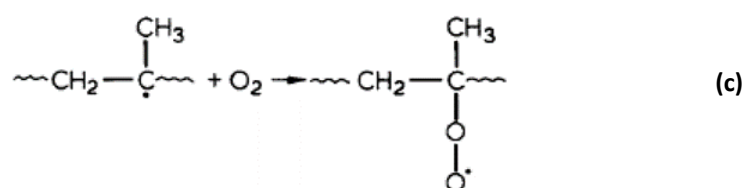
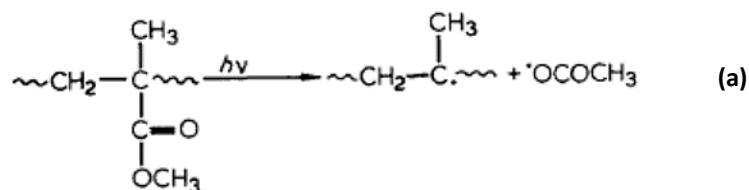
**Appendix A. Primary photooxidation routes of PMMA relating to the movement of free radicals**


Figure 1. Small radicals formed by cleavage of the ester side group (methoxycarbonyl) (a). The small radical formed can abstract hydrogen from the methylene methyl group in the PMMA backbone to give a secondary alkyl radical (b). In presence of oxygen, the alkyl radical rapidly reacts with it to give a peroxy radical (c). When both peroxy radicals are tertiary, a non-terminating interaction occurs to give alkoxy radicals (d) (Dickens *et al.* 1984, p. 710-711).

In PMMA, main chain scission can take place via two energy-related processes: direct main chain scission occurring on exposure to wavelengths of 300 nm and ester side chain scission via a two-step process. Firstly, a radical is formed by chain scission of the C=C double bond and the removal of the ester side group (methoxycarbonyl) (Fig.2.18a). The small methoxy and carbomethoxy radicals formed from the decomposition of the PMMA ester side group can abstract further hydrogen from the methylene or methyl groups in the PMMA backbone, forming secondary alkyl radicals (Fig.2.18b). These rapidly react with oxygen – when available – to give peroxy radicals (Fig.2.18c) (Williams 1993; Nicholson 2006). Their formation, in theory requires no light and can be induced both thermally, as temperature approaches the T<sub>g</sub> of PMMA, and photo-chemically (Feller 1994a). Peroxy radicals are not sufficiently reactive to abstract hydrogen from PMMA, but will interact with other peroxy radicals (Gupta *et al.* 1980). When both peroxy radicals are tertiary, a non-terminating interaction occurs to give

alkoxyl radicals (Fig.2.18d). When at least one of the radicals is not tertiary, they can combine at room temperature (Gupta *et al.* 1980) to give an alcohol, a ketone or aldehyde, and no further chain scission.

## **Appendix B. Conservation survey questionnaire & answers**

\*The correspondence has been edited to omit personal data.

### Email questionnaire

RE: cleaning of plastics/PhD

Please let me introduce myself, my name is Stefani Kavda and I recently started my PhD in the cleaning of plastics in design in UCL Qatar, under the supervision of Dr. Stavroula Golfomitsou (Coordinator and Lecturer in Conservation Studies UCL Q) and Dr. Emma Richardson (Lecturer in Materials, Department of History of Art, UCL).

In this initial stage I am refining my research topic, which aims to examine the behaviour of plastics towards (surface) cleaning (agents, systems and application methods) from soiling.

Cleaning treatments are poorly developed and in order to render my research more focused and efficient, the testing of different methods and materials that correspond to actual cleaning approaches routinely used by conservators is needed. Through this informal email I seek your help in locating key problems when working with plastic museum objects.

I would be very interested in problems you face when cleaning plastics:

- types of plastics that are more problematic/ harder to clean (in terms of their chemical properties or colour),
- a specific plastic (or family of plastics) that more commonly requires cleaning amongst objects in your museum's collection,
- types of dirt that you are often called to remove,
- plastics that demonstrate dirt more than others (maybe because of their colour?),
- issues that are common/reoccurring on more (than one) types of plastics.

Please feel free to comment and describe your experience, or anything that might come into mind.

I would very much appreciate your time and support.

Answer 1: Private practice, Netherlands and Germany

Dear Stefani Kavda,

firstly I want to wish you all the best with your research.

To be honest I find it a bit tough to answer your questions, since I haven't got much time to think about such a broad subject. I could imagine it might be easier if you would interview conservators that you know personally, or from collections that you might have access to, by appointment. Anything I would tell you would be a bit random and a bit short. Therefore, I'm not sure if that would be of any real use to you and to your research.

Personally I have not encountered many problems with plastic objects and their cleaning.

Concerning (plastic) sculpture in museum collections, very common problems are: accumulation of dust, visitors touching objects or walking into them (rubs from shoes, fingerprints etc), as well as light exposure.

I would always try to diminish all three by applying risk assessment before installing those objects.

When needed, take measurements like installing objects under a hood, keeping visitors at a distance and keeping lux levels and environmental fluctuations very low. Same goes for objects going on loan. In storage, you would need to know what plastic you are dealing with and then take appropriate measurements. Setting up a project to detect all plastics in your collection by FTIR or otherwise (preferably without sampling) is a big undertaking but would be a necessary part of the risk assessment, otherwise you don't know what types of plastics you are dealing with, each with their own problematic. A part of this would also be artist interviews about the production of the work, and determining the meaning or value of the plastic elements within the work. Cleaning is not always wanted or needed, and as a conservator you might wish to proceed differently.

Apologies for not answering your very specific questions, but I hope you get an idea of my work in large museum collections.

PS

you probably have come across the European Project POPART, which also dealt with cleaning methodologies for plastics in art and design: <http://popart-highlights.mnhn.fr/> Techniques for cleaning as commonly used by conservators were the objective in this study, and included: cleaning agents, wet cleaning and dry cleaning, products like sponges, cloth, cotton etc and their effect on the surface of plastics (scratching, matte and glossy surfaces), loss of plasticizer and surface roughness on micro-level, common types of soiling etc, all applied to plastics commonly found in art and design collections. Since then research continued on these subjects, for example as presented at Future Talks.

However, as I mentioned before, I have been much more involved in preventing dirt than actual cleaning (except dusting) of plastics in museum collections and I am convinced that this is the best way to work with collections. It is better for the objects most of the time. Still, this study was very helpful in raising awareness for the vulnerable surfaces of plastic objects.

I am curious to hear about the development of a thesis for your research, Please inform me about your findings.

Answer 2: Museum of Modern Art, New York

Dear Stefani,

My apologies for my tardy reply but I have been swamped. See my answers below in red.

I would be very interested in problems you face when cleaning plastics, i.e:

- types of plastics that are more problematic/ harder to clean (in terms of their chemical properties or colour) Polyurethanes are the most problematic and of course the early cellulose acetate and nitrate.
- a specific plastic (or family of plastics) that more commonly requires cleaning amongst objects in your museum's collection. I would say they are mostly the same since we have a good HVAC system that filters out a lot of the dirt. We do find that lighter coloured plastics will show the dirt more of course.
- types of dirt that you are often called to remove, I have not analyzed the dirt but it is primarily dust and soiling from the museum visitors and in some cases when someone has touched the object therefore it would be more oily or greasy.
- plastics that demonstrate dirt more than others (maybe because of their colour?) I am not sure about this?
- issues that are common/reoccurring on more (than one) types of plastics. most plastic degrade and the first visual sign is a shift in colour and mostly yellowing.
- In terms of the collections that you have worked with, if you were to point out one plastic (or maximum a couple of them) that is the most common throughout each collection, which would that be? And which type of object is the most abundant? When I was a student at the Victoria and Albert Museum/RCA Program in the 1990s I did a survey of their Design Collection and then when I started here at MoMA I also was part of a survey and the results of the types of plastics was very similar for Museum Design Collections. I wrote my thesis at the RCA on the storage of objects in design collections and highlighted 4 problematic polymers in the V&A's collection. Polyvinyl Chloride, polyurethane, natural rubber and cellulose nitrate. MoMA's collection is very similar and the problems are paralleled. My MA thesis is available, but it is very dated and frankly at this stage of my career I think not that informative. I do not have it as a digital file as at that time it was only presented in hard copy. I am happy to speak to you on the telephone if that would be helpful. So please feel free to call.

Answer 3: Die Neue Sammlung, Munich

I would be very interested in problems you face when cleaning plastics, i.e:

- types of plastics that are more problematic/ harder to clean (in terms of their chemical properties or colour)

plastics with less reactive surfaces like for example PE, PP. Because of the low surface energy they both are more difficult to clean and to bond. Moreover high-gloss, or transparent plastic surfaces are quite delicate to clean. The risk of producing matt stains or scratches and the like has to be considered.

In general you could say that the following are more prone to 'get dirty' than others:

CA, HDPE, HIPS, PMMA, soft PVC, soft PUR foam

- a specific plastic (or family of plastics) that more commonly requires cleaning amongst objects in your museum's collection

see above

- types of dirt that you are often called to remove

on show: mostly fingerprints. in the studio: plasticisers, fat residues, loose dust, fixed dust, oily products, waxy products, pencil and paint markers, chewing gum...

- plastics that demonstrate dirt more than others (maybe because of their colour?)

high-gloss, transparent, smooth surface plastics, foams

#### Answer 4: Museum Tinguely, Basel

Dear Stefani,

I am terribly sorry to have dropped the ball. Your email request had slipped off my virtual desktop by the time I had returned from the US, for which I do apologize.

Even more so, I am afraid that the practice at Museum Tinguely will not be of help to you, in narrowing and determining the actual type of plastic you will be focussing on. Let me explain:

Our Museum Tinguely (MT) was instituted just about 20 years ago, after the death of Jean Tinguely, who by then had become an internationally known artist of kinetic art. His sculptures (which could be called "pieces") are extremely diverse, partially because Tinguely built many of them at a rapid speed, just in time for an exhibition. Quality of craftsmanship was not his main concern. Check out the collection at our website:

[http://www.tinguely.ch/en/museum\\_sammlung/sammlung.1980-1991.html](http://www.tinguely.ch/en/museum_sammlung/sammlung.1980-1991.html)

In his later years, when he started adding found objects (in form of bits and pieces from trash, scrap, factory junk and otherwise "useless" stuff), just a few items made of polymers were used to enhance his work. The overwhelming amount of his prolific oeuvre is compiled of metallic structures, mostly made of iron components, with additional elements, made of a large variety of materials, though predominantly metal and wood.

The most common issues we have to deal with are caused by electrical motors, transmission of forces and wear as a consequence of movement. As you can imagine, the kinetic approach leads to friction > squeaking, weeping, rattling, even intentionally banging sounds, wearing down the (often non-existing) bearings.

On rare occasion, we encounter plastics of sorts - usually former trashed items, which Tinguely found, giving them another life: One example is a vacuum cleaner hose, which is attached to one of the sculptures of the ensemble called "Mengele Totentanz" - which you might spot briefly (dangling) at sec 45 in this short YouTube snippet: <https://www.youtube.com/watch?v=DKdTF77RoxU>

The hose as broken by now and we are trying to stabilize it. One day, is likely to be substituted for an identical, but recent vacuum hose, providing the actual length. Cleaning of it, has not be an issue, since it can be done dry and nearly superficial.

In other words: Since movement (and the continuation of it) was one of Tinguely's major intentions, the museum has been concentrating its effort on maintaining the concept of ("Bewegung" - movement) alive. In fact, the resulting dilemma of giving up of (highly valuable) original materiality is an extremely interesting one...though it may not be of relevance for your search of finding the most appropriate polymer to focus on in your research.

There are just a couple of items that might be of interest though, which I do want to mention: Pit Stop, contains some elements of fiberglass reinforced polymer (probably polyester, though untested): [http://www.tinguely.ch/en/museum\\_sammlung/sammlung.1980-1991\\_019.html](http://www.tinguely.ch/en/museum_sammlung/sammlung.1980-1991_019.html)

With Tinguely's work it is of obvious importance to always keep the danger of potential over cleaning in mind. Moist, or even more so solvent cleaning is therefore reduced to an absolute minimum (avoided on a general basis).

Meta-Harmonie 2, is a long term loan item from Emanuel Hoffmann-Stiftung on display at MT. It contains an old, regular, upright) piano, which you can check out here: <https://www.youtube.com/watch?v=S0rVxhYFlwM>

The piano is being played mechanically (or rather hammered) by three "players", a wooden Pinocchio, a plastic clog, and a plastic Walt Disney character, a Dewey figure (located all the way towards the back, activated at sec 25 in the snippet). That figure has suffered immensely from mechanical stress over the years, with its foot/leg shattered. Currently that mechanism has been deactivated, to prevent further damage from happening to the figure.

But more interestingly for you would be that the plasticizer has migrated to the surface, attracting all sorts of surface grime, while disfiguring the Dewey-doll completely. One of the future projects is to decide (together with the lending institution), whether we will attempt to clean Dewey, or substitute the figure for a very similar one which we purchased some time ago. The trouble is that there is far too little time for (interesting) conservation problems like that, since the everyday issues of taking down and setting up contemporary exhibitions, and the related care for the loan items there, is taking up just about all of our time. Indeed, we do regret, that care for the permanent collection is pushed to the back burner far too often.

And finally, we are caring for a couple sculptures by Niki de Saint-Phalle, consisting of FRP. One of them has been treated recently by a freelance conservator. If this is more up your alley, I could send you the report of "Gwendolyn" from the early 1990s...

I am sorry to not be of greater help. Please feel free to ask any further questions, if any of this seems more relevant for your studies, would you.

#### Answer 5: British Museum, London

Dear Stefani,

Your dissertation sounds very interesting.

I am sure that you have come across the POPART publication which was published as part as a Euro-wide project into the conservation of plastics. If not it could be of interest to you.

On the whole we don't have a lot of problems in cleaning plastics in the British Museum.

Plastics in storage are usually covered and so should not get dirty. Although of course they may need a light clean for display.

Before any cleaning takes place, the nature of the dirt should be identified. Is it dust from the environment? – this can be removed

Is it part of the history of the object?- it may be considered important to retain this information eg a sign of use from an ethnographic context and the dirt would not normally be removed.

If objects are on display for a long time they might acquire some dust which can usually be removed with a vacuum cleaner and small very soft brush. This may also be the case for an object that has been taken out of storage for display or loan. If further cleaning is required, this is usually done by cleaning with deionised water and cotton wool buds (as suggested in POPART approach).

Obviously if we had a plastic that was sensitive to water we would take a different approach but hasn't been the case recently.

I remember some years ago cleaning a cellulose nitrate puppet with white spirit since there was a problem with other solvents.

I hope that this information is useful and I wish you all the best with your PhD.

#### Answer 6: Victoria and Albert Museum, London

Dear Ms Stefani

Thank you for your email. Unfortunately I do not think that I am in a position to be much help as I am not a conservator but a conservation scientist and therefore do not interact a lot directly with cleaning objects. The information that you require regarding the cleaning of different types of plastics is probably best found in the results of the Popart project. Some of these are available online as pdfs. I would also suggest that you send a query to the ConsDist List and ask for the experience of conservators dealing directly with plastic objects.

<http://popart-highlights.mnhn.fr/collection-survey/what-is-the-condition-of-the-collection/index.html>

[http://popart-highlights.mnhn.fr/wp-](http://popart-highlights.mnhn.fr/wp-content/uploads/5_Active_conservation/2_Studies_in_cleaning_plastics/5_2_StudiesInCleaningPlastics.pdf)

[content/uploads/5 Active conservation/2 Studies in cleaning plastics/5 2 StudiesInCleaningPlastics.pdf](http://popart-highlights.mnhn.fr/wp-content/uploads/5_Active_conservation/2_Studies_in_cleaning_plastics/5_2_StudiesInCleaningPlastics.pdf)

I hope that this information is of some use.

#### Answer 7: Science Museum, London

Hi Stefani,

Okay, now to answer some of your questions:

**1) types of plastics that are more problematic/ harder to clean (in terms of their chemical properties or colour)** - cellulose nitrate is a pain, as is bakelite. More modern plastics are generally a lot easier to deal with, since we know we can use some solvents, and we know what they'll be stable against.

**2) a specific plastic (or family of plastics) that more commonly requires cleaning amongst objects in your museum's collection** - because we have an industrial collection, we see a lot of bakelite and hard rubber. Both of those have tricky aspects - it's hard to remove accretions, and any solvents will change the colour of the plastic (fading, making light 'halos', etc).

**3) types of dirt that you are often called to remove** - we find a lot, with older materials, that there's a thick, black, greasy type of soil that is due to the use of coal-burning heat. This crops up on plastics from the early 20th century, which are already tricky to clean, and because it's oily, is very difficult to remove. Other than that, we get a lot of loose dust. This is usually fairly easily removed with a microfibre cloth or the equivalent, but I worry about the scratching and potential changes micro-scratches can induce.

**4) plastics that demonstrate dirt more than others (maybe because of their colour?)** - Yes, lighter plastics show the dirt quite a lot, but light dirt shows up on dark plastics just as much. I don't know that any specific plastic or colour sticks out to me in terms of showing dirt, but I'll let you know if I notice anything!

**5) issues that are common/reoccurring on more (than one) types of plastics** - Greasy surface dirt is a problem on a ton of different materials, not just limited to plastics. Cracking/crazing are common, and the risk of exacerbating these by cleaning the surface is a constant worry.

**6) In terms of the collections that you have worked with, if you were to point out one plastic (or maximum a couple of them) that is the most common throughout each collection, which would that be? And which type of object is the most abundant?** I've really only worked with the Science Museum collections with regards to plastics, so I don't have a lot to compare against. We have a LOT of bakelite - industrial collections tend to have the hard workers, and it was so frequently used as an electrical



insulator that it's everywhere! PVC is constantly used and a pain in the butt, too. With a more modern collection, I imagine that ABS would be fairly common, but I have no proof of that.

Please let me know if you have any other questions! Hope that helps!

#### Answer 8: Die Neue Sammlung, Munich

Hi Stefani,

please excuse my late response.

Now to your PhD thesis, congratulations what an interesting topic and I have been thinking of how I clean and how I approach cleaning plastic surface. It is a tricky one. Literature I am still using when I am approaching cleaning plastics is, Friderike Waentics: 'Plastics in Art' and Yvonne Shashouas 'Conservation of plastics' and the PopArt Project. Cleaning plastics is dependent on so many different aspects. Which plastic, how aged, how used it is. How damaged it is and how new it is. Difficult one is often to remove degradation of plastisizers (PVC) or aged CN and CA with its degradation products. Tricky are the surfaces of aged fiber glas reinforced plastics. Tricky is also surface damages on monochrome surfaces, like scratches or dents - maybe you remember the airbrush retouching workshop at the last Future Talks conference, this is sort of dealing with this topic and the difficulty you find in design objects with these perfect monochrome surfaces.

When it comes to approaching a treatment strategy, I look at the regular dry cleaning methods, like brushes and rubbers and test.

Wet cleaning - depends on the solubility parameters. And I have tried and used gels on PE- not very successful though.

An issue with the many monochrome industrial produced surfaces, like ABS or polycarbonate you have to be careful to not disturb the gloss.

This is a quick answer and will there be more coming to my mind, I will let you know. I keep my fingers crossed and please ask, if you have questions.

#### Answer 9: Fondazione Plart, Naples

Please find my answers below your questions.

I would be very interested in problems you face when cleaning plastics, i.e:

- types of plastics that are more problematic/ harder to clean (in terms of their chemical properties or colour)

(Aged) cellulose nitrate is very sensitive to abrasion, water and solvents; PUR is problematic to clean due to its porous structure and electrical attraction to small and loose particles; it's hard to reach evenness in cleaning on vast, light and monochrome areas; I have a hard time removing stains on more porous plastics

- a specific plastic (or family of plastics) that more commonly requires cleaning amongst objects in your museum's collection

Phenolic resin, PVC, PMMA

- types of dirt that you are often called to remove

dust, moulds, aged tape, aged labels

- plastics that demonstrate dirt more than others (maybe because of their colour?)

Transparent plastics, plasticized PVC

- issues that are common/reoccurring on more (than one) types of plastics.

cyclic loss of plasticizer due to migration - also after cleaning - in plasticized and aged plastics; moulds on phenolic resins;

### Answer 10: Fondazione Plart, Naples

Tipi di plastica che sono più problematici / più difficile da pulire (in termini di proprietà chimiche o colore)

Dagli interventi di pulitura effettuati al Plart, ho riscontrato che alcuni tipi di plastica sono più delicati e bisogna fare maggiore attenzione durante le operazioni di pulitura.

Il nitrato di cellulosa è sensibile ai solventi (es: ethanol) e un loro scorretto utilizzo può provocare alterazioni della superficie come scolorimenti / sbiancamenti e opacizzazione.

Molto sensibile è anche il polistirene, tende anch'esso a sbiancare ma può essere risolto con il white spirit. Il polivinilcloruro manifesta perdita dei plastificanti e dei coloranti con chalking in superficie, quindi durante le operazioni di pulitura si possono estrarre ulteriormente gli additivi e avere un effetto pulito ma che svanisce a breve termine.

Il poliuretano, data la sua struttura cellulare, è molto delicato, attrae elettrostaticamente le polveri, e quando è in avanzato stato di degrado è fragile e si rischia di portare via materiale con pennelli o aspirapolvere.

Una plastica specifica (o famiglia di materie plastiche), che richiede più comunemente pulizia tra gli oggetti della collezione del museo,

Tutte le plastiche richiedono manutenzione costante, ad esempio il polimetilmetacrilato e il polivinilcloruro attraggono la polvere.

I tipi di sporco che si sono spesso chiamati a rimuovere,

Polvere, residui di natura organica, adesivi, essudati, muffe.

Plastiche che dimostrano la sporcizia più di altri (? Forse a causa del loro colore),

Ho riscontrato che la bachelite a causa del suo colore scuro, può apparire pulita, ma in realtà effettuando la pulitura ha molti depositi nero/giallastri che continuano ad essere estratti dal tamponcino dopo svariati passaggi.

Problemi che sono comuni / ripetersi in più (di uno) tipi di plastica.

I problemi comuni sono i residui di vecchie etichettature e depositi di polvere.

abbiamo valutato che la plastica maggiormente presente nella nostra collezione è la bachelite, mentre gli oggetti più frequenti sono le radio e le scatoline.

#### Answer 10: Hamburger Kunsthalle, Hamburg

Dear Stefani Kavda,

sorry for my late reply. I am also sorry, that it will not be of much help, I guess.

I don't have much practical experience in cleaning plastics, so there is not much practical feedback that I could give you, looking at your questions. But it would be interesting to read more about your findings, once they have been settled. I hope you have received interesting feedback from your email letter, which I guess, you have sent out to many other participants of the Future Talks Attendants List. I hope you have found a possible collaboration among this feedback, because I do think that you will need a strong collaboration with a conservator that is working in practice in order to find out more about the cleaning of plastics.

I look forward to hearing from your research, once it is published and wish you good luck with this project.

#### Answer 11: Collector, UK

Hello Stefani

This sounds like an interesting and important research but I don't think I will be able to help very much.

I never clean plastics as a conservator, just as a collector.

These days I collect only plastic play money and clean where necessary with cotton bud moistened with saliva !! I did say that I am not a conservator!

BUT, I still think that the whole area of cleaning plastics is important and good initial work was done in the POPART project with which I was involved.

Some initial thoughts.

Plastics tend to hold static charges and so attract airborne dust more than most materials and simple cleaning often generates more static making the problem worse.

Textured surfaces are common in plastics and they present further problems for cleaning.

Some materials are affected by solvents, casein and water for example.

Many plastics have soft surfaces and are easily scratched with cleaning cloths and other cleaning products.

Cellular plastics – big issues!

Plastics are frequently painted.

Some solvents can help initiate degradation – e.g. water with Cellulose Nitrate

Some plastics can be marked by water – e.g. Vulcanite

Initial stages of degradation often alter the surface properties of plastics

I am sure that there are lots of other factors to be considered, but no-one said it was simple.

Answer 12: Tate, London

Hi Stefani,

I'm more than happy to help where I can and glad to hear that you will be focussing on the cleaning of plastics as this is still an area which needs to be refined.

Initially I can point you towards the POPART on the preservation of plastic artefacts in museum collections. This was an overarching study which carried out an overall survey on condition of plastic objects in collections as well as degradation processes and identification. In particular for your research they carried out a lot of research into active conservation and in particular cleaning which I think would be great place for you to start: <http://popart-highlights.mnhn.fr/>

Another project which is being carried out at various international art museums is the CAPS project which is looking at the cleaning of acrylic paint surfaces: [http://www.getty.edu/conservation/our\\_projects/education/caps/](http://www.getty.edu/conservation/our_projects/education/caps/)

As far as my experience with cleaning plastics I would say that I have worked with all kinds of plastics in various collections including social history, scientific and medical collections and art collections but in particular for cleaning I would say PVC, Perspex, acrylic paint, latex and polyester resin. These are the plastics most associated with contemporary art and contemporary artefacts and therefore have a certain expectation to look clean and free of any deterioration.

The plastics which are the hardest to clean I would say fall into three categories:

- 1) those that have already started to deteriorate and cleaning them may remove the material itself or cause irreversible damage e.g. cellulose nitrate which has already started to discolour.
- 2) highly polished or transparent surfaces as the possibility of being scratched or the high gloss finished being lost is very high. e.g. Perspex
- 3) very sensitive polymers which react to any interaction either from solvent, water, detergent, mechanical cleaning. For example natural rubber is very volatile.

The type of dirt I commonly find is surface dust which has built up over time in storage or while on display. Due to the nature of many polymers this generally quickly adheres to the surface either due to plasticiser loss causing the surface to become tacky or the natural surface of the polymer allows the dirt to become quickly ingrained e.g. latex. This can be very difficult to remove and will make the surface look grey and dull overall.

Also adhesive tape or adhesive residue is often found on plastic collections and again can be very difficult to remove as generally solvents aren't appropriate for plastics (although look at POPART for changing view on this).

I hope this is enough information for helping to start you off and please feel free to ask any more questions. I would say that I was quite interested in the cleaning and overall care of latex as this is a material quite often found in contemporary art and more often than not would be put on open display causing a build up of surface dirt which is very difficult to remove. Louise Bourgeois and Eva Hesse are two artists that use latex.

Very best of luck with your research and I look forward to seeing how it develops.

Answer 13: Museum of Design in Plastics (MoDiP), Bournemouth

Dear Stefani,

Thank you for your enquiry. I regret that we do not employ conservators in our museum. We are a very small museum team within the university and our resources are currently very limited. I am sorry that I am unable to help you with your request.

Best wishes

Answer 14: Private practice, Paris

Dear Stefani,

Thank you for sharing this research project, in which I wish you most success.

I take the liberty of forwarding your email to my colleague, the actual leader and main researcher of the project on cleaning gel systems you read about in FT prints, and a contemporary art and design conservator who also wrote her Master thesis on Plastics cleaning.

I, for my part, will try and answer your questions, hoping to help you in sorting out the different topics of the subject. I also invite you (if not already done) to consult the prints of the PoPArT Project that took place from 2008 to 2012.

**Appendix C. Mounting samples in the Atlas ageing chamber**

Atlas specimen holders (RD – 3T) used in the Ci3000 weathering chamber, were in the form of an open frame, leaving samples exposed and allowing free flow of air against their front and back surfaces (Fig.14). Holders were made from stainless steel that didn't affect the results of the exposure. The absence of backing was strategic. When dealing with transparent samples, a backing can affect radiation absorption (ISO 4892-2; Wypych 2013). The enclosure of Ci3000 contained a single tier specimen rack in the form of a cylindrical frame (Fig.15) onto which the sample holders are hooked (where marked with red) and provision for air passing over the samples to regulate temperature. The rack accommodated 19 specimen holders at a time, with 10 samples in each holder (total 190 samples per ageing cycle). The lamp was placed such that the quantity of radiation received by the specimens would not vary more than  $\pm 10\%$  over the entire area of exposure. The radiation distribution was improved by rotation of the cylindrical frame carrying the specimen holders around the light source.

Samples were divided in two groups: PMMA samples undergoing artificial ageing and unaged samples. Each group had alpha-numeric classification system organised in a progressive order, starting from 1. The aged samples were labelled numerically, while unaged samples were accompanied by a 'U' standing for 'unaged', followed by the number. Labelling was performed with a very thin, black permanent marker that withstood the exposure and did not affect the PMMA surface. Samples were handled with gloves to avoid deposited oils that act as UV absorbers and contain contaminants that would affect the polymer degradation (ISO 877-1). Samples were mounted on the holders with nylon thread carefully placed on the edges of the samples (Fig.16), in such a manner that there were no loose samples and no additional applied stresses (BS 2782-5). At the same time, the choice of nylon proved beneficial, because due to its transparent nature, it allowed total exposure of the PMMA sample surfaces. The chamber had a viewing window that allowed regular inspection and monitoring of samples on the specimen rack during ageing cycles.



Figure 34. Specimen holder RD - 3T.

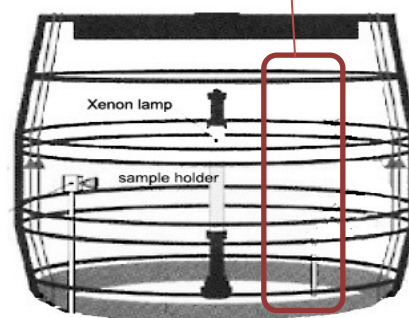


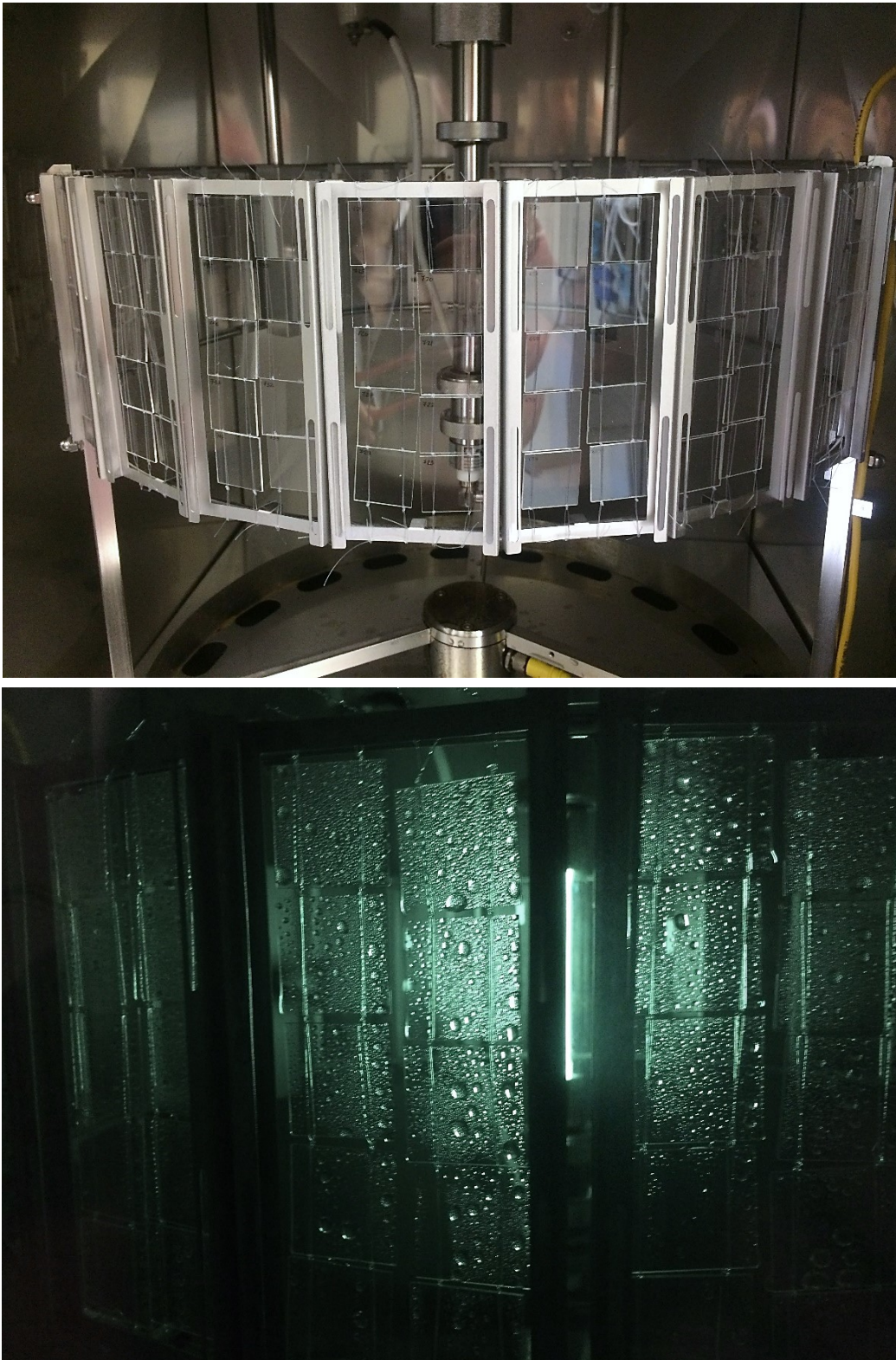
Figure 3. Specimen rack/cylindrical frame.



Figure 4. Tying samples with nylon thread on the sample holders.



*Figure 5. PMMA samples mounted on RD – 3T Atlas specimen holders with nylon thread tied on their edges.*



*Figure 6. RD – 3T specimen holders hooked on the specimen rack (cylindrical frame) before ageing (top) and during the wet ageing cycle (bottom).*



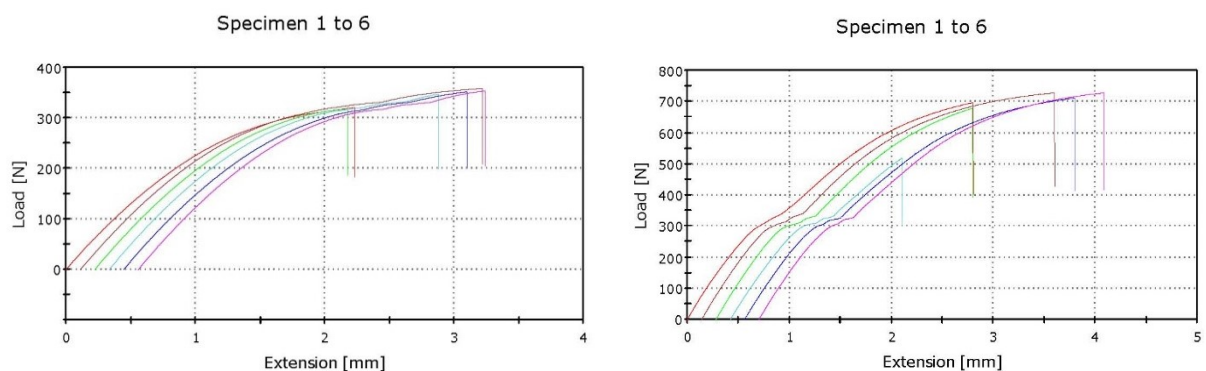
### Appendix D. Preliminary tensile test: fine tuning the method

Two sets of preliminary tensile tests were conducted on 1.0 mm thick PMMA samples to:

- establish whether the breaking loads of the samples were within the tolerance of the instrument, namely 2000 Newton (N).
- determine the relationship between sample width and breaking load. The hypothesis was that width of samples is proportionate to their load. This subsequently led to the determination of the experimental parameters (sample size, extension speed, grip strength) and a methodology for the main tensile analysis presented in the following section.
- determine whether PMMA's orientation was the same in all directions of a sample, as anticipated (BS2782-9 Method 941:1990) due to the isotropic nature of amorphous PMMA. Orientation has a prominent effect on mechanical properties (Chartoff *et al.* 2008), and consequently on the homogeneity of samples, rendering this test essential. Extreme changes in processing conditions and manufacturing could alter the material behaviour and produce different types or distributions of orientation within the sample (BS2782-9 Method 941:1990). If the orientation would indeed be the same in all directions, this would mean that it could be disregarded. Moreover, it would allow for reproducibility of results when testing the exponentially aged PMMA samples in the forthcoming main tensile study.

Parameters were kept constant so to define the error and deviation of results, ensuring homogeneity in samples. Tests were run in multiple replicates to examine the repeatability of their breaking point.

#### Width test



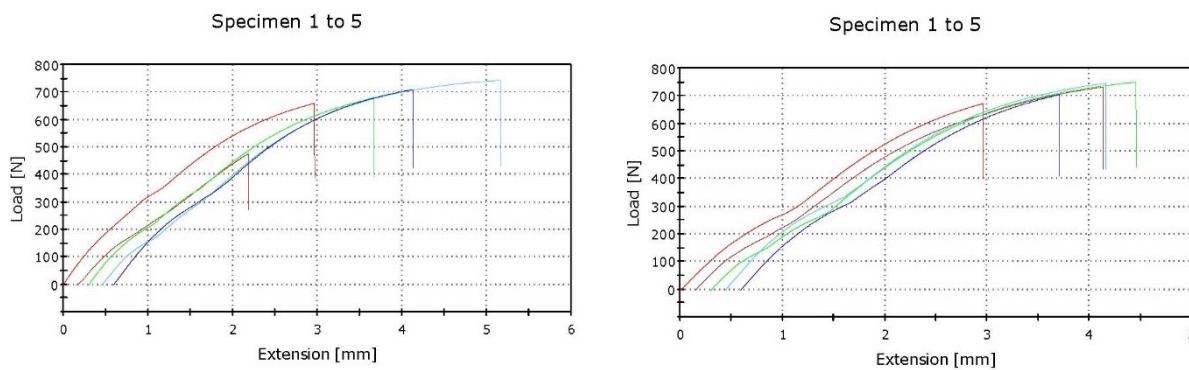
Graph 1. Width test with six replicates: (left) 5 mm set – (right) 10 mm set.

The Width test employed two sets of six samples each: one set measuring 5 mm width and another set measuring 10 mm width, and 100 mm long, in order to examine the relation of PMMA samples with breaking load and proportion. Based on the resulting load-elongation

curves (Graph 4.1), samples 5 mm and 10 mm wide provided similar load-elongation curves with similar patterns and a yield at about 300 N, with the 5 mm wide showing slightly more consistency.

### Orientation test

The Orientation test investigated the importance of the direction of cut and employed two sets of five samples each (50 x 10 mm), cut in two different directions: one parallel and one perpendicular to the initial sheet supplied. The directions were arbitrarily named X and Y axis, respectively, since the initial direction of cut was unknown. The direction of testing was defined as the direction of the long axis of the sample. The Y axis samples displayed greater consistency (StDev 33.1) than the X axis samples (StDev 105.3) (Graph 4.2). This demonstrated that the direction of cut influenced the mechanical behaviour of samples, and in turn suggested that the molecular orientation of the material was not the same in all directions. The tested PMMA resembled an oriented amorphous structure, possibly resulting from drawing, a process that forces molecules to align, changing the mechanical properties of a material from one dimension to the other (Callister and Rethwisch 2014). This process gives rise to strengthening and stiffening effects, which improve the tensile strength of the drawn PMMA relative to that of unoriented material. This increased strength became visible with application of load in the Y axis direction of drawing (direction of orientation), which showed higher load than samples cut in the opposite direction (Graph 4.3 – see Y axis).



*Graph 2. Orientation test with five replicates: X axis set (left) – Y axis set (right).*

The shorter samples (50 mm long) were more prone to breaking near the edge of grips than the longer samples (100 mm), used in the Width test, mostly breaking within the gauge length (Fig.4.3). One interpretation is that the longer samples had more material to distribute the load along the grips. Hence, it was recommended that samples for the main tensile test should be at least 100 mm long, for more consistent results. Samples breaking in the grips or at some obvious flaw areas were discarded and excluded from the measurements.

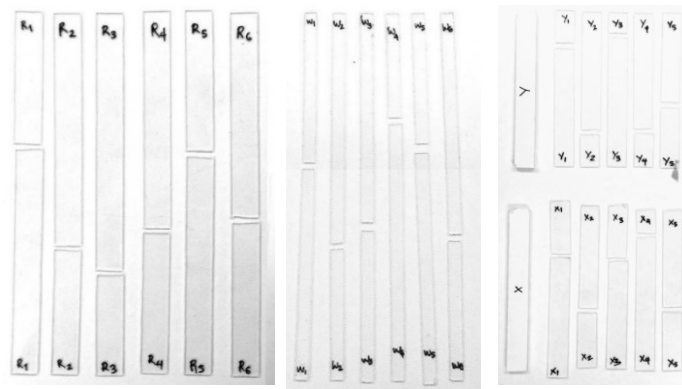


Figure 7. PMMA replicates after tensile testing. From left to right: (R) Width test 10mm, (W) Width test 5mm, Orientation tests Y and X axes.

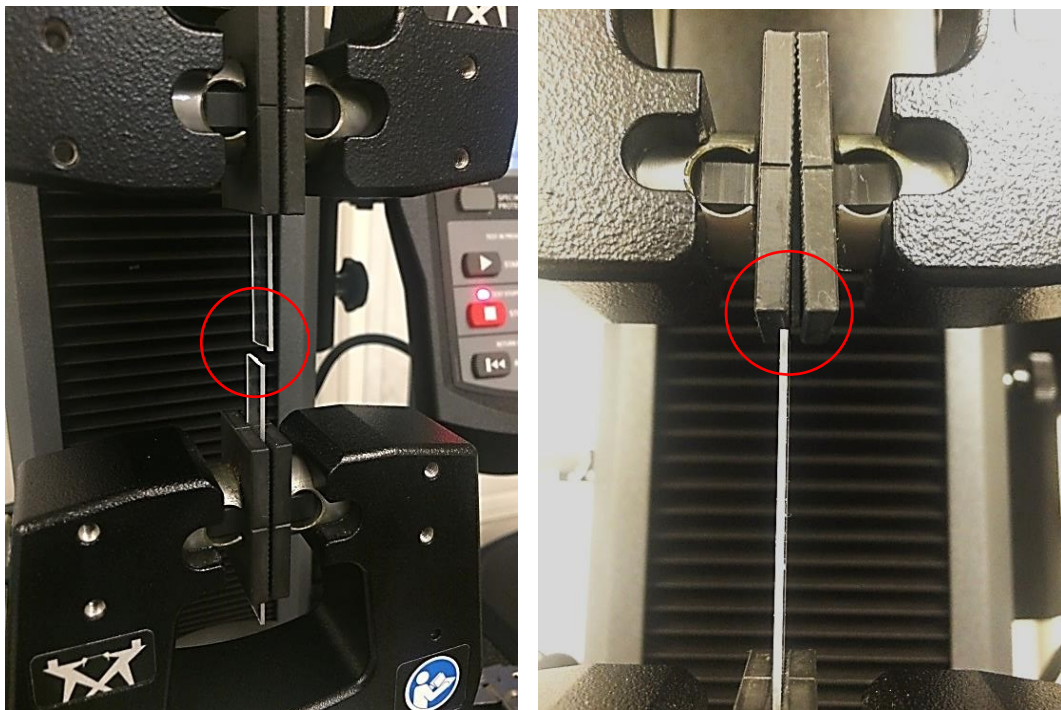
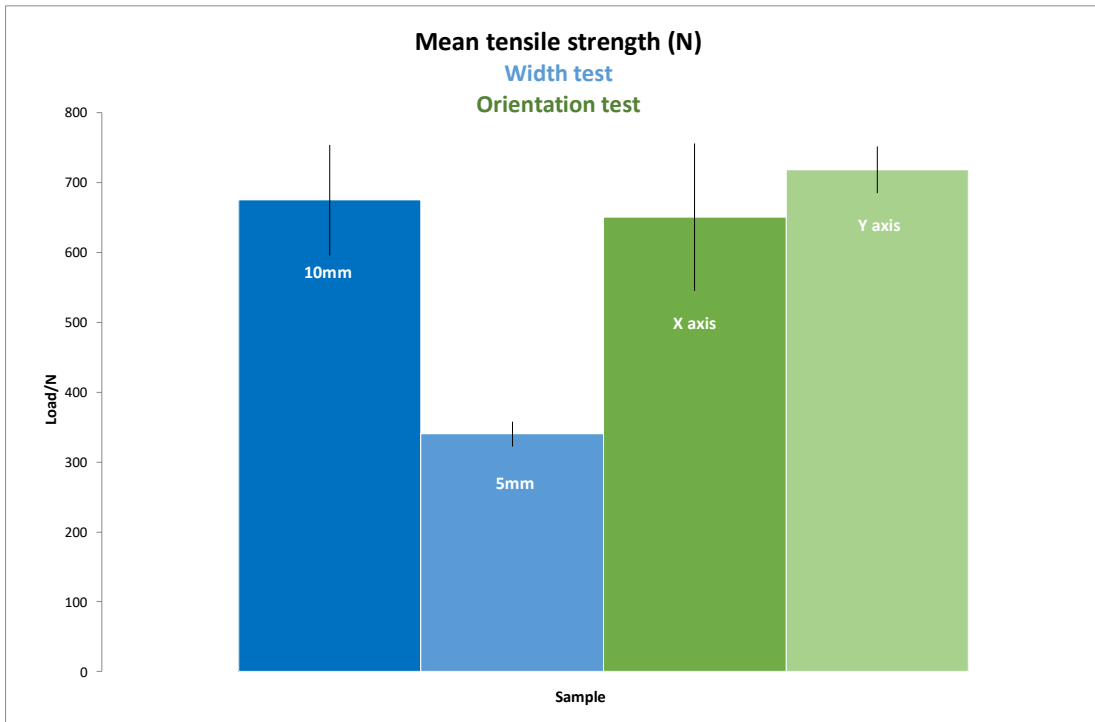


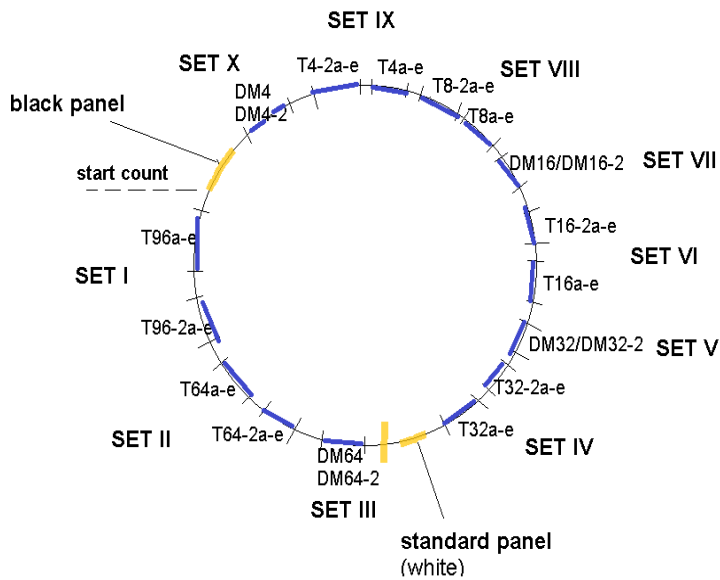
Figure 8. Sample broken within the gauge length (left) – sample broken near the edge of grips (right).

An overall observation was that PMMA samples in both tests (Width and Orientation) broke within the load range (max load: 2000 N) of the instrument, rendering the technique suitable for the purpose of this study. The 10 mm wide samples broke at around 700 N, while the 5 mm wide broke at around 300-350 N (Graph 4.3). This confirmed that the dimensions of a sample are proportional to the load and that by halving the sample width, its load was also halved. This meant that exact sample dimensions were inconsequential, and measurements of load could be extrapolated from the results.



Graph 4.3. Mean tensile strength (load/N) of the PMMA replicates tested in the Width test (10 mm and 5 mm) and the Orientation test (X and Y axes).

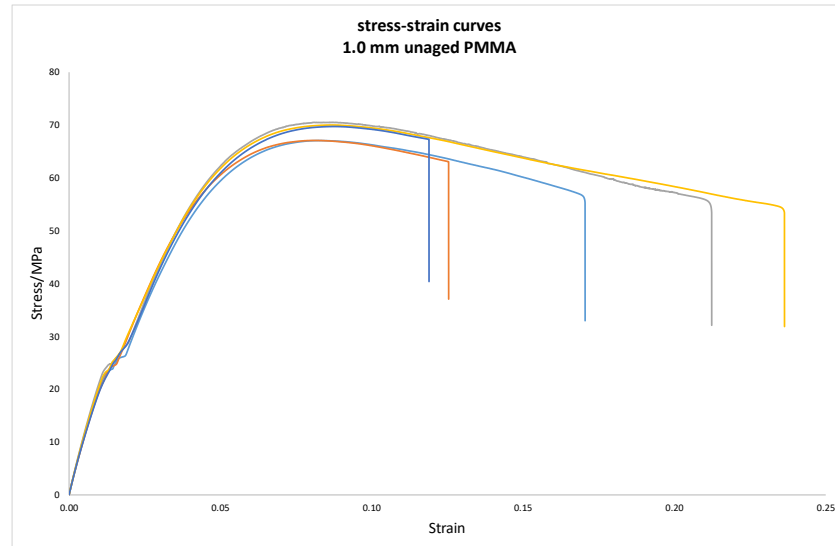
**Appendix E. Diagram of the mounting positions of PMMA samples in the Atlas chamber for exponential ageing.**



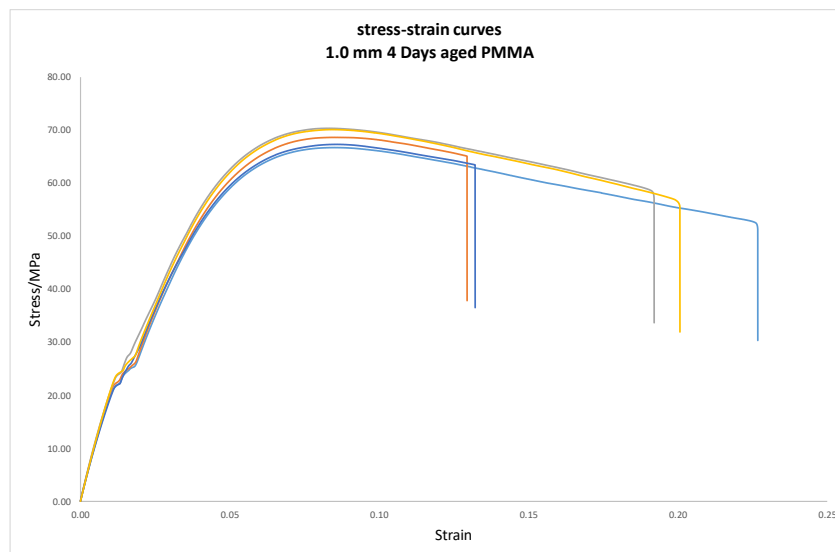
- SET I: 96 days, 2 holders, 5 samples each
- SET II: 64 days, 2 holders, 5 samples each
- SET III: DMA 64 days, 1 holder, 2 samples
- SET IV: 32 days, 2 holders, 5 samples each
- SET V: DMA 32 days, 1 holder, 2 samples
- SET VI: 16 days, 2 holders, 5 samples each
- SET VII: DMA 16 days, 1 holder, 2 samples
- SET VIII: 8 days, 2 holders, 5 samples each
- SET IX: 4 days, 2 holders, 5 samples each
- SET X: DMA 4 days, 1 holder, 2 samples

**Appendix F. Tensile test of exponentially aged material**

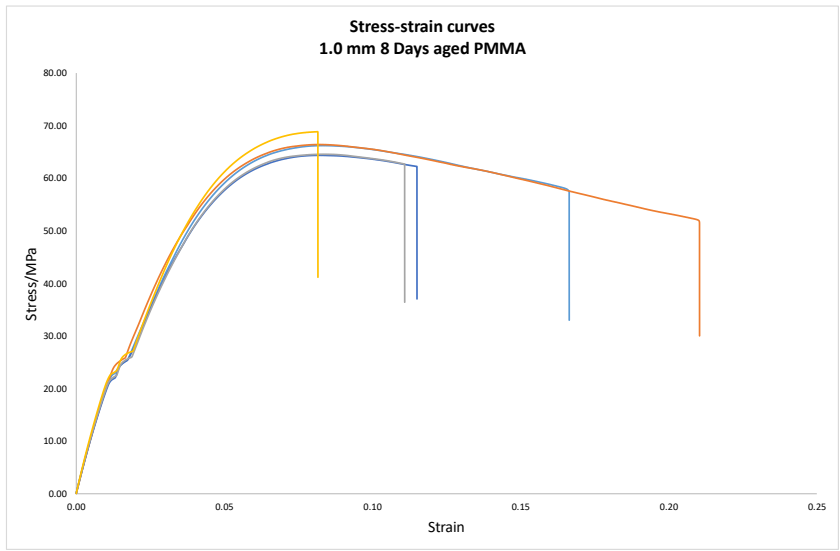
Stress-strain curves of all 5 replicates for each set of unaged and exponentially 1.0 mm UV-aged PMMA.



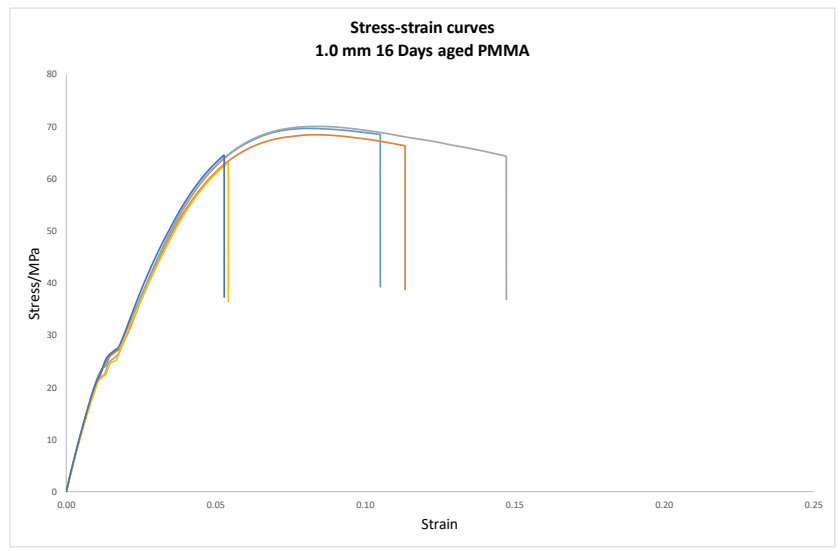
*Graph 4. Stress-strain curves of 1.0 mm: unaged PMMA.*



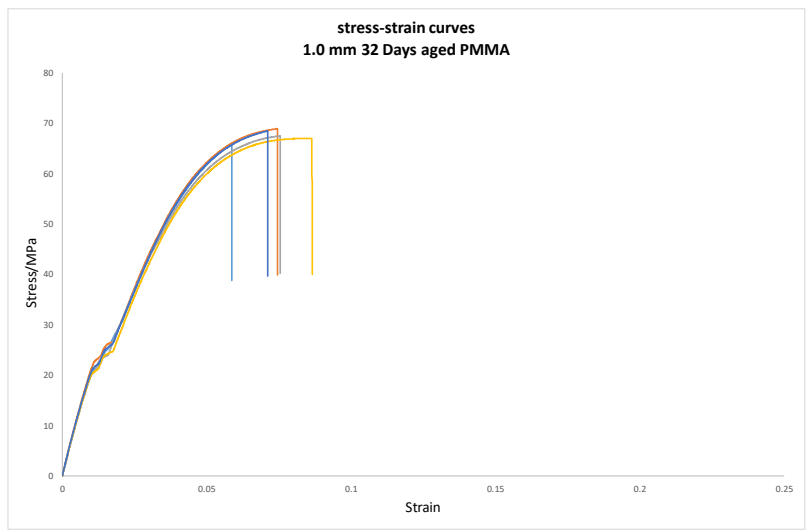
*Graph 5. Stress-strain curves of 1.0 mm: 4 days UV-aged PMMA.*



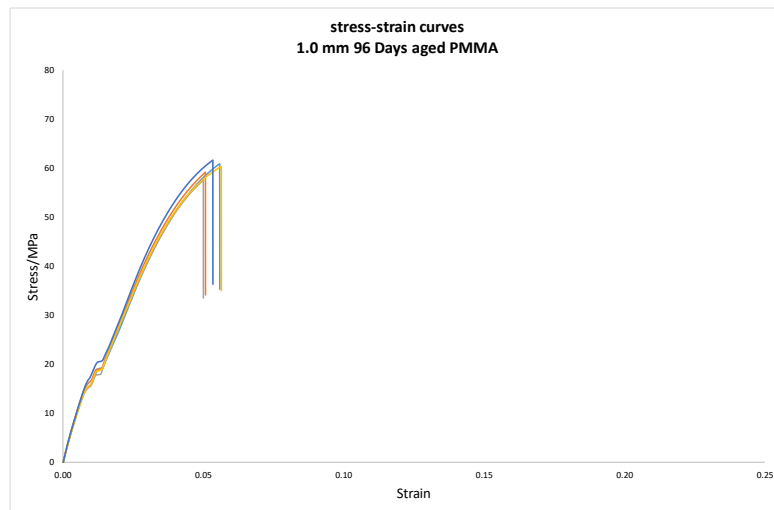
Graph 6. Stress-strain curves of 1.0 mm: 8 days UV-aged PMMA.



Graph 7. Stress-strain curves of 1.0 mm: 16 days UV-aged PMMA.

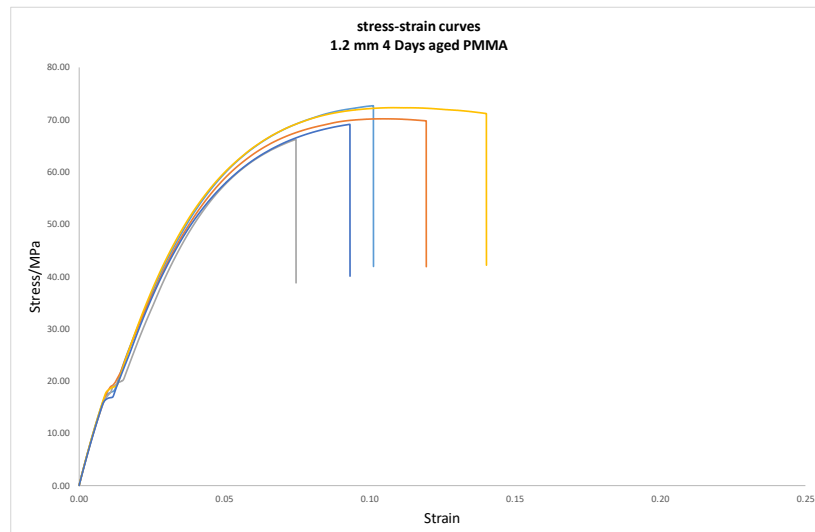


Graph 8. Stress-strain curves of 1.0 mm: 32 days UV-aged PMMA.

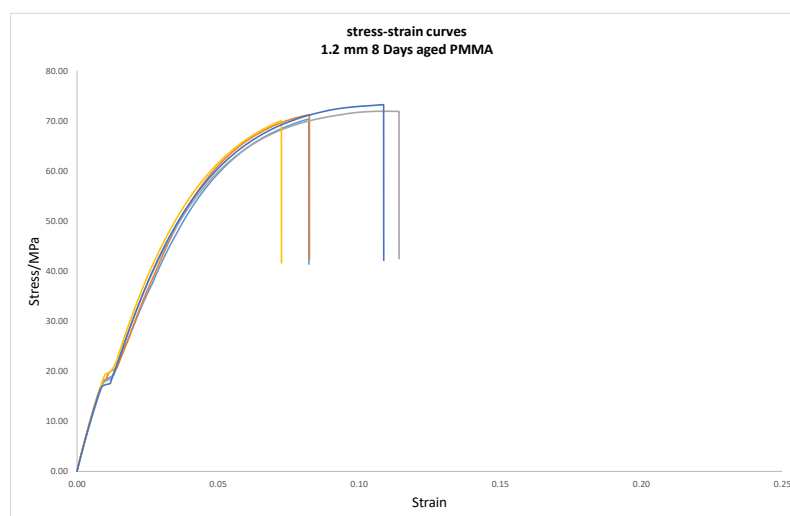


*Graph 9. Stress-strain curves of 1.0 mm: 96 days UV-aged PMMA.*

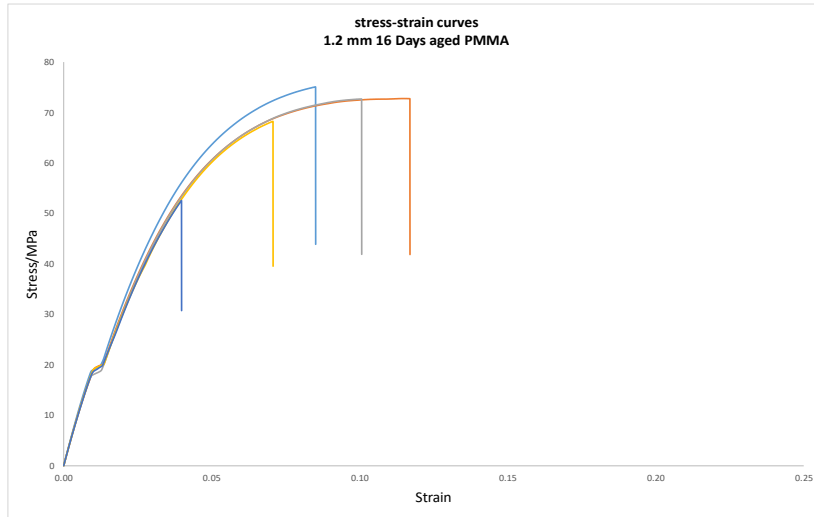
Stress-strain curves of all 5 replicates for each set of unaged and exponentially 1.2 mm UV-aged PMMA.



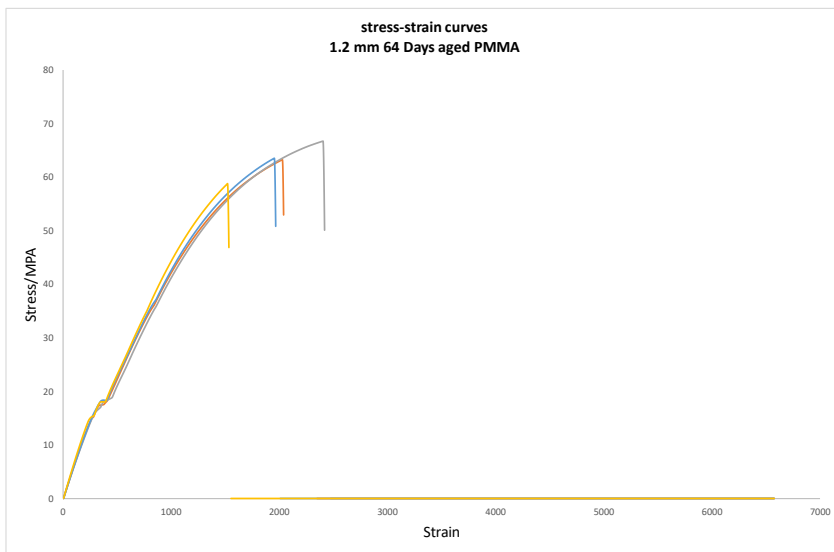
*Graph 10. Stress-strain curves of 1.2 mm: 4 days UV-aged PMMA.*



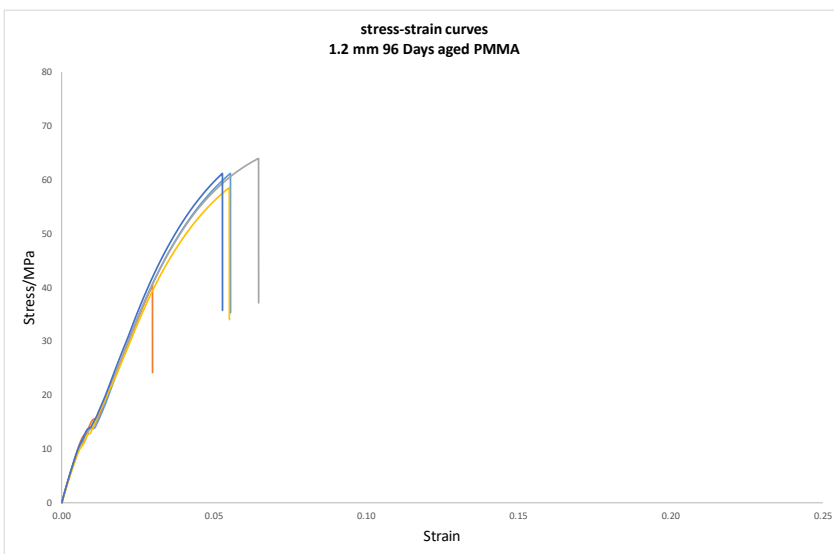
*Graph 11. Stress-strain curves of 1.2 mm: 8 days UV-aged PMMA.*



Graph 12. Stress-strain curves of 1.2 mm: 16 days UV-aged PMMA.



Graph 13. Stress-strain curves of 1.2 mm: 64 days UV-aged PMMA.



Graph 14. Stress-strain curves of 1.2 mm: 96 days UV-aged PMMA.



### Appendix G. Residues on received samples & pre-washing

See here for pre-washing tests of samples, ATR-FTIR characterization of the backing, adhesive tape and protective film residues.



*Figure 9. PMMA coupons as received on the black hard-plastic.*

PMMA samples received by Goodfellow Inc. were attached to a black, hard-plastic backing by



*Figure 10. Coupons immediately after being removed from the black hard-plastic. Transparent and black (dust) residues are visible on all the coupons.*

means of transparent adhesive tape and were protected with a transparent film (Fig.4). It was apparent that PMMA material was first attached on this hard-plastic backing as a sheet (400 x 400 mm) with protective film, prior to the coupons being cut. This theory was supported by the scrap material found between all rows of coupons and traces of residual packaging seen as dust generated by cutting and subsequently deposited on the samples (Fig.5). The source of dust was speculated to derive

from cutting the PMMA and the protective film due to their transparent dust, as well as the hard-plastic backing

due to its black dust (Fig.5). On both sides of each sample was a sticky residue, on one side it

originated from the adhesive tape that kept coupons secured on the backing, and on the other side from the protective film. This stickiness exacerbated the adhesion of residual dust on their surfaces.

### ATR-FTIR residue characterisation

To characterize the residues from the adhesive tape, the backing and the protective film, ATR-FTIR analysis was performed on all materials and both sides of samples.

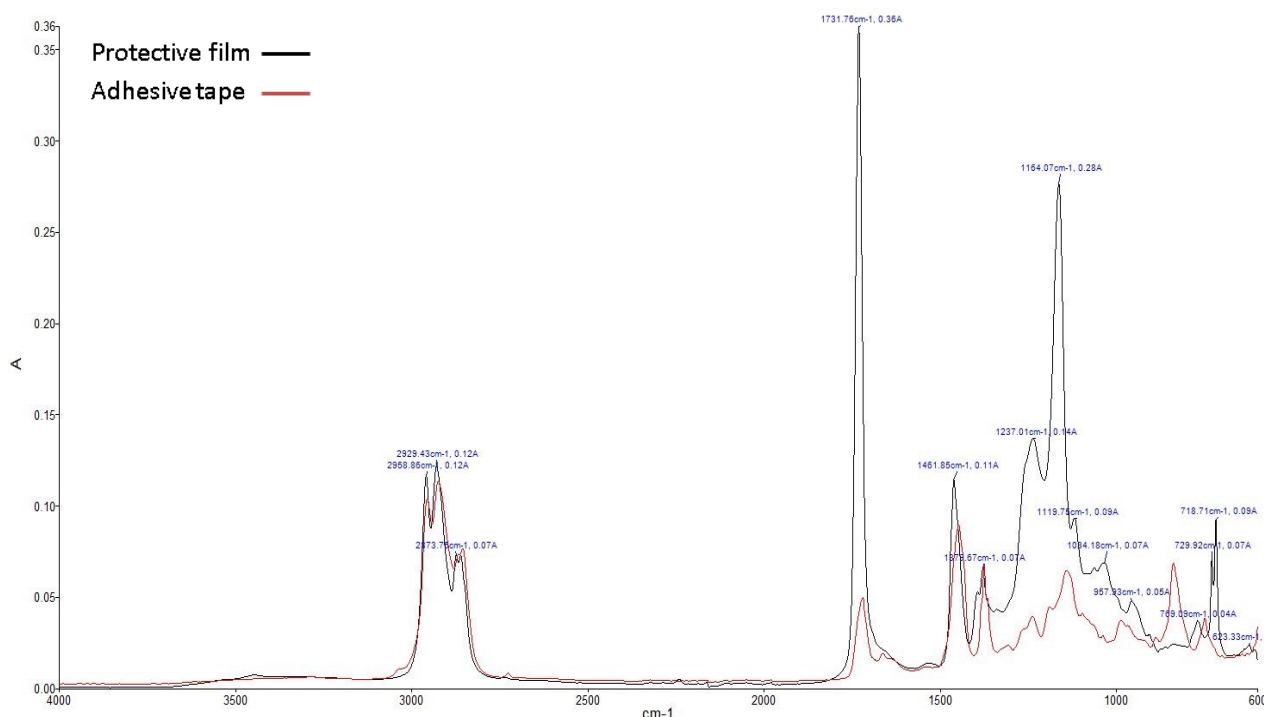


Figure 11. Spectra of transparent adhesive tape (red line) used to hold PMMA coupons on a black, hard-plastic backing and transparent film protecting (black line) the coupons.

Spectra of the adhesive tape and the protective film (Fig.6) appear to be comparable with similar spectral features between 4000-800  $\text{cm}^{-1}$  (Table 1). Interpretation of the spectra reveals the presence of characteristic absorption bands attributed to functional groups present in poly (vinyl acetate) (PVAC). The presence of peaks at around 2955  $\text{cm}^{-1}$ , 2930  $\text{cm}^{-1}$  and 2870  $\text{cm}^{-1}$  are associated with stretching of  $\text{CH}_3$ ,  $\text{CH}_2$  and  $\text{CH}_3$  groups, respectively. The strong absorption band centred at 1730  $\text{cm}^{-1}$  is attributed to the C–O stretching vibration of the acetate ester group ( $\text{CH}_3\text{COO-R}$ ) (Toja *et al.* 2013). Peaks at around 1460  $\text{cm}^{-1}$  and 1375  $\text{cm}^{-1}$  are assigned to the stretching vibration of  $\text{CH}_3$  groups in the acetate substituent, 1238  $\text{cm}^{-1}$  to the stretch mode of C–O–C vibrations, and 1080  $\text{cm}^{-1}$  to the CH–O of the acetate ester group. All these peaks confirm the presence of PVAC (Toja *et al.* 2012; Toja *et al.* 2013) as the base material of both the adhesive tape and the film.

The possibility of phthalate-based additives in the PVAC-based materials is proposed due to the absorption at 2955  $\text{cm}^{-1}$  ( $\text{CH}_2$ ), 2870  $\text{cm}^{-1}$  ( $\text{CH}_3$ ), 1730  $\text{cm}^{-1}$  ( $\text{C}-\text{O}$ ), 1460  $\text{cm}^{-1}$  ( $\text{CH}_3$ ), 1120  $\text{cm}^{-1}$  ( $\text{C}-\text{O}-\text{C}$ ) and 1080  $\text{cm}^{-1}$  ( $\text{CH}-\text{O}$ ), commonly ascribed to dibutyl phthalate plasticizers (DBP) (Toja *et al.* 2012). The adhesive tape shows an additional diagnostic peak of dibutyl phthalate at around 1660  $\text{cm}^{-1}$ , assigned to skeletal vibrations of the aromatic ring. Absence of the latter diagnostic peak and at around 1578  $\text{cm}^{-1}$  (skeletal vibrations of the aromatic ring) in the protective film spectrum, reduces the chances of a phthalate-based additive in the protective film.

Spectra of both sides of PMMA coupons, analysed after detachment from the backing and removal of the protective film, strictly shows peaks attributed to PMMA. Since visual examination confirmed traces of residual black packaging and transparent protective materials it is apparent that these residues are beyond the detection limit of the ATR-FTIR instrument.

Adhesive tape on backing and protective film Diagnostic IR absorptions and assignments	
Wavenumber ( $\text{cm}^{-1}$ )	Tentative band assignment
2955, 2870	$\text{CH}_3$
2930	$\text{CH}_2$
1730	$\text{C}-\text{O}$ (acetate ester group)
1460, 1375	$\text{CH}_3$ (acetate ester group)
1238	$\text{C}-\text{O}-\text{C}$
1080	$\text{CH}-\text{O}$ (acetate ester group)

*Table 1. Assignments of diagnostic IR absorption bands of transparent adhesive tape holding PMMA coupons on a black, hard-plastic backing and transparent film protecting the coupons. Adhesive tape and protective film analysed with ATR-FTIR exhibit similar absorptions.*

### Visual assessment

PMMA coupons were mounted in the Atlas weathering chamber without any preparation or pre-washing treatment and exposed to UV radiation for 32 days. Macroscopic examination showed that the residual black spots from the hard-plastic backing were removed during ageing. This was attributed to the wet cycles of the ageing which could have washed off some residues. Under the stereomicroscope, aged PMMA surfaces did not look pristine, nor residue-free. Some residues visible only under magnification, were identified as tiny remains of a yellowish hue, that formed circular deposits (Fig.7a). Higher magnification revealed that these were adhesive tape residues that had dried, formed bubbles or crystallised during UV exposure

(Fig.7b, c). These could be easily removed with the mechanical action of a bamboo skewer confirming that they were surface deposits and not chemical damage. Some transparent remains from the protective film were also visible. Consequently, it was considered essential to pre-wash PMMA coupons before artificial ageing in order to remove residues and avoid interference in the cleaning experiments.

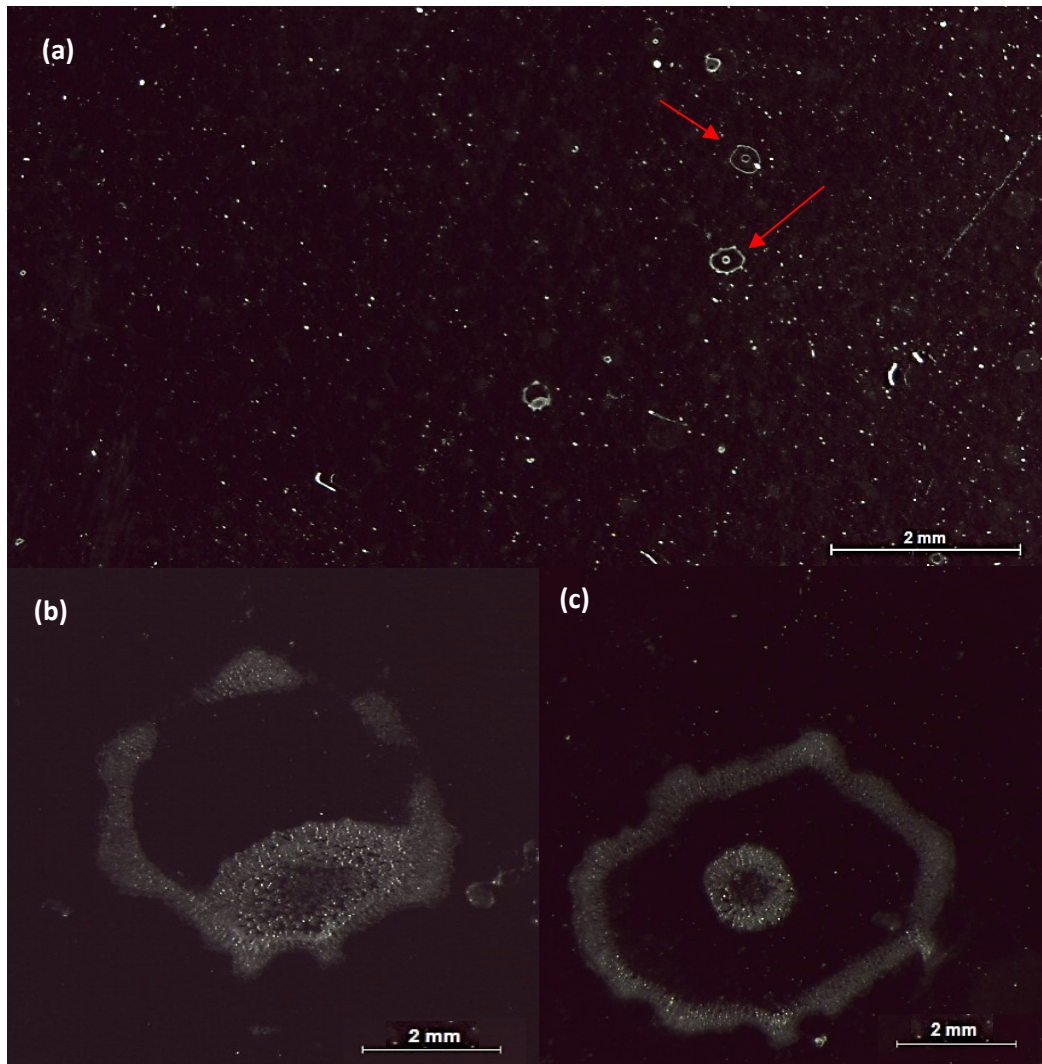


*Figure 12. Microimages of PMMA coupons aged under UV for 32 days, without pre-washing for removal of adhesive tape, backing and protective film residues (top image: 73x). Transparent adhesive remains appear to have dried or crystallised (bottom images: 1200x).*

#### Residue removal: prewashing

Prewashing tests on PMMA coupons aimed at identifying the safest and most efficient method to remove the residues, while avoiding damage to the PMMA surface. Tests included: wiping with a dry tissue, wiping with a tissue moistened with ethanol, compressed air, washing in an ultrasonic bath in deionised water or ethanol or rinsing with deionized water. Stereomicroscopy before and after each treatment documented changes in the samples' topography.

Tests carried out by wiping a dry tissue or an ethanol-moistened tissue were considered aggressive due to their mechanical action. Compressed air failed to completely remove residues and left surfaces with blemished areas. Samples were placed in an ultrasonic bath in glass beakers containing deionised water or ethanol and were cleaned via high intensity vibrations for 1 minute. They were subsequently blotted with tissue and dried under compressed air. Visual observation showed that both ethanol and water left surfaces equally clean and free from damage (Fig.8). Use of a wash bottle to rinse the samples with deionized water had equally good visual results as ultrasonic cleaning. Rinsing one coupon at a time with a wash bottle was more time-consuming than simultaneously cleaning a batch of coupons in a bath, thus the latter was selected.

ATR-FTIR analysis of samples before and after ultrasonic cleaning in deionised water and ethanol (Fig.9) showed no chemical alteration to the surfaces. Given that deionised water and ethanol performed similarly, and ethanol has been earlier documented to occasionally cause leaching of MMA monomer and surface opacity, deionised water was chosen as the least aggressive.

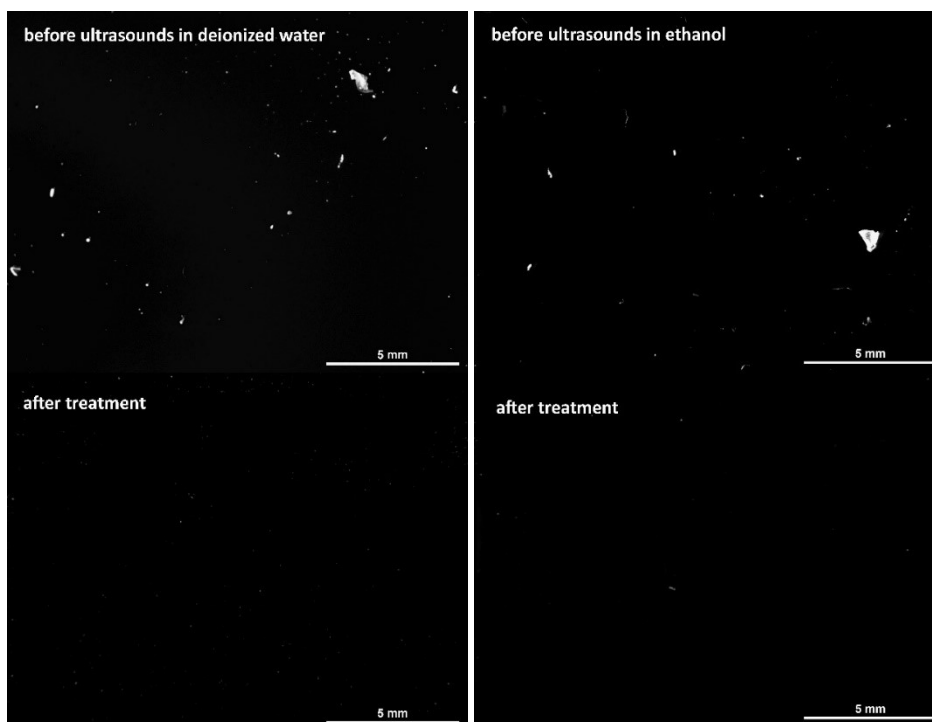


*Figure 13. Microimages (x40) of PMMA coupons after cleaning in an ultrasonic bath of deionised water (left) and ethanol (right), blotting with tissue and drying with compressed air. All surfaces are clean and free from damage.*

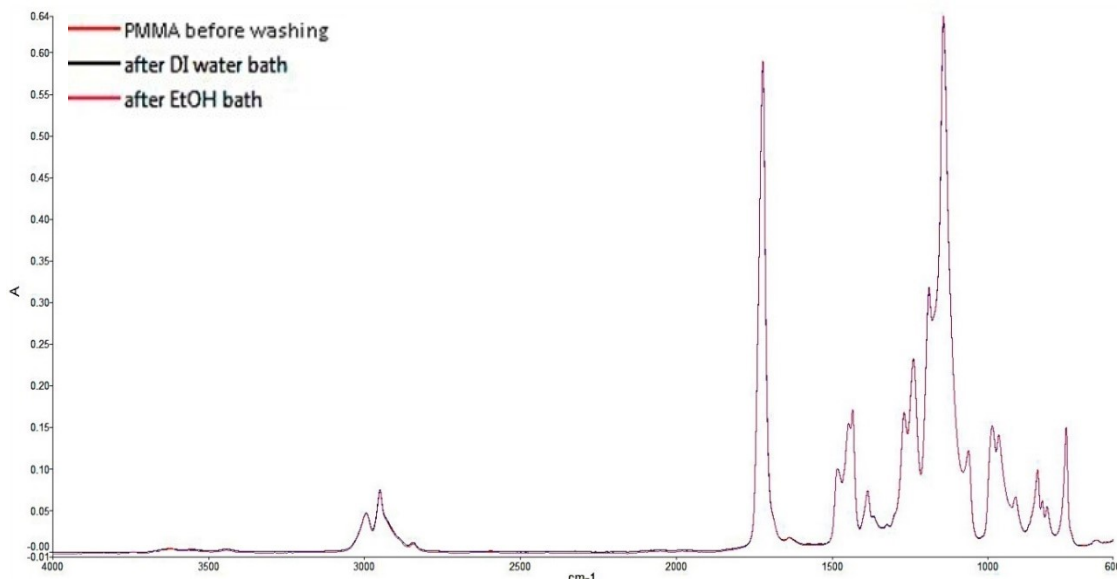


Figure 14. Spectra of PMMA coupons before and after ultrasonic cleaning in deionised water and ethanol. The untreated control is included for comparison.

**Appendix H. Conditioning of samples & weighing protocol**

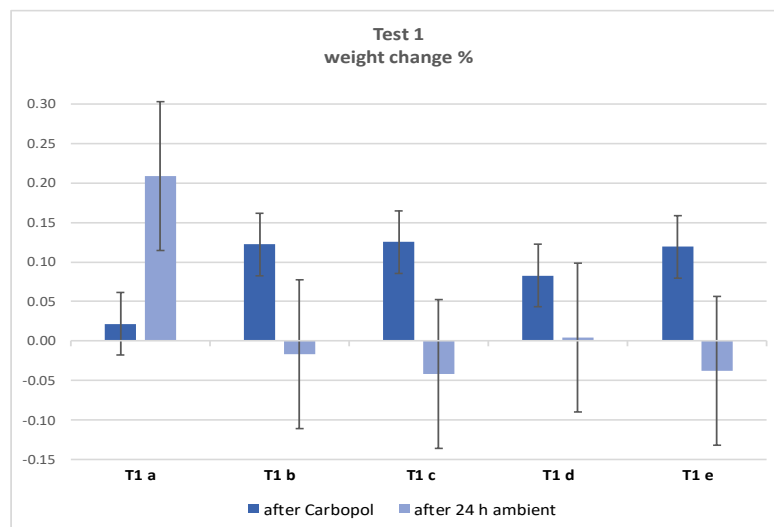
After having established a prewashing method for removal of all residues from the backing, tape and the protective film, the acclimatising/conditioning of samples was in order. By measuring differently buffered samples weight, it was aimed to understand how different conditioning methods would affect PMMA, and whether variations in mass could be moderated. To define the most suitable method that would allow samples to dry in the most consistent manner, trials were performed. Prewashed and subsequently treated replicates were exposed to different environments (Table 2.). Carbopol hydrogel was selected as it was documented to leave PMMA samples with the most extreme weight changes, ideal for testing buffering methods. Carbopol treatments lasted 60 minutes and followed by clearing with three separate wet washes with moistened cotton swabs in deionized water. All replicates were weighed before and after each stage.

test 1	prewashing	Carbopol	Ambient 24h			
test 2	prewashing	silica gel 24h	Carbopol	Silica gel 24h	Ambient 24 h	
test 3	prewashing	silica gel 24h	Ambient 24h	Carbopol	silica gel 24h	Ambient 24h
test 4	prewashing	buffered box 24h	Carbopol	buffered box 24h		
test 5	Ambient Day 1	Ambient Day 2	Ambient day 3	Ambient day 4	Ambient day 5	Ambient day 6
test 6	buffered box day 1	buffered box day 2	buffered box day 3	buffered box day 4	buffered box day 5	

Table 2. Tests of conditioning samples in different environments.

## Test 1

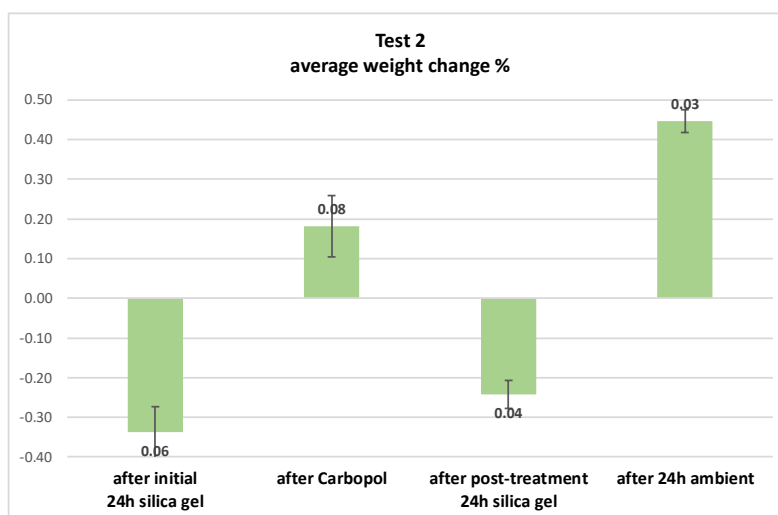
- Ultrasonic prewashing of replicates
- Treatment with Carbopol hydrogel
- Samples were then left to stand in ambient (laboratory) conditions for 24 hours
- Weight measurements showed very inconsistent weight changes (StDev 0.09 %), exhibiting large deviations
- The pattern of weight changes was random, fact which was attributed to the uncontrollable ultrasonic washing and inconsistencies in Carbopol hydrogel treatment.



*Graph 15. Test 1 examining the weight changes in PMMA replicates after being for 24 hours in ambient condition.*

## Test 2

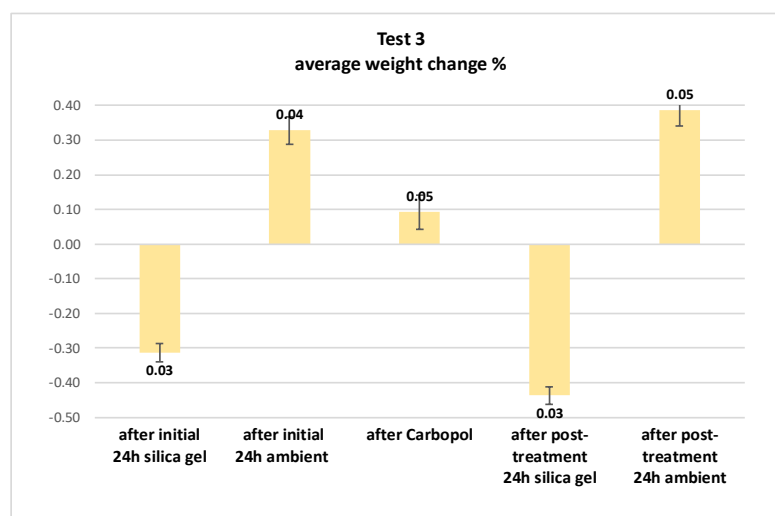
- Ultrasonic prewashing of replicates
- Storage in an airtight container with silica gel for 24 hours
- Treatment with Carbopol hydrogel
- Storage in silica gel for 24 hours
- Exposure to ambient (laboratory) conditions for 24 hours
- Weight measurements showed weight loss both times after storage in silica gel for 24 hours.
- While in ambient (laboratory) conditions, samples regained some of the weight lost during exposure to silica gel, possibly by reabsorbing room moisture.
- Improved weight consistency (StDev 0.03 %) after 24 hours in ambient conditions, compared to Test 1. This was attributed to the prior conditioning of samples in a silica gel environment.
- Averaged weight changes  $\pm 0.4$  %.



Graph 16. Test 2 examining the weight changes in PMMA replicates after being kept in an airtight environment with silica gel for 24 hours and then in ambient condition for another 24 hours.

### Test 3

- Ultrasonic prewashing of replicates
- Storage in an airtight container with silica gel for 24 hours
- Exposure to ambient (laboratory) conditions for another 24 hours
- Treatment with Carbopol hydrogel
- Storage in silica gel for 24 hours
- Exposure to ambient (laboratory) conditions for another 24 hours
- Ambient conditions for 24 more hours.
- Weight measurements were similar to results in Test 2
- Weight changes after silica gel were more consistent (StDev 0.03 %) than after ambient conditions (StDev 0.04 % and 0.05 %).

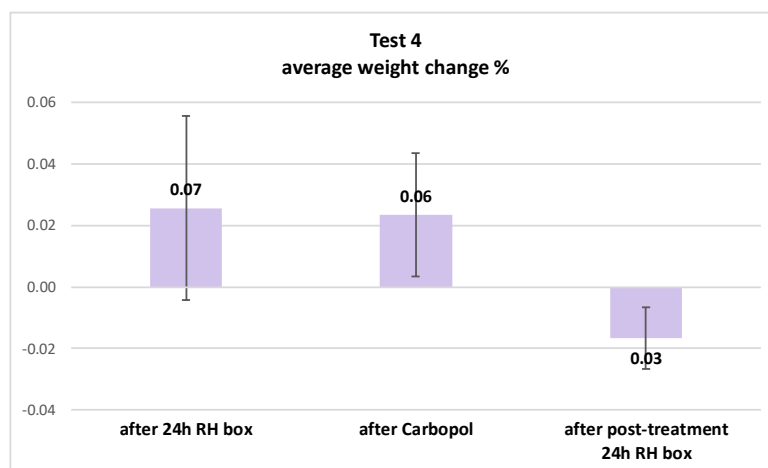


Graph 17. Test 3 examining the weight changes in PMMA replicates after being kept in an airtight environment with silica gel for 24 hours and then in ambient condition for another 24 hours.



## Test 4

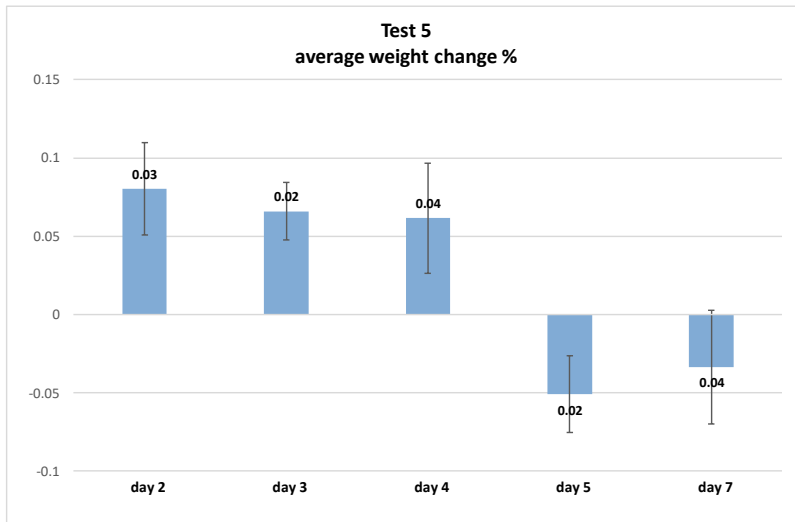
- Ultrasonic prewashing of replicates
- Storage in an acrylic box for 24 hours. The box was buffered with preconditioned Prosorb humidity control cassettes, with vapour permeable non-woven panels, prefilled with Prosorb beads, to keep relative humidity (RH) constant at 50 %  $\pm$  5 %. Beads would absorb and desorb water vapour, as appropriate, to stabilise RH. The acrylic case was sealed, and samples were handled through a 'window' opening.
- Treatment with Carbopol hydrogel
- Storage in an acrylic box for 24 hours
- Weight measurements were very inconsistent (StDev 0.07 %) after the first 24 hours
- After treatment and the second buffering in the acrylic box, weight fluctuations were much steadier (StDev 0.03 %).
- Even though samples showed both weight gain and loss, overall, they displayed the smallest in average weight change of  $\pm$  0.01 %.



Graph 18. Test 4 examining the weight changes in PMMA replicates after being placed in an acrylic box buffered with Presorb maintaining RH constant at 55 %.

## Test 5

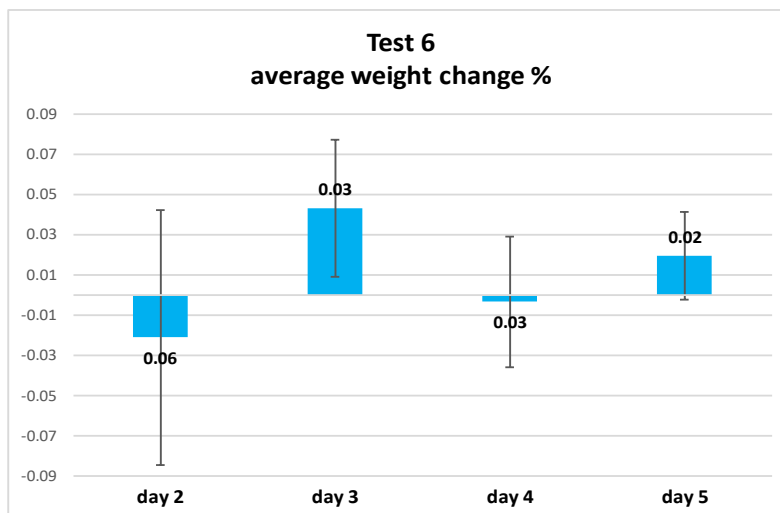
- Ultrasonic prewashing of replicates
- Exposure to ambient (laboratory) conditions for 7 days.
- Weight measurements, repeated every 24 hours, showed that up to day 4, samples consistently gained weight, which started to decrease from day 5 onwards. No stabilization of fluctuations was reached within one week in ambient conditions.
- Exposure to ambient (laboratory) conditions showed uncontrollable daily weight changes that reflected environmental fluctuations. Samples on average gained/lost  $\pm$  0.06 % weight.



Graph 19. Test 5 examining the daily weight changes in PMMA replicates being kept in ambient condition for 7 days.

Test 6

- Ultrasonic prewashing of replicates
- Storage in the RH acrylic box for 24 hours for 5 days
- Weight measurements, repeated every 24 hours, showed that changes after the first 24 hours were the most inconsistent among all tested days (StDev 0.06 %). This was attributed to the effect of ultrasonic washing. After day 2 in the buffered weight fluctuations were stabilised (roughly StDev 0.025 %). Samples in this test displayed among the smallest in average weight gain/loss of  $\pm 0.03$  %.



Graph 20. Test 6 examining the daily weight changes in PMMA replicates being placed in an acrylic box buffered with Presorb maintaining RH constant at 55% for 5 days.

To support the information obtained from the conditioning tests, the fluctuations of relative humidity experienced by PMMA replicates during the different conditioning methods

tested, were monitored with iButton miniature data loggers. iButton data obtained from the RH buffered box (Fig.10) indicated that the RH was very stable at ca. 55 % throughout the test, with a minor fluctuation of  $\pm 5$  % (min: 54.7 %, max: 58.3 %, average: 56 %). It was noted that these values were higher than anticipated, as the Prosorb cassette was preconditioned to keep RH at 50 %. A second datalogger was used to confirm the RH in the box, showing levels between ca. 52-54 %. The iButton placed in the laboratory showed that in ambient conditions (Fig.11), RH reached very high levels (ca. 75 %) with a lot of fluctuation. Some days the RH fluctuated between 35 and 63 %. Such large fluctuations over  $\pm 5$  % could result detrimental for PMMA that, as most plastics, would benefit from a stable RH maintained around 50 % (Shashoua 2014).

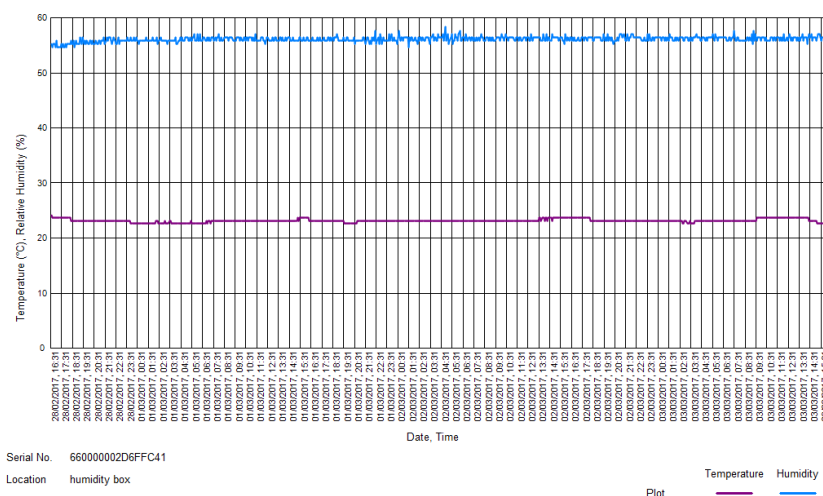


Figure 15. iButton data of RH buffered box with Prosorb preconditioned at 50 %, showing a stable RH at 55 %.

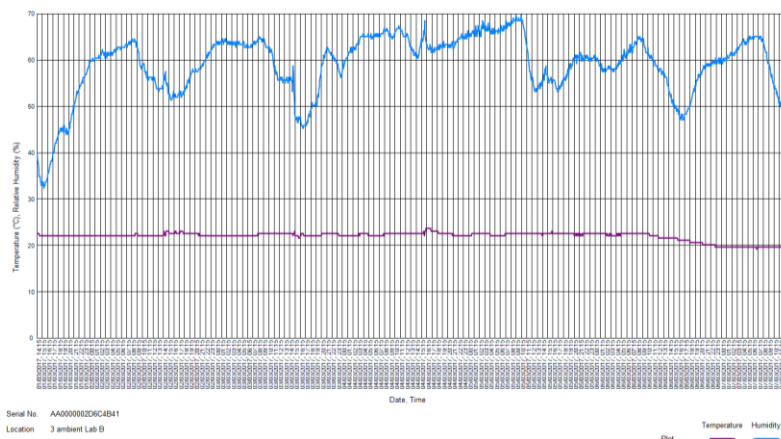


Figure 16. iButton data of the ambient laboratory environment, showing very high RH levels and large fluctuations.

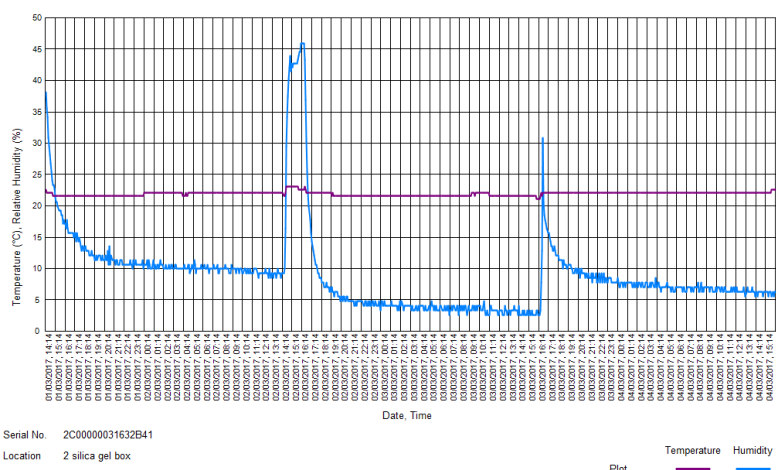
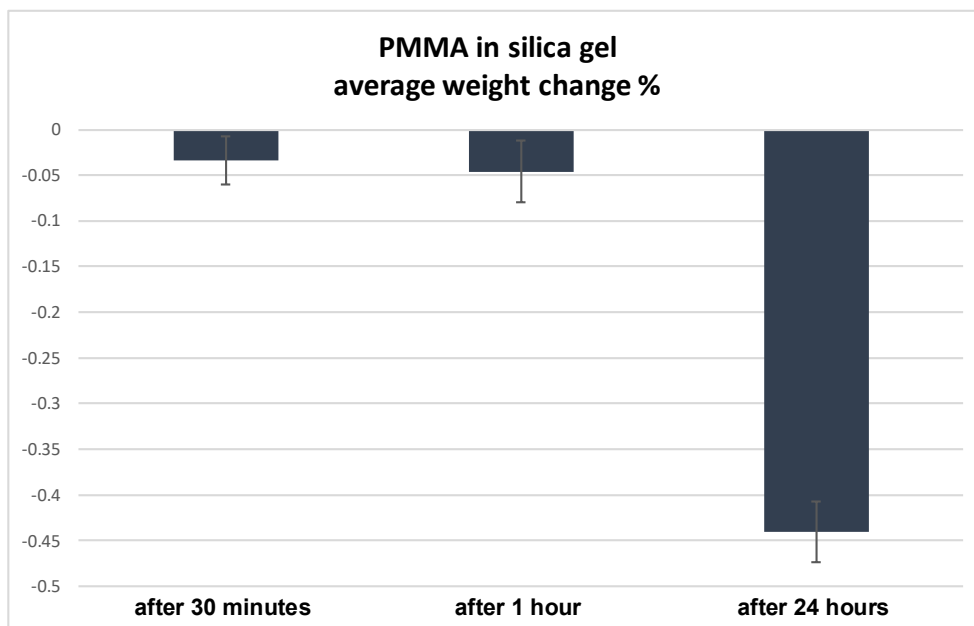


Figure 17. iButton data of airtight container with silica gel, showing very low RH levels.

iButton data obtained from the airtight container with silica gel (Fig.12) revealed that RH instantly dropped to ca. 10 % and some days reached as low as 5 %. Use of silica gel in contact with plastics was documented to absorb polymer degradation products (Baker *et al.* 2015), or polymer components, such as plasticizer, specifically in reference to PVA (Shashoua 2001) and cellulose acetate (Shashoua 2012a). Even though silica gel has been widely used for adsorption of water vapour, lack of research and storage recommendations for PMMA museum objects rendered its use complicated.



Graph 21. Weight change % averaged from 10 unwashed PMMA replicates placed in airtight container with silica gel and weighed after 30 minutes, 1 hour and 24 hours.

An additional test was carried out to understand the effect of silica gel on PMMA. New, unwashed PMMA coupons (n=10 samples) were placed in an airtight container with silica gel and were weighed after 30 minutes, 1 hour and 24 hours. Results showed that silica gel

was harmful to PMMA, as samples very consistently lost on average -0.45 % of their weight within 24 hours. This effect was attributed to the non-selective adsorption of the silica gel (Shashoua 2012a), which rendered its use uncontrollable. Furthermore, RH levels of 5 and 10 % were too low for PMMA.

The exact, numeric weight values of gravimetric measurements were not the focus of this study, but it was interesting to document the comparative behaviour of PMMA. Most importantly, these tests aimed to locate methods offering the most suitable environment for conditioning of PMMA samples, after ultrasonic cleaning (pre-washing), artificial UV ageing, dirt application and cleaning treatment. Summarizing the aforementioned points, the use of silica gel was rejected for being possibly harmful, with uncertain effectiveness and for causing large weight loss of PMMA. Ambient conditions caused weight gain of samples and allowed RH to reach very high levels with a lot of fluctuation, thus it was also rejected.

The buffered box, with the help of preconditioned Prosorb cassettes, offered very stable RH levels at ca. 55 %, with acceptable fluctuations less than  $\pm 5$  %, and the lowest deviation of PMMA sample weight, among tested methods. All tests indicated that for the first 24 hours after ultrasonic cleaning, PMMA always exhibited the most inconsistencies in weight, regardless conditioning method. High deviations were also observed during the first 24 hours with samples placed in the RH straight after prewashing. It was noticed though, that the fluctuations became more consistent after 48 hours. Therefore, it was suggested that PMMA coupons be conditioned in the RH box for 48 hours after prewashing in ultrasonic bath and prior to weighing, and 24 hours after UV ageing (and before treatment), after dirt application and after cleaning treatment, prior to their weighing.



*Figure 18. Prosorb humidity control cassettes, preconditioned to keep relative humidity (RH) constant at the desirable level.*

## Appendix I. Physical characteristics of gels

Agar and Gellan gels were physical, rigid, brittle, strain-stiffening with well-defined shapes. They were prepared in pre-formed sheets that rendered application and removal very easy, thus minimizing mechanical stress. Gels could only make contact because the PMMA surfaces were completely flat and planar. Glass weights were placed on the gels to increase contact with the PMMA surfaces. The nature of rigid gels also represents the main limit to their use; given their rigidity it may be difficult to obtain good contact on surfaces that are not perfectly flat (Cremonesi 2010). To overcome this limitation in other studies Agar gels have been applied semi-solid, in a fluid state, turning solid on contact with the surface (Cremonesi and Casoli 2017). In this study, rigid gels used in the cleaning experiments scored the highest CARS in categories '*Ease of use*' and '*Control*', regarding handling of the treatments, because they were very easy to place and to remove from PMMA samples.

Agar and Gellan gels form hydrogen-bonded bundles of polymer chains having porous regions within which water can diffuse. Their pore size depends on their grade, concentration, and preparation method. Published NMR data indicate that the water mobility inside the polysaccharidic network of Agar gels and the water content in the pores strictly depends on the gel concentration (Bertasa *et al.* 2017). Similar research demonstrates that pores in 4 wt.% Agar gels are smaller and limit water diffusion compared to pores found at smaller concentrations (i.e. 1 wt.%) (Angelova *et al.* 2016a). The implication being that in practice lower concentrations of Agar, such as a 2 wt.% used in the present study, would be less rigid and more easily release water than stiffer gels formed by higher concentrations (i.e. 5 wt.%). However, the harder the gel the less readily it would conform to textured surfaces with limited adhesion and high retention of water.

In cases where the pH drops below 6.0, precipitation (flocculation) of the Agar can take place (Wolbers 2017). This is a process by which fine particulates are caused to clump together into a floc. Moreover, polysaccharide Agar and Gellan gels are capable of a physical process termed syneresis. This meant that they can spontaneously exude/release free liquid (water) through their gel surface on standing or with an applied force (Wolbers 2017). Besides, rigid gels such as Agar and Gellan tend to exhibit higher syneresis than softer, more flexible gels (Wolbers 2017), such as Carbopol and PVA.

PAA-based Carbopol/Ethomeen and Pemulen/TEA gels were quite tacky and with a paste consistency that is very easy to uniformly spread. However, due to their paste-like nature and high level of adhesion, they would adhere to the treated surfaces becoming uncontrollable and difficult to remove without leaving greasy residues. For this reason, samples after Carbopol and Pemulen gels scored satisfactory CARS in '*Ease of use*', but very

poorly in the 'Control' category. Unlike rigid polysaccharidic Agar and Gellan and putty-like PVA/borax, Carbopol and Pemulen gels required some mechanical action in the form of wiping with a soft Teflon spatula, in order to be removed, possibly giving them a head start in cleaning efficiency compared to the other gel treatments.

Carbopol/Ethomeen exhibited the lowest viscosity among gels used in the present cleaning experiments, having the lowest horizontal and vertical hold. Pemulen/TEA hydrogels and solvent gels with the alcohols EtOH and IPA exhibited this paste-like consistency earlier mentioned, but gels coupled with PET showed improved consistency and viscoelasticity and did not dissociate as much as the other gels with EtOH, IPA and water. This was attributed to the chemical nature of Pemulen that when mixed with a non-polar solvent, formed an emulsion. Pemulen/PET emulsion-gels presented better retention properties, hence were more consistent, malleable and able to be removed as intact pieces.

PVA/borax gels were highly viscous polymeric solutions with transient crosslinks with a finite relaxation time that offered them their ability to retract. The gels were self-healing and mouldable, yet at the same time, strain-stiffening and elastic (Angelova *et al.* 2016a; Riedo *et al.* 2015). The combination of these characteristics yielded a soft, putty-like, malleable material that could be moulded, reformed and conformed to surfaces, while maintaining its shape (Angelova *et al.* 2015; Angelova *et al.* 2017a). PVA gels were placed on sample surfaces with a soft Teflon spatula and uniformly spread/flattened with glass slides, also acting as barriers limiting solvent evaporation. Their unique mixture of mechanical properties and the labile nature of the crosslinks offered limited adhesion to the treated surface (Angelova *et al.* 2016a) that, not only allowed them to be completely removed, but rendered them easily 'peelable'. Their self-healing property required some barrier/weight to hold them in place for the duration of the treatments, otherwise they would start retracting and eventually lose contact with the substrate. PVA gels did not dissociate during cleaning, and they were often recorded to have successfully peeled off synthetic sebum soil along. With some manipulation of the gel, PVA offered absolute control of the targeted area to treat. For these reasons samples treated with PVA received the highest CARS score for 'Ease of use' and 'Control'.

Appendix J. Smoothing of NMR MOUSE data

		TABLE I									
CONVOLUTES	SMOOTHING		QUADRATIC		CUBIC		A20	A30			
POINTS	25	23	21	19	17	15	13	11	9	7	5
-12	-253										
-11	-138	-42									
-10	-33	-21	-171								
-09	62	-2	-76	-136							
-08	147	15	9	-51	-21						
-07	222	30	84	24	-6	-78					
-06	287	43	149	89	7	-13	-11				
-05	322	54	204	144	18	42	0	-36			
-04	387	63	249	189	27	87	9	9	-21		
-03	422	70	284	224	34	122	16	44	14	-2	
-02	447	75	309	249	39	147	21	69	39	3	-3
-01	462	78	324	264	42	162	24	84	54	6	12
00	467	79	329	269	43	167	25	89	59	7	17
01	462	78	324	264	42	162	24	84	54	6	12
02	447	75	309	249	39	147	21	69	39	3	-3
03	422	70	284	224	34	122	16	44	14	-2	
04	387	63	249	189	27	87	9	9	-21		
05	322	54	204	144	18	42	0	-36			
06	287	43	149	89	7	-13	-11				
07	222	30	84	24	-6	-78					
08	147	15	9	-51	-21						
09	62	-2	-76	-136							
10	-33	-21	-171								
11	-138	-42									
12	-253										
NORM	5175	8059	3059	2261	323	1105	143	429	231	21	35

Figure 19. Table with convolutes for smoothing the sum of the signal amplitude by using Savitzky-Golay filtering with a 9-point convolute (window). For cubic or quadratic function, the set of integers were shown in this table for up to 25 points. The appropriate normalizing factors for the 9-point smoothing used here were highlighted in red; The noise was reduced approximately as the square root of the number of points (After Savitzky-Golay 1964, p. 1631).

Although the NMR data were optimized by increasing the number of scans, interference was still present as background noise, hindering the detection of changes in the graphs before and after treatment. Given that it was already hard to detect liquid movement in the PMMA samples due to their stiffness, the visual data were further enhanced by using Savitzky-Golay filtering with a 9-point convolute (window) to smooth the sum of the signal amplitude (Richardson *et al.* 2017). Computational methods can be used for the removal of random noise, under two prerequisites (Savitzky and Golay 1964): that the points to be smoothed are at a fixed, uniform interval – in NMR each data point is obtained at the same time interval, and that the curves formed by graphing the data points are continuous and roughly smooth – which is the case in NMR. Savitzky-Golay smoothing is based on the concept of a convolute and a convolutional function, where a mathematical operation is employed to produce a third function from two functions. According to it, the noise is reduced approximately as the square root of the number of points used (here 9-point smooth) (Savitzky and Golay 1964).



## Appendix K. Gel recipes

### Agar and Gellan

Agar and Gellan gels both followed the same preparation method and recipes. Agar powder (Sigma-Aldrich®) was dispersed and mixed in deionized water at room temperature (2 wt.%, 0.9 g in 45 mL water). The solution was heated until it came to boiling (approx. 90 °C) (Sansonetti *et al.* 2012). Gellan gum (Albert y Ferran Adrià, <http://www.albertyferranadria.com/eng/texturas-info.html>) was prepared in deionized water and heated to boiling conditions (2 wt.%, 0.9 g in 45 mL). Once left to cool, both solutions were re-heated a second time to improve the water retention properties of the gels (Cremonesi 2010, 181). The pH of Agar was measured at around 7.0 (neutral) using a pH indicator strip, whereas Gellan formed a slightly acidic solution (pH 6.0). Both solutions, once prepared in beakers with magnetic stirrers on a hot plate to boiling conditions (approx. 90 °C), were poured into rectangular containers and allowed to cool down to room temperature in order to gellify. They would usually start to solidify between 32-45 °C. The gels were 2-3 mm thick and further cut into smaller rectangular pieces in the size of the PMMA samples (25 x 25 mm).

The same procedure was repeated for the solvent gels in 20/80 wt.% solvent/deionized water mixtures (2 wt.%, 0.9 g in 36 mL water and 9 mL solvent). Solvents were added following the removal of solutions from the hot plate the second time and during their cooling. It was essential to avoid heating of the solvents because of their high flammability. In addition, solvents would readily evaporate at increased temperatures and the gels would lose their anticipated cleaning efficiency. Gels were refrigerated in resealable polyethylene zip lock bags until use to counter the biodeterioration of these natural biopolymers (Wolbers 2017).

### Carbopol EZ 2/Ethomeen C-25

After empirical testing of a variety of recipes, a formula by Stavroudis and Blank (1989) was prepared. Carbopol EZ 2 (Kremer) was mixed in deionized water and stirred continuously until smooth (2 wt.%, 0.4 g in 20 mL) and was left to stand overnight to fully disperse. The following day 4 mL Ethomeen C-25 (Kremer) was gradually added to the dispersion until a basic solution (pH 8.0) was reached and a less tacky and consistent paste mixture was formed. For the solvent gels, recipes were made by mixing 0.4 g in 4 mL solvent and 16 mL water. Mixtures were left to stand overnight and the next day 4 mL Ethomeen was added into the dispersion and constantly stirred. All Carbopol gels were prepared in glass jars and left sealed to stand overnight to fully disperse and become uniform in texture and appearance. It was recommended to stir the gels before each use to promote homogeneous re-partition of the

Ethomeen base in the polymeric macromolecular network (Hennen *et al.* 2017). Carbopol/Ethomeen with water and alcohols were yellow or amber in colour, due to the discolouration of Ethomeen (Stavroudis 2017), while the emulsion formed by mixing with PET had a milky or cloudy effect.

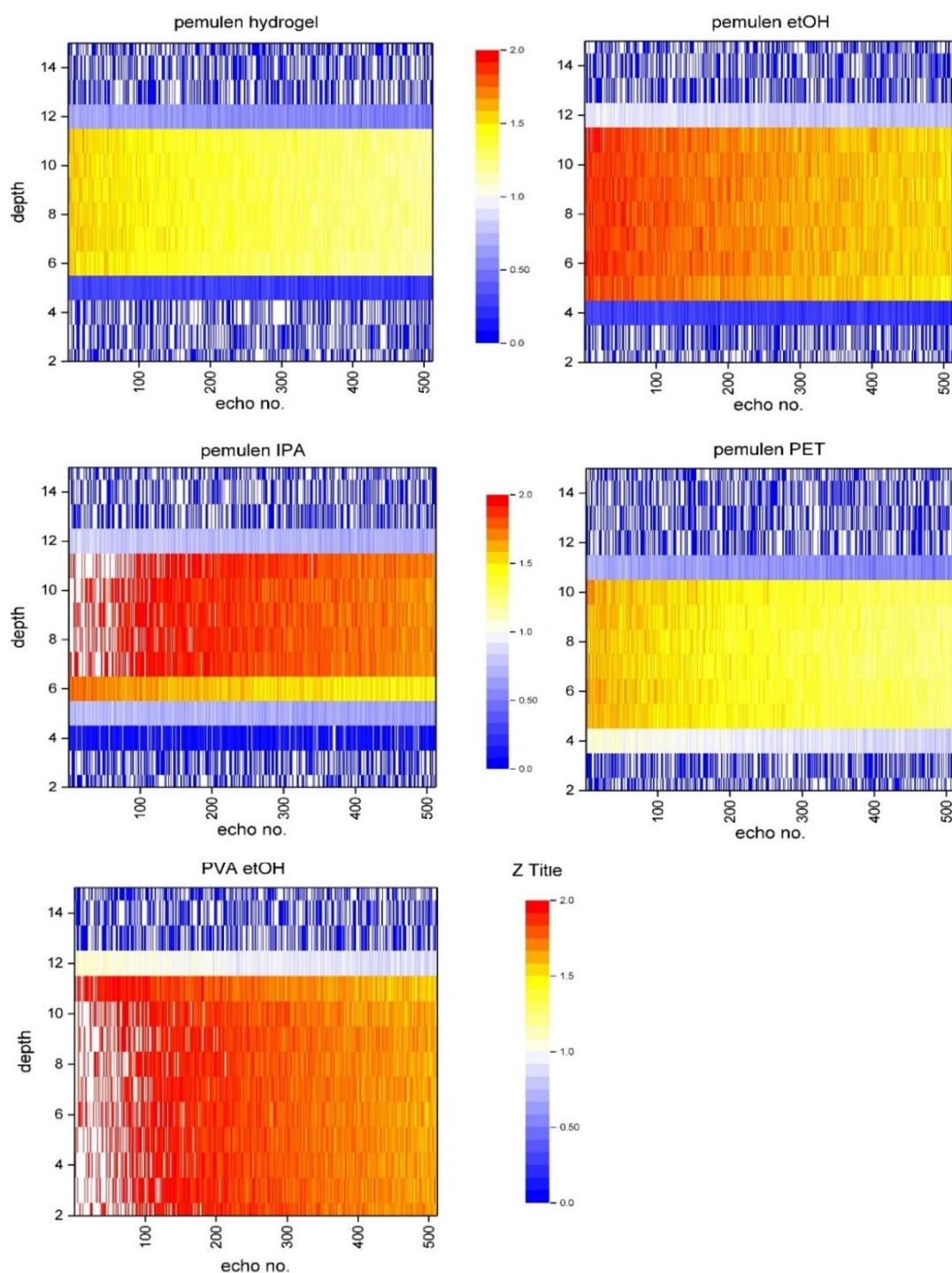
#### Pemulen TR-2/Triethanolamine

For the current study the gel was prepared in two stages. First Pemulen™ TR-2 was gradually added in deionized water with constant stirring (1 wt.%, 0.2 g in 10 mL water). Separately, a solution of liquid TEA was also prepared in deionized water (5 wt.%, 1 g in 10 mL water). The two dispersions were mixed together and hand stirred creating a weak basic gel (pH 8.0). Use of a miniature balloon whisk was recommended in order to reach a smoother consistency (Ravenel 2012). To prepare the solvent gels Pemulen was diluted in 20/80 wt.% solvent/deionized water (1 wt.%, 0.2 g Pemulen in 2 mL solvent and 8 mL water) and a separate solution of TEA in deionized water (5 wt.%, 1 g in 8 mL) was prepared. The two solutions were mixed and 2 mL solvent was added. The gels were energetically shaken until all the solvent was incorporated into the system. Even once thoroughly mixed, Pemulen would form lumps of concentrated polymer, which would disperse with time. To allow that to happen, Pemulen gels were left to stand overnight in sealed glass jars prior to their use.

#### 80 % PVAc/Borax

An 80% hydrolysed PVA (Poval PVA-424, Kuraray Co., Ltd.) in powder form was allowed to sit undisturbed in deionized water for 30 minutes (4 wt.%, 0.2 g in 3.75 g water). In a separate container borax (sodium tetraborate decahydrate, Sigma-Aldrich®) in powder form was mixed in deionized water with the assistance of some heat (1 wt.%, 0.05 g in 1 g water). Once the polymer had swollen and become transparent, the PVA/water mixture was stirred – without the application of heat - for the polymer to fully dissolve. Borax was then added to the polymer and stirred vigorously with a spatula until a homogeneous gel was formed. Solvent gels were prepared by dispersing the 4 wt.% 80 % hydrolysed PVA in 20/80 wt% solvent/deionized water mixtures (0.2 g PVA in 0.95 g solvent and 2.8 g water). The next steps followed the same procedures as for preparation of the hydrogel.

## Appendix L. NMR MOUSE profile scans of gel systems



Graph 22. 2D colour-intensity contour heat maps of the gel systems used in the final experiment. The gels were placed between microscope glass slides to assist with the definition of the interfaces. Gels with alcohols etOH and IPA displayed the highest proton density. Pemulen with etOH and IPA, along with PVA etOH, exhibited similar relaxation behaviors. Pemulen with H<sub>2</sub>O and PET showed a weaker proton density, and again their behaviors were comparable. None of the solvent gels had fully relaxed by the 512<sup>th</sup> echo, suggesting very long relaxation times.

**Appendix M. Preliminary cleaning experiments on unaged, unsoiled PMMA samples**

The preliminary cleaning experiments carried out on unaged PMMA samples aimed to assess the damage potential, rather than the effectiveness, of the individual gel cleaning methods encountered in the literature. Samples were studied in their unaged condition to collect control data. Implications of degradation were examined in later experiments. Since the interaction between variables was expected, understanding the effect of single factors, before proceeding to more complicated experimental designs was necessary. Therefore, three smaller experiments were designed to examine the impact of individual cleaning materials, seen here as hydrogels and non-gellated, free flowing liquid solvents, as well as their interaction and damage potential when combined in one cleaning system. All experiments were assessed with respect to application time.

**Experimental design**

The factors initially considered critical for cleaning PMMA were type of gel, solvent and application time. The experiments were statistically designed to examine them individually and in combination. Once these factors and their levels will be tested, the following experiments will address additional factors and/or levels, rendering the experimental design more complex. Following the preliminary experiments, further variables such as surface condition of PMMA, type and condition of surface dirt will be interrogated.

The experiments were two-factorial, therefore consisting of two factors examined at a time. Overall three factors, Gels, Solvents and Application time, were studied at multiple levels (general two-factorial design) as laid out in Table 3. The two-factorial experimental design generated three smaller scale experiments:

- Effect of hydrogels Agar, Gellan, Carbopol, Pemulen and PVA and their interaction with application times (5 and 60 minutes).
- Effect of free solvents H<sub>2</sub>O, EtOH, IPA and PET, in relation to application times (5 and 60 minutes).
- Interaction of Gels and Solvents, previously examined in isolation, combined as solvent-based gel systems.

**Preliminary Experiment on unaged, unsoiled PMMA: 2 and 3 replicates**

Experimental Variables			
Factor	A. Gels	B. Solvents	C. Application time
Levels	1. Agar	1. Deionised water (H <sub>2</sub> O)	1. 5 minutes
	2. Gellan	2. Ethanol (EtOH)	2. 60 minutes
	3. Carbopol®+Ethomeen	3. Isopropanol (IPA)	
	4. Pemulen™ TR2+TEA	4. Petroleum ether (PET)	
	5. PVA/Borax		

*Table 3. Experimental variables in the two-factorial design used for the preliminary cleaning experiments of unaged and unsoiled PMMA.*

**Sample preparation**

These preliminary cleaning experiments were performed on new, transparent PMMA square coupons (25 x 25 x 1.0 mm) pre-washed in ultrasonic bath with deionised water. The experiments with hydrogels and free-standing solvents were run in triplicate, whereas solvent gels in duplicates. Each experiment consisted of 24 iterations for a total of 72 samples used in this preliminary experiment. The (hydro/solvent) gels were applied and removed with a soft Teflon spatula, while the free solvents were applied as 3 drops with a micropipette (ca. 0,14 mL) and removed/blotted by rolling a cotton swab. Samples were confined with a plastic cover during treatment, to limit evaporation of free and gellated solvents. In all three experiments, treatments were followed by a post-treatment cleaning consisting of rolling 3 consecutive, moistened cotton swabs followed by a dry one.

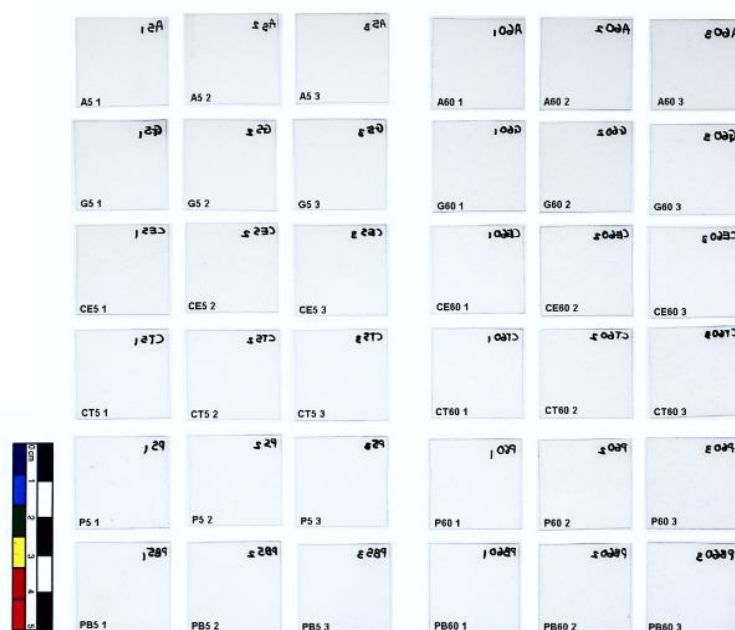


*Figure 20. Documentation of unaged and unsoiled PMMA samples before treatment with hydrogels, free solvents or solvent gels for 5 or 60 minutes. The samples were labelled at the back.*

## Results and interpretation

### Free solvents

#### Stereomicroscopy under raking light

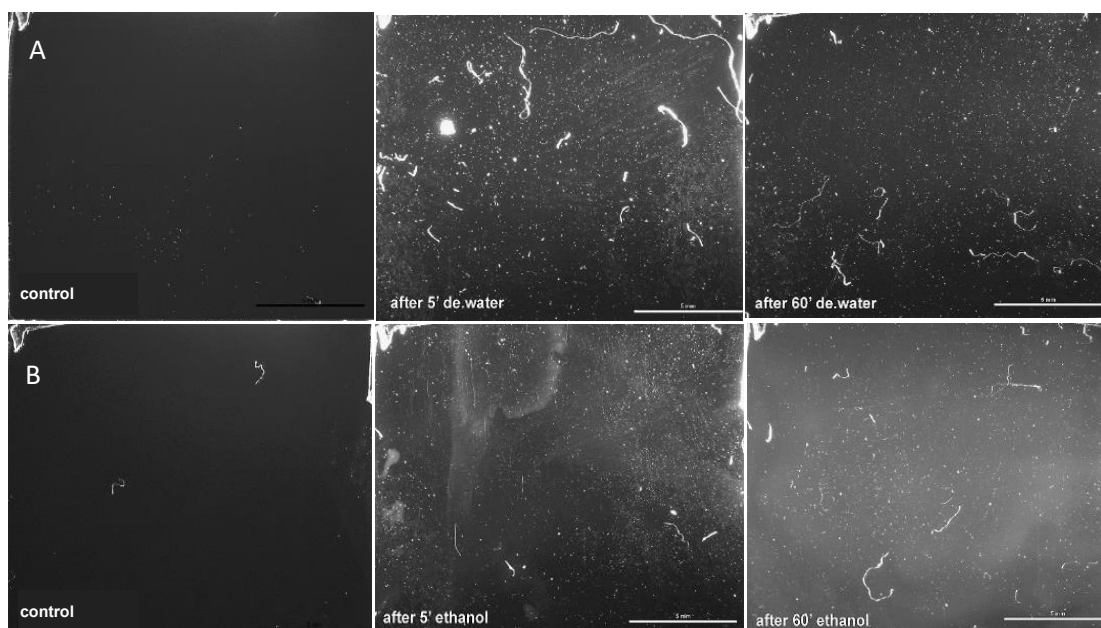


*Figure 21. Stereomicroscopic images of unaged PMMA controls and samples treated with solvents for 5 and 60 minutes under raking light (x78.1).*

H<sub>2</sub>O left transparent PMMA samples in good condition with limited regions of opacity, transparency, independent of application time (Fig.21 A). EtOH caused the formation of non-uniform surface opacity and induced abrasions, which were obscured after 60 minutes due to the extent of surface opacity (Fig.21 B). IPA caused a similar effect to EtOH, resulting in loss of transparency. After prolonged application (60 minutes) damage was exacerbated. PET caused surfaces to visually appear greasy. The post-treatment clearance with 3 separate H<sub>2</sub>O-moistened swabs rolled over the samples left cotton fibre residues (Fig.21 A).

#### SEM imaging

Under the SEM, H<sub>2</sub>O left PMMA surfaces looking unchanged resembling the PMMA control sample (Fig.22 A). The high magnification of SEM allowed for the extensive areas of non-uniform loss of surface transparency in the etOH to be identified as fine particulate deposit (Fig.22 B-C). The same phenomenon was caused by IPA; Opaque areas showing a fine deposit of particulate matter. Although PET was seen to leave a slightly greasy residue under the stereomicroscope, this was not apparent under the SEM. Surfaces were relatively clean, free from abrasions, with limited loss of transparency. It has been speculated that the magnification was so high that it was not possible to distinguish the greasy layer.

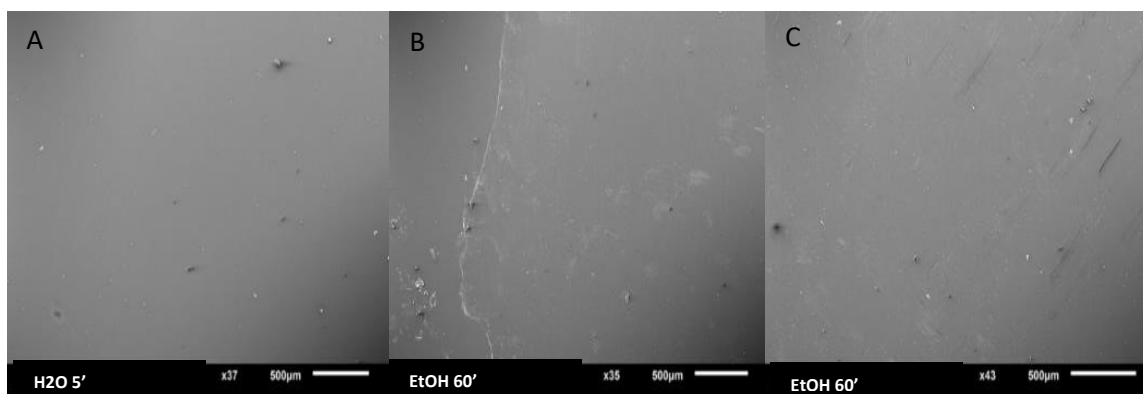
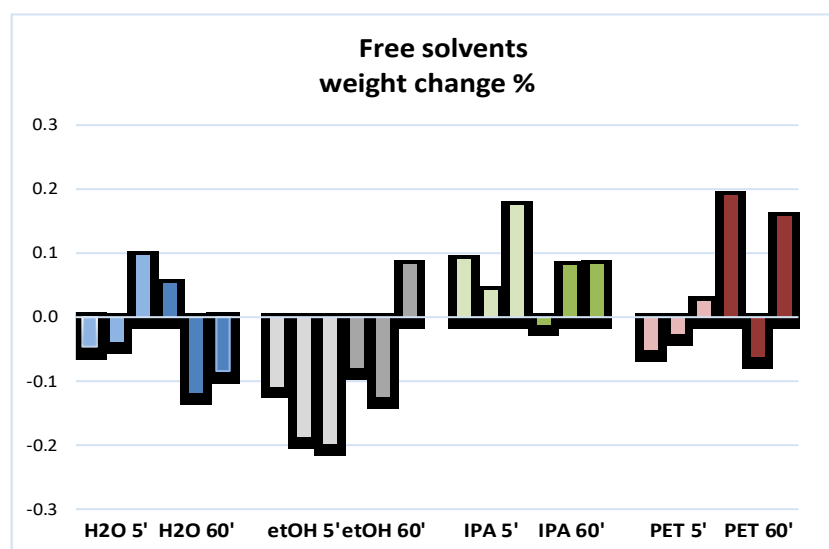


Figure 22. SEM micrographs: A: H<sub>2</sub>O left new PMMA as pristine as the PMMA control sample. B-C: EtOH caused fine deposits and surface opaqueness.

Weight change

Application of H<sub>2</sub>O caused inconsistent low level weight changes (both gain and loss). EtOH instigated the largest and most consistent weight loss, while IPA consistently caused weight gain. Application time of neither EtOH nor IPA affected the cleaning result. Shorter times (5 minutes) of PET application exhibited the least change and variance among all solvent-treated samples, whereas prolonged application (60 minutes) caused large weight gain in two samples.



Graph 23. Weight change % of unaged PMMA samples (in triplicate) treated with free solvents for 5 and 60 minutes. Changes % are relative to the starting/initial weight.

Conclusions

Free H<sub>2</sub>O caused inconsistent weight changes, but visually left new PMMA surfaces unchanged, confirmed under high magnification. EtOH caused weight loss, whereas IPA weight gain, both in a consistent fashion. Both organic solvents visually left PMMA in a similar condition, causing loss of transparency, identified as fine deposits under the SEM. Application time of the free

solvents generally did not affect the surface condition. The 60-minute applications caused inconsistent weight changes. Visually, free PET left surfaces in a better condition.

## **Hydrogels**

### Stereomicroscopy under raking light

Agar hydrogels left samples in a good condition; Surfaces exhibited limited loss of transparency and most importantly minor abrasions. Gellan hydrogels had a similar impact on the PMMA as Agar hydrogels. Application of Carbopol for 5 minutes left samples heavily impaired, bearing numerous scratches, while after 60 minutes surfaces appeared somewhat smoother. Application of Pemulen after both application times left PMMA equally impaired; Loss of transparency and cotton fibre residues trapped on what gave the impression to be a greasy surface to the naked eye. PVA hydrogels left PMMA surfaces in a satisfactory condition: clear and with minute gel residues sporadically visible.



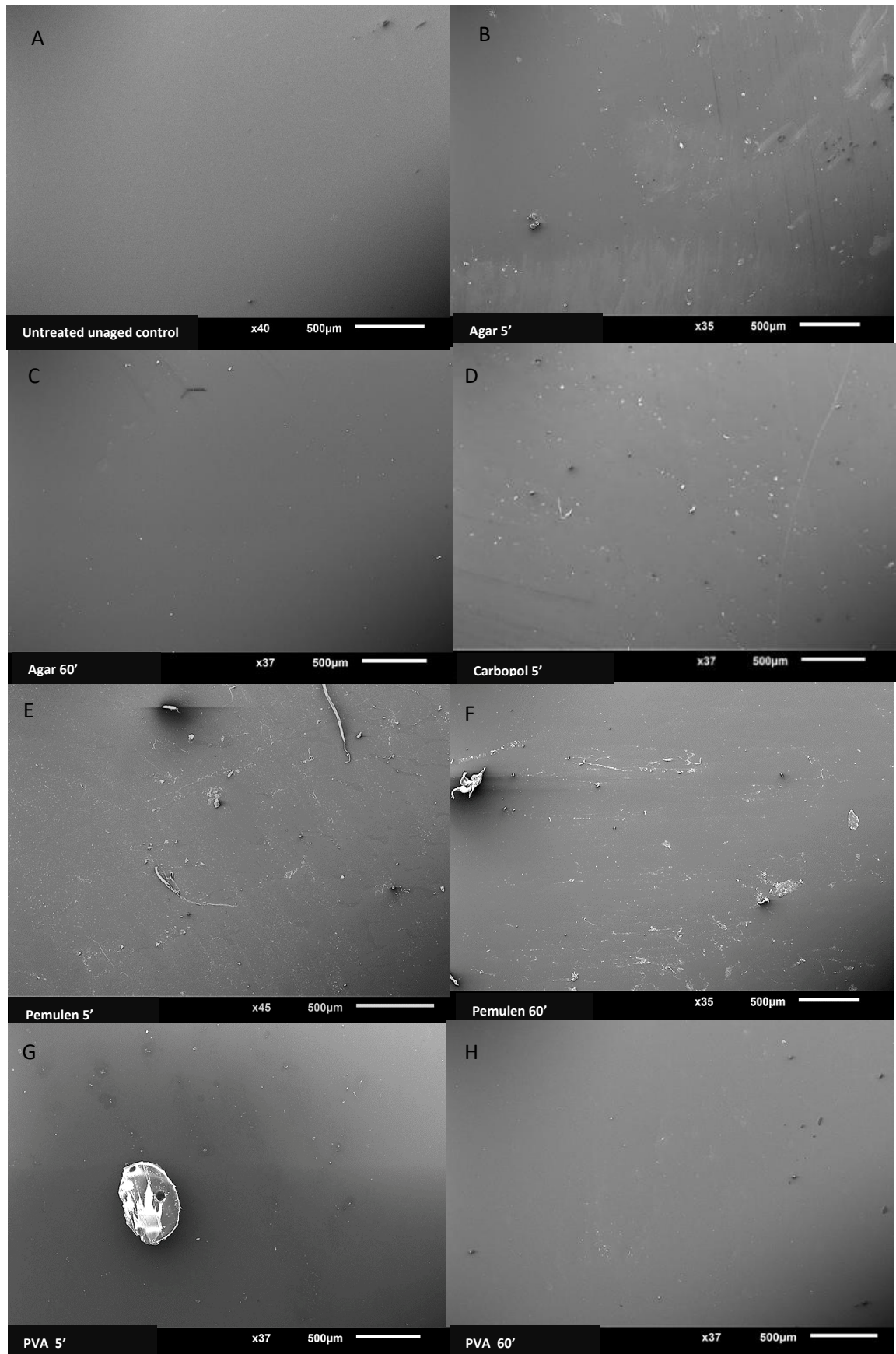


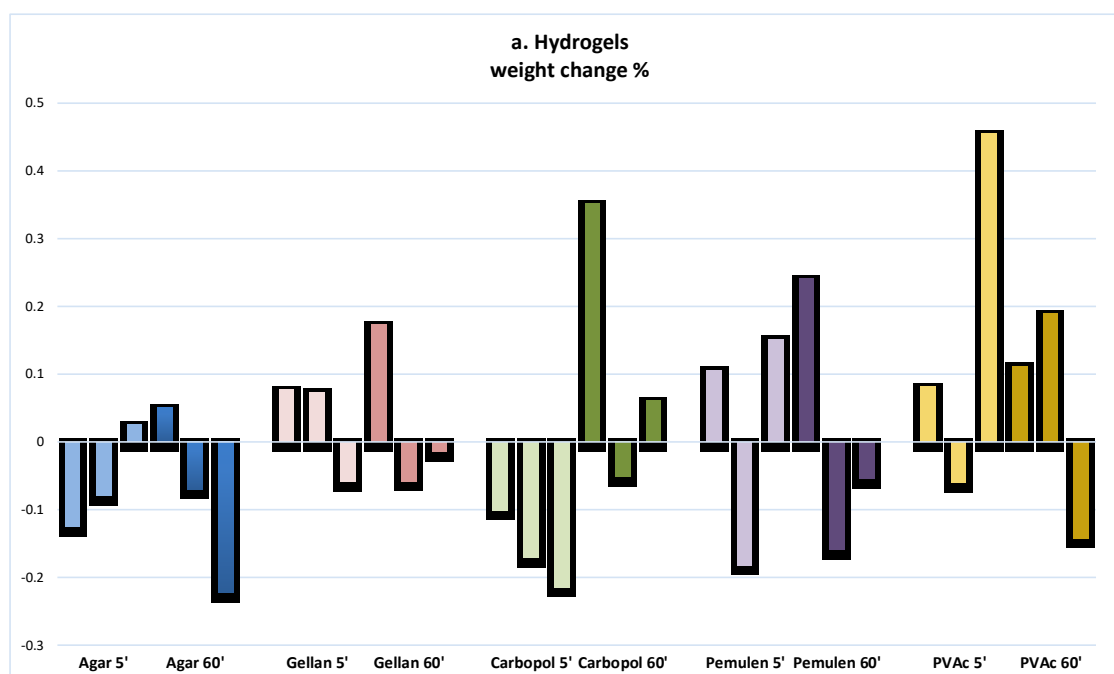
*Figure 23. SEM micrographs: A: New PMMA control sample with pristine surface. B-C: Agar hydrogel left surfaces in good condition. D: Carbopol hydrogel left limited gel residues and some stains. E-F: Pemulen hydrogel left surfaces with inferior condition with a large amount of gel residue. G-H: PVA hydrogels caused some areas resembling discolouration.*

### SEM imaging

Overall, hydrogels deposited negligible residues on the treated samples, as confirmed by SEM. Agar (Fig.23 B-C) left surfaces in a satisfactory condition. Gellan hydrogels behaved similarly to Agar. Carbopol deposited limited gel residues, abraded the PMMA and caused some areas to appear dull and opaque, as if discoloured (Fig.23 D). Pemulen hydrogels deposited a greater quantity of residue compared to other hydrogels, visible as thin gel layers covering PMMA surface areas (Fig.23 E-F). PVA hydrogels caused sporadic loss of transparency and some waterlines (areas that resembled droplets of liquid that had evaporated) (Fig.23 G-H).

### Weight changes

Overall, the results were inconsistent and did not allow clear conclusion to be drawn (Graph 25). Agar hydrogels primarily caused samples to lose weight, with longer applications (60 minutes) causing greater loss. Gellan hydrogels displayed greater consistency of PMMA weight change amongst hydrogels, with a tendency to gain weight. The 5-minute application of Carbopol hydrogels induced the greatest weight loss, while application of 60 minutes caused large inconsistencies. Pemulen hydrogels caused a variable response, independent of application time. PVA hydrogels caused the largest weight gain among hydrogels and were inconsistent indicating that they cannot be used in a repeatable fashion on PMMA.



Graph 24. Weight change % of unaged PMMA samples (in triplicate) treated with hydrogels for 5 and 60 minutes. Changes % are normalised to the starting/initial weight.

## **Conclusions**

I might be tempted to suggest that the lack of systematic response might indicate unpredictable treatment if used in conservation of PMMA. There was no clear pattern indicating if with increased application time cleaning an important factor, or if the action of a particular hydrogel was more/less controllable. Microscopic observations indicated that Agar and Gellan hydrogels performed well, leaving treated surfaces in a good condition. Pemulen on the other hand performed the poorest, depositing significant amounts of gel residues. Carbopol hydrogels left some gel residues and caused some loss of surface transparency. PVA also caused opacity of the surface.

## **Solvent-gels**

### **Stereomicroscopy under raking light**

Hydrogels were discussed previously. This section discusses gels coupled with EtOH, IPA and PET. Agar solvent gels reduced the extensive opaqueness and abrasions induced in PMMA by EtOH and IPA, although still visible to some degree (Fig.24 A). Agar PET exhibited similarities with the application of the free solvent: surfaces visually appeared greasy, but microscopic observation showed they were left in a good condition. Gellan solvent gels induced a similar result to Agar solvent gels, reducing the damaging effect of free solvents. Carbopol solvent gels left PMMA in an equally poor visual condition compared to free solvents, particularly after Carbopol EtOH; Intense loss of transparency and opaqueness to the samples, accompanied by abrasions (Fig.24 B). Pemulen solvent gels left PMMA in a similar visual condition as Carbopol solvent gels causing intense scratching (Fig.24 C). Therefore, Carbopol and Pemulen gels did not regulate the effect of solvents. PVA solvent gels left PMMA free from abrasions. PVA with EtOH and IPA caused loss of transparency (Fig.24 D), similar to the application of free solvents.

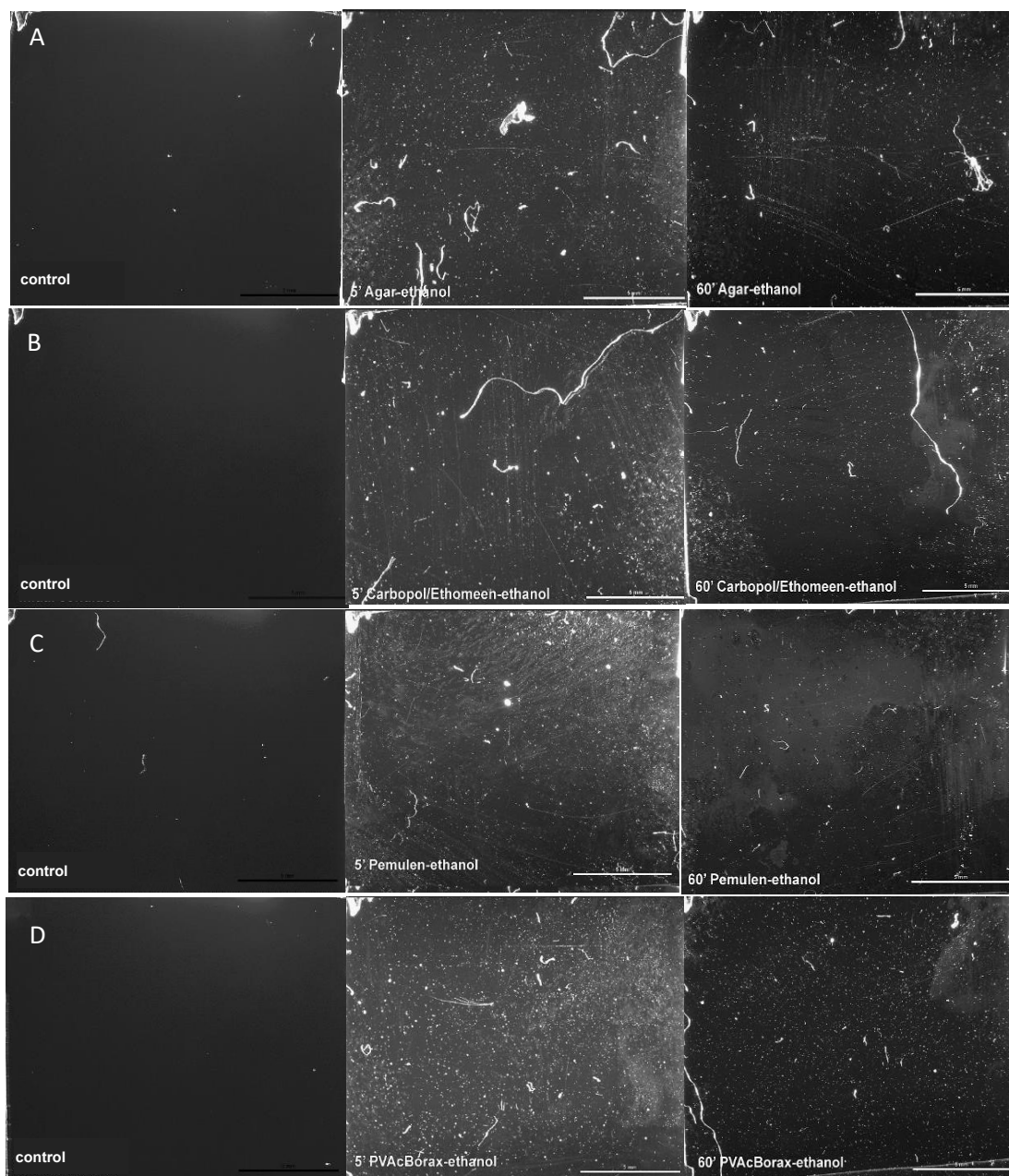


Figure 24. Stereomicroscopic images under raking light (x78.1) of unaged PMMA samples treated with solvent gels for 5 and 60 minutes. A: Agar EtOH, B: Carbopol EtOH, C: Pemulen EtOH and D: PVA EtOH.

#### SEM imaging

Agar and Gellan solvent gels deposited very negligible to no residues on the treated samples, which was confirmed by SEM (images not shown). By comparison, Carbopol and Pemulen solvent gels deposited extensive residue, and caused loss of transparency (Fig.2 A-B). Under high magnification, Pemulen residues were identified as deposits of gel. Observation of the opaque surfaces determined the presence of fine depositions of particulate matter. PVA solvent gels deposited negligible to no residues on the treated samples, as confirmed by SEM,

and caused limited surface opaqueness (Fig.25 C). With the exception of rigid, pre-formed Agar and Gellan gels, all other gels with EtOH and IPA caused severe abrasions.

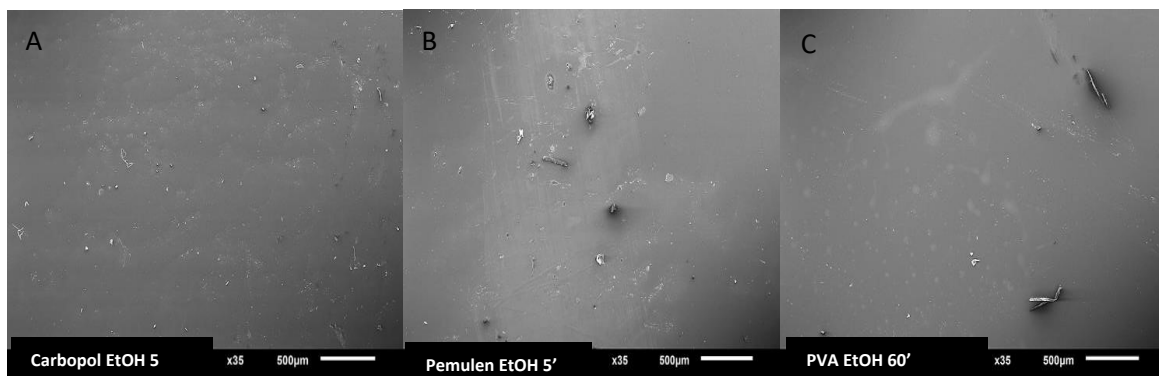
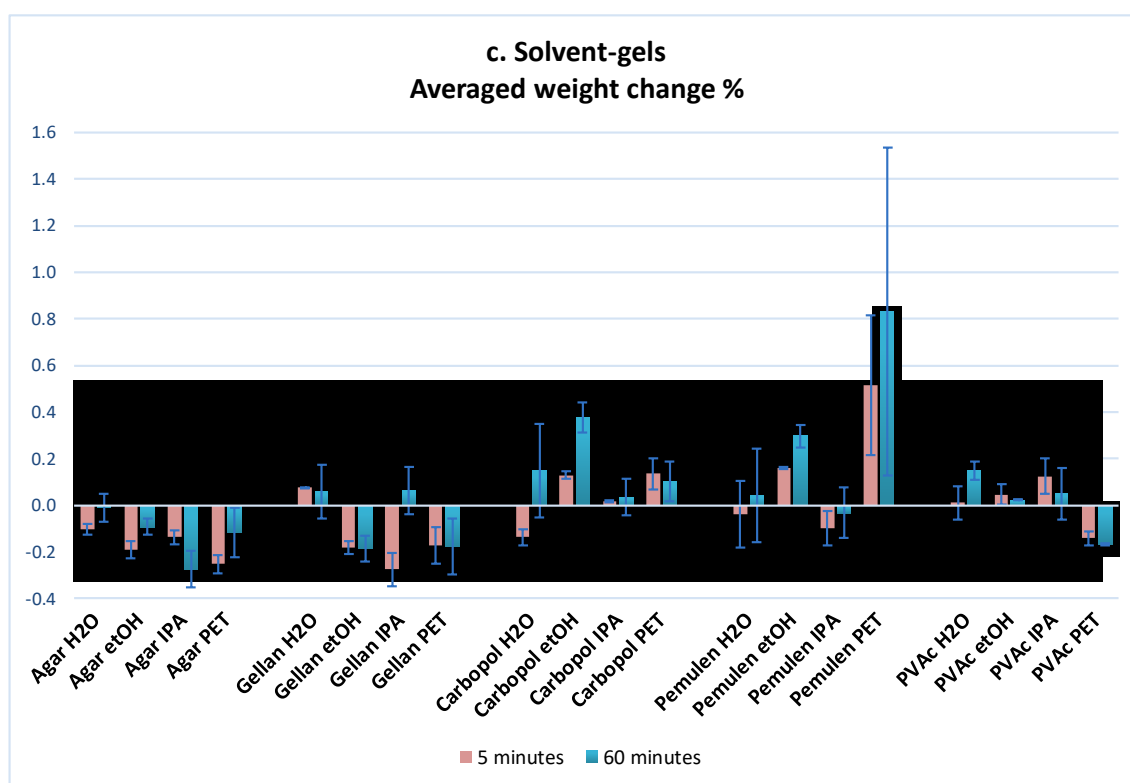


Figure 25. SEM micrographs. A-B: Carbopol and Pemulen with EtOH for 5 minutes caused loss of transparency and deposited gel residues on new PMMA. C: PVA EtOH for 60 minutes although caused limited areas of opaqueness and deposited negligible gel residues, left surfaces in an overall satisfactory visual condition.



Graph 25. Average weight change % of unaged PMMA samples (in duplicate) treated with solvent-gels for 5 and 60 minutes. Pink bars represent samples treated for 5 minutes and blue bars represent samples treated for 60 minutes. Changes % are normalised to the starting/initial weight. Error bars show the standard deviation.

Weight change

Solvent gels with the exception of Gellan hydrogel caused weight loss in a consistent manner. Carbopol with H<sub>2</sub>O and EtOH caused large, inconsistent weight changes, whereas with IPA and

PET it caused negligible and consistent gains. Pemulen solvent gels caused the most extreme weight changes, with Pemulen PET inducing the largest gain among solvent gels. PVA solvent gels caused the smallest weight changes. The within group deviations were low, showing the highest consistency in results along with the Agar solvent gels.

### Discussion

The three small-scale experiments carried out here helped to understand gaps in methodology and execution of this type of cleaning experiment. The results, even if somewhat inconsistent, led to the understanding that duplicates and triplicates were insufficient to draw definite conclusions and trends in relation to the cleaning methods and materials. This outcome was imperative to identify at an early stage of the research. More replicates would be essential to showcase the general trend of the treated samples' behaviour and identify outliers.

The presence of gel thickeners was shown to influence the action of solvents, in some cases by exhibiting a satisfactory performance and in others by increasing the surface damage and residue deposition. For example, the action of EtOH and IPA was more controlled in rigid Agar and Gellan gels than when applied with cotton swabs. By comparison, when the same solvents were added to Carbopol and Pemulen gels, cleaning was less efficient comparing to their application with cotton swabs. Some of these preliminary results showed a positive influence of gels on the effect of cleaning, indicating that the solvent gel systems were promising compared to other application methods. One observation was that generally no swelling was macroscopically visible in any of the treated samples. Changes in the optical and physical properties of the treated PMMA surfaces were further scrutinised in the following experiments.

Ideally there would be no weight changes after treatment, especially in the current experiment where there was no foreign surface matter/dirt. This would be an indication that the solvent gel action had no effect to the original material. Later experiments explored whether more than one process might occur concurrently, as bulk gravimetric analysis overlooks the possibility of simultaneous extraction and deposition of material. Results of py-GC/MS (discussed in Chapter 4) were used to support interpretation of the behaviour of PMMA additive components and their interaction with cleaning materials.

**Appendix N. Macroscopic observation of PMMA samples synthetic sebum soil treated with gels for 5 & 60 minutes.**

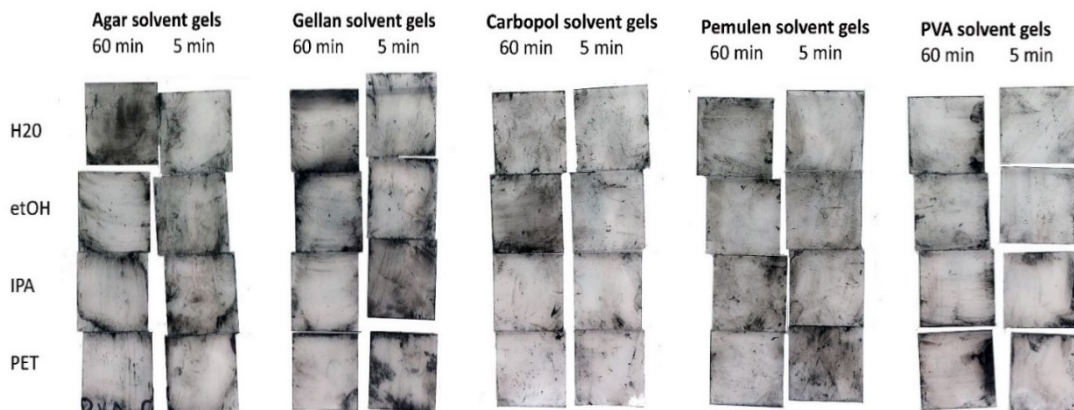
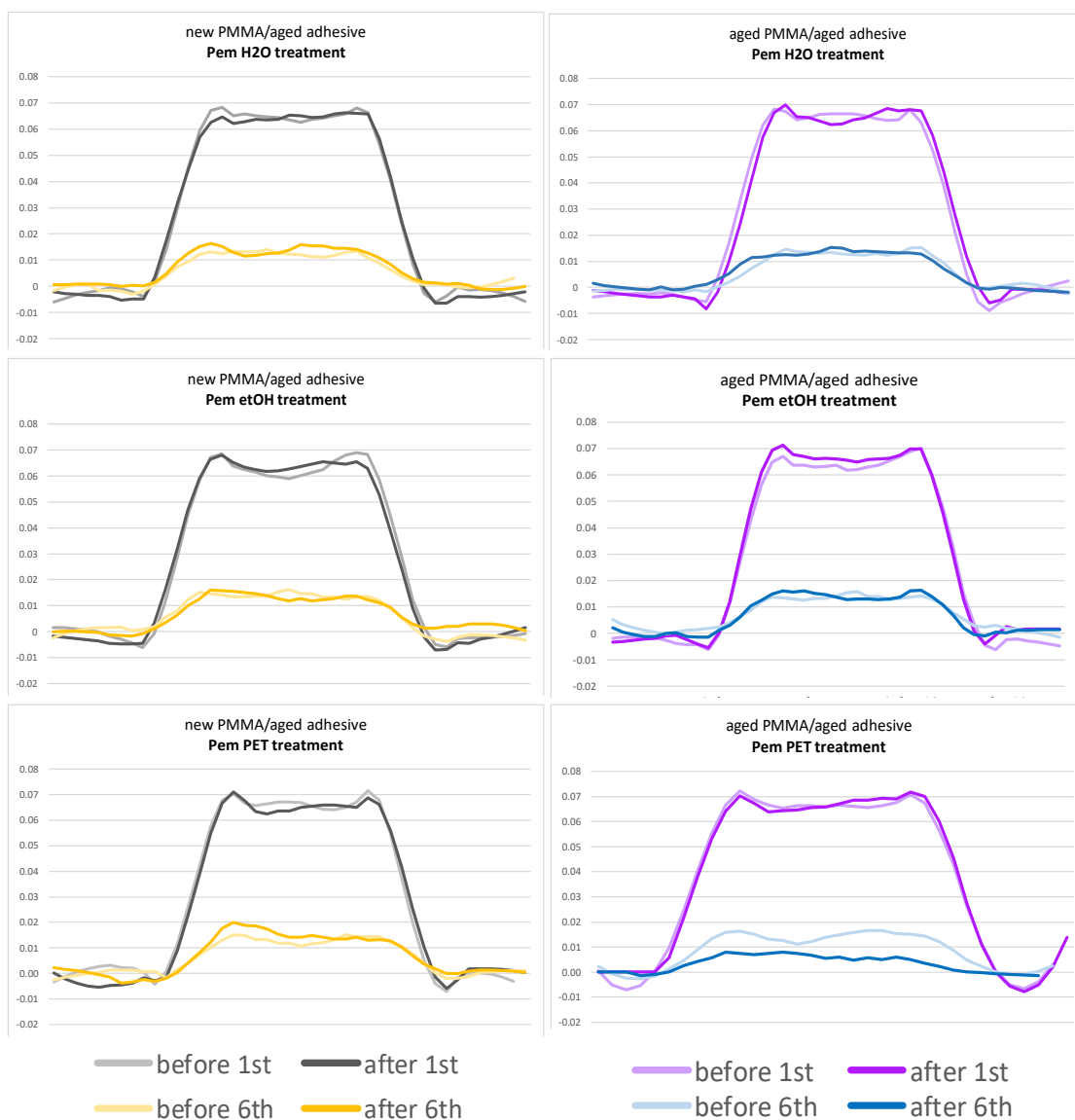


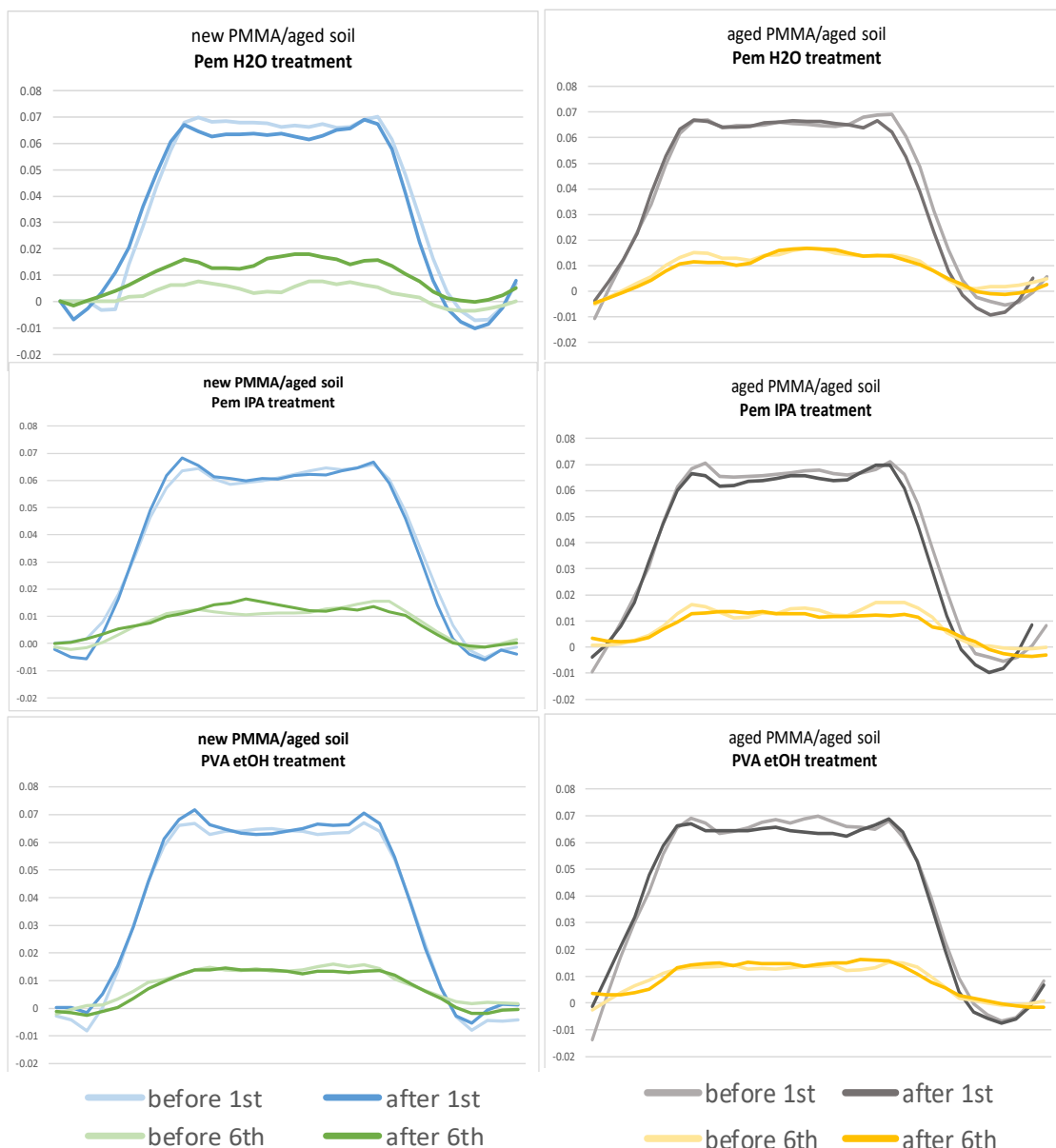
*Figure 26. New PMMA samples (n=40) with synthetic sebum soil after cleaning with gel-based treatments for 5 and 60 minutes. The aim of this preliminary cleaning trial was to test the impact of time on the cleaning outcome. The picture was not very representative due to black, soil residues left on the back side of the transparent, treated samples as a result of sample handling.*

**Appendix O. NMR results of 2<sup>nd</sup> replicates: line graphs of profile scans after gel treatment**



*Graph 26. Smoothed line graphs of NMR profile scans before and 24 h after gel treatment on new (left) and aged (right) PMMA samples with aged spray adhesive (2<sup>nd</sup> replicate). Treatments consisted of Pemulen H2O, Pemulen etOH and Pemulen PET. Profile scans of new samples are in black (1<sup>st</sup> echo) and yellow (6<sup>th</sup> echo) tones, while aged samples are in purple (1<sup>st</sup> echo) and blue (6<sup>th</sup> echo) tones.*





Graph 27. Smoothed line graphs of NMR profile scans before and 24 h after gel treatment on new (left) and aged (right) PMMA samples with aged synthetic sebum oil (2<sup>nd</sup> replicate). Treatments consisted of Pemulen H2O, Pemulen IPA and PVA etOH. Profile scans of new samples are in blue (1<sup>st</sup> echo) and green (6<sup>th</sup> echo) tones, while aged samples are in black (1<sup>st</sup> echo) and yellow (6<sup>th</sup> echo) tones.

## Appendix P. Msheireb Arts Centre, Doha

### Collection & historical context

The three acrylic three-dimensional objects under study were retrieved from the Msheireb Arts Centre (MAC) located in the Msheireb district, today's oldest part of the capital of Qatar, Doha. The objects belong to a collection that is attributed to an artist initiative called 'Sadaa Al Thikrayat', which translates to Echo Memory (Ghummakkad 2013). The collection consists of objects that were salvaged/found in the downtown district that was established in the mid-1940's in the vicinity of a well, giving it its name 'place of sweet water'. The Msheireb area was at the time inhabited by a migrant community of labour workers (ca. 20,000, in their majority

from South Asia), merchants and pearl divers who lived and worked in Qatar (Ghummakkad 2013). In 2010 these people were evicted, and the area was demolished in order to be re-developed/regenerated into a major construction project known as Msheireb Downtown Project (Barbour 2012).

The Echo Memory Collection aimed to document the life and local architecture of the people who previously inhabited Msheireb. The items left behind, countless personal possessions and indications of individual contributions to the development of the country constitute the collection of today's MAC (Ben Barbour, personal communication 2015). These objects, roughly estimated to be between 3,000-4,000 (Exell 2016), include anything from personal effects to commercial artefacts and remains of the wrecked buildings, and were collected by members of the project including artists, construction workers and other employees working on the site. The collected objects, including the neon shop sign and the lamp shades, are reminiscence of these people, who comprise ca. 60 % of the Qatari population today.



*Figure 27. View of other objects in the collection in the MAC storage rooms. Disposable plastic spoons (a) and cups (b) placed in damaged cardboard boxes on shelves.*



*Figure 28. Plastic lamp shades of different shapes and sizes along with the lamp shades under examination here, placed on shelves unprotected and in direct sunlight.*



*Figure 29. View of plastic illuminated shop signs in the collection in the MAC storage rooms, placed directly on the floor and in direct sunlight (a, b). The shop sign under examination in its original location, before relocation to UCL Q lab.*

The collection is partially stored in MAC and partially exhibited at the Msheireb Museums. Since the opening of the Museums in 2016, MAC has been functioning as a storage for the Echo Memory collection objects that were not chosen for display in the Museums. In the storage, a wide range of materials made of paper, plastic, metal, wood, ceramic, glass and textile can be found. Plastics comprise 20 % of the collection in these storerooms. The MAC is located in an only-girls school that was abandoned in 2005 (Ghummakkad 2013; Exell 2016). The building is old and has not been refurbished, with its classrooms serving as the storages. The storerooms are not purpose-built and their condition is inadequate for housing objects.

Organic and inorganic materials are placed in storerooms with many unsealed windows, no sun protection and often broken, allowing flow of particulate matter and insects. MAC is situated in the most polluted area in Doha with construction sites as well as heavy use

of motor vehicles and traffic, resulting in high levels of pollutants. Doha is surrounded by desert which is responsible for sand particulates and by sea, which means that humidity is present in high levels. It has a hot desert weather with very high temperature levels, all year round. The door is often kept open and even when closed, there is wide gap between it and the floor, which allows dirt and leaves from the garden outside into the room. The materials are placed everywhere in the room, into disorder, on the floor and on metal shelving units placed on the floor without any further support. Fig.29-31 depict the situation of the MAC.

#### **Appendix Q. Characterisation of objects with ATR-FTIR analysis**

There was a lot of signal interference from the surface matter (dust, dirt) on the lamp shades, which resulted in detection of inorganic matter (dust) and rendered absorption of the substrate material very poor. To allow for analysis, spots to be analysed were previously lightly dusted. Analysis was performed with 32 scans at ambient temperature and pressure with a zinc selenide (ZnSe)/diamond Universal ATR Sampling Accessory (Perkin Elmer FT-IR/NIR Frontier) between 4000 and 600  $\text{cm}^{-1}$  (mid-IR region), with a resolution of 4  $\text{cm}^{-1}$  and a maximum penetration depth of the IR beam into the specimen at 3-4  $\mu\text{m}$ .

A detailed list of all absorbed peaks and their band assignments is found in Table 4. The spectra (Fig.27-28) obtained from all three objects were very characteristic of PMMA. The most characteristic absorption bands were peaks 1723  $\text{cm}^{-1}$ , 1270/1240  $\text{cm}^{-1}$  and 1190/1144  $\text{cm}^{-1}$ . The strongest absorption bands in the spectrum appeared in the stretching region between 3000-2800  $\text{cm}^{-1}$  due to  $\text{CH}_2/\text{CH}_3$  vibrations; 1800-1600  $\text{cm}^{-1}$  due to carbonyl absorption; 1300-1000  $\text{cm}^{-1}$  assigned to C–C–O stretching and in the bending range 1500-1400  $\text{cm}^{-1}$  due to C–H bonds.

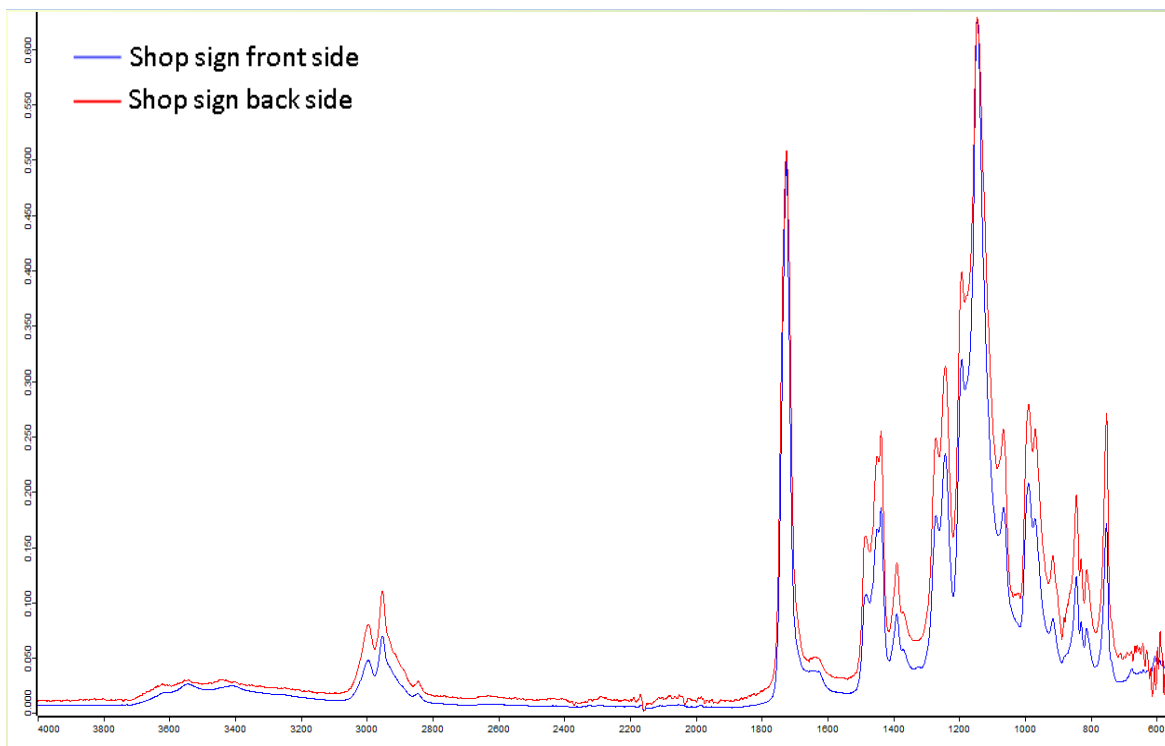


Figure 30. ATR-FTIR spectra of front (blue) and back side (red) of PMMA shop sign.

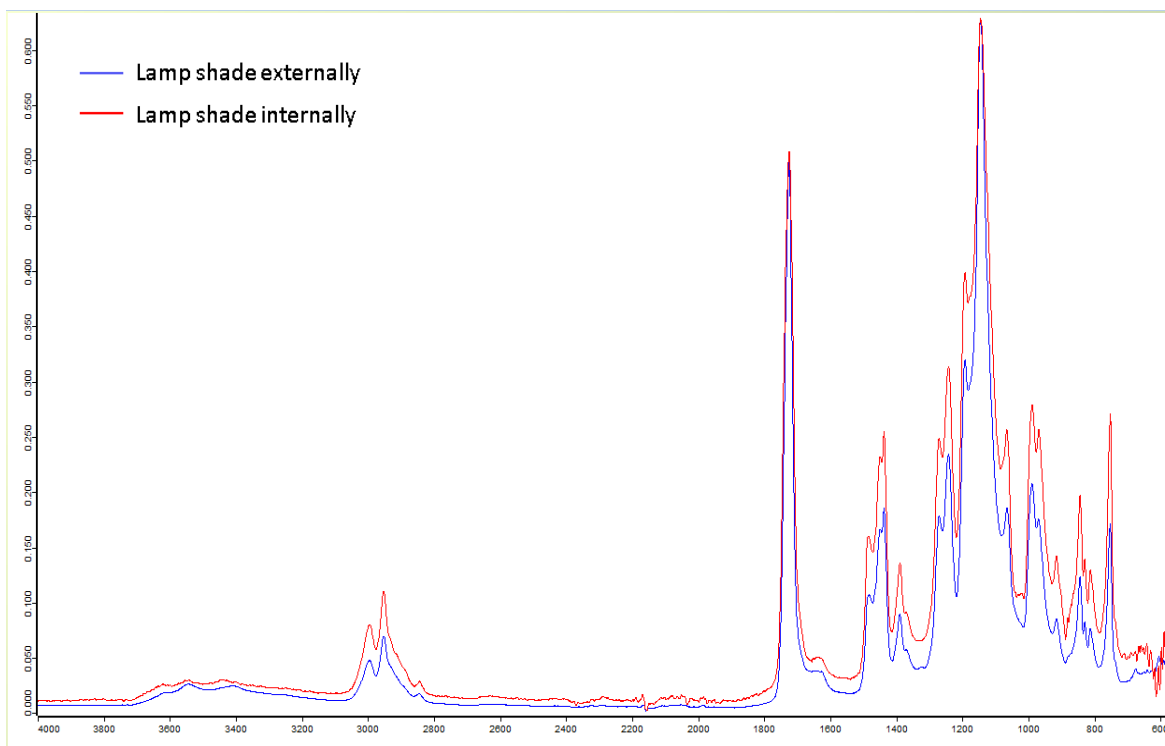


Figure 31. FTIR ATR spectra of external (blue) and internal side (red) of both PMMA lamp shades.

IR absorptions and assignments of neon shop sign and lamp shades	
Wavenumber (cm <sup>-1</sup> )	Band assignment
2995, 2950	Symmetric and asymmetric C–H
2920, 2850	stretch
1723	C–H stretch
1640	C=O stretch
1483, 1435	C=C stretch
1447, 1387	C–H scissoring
1270, 1240	C–H stretch
1190, 1144	C–C–O stretch
1063	C–O–C stretch
986, 965	C–C skeletal stretch
912, 826, 810	C–CH <sub>3</sub> bend
840, 749	C–H rock
	C–H torsion

*Table 4. Assignments of diagnostic IR absorptions of the neon shop sign and the two lamp shades analysed with ATR FTIR.*

## Appendix R. Treatment reports of Msheireb Art Centre case studies

### Neon shop sign C550

#### Documentation

Conservation Lab Number: C550

Brief Description: Plastic neon sign

Owner/Collection Name: Msheireb Art Centre (MAC)

Object Type: Illuminated shop sign

Material Type: PMMA, neon lamp

Dimensions: 970 x 550 mm (max length x max width), thickness: 6 mm

### Materials and technology

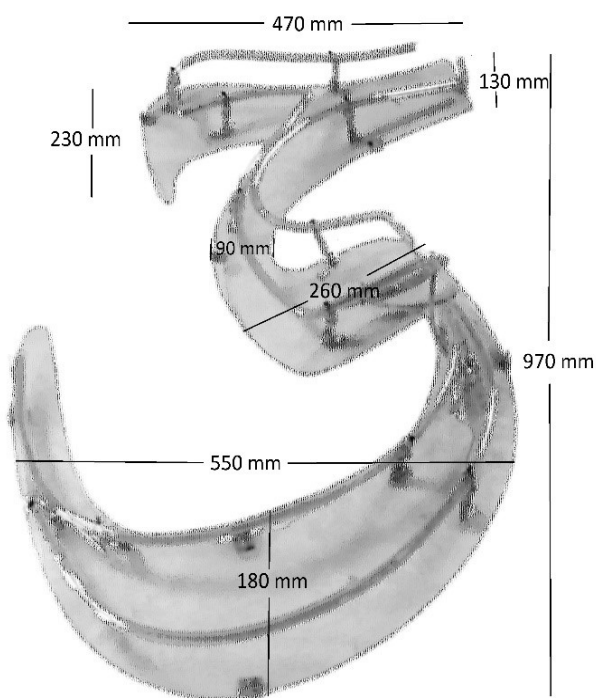


Figure 32. Measurements of the shop sign C550.

The object consisted of a transparent, 6 mm thick PMMA sheet of roughly a meter by half, and glass tubes with an outer diameter of 12 mm. There were two sets of glass tubes mounted on glass clips/supports via wires (Fig.33 b), which were in turn held in place by metallic holders screwed on the acrylic sheet. The façade bearing the glass tubes was postulated to be the front side that reads the Arabic word *حي* (*hayy or hiyy*) consisting of the letters *ح* and *ي* (from right to left) translating into 'neighbourhood'. The sign was shaped according to Arabic calligraphy. More

metallic supports (Fig.34) were found on the sides of the acrylic sheet, also screwed on the sign. These were possibly used to mount/hang the sign on a wall/high location.

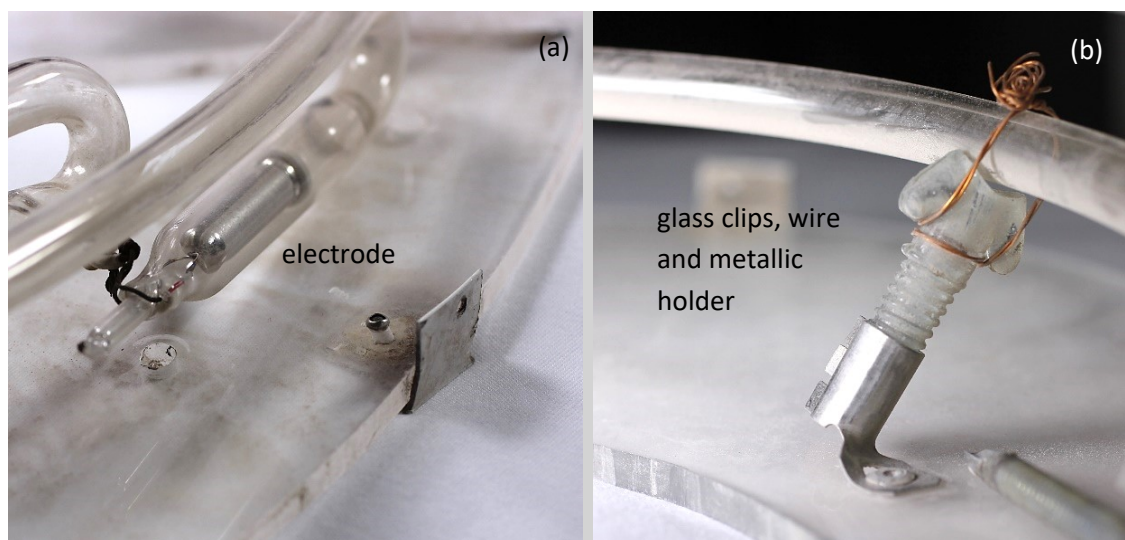
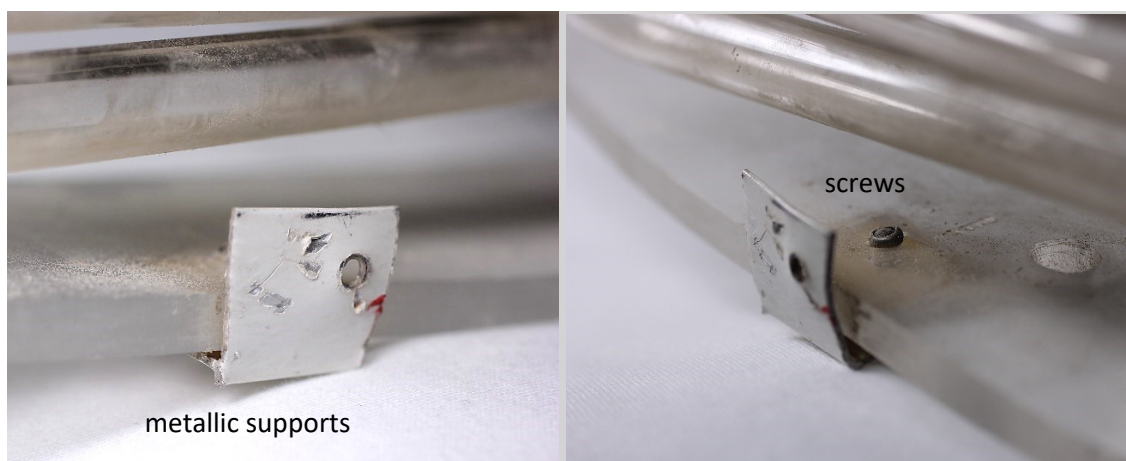


Figure 33. The glass casing contains one of the electrodes found at each end of the glass tube (a). The glass clips/supports holding the glass tube via wiring, which are in turn held in place by metallic holders screwed on the acrylic sheet (b) of the shop sign C550.

The glass tubes were the remains of neon lights, which were now broken in several places, thus not functional. Neon lights are a type of cold cathode gas-discharge light sealed in glass tubes filled with the gas at a low pressure, in partial vacuum. The glass casing contains electrodes at each end of the tube (Fig.33 a) and electrical current used to make the electrodes glow a characteristic orange/red light. The glass tubes require heating up to 650 °C to bend in the desired shapes and form letters (a technique similar to glass blowing). Neon lighting was developed in 1910 and has since been commonly employed for multicoloured glowing signage around the world.



*Figure 34. Metallic supports screwed on the sides of the acrylic sheet, possibly used to mount the sign C550 on a wall.*

The sign حى was cast or extruded into a flat sheet, possibly synthesised by bulk polymerisation. If cast, PMMA was mixed in a form or mould, between two glass plates, while if extruded, it was continuously pushed through a horizontal form. In both processes a radical initiator is added to the pure liquid monomer MMA and the reaction is initiated via energy input (i.e. heat or irradiation). This falls under the chain-growth polymerisation, which means that synthesis is a radical reaction that consists of 3 steps, initiation, propagation and termination, and the growth of the polymer occurs only at the end of the chain(s). The edges of the sign visually appeared unpolished/matte and frosted with indentations (unevenly cut) (Fig.35), suggesting mechanical cutting by direct contact of tool to sheet and means of raw machining.

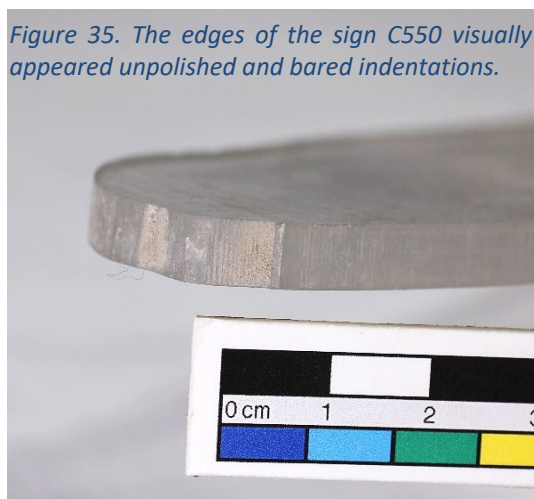


*Figure 35. The edges of the sign C550 visually appeared unpolished and bared indentations.*



### Condition assessment

The acrylic sheet of the sign was structurally complete, whereas the neon glass tubes appeared broken in three areas with some parts missing (Fig.36 c). The object was heavily soiled (Fig.36 a-b). Both the sheet and the glass tubes were clear/transparent, allowing the foreign matter covering their surfaces to visually appear darkened and yellowed. Screws holding the glass tubes and the metallic supports (mounts) on the sheet caused cracking of the sign (Fig.36 d) due to mechanical pressure. Some cracks were smaller than others, while some ran through large surface areas. Due to increased surface soiling it was hard to confirm the presence of scratches, material loss and other surface defects.

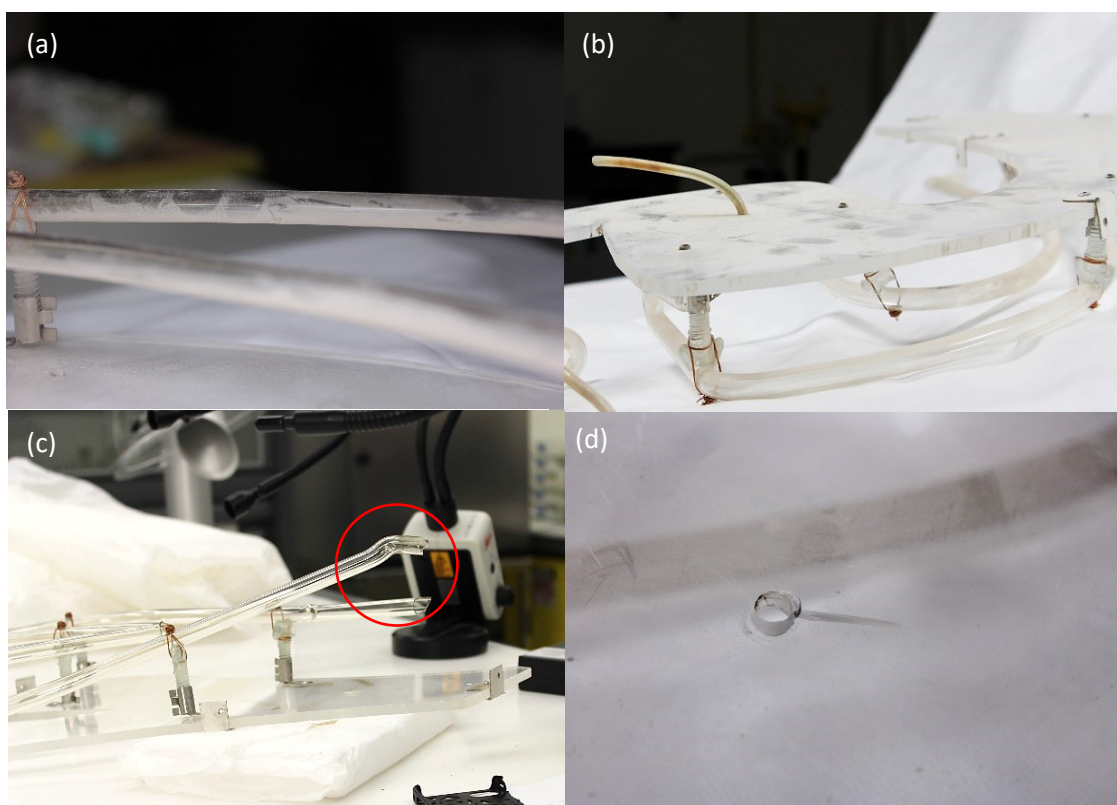


*Figure 36. Heavy soiling visible on the surface of the glass tubes and the sign C550 (a-b). Broken glass tube with missing part (c). Cracking of the acrylic sign due to mechanical pressure of (missing) screws (d).*

### Treatment

The two sides of the sign were treated differently to allow for direct comparisons and assess the physical properties of the gels as well as their impact on cleaning. One side was treated with 1 % Pemulen:5 % triethanolamine with deionised water, prepared according to Stavroudis (2012), and the other side with 80 % PVA/borax (5%:1%) with ethanol/deionised water (20/80 wt.%), prepared according to Angelova *et al.* (2016). All treatments lasted 3 minutes and were

repeated 3 times, followed by clearance with multiple cotton swabs moistened with deionised water, linearly rolled towards one direction.

### Lamp shade C553

#### Documentation

Conservation Lab Number: C553

Brief Description: Plastic lamp/light shade

Owner/Collection Name: Msheireb Art Centre (MAC)

Object Type: Lighting

Material Type: PMMA

Dimensions: 200 x 200 x 100 mm, thickness: 4 mm

#### Materials and technology

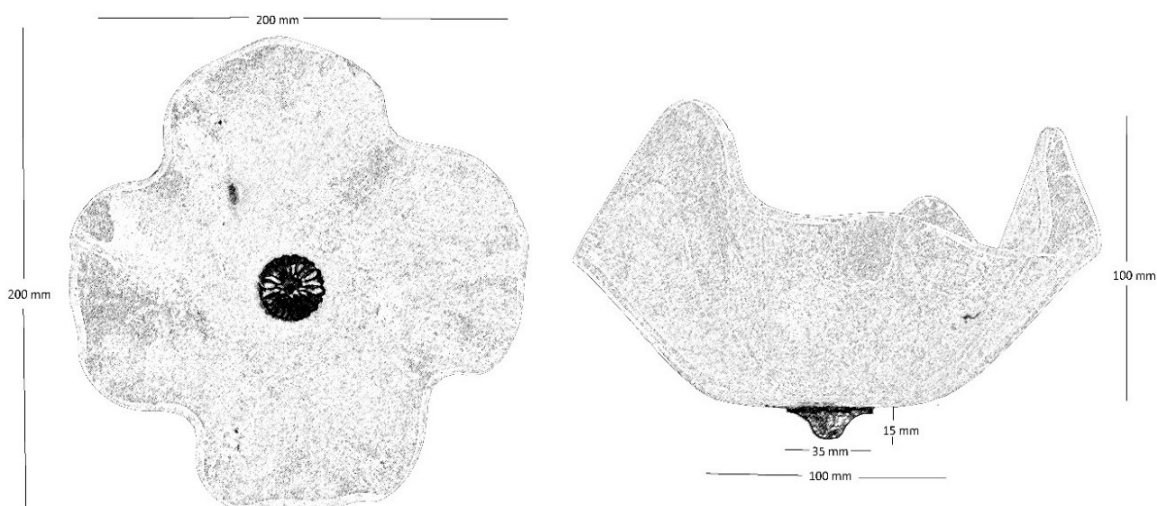


*Figure 37. Drawing of lamp shade C553 showing its measurements.*

The object consisted of a transparent, 4 mm thick PMMA of 200 x 200 mm (Fig.37), shaped like a flower with many folds. In its centre, a metallic element was visible from both sides of the lamp. In the internal surface this element bared decoration resembling flowery patterns, while on the external side it was broken indicating a missing part. It was postulated that the internal surface was facing upwards with the broken metallic element functioning as its base, possibly standing on a rod/stand from which it had now been detached. This lamp shade appeared to be decorative, as it had no fitting for light bulbs or any electrical wiring. It may have been part of a larger lighting complex, a hypothesis which was enhanced by the fact that there were two identical shades (C553 and C554). The shade was made via casting in a mould as a liquid resin

through bulk polymerisation. The edges of the hardened object were smoothly finished (Fig.38 a) and did not show any signs of machining, supporting the theory of a moulded object.

#### Condition assessment

The light shade was structurally complete. The metallic element displayed a shattered edge on the bottom of the shade (externally), indicating that there was a rod-like stand, possibly a metallic structure, supporting the shade. The object was heavily soiled, especially internally, rendering it darkened. Three transparent self-adhesive (duck) tapes were visible on the external surface (Fig.38 b); They had been vertically adhered and did not seem to offer any static support as they were not holding/bonding any parts. Neither the tapes, nor their adhesive, had yellowed. Some cracking was visible on the curvy part of the shade, just about where the folds started. These cracks had a cyclical pattern, seen also in the other shade (C554), and were the result of mechanical pressure due to the shape and weight of the folds. Due to increased surface soiling it was hard to confirm the presence of scratches, material loss and other surface defects.

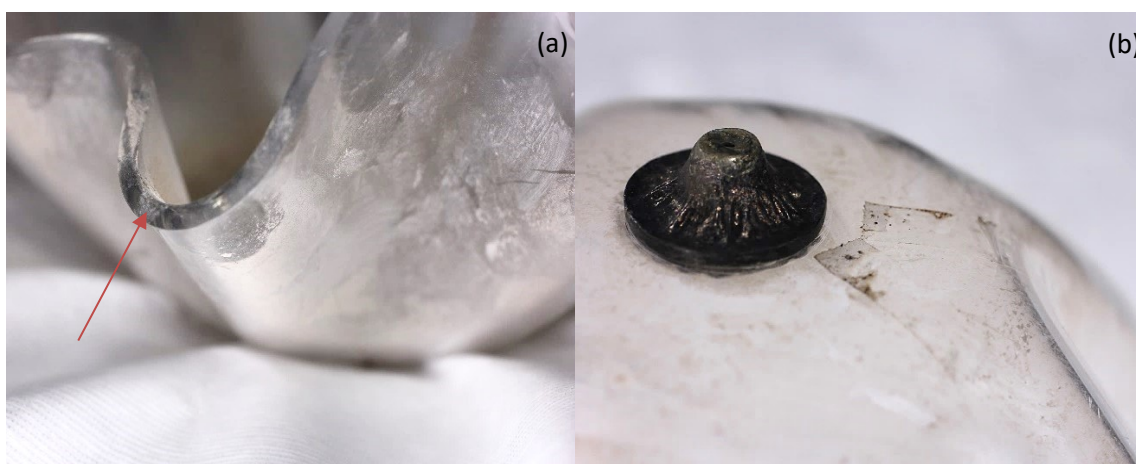


*Figure 38. Smoothly finished edges of object C553 supporting it was moulded (a). Heavy soiling visible on the surface of the lamp shade, as well as three transparent, adhesive tapes (b).*

#### Treatment

Cleaning of the light shade was carried out with 1 % Pemulen:5 % triethanolamine with deionised water. The metallic element was treated with PVA ethanol and removal of each of the three tapes were removed with different Pemulen solvent gels. The Pemulen hydrogel was applied with a soft Teflon spatula in large areas (blocks). Similar to the shop sign, removal of Pemulen was carried out with soft wiping and moistened cotton swabs. The removed gels, after the first two applications were too dirty to be reused, with visible dark, soil particles. This meant that the gels were successful at removing all the (loose) soil. As previously seen,

clearance of the treated surface with swab rolling visibly picked up dirt along with the Pemulen residue. The majority of the dirt was successfully removed after two applications. After the third application, the hydrogel removed after treatment completion was clear, without visible soil.



*Figure 39. Treatment of metallic element of lamp shade C553 with PVA ethanol. PVA gel removed after 1<sup>st</sup> application with imprint of the metallic element. Dirt remains entrapped in crevices after treatment.*

The metallic element was cleaned with 80 % PVA/borax (5%:1%) with ethanol/deionised water (20/80 wt.%) (Fig.39). PVA was chosen for this due to its advantageous properties of being highly viscous and elastic, forming one large molecule that does not leave residues and the ability to conform to multi-dimensional and complex surfaces. The runny consistency of Pemulen would be problematic to clear. After the first application the gel successfully lifted a lot of black dirt, visible on the removed PVA due to its transparent nature. After the third application, the crevices of the metallic element still showed dirt remains, which were removed with the mechanical action of a bamboo skewer.

**Lamp shade C554**Documentation

Conservation Lab Number: C554

Brief Description: Plastic lamp/light shade

Owner/Collection Name: Msheireb Art Centre (MAC)

Object Type: Lighting

Material Type: PMMA

Dimensions: 200 x 200 x 100 mm, thickness: 4 mm

Materials and technology

The object is identical to lamp shade C553. For information about dimensions and technology refer to 'Materials and technology' of light shade C553.

Condition assessment

The light shade was structurally complete. Similar to shade C553, the metallic element displayed a shattered edge on the bottom of the shade (externally). The object was heavily soiled. The internal side bared visibly more dirt and dust deposits (Fig.40). Some cracks with a cyclical pattern, seen also in shade C553, were visible on the curvy part of the shade. Due to increased surface soiling it was hard to confirm the presence of scratches, material loss and other surface defects.



*Figure 40. Heavy soiling visible on the surface of lamp shade C554.*

Treatment

Cleaning was carried out with 1 % Pemulen:5 % TEA with isopropanol/deionised water (20/80 wt.%) (Fig.11.29 a-b). After two applications, the removed gels were too dirty to be reused (Fig.11.30 a), indicating that the gel was successful at removing all (loose) soil. Clearance with swab rolling was remarkable, as seen in all previously treated objects with Pemulen. The majority of the dirt was successfully removed after two applications (Fig.11.29 c). The same

result was seen on lamp shade C553 treated with Pemulen hydrogel. After the third application, Pemulen was clear, without visible soil. The metallic element was cleaned with 80 % PVA/borax (5%:1%) with ethanol/deionised water (20/80 wt.%), following the same treatment steps used for the metallic element of shade C553.



*Figure 41. Images of the author during treatment of the case studies in the UCL Qatar Conservation laboratories.*

## BIBLIOGRAPHY

---

- Abar, F., Abadyan M. and Aghazade J., 2015. Effects of surface quality and loading history on fatigue life of laser-machined poly(methyl methacrylate). *Materials and Design* 65/: 473–481.
- Aboueiezz, M. and Waters P. F., 1978. *Studies on the Photodegradation of Poly(Methyl Methacrylate)*. Washington, DC: U.S. DEPARTMENT OF COMMERCE National Technical Information Service.
- Adam, C., Lacoste J. and Lemaire J., 1989. Photo-oxidation of elastomeric materials. Part I. Photo-oxidation of polybutadienes. *Polymer Degradation and Stability* 24:185–200, 29: 305–20/Part IV.
- Affolter, S., 2015. *Long-Term Behaviour of Thermoplastic Materials*. Interstate University NTB. Available at: <http://institute.ntb.ch/mnt/kompetenzen/polymericstnb> (accessed 5 December 2015).
- Aguilar-Sánchez, B. and Buentello-Martínez R., 2017. Agarose gels with methyl ethyl ketone for cleaning a 19th-century document. In: Angelova L, Ormsby BA, Townsend JH and Wolbers R (eds) *Gels in the conservation of art*. London, England: Archetype Publications.
- Aguilar-Vega, M., 2013. Structure and Mechanical Properties of Polymers. In: Saldívar-Guerra E and Vivaldo-Lima E (eds) *Handbook Of Polymer Synthesis, Characterization, And Processing*. Hoboken, New Jersey: John Wiley & Sons, Inc, 425–434.
- AIC-BPG, 1992. 14 Surface Cleaning, Adhesives. *Book and Paper Group AIC: Paper Conservation Catalogue*. Washington DC: American Institute for the Conservation of Historic and Artistic Works (AIC).
- Akhurst, S., 2008. Design and Sustainability. In: Keneghan B and Egan L (eds) *Plastics: looking at the future and learning from the past: papers from the conference held at the Victoria and Albert Museum, London: 23-25 May 2007*. London, United Kingdom: Archetype Publications Ltd, 160-162.
- Albus, S., Bonten C., Kessler K., Rossi G. and Wessel T., 2008. *Plastic Art - A Precarious Success Story*. Germany: The AXA Art Conservation Project.
- Alves, N. M., Gómez Ribelles J. L., Gómez Tejedor J. A. and Mano J. F., 2004. Viscoelastic Behavior of Poly(methyl methacrylate) Networks with Different Cross-Linking Degrees. *Macromolecules* 37/: 3735-3744.
- Andersson, Ö., 2012. Statistics for Experiments. *Experiment!: Planning, Implementing and Interpreting*. John Wiley & Sons, 139-173.
- Andrady, A. L. and Neal M. A., 2009. Applications and Societal Benefits of Plastics. *Philosophical Transactions: Biological Sciences* 364/1526: 1977-1984.

- Andrews, E. H. and Bevan L., 1972. Mechanics and mechanism of environmental crazing in a polymeric glass. *Polymer* 13/7: 337-346.
- Angelova, L., Berrie B. H., deGhetaldi K., Kerr A. and Weiss R. G., 2015. Partially hydrolyzed poly(vinyl acetate)-borax based gel-like materials for conservation of art: Characterization and applications. *Studies in Conservation* 60/4.
- Angelova, L., Carretti E., Berrie B. H. and Weiss R. G., 2017a. Poly(vinyl alcohol)-borax 'gels': a flexible cleaning option. In: Angelova L, Ormsby BA, Townsend JH and Wolbers R (eds) *Gels in the conservation of art*. London, England: Archetype Publications, 231-236.
- Angelova, L., Ormsby B. A. and Richardson E., 2016a. Diffusion of water from a range of conservation treatment gels into paint films studied by unilateral NMR. Part I: Acrylic emulsion paint. *Microchemical Journal* 124/: 311–320.
- Angelova, L., Sofer G. and Ormsby B. A., 2016b. *A conservation challenge, an Op art sculpture, and a mystery artist*. Available at: <https://www.tate.org.uk/about-us/projects/nanorestart/conservation-challenge-op-art-sculpture-and-mystery-artist> (accessed 13 December 2018).
- Angelova, L., Sofer G. and Ormsby B. A., 2017b. *The Results Are In. The treatment of Op Structure by Michael Dillon*. Available at: <https://www.tate.org.uk/about-us/projects/nanorestart/results-are> (accessed 13 December 2018).
- Angelova, L. V., 2013. Gels From Borate-Crosslinked Partially Hydrolyzed Poly(Vinyl Acetate)s: Characterization Of Physical And Chemical Properties And Applications In Art Conservation. Ph.D. thesis. Faculty of the Graduate School of Arts and Sciences - Chemistry. Washington, DC: Georgetown University.
- Angelova, L. V., Terech P., Natali I., Dei L., Carretti E. and Weiss R. G., 2011. Cosolvent gel-like materials from partially hydrolyzed poly(vinyl acetate)s and borax. *Langmuir* 27/.
- Anzani, M., Berzioli M., Cagna M., Campani E., Casoli A., Cremonesi P., Fratelli M., Rabbolini A. and Riggiardi D., 2008. Gel rigidi di Agar per il trattamento di pulitura di manufatti in gesso/Use of Rigid Agar Gels for Cleaning Plaster Object. *Quaderni del Cesmar* 7, 6/II.
- Archer, N. E., Charles Y., Elliott J. A. and Jickells S., 2005. Changes in the lipid composition of latent fingerprint residue with time after deposition on a surface. *Forensic Science International* 154/2: 224-239.
- Armisen, R. and Galatas F., Production and utilization of products from commercial seaweeds. Chapter 1 - Production, Properties And Uses Of Agar. In: Department FaA (ed). Spain: FAO Corporate Document Repository.
- Arnold, J. C., 1998. The effects of diffusion on environmental stress crack initiation in PMMA. *Journal of Materials Science* 33/: 5193 – 5204.



- Arnoult, C., Di Martino J. and Ruch D., 2012. Prediction and limitation of polymer degradation in Environmental SEM. *Ultramicroscopy* 122/: 32-36.
- Asensio, R. C., SanAndrésMoya M., delaRoja J. M. and Gómez M., 2009. Analytical characterization of polymers used in conservation and restoration by ATR-FTIR spectroscopy. *Analytical and Bioanalytical Chemistry* 395/: 2081–2096.
- Ashby, M. F. and Jones D. R. H., 2012. *Engineering Materials 1 (Fourth Edition) An Introduction to Properties, Applications and Design*. Oxford: Butterworth-Heinemann.
- Askeland, D. R. and Fulay P. P., 2010. *Essentials of Materials Science and Engineering*. Stanford, USA: Cengage Learning.
- Astbury, J., 2018. Mies van der Rohe: the modernist architect who led the Bauhaus to its end. *Dezeen Magazine*. Available at: <https://www.dezeen.com/2018/11/19/mies-van-der-rohe-modernist-architect-third-director-bauhaus-100/> (accessed 3 March 2020).
- ASTME1640-07, Standard Test Method for Glass Transition Temperature (DMA Tg) of Polymer Matrix Composites by Dynamic Mechanical Analysis (DMA).
- Awada, H. and Daneault C., 2015. Chemical Modification of Poly(Vinyl Alcohol) in Water. *Applied Sciences* 5/: 840-850.
- Ayre, W. N., Denyer S. P. and Evans S. L., 2014. Ageing and moisture uptake in polymethyl methacrylate (PMMA) bone cements. *Journal of the Mechanical Behaviour of Biomedical Materials* 32/: 76-88.
- Bacci, M., 2000. UV-VIS-NIR, FT-IR and FORS Spectroscopies. In: Ciliberto E and Spoto G (eds) *Modern analytical methods in art and archaeology* New York; Chichester: Wiley, 321-362.
- Baglioni, M., Chelazzi D., Giorgi R. and Poggi G., 2013. Colloid and Materials Science for the Conservation of Cultural Heritage: Cleaning, Consolidation, and Deacidification. *Langmuir* 29/: 5110–5122.
- Baglioni, P., Dei P., Carretti E. and Giorgi R., 2009. Gels for the Conservation of Cultural Heritage. *Langmuir* 25/15: 8373–8374.
- Baij, L., Keune K., Hermans J., Noble P. and Iedema P., 2017. Time-dependent ATR-FTIR studies on the release of solvents from cleaning gels into model systems of oil paint binding media In: Angelova L, Ormsby BA, Townsend JH and Wolbers R (eds) *Gels in the conservation of art*. London, England: Archetype Publications, 316-321.
- Balcar, N., Barabant G., Bollard C., Kuperholc S., Laganà A., Van Oosten T., Segel K. and Shashoua Y., 2012. Studies in active conservation of plastic artefacts in museums- Studies in cleaning plastics. In: Lavédrine B, Fournier A and Martin G (eds) *Preservation of Plastic Artefacts in Museum Collections*. Comité des travaux historiques et scientifiques - CTHS, 225-269.

- Ballenger, V., Kaltenecker-Commerçon J., Verdu J. and Tordjeman P., 1997. Interactions of solvents with poly(methyl methacrylate). *Polymer* 38/16: 4175-4184.
- Barbour, B., 2012. Salvaging Memory: The Msheireb Arts Centre (MAC) and the Echo Memory Project. Unpublished essay.
- Barker, M., 1999. Part Two: Defining Plastics. In: Quye A and Williamson C (eds) *Plastics: Collecting And Conserving* Edinburgh: NMS Publishing Limited, 23-33.
- Barkovic, M., Diamond O. and Cross M., 2017. The use of agar gel for treating water stains on an acrylic canvas. In: Angelova L, Ormsby BA, Townsend JH and Wolbers R (eds) *Gels in the conservation of art*. London, England: Archetype Publications, 51-56.
- Barros García, J. M., 2015. Re-evaluating the roles of the cleaning process in the conservation of paintings. *Ge-Conservacion* 7/: 14-23.
- Barrie, J. A. and Platt B., 1963. The diffusion and clustering of water vapour in polymers. *Polymer* 4/: 303-313.
- Barrueso-Martinez, M. a. L., Ferrandiz-Gomez T. D. P., Romero-Sanchez M. a. D. and Martin-Martinez J. M., 2003. Characterization of eva-based adhesives containing different amounts of rosin ester or polyterpene tackifier. *The Journal of Adhesion* 79/8-9: 805-824.
- Basavarajappa, S., Al-Kheraif A. A. A., ElSharawy M. and Vallittu P. K., 2016. Effect of solvent/disinfectant ethanol on the micro-surface structure and properties of multiphase denture base polymers. *Journal of the Mechanical Behavior of Biomedical Materials* 54/Supplement C: 1-7.
- Bechthold, T., 2005. Wet look in 1960s furniture design: degradation of polyurethane-coated textile carrier substrates. In: Rogerson C and Garside P (eds) *The Future of the 20th Century: Collecting, Interpreting and Conserving Modern Materials*. London: Archetype 128-132.
- Bechthold, T., 2009. Stiletto. Double-sided problems with a self-adhering, flexible PVC-film. In: Bechthold T (ed) *Future Talks 009: The Conservation of Modern Materials in Applied Arts and Design*. Munich, 103-108.
- Belfiore, L. A., 2010. *Physical Properties of Macromolecules*. Hoboken, NJ, USA: John Wiley & Sons, Inc.
- Bellucci, R., Cremonesi P. and Pignagnoli G., 1999. A Preliminary Note on the Use of Enzymes in Conservation: The Removal of Aged Acrylic Resin Coatings with Lipase. *Studies in Conservation* 44/4: 278-281.
- Belmares, M., Blanco M., Goddard W. A., Ross R. B., Caldwell G., Chou S.-H., Pham J., Olofson P. M. and Thomas C., 2004. Hildebrand and Hansen Solubility Parameters from

- Molecular Dynamics with Applications to Electronic Nose Polymer Sensors. *Journal of Computational Chemistry* 25/15: 1814-1826.
- Belokon, Z. S., Skorobogatova A. Y., Gribkova N. Y., Arzhakov S. A., Bakeyev N. F., Kozlov P. V. and Kabanov V. A., 1976. Mechanical properties of crosslinked polymethacrylate glass. *Polymer Science U.S.S.R.* 18/12: 3171-3180.
- Ben Halima, N., 2016. Poly(vinyl alcohol): review of its promising applications and insights into biodegradation. *RSC Advances* 6/46: 39823-39832.
- Bensaid, M. O., Ghalouci L., Hiadsi S., Lakhdari F., Benharrats N. and Vergoten G., 2014. Molecular mechanics investigation of some acrylic polymers using SPASIBA force field. *Vibrational Spectroscopy* 74/: 20–32.
- Bensaude-Vincent, B., 2013. Plastics, materials and dreams of dematerialization. In: Gabrys J, Hawkins G and Michael M (eds) *Accumulation: The Material Politics of Plastic*. Routledge, 17-29.
- Bertasa, M., Chiantore O., Poli T., Riedo C., diTullio V., Canevali C., Sansonetti A. and Scalarone D., 2017. A study of commercial agar gels as cleaning materials. In: Angelova L, Ormsby BA, Townsend JH and Wolbers R (eds) *Gels in the conservation of art*. London, England: Archetype Publications, 11-18.
- Bettencourt, A., Calado A., Amaral J., Vale F. M., Rico J. M. T., Monteiro J., Montemor M. F., Ferreira M. G. S. and Castro M., 2002. The effect of ethanol on acrylic bone cement. *International Journal of Pharmaceutics* 241/1: 97-102.
- Bibire, L.-E. and Carja G., 2013. Chapter 5. Composites Based on Polymers – Layered Double Hydroxides Anionic Clays. In: Bercea M (ed) *Polymer Materials with Smart Properties*. New York: Nova Science Publishers, 117-136.
- Biroš, J., Larina T., Trekoval J. and Pouchlý J., 1982. Dependence of the glass transition temperature of poly (methyl methacrylates) on their tacticity. *Colloid and Polymer Science* 260/1: 27-30.
- Blank, S., 1990. An Introduction to Plastics and Rubbers in Collections. *Studies in Conservation* 35/2: 53-63.
- Blüher, A., Haller U., Banik G. and Thobois E., 1995. The Application of Carbopol™ Poultrices on Paper Objects. *Restaurator* 16/: 234-247.
- Blümich, B., Casanova F., Perlo J., Presciutti F., Anselmi C. and Doherty B., 2010. Noninvasive Testing of Art and Cultural Heritage by Mobile NMR. *Accounts of chemical research* 43/: 761-770.
- Bobalek, E. G., Henderson J. N., Serafini T. T. and Shelton J. R., 1959. Chemical Degradation and Mechanical Testing of Polyethylenes. *Journal of Applied Polymer Science* 11/5: 210-215.

- Bodurov, I., Vlaeva I., Yovcheva T., Dragostinova V. and Sainov S., 2013. Surface properties of PMMA films with different molecular weights. *Bulgarian Chemical Communications, Special Issue B 45/*: 77-80.
- Bogdanova, L. M., Irzfiak V. I. and Rozenberg B. A., 1986. Contribution Of A Diffusional Mechanism To The Relaxation Of Free Volume In Amorphous Polymers. *Polymer Science U.S.S.R.* 28/7: 1690-1697.
- Bollard, C., Kuperholc S. and Barabant G., 2011. Effects of cleaning gel systems on plastics. A preliminary study on plasticized poly(vinyl chloride). In: Bechthold T (ed) *Future Talks 011 Technology and Conservation of Modern Materials in Design*. Munich, 119-126.
- Bonaldo, M., 2015. Investigations in the Use of a Rigid Hydrogel Gellan Gum in the Making of Cleaning Systems for Sensitive Acrylic Paint Surfaces. Queen's University.
- Boone, H. N. and Boone D. A., 2012. Analyzing Likert Data. *Journal of Extension* 50/2.
- Bortolotti, V., Camaiti M., Casieri C., De Luca F., Fantazzini P. and Terenzi C., 2006. Water absorption kinetics in different wettability conditions studied at pore and sample scales in porous media by NMR with portable single-sided and laboratory imaging devices. *Journal Of Magnetic Resonance* 181/2: 287-295.
- Botti, L., Corazza A., Iannuccelli S., Placido M., Residori L., Ruggiero D., Sotgiu S., Tireni L., Berzioli M., Casoli A., Isca C. and Cremonesi P., 2011. Evaluation of cleaning and chemical stabilization of paper treated with a rigid hydrogel of gellan gum by means of chemical and physical analyses. In *ICOM-CC 16th Triennial Conference: preprints. Lisbon 19–23 September 2011*, ed. J. Bridgland. Almada: Critério Produção Gráfica, Lda.
- Bourhis, E. L., 2014. *Glass: Mechanics and Technology*. Weinheim, Germany: Wiley-VCH Verlag GmbH & Co. KGaA.
- Bowden, P. B. and Jukes A., 1972. The Plastic Flow of Isotropic Polymers. *Journal of Materials Science* 7/: 52-63.
- Bower, D. I., 2002. *An Introduction to Polymer Physics*. Cambridge, UK: Cambridge University Press.
- Brancaleon, L., Bamberg M. P. and Kollias N., 2000. Spectral Differences between Stratum Corneum and Sebaceous Molecular Components in the Mid-IR. *Applied Spectroscopy* 54/8: 1175-1182.
- Brancaleon, L., Bamberg M. P., Sakamaki T. and Kollias N., 2001. Attenuated Total Reflection–Fourier Transform Infrared Spectroscopy as a Possible Method to Investigate Biophysical Parameters of Stratum Corneum In Vivo. *Journal of Investigative Dermatology* 116/3: 380-386.
- Braun, D., 2009. Origins and Development of Initiation of Free Radical Polymerization Processes. Review article. *International Journal of Polymer Science*.

- Broughton, W. R., Dean G., Maxwell A. S. and Sims G. D., 2005. Review of accelerated ageing methods and lifetime prediction techniques for polymeric materials. Middlesex, UK: National Physical Laboratory.
- Brown, J. E. and Kashiwagi T., 1996. Gas phase oxygen effect on chain scission and monomer content in bulk poly(methyl methacrylate) degraded by external thermal radiation. *Polymer Degradation and Stability* 52/: 1-10.
- Bryant, W. M. D., 1947. Polythene fine structure. *Journal Of Polymer Science* 2/6: 547-564.
- Brydson, J. A., 1999. *Plastics Materials (Seventh Edition)*. Oxford: Butterworth-Heinemann.
- BS2782-3: Methods 320A to 320F: 1976, Methods of testing plastics. Mechanical properties. Tensile strength, elongation and elastic modulus.
- BS2782-9 Method 941: 1990, Methods of testing plastics. Sampling and test specimen preparation. Determination of maximum reversion of amorphous thermoplastics moulding materials.
- Budai-Szűcs, M., 2008. Formulation and Investigation of Gel-Emulsions Containing Polymeric Emulsifiers. Ph.D. Thesis. Department of Pharmaceutical Technology. University of Szeged.
- Burchill, P. J. and Stacewicz R. H., 1982. Effect of water on the crazing of a crosslinked poly(methylmethacrylate). *Journal of Materials Science Letters* 1/10: 448-450.
- Burke, J., 2008. Solubility Parameters: Theory and Application. *Conservation Online (CoOl)*. Available at: <http://cool.conservation-us.org/byauth/burke/solpar/solpar2.html> (accessed 15 May 2016).
- Burnstock, A. and Kieslich T., 1996. A study of the clearance of solvent gels used for varnish removal from paintings. In *Icom Committee for Conservation: 11th Triennial Meeting, Edinburgh, 1-6 September 1996*, ed. J. Bridgland. London: James and James.
- Bützer, J., 2002. Pratone- The Restoration of a Nineteenseventies Polyurethane Flexible Foam Designer Seat. In: Van Oosten T, Shashoua Y and Waentig F (eds) *Plastics in Art: History, Technology, Preservation*. Munich, Germany: Siegl's Fachbuchhandlung.
- Buys, S. and Oakley V., 1993. *Conservation and Restoration of Ceramics*. Oxford: Butterworth-Heinemann.
- Cadd, S., Islam M., Manson P. and Bleay S., 2015. Fingerprint composition and aging: A literature review. *Science & Justice* 55/4: 219-238.
- Callister, W. D. and Rethwisch D. G., 2014. *Materials Science and Engineering*. USA: John Wiley & Sons.
- Caminati, G., 2013. Cultural Heritage Artefacts and Conservation: Surfaces and Interfaces. In: Baglioni P and Chelazzi D (eds) *Nanoscience for the Conservation of Works of Art*. Cambridge, UK: The Royal Society of Chemistry, 1-48.

- Cao, M., Liu X., Luan J. and Zhang X., 2014. Characterization of physicochemical properties of carboxymethyl agar. *Carbohydrate Polymers* 111/Supplement C: 449-455.
- Caple, C., 2000. *Conservation Skills: Judgement, Method and Decision Making*. London and New York: Routledge.
- Caple, C., 2011. The aims of conservation. In: Richmond A and Bracker A (eds) *Conservation: Principles, Dilemmas and Uncomfortable Truths*. London: Routledge and the V&A Museum, 25-31.
- Carifio, J. and Perla R. J., 2007. Ten Common Misunderstandings, Misconceptions, Persistent Myths and Urban Legends about Likert Scales and Likert Response Formats and their Antidotes. *Journal of Social Sciences* 3/3: 106-116.
- Carretti, E., Bonini M., Dei L., Berrie B. H., Angelova L. V., Baglioni P. and Weiss R. G., 2010a. New Frontiers in Materials Science for Art Conservation: Responsive Gels and Beyond. *Accounts of chemical research* 43/6: 751-760.
- Carretti, e., Dei I., Macherelli A. and Weiss R. G., 2004. Rheoreversible Polymeric Organogels: The Art of Science for Art Conservation. *Langmuir* 20/20: 8414-8418.
- Carretti, E., Dei L., Weiss R. G. and Baglioni P., 2008. A new class of gels for the conservation of painted surfaces. *Journal of Cultural Heritage* 9/4: 386-393.
- Carretti, E., Natali I., Matarrese C., Bracco P., Weiss R. G., Baglioni P., Salvini A. and Dei L., 2010b. A new family of high viscosity polymeric dispersions for cleaning easel paintings. *Journal of Cultural Heritage* 11/4: 373-380.
- Carretti, E., Salvadori B., Baglioni P. and Dei L., 2005. Microemulsions and Micellar Solutions for Cleaning Wall Painting Surfaces. *Studies in Conservation* 50/2: 128-136.
- Casoli, A., Cremonesi P., Isca C., Groppetti R., Pini S. and Senin N., 2013. Evaluation of the effect of cleaning on the morphological properties of ancient paper surface. *Cellulose* 29/: 2027-2043.
- Casoli, A., Di Diego Z. and Isca C., 2014. Cleaning painted surfaces: evaluation of leaching phenomenon induced by solvents applied for the removal of gel residues. *Environmental Science and Pollution Research* 21/: 13252-13263.
- Çaykara, T. and Güven O., 1999. UV degradation of poly(methyl methacrylate) and its vinyltriethoxysilane containing copolymers. *Polymer Degradation and Stability* 65/2: 225-229.
- Cecchini, C. and Hansen A., 2014. *Polymeric materials in art and design: an Italian interdisciplinary experience*.
- Chalal, S., Haddadine N., Bouslah N., Souilah S., Benaboura A., Barille R. and Haroun A., 2014. Preparation Characterization and Thermal Behaviour of Carbopol-TiO<sub>2</sub> Nanocomposites. *Open Journal of Organic Polymer Materials* 4/: 55-64.

- Charola, E. and Koestler R. J., 2006. Methods in Conservation. In: May E and Jones M (eds) *Conservation Science: Heritage Materials*. Cambridge: RSCPublishing.
- Chartoff, R. P., Menczel J. D. and Dillman S. H., 2008. Dynamic Mechanical Analysis (DMA). In: Menczel JD and Prime RB (eds) *Thermal Analysis of Polymers*. John Wiley & Sons, Inc., 387-495.
- Chiantore, O. and Rava A., 2012. *Conserving Contemporary Art: Issues, Methods, Materials, and Research*. Los Angeles: The Getty Conservation Institute.
- Chiantore, O., Trossarelli L. and Lazzari M., 2000. Photooxidative degradation of acrylic and methacrylic polymers. *Polymer* 41/: 1657–1668.
- Chinn, S. C., Herberg J. L., Gjersing E. L., Cook A., Sawvel A. M., Maxwell R. S., Wheeler H. and Wilson M., 2006. Magnetic Resonance Based Diagnostics for Polymer Production and Surveillance. *Conference for Aging and Stockpile Stewardship*. Los Alamos, NM, United States.
- Choi, J. O., Moore J. A., Corelli J. C., Silverman J. P. and Bakhru H., 1988. Degradation of poly(methylmethacrylate) by deep ultraviolet, x-ray, electron beam, and proton beam irradiations. *Journal of Vacuum Science & Technology B* 6/6: 2286-2289.
- Choudhury, I. A. and Shirley S., 2010. Laser cutting of polymeric materials: An experimental investigation. *Optics & Laser Technology* 42/3: 503-508.
- Chuanfu, C., Changyu R. and Fu X., 1994. Stereoregularity of poly (methyl methacrylate) obtained with chiral anionic complex initiator. *Chinese Journal of Polymer Science* 13/1: 91-96.
- Chuang, Y.-F., Wu H.-C., Yang F., Yang T.-Y. and S L., 2016. Cracking and healing in poly(methyl methacrylate): effect of solvent. *Journal of Polymer Research* 24/2.
- Chung, H., Kim T., Park G. and Chung I., 2015. Synthesis of Thermally Stable Waterborne Acrylic Pressure Sensitive Adhesives (PSAs) for Application to LCD Devices. *Molecular Crystals and Liquid Crystals* 617/1: 82-91.
- Coates, J., 2000. Interpretation of Infrared Spectra, A Practical Approach. *Encyclopedia of Analytical Chemistry*: 10815–10837.
- Coghlan, A., 1996. Tragedy in toytown - Teddy's gone gooey, Barbie's broken out in green blotches and there's snow all over your favourite videos. What's going on, asks a traumatised Andy Coghlan. *New Scientist*.
- Comiotto, A. and Egger M., 2009. Naum Gabo's sculpture 'Construction in Space: Crystal' (1937): Evaluating a suitable bonding strategy for stress loaded poly(methyl methacrylate). In: Bechthold T (ed) *Future Talks 009: The Conservation of Modern Materials in Applied Arts and Design*. Munich, 61-69.

- Considine, B., Leonard M., Podany J., de Tagle A., Khandekar N. and Levin J., 2000. Finding a Certain Balance: A Discussion about Surface Cleaning. *Conservation Perspectives, The GCI Newsletter* 15/3.
- Cooper, D. A., 2012. Effects of Chemical and Mechanical Weathering Processes on the Degradation of Plastic Debris on Marine Beaches. Ph.D thesis. Geology. Ontario, Canada: The University of Western Ontario.
- Cooper, W. J., Krasicky P. D. and Rodriguez F., 1986. Dissolution Rates of Poly(Methyl Methacrylate) Films in Mixed Solvents. *Journal of Applied Polymer Science* 31/: 65-73.
- Cowie, J. M. G., 1991. *Polymers: Chemistry and Physics of Modern Materials*. CRC Press.
- Cowie, J. M. G., Mohsin M. A. and McEwen I. J., 1987. Alcohol-water cosolvent systems for poly(methyl methacrylate). *Polymer* 28/9: 1569-1572.
- Cremonesi, P., 2010. Rigid Gels and Enzyme Cleaning. In: Mecklenburg MF, Charola AE and Koestler RJ (eds) *New Insights into the Cleaning of Paintings Proceedings from the Cleaning 2010 International Conference*. Universidad Politécnic de Valencia and Museum Conservation Institute: Smithsonian Institution Scholarly Press, 179-184.
- Cremonesi, P., 2015. Surface cleaning? Yes, freshly grated Agar gel, please. *Studies in Conservation*: 1-6.
- Cremonesi, P. and Casoli A., 2017. Thermo-reversible rigid agar hydrogels: their properties and action in cleaning. In: Angelova L, Ormsby BA, Townsend JH and Wolbers R (eds) *Gels in the conservation of art*. London, England: Archetype Publications, 19-28.
- Creswell, J. W., 2014. *Research Design: qualitative, quantitative, and mixed methods approaches*. London, UK: Sage Publications.
- Crichton, J. S., 1988. Degradation of Polymeric Materials. *Modern Organic Materials: preprints of contributions to the modern organic materials meeting held at the University of Edinburgh 14 & 15 April 1988*. Edinburgh: Scottish Society for Conservation and Restoration, 11-19.
- Croxton, R. S., Baron M. G., Butler D., Kent T. and Sears V. G., 2010. Variation in amino acid and lipid composition of latent fingerprints. *Forensic Science International* 199/1: 93-102.
- Czech, Z., 2006. Solvent-based pressure-sensitive adhesives for removable products. *International Journal of Adhesion and Adhesives* 26/6: 414-418.
- Czech, Z., Kowalczyk A. and Swiderska J., 2011. Pressure-Sensitive Adhesives for Medical Applications. In: Akyar I (ed) *Wide Spectra of Quality Control*. 309-332.
- Czech, Z., Loclair H. and Wesolowska M., 2007. Photoreactivity Adjustment Of Acrylic Psa. *Reviews on Advanced Materials Science* 14/: 141-150.
- Czech, Z., Pelech R. and Zych K., 2009. *Thermal decomposition of acrylic pressure-sensitive adhesives*.



- De Rosa, C. and Auriemma F., 2014. *Crystals and crystallinity in polymers: diffraction analysis of ordered and disordered crystals*. Hoboken, New Jersey: Wiley.
- Debik, J., Kaltenbruner G. and Steiner K., 2013. The challenge of conserving a mechanically damaged poly(methyl methacrylate) (PMMA) object - adhering and filling. The conservation of a multiple by Arturo Schwartz and Marcel Duchamp, Part II. In: Bechthold T (ed) *Future Talks 013: Lectures and Workshops on Technology and Conservation of Modern Materials in Design*. Munich, 195-202.
- Deegan, R. D., Bakajin O., Dupont T., Huber G., Nagel S. R. and Witten T. A., 2000. Contact line deposits in an evaporating drop. *Physical review. E, Statistical physics, plasmas, fluids, and related interdisciplinary topics* 62/: 756-765.
- deGhetaldi, K., Baade B., Voras Z. and Wroczynski E., 2017. Resurrecting a giant: using solvent gels and aqueous systems to restore Villanova University's *Triumph of David*. In: Angelova L, Ormsby BA, Townsend JH and Wolbers R (eds) *Gels in the conservation of art*. London, England: Archetype Publications, 157-164.
- DeGroot, S., Laganà A., VanOosten T., VanKeulen H. and Palmeira M., 2011. The wear and tear of polyurethane elastomers. Investigation into properties, degradation and treatments. In: Bechthold T (ed) *Future Talks 011 Technology and Conservation of Modern Materials in Design*. Munich, 89-98.
- Dei, L., 2013. Conservation Treatments: Cleaning, Consolidation and Protection. In: Baglioni P and Chelazzi D (eds) *Nanoscience for the Conservation of Works of Art*. Cambridge, UK: The Royal Society of Chemistry, 77-92.
- Del Federico, E., Centeno S. A., Kehlet C., Currier P., Stockman D. and Jerschow A., 2010. Unilateral NMR applied to the conservation of works of art. *Anal Bioanal Chem* 396/: 213-220.
- Dellaportas, P., Papageorgiou E. and Panagiaris G., 2014. Museum factors affecting the ageing process of organic materials: review on experimental designs and the INVENVORG project as a pilot study. *Heritage Science* 2/1: 2.
- DeLoach, R., 2010. Analysis of Variance in the Modern Design of Experiments. *48th AIAA Aerospace Sciences Meeting Including the New Horizons Forum and Aerospace Exposition*. Orlando, Florida.
- Derrick, M., Stulik D. and Landry J. M., 1999. *Infrared Spectroscopy in Conservation Science*. Los Angeles: The Getty Conservation Institute.
- Diani, J., Gilormini P. and Arrieta J. S., 2015. Direct experimental evidence of time-temperature superposition at finite strain for an amorphous polymer network. *Polymer* 58/: 107-112.

- Dickens, B., Martin J. W. and Waksman D., 1984. Thermal and photolytic degradation of plates of poly(methyl methacrylate) containing monomer. *Polymer* 25/5: 706-715.
- Dickens, B., W M. J. and Waksman D., 1986. Analysis of Damage Profiles in Poly(methyl methacrylate) in Terms of Oxygen Diffusion and Consumption. *Polymer Degradation and Stability* 15/: 265-279.
- DiTullio, V., Gioventù E., Proietti N., Luvidi L., Mecchi A. M. and Capitani D., 2017. A study of water mobility in hydrogels suitable for biocleaning mural paintings: a unilateral NMR study. In: Angelova L, Ormsby BA, Townsend JH and Wolbers R (eds) *Gels in the conservation of art*. London, England: Archetype Publications, 327-330.
- Divoux, T., Mao B. and Snabre P., 2014. Syneresis and delayed detachment in agar plates. *Soft Matter* 11/8.
- Dixit, M., Gupta S., Mathur V., Rathore K. S., Sharma K. and Saxena N. S., 2009a. Study Of Glass Transition Temperature Of Pmma And Cds-Pmma Composite. *Chalcogenide Letters* 6/3: 131-136.
- Dixit, M., Mathur V., Gupta S., Baboo M., Sharma K. and Saxena N. S., 2009b. Investigation of miscibility and mechanical properties of PMMA/PVC blends. *Optoelectronics And Advanced Materials – Rapid Communications* 3/10: 1099 - 1105.
- Diz, E. L. and Spragg R., 2010. Investigating Phase Transitions with Variable Temperature ATR. Available at: [https://www.perkinelmer.com/lab-solutions/resources/docs/APP\\_PhaseExtractionATR.pdf](https://www.perkinelmer.com/lab-solutions/resources/docs/APP_PhaseExtractionATR.pdf) (accessed 26 November 2017).
- Doherty, B., Presciutti F., Sgamellotti A., Brunetti B. G. and Miliari C., 2014. Monitoring of optimized SERS active gel substrates for painting and paper substrates by unilateral NMR profilometry. *Journal of Raman Spectroscopy* 45/11-12: 1153-1159.
- Domagalski, N. R., Mack B. C. and Tabora J. E., 2015. Analysis of Design of Experiments with Dynamic Responses. *Organic Process Research & Development* 19/: 1667-1682.
- Domingues, J. A. L., Bonelli N., Giorgi R., Fratini E. and Baglioni M., 2013a. Innovative Method For The Cleaning Of Watersensitive Artifacts: Synthesis And Application Of Highly Retentive Chemical Hydrogels. *International Journal Of Conservation Science* 4/: 715-722.
- Domingues, J. A. L., Bonelli N., Giorgi R., Fratini E., Gorel F. and Baglioni P., 2013b. Innovative Hydrogels Based on Semi-Interpenetrating p(HEMA)/PVP Networks for the Cleaning of Water-Sensitive Cultural Heritage Artifacts. *Langmuir* 29/: 2746-2755.
- Donth, E. and Michler G. H., 1989. Discussion of craze formation and growth in amorphous polymers in terms of the multiplicity of glass transition at low temperatures. *Colloid and Polymer Science* 267/7: 557-567.

- Dorge, V., 2000. The Gels Cleaning Research Project. *Conservation Perspectives, The GCI Newsletter* 15/3.
- Duan, G., Zhang C., Li A., Yang X., Lu L. and Wang X., 2008. Preparation and Characterization of Mesoporous Zirconia Made by Using a Poly (methyl methacrylate) Template. *Nanoscale Research Letters* 3/: 118–122.
- Duboisset, F., 2011. American Modernism. A MAA Chair by George Nelson (1958). Technical Study, Consolidation and Protection of Natural Rubber. In: Bechthold T (ed) *Future Talks 011 Technology and Conservation of Modern Materials in Design*. Munich, 75-79.
- Duncan, J., 2007. Principles and Applications of Mechanical Thermal Analysis. In: Gabbott P (ed) *Principles and Applications of Thermal Analysis*. Blackwell Publishing, 120-163.
- Duncan, T. T., Berrie B. H. and Weiss R. G., 2017. A comparison between gel and swab cleaning: physical changes to delicate surfaces. In: Angelova L, Ormsby BA, Townsend JH and Wolbers R (eds) *Gels in the conservation of art*. London, England: Archetype Publications, 250-256.
- Duplat, V., Bartoletti A. and Ormsby B. A., 2018. *The Removal of Pressure Sensitive Tape from Works of Art on Paper. A Workshop by Antonio Mirabile*. Available at: <https://www.tate.org.uk/about-us/projects/nanorestart/pst-removal-workshop> (accessed 18 December 2018).
- Dybal, J. and Krimm S., 1990. Normal-mode analysis of infrared and Raman spectra of crystalline isotactic poly(methyl methacrylate). *Macromolecules* 23/5: 1301-1308.
- Dybal, J., Štokr J. and Schneider B., 1983. Vibrational spectra and structure of stereoregular poly(methyl methacrylates) and of the stereocomplex. *Polymer* 24/8: 971-980.
- Edmonds, W. A. and Kennedy T. D., 2017. *An Applied Guide to Research Designs. Quantitative, Qualitative, and Mixed Methods*. Thousand Oaks, California: Sage Publications.
- Ehrenstein, G. W., Riedel G. and Trawiel P., 2004. *Thermal Analysis of Plastics. Theory and Practice*. Munich: Carl Hanser Verlag.
- El-Hefian, E. A., Nasef M. M., Hamid A. and Yahaya A. H., 2012. Preparation and Characterization of Chitosan/Agar Blended Films: Part 1. Chemical Structure and Morphology. *E-Journal of Chemistry* 9/3: 1431-1439.
- Ennis, C. P. and Kaiser R. I., 2010. Mechanistical studies on the electron-induced degradation of polymethylmethacrylate and Kapton. *Physical Chemistry Chemical Physics* 12/: 14902–14915.
- Etherington, R., 2013. V&A acquires Katy Perry false eyelashes as part of new "rapid response collecting" strategy. *Dezeen Magazine*. Available at: <http://www.dezeen.com/2013/12/18/rapid-response-collecting-victoria-and-albert-museum-kieran-long/> (accessed Sunday 16 March 2015).

- Etienne, S. and David L., 2007. Long-term physical ageing of amorphous polymers. *Philosophical Magazine: Tenth International Workshop on Disordered Systems* 87/3-5: 417-424.
- Ettwein, F., Rohrer-Vanzo V., Langthaler G., Werner A., Stern T., Moser O., Leitner R. and Regenfelder K., 2017. Consumer's perception of high gloss furniture: instrumental gloss measurement versus visual gloss evaluation. *European Journal of Wood and Wood Products*.
- Eve, S. and Mohr J., 2009. Study of the surface modification of the PMMA by UV-radiation. *Procedia Engineering* 1/: 237–240.
- Eve, S. and Mohr J., 2010. Effects of UV-irradiation on the thermo-mechanical properties of optical grade poly(methyl methacrylate). *Applied Surface Science* 256/9: 2927–2933.
- Exell, K., 2016. *Modernity and the Museum in the Arabian Peninsula*. Taylor & Francis.
- Feldman, D., 2008. Polymer History. *Designed Monomers and Polymers* 11/1: 1-15.
- Feller, R. L., 1994a. *Accelerated Aging: Photochemical and Thermal Aspects*. USA: The J. Paul Getty Trust.
- Feller, R. L., 1994b. Aspects of Chemical Research in Conservation: The Deterioration Process. *Journal of the American Institute for Conservation* 33/2: 91-99.
- Fife, G., Stabik B., Kelley A., King J., Blümich B., Hoppenbrouwers R. and Meldrum T., 2014. Characterization of aging and solvent treatments of painted surfaces using single-sided NMR. *Magnetic resonance in chemistry* 53/1: 58-63.
- Finkelstein, N. H., 2008. *Plastics*. New York: Marshal Cavendish.
- Fisher, T., 2008. Plastics in Everyday Life: Polymorphous (In)authenticity. In: Keneghan B and Egan L (eds) *Plastics: looking at the future and learning from the past: papers from the conference held at the Victoria and Albert Museum, London: 23-25 May 2007*. London, United Kingdom: Archetype Publications Ltd, 145-152.
- Foreman, J., 1997. Dynamic Mechanical Analysis of Polymers. Reprinted from American Laboratory January 1997. TA Instruments.
- Foreman, P. B., Shah S. M., Chandran R. and Eaton P. S., 2003. Rubber-acrylic adhesive formulation. Available at: <https://patents.google.com/patent/US6642298B2/en>.
- Freile-Pelegrin, Y., Madera-Santana T., Robledo D., Veleza L., Quintana P. and Azamar J. A., 2007. Degradation of agar films in a humid tropical climate: Thermal, mechanical, morphological and structural changes. *Polymer Degradation and Stability* 92/.
- Freinkel, S., 2011. *Plastic : a toxic love story*. Boston: Houghton Mifflin Harcourt.
- Fricke, A. L., 2016. The conservation of polymeric materials in museum collections using advanced surface science and surface analysis techniques. Ph.D. Thesis. Department of Materials. Imperial College London.

- García Fernández-Villa, S., Moya M. and Blasco S., 2012. Industrial development of plastics and 20th-century art: new synergies.
- Gates, T. S. and Grayson M. A., 1999. On The Use Of Accelerated Aging Methods For Screening High Temperature Polymeric Composite Materials. *American Institute of Aeronautics and Astronautics 2/*: 925-935.
- Ghosh, A., 2010. Degradation of polymer/substrate interfaces – an attenuated total reflection Fourier transform infrared spectroscopy approach. Chemistry. Ohio State University.
- Ghumakkad, 2013. *Msheireb Arts Center: An Oasis in a Desert*. Available at: <https://ghummakkad.wordpress.com/2013/11/23/msheireb-arts-center-an-oasis-in-a-desert/> (accessed 8 March 2018).
- Gilbert, A. S., Pethrick R. A. and Phillips D. W., 1977. Acoustic relaxation and infrared spectroscopic measurements of the plasticization of poly(methyl methacrylate) by water. *Journal of Applied Polymer Science 21/2*: 319-330.
- Giorgi, R. and Carretti E., 2013. Cleaning III: Applications and Case Studies. In: Baglioni P and Chelazzi D (eds) *Nanoscience for the Conservation of Works of Art*. Cambridge, UK: The Royal Society of Chemistry, 225-251.
- Giorgi, R., Domingues J. A. L., Bonelli N. and Baglioni P., 2013. Semi-interpenetrating p(HEMA)/PVP hydrogels for the cleaning of water-sensitive painted artifacts: Assessment of release and retention properties. In: Rogerio-Candelera MA, Lazzari M and Cano E (eds) *Science and Technology for the Conservation of Cultural Heritage*. London: Taylor & Francis Group, 291-294.
- Girod, A., Xiao L., Reedy B., Roux C. and Weyermann C., 2015. Fingerprint initial composition and aging using Fourier transform infrared microscopy ( $\mu$ -FTIR). *Forensic Science International 254/*: 185-196.
- Goga, N. O., Demco D. E., Kolz J., Ferencz R., Haber A., Casanova F. and Blümich B., 2008. Surface UV aging of elastomers investigated with microscopic resolution by single-sided NMR. *Journal Of Magnetic Resonance 192/1*: 1-7.
- Golfomitsou, S. and Merkel J. F., 2004. Synergistic effects of corrosion inhibitors for copper and copper alloy archaeological artefacts. *Proceedings of Metal 2004*. Canberra: National Museum of Australia, 344-368.
- Gorassini, A., Adami G., Calvini P. and Giacomello A., 2016. ATR-FTIR characterization of old pressure sensitive adhesive tapes in historic papers. *Journal of Cultural Heritage 21/Supplement C*: 775-785.
- Gorel, F., 2010. Assessment of agar gel loaded with micro-emulsion for the cleaning of porous surfaces. *CeROArt*. Available at: <http://ceroart.revues.org/1827> (accessed 18 Jan 2014).

- Graner, S., 2009. Work in progress - Practical experience in the conservation of high-gloss polyester resin and flexible polyvinyl chloride based on exemplary cases. In: Bechthold T (ed) *Future Talks 009: The Conservation of Modern Materials in Applied Arts and Design*. Munich, 79-84.
- Grassie, N. and Melville H. W., 1947. C-Degradation. The mechanism of the thermal degradation of polymethyl methacrylate. *Discussions of the Faraday Society* 2/0: 378-383.
- Grattan, D., 1993. Degradation Rates for Some Historic Polymers and the Potential of Various Conservation Measures for Minimizing Oxidative Degradation. In: Grattan D and Institute CC (eds) *Saving the twentieth century: the conservation of modern materials: proceedings of a conference Symposium 91: Saving the Twentieth Century, Ottawa, Canada, 15 to 20 September, 1991*. Ottawa, Canada, 351-361.
- Grohens, Y., Castelein G., Carriere P., Spevacek J. and Schultz J., 2001. Multiscale Aggregation of PMMA Stereocomplexes at a Surface: An Atomic Force Microscopy Investigation. *Langmuir* 17/: 86-94.
- Grohens, Y., Prud'homme R. E. and Schultz J., 1998. Cooperativity in Backbone to Side-Chain Conformational Rearrangements in Stereoregular PMMA. *Macromolecules* 31/8: 2545-2548.
- Gschwind, M., 1950. Plastics in 1950. *Fortune* 56: 108-119.
- Guerrero-Santos, R., Saldívar-Guerra E. and Bonilla-Cruz J., 2013. Free Radical Polymerization. In: Saldívar-Guerra E and Vivaldo-Lima E (eds) *Handbook Of Polymer Synthesis, Characterization, And Processing*. Hoboken, New Jersey: John Wiley & Sons, Inc, 65-83.
- Gugumus, F., 1990. Photooxidation of polymers and its inhibition. In: Pospisil J and Klemchuk PP (eds) *Oxidation Inhibition in Organic Materials, Volume II*. Florida: CRC Press, 29-162.
- Gulrez, S. K. H., Al-Assaf S. and O'Phillips G., 2011. Hydrogels: Methods of Preparation, Characterisation and Applications In: Carpi A (ed) *Progress in Molecular and Environmental Bioengineering - From Analysis and Modeling to Technology Applications*. Rijeka, Croatia and Shanghai, China: InTech, 117-150.
- Gupta, A., Liang R., Tsay F. D. and Moacanin J., 1980. Characterization of a Dissociative Excited State in the Solid State: Photochemistry of Poly(methyl methacrylate). Photochemical Processes in Polymeric Systems. *Macromolecules* 13/: 1696-1700.
- Guthausen, A., Zimmer G., Blümmler P. and Blümich B., 1998. Analysis of Polymer Materials by Surface NMR via the MOUSE. *Journal Of Magnetic Resonance* 130/1: 1-7.

- Haider, K. S. and Van Oosten T., 2009. Plastic Bags - Research into Polyethylene Bags of the Series 'Bicycles' by Andreas Slominski. In: Bechthold T (ed) *Future Talks 009: The Conservation of Modern Materials in Applied Arts and Design*. Munich, 41-48.
- Haillant, O., Fromageot D. and Lemaire J., 2004. Experimental techniques in studies of photostability. In: Strlič M and Kolar J (eds) *Ageing and Stabilization of Paper*. Ljubljana, Slovenia: National and University Library.
- Harvey, C. J., LeBouf R. F. and Stefaniak A. B., 2010. Formulation and stability of a novel artificial human sweat under conditions of storage and use. *Toxicology in Vitro* 24/6: 1790-1796.
- Hawkes, R., 2013. 'Gel Media in Aqueous Cleaning Methods on Paper': a lecture by Professor Richard Wolbers, University of Delaware, presented at the Wellcome Institute, London, June 19th 2013. The Icon Book & Paper Gathering. (accessed 05 June 2016).
- Hayden, H. W., Moffatt W. G. and Wulff J., 1967. *The Structure and Properties of Materials Volume III: Mechanical Behavior*. New York: John Wiley and Sons.
- Hedley, G., 1994. Cleaning and meaning: The Ravished Image reviewed. In: Knell S (ed) *Care of Collections*. London: Routledge.
- Hennen, S., Mederos-Henry F., deBoulard C., Espinosa M. F. and Cremonesi P., 2017. The influence of organic and inorganic alkalis on the formulation and properties of Pemulen TR-2 gels. In: Angelova L, Ormsby BA, Townsend JH and Wolbers R (eds) *Gels in the conservation of art*. London, England: Archetype Publications, 165-171.
- Higuchi, Y., 2015. Observation of Environmental Stress Cracking in Polymethylmethacrylate by Using the Chemiluminescence Method. *Materials Sciences and Applications* 6/: 1084-1088.
- Hinton, P. R., 2004. *Statistics explained*. London and New York: Routledge.
- Hodin, J. I., 2009. Can Museums Collect New Media Art?: The Need For A Paradigm Shift In Museum Conservation. Master's Degree. Sotheby's Institute of Art – New York/University of Manchester.
- Holland, B. J. and Hay J. N., 2001. The kinetics and mechanisms of the thermal degradation of poly(methyl methacrylate) studied by thermal analysis-Fourier transform infrared spectroscopy. *Polymer* 42/11: 4825-4835.
- Holländer, A., 2009. Aging of plastics - What can we do about it? In: Bechthold T (ed) *FUTURE TALKS 009: The Conservation of Modern Materials in Applied Arts and Design*. Munich, 26-31.
- Hoogenboom, R., Becer C. R., Guerrero-Sanchez C., Hoepfner S. and Schubert U. S., 2010. Solubility and Thermoresponsiveness of PMMA in Alcohol-Water Solvent Mixtures. *Australian Journal of Chemistry* 63/8: 1173-1178.

- Hub, C., Harton S. E., Hunt M. A., Fink R. and Ade H., 2007. Influence of Sample Preparation and Processing on Observed Glass Transition Temperatures of Polymer Nanocomposites. *Journal of Polymer Science: Part B: Polymer Physics* 45/: 2270–2276.
- Huggett, R., Brooks S. C. and Sadler R., 1984. Stereochemistry of poly(methy methacrylate) acrylic resin denture base material. *Biomaterials* 5/: 118-119.
- Hutchinson, J. M., 1995. Physical aging of polymers. *Progress in Polymer Science* 20/4: 703-760.
- Iannuccelli, S. and Sotgiu S., 2010. Wet Treatments of Works of Art on Paper with Rigid Gellan Gels. In *ICOM-CC Graphic Documents Working Group – Interim Meeting: Choices in Conservation Practice Versus Research*. Copenhagen, 25-39.
- ICF Consulting, 2006. Technical Evaluation Report: Gellan Gum - Handling/Processing. Program UNO. Available at: <http://www.ams.usda.gov/AMSv1.0/getfile?docName=STELPRDC5057602> (accessed 19 Feb 2014).
- Ignell, S., Kleist U. and Rigdahl M., 2010. Evaluating contrast gloss of textured polymeric surfaces. *Polymer Engineering & Science* 50/11: 2114-2121.
- Ionita, D., Cristea M. and Banabic D., 2015. Viscoelastic behavior of PMMA in relation to deformation mode. *Journal of Thermal Analysis and Calorimetry* 120/3: 1775-1783.
- Islam, M. T., Rodríguez-Hornedo N., Ciotti S. and Ackermann C., 2004. Fourier transform infrared spectroscopy for the analysis of neutralizer-carbomer and surfactant-carbomer interactions in aqueous, hydroalcoholic, and anhydrous gel formulations. *The AAPS Journal* 6/4: 61-67.
- ISO 877-1:2010, Plastics - Methods of exposure to solar radiation - Part 1: General guidance.
- ISO 877-2:2009, Plastics -- Methods of exposure to solar radiation -- Part 2: Direct weathering and exposure behind window glass.
- ISO 4892-1:2016, Plastics - Methods of exposure to laboratory light sources - Part 1: General guidance.
- ISO 4892-2:2013, Plastics -- Methods of exposure to laboratory light sources -- Part 2: Xenon-arc lamps.
- ISO 4892:1981, Plastics -- Methods of exposure to laboratory light sources.
- ISO 20753:2014, Plastics. Test specimens.
- Jakubowicz, I., 2001. Material Behaviour. Effects of artificial and natural ageing on impact-modified poly(vinyl chloride) (PVC). *Polymer testing* 20/: 545–551.
- Jamieson, S., 2004. Likert scales: how to (ab)use them. *Medical Education* 38/: 1212–1218.
- Javidi, A., Rieger U. and Eichlseder W., 2008. The effect of machining on the surface integrity and fatigue life. *International Journal of Fatigue* 30/: 2050–2055.



- Jiang, M., Zhu J., Chen C., Lu Y., Ge Y. and Zhang X., 2016. Poly(vinyl Alcohol) Borate Gel Polymer Electrolytes Prepared by Electrodeposition and Their Application in Electrochemical Supercapacitors. *ACS Applied Materials and Interfaces* 8/: 3473–3481.
- Johnston, A. and Rogers K., 2017. The Effect of Moderate Temperatures on Latent Fingerprint Chemistry. *Applied Spectroscopy* 71/9: 2102-2110.
- Jones, A., Clemmet M., Highton A. and Golding E., 1999. *Access to Chemistry*. Cambridge, UK: The Royal Society of Chemistry (RSC).
- Jones, S. and Holden J., 2008. *It's a material world: caring for the public realm*. London: Demos.
- Jonge, P. d., VanOosten T., Keune P. and Lorne A., 2005. Piero Gilardi Still Life of Watermelons. In: Hummelen I and Sillé D (eds) *Modern art: who cares?: an interdisciplinary research project and an international symposium on the conservation of modern and contemporary art*. London, United Kingdom: Archetype Publications Ltd., 136-148.
- Kaczmarek, H. and Chaberska H., 2006. The influence of UV-irradiation and support type on surface properties of poly(methyl methacrylate) thin films. *Applied Surface Science* 252/23: 8185–8192.
- Kaczmarek, H., Gałka P. and Kowalonek J., 2010. Influence of a photoinitiator on the photochemical stability of poly(methyl methacrylate) studied with fourier transform infrared spectroscopy. *Journal of Applied Polymer Science* 115/3: 1598-1607.
- Kambe, H., Watanabe H., Nagatomo S. and Itoh Y., 1977. Degradation of poly (methyl methacrylate) by flash irradiation. *Polymer* 18/10: 1063-1067.
- Kane, C. L., 2015. Plastic Shine: From Prosaic Miracle To Retrograde Sublime. *e-flux special issue 'Politics of Shine'*.
- Kargin, V. A., 1958. Structure and Phase State of Polymers. *Journal Of Polymer Science*: 247-258.
- Kawagoe, M. and Morita M., 1994. Fracture mechanisms of poly(methyl methacrylate) under static torsion in alcohol environments. *Journal of Materials Science* 29/22: 6041-6046.
- Kehlet, C., 2013. Non-invasive investigation of polymeric materials using nuclear magnetic resonance. In: Bechthold T (ed) *Future Talks 013: Lectures and Workshops on Technology and Conservation of Modern Materials in Design* Munich, 11-16.
- Kehlet, C., DeFederico E., Schahbaz H., Catalano A., Dittmer J. and Nielsenc N. C., 2013. Non-invasive characterization of polymeric materials in relation to art conservation using unilateral NMR combined with multivariate data analysis. *Analytical Methods* 5/: 4480–4486.
- Khan, M. I., Tabussum S., Doedens R. J., Golub V. O. and O'Connor C. J., 2004. Functionalized Metal Oxide Clusters: Synthesis, Characterization, Crystal Structures, and Magnetic

- Properties of a Novel Series of Fully Reduced Heteropolyoxovanadium Cationic Clusters Decorated with Organic Ligands. *Inorganic Chemistry* 43/: 5850–5859.
- Khandekar, N., 2000. A survey of the conservation literature relating to the development of aqueous gel cleaning on painted and varnished surfaces. *Reviews in Conservation* 1/: 10-20.
- Khandekar, N., 2004a. Gelled Systems: Theory and Early applications. In: Dorge V (ed) *Solvent Gels for the Cleaning of Works of Art: The Residue Question*. The Getty Conservation Institute.
- Khandekar, N., 2004b. Introduction. In: Dorge V (ed) *Solvent Gels for the Cleaning of Works of Art: The Residue Question*. The Getty Conservation Institute.
- Khanjian, H., Stulik D. and Miller D., 2004. Reserach into Solvent Residues. In: Dorge V (ed) *Solvent Gels for the Cleaning of Works of Art: The Residue Question*. The Getty Conservation Institute.
- Kirwan, L. J., Fawell P. D. and vanBronswijk W., 2003. In Situ FTIR-ATR Examination of Poly(acrylic acid) Adsorbed onto Hematite at Low pH. *Langmuir* 19/: 5802-5807.
- Knuutinen, U. and Kyllonen P., 2006. Two case studies of unsaturated polyester composite art objects.
- Koleva, M., 2013. Cast Products and Mould Designer Skills at the European Context (CAE-DS): Poly(methyl methacrylate) PMMA. Technical University of Gabrovo
- Kronkright, D., 2009. Book review of: *Solvent Gels For The Cleaning Of Works Of Art: The Residue Question*, and: *Cleaning Painted Surfaces: Aqueous Methods*. *Journal of the American Institute for Conservation* 48/1: 83-96.
- Kwamen, D. R. T., 2014. Solvent and Plasticizer effects in Solid Polymers by NMR. PhD. Faculty of Mathematics, Computer Science and Natural Sciences. RWTH Aachen University.
- Labidi, N. S. and Djebaili A., 2008. Studies of The Mechanism of Polyvinyl Alcohol Adsorption on The Calcite/Water Interface in The Presence of Sodium Oleate. *Journal of Minerals & Materials Characterization & Engineering* 7/2: 147-161.
- Laganà, A., 2008. I materiali plastici: poliuretano, polimetilmetacrilato e polivinilcloruro. Tre casi di studio. *Bollettino ICR - Istituto Centrale per il Restauro* 16-17/: 101-134.
- Laganà, A. and Van Oosten T., 2009. Investigation into a suitable method for adhering damaged works of art made of transparent unsaturated polyester. In: Bechthold T (ed) *FUTURE TALKS 009: The Conservation of Modern Materials in Applied Arts and Design* Munich.
- Laganà, A. and vanOosten T., 2011. Back to transparency, back to life: research into the restoration of broken transparent unsaturated polyester and poly(methyl

- methacrylate) works of art. In *ICOM-CC 16th Triennial Conference: preprints. Lisbon 19–23 September 2011*, ed. J. Bridgland. Almada: Critério Produção Gráfica, Lda.
- Laganà, A., Langenbacher J., Rivenc R., Caro M., Dion V. and Learner T., 2017. The Future of Looking Younger: A New face for PMMA. Research into fill materials to repair poly (methyl methacrylate) in contemporary objects and photographs. In *ICOM-CC 17th Triennial Conference: preprints, Copenhagen, 4–8 September 2017*, ed. J. Bridgland, art. 0906. Paris: International Council of Museums.
- Lai, C.-H., 1992. Physical ageing and dimensional changes of acrylate polymers. Ph.D. Physical and Inorganic Chemistry. The University of Adelaide.
- Lambert, S., 2012. Plastics - Why not? A Perspective from the Museum of Design in Plastics. In: Were G and King JCH (eds) *Extreme Collecting: Challenging Practices for 21st Century Museums*. Oxford: Berghahn Books, 168-180.
- Lampman, S., 2003. *Characterization and Failure Analysis of Plastics*. ASM International.
- Lantry, D. N., 2001 Archives and Collections, Dress for Egress: The Smithsonian National Air and Space Museum's Apollo Spacesuit Collection. *Journal of Design History* 14/4.
- Laurenson, P., 2006. Authenticity, Change and Loss in the Conservation of Time-Based Media Installations. *TATE PAPERS*.
- Lavédrine, B., Rivenc R. and Schilling M., 2009. POPART: an international research project on the conservation of plastics. *Conservation perspectives: the GCI newsletter* 24/2: 10-12.
- Lavédrine, B. and Shashoua Y., 2012. Foreword by Bertrand Lavédrine, project coordinator and Yvonne Shashoua, conservation scientist. In: Lavédrine B, Fournier A and Martin G (eds) *Preservation of Plastic Artefacts in Museum Collections*. Comité des travaux historiques et scientifiques - CTHS, 11-14.
- Lazzari, M., Ledo-Suárez A., López T., Scalarone D. and López-Quintela M. A., 2011. Plastic matters: an analytical procedure to evaluate the degradability of contemporary works of art. *Analytical and Bioanalytical Chemistry* 399/9: 2939-2948.
- Learner, T., 2012. Modern paints. In: Hill-Stoner J and Rushfield R (eds) *Conservation of Easel Paintings*. London and New York: Routledge, 242-251.
- Learner, T., Rivenc R. and Richardson E., 2011. *From Start To Finish: De Wain Valentine's Gray Column*. Los Angeles: The Getty Conservation Institute.
- Lee, H. B., Khang G. and Lee J. H., 2003. Polymeric Biomaterials. In: Park JB and Bronzino JD (eds) *Biomaterials: Principles and Applications*. Florida: CRC Press.
- Lenz, E., 2012. New Materials, New Approaches. Exhibition Catalog. In: D. Wigmore Fine Art I (ed).
- Levine, H. and Slade L., 1988. Water as a plasticizer: Physico-chemical aspects of low moisture polymeric systems. 79-185.

- Lim, X., 2018. These Cultural Treasures Are Made of Plastic. Now They're Falling Apart. *The New York Times*. Available at: <https://www.nytimes.com/2018/08/28/science/plastics-preservation-getty.html> (accessed 9 April 2020).
- Lister, T. and Renshaw J., 2004. *Conservation Chemistry- an introduction*. London: Royal Society of Chemistry.
- Liu, J., Wang J., Li H., Shen D., Zhang J., Ozaki Y. and Yan S., 2006. Epitaxial Crystallization of Isotactic Poly(Methyl Methacrylate) on Highly Oriented Polyethylene. *The Journal of Physical Chemistry B* 110/2: 738-742.
- Loehnert, S., 2010. About Statistical Analysis of Qualitative Survey Data. *International Journal of Quality, Statistics, and Reliability*.
- Lorne, A., 1999. The poly(methyl methacrylate) objects in the collection of The Netherlands Institute for Cultural Heritage. In ICOM-CC 12th Triennial Meeting: preprints Volume II, Lyon, 29 August-3 September 1999, ed. J. Bridgland. London: James and James.
- Luo, D., 1994. Tacticity effect on miscibility of polymer blends.
- Luo, D., Pearce E. M. and Kwei T. K., 1993. Miscibility of stereoregular poly(methyl methacrylates) with poly(styrene-co-p-(hexafluoro-2-hydroxy-2-propyl)styrene). *Macromolecules* 26/23: 6220-6225.
- Maitra, J. and Shukla V. K., 2014. Cross-linking in Hydrogels - A Review. *American Journal of Polymer Science* 4/2: 25-31.
- Malacarne-Zanon, J., Pashley D. H., Agee K. A., Foulger S., Alves M. C., Breschi L., Cadenaro M., Garcia F. P. and Carrilho M. R., 2009. Effects of ethanol addition on the water sorption/solubility and percent conversion of comonomers in model dental adhesives. *Dental Materials* 25/10: 1275-1284.
- Mandarim de Lacerda, M. E., 2010. The use of plastic in utilitarian and functional design objects. Master's Thesis. Art. Iowa: University of Iowa.
- Mark, J. E., Eisenberg A., Graessley W. W., Mandelkern L., Samulski E. T., Koenig J. L. and Wignall G. D., 1993. *Physical Properties of Polymers (Acs Professional Reference Books)*. Washington: American Chemical Society.
- Martin, J. W., Dickens B., Waksman D., Bentz D. P., Byrd W. E., Embree E. and Roberts W. E., 1987. Thermal degradation of poly(methyl methacrylate) at 50°C to 125°C. *Journal of Applied Polymer Science* 34/1: 377-393.
- Martinez-Vega, J. J., Trumel H. and Gacougnolle J. L., 2002. Plastic deformation and physical ageing in PMMA. *Polymer* 43/18: 4979-4987.
- Mason, M., 2011. The impact of World War II on women's fashion in the United States and Britain. Master's Thesis. Department of Theatre. University of Nevada.

- Maxwell, A., Broughton W., Dean G. and Sims G., 2005. *Review of Accelerated Ageing Methods and Lifetime Prediction Techniques for Polymeric Materials*.
- Mazzuca, C., Micheli L., Carbone M., Basoli F., Cervelli E., Iannuccelli S., Sotgiu S. and Palleschi A., 2014. Gellan hydrogel as a powerful tool in paper cleaning process: A detailed study. *Journal of Colloid and Interface Science* 416/: 205-211.
- McDonagh-Smith, A., Arnold J. C. and Isaac D. H., 2001. Thermal stresses and orientations in acrylic sheet. *Polymer Engineering & Science* 41/10: 1771-1782.
- McGlinchey, C., 1993. The Physical Aging of Polymeric Materials. In: Grattan D and Institute CC (eds) *Saving the twentieth century: the conservation of modern materials: proceedings of a conference Symposium 91: Saving the Twentieth Century, Ottawa, Canada, 15 to 20 September, 1991*. Ottawa, Canada: Canadian Conservation Institute, 113-121.
- McKibbin, C., Allington-Jones L. and Verveniotou E., 2017. Giant sequoia: an extraordinary case study involving Carbopol gel. In: Angelova L, Ormsby BA, Townsend JH and Wolbers R (eds) *Gels in the conservation of art*. London, England: Archetype Publications, 172-176.
- McNeill, I. C., Ahmed S. and Memetea L., 1995. Thermal degradation of vinyl acetate—methacrylic acid copolymer and homopolymers. I. An FTIR spectroscopic investigation of structural changes in the degrading material. *Polymer Degradation and Stability* 47/3: 423-433.
- Meijer, H. E. H. and Govaert L. E., 2005. Mechanical performance of polymer systems: The relation between structure and properties. *Progress in Polymer Science* 30/8–9: 915-938.
- Meikle, J. L., 1992. Into the Fourth Kingdom: Representations of Plastic Materials (1920-1950). *Journal of Design History* 5/3: 173-182.
- Meikle, J. L., 1998. Material Virtues: On the Ideal and the Real. *Journal of Design History* 11/3: 191-199.
- Meldrum, T., 2013. NMR Fundamentals I. Introduction through Relaxation. Volterra Summer School.
- Mess, A., Vietzke J.-P., Rapp C. and Francke W., 2011. Qualitative Analysis of Tackifier Resins in Pressure Sensitive Adhesives Using Direct Analysis in Real Time Time-of-Flight Mass Spectrometry. *Analytical Chemistry* 83/19: 7323-7330.
- Meyers, G., Badami A., Rozeveld S., Cieslinski B., Todd C., Wood C., Rothe D., Heeschen W. and Mitchell G., 2011. Microscopy Characterization of Porous Polymer Materials. In: Silverstein MS, Cameron NR and Hillmyer MA (eds) *Porous Polymers*. UK: John Wiley & Sons, Inc.

- Michalski, S. and Rossi-Doria M., 2011. Using decision diagrams to explore, document, and teach treatment decisions, with an example of their application to a difficult painting consolidation treatment. In *ICOM-CC 16th Triennial Conference: preprints. Lisbon 19–23 September 2011*, ed. J. Bridgland. Almada: Critério Produção Gráfica, Lda.
- Michler, G. H., 1989. Crazes in amorphous polymers I. Variety of the structure of crazes and classification of different types of crazes. *Colloid and Polymer Science* 267/5: 377-388.
- Mijović, J., Nicolais L., D'Amore A. and Kenny J. M., 1994. Principal features of structural relaxation in glassy polymers. A Review. *Polymer Engineering & Science* 34/5: 381-389.
- Miller-Chou, B. A. and Koenig J. L., 2003. A review of polymer dissolution. *Progress in Polymer Science* 28/: 1223–1270.
- Miller, Z., Whitby G. and Garside P., 2017. Investigating the ability of phytate gel systems to treat iron gall ink at the British Library. In: Angelova L, Ormsby BA, Townsend JH and Wolbers R (eds) *Gels in the conservation of art*. London, England: Archetype Publications.
- Min, K., Silberstein M. N. and Aluru N. R., 2014. Crosslinking PMMA: Molecular Dynamics Investigation of the Shear Response. *Journal of Polymer Science Part B Polymer Physics* 52/6.
- Minolta, K., 2017. *Understanding Gloss Standards & Units*. Available at: <https://sensing.konicaminolta.us/blog/understanding-gloss-standards-units/> (accessed 13 March 2017).
- Mishra, S. and Keten S., 2013. Atomistic simulation based prediction of the solvent effect on the molecular mobility and glass transition of poly (methyl methacrylate). *Applied Physics Letters* 102/4: 041903.
- Mitsuoka, T., Torikai A. and Fueki K., 1993. Wavelength sensitivity of the photodegradation of poly(methyl methacrylate). *Journal of Applied Polymer Science* 47/: 1027–1032.
- Mittermeier, C., Johlitz M. and Lion A., 2015. A thermodynamically based approach to model physical ageing of amorphous polymers. *Archive of Applied Mechanics* 85/8: 1025-1034.
- Moncrieff, A. and Weaver G., 1987. *Science for Conservators, Volume 1: An introduction to Materials*. Museums & Galleries Commission and Routledge.
- Moncrieff, A. and Weaver G., 1992. *Science for Conservators, Volume 2: Cleaning*. Museums & Galleries Commission and Routledge.
- Moore, G. and Griffith, C. A., 2006. Laboratory evaluation of the decontamination properties of microfibre cloths. *Journal of Hospital Infection* 64/4: 379-385.

- Morales-Muñoz, C., 2011. Spectrocolorimetric and microscopic techniques for the evaluation of plasticized PVC cleaning: a case study applicable to three-dimensional objects at museums. *Journal of Microscopy* 243/3: 257-266.
- Morales-Muñoz, C., 2010. Surface modification of plasticized PVC by dry cleaning methods: Consequences for artworks. *Applied Surface Science* 256: 3567–3572.
- Morgan, E., 1991a. *Chemometrics: Experimental Design*. Chichester, England: John Wiley & Sons.
- Morgan, J., 1991b. *Conservation of Plastics: An introduction*. London: The Conservation Unit of the Museums & Galleries Commission and the Plastics Historical Society.
- Müller-Wuesten, D., 2011. Art and motion. The conservation of the motor-driven Olympia-sculpture designed by Hans-Michael Kassel in 1972. In: Bechthold T (ed) *Future Talks 011 Technology and Conservation of Modern Materials in Design*. Munich, 153-158.
- Mumok, 2013. Dan Flavin - Lights. In: Wien MMKSL (ed).
- Muzeau, E., Vigier G. and Vassoille R., 1994. Physical aging phenomena in an amorphous polymer at temperatures far below the glass transition. *Journal of Non-Crystalline Solids*.
- N'Diaye, M., Pascaretti-Grizon F., Massin P., Baslé M. F. and Chappard D., 2012. Water Absorption of Poly(methyl methacrylate) Measured by Vertical Interference Microscopy. *Langmuir* 28/31: 11609-11614.
- Nagai, H., 1963. Infrared Spectra of Stereoregular Polymethyl Methacrylate. *Journal of Applied Polymer Science* 7/: 1697-1714.
- Nagai, H., Watanabe H. and Nishioka A., 1962. Infrared spectra of deuterated polymethyl methacrylates. *Journal Of Polymer Science* 62/174: S95-S98.
- Nagai, N., Matsunobe T. and Imai T., 2005. Infrared analysis of depth profiles in UV-photochemical degradation of polymers. *Polymer Degradation and Stability* 88/2: 224-233.
- Nagy, E. E., Landgrebe B. and Smith S. M., 2011. Treatment of Donald Judd's Untitled 1977: Retention of the original acrylic sheets. *Objects Specialty Group Postprints* 18/: 113-125.
- Natali, I., Carretti E., Angelova L., Baglioni P., Weiss R. G. and Dei L., 2011. Structural and Mechanical Properties of "Peelable" Organoaqueous Dispersions with Partially Hydrolyzed Poly(vinyl acetate)-Borate Networks: Applications to Cleaning Painted Surfaces. *Langmuir* 27/: 13226–13235.
- Negm, N. A., El-Faragy A. F., Tawfik S. M., Abdelnour A. M., Hefni H. H. and Khowdiary M. M., 2003. Synthesis, Surface and Thermodynamic Properties of Substituted

- Polytriethanolamine Nonionic Surfactants. *Journal of Surfactants and Detergents* 16/: 333–342.
- Nekkanti, V., Marwah A. and Pillai R., 2015. Media milling process optimization for manufacture of drug nanoparticles using design of experiments (DOE). *Drug Development and Industrial Pharmacy* 41/1: 124-130.
- Nemat-Nasser, S., Amirkhizi A., Holtzworth K., Jia Z., Nantasetphong W. and Song Y., 2015. Modification and Engineering of HSREP to Achieve Unique Properties. *Elastomeric Polymers with High Rate Sensitivity*. Elsevier, 319-345.
- Newman, T. R., 1965. Plastics: An Infant in Art. *Art Education* 18/7: 20-24.
- Nicholson, J. W., 2006. *The Chemistry of Polymers*. Cambridge, UK: The Royal Society of Chemistry.
- Nilsen, S. K., Dahl I., Jørgensen O. and Schneider T., 2002. Micro-fibre and ultra-micro-fibre cloths, their physical characteristics, cleaning effect, abrasion on surfaces, friction, and wear resistance. *Building and Environment* 37/12: 1373-1378.
- Norman, G., 2010. Likert scales, levels of measurement and the “laws” of statistics. *Advances in Health Sciences Education* 15/: 625–632.
- Oddy, A., 1999. Does Reversibility Exist in Conservation? In: Oddy A and Carroll S (eds) *Occasional Paper No.135: Reversibility - Does it Exist?* London: British Museum 1-5.
- Oligschläger, D., Kupferschläger K., Poschadel T., Watzlaw J. and Blümich B., 2014. Miniature mobile NMR sensors for material testing and moisture monitoring. *The Open-Access Journal for the Basic Principles of Diffusion Theory, Experiment and Application* 22/8: 1-25.
- O'Reilly, J. M., Bair H. E. and Karasz F. E., 1982. Thermodynamic properties of stereoregular poly(methyl methacrylate). *Macromolecules* 15/4: 1083-1088.
- O'Reilly, J. M. and Mosher R. A., 1981. Conformational energies of stereoregular poly(methyl methacrylate) by Fourier transform infrared spectroscopy. *Macromolecules* 14/3: 602-608.
- O'Reilly, J. M. and Mosher R. A., 1983. Functional groups in carbon black by FTIR spectroscopy. *Carbon* 21/1: 47-51.
- Ortíz-Rodríguez, E., 2013. Polymer Rheology. In: Saldívar-Guerra E and Vivaldo-Lima E (eds) *Handbook Of Polymer Synthesis, Characterization, And Processing*. Hoboken, New Jersey: John Wiley & Sons, Inc, 435–449.
- Otero-Pailos, J., 2007. Conservation Cleaning / Cleaning Conservation. *Editorial* 4/1: III-VIII.
- Ouano, A. C. and Carothers J. A., 1980. Dissolution dynamics of some polymers: Solvent-polymer boundaries. *Polymer Engineering & Science* 20/2: 160-166.



- Øysæd, H., 1990. Dynamic mechanical properties of multiphase acrylic systems. *Journal of Biomedical Materials Research* 24/8: 1037-1048.
- Paltridge, B. and Phakiti A., 2010. Continuum companion to Research Methods in Applied Linguistics. Continuum International Publishing.
- Papanu, J. S., Hess D. W., Soane D. S. and Bell A. T., 1989. Dissolution of Thin Poly(methyl methacrylate) Films in Ketones, Binary Ketone/Alcohol Mixtures, and Hydroxy Ketones. *Journal of The Electrochemical Society* 136/10: 3077-3083.
- Passaglia, E., 1987. Crazes and fracture in polymers. *Journal of Physics and Chemistry of Solids* 48/11: 1075-1100.
- Patel, M. M., Smart J. D., Nevell T. G., Ewen R. J., Eaton P. J. and Tsibouklis J., 2003. Mucin/Poly(acrylic acid) Interactions: A Spectroscopic Investigation of Mucoadhesion. *Biomacromolecules* 4/: 1184-1190.
- Pavitt, J., 1998. Review of Early plastics: Perspectives 1850-1950. *Journal of Design History* 11/2: 175-177.
- Pavitt, R., 2012. Cleaning of painted surfaces - Wolbers strikes again! A Workshop Review. *News in Conservation IIC*, 32. Available at: [https://www.iiconservation.org/system/files/publications/journal2012b2012\\_5.pdf](https://www.iiconservation.org/system/files/publications/journal2012b2012_5.pdf) (accessed 19 Jan 2014).
- Pavlidou, E., 2013. The Role of Microscopy Techniques in the Study of Cultural Heritage Materials. In: Varella EA (ed) *Conservation science for the cultural heritage: applications of instrumental analysis*. Heidelberg: Springer Verlag.
- PCE Instruments, 2018. *Gloss Meter IG-331*. Available at: <https://www.industrial-needs.com/technical-data/gloss-meter-ig-331.htm> (accessed 13 April 2017).
- Peacock, A. J. and Calhoun A., 2006. *Polymer Chemistry - Properties and Applications*. Munich: Hanser Publishers.
- Pearce, S., 2012. Knowing the New. In: Were G and King JCH (eds) *Extreme Collecting: Challenging Practices for 21st Century Museums*. Oxford: Berghahn Books, 93-101.
- Pereira, L., Sousa A., Coelho H., Amado A. M. and Ribeiro-Claro P. J. A., 2003. Use of FTIR, FT-Raman and <sup>13</sup>C-NMR spectroscopy for identification of some seaweed phycocolloids. *Biomolecular Engineering* 20/: 223-228.
- PerkinElmer, 2011. Application Note. Thermal Analysis.
- PerkinElmer, 2013. Dynamic Mechanical Analysis (DMA).
- Peterson, J. D., Vyazovkin S. and Wight C. A., 1999. Stabilizing effect of oxygen on thermal degradation of poly(methyl methacrylate). *Macromolecular Rapid Communications* 20/: 480-483.

- Pethrick, R. A., Amornsakchai T. and North A. M., 2011. *Introduction to Molecular Motion in Polymers*. Scotland, UK: Whittles Publishing.
- Piccarolo, S. and Titomanlio G., 1982. Synergism in the swelling and solubility of poly(methyl methacrylate) in presence of ethanol/water mixtures. *Die Makromolekulare Chemie, Rapid Communications* 3/6: 383-387.
- Pickett, J. E., 2018. Weathering of Plastics. In: Kutz M (ed) *Handbook of Environmental Degradation of Materials*. Oxford, UK: Elsevier, 163-182.
- Placido, A. J., 2010. Characterization Of Poly(Methylmethacrylate Basednanocomposites Enhanced Withcarbon Nanotubes. Masters Thesis. Chemical Engineering. Lexington, Kentucky: University of Kentucky.
- Plastics Historical Society, 2015. *The conservation of plastics*. Available at: [http://plastiquarian.com/?page\\_id=14326](http://plastiquarian.com/?page_id=14326) (accessed 18 March 2020).
- Ploeger, R., Verteramo R. and Chiantore O., 2009. 'Figura N.37' By Antonio Bueno: A Plastic Conservation Case Study From the Modern Art Gallery (GAM) of Turin, Italy. In: Bechthold T (ed) *Future Talks 009: The Conservation of Modern Materials in Applied Arts and Design*. Munich, 195-199.
- Polyakov, V. A. and Perov Y. Y., 1988. Experimental Methods Of Evaluating The Edge Effect - Review. *Mekhanika Kompozitnykh Materialov (translated)* 2/: 318-331.
- PolymerScienceLearningCenter, 2019. *Poly(methyl methacrylate)*. Available at: <https://pslc.ws/macrog/pmma.htm> (accessed 27 March 2015).
- Praiboon, J., Chirapart A., Akakabe Y., Bhumibhamond O. and Kajiwarac T., 2006. Physical and Chemical Characterization of Agar Polysaccharides Extracted from the Thai and Japanese Species of Gracilaria. *Science Asia* 32/Supplement 1: 11-17.
- Praticò, Y., Caruso F., Wangler T. and Flatt R. J., 2016. Statistical Analysis At The Service Of Conservation Practice: Doe For The Optimisation Of Stone Consolidation Procedures. In: Hughes JJ and Howind T (eds) *SCIENCE AND ART: A FUTURE FOR STONE Proceedings Of The 13th International Congress On The Deterioration And Conservation Of Stone*. Paisley, Scotland: University of the West of Scotland, 923-930.
- Pudney, P. D. A., Mutch K. J. and Zhu S., 2009. Characterising the phase behaviour of stearic acid and itstriethanolamine soap and acid–soap by infrared spectroscopy. *Physical Chemistry Chemical Physics* 11/: 5010–5018.
- Pugliese, M. and Waentig F., 2012. Foreword of Marina Pugliese, art historian and Friederike Waentig, restorer. In: Lavédrine B, Fournier A and Martin G (eds) *Preservation of Plastic Artefacts in Museum Collections*. Paris, France: Editions du Comité des travaux historiques et scientifiques, 23-24.

- Qayyum, M. M. and White J. R., 1987. Plastic fracture in weathered polymers. *Polymer* 28/3: 469-476.
- Quye, A. and Keneghan B., 1999. Chapter Five: Degradation. In: Quye A and Williamson C (eds) *Plastics: Collecting And Conserving* Edinburgh: NMS Publishing Limited.
- Quye, A. and Williamson C., 1999. *Plastics: collecting and conserving*. Edinburgh, United Kingdom: National Museums of Scotland.
- Quye, A., Littlejohn D., Pethrick R. A. and Stewart R. A., 2011. Accelerated ageing to study the degradation of cellulose nitrate museum artefacts. *Polymer Degradation and Stability* 96/10: 1934-1939
- Rai, V. N., Mukherjee C. and Jain B., 2016. Optical Properties (Uv-Vis And Ftir) Of Gamma Irradiated Polymethyl Methacrylate (PMMA). <https://arxiv.org › physics>.
- Ravenel, N., 2010. Pemulen® TR-2: An Emulsifying Agent with Promise. *WAAC Newsletter* 32/3: 10-12.
- Read, B. E., Tomlins P. E. and Dean G. D., 1990. Physical ageing and short-term creep in amorphous and semicrystalline polymers. *Polymer* 31/7: 1204-1215.
- Reedy, T. J. and Reedy C. L., 1994. Statistical Analysis In Conservation Science\*. *Archaeometry* 36/1: 1-23.
- Reusch, W., 2013. *Polymers*. Available at: <https://www2.chemistry.msu.edu/faculty/reusch/VirtTxtJml/polymers.htm> (accessed 22 September 2016).
- Rhyne, C. S., 2006. Clean Art? *JAIC Online, Journal of the American Institute for Conservation* 45/: 165-170.
- Ribelles, J. L. G. and Calleja R. D., 1984. Effect of the cooling rate in the formation of glass on the  $\alpha$  and  $\beta$  relaxations of some amorphous polymers. *Polymer Engineering & Science* 24/15: 1202-1204.
- Richardson, E., Woolley E., Corda K., Julien-Lees S., Pinchin S. and Roberts Z., 2017. *In Situ* Characterisation Of Readhesion Treatments For Ceiling Paintings Using Unilateral NMR. *Insight - Non-Destructive Testing and Condition Monitoring* 59/5: 249-255.
- Riedo, C., Caldera F., Poli T. and Chiantore O., 2015. Poly(vinylalcohol)-borate hydrogels with improved features for the cleaning of cultural heritage surfaces. *Heritage Science* 3/1: 23.
- Rivenc, R., Richardson E. and Learner T., 2011. The LA Look from Start to Finish: Materials, Processes and Conservation of Works by the Finish Fetish Artists. In *ICOM-CC 16th Triennial Conference: preprints. Lisbon 19–23 September 2011*, ed. J. Bridgland. Almada: Critério Produção Gráfica, Lda.
- Rogers, H., 2005. A Brief History of Plastic. *The Brooklyn Rail*.

- Rogerson, C., 2009. Preserving Jewellery Created from Plastics and Rubber: Application of Materials and Interpretation of Objects. Ph.D. London: The Royal College of Art.
- Rositani, F., Antonucci P. L., Minutoli M., Giordano N. and Villari A., 1987. Infrared analysis of carbon blacks. *Carbon* 25/3: 325-332.
- Ross-Murphy, S. B., 1987. Special issue: 2nd International Workshop on Plant Polysaccharides Physical gelation of biopolymers. *Food Hydrocolloids* 1/5: 485-495.
- Rossi, F., Santoro M., Casalini T., Veglianese P., Masi M. and Perale G., 2011. Characterization and Degradation Behavior of Agar–Carbomer Based Hydrogels for Drug Delivery Applications: Solute Effect. *International Journal of Molecular Sciences* 12/6: 3394-3408.
- Rovetta, T., Bianchin S., Salemi G. and Favaro M., 2014. The case study of an Italian contemporary art object: Materials and state of conservation of the painting "Ragazzo seduto" by Remo Brindisi. *Journal of Cultural Heritage* 15/: 564-568.
- Rühli, F. J., Böni T., Perlo J., Casanova F., Baias M., Egarter E. and Blümich B., 2007. Non-invasive spatial tissue discrimination in ancient mummies and bones in situ by portable nuclear magnetic resonance. *Journal of Cultural Heritage* 8/3: 257-263.
- SAFETYDATASHEET, 2018. BYK-358 N. BYK Additives & Instruments.
- Sahoo, S., Chakraborti C. K., Behera P. K. and Mishra S. C., 2012. FTIR and Raman Spectroscopic Investigations of a Norfloxacin/Carbopol934 Polymeric Suspension. *Journal of Young Pharmacists : JYP* 4/3: 138-145.
- Sale, D., 2011. Yellowing and appearance of conservation adhesives for poly (methyl methacrylate): A reappraisal of 20-year-old samples and test methods. *Adhesives & Consolidants for Conservation: Research and Applications*. Ottawa, Canada: Canadian Conservation Institute (CCI), 1-19.
- Sale, D., 1993. An evaluation of eleven adhesives for repairing poly(methyl methacrylate) objects and sculpture. In: Grattan D and Institute CC (eds) *Saving the twentieth century: the conservation of modern materials: proceedings of a conference Symposium 91: Saving the Twentieth Century, Ottawa, Canada, 15 to 20 September, 1991*. Canada: Canadian Conservation Institute, 325-340.
- Salzer, R., 2013. Infrared and Raman Spectroscopy. In: Varella EA (ed) *Conservation science for the cultural heritage: applications of instrumental analysis*. Heidelberg: Springer Verlag.
- Samiey, B. and Ashoori F., 2012. Adsorptive removal of methylene blue by agar: effects of NaCl and ethanol. *Chemistry Central Journal* 6/1: 14.
- Sandino, L., 2004. Here Today, Gone tomorrow: Transient Materiality in Contemporary Cultural Artefacts. *Journal of Design History* 17/3: 283-293.

- Sansonetti, A., Casati M., Striova J., Canevali C., Anzani M. and Rabbolini A., 2012. A Cleaning Method Based On The Use Of Agar Gels: New Tests And Perspectives. *12th International Congress on the Deterioration and Conservation of Stone*. New York: Columbia University.
- Saunders, S. and Kirby J., 2001. A comparison of light-accelerated ageing regimes in some galleries and museums. *The Conservator* 25/1: 95-104.
- Savitzky, A. and Golay M. J. E., 1964. Smoothing and Differentiation of Data by Simplified Least-Squares Procedures. *Analytical Chemistry* 36/8: 1627-1639.
- Schaeffer, T. T., 2001. *Effects of Light on Materials in Collections: Data on Photoflash and Related Sources*. USA The J. Paul Getty Trust.
- Schlenker, B. R., 1969. *Introduction to Materials Science*. Australasia: John Wiley & Sons.
- Schulz, H., Özkan G., Baranska M., Krüger H. and Özcan M., 2005. Characterisation of essential oil plants from Turkey by IR and Raman spectroscopy. *Vibrational Spectroscopy* 39/: 249–256.
- Scialla, S., 2006. The Formulation of Liquid Household Cleaners. In: Showell MS (ed) *Handbook of Detergents, Part D: Formulation*. Boca Raton, FL: CRC Press.
- Scott, C. L., 2012. The Use of Agar as a Solvent Gel. *40th Annual Meeting - Research and Technical Studies Specialty Group Postprints* Albuquerque, NM: Research and Technical Studies Specialty Group (RATS) and The American Institute for Conservation of Historic and Artistic Works (AIC), 138-173.
- Shahidzadeh, N., Schut M. F. L., Desarnaud J., Prat M. and Bonn D., 2015. Salt stains from evaporating droplets. *Scientific Reports* 5/10335.
- Shashoua, Y., 1999. Back to plastics. In: Oddy WA and Carroll S (eds) *Reversibility: does it exist?* London, United Kingdom: British Museum, 29-32.
- Shashoua, Y., 2006. Plastics. In: May E and Jones M (eds) *Conservation Science: Heritage Materials*. Cambridge: RSC Publishing.
- Shashoua, Y., 2008. *Conservation of Plastics: materials science, degradation and preservation*. Oxford: Butterworth-Heinemann.
- Shashoua, Y., 2012a. Conservation Adsorbents—How Effective Are They For Plastics? *Soft Materials and Hard Plastics in Art: Characterization, Degradation and Conservation*. Northwestern University: Art Institute Chicago.
- Shashoua, Y., 2012b. Studies in active conservation of plastic artefacts in museums- Introduction. In: Lavédrine B, Fournier A and Martin G (eds) *Preservation of Plastic Artefacts in Museum Collections*. Comité des travaux historiques et scientifiques, 219-223.

- Shashoua, Y., 2014. A safe place Storage strategies for Plastics. *Conservation Perspectives, The GCI Newsletter Conservation of Plastics/*.
- Shashoua, Y., Liss-Petersen A. and Rapoport E., 2009. The price of pristine PMMA. In: Bechthold T (ed) *FUTURE TALKS 009: The Conservation of Modern Materials in Applied Arts and Design*. Munich, 51-58.
- Shaw, M. T. and MacKnight W. J., 2005. *Introduction to Polymer Viscoelasticity*. Hoboken, NJ, USA: John Wiley & Sons, Inc.
- Shimadzu, 2019. *ATR Precautions*. Available at: <https://www.shimadzu.com/an/ftir/support/ftirtalk/letter1/atr1.html> (accessed 5 June 2019).
- Shin, H. S., Jung Y. M., Oh T. Y., Chang T., Kim S. B., Lee D. H. and Noda I., 2002. Glass Transition Temperature and Conformational Changes of Poly(methyl methacrylate) Thin Films Determined by a Two-Dimensional Map Representation of Temperature-Dependent Reflection-Absorption FTIR Spectra. *Langmuir* 18/: 5953-5958.
- Shin, H. S., Lee H., Jun C.-H., Jung Y. M. and Kim S. B., 2005. Transition temperatures and molecular structures of poly(methyl methacrylate) thin films by principal component analysis: comparison of isotactic and syndiotactic poly(methyl methacrylate). *Vibrational Spectroscopy* 37/1: 69-76.
- Shungu, D., Valiant M., Tutlane V., Weinberg E., Weissberger B., Koupal L., Gadebusch H. and Stapley E., 1983. GELRITE as an Agar Substitute in Bacteriological Media. *Applied and Environmental Microbiology* 46/4: 840-845.
- Silverwood, R. J., Tabatabaei H. and Ajji A., 2014. *Peelable - Resealable Films: FTIR Characterisation and Peel Strength*. Society of Plastics Engineers.
- Simms, M., 2015. Helen Pashgian: Light Invisible. *CAA Reviews*.
- Singer, E. and Couper M. P., 2017. Some Methodological Uses of Responses to Open Questions and Other Verbatim Comments in Quantitative Surveys. *Methods, data, analyses* 11/2: 115-134.
- Singh, B. and Sharma N., 2008. Mechanistic implications of plastic degradation. *Polymer Degradation and Stability* 93/3: 561-584.
- Snijders, E., Weerdenburg S. and Timmermans R., 2011. The treatment of a polyurethane rigid foam floor piece by Ger van Elk: a study in the conservation of plastics. In *ICOM-CC 16th Triennial Conference: preprints. Lisbon 19–23 September 2011*, ed. J. Bridgland. Almada: Critério Produção Gráfica, Lda.
- Söderman, O. and Stilbs P., 1994. NMR studies of complex surfactant systems. *Progress in Nuclear Magnetic Resonance Spectroscopy* 26/: 445-482.

- Song, J., Fischer C. H. and Schnabel W., 1992. Thermal oxidative degradation of poly(methyl methacrylate). *Polymer Degradation and Stability* 36/3: 261-266.
- Sperling, L. H., 2006. *Introduction to Physical Polymer Science*. Hoboken, NJ, USA: John Wiley & Sons, Inc.
- Spoljaric, S., Salminen A., Luong N. D. and Seppälä J., 2014. Stable, self-healing hydrogels from nanofibrillated cellulose, poly(vinyl alcohol) and borax via reversible crosslinking. *European Polymer Journal* 56/: 105-117.
- Spyratou, E., Asproudis I., Tsoutsi D., Bacharis C., Moutsouris K., Makropoulou M. and Serafetinides A. A., 2010. UV laser ablation of intraocular lenses: SEM and AFM microscopy examination of the biomaterial surface. *Applied Surface Science* 256/8: 2539-2545.
- Stansbury, J. W. and Dickens S. H., 2001. Determination of double bond conversion in dental resins by near infrared spectroscopy. *Dental Materials* 17/: 71-79.
- Stavroutis, C., 2012. Pemulen Revised: pHuck the pH Meter. *WAAC Newsletter* 34/2.
- Stavroutis, C., 2014. Pemulen TR-2: the once and future king (of conservation). *WAAC Newsletter* 36/2: 10-11.
- Stavroutis, C., 2017. Gels: evolution in practice. In: Angelova L, Ormsby BA, Townsend JH and Wolbers R (eds) *Gels in the conservation of art*. London, England: Archetype Publications, 209-217.
- Stavroutis, C. and Blank S., 1989. Solvents & Sensibility. *Western Association for Art Conservation (WAAC) Newsletter* 11/2: 2-10.
- Stefaniak, A. B., Harvey C. J. and Wertz P. W., 2010. Formulation and stability of a novel artificial sebum under conditions of storage and use. *International Journal of Cosmetic Science* 32/5: 347-355.
- Struik, L. C. E., 1977. Physical aging in plastics and other glassy materials. *Polymer Engineering & Science* 17/3: 165-173.
- Stuart, B., 2004. *Infrared Spectroscopy: Fundamentals and Applications*. Chichester, UK: Wiley.
- Stuart, B., 2007. *Analytical Techniques in Materials Conservation*. England: Wiley.
- Subbiah, S. and Melkote S. N., 2013. Engineering Materials for Micro Cutting. In: Cheng K and Huo D (eds) *Micro-Cutting: Fundamentals and Applications*. John Wiley & Sons.
- Suenson-Taylor, K. and Sully D., 1996. The Use of Condition Score to Determine Glycerol Concentration in the Treatment of Waterlogged Archaeological Leather. An Empirical Solution. In: Hoffmann P, Grant T, Spriggs JA and Daley T (eds) *Proceedings of the 6th ICOM Group on Wet Organic Archaeological Materials Conference*. York, 157-172.
- Suenson-Taylor, K., Sully D. and Orton C., 1999. Data in Conservation: The Missing Link in the Process. *Studies in Conservation* 44/3: 184-194.

- Sullivan, M. S., Duncan T. T., Berrie B. H. and Weiss R. G., 2017. Rigid polysaccharide gels for paper conservation: a residue study. In: Angelova L, Ormsby BA, Townsend JH and Wolbers R (eds) *Gels in the conservation of art*. London, England: Archetype Publications, 42-50.
- Sun, M., Zou J., Zhang H. and Zhang B., 2014. Measurement of reversible rate of conservation materials based on gel cleaning approach. *Journal of Cultural Heritage*: 1-9.
- Sutherland, K., 2001. Solvent extractable components of oil paint films. Ph.D. thesis. Van 't Hoff Institute for Molecular Sciences (HIMS). Amsterdam: University of Amsterdam (UvA).
- Sutherland, K. and Phenix A., 2001. The cleaning of paintings: effects of organic solvents on oil. *Reviews in Conservation International Institute for Conservation of Historic and Artistic Works (IIC) 2/*.
- Szakonyi, G. and Zelkó R., 2012. The effect of water on the solid state characteristics of pharmaceutical excipients: Molecular mechanisms, measurement techniques, and quality aspects of final dosage form. *International Journal of Pharmaceutical Investigation 2/1*: 18-25.
- Szmelter, I., 2009. Theory and Practice of the Preservation of Modern and Contemporary Art: complex tangible and intangible heritage. In: Schädler-Saub U and Weyer A (eds) *Theory and practice in the conservation of modern and contemporary art: reflections on the roots and the perspectives*. Hildesheim: Archetype, 101-119.
- Taylor, A. J., 2018. Alexander Calder's Industrial Revolution. *Architecture, Industry and World Peace*: 181-185.
- Teutonico, J., 2006. The Gels Cleaning Research Project. *Conservation Perspectives, The GCI Newsletter 21/2*: 7.
- Tham, W. L., Chow W. S. and Mohd-Ishak Z. A., 2010. Simulated body fluid and water absorption effects on poly(methyl methacrylate)/hydroxyapatite denture base composites. *eXPRESS Polymer Letters 4/9*: 517–528.
- The Solomon R. Guggenheim Foundation, 2020. *László Moholy-Nagy*. Available at: <https://www.guggenheim.org/artwork/artist/laszlo-moholy-nagy> (accessed 3 April 2020).
- Tobing, S. D. and Klein A., 2001. Molecular parameters and their relation to the adhesive performance of acrylic pressure-sensitive adhesives. *Journal of Applied Polymer Science 79/12*: 2230-2244.
- Todica, M., Stefan R., Pop C. V. and Olar L., 2015. IR and Raman Investigation of Some Poly(acrylic) Acid Gels in Aqueous and Neutralized State. *ACTA PHYSICA POLONICA A 128/1*: 128-135.



- Toja, F., Nevin A., Comelli D., Levi M., Cubeddu R. and Toniolo L., 2011a. Fluorescence and Fourier-transform infrared spectroscopy for the analysis of iconic Italian design lamps made of polymeric materials. *Analytical Chemistry for Cultural Heritage* 399/: 2977–2986.
- Toja, F., Nevin A., Comelli D. and Toniolo L., 2011b. Novel Applications of Molecular Spectroscopy and Imaging for the Analysis of Design Objects in ABS. In: Bechthold T (ed) *Future Talks 011 Technology and Conservation of Modern Materials in Design*. Munich, 241-248.
- Toja, F., Saviello D., Nevin A., Comelli D., Lazzari M., Valentini G. and Toniolo L., 2013. The degradation of poly(vinyl acetate) as a material for design objects: A multi-analytical study of the Cocoon lamps. Part 2. *Polymer Degradation and Stability* 98/: 2215-2223.
- Tokiwa, Y., Calabia B., Ugwu C. and Aiba S., 2009. Biodegradability of Plastics. *International Journal of Molecular Sciences* 10/9: 3722-3742.
- Torikai, A. and Hasegawa H., 1998. Wavelength effect on the accelerated photodegradation of polymethylmethacrylate. *Polymer Degradation and Stability* 61/: 361-364.
- Torikai, A., Hattori T. and Eguchi T., 1995. Wavelength effect on the photoinduced reaction of polymethylmethacrylate. *Journal of Polymer Science Part A: Polymer Chemistry* 33/: 1867-1871.
- Torikai, A., Ohno M. and Fueki K., 1990. Photodegradation of poly(methyl methacrylate) by monochromatic light: Quantum yield, effect of wavelengths, and light intensity. *Journal of Applied Polymer Science* 41/: 1023–1032.
- Tortajada-Hernando, S. and Blanco-Dominguez M. M., 2013. Cleaning plaster surfaces with agar-agar gels: evaluation of the technique. *Ge-conservación - Grupo Español IIC* 4/: 111-126.
- Tran, H. H., Wu W. and Lee N. Y., 2013. Ethanol and UV-assisted instantaneous bonding of PMMA assemblies and tuning in bonding reversibility. *Sensors and Actuators B: Chemical* 181/: 955-962.
- Tretinnikov, O. N., 1999. Wettability and microstructure of polymer surfaces: stereochemical and conformational aspects. *Journal of Adhesion Science and Technology* 13/10: 1085-1102.
- Tretinnikov, O. N., 2003. Conformational characteristics of stereoregular PMMA and of the stereocomplex: new insights from FTIR measurements. *Macromolecular symposia* 203/1: 57-70.
- Tretinnikov, O. N. and Ohta K., 1998. Surface Segregation in Stereochemically Asymmetric Polymer Blends. *Langmuir* 14/4: 915-920.

- Tretinnikov, O. N. and Zhibankov R. G., 1991. The molecular structure and glass-transition temperature of the surface layers of films of poly(methyl methacrylate) according to infrared spectroscopy data. *Journal of Materials Science Letters* 10/17: 1032-1036.
- Trivedi, T. J. and Kumar A., 2014. Efficient Extraction of Agarose from Red Algae Using Ionic Liquids. *Green and Sustainable Chemistry* 4/: 190-201.
- Troiano, F., Vicini S., Gioventù E., Lorenzi P. F., Improta C. M. and Cappitelli F., 2014. A methodology to select bacteria able to remove synthetic polymers. *Polymer Degradation and Stability* 107/: 321-327.
- Tsang, J.-s. and Erhardt D., 1992. Current Research on the Effects of Solvents and Gelled and Aqueous Cleaning Systems on Oil Paint Films. *JAIC Online, Journal of the American Institute for Conservation* 31/1: 87-94.
- Turner, D. T., 1982. Polymethyl methacrylate plus water: sorption kinetics and volumetric changes. *Polymer* 23/2: 197-202.
- Ulrich, K., Centeno S. A., Arslanoglu J. and Del Federico E., 2011. Absorption and diffusion measurements of water in acrylic paint films by single-sided NMR. *Progress in Organic Coatings* 71/3: 283-289.
- Umney, N. and Rivers S., 2003. *Conservation of Furniture*. Oxford, UK: Butterworth-Heinemann.
- Urbaniak-Domagala, W., 2012. Advanced Aspects of Spectroscopy: The Use of the Spectrometric Technique FTIR-ATR to Examine the Polymers Surface. Department of Material and Commodity Sciences and Textile Metrology. Poland: Technical University of Lodz.
- Van Oosten, T., 2002. Crystals and Crazes: Degradation in Plastics Due to Microclimates. In: Van Oosten T, Shashoua Y and Waentig F (eds) *Plastics in Art: History, Technology, Preservation*. Munich, Germany: Siegl's Fachbuchhandlung, 80-88.
- Van Oosten, T., 2011. *PUR Facts: Conservation of Polyurethane Foam in Art and Design*. Amsterdam University Press.
- Van Oosten, T. and Huys F., 2005. The "Aeromodeller OO-PL" : the conservation of a PVC balloon. In *ICOM-CC 14th Triennial Meeting: preprints, The Hague, 12-16 September 2005*, ed. LEarthscan Ltd.
- Varanese, D. V., 1998. *The Fundamentals of Selecting Pressure-Sensitive Adhesives Medical Plastics and Biomaterials*. Available at: <https://www.mddionline.com/fundamentals-selecting-pressure-sensitive-adhesives-0> (accessed 4 June 2018).
- Varlot, K., Martin J., Gonbeau D. and Quet C., 1999. Chemical bonding analysis of electron-sensitive polymers by EELS. *Polymer* 40/: 5691-5697.

- Varshosaz, J., Reza Zaki M., Minaiyan M. and Banoozadeh J., 2015. *Preparation, Optimization, and Screening of the Effect of Processing Variables on Agar Nanospheres Loaded with Bupropion HCl by a D-Optimal Design*.
- Verma, A. and Pandit J. K., 2011. Rifabutin loaded floating gellan gum beads: In vitro and in vivo evaluation. *African Journal of Pharmacy and Pharmacology* 5/5: 589-595.
- Villalobos, M. A. and Debling J., 2013. Bulk and Solution Processes. In: Saldívar-Guerra E and Vivaldo-Lima E (eds) *Handbook Of Polymer Synthesis, Characterization, And Processing*. Hoboken, New Jersey: John Wiley & Sons, Inc, 273–294.
- Waentig, F., 2008a. *Plastics in Art*. Petersberg, Germany: Michael Imhof Verlag.
- Waentig, F., 2008b. Educating Conservation of Modern Materials: case studies. In: Keneghan B and Egan L (eds) *Plastics: looking at the future and learning from the past: papers from the conference held at the Victoria and Albert Museum, London: 23-25 May 2007*. London, United Kingdom: Archetype Publications Ltd, 52-58.
- Ward, I. M. and Sweeney I., 2013. *Mechanical Properties of Solid Polymers*. West Sussex: John Wiley & Sons.
- Ward, G. W. R., 2008. *The Grove Encyclopedia of Materials and Techniques in Art*. New York: Oxford University Press.
- Warda, J., Brückle I., Bezúr A. and Kushel D., 2007. Analysis of Agarose, Carbopol, and Laponite Gel Poultices in Paper Conservation. *JAIC Online, Journal of the American Institute for Conservation* 46/3: 263-279.
- Weissman, S. A. and Anderson N. G., 2014. Design of Experiments (DoE) and Process Optimization. A Review of Recent Publications. *Organic Process Research & Development*.
- Wertz, P. W., 2009. Human synthetic sebum formulation and stability under conditions of use and storage. *International Journal of Cosmetic Science* 31/1: 21-25.
- Wheeler, A., 2015. *An Interview With Iconic Artist Bruce Beasley On 3D Printing Sculptures*. Available at: <https://3dprintingindustry.com/news/an-interview-with-iconic-artist-bruce-beasley-on-3d-printing-sculptures-42536/> (accessed 9 January 2020).
- Wiles, D. M., 1993. Changes in polymeric materials with time. In: Grattan DW and Institute CC (eds) *Saving the twentieth century: the conservation of modern materials: proceedings of a conference Symposium 91: Saving the Twentieth Century, Ottawa, Canada, 15 to 20 September, 1991*. Ottawa, Canada: Canadian Conservation Institute, 105-112.
- Williams, S., 2019. Care of objects made from rubber and plastic. *CCI Notes Series 15 (Modern Materials and Industrial Collections)*, 15. Available at: <https://www.canada.ca/en/conservation-institute/services/conservation-preservation-publications/canadian-conservation-institute-notes/care-rubber-plastic.html> (accessed 17 March 2020).

- Williams, S. R., 1993. Composition Implications of Plastic Artifacts: A Survey of Additives and Their Effects on the Longevity of Plastics. In: Grattan D and Institute CC (eds) *Saving the twentieth century: the conservation of modern materials: proceedings of a conference Symposium 91: Saving the Twentieth Century, Ottawa, Canada, 15 to 20 September, 1991*. Ottawa, Canada: Canadian Conservation Institute, 134-153.
- Winkelmeyer, I., 2002. Perfection for an instant restoration of a polyurethane soft sculpture by John Chamberlain. In: Van Oosten T, Shashoua Y and Waentig F (eds) *Plastics in Art: History, Technology, Preservation*. Munich, Germany: Siegl's Fachbuchhandlung.
- Winther, T., Bannerman J., Skogstad H., Wikström L., Sandström T. and Brynnel U., 2013. Practical Aspects of the Testing and Use of Adhesives of Polystyrene. In: Bechthold T (ed) *Future Talks 013: Lectures and Workshops on Technology and Conservation of Modern Materials in Design. Munich, 19-26*. Munich, 115-120.
- Wochnowski, C., Eldin M. A. S. and Metev S., 2005. UV-laser-assisted degradation of poly(methyl methacrylate). *Polymer Degradation and Stability* 89/: 252-264.
- Wolbers, R., 2000. *Cleaning Painted Surfaces: Aqueous Methods*. London: Archetype Publications.
- Wolbers, R., 2013. The Use of Gels in Aqueous Conservation of Paper. Available at: <http://www.youtube.com/watch?v=R3qvho8SFdc> (accessed 20 Feb 2014).
- Wolbers, R., 2017. Terminology and properties of selected gels. In: Angelova L, Ormsby BA, Townsend JH and Wolbers R (eds) *Gels in the conservation of art*. London, England: Archetype Publications, 381-394.
- Wollny, K., 2006. DMTA investigation of a polymethyl methacrylate (PMMA) over a temperature range of -150 °C to 160 °C. *Application Note Physica Rheometers*. Anton Paar Germany GmbH.
- Wu, Y., 2014. Pressure Sensitive Adhesives based on Oleic Acid. Wood Science and Chemical Engineering. Oregon State University.
- Wypych, G., 2013. *Handbook of Material Weathering*. Toronto: ChemTec Publishing.
- Wypych, G. and Faulkner T., 1999. Basic parameters in weathering studies. In: Wypych G (ed) *Weathering of Plastics - Testing to Mirror Real Life Performance*. Norwich, NY: William Andrew Publishing/Plastics Design Library.
- Xie, F., Yu L., Chen L. and Li L., 2008. A new study of starch gelatinization under shear stress using dynamic mechanical analysis. *Carbohydrate Polymers* 72/: 229-234.
- Yip, V., 2015. The conservation of two contemporary Chinese woodblock prints using Gellan gum. *The International Institute for Conservation of Historic and Artistic Works*. Available at: <https://www.iiconservation.org/node/5733> (accessed 05 June 2016).

- Yun, M., Yim C., Jung N., Kim S., Thundat T. and Jeon S., 2011. Nanomechanical Thermal Analysis of Photosensitive Polymers. *Macromolecules* 44/24: 9661–9665.
- Zhao, R., Chen C.-Z., Li Q.-F. and Luo W., 2008. Effects of stress and physical ageing on nonlinear creep behavior of poly(methyl methacrylate) *Journal of Central South University of Technology* 15/s1: 582-588.
- Zhao, Y., Wang C. C., Huang W. M. and Purnawali H., 2013. Ethanol Induced Shape Recovery and Swelling in Poly(methyl methacrylate) and Applications in Fabrication of Microlens Array. *Advances in Science and Technology*.
- Zięba-Palus, J., 2007. The usefulness of infrared spectroscopy in examinations of adhesive tapes for forensic purposes. *Forensic Science and Criminology* 2/2: 1-9.
- Zolotarev, V. M., Volchek B. Z. and Vlasova E. N., 2006. Optical constants of industrial polymers in the IR region. *Optics and Spectroscopy* 101/5: 716-723.
- Zumdahl, S. and Zumdahl S., 2010. *Chemistry*. USA: Brooks Cole.